

Dayong Wang

Molecular
Toxicology in
*Caenorhabditis
elegans*

 Springer

Molecular Toxicology in *Caenorhabditis elegans*

Dayong Wang

Molecular Toxicology
in *Caenorhabditis elegans*

 Springer

Dayong Wang
School of Medicine
Southeast University
Nanjing, China

ISBN 978-981-13-3632-4 ISBN 978-981-13-3633-1 (eBook)
<https://doi.org/10.1007/978-981-13-3633-1>

Library of Congress Control Number: 2018966331

© Springer Nature Singapore Pte Ltd. 2019

This work is subject to copyright. All rights are reserved by the Publisher, whether the whole or part of the material is concerned, specifically the rights of translation, reprinting, reuse of illustrations, recitation, broadcasting, reproduction on microfilms or in any other physical way, and transmission or information storage and retrieval, electronic adaptation, computer software, or by similar or dissimilar methodology now known or hereafter developed.

The use of general descriptive names, registered names, trademarks, service marks, etc. in this publication does not imply, even in the absence of a specific statement, that such names are exempt from the relevant protective laws and regulations and therefore free for general use.

The publisher, the authors, and the editors are safe to assume that the advice and information in this book are believed to be true and accurate at the date of publication. Neither the publisher nor the authors or the editors give a warranty, express or implied, with respect to the material contained herein or for any errors or omissions that may have been made. The publisher remains neutral with regard to jurisdictional claims in published maps and institutional affiliations.

This Springer imprint is published by the registered company Springer Nature Singapore Pte Ltd.
The registered company address is: 152 Beach Road, #21-01/04 Gateway East, Singapore 189721, Singapore

Preface

Model animal *Caenorhabditis elegans* has been successfully used in toxicological study of various environmental toxicants or stresses. The basic knowledge system on model organism toxicology has been gradually established in *C. elegans*. With engineered nanomaterials as typical environmental toxicants, this has been described in the published book *Nanotoxicology in Caenorhabditis elegans*. In *C. elegans*, besides the cellular and developmental processes, the molecular events and the related signaling pathways are conserved to a great degree with those in mammals and in human beings. More importantly, *C. elegans* has been proven to be very sensitive to environmental exposures and can be employed to assess the potential toxicity of environmental toxicants at environmentally relevant concentrations. As a classic model animal, *C. elegans* has the well-described genetic and developmental backgrounds and the rich and available genetic resources based on the past half of century study. These backgrounds provide the strong basis for our establishing the knowledge system of molecular toxicology in nematodes. During the past 20 years, a large amount of data on the molecular toxicology has been obtained in *C. elegans*.

C. elegans is a tiny model animal. With the aid of a series of sensitive sublethal endpoints, it has the potential for understanding the response to environmental toxicants or stresses or the toxicity induction by environmental toxicants or stresses at the whole animal level. Therefore, the introduced knowledge system on the molecular toxicology in this book has been mainly organized at the whole animal level in nematodes.

In this book, we have raised three important concerns. The first concern is the definition and the association between molecular basis for toxicity in environmental toxicant- or stress-exposed nematodes and the molecular basis for transgenerational toxicity of environmental toxicants and stresses. The second concern is the definition and the association between protective molecular response to environmental toxicants and stresses and molecular basis for toxicity induction of environmental toxicants or stresses. The third concern is the definition and the association between molecular signals and epigenetic signals required for the regulation of toxicity of environmental toxicants or stresses.

Based on these concerns, in Chaps. 1 and 2, we first introduced the molecular basis for oxidative stress and reduced lifespan caused by environmental toxicants or stresses. In Chaps. 3, 4, 5, 6, 7 and 8, we introduced some important signaling pathways (oxidative stress-related, MAPKs, insulin and the related, development-related, cell death and DNA damage-related, and metabolism-related) involved in the regulation of toxicity of environmental toxicants or stresses. In Chaps. 9, 10, 11 and 12, we introduced the important roles of protective response signals, G-protein-coupled receptors and ion channels and downstream cytoplasmic signals, specific molecular signals, and epigenetic regulation signals in regulating the toxicity of environmental toxicants or stresses. In Chap. 13, we introduced and discussed the values and the limitations of normally used strategies to screen and to identify new genetic loci involved in the regulation of toxicity of environmental toxicants or stresses. Finally, in Chaps. 14 and 15, we introduced the molecular basis for adaptive response and transgenerational toxicity induced by environmental toxicants or stresses.

Nanjing, China

Dayong Wang

Contents

1	Molecular Basis for Oxidative Stress Induced by Environmental Toxicants in Nematodes	1
1.1	Introduction	1
1.2	Evidence for the Direct Association of Oxidative Stress with Toxicity of Environmental Toxicants	2
1.2.1	Induction of Oxidative Stress in Targeted Organs of Environmental Toxicants	2
1.2.2	Pharmacological Evidence for the Association of Oxidative Stress and Toxicity Formation of Environmental Toxicants	3
1.2.3	Association of Induction of Oxidative Stress in Intestine and Toxicity Formation in Other Targeted Organs	3
1.3	Molecular Machinery for the Activation of Oxidative Stress in Nematodes	5
1.3.1	Role of GAS-1 in the Activation of Oxidative Stress	5
1.3.2	Role of MEV-1 in the Activation of Oxidative Stress	6
1.3.3	Role of ISP-1 in the Activation of Oxidative Stress	7
1.3.4	Role of CLK-1 in the Activation of Oxidative Stress	8
1.4	Response Signals with the Functions to Defend Against the Oxidative Stress	9
1.4.1	Superoxide Dismutases (SODs)	9
1.4.2	Catalases (CATs)	10
1.4.3	Insulin Signaling	10
1.4.4	SKN-1/Nrf Signaling	12
1.5	Systematic Identification of Novel Genes Required for the Regulation of Oxidative Stress	16
1.5.1	Functional Genomic Approach to Identify Novel Genes Required for the Regulation of Oxidative Stress	16

1.5.2	Identification of Genes Required for the Regulation of Oxidative Stress or Stress Response Based on the Translocation of Environmental Toxicant	16
1.6	Molecular Basis for Induction of Oxidative Stress in Nematodes Exposed to Environmental Toxicants	22
1.6.1	Alteration in Primary Molecular Mechanism for the Control of Oxidative Stress Induced by Environmental Toxicants	22
1.6.2	Induction of Expression for Proteins with the Functions to Defend Against the Oxidative Stress Induced by Environmental Toxicants	23
1.6.3	Suppression in Expressions of Genes Mediating the Protection Response Defending Against Oxidative Stress in Nematodes After Chronic Exposure to Certain Environmental Toxicants	23
1.6.4	Induction of Expression for SOD Proteins in Environmental Toxicant-Exposed Nematodes Without Obvious Activation of Oxidative Stress	24
1.6.5	Molecular Signals Involved in the Regulation of Induction of Oxidative Stress in Nematodes Exposed to Environmental Toxicants	26
1.7	Perspectives	26
	References	27
2	Molecular Basis for Reduced Lifespan Induced by Environmental Toxicants or Stresses	31
2.1	Introduction	31
2.2	Molecular Basis for Longevity Control	32
2.2.1	Insulin Signaling Pathway	32
2.2.2	Dietary Intake Signaling Pathway	34
2.2.3	Mitochondrial Respiration Signaling Pathway	35
2.2.4	Germline Signaling Pathway	36
2.2.5	Interaction Among Different Signaling Pathways	38
2.3	Environmental Toxicants or Stresses Reduce Lifespan by Affecting the Molecular Basis for Longevity	38
2.3.1	Environmental Toxicants or Stresses Reduce Lifespan by Affecting the Insulin Signaling Pathway	38
2.3.2	Environmental Toxicants or Stresses Reduce Lifespan by Affecting the Mitochondrial Respiration Signaling Pathway	40
2.3.3	Environmental Toxicants or Stresses Reduce Lifespan by Affecting Certain MicroRNAs-Mediated Molecular Signals	42

2.4	Innate Immune Response Is Involved in the Regulation of Longevity Reduction in Nematodes Exposed to Environmental Toxicants or Stresses	44
2.5	Genetic Identification of Genes and Signaling Cascade in the Regulation of Toxicity on Lifespan by Environmental Toxicants or Stresses	48
2.6	Environmental Toxicants or Stresses Reduce Lifespan by Affecting Signaling Pathways Associated with the Stress Response	50
2.7	Perspectives	53
	References	53
3	Roles of Oxidative Stress-Related Molecular Signals in the Regulation of Toxicity of Environmental Toxicants or Stresses	59
3.1	Introduction	59
3.2	Roles of Mitochondrial Complex Signals in the Regulation of Toxicity of Environmental Toxicants or Stresses	60
3.2.1	Complex I (NADH Ubiquinone Oxidoreductase)	60
3.2.2	Complex II (Succinate Ubiquinone Oxidoreductase)	65
3.2.3	Complex III	67
3.2.4	Complex IV	71
3.2.5	Coenzyme Q (Ubiquinone, CoQ) Synthesis	71
3.3	Roles of SODs in the Regulation of Toxicity of Environmental Toxicants or Stresses	75
3.3.1	SOD-1	75
3.3.2	SOD-2 and SOD-3	76
3.3.3	SOD-4	78
3.3.4	SOD-5	81
3.4	Roles of CTL Proteins in the Regulation of Toxicity of Environmental Toxicants or Stresses	81
3.5	Roles of GST Proteins in the Regulation of Toxicity of Environmental Toxicants or Stresses	82
3.6	Perspectives	83
	References	85
4	Functions of MAPK Signaling Pathways in the Regulation of Toxicity of Environmental Toxicants or Stresses	89
4.1	Introduction	89
4.2	p38 MAPK Signaling Pathway	90
4.2.1	Exposure to Environmental Toxicants or Stress Dysregulates the Expression of p38 MAPK Signal	90
4.2.2	p38 MAPK Signaling Pathway Regulates the Toxicity of Environmental Toxicants or Stresses	93

4.2.3	Intestinal Signaling Cascade of p38 MAPK Signaling Pathway Regulates the Toxicity of Environmental Toxicants or Stresses	94
4.2.4	SKN-1 Acts as an Important Target for Intestinal PMK-1 in Regulating the Toxicity of Environmental Toxicants or Stresses	96
4.2.5	ATF-7 Acts as Another Important Target for Intestinal PMK-1 in Regulating the Toxicity of Environmental Toxicants or Stresses	97
4.2.6	Role of Antimicrobial Proteins as the Targets for PMK-1 in Regulating the Toxicity of Environmental Toxicants or Stresses	100
4.2.7	Upregulators of p38 MAPK Signaling Pathway in Response to Environmental Toxicants or Stresses	100
4.3	JNK Signaling Pathway	104
4.3.1	Exposure to Environmental Toxicants or Stress Dysregulates the Expression of JNK MAPK Signal	106
4.3.2	JNK MAPK Signaling Pathway Regulates the Toxicity of Environmental Toxicants or Stresses	106
4.4	ERK Signaling Pathway	107
4.4.1	Exposure to Environmental Toxicants or Stress Dysregulates the Expression of ERK MAPK Signal	107
4.4.2	ERK MAPK Signaling Pathway Regulates the Toxicity of Environmental Toxicants or Stresses	108
4.4.3	Signaling Cascade of ERK MAPK Signaling Pathway in the Regulation of Toxicity of Environmental Toxicants or Stresses	109
4.4.4	Identification of Potential Downstream Targets for Neuronal MPK-1 in Regulating the Toxicity of Environmental Toxicants or Stresses	110
4.4.5	Identification of Upstream Regulators for ERK MAPK Signaling Pathway in Regulating the Toxicity of Environmental Toxicants or Stresses	110
4.5	Perspectives	112
	References	112
5	Functions of Insulin and the Related Signaling Pathways in the Regulation of Toxicity of Environmental Toxicants or Stresses	117
5.1	Introduction	117
5.2	Environmental Toxicants or Stresses Dysregulate the Expression of Insulin Signaling Pathway	118
5.3	The Insulin Signaling Pathway Regulates the Toxicity of Environmental Toxicants or Stresses	119

- 5.4 Genetic Interactions of Genes in the Insulin Signaling Pathway in Regulating the Toxicity of Environmental Toxicants or Stresses 119
- 5.5 Targets of DAF-16 in Regulating the Toxicity of Environmental Toxicants or Stresses 121
 - 5.5.1 SOD-3 121
 - 5.5.2 Antimicrobial Proteins 123
 - 5.5.3 MTL-1 and MTL-2 124
 - 5.5.4 NATC-1 124
 - 5.5.5 HSF-1 126
 - 5.5.6 Genetic Interaction Between SOD-3 and Antimicrobial Proteins in the Regulation of Toxicity of Environmental Toxicants or Stresses 128
- 5.6 Upregulators of Insulin Signaling Pathway in Regulating the Toxicity of Environmental Toxicants or Stresses 129
 - 5.6.1 SMK-1 131
 - 5.6.2 AAK-2 133
 - 5.6.3 JNK-1 133
 - 5.6.4 HCF-1 137
 - 5.6.5 SIR-2.1/SIRT1 138
 - 5.6.6 PRDX-2 138
- 5.7 Genetic Interaction Between SKN-1 and DAF-16 or DAF-2 in Regulating the Toxicity of Environmental Toxicants or Stresses 141
- 5.8 Perspectives 143
- References 143
- 6 Functions of Development-Related Signaling Pathways in the Regulation of Toxicity of Environmental Toxicants or Stresses 147**
 - 6.1 Introduction 147
 - 6.2 Wnt Signaling Pathway 148
 - 6.2.1 Involvement of Certain Wnt Ligands in Regulating the Toxicity of Environmental Toxicants or Stresses 148
 - 6.2.2 Genetic Interactions of Wnt Ligands in Regulating the Toxicity of Environmental Toxicants or Stresses 148
 - 6.2.3 Involvement of Canonical Wnt/ β -Catenin Signaling Pathway in Regulating the Toxicity of Environmental Toxicants or Stresses 151
 - 6.2.4 Role of HMP-2 in the Regulation of Toxicity of Environmental Toxicants or Stresses 152
 - 6.2.5 Identification of Downstream Targets for β -Catenin BAR-1 in Regulating the Toxicity of Environmental Toxicants or Stresses 154

6.2.6	Genetic Interactions Between β -Catenin BAR-1 and Other Signaling Pathways in Regulating the Toxicity of Environmental Toxicants or Stresses	156
6.3	TGF- β Signaling Pathway	157
6.3.1	DBL-1-Mediated TGF- β Signaling Pathway	157
6.3.2	DAF-7-Mediated TGF- β Signaling Pathway	159
6.4	Notch Signaling Pathway	161
6.4.1	Role of GLP-1 in the Regulation of Toxicity of Environmental Toxicants or Stresses	161
6.4.2	Genetic Interaction Between GLP-1 and Insulin Signal in the Regulation of Toxicity of Environmental Toxicants or Stresses	163
6.5	Developmental Timing Control-Related Signals	165
6.5.1	Involvement of <i>let-7</i> in Regulating the Toxicity of Environmental Toxicants or Stresses	165
6.5.2	Tissue-Specific Activity of <i>let-7</i> in the Regulation of Toxicity of Environmental Toxicants or Stresses	167
6.5.3	Downstream Targets of <i>let-7</i> in the Regulation of Toxicity of Environmental Toxicants or Stresses	167
6.5.4	Identification of Downstream Targets for HBL-1 in Regulating the Toxicity of Environmental Toxicants or Stresses	171
6.5.5	Genetic Interaction Between LIN-41 and ALG-1 or ALG-2 in Regulating the Toxicity of Environmental Toxicants or Stresses	173
6.5.6	Feedback Loop Formed by <i>let-7</i> and Its Direct Targets During the Control of ENMs Toxicity	173
6.6	Perspectives	174
	References	176
7	Functions of Cell Death and DNA Damage-Related Signaling Pathways in the Regulation of Toxicity of Environmental Toxicants or Stresses	181
7.1	Introduction	181
7.2	Apoptosis Signaling Pathway	182
7.2.1	Involvement of Core Apoptosis Signaling Pathway in the Control of Toxicity of Environmental Toxicants or Stresses	182
7.2.2	Upregulators of Core Apoptosis Signaling Pathway in Regulating the Toxicity of Environmental Toxicants or Stresses	183
7.2.3	Targets of Core Apoptosis Signaling Pathway in Regulating the Toxicity of Environmental Toxicants or Stresses	186

7.3	DNA Damage Signaling Pathway	187
7.3.1	Involvement of Core DNA Damage Signaling Pathway in the Control of Toxicity of Environmental Toxicants or Stresses	187
7.3.2	Upregulators of Core DNA Damage-Related Signaling Pathway in Regulating the Toxicity of Environmental Toxicants or Stresses	189
7.4	DNA Replication Stress-Related Signal	193
7.4.1	Involvement of ATR Signaling Pathway in the Regulation of DNA Replication Stress Induced by Environmental Toxicants or Stresses	194
7.4.2	Cell-Type-Specific Responses to DNA Replication Stress Induced by Environmental Toxicants or Stresses	196
7.5	Telomere-Related Signal	196
7.6	Perspectives	197
	References	199
8	Functions of Metabolism-Related Signaling Pathways in the Regulation of Toxicity of Environmental Toxicants or Stresses	203
8.1	Introduction	203
8.2	Functions of Fat Metabolic Sensors in the Regulation of Toxicity of Environmental Toxicants or Stresses	205
8.2.1	SBP-1	206
8.2.2	NHR-49	206
8.2.3	MDT-15	209
8.2.4	NHR-80	217
8.3	AMPK Signaling Pathway	217
8.4	ACC and FAS	218
8.5	FAT-6 and FAT-7	219
8.6	Role of ELO Proteins in the Regulation of Toxicity of Environmental Toxicants or Stresses	219
8.7	Role of Fatty Acid Transport Protein ACS-22 in the Regulation of Toxicity of Environmental Toxicants or Stresses	219
8.7.1	ACS-22 Regulate the Intestinal Barrier in Nematodes	219
8.7.2	Mutation of <i>acs-22</i> Causes a Susceptibility to the Toxicity of Environmental Toxicants of Stresses	221
8.7.3	Mutation of <i>acs-22</i> Disrupts the Beneficial Function of LAB in Preventing the Toxicity of Environmental Toxicants or Stresses	221
8.8	Perspectives	223
	References	228

9	Functions of Protective Response-Related Signaling Pathways in the Regulation of Toxicity of Environmental Toxicants or Stresses	231
9.1	Introduction	231
9.2	Neurotransmitters	232
9.2.1	Involvement of Neurotransmitter Signals in the Regulation of Toxicity of Environmental Toxicants or Stresses	232
9.2.2	Genetic Interactions of Neurotransmitter Signals in the Regulation of Toxicity of Environmental Toxicants or Stresses	233
9.2.3	Serotonin Response to Environmental Toxicants or Stresses	236
9.2.4	Neurotransmitter Receptors	237
9.2.5	Function of Neurotransmission in the Regulation of Toxicity of Environmental Toxicants or Stresses	240
9.3	Antimicrobial Proteins	241
9.3.1	Response of Antimicrobial Proteins to the Toxicity of Environmental Toxicants or Stresses	241
9.3.2	Molecular Control of Toxicity of Environmental Toxicants or Stresses by Antimicrobial Proteins	244
9.4	Mitochondrial UPR	244
9.4.1	Induction of Mitochondrial UPR in Nematodes Exposed to Environmental Toxicants or Stresses	244
9.4.2	Molecular Basis for Mitochondrial UPR Induced by Environmental Toxicants or Stresses	248
9.4.3	Targets of Mitochondrial UPR Signaling Pathway in Nematodes Exposed to Environmental Toxicants or Stresses	253
9.5	Endoplasmic Reticulum (ER) UPR	258
9.5.1	Induction of ER UPR in Nematodes Exposed to Environmental Toxicants or Stresses	258
9.5.2	Molecular Basis for ER UPR Induced by Environmental Toxicants or Stresses	261
9.5.3	Targets of ER UPR Signaling Pathway in Nematodes Exposed to Environmental Toxicants or Stresses	266
9.5.4	Upregulators of ER UPR Signaling Pathway in Nematodes Exposed to Environmental Toxicants or Stresses	267
9.6	Autophagy	274
9.6.1	Induction of Autophagy in Nematodes Exposed to Environmental Toxicants or Stresses	274
9.6.2	Molecular Control of Autophagy in Nematodes Exposed to Environmental Toxicants or Stresses	274
9.7	Perspectives	288
	References	289

10	Functions of G-Protein-Coupled Receptors and Ion Channels and the Downstream Cytoplasmic Signals in the Regulation of Toxicity of Environmental Toxicants or Stresses	293
10.1	Introduction	293
10.2	GPCRs	294
10.2.1	Epidermal DCAR-1	294
10.2.2	Intestinal FSHR-1	297
10.2.3	Neuropeptide Receptors	300
10.2.4	Neuronal SRH-220	308
10.3	Ion Channels	310
10.3.1	Cyclic Nucleotide-Gated Ion Channels	310
10.3.2	Voltage-Gated Calcium Ion Channel UNC-2	310
10.3.3	Potassium Ion Channel KVS-1	311
10.3.4	Chloride Intracellular Channel EXL-1	313
10.4	ARR-1/Arrestin	313
10.5	G-Proteins	316
10.5.1	Gq α Signaling	316
10.5.2	Go α Signaling	316
10.6	PLC-DAG-PKD Signaling	318
10.6.1	PLC-PKD-TFEB Signaling Cascade	318
10.6.2	DKF-2	319
10.6.3	Association with p38 MAPK Signaling	320
10.7	Ca ²⁺ Signaling	322
10.7.1	UNC-31	322
10.7.2	CRT-1	322
10.8	Perspectives	323
	References	324
11	Discussion on Specificity of Molecular Signals in Response to Certain Environmental Toxicants or Stresses	327
11.1	Introduction	327
11.2	Heavy Metal Response Signaling	328
11.2.1	Molecular Signaling for Heavy Metal Response	328
11.2.2	Regulation of Toxicity of Other Environmental Toxicants by MTL-1 and MTL-2	332
11.3	Heat Shock Response Signaling	335
11.3.1	Molecular Signaling for Heat Shock Response	335
11.3.2	Regulation of Toxicity of Other Environmental Toxicants by Heat Shock Proteins	336
11.3.3	Regulation of Toxicity of Other Environmental Toxicants by HSF-1	336
11.4	Hypoxia Response Signaling	340
11.4.1	Molecular Signaling for Hypoxia Response	340
11.4.2	Regulation of Toxicity of Other Environmental Toxicants by HIF-1 and EGL-9	343
11.5	Perspectives	345
	References	347

12	Epigenetic Regulation of Toxicity of Environmental Toxicants or Stresses	351
12.1	Introduction	351
12.2	Methylation Regulation	352
12.2.1	Methylation of Histone H3K4	352
12.2.2	Methylation of Histone H3K9	355
12.2.3	Methylation of HIS-24K14	359
12.2.4	Methylated Glycans	361
12.3	Histone Acetylation Regulation	361
12.3.1	MYST Family Histone Acetyltransferase Complex	361
12.3.2	N-Terminal Acetyltransferase C (NAT) Complex	365
12.3.3	CBP-1	365
12.4	miRNA Regulation	368
12.4.1	Dysregulated miRNAs by Environmental Toxicants or Stresses	368
12.4.2	Functions of miRNAs in Response to Environmental Toxicants or Stresses and the Underlying Molecular Mechanisms	369
12.4.3	The mRNAs–miRNA Network Involved in the Regulation of Toxicity of Environmental Toxicants or Stresses	379
12.5	lncRNA Regulation	382
12.5.1	Dysregulation of lncRNAs by Environmental Toxicants or Stresses	382
12.5.2	Effect of Ascorbate or Paraquat Treatment on lncRNA Profiling in Nematodes Exposed to Environmental Toxicants or Stresses	382
12.5.3	Effects of PEG Modification or FBS Surface Coating on Graphene Oxide-Induced lncRNA Profiling	382
12.5.4	The lncRNA–miRNA Network Involved in the Regulation of Toxicity of Environmental Toxicants or Stresses	384
12.5.5	Functional Analysis of <i>linc-37</i> and <i>linc-14</i> in Regulating the Toxicity of Environmental Toxicants or Stresses	385
12.6	Perspectives	387
	References	387
13	Strategies to Screen and to Identify New Genetic Loci Involved in the Regulation of Toxicity of Environmental Toxicants or Stresses	391
13.1	Introduction	391
13.2	Transcriptomic Screen and Identification of New Genetic Loci Involved in the Regulation of Toxicity of Environmental Toxicants or Stresses	392

13.3	Proteomic Screen and Identification of New Genetic Loci Involved in the Regulation of Toxicity of Environmental Toxicants or Stresses	396
13.4	Forward Genetic Screen and Identification of New Genetic Loci Involved in the Regulation of Toxicity of Environmental Toxicants or Stresses	397
13.5	Reverse Genetic Screen and Identification of New Genetic Loci Involved in the Regulation of Toxicity of Environmental Toxicants or Stresses	400
13.5.1	Using a Certain Number of Mutants to Screen and to Identify Genetic Loci Involved in the Regulation of Toxicity of Environmental Toxicants or Stresses	400
13.5.2	Using RNAi Knockdown Technique to Screen and to Identify Genetic Loci Involved in the Regulation of Toxicity of Environmental Toxicants or Stresses	404
13.6	Perspectives	404
	References	406
14	Molecular Basis for Adaptive Response to Environmental Toxicants or Stresses	411
14.1	Introduction	411
14.2	Molecular Alterations During the Formation of Adaptive Response	412
14.3	Molecular Signaling Pathways Involved in the Regulation of Adaptive Response Induction	413
14.3.1	Insulin Signaling Pathway	413
14.3.2	SKN-1/Nrf	415
14.3.3	ERK MAPK Signaling Pathway	415
14.3.4	Apoptosis Signaling Pathway	417
14.3.5	Catalases and RNA Interference	418
14.3.6	RAD-1 and RAD-2	420
14.3.7	Metallothioneins (MTs)	421
14.3.8	20S Proteasome	421
14.3.9	HPL-2 and Endoplasmic Reticulum Unfolded Protein Response (ER UPR)	423
14.3.10	Germline Signals	424
14.4	Perspectives	426
	References	427
15	Molecular Basis for Transgenerational Toxicity Induction of Environmental Toxicants or Stresses	429
15.1	Introduction	429
15.2	Molecular Alterations During the Formation of Transgenerational Toxicity of Environmental Toxicants or Stresses	430

- 15.2.1 Environmental Toxicant- or Stress-Induced Transgenerational Gene Expression Profiles 430
- 15.2.2 Environmental Toxicant- or Stress-Induced Transgenerational microRNA (miRNA) Expression Profiles 431
- 15.3 Crucial Role of Intestinal Barrier Against the Formation of Transgenerational Toxicity of Environmental Toxicants or Stresses 431
- 15.4 Molecular Signals for RNA Inheritance Are Involved in the Regulation of Transgenerational Toxicity of Environmental Toxicants or Stresses 434
 - 15.4.1 RNA Inheritance and Transgenerational Toxicity of Heat Stress 434
 - 15.4.2 RNA Inheritance and Transgenerational Toxicity of Pathogen Infection 435
- 15.5 Epigenetic Regulation of Transgenerational Toxicity of Environmental Toxicants or Stresses 436
 - 15.5.1 Role of H3K4 Dimethylation 436
 - 15.5.2 Role of H3K9 Methylation 439
- 15.6 Transgenerational Hormesis and Insulin Signaling Pathway 440
- 15.7 Perspectives 441
- References 444

Chapter 1

Molecular Basis for Oxidative Stress Induced by Environmental Toxicants in Nematodes



Abstract Oxidative stress plays an important role in the toxicity induction of environmental toxicants or stresses in nematodes. Usually, this is the first cellular mechanism needed to be clarified for the toxicity formation of certain environmental toxicants or stresses. We here systematically introduced both the molecular machinery for the activation of oxidative stress and the response signals with the functions to defend against the oxidative stress in nematodes. Moreover, we explained the molecular basis for the induction of oxidative stress in nematodes exposed to environmental toxicants.

Keywords Molecular basis · Oxidative stress · Environmental toxicant · *Caenorhabditis elegans*

1.1 Introduction

Oxidative stress is normally considered to play a pivotal role in the toxicity induction of environmental toxicants or stresses in organisms, including the nematodes. That is, induction of oxidative stress acts as an important cellular mechanism for the toxicity formation of environmental toxicants or stresses in nematodes. Usually, the first cellular mechanism for the toxicity formation of certain environmental toxicants or stresses needed to be clarified is to determine the association between the toxicity formation of examined environmental toxicant or stress and the induction of oxidative stress.

With the concern on the important role of oxidative stress in toxicity induction of environmental toxicants or stresses, we here first introduced the evidence for the direct association of oxidative stress with toxicity of environmental toxicants in nematodes. Moreover, we systematically introduced both the molecular machinery for the activation of oxidative stress and the response signals with the functions to defend against the oxidative stress in nematodes. Finally, we introduced and explained the molecular basis for induction of oxidative stress in nematodes exposed to environmental toxicants.

1.2 Evidence for the Direct Association of Oxidative Stress with Toxicity of Environmental Toxicants

1.2.1 Induction of Oxidative Stress in Targeted Organs of Environmental Toxicants

With the heavy metal of Hg as an example of environmental toxicants, the toxic effects of Hg exposure on development of male nematodes were examined. Acute exposure to Hg (from L3 larvae for 24 h) at the concentration of 0.5 mg/L significantly reduced the number of rays formed surrounding the tail [1]. Acute exposure to Hg at the concentration of 9.8 mg/L further severely decreased the number of rays [1]. Moreover, acute exposure to Hg at the concentration of 19.3 or 29.5 mg/L severely reduced both the number of rays and the size of fan in male nematodes [1]. In nematodes exposed to Hg at the concentration of 39.7 mg/L, no rays and no obvious fan could be observed in male nematodes [1]. Meanwhile, the obvious induction of reactive oxygen species (ROS) production was detected in the fans of tails in male nematodes after exposure to Hg at concentrations more than 0.5 mg/L (Fig. 1.1) [1]. The strong induction of ROS production was also observed in the intestine of male nematodes exposed to Hg at concentrations more than 0.5 mg/L (Fig. 1.1) [1]. These results imply the close correlation of induction of ROS production in the fans of tails with the formation of abnormal male-specific structures in nematodes after Hg exposure.

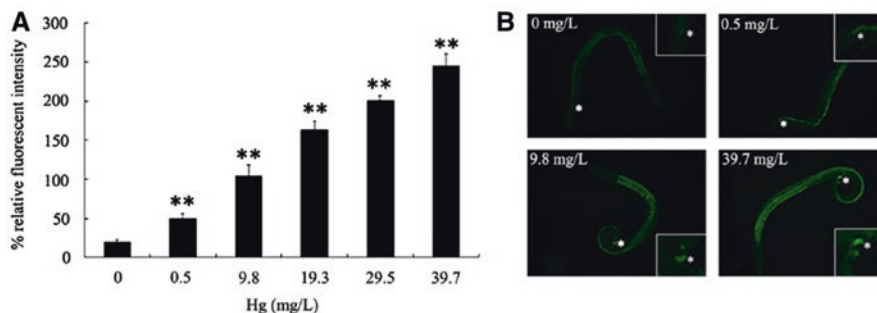


Fig. 1.1 ROS production in male nematodes exposed to Hg [1]. (a) ROS production in tails of male nematodes exposed to Hg at different concentrations. Bars represent means \pm SEM. ** $P < 0.01$ vs 0 mg/L. (b) Representative images of ROS production. Asterisks indicate the position of male tails

1.2.2 Pharmacological Evidence for the Association of Oxidative Stress and Toxicity Formation of Environmental Toxicants

Antioxidant administration is a powerful strategy used for decreasing the free radical-induced oxidative damage. To confirm the direct association between the induction of oxidative stress and the toxicity of Hg exposure on the development of male-specific structures, the male nematodes were pretreated with vitamin E (200 mg/mL), a potent antioxidant, for 24 h at the L2-larval stage. After that, the male nematodes were exposed to Hg (9.8 mg/L) for 24 h at the L3-larval stage. Vitamin E treatment alone cannot induce the obvious ROS production in male tails [1]. Pretreatment with the vitamin E could obviously prevent the induction of severe ROS production in fans in tails of nematodes exposed to Hg (9.8 mg/L) (Fig. 1.2) [1]. Meanwhile, pretreatment with the vitamin E could obviously prevent the formation of high percentage of abnormal males and severe deficit in male-specific structures in tails in nematodes exposed to Hg (9.8 mg/L) (Fig. 1.2) [1]. This pharmacological data provides an important evidence for the direct association between the induction of oxidative stress and the Hg toxicity on development of male-specific structures in nematodes.

1.2.3 Association of Induction of Oxidative Stress in Intestine and Toxicity Formation in Other Targeted Organs

Besides the direct induction of oxidative stress in the targeted organs, another possibility also exists. That is, a close association of induction of oxidative stress in the intestine and toxicity formation in other targeted organs may be formed in nematodes. With multiwalled carbon nanotubes (MWCNTs), carbon-based engineered nanomaterials (ENMs), as an example, prolonged exposure (from L1-larvae to adult day 1) to MWCNTs at concentrations more than 0.1 $\mu\text{g/L}$ could induce the significant intestinal ROS production (Fig. 1.3) [2]. Meanwhile, prolonged exposure to MWCNTs at concentrations more than 0.1 $\mu\text{g/L}$ also significantly reduced the brood size (Fig. 1.3) [2]. Nevertheless, we did not detect the obvious induction of ROS production in reproductive organs of nematodes [2]. In nematodes, the reproductive organs such as spermatheca are the important secondary targeted organs for MWCNTs (Fig. 1.3) [2]. Therefore, the induction of oxidative stress in the intestine may potentially further contribute to the toxicity formation of environmental toxicants in other targeted organs in nematodes.

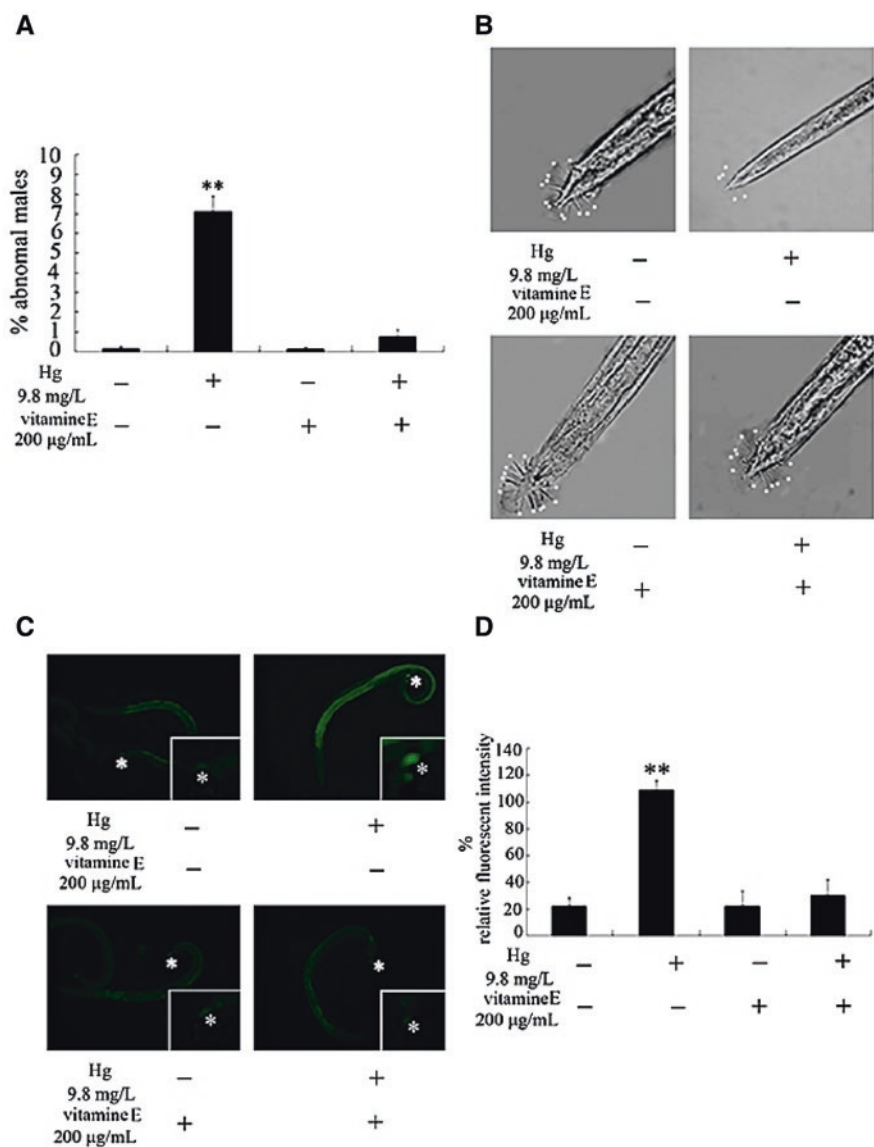


Fig. 1.2 Effects of vitamin E pretreatment on the development of male-specific structures in nematodes exposed to Hg [1]. (a) Effects of vitamin E pretreatment on the formation of abnormal males induced by Hg exposure. (b) Effects of vitamin E pretreatment on the development of male-specific structures induced by Hg exposure. (c) Representative images of ROS production. Asterisks indicate the position of male tails. (d) Effects of vitamin E pretreatment on the ROS production induced by Hg exposure. Bars represent means \pm SEM. ** $P < 0.01$

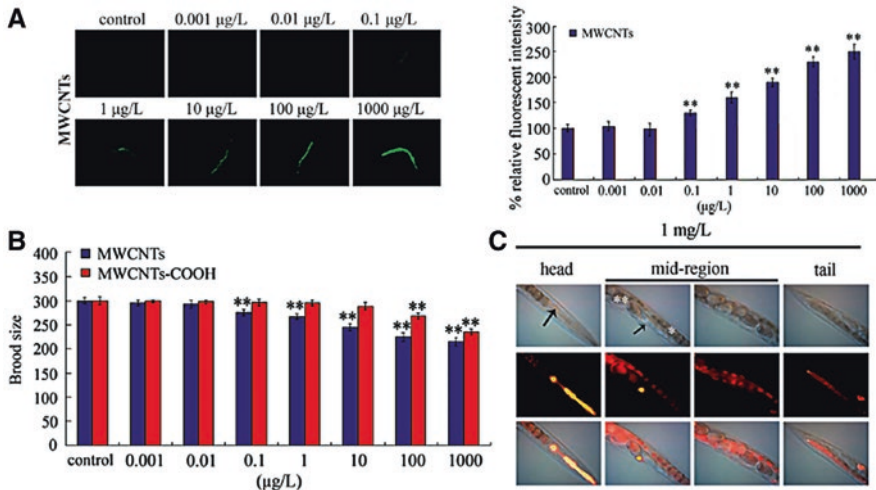


Fig. 1.3 Toxicity of MWCNTs on nematodes after prolonged exposure [2]. (a) Toxicity of MWCNT exposure in inducing intestinal ROS production. (b) Toxicity of MWCNT exposure in reducing brood size. (c) Distribution and translocation of MWCNTs labeled with Rho B. Arrowheads indicate the pharynx and the spermatheca, respectively, at the head region or mid-region of nematodes. The intestine (*) and the embryos (**) in the mid-region are also indicated. Prolonged exposure was performed from L1-larvae to adult day 1. Bars represent mean \pm SEM. ** $P < 0.01$ vs control

1.3 Molecular Machinery for the Activation of Oxidative Stress in Nematodes

The superoxide anion ($O_2^{\cdot-}$) can generate several types of toxic ROS, which will further lead to the toxic effects on nematodes at different aspects. In organisms, the major source of superoxide anion is the electron transport in mitochondrion. Electron transport is normally mediated by five complexes (complexes I–V) embedded in the inner membrane of the mitochondrion.

1.3.1 Role of *GAS-1* in the Activation of Oxidative Stress

In nematodes, *gas-1* encodes a subunit of mitochondrial complex I. Mutation of *gas-1* did not affect the physical structure in mitochondria [3]. In contrast, mutation of *gas-1* decreased the complex I-dependent mitochondrial metabolism as indicated in alterations in the rates of both oxidative phosphorylation and electron transport [3]. The rates of oxidative phosphorylation were significantly decreased in *gas-1* mutant nematodes [4]. The *gas-1* mutant shows the hypersensitive property to oxygen and shortened lifespan [4].

In *gas-1* mutant nematodes, the significantly elevation in mitochondrial matrix oxidant burden was detected, which may be closely associated with the limited superoxide scavenging capacity and the decreased mitochondria content, as well as the membrane potential [5].

In nematodes, *gas-1* is mainly expressed in the mitochondria of neuromuscular system [3]. Importantly, it has been shown that GAS-1 can act at the presynaptic to regulate different biological processes [3].

In nematodes, *nuo-6* encodes another subunit of mitochondrial NADH dehydrogenase (ubiquinone) complex (complex I). However, mutation of *nuo-6* decreased the electron transport and increased the longevity [6]. The generation of superoxide was elevated in *nuo-6* mutant nematodes, although the overall ROS levels were not and the oxidative stress was low in *nuo-6* mutant nematodes [6]. More importantly, it is considered that this elevation is required for the increase in longevity, since this could be abolished by the antioxidants and phenocopied by mild treatment with prooxidant paraquat [6]. The increased superoxide generation may act as a signal in young *nuo-6* mutant to trigger the changes of gene expression so as to prevent or attenuate the effects of the subsequent aging [6]. That is, the superoxide generated in the *nuo-6* mutant may act as a protective signal in response to the damage during the aging process.

1.3.2 Role of MEV-1 in the Activation of Oxidative Stress

Mitochondrial succinate–ubiquinone reductase (complex II) functions to catalyze the electron transport from succinate to ubiquinone. This complex II contains succinate dehydrogenase (SDH), flavin protein, iron–sulfur protein, and two other subunits containing cytochrome *b560*. In nematodes, *mev-1* encodes an ortholog of succinate dehydrogenase cytochrome *b560* subunit of the complex II that is required for the oxidative phosphorylation. SDH, the catalytic component of complex II, is normally anchored to the inner membrane of mitochondrion with the cytochrome *b560*. Nevertheless, the SDH activity in *mev-1* mitochondrial fraction was identical to that of wild-type nematodes [7]. In contrast, the complex II activity in the *mev-1* membrane fraction was significantly reduced by more than 80% [7]. These results imply that mutation of *mev-1* may affect neither the SDH anchoring to the mitochondrial membrane nor the SDH activity. The MEV-1 may potentially compromise the ability of complex II to participate in the electron transport. That is, cytochrome *b560*, the *mev-1* gene product, can participate directly into the transporting electrons from SDH to CoQ. The cytochrome *b560* has three membrane-spanning domains, and the substitution of glutamic acid for glycine could affect the ability of iron to accept and relinquish the electrons.

The ability of complex II to catalyze the electron transport from succinate to ubiquinone is compromised in *mev-1* mutant nematodes, which may result in the indirect increase in the superoxide levels and the oxygen hypersensitivity, as well as

the premature aging [8]. At least for the longevity control, the evidence was raised that the MEV-1 may govern the aging rate by modulating the cellular response to oxidative stress [8]. In *mev-1* mutant nematodes, an overproduction of superoxide anion from the mitochondria and a reciprocal reduction in glutathione content were detected [8]. Although the superoxide anion is normally produced at complexes I and III in the electron transport system under normal conditions, the mutation of *mev-1(kn1)* could increase the superoxide anion production at the complex II itself (as indicated by an attendant decrease in glutathione levels) rather than at the complexes I and III [8]. Additionally, the *mev-1* mutant nematodes had metabolic changes as indicated by the lactate level with twofold higher than that in wild-type nematodes [8]. In nematodes, the Cyt-1/ceSDHC may play an important role not only in the energy metabolism but also in the superoxide anion production.

1.3.3 Role of ISP-1 in the Activation of Oxidative Stress

In organisms, the mitochondrial complex III functions to catalyze the electron transfer from ubiquinol to cytochrome c. The complex III contains three subunits, cytochrome b, the iron–sulfur protein, and cytochrome c1, to catalyze the redox reactions. In nematodes, *isp-1* encodes a “Rieske” iron–sulfur protein subunits of complex III of the mitochondrial respiratory chain. The prolines are important structurally to make the peptide backbone locally rigid, and *isp-1(qm150)* is a point mutation at residue 225 that changes the proline into a serine [9]. This mutation may affect the properties of the iron–sulfur center directly through a local distortion of the structure and the redox potential. The electron transfer from ubiquinol at its binding site on cytochrome b to cytochrome c1 is involved in the conformation of head of the ISP carrying the 2Fe-2S group [9].

In the *isp-1* mutant nematodes, the decrease in electron transport, the reduction in oxygen consumption, and the resistance to oxidative stress were observed [6, 9]. In *isp-1* mutant nematodes, the generation of superoxide was elevated [6]. The increased superoxide generation in *isp-1* mutant nematodes was also abolished by the antioxidants and phenocopied by mild treatment with the prooxidant paraquat [6]. Moreover, an increased lifespan was detected in the *isp-1* mutant nematodes [9]. Nevertheless, the effects of ISP-1 and DAF-2, an insulin receptor, on longevity were not additive in nematodes [9].

In nematodes, the elevated ROS levels in *isp-1* mutant nematodes may induce an activation of multiple stress response pathways [10]. These pathways include those of mitochondrial unfolded protein response, SKN-1-mediated stress response, and hypoxia response [10]. Mutation of *isp-1* could further increase the expression of specific antioxidant enzymes, such as the superoxide dismutase genes *sod-3* and *sod-5* [10]. Meanwhile, mutation of *sod-3* or *sod-5* decreased the lifespan and exacerbated the slow physiologic rates in *isp-1* mutant nematodes [10].

1.3.4 Role of CLK-1 in the Activation of Oxidative Stress

1.3.4.1 Mitochondrial CLK-1

In nematodes, *clk-1* encodes a ubiquinone (UQ) (coenzyme Q) biosynthesis protein COQ7. UQ is a lipophilic redox-active molecule and an electron carrier in the mitochondrial electron transport chain. Normally, the electron transfer via the UQ involves the formation of semi-ubiquinone radicals and the generation of superoxide radicals upon reaction with oxygen. In contrast, the UQ in the reduced form can serve as a lipid-soluble antioxidant to protect the cells from lipid peroxidation. In the *clk-1* mutant nematodes, no detectable levels of UQ could be observed [11]. Meanwhile, the UQ biosynthesis intermediate, demethoxyubiquinone (DMQ9), was present at a high level in *clk-1* mutant nematodes [11]. In the *clk-1* mutant nematodes, the DMQ9 may act as an electron carrier in the respiratory chain, since the activities of NADH–cytochrome c reductase and succinate–cytochrome c reductase were similar to those in wild-type nematodes [11].

In the *clk-1* mutant nematodes, the rates of oxidative phosphorylation were decreased; however, the lifespan was increased [12]. Moreover, it has been reported that mutation of *sod-2* resulted in the increase in lifespan in *clk-1* mutant nematodes; however, mutation of either of the two cytoplasmic *sod* genes, *sod-1* or *sod-5*, decreased the lifespan of *clk-1* mutant nematodes [12]. Additionally, the increase in mitochondrial superoxide levels by mutation of *sod-2* or treatment with paraquat could still cause the increase in lifespan in *clk-1*; *sod-1* double mutants [12]. These results imply that the elevated ROS in the mitochondria can act to increase lifespan, whereas the elevated ROS in the cytoplasm may decrease the lifespan of nematodes.

1.3.4.2 Nuclear CLK-1

Besides this, recently a distinct nuclear form of CLK-1 was further identified in nematodes. This nuclear CLK-1 may mediate a retrograde signaling pathway in response to the mitochondrial ROS by acting as a barometer of oxidative metabolism [13]. The nuclear CLK-1 can regulate both the mitochondrial ROS metabolism and the mitochondrial unfolded protein response by modulating the corresponding gene expression [13]. That is, the basal levels of ROS produced by the mitochondria may direct a pool of CLK-1 to the nucleus where it regulates the expression of genes associated with both the mitochondrial ROS metabolism and the mitochondrial unfolded protein response and lowers the ROS level [13]. The lowered ROS further results in the predominant localization of CLK-1 in the mitochondria and induces the return to basal ROS production, which will be helpful for maintaining the mitochondrial homeostasis [13]. Therefore, a respiratory enzyme exists in the nucleus to regulate both the mitochondrial stress responses and the longevity in nematodes.

1.4 Response Signals with the Functions to Defend Against the Oxidative Stress

1.4.1 Superoxide Dismutases (SODs)

The SOD activity can be detected in the extracts of nematodes, and the SODs have been well known to protect the cells or organisms from oxidative stress by catalytically removing the superoxide radical ($^{\bullet}\text{O}_2^-$). For example, dauer is a developmental state for larvae adapting the environmental stresses or starvation. The extracts of dauer larvae had 17.1 units SODase per milligram protein, whereas obligate larvae and young adults had 4.3 and 3.8 units SODase per milligram, respectively [14]. Additionally, the ratio of SODase to oxygen consumption was markedly increased in dauer larvae compared with that in young adults, implying that this elevated SODase might contribute to an increased resistance to certain environmental stresses [14].

1.4.1.1 SOD-1

In nematodes, *sod-1* encodes a cytoplasmic copper/zinc superoxide dismutase. The SOD-1 activity has been implicated in the increase in lifespan of dauer larvae, because its activity was the highest at this developmental stage compared with others [14]. In *sod-2* mutant, both the cytosolic $^{\bullet}\text{O}_2^-$ level and the mitochondrial $^{\bullet}\text{O}_2^-$ level were significantly increased [14], implying that both cytosolic SOD-1 and mitochondrial SOD-1 are required for the detoxification of $^{\bullet}\text{O}_2^-$ [15].

1.4.1.2 SOD-2 and SOD-3

In nematodes, *sod-2* and *sod-3* encode mitochondrial iron/manganese superoxide dismutases. Both SOD-2 and SOD-3 function to defend against the oxidative stress and to promote the normal lifespan [5].

Both *sod-2* expression and *sod-3* expression were diminished by mutation of *daf-16* encoding a FOXO transcriptional factor in the insulin signaling pathway. Nevertheless, the increased longevity was observed in *sod-2(ok1030)* or *sod-2(gk257)* mutant which has the decreased Mn-SOD scavenging capacity and increased mitochondrial matrix oxidant burden [5, 16]. In *sod-2* or *sod-3* mutant, the mild compensatory upregulation of other *sod* genes was even detected [5, 16]. Mutation of *sod-2* even increased the lifespan in *clk-1* mutant, but it clearly decreased the lifespan of *isp-1* mutant [16].

1.4.1.3 SOD-4

In nematodes, *sod-4* encodes an extracellular $\text{Cu}^{2+}/\text{Zn}^{2+}$ superoxide dismutase. SOD-4 is expressed in the nervous system, intestine, and rectal gland cells. The *sod-4* expression was also significantly upregulated in dauers [14].

In nematodes, although the *sod* genes were not required for the longevity of *daf-2* insulin/IGF-1 receptor mutant, mutation of *sod-4* enhanced the longevity and the constitutive diapause in *daf-2* mutant [17].

1.4.1.4 SOD-5

sod-5 encodes a cytoplasmic $\text{Cu}^{2+}/\text{Zn}^{2+}$ superoxide dismutase. The *sod-5* expression could be increased in *sod-1* mutant [5, 16], implying the possible functional compensation between SOD-1 and SOD-5. Both SOD-3 and SOD-5 may act as direct targets for DAF-16 due to the existence of DAF-16 binding element on the promoter regions for these genes.

1.4.2 Catalases (CATs)

In nematodes, *ctl-1*, *ctl-2*, and *ctl-3* encode the catalases, antioxidant enzymes that protect the cells from the damage of oxidative damage. CTL-1 is predicted to be a cytosolic catalase. CTL-2 is observed to be mainly located in the peroxisomes of intestinal epithelial cells. The altered peroxisome morphology was observed in *ctl-2* mutant nematodes [18] and suggests the possible changes in peroxisomal function, including increased ROS production.

CTL-1 and CTL-2 could be negatively regulated by DAF-2-mediated insulin signaling [18]. The *ctl-1* mutant has no obvious effect on either nematode aging or egg-laying capacity; however, the *ctl-2* mutant exhibits progeric phenotype and decreased egg-laying capacity [18]. Mutation of *ctl-2* could reduce the lifespan of long-lived *daf-2* or *clk-1* mutant and accelerates the onset of its egg-laying period [18].

1.4.3 Insulin Signaling

1.4.3.1 Role of Insulin Signaling in the Activation of Oxidative Stress

In the insulin signaling pathway, AGE-1 is the downstream target of insulin receptor DAF-2. Mutation of *age-1* was resistant to the oxidative stress [19]. Meanwhile, both the activity of (SOD) and the activity of catalase exhibited an age-dependent increase in *age-1* mutant [19], which suggests that the signaling cascade of

DAF-2-AGE-1 regulates the activation of oxidative stress by negatively regulating the SOD and catalase activities. It has been further found that the expression of *sod-3* encoding a Mn-SOD was increased by *daf-2* mutation, which is regulated by the insulin-like signaling pathway [20], suggesting that the DAF-2 may regulate the longevity and the oxidative stress by affecting Mn-SOD-associated antioxidant defense system. Nevertheless, in wild-type and *age-1* dauer larvae, only elevated levels of the SOD activity, but not of the catalase activity, could be detected [19].

The forkhead transcription factor DAF-16 is negatively regulated by the DAF-2-AGE-1 signaling cascade in the insulin signaling pathway. Under the normal conditions, the DAF-16 protein is normally located in the cytoplasm. However, under the oxidative stress or certain environmental stress, the DAF-16 would be translocated into the nuclei [21]. Additionally, the DAF-16 could be constitutively accumulated in the nuclei of *mev-1* or *gas-1* mutant nematodes even under the normal conditions, which could be recovered by the supplementation of the antioxidant coenzyme Q10 (Fig. 1.4) [21].

Besides the oxidative stress or the environmental stress, it has also reported that SOD-3, a superoxide dismutase regulated by DAF-16, could be induced in intestinal cells after the infection with pathogenic bacteria [22]. Moreover, both the SOD-3 and the CTL-2 were required for DAF-16-mediated resistance to infection with pathogenic bacteria [22]. Therefore, the nematodes may potentially respond to the pathogen infection by producing intestinal ROS while simultaneously inducing a DAF-16-dependent oxidative stress response to protect adjacent tissues from the damage from the infection [22].

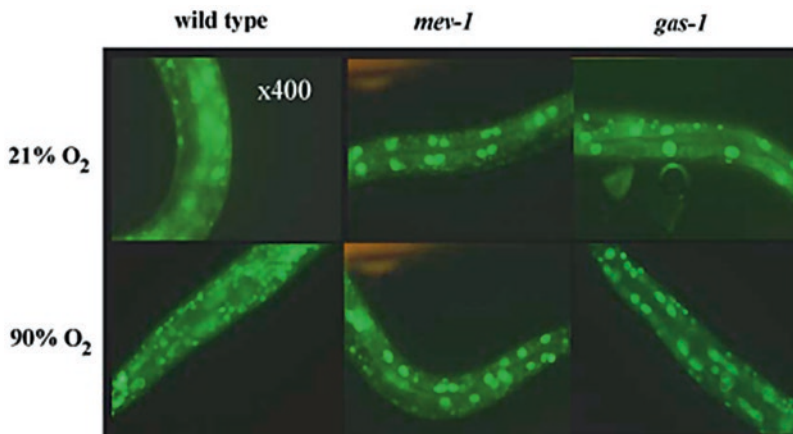


Fig. 1.4 Localization of DAF-16::GFP in wild type, *mev-1* and *gas-1* L2 larvae under atmospheric conditions (21% oxygen) or 90% oxygen [21]

1.4.3.2 Interaction Between β -Catenin/BAR-1 and DAF-16 in the Regulation of Oxidation Stress

In nematodes, β -catenin/BAR-1 is a transcriptional factor in the Wnt signaling pathway. It has been shown that mutation of *bar-1* could reduce the activity of DAF-16 in dauer formation and lifespan [23]. Moreover, BAR-1 was required for the oxidative stress-induced expression of SOD-3, a DAF-16 target [23]. The association of β -catenin with FOXO could be enhanced in cells exposed to the oxidative stress [23]. These observations demonstrate the important association of β -catenin with FOXO in the regulation of oxidative stress [23].

1.4.3.3 Identification of Upstream Regulator of DAF-2 in the Regulation of Oxidative Stress

In nematodes, mutation of *pcm-1* encoding a protein L-isoaspartyl methyltransferase induced a susceptibility to oxidative stress, since treatment with paraquat, a ROS generator, resulted in the more severe developmental delay at the second larval stage in *pcm-1* mutants than in wild-type nematodes [24]. This effect could be reversed by the administration with vitamin C, implying that the observed developmental delay and the egg-laying defects may be resulted from the oxidative stress [24]. Genetic interaction assay further indicated that mutation of *daf-2* could inhibit the Egl phenotype in *pcm-1* mutant treated with juglone, suggesting that the PCM-1 is involved in the control of cellular responses by acting an upstream regulator of DAF-2 in the insulin signaling pathway [24].

1.4.4 SKN-1/Nrf Signaling

1.4.4.1 Role of SKN-1 in the Regulation of Oxidative Stress

In nematodes, the SKN-1/Nrf plays a pivotal role in resisting the oxidative stress [25]. The *skn-1* mutants were sensitive to oxidative stress and showed the reduced longevity [25]. SKN-1 is expressed in both the ASI sensory neurons and the intestine. The SKN-1::GFP would be translocated and accumulated into the nucleus in response to the oxidative stress [25].

During the regulation of oxidative stress, the activity of SKN-1 is normally regulated by its phosphorylation modification. For the modification of SKN-1, it has been further suggested recently that SKN-1 could also be *O*-GlcNAcylated at Ser470 and Thr493 by *O*-GlcNAc transferase OGT-1. Under the condition of oxidative stress, SKN-1 was highly *O*-GlcNAcylated, which resulted in the decrease in GSK-3-mediated phosphorylation at Ser483 adjacent to the *O*-GlcNAcylated residues (Ser470 and Thr493) [26]. In nematodes, disruption of *O*-GlcNAc modification on SKN-1 could inhibit the SKN-1 accumulation in the intestinal

nuclei and decreased the activities of SKN-1 in modulating the lifespan and being against the oxidative stress [26]. That is, a cross talk between the phosphorylation and the *O*-GlcNAcylation for SKN-1 may exist in the regulation of oxidative stress and lifespan in nematodes.

1.4.4.2 Identification of Downstream Targets for Transcriptional Factor SKN-1 in the Regulation of Oxidative Stress

First of all, it has been well known that the SKN-1/Nrf can modulate the oxidative stress by regulating the phase II detoxification genes, such as *gcs-1* and *gst-4*, through constitutive and stress-inducible mechanisms during the postembryonic stages [25].

Besides this, it has been further suggested that the expressions of totally 810 genes could be controlled by the SKN-1/Nrf2 using the whole transcriptome RNA sequencing technique [27]. Among these genes, *nlg-1* encodes a synaptic cell adhesion molecule neuroligin, which acts as a direct target of SKN-1 [27]. Pharmacological treatments to induce the oxidative stress could increase the synaptic abundance of NLG-1 [27]. The increasing *nlg-1* dosage was correlated with the increased survival in response to the oxidative stress [27]. In contrast, genetic inactivation of *nlg-1* reduced the survival and suppressed the resistance of nematodes to oxidative stress [27]. That is, neuronal SKN-1 activation may potentially confer a protection mechanism for nematodes in response to environmental stresses by affecting the function of neuroligin [27].

1.4.4.3 Identification of Upstream Regulators for SKN-1 in the Regulation of Oxidative Stress

1.4.4.3.1 DAF-16

In nematodes, the *skn-1* expression could be activated by the DAF-16 in the insulin signaling pathway [28]. Nevertheless, the SKN-1 was required for the oxidative stress but not the increased lifespan induced by overexpression of DAF-16 [28]. Meanwhile, it was noted that the DAF-16 overexpression could rescue the short lifespan of *skn-1* mutants but not their susceptibility to oxidative stress [28]. Therefore, the function of SKN-1 in promoting longevity may through a different mechanism from that in protecting against the oxidative damage in nematodes.

1.4.4.3.2 PMK-1

PMK-1 is a p38 MAPK in the p38 MAPK signaling pathway, an integral part of the response of nematodes to a variety of environmental stresses. After exposure to the oxidative stress, the PMK-1 could phosphorylate the SKN-1 and causes the

translocation and accumulation of SKN-1 in the intestine nuclei, where SKN-1 activated the transcription of *gcs-1* encoding a phase II detoxification enzyme [29].

1.4.4.3.3 BLI-3

In nematodes, the ROS could be generated during infection by Duox1/BLI-3, a dual oxidase [30]. Meanwhile, bacterial pathogen infection increased the expression of SKN-1 in the intestine [30]. Mutation of *skn-1* decreased the resistance of nematodes to pathogen infection, whereas increasing SKN-1 activity would augment the resistance of nematodes to pathogen infection [30]. NSY-1, SEK-1, and PMK-1 in the p38 MAPK signaling pathway were all required for the activation of SKN-1 during the pathogen infection [30]. Moreover, it has been shown that the ROS produced by BLI-3 was the important source for SKN-1 activation via the p38 MAPK signaling pathway during the pathogen infection [30]. That is, ROS generation by BLI-3 may activate a protective SKN-1 response via the p38 MAPK signaling in pathogen-infected nematodes.

1.4.4.3.4 SKR-1/2 and WDR-23

In mammals, the Nrf2 is regulated in part by the redox sensor repressor protein of Keap1. In nematodes, new genes required for activation of the core SKN-1 target gene *gst-4* induced by treatment of juglone were identified using genome-wide RNAi screening [31]. Among these candidate regulators, mutation of *skr-1/2* encoding the homologs of yeast and mammalian Skp1 inhibited the induction of SKN-1-dependent detoxification genes and reduced the resistance of nematodes to prooxidants without decreasing the p38 MAPK activation [31]. Moreover, during the control of oxidative stress, SKR-1/2 further acted upstream of the WD40 repeat protein WDR-23, which binds to and inhibits the SKN-1 [31]. Therefore, the signaling cascade of SKR-1/2-WDR-23 is a novel p38 MAPK-independent signaling mechanism that activates the SKN-1 [31].

1.4.4.3.5 ELT-3

Using a transcription factor library to identify genes required for activation of SKN-1 target *gst-4* in *brap-2* mutants, ELT-3, a GATA transcription factor, was identified as a positive regulator of *gst-4p::gfp* expression [32]. In nematodes, the ELT-3 interacted with the SKN-1 to activate the *gst-4* transcription [32]. Moreover, ELT-3 was required for the lifespan extension of nematodes overexpressing the SKN-1 [32].

1.4.4.3.6 GSK-3

Under the normal conditions, phosphorylation by glycogen synthase kinase-3 (GSK-3) could prevent SKN-1 from the accumulation in nuclei [33]. If this inhibition was blocked, the background levels of p38 MAPK signaling were still required for the SKN-1 function. Therefore, GSK-3 inhibits SKN-1 activity in the intestine and influences redox conditions.

1.4.4.3.7 MDT-15

MDT-15, a subunit of the conserved mediator complex, was required for the oxidative stress responses [34]. More importantly, MDT-15 was required for SKN-1 expression [34]. MDT-15 was also required for the expression of genes in SKN-1-dependent and SKN-1-independent fashions downstream of insulin/IGF-1 signaling [34]. In nematodes, the MDT-15 directly binds to the SKN-1 through a region distinct from the classical transcription factor-binding KIX-domain [34].

1.4.4.3.8 MKK-4, IKK ϵ -1, NEKL-2, and PDHK-2

Based on the RNAi suppression screen to identify additional kinases acting in the activation of SKN-1 in response to oxidative stress, four kinases, MKK-4, IKK ϵ -1, NEKL-2, and PDHK-2, were further identified [35]. These kinases were required for the nuclear localization of SKN-1 in response to oxidative stress in nematodes [35]. Moreover, mutation of two of these kinase genes, such as *pdhk-2* and *nekl-2*, could result in a shorter lifespan and increased sensitivity to arsenite stress [35].

1.4.4.3.9 IRE-1

In nematodes, IRE-1, an endoplasmic reticulum (ER) transmembrane protein, has the function in maintaining the ER homeostasis by initiating unfolded protein response (UPRER) [36]. The ROS generated at the ER or by mitochondria could sulfenylate a cysteine within the IRE-1 kinase activation loop, which inhibited the IRE-1-mediated UPRER, initiated the p38 MAPK/SKN-1 antioxidant response, and increased the stress resistance and the lifespan [36]. That is, IRE-1 has an important function as a cytoplasmic sentinel that potentially activates p38 MAPK and SKN-1.

1.4.4.3.10 HCF-1

HCF-1, a host cell factor-1, is a regulator for DAF-16 in the regulation of both longevity and stress response [37]. Moreover, HCF-1 prevented the nuclear accumulation of SKN-1 and inhibited the transcriptional activation of SKN-1, as well as its targeted genes [37]. Additionally, the function of SKN-1 in enhancing oxidative stress resistance could be incurred by *hcf-1* mutation [37].

1.5 Systematic Identification of Novel Genes Required for the Regulation of Oxidative Stress

1.5.1 *Functional Genomic Approach to Identify Novel Genes Required for the Regulation of Oxidative Stress*

In order to perform this functional genome screen, synchronized L1-larvae of *rrf-3(pk1426)* strain were fed with bacteria expressing dsRNA corresponding to the examined genes [38]. Upon reaching to the L4 larval stage (day 0), the nematodes were treated with paraquat (80 mM), and then the survival of animals was monitored in every other day (from day 3 to day 15) [38]. The identified candidate genes are shown in Table 1.1. Based on this gene list, at least a partial functional overlap between the processes of ROS resistance and regulation of lifespan may exist. About ~30% of the aging genes identified here were involved in mitochondrial function [38]. These included those genes encoding components for the respiratory chain, mitochondrial ribosomes, ADP/ATP carriers, and molecules involved in mitochondrial protein synthesis (Table 1.1) [38].

1.5.2 *Identification of Genes Required for the Regulation of Oxidative Stress or Stress Response Based on the Translocation of Environmental Toxicant*

Besides the phenotypic analysis, another strategy to identify the genes required for the regulation of oxidative stress or stress response is based on the translocation of environmental toxicant, such as the graphene oxide (GO), a carbon-based nanomaterial [39]. Activation of oxidative stress is an important cellular contributor to GO toxicity formation in nematodes [40]. Based on the translocation pattern of GO/Rho B, seven genes were identified to be required for the GO toxicity and translocation of GO [39]. Among these seven genes, mutation of *hsp-16.48*, *gas-1*, *sod-2*, *sod-3*, or *aak-2* resulted in the greater GO translocation into the body and toxicity on the functions of both primary targeted organs, such as the intestine, and secondary targeted organs, such as the neurons and reproductive organs (Fig. 1.5) [39]. In

Table 1.1 Paraquat resistance assay for the RNAi clones [38]

Predicted gene	Domain and function	Survival (%)							Mean survival (\pm SEM)	P-value	Relative resistance (%)
		Day 0	Day 3	Day 5	Day 7	Day 9	Day 9	Day 9			
Genes on Chrom III											
Vector	Negative control	100	64	3	0	0	0	0	4.28 (\pm 0.13)	100	
daf-2	Positive control	100	90	77	64	27	27	27	8.32 (\pm 0.36)	<0.0001	194
C40H1.5	Transthyretin-like family	100	66	26	9	4	4	4	5.02 (\pm 0.28)	0.0164	117
Y111B2C.m	epc-1, polycomb enhancer protein	100	93	70	43	6	6	6	7.13 (\pm 0.29)	<0.0001	167
Y76A2B.1	pod-1, coronin-like, actin-binding protein	100	55	24	7	0	0	0	4.68 (\pm 0.20)	0.1031	109
Y76A2B.3	Long-chain acyl-coA synthetase	100	76	22	5	5	5	5	5.07 (\pm 0.29)	0.0067	118
Y119D3_446.d	Glycolipid transferase	100	72	24	7	1	1	1	5.03 (\pm 0.19)	0.0031	118
Y55D5A_391.b	daf-2, insulin/IGF-1 receptor	100	71	18	18	7	7	7	5.23 (\pm 0.31)	0.0083	122
Y71H2_390.d	SNAP-25 interacting protein, exocytosis	100	62	31	17	12	12	12	5.36 (\pm 0.41)	0.0110	125
Y53G8A_1734.d	ral-1, Ras-like GTPase, related to Ral-1	100	82	39	9	2	2	2	5.56 (\pm 0.25)	<0.0001	130
T28D6.4	Ankyrin repeat	100	91	60	38	12	12	12	6.95 (\pm 0.35)	<0.0001	162
K12H4.5	Phosphatidylserine decarboxylase	100	92	71	41	11	11	11	7.27 (\pm 0.25)	<0.0001	170
T28A8.6		100	70	24	7	4	4	4	5.02 (\pm 0.29)	0.0137	117
C29F9.7	pat-4, integrin-linked kinase	100	76	55	38	17	17	17	6.73 (\pm 0.40)	<0.0001	157
Y66A7A1		100	52	33	4	0	0	0	9.00 (\pm 0.29)	0.0572	210
Y71H2_388.c	PP2A regulatory subunit (cytochrome C oxidase subunit)	100	82	48	2	0	0	0	5.57 (\pm 0.20)	<0.0001	130
F54D8.2	Cytochrome c oxidase subunit VIa	100	70	41	22	3	3	3	5.62 (\pm 0.27)	<0.0001	131
F56D2.1	Mitochondrial processing peptidase	100	55	17	3	0	0	0	4.46 (\pm 0.20)	0.4303	104
K04G7.4	Nuo-4, NADH: ubiquinone oxidoreductase	100	78	55	4	0	0	0	5.06 (\pm 0.23)	<0.0001	118
T20H4.5	Ubiquinone Fe-S protein	100	99	89	45	2	2	2	7.58 (\pm 0.18)	<0.0001	177
T26A5.3	Tag-99, NADH: ubiquinone oxidoreductase	100	60	31	7	0	0	0	4.91 (\pm 0.25)	0.0138	115

(continued)

Table 1.1 (continued)

Predicted gene	Domain and function	Survival (%)							Mean survival (\pm SEM)	P-value	Relative resistance (%)
		Day 0	Day 3	Day 5	Day 7	Day 9	Day 11	Day 13			
W09D10.3	Mitochondrial ribosomal protein L12	100	56	31	25	13	5.45 (\pm 0.42)	0.0157	127		
T28D6.2	tba-7, tubulin alpha	100	45	17	1	0	4.24 (\pm 0.13)	0.9887	99		
Y56A3A19	Acyl carrier protein/NADH:ubiquinone oxidoreductase	100	70	47	20	3	5.74 (\pm 0.31)	<0.0001	134		
Y37D8A18	Mitochondrial ribosomal protein 510	100	58	21	5	1	4.67 (\pm 0.21)	0.1395	109		
Y43F4B.7	Amino acid transporter	100	49	7	2	0	4.12 (\pm 0.17)	0.4032	96		
T27E9.1	Tag-61, mitochondrial ADP/ATP carrier protein	100	87	58	29	11	6.51 (\pm 0.39)	<0.0001	152		
Y71H2_378.a	Mitochondrial translation elongation factor Tu	100	97	94	89	72	11.46 (\pm 0.29)	<0.0001	268		
Y119D3_463.b	Cytochrome c heme binding site	100	63	9	0	0	4.37 (\pm 0.18)	0.6166	102		
Y39A3C_82.a		100	72	34	16	10	5.7 (\pm 0.28)	<0.0001	133		
Y53G8A_1734.g		100	85	51	20	2	6.07 (\pm 0.32)	<0.0001	142		
Y53G8A_2702.a		100	96	68	36	13	7.17 (\pm 0.30)	<0.0001	168		
Y53G8A_9248.b		100	67	44	33	11	6.05 (\pm 0.39)	<0.0001	141		
Y53G8A_9248.c	NADH: ubiquinone oxidoreductase	100	71	43	26	11	5.98 (\pm 0.32)	<0.0001	140		
Y53G8A_9248.d	NADH: ubiquinone oxidoreductase	100	84	44	11	1	5.74 (\pm 0.22)	<0.0001	134		
Y71H2_388.d	NADH: ubiquinone oxidoreductase	100	92	45	4	0	5.72 (\pm 0.21)	<0.0001	134		
F09G8.3	Mitochondrial ribosomal protein S9	100	88	71	65	25	7.93 (\pm 0.31)	<0.0001	185		
Y71H2_385.b		100	75	56	50	13	6.79 (\pm 0.42)	<0.0001	159		
Genes on Chrom IV											
Vector	Negative control	100	42	7	3	0	4.02 (\pm 0.12)		100		
daf-2	Positive control	100	92	73	56	28	8.36 (\pm 0.40)	<0.0001	208		
R02D3.6	Gr1-19, ground-like domain	100	47	17	11	5	4.55 (\pm 0.26)	0.0365	113		
W03G1.7	asm-3, acid sphingomyelinase	100	75	43	24	19	6.59 (\pm 0.39)	<0.0001	164		
F09C11.1		100	47	19	6	3	4.46 (\pm 0.025)	0.0698	111		

F41A4.1	PAM domain	100	52	14	3	1	4.37 (±0.15)	0.0726	109
F42A6.1	Olfactory receptor	100	67	17	8	8	4.94 (±0.32)	0.0006	123
B0546.3	Yippee, putative zinc-binding protein	100	35	15	4	4	4.16 (±0.30)	0.703	103
W07G9.1		100	64	30	16	12	5.55 (±0.42)	<0.0001	138
F28F9.4	aat-8, amino acid transporter	100	64	37	24	10	5.73 (±0.35)	<0.0001	143
C46G7.2		100	38	3	0	0	3.77 (±0.14)	0.2690	94
K07H8.8		100	68	24	9	6	5.14 (±0.21)	<0.0001	128
F49C12.9	Ubiquitin-associated domain	100	47	17	8	2	4.46 (±0.30)	0.1004	111
F56D5.5	Golgi matrix protein	100	81	38	17	7	5.96 (±0.28)	<0.0001	148
T05A1.5	Solute carrier protein, transporter	100	87	55	44	29	7.69 (±0.48)	<0.0001	191
ZK792.2	inx-8, gap junction protein	100	80	59	43	35	7.77 (±0.55)	<0.0001	193
ZK792.3	inx-9, gap junction protein	100	35	17	17	17	5.06 (±0.55)	0.0541	126
R10H10.2	spe-26, Kelch motif, actin-binding protein	100	68	45	18	8	5.78 (±0.34)	<0.0001	144
R10H10.7	A conserved, uncharacterized domain	100	65	32	13	0	5.60 (±0.39)	<0.0001	139
C42C1.3		100	46	25	11	4	4.67 (±0.30)	0.0175	116
F49E11.3	amt-2, ammonia permease	100	42	12	8	4	4.26 (±0.28)	0.2962	106
Y45F10D.8	WD repeat protein	100	92	72	57	36	8.58 (±0.41)	<0.0001	213
Y51H4A.m		100	55	37	29	24	6.29 (±0.39)	<0.0001	156
W03G1.5	<i>Drosophila</i> larval cuticle structural component	100	44	27	8	0	4.54 (±0.21)	0.0176	113
F52C12.5	elt-6, erythroid-like transcription factor	100	87	60	33	20	7.04 (±0.43)	<0.0001	175
B0496.8	tag-224, LIM domain, PET domain	100	83	55	36	23	7.51 (±0.36)	<0.0001	187
F33D4.5	Ribosomal protein L1p/L10e family	100	92	77	64	50	9.00 (±0.32)	<0.0001	224
C28C12.9	gei-9, acyl CoA dehydrogenase	100	67	34	16	4	5.38 (±0.28)	<0.0001	134
F28D1.7	rps-23, ribosomal protein small subunit	100	79	30	6	0	5.25 (±0.17)	<0.0001	134
Y41E3.4	ers-1, glutaminyl-tRNA synthetase	100	79	26	21	10	5.69 (±0.40)	<0.0001	142
T05E11.1	rps-5, ribosomal protein small subunit	100	77	40	0	0	5.34 (±0.13)	<0.0001	133

(continued)

Table 1.1 (continued)

Predicted gene	Domain and function	Survival (%)						Mean survival (\pm SEM)	P-value	Relative resistance (%)
		Day 0	Day 3	Day 5	Day 7	Day 9	Day 9			
Y57G11C.17	hhat-2, hedgehog acyltransferase	100	70	10	10	5	4.85 (± 0.25)	0.0002	121	
T22B11.5	2-oxoglutarate dehydrogenase, TCA cycle	100	48	40	24	8	5.35 (± 0.40)	<0.0001	133	
F13B6.1	Mucin (weak homology)	100	60	40	8	0	5.13 (± 0.22)	<0.0001	128	
F08B4.7	Small nuclear ribonucleoprotein polypeptide C	100	53	12	3	0	4.32 (± 0.16)	0.1311	107	
F01G10.1	Transketolase, sugar phosphate metabolism	100	52	13	4	4	4.42 (± 0.28)	0.0926	110	
F58B3.5	mrs-1, methionyl-tRNA synthetase	100	92	75	60	35	8.52 (± 0.29)	<0.0001	212	
C39E9.6	Defense-related protein, SCP domain	100	44	17	2	0	4.21 (± 0.24)	0.4322	105	
LLC1.3	Pyruvate, a-ketoglutarate dehydrogenase	100	91	85	66	14	8.00 (± 0.29)	<0.0001	199	
Y69A2A_2991.c	Protein tyrosine phosphatase	100	60	35	24	15	5.83 (± 0.35)	<0.0001	145	
F29C4.2	Cytochrome c oxidase polypeptide	100	68	34	12	0	5.21 (± 0.32)	<0.0001	130	
K08F11.4	Year-1, tyrosyl-tRNA synthetase (mitochondrial)	100	93	88	72	60	9.97 (± 0.40)	<0.0001	248	
E04A4.7	Cytochrome c	100	98	76	45	26	8.28 (± 0.34)	<0.0001	206	
F42A9.5	cyp-33E2, cytochrome P450 family	100	71	39	24	14	6.01 (± 0.32)	<0.0001	150	
C47E12.2	Mitochondrial ADP/ATP carrier protein	100	74	62	56	50	8.92 (± 0.66)	<0.0001	222	
F21D5.8	Mitochondrial 28S ribosomal protein S33	100	71	38	30	21	6.53 (± 0.36)	<0.0001	162	
C33A12.1	NADH: ubiquinone oxidoreductase	100	64	49	29	12	6.03 (± 0.34)	<0.0001	150	
ZK809.3	NADH: ubiquinone oxidoreductase	100	85	55	40	25	6.39 (± 0.25)	<0.0001	159	
Y57G11C.12	nuo-3, NADH: ubiquinone oxidoreductase	100	87	74	68	29	8.19 (± 0.28)	<0.0001	204	
Y55F3B_743.b	Mitochondrial ribosomal protein	100	63	35	17	6	5.42 (± 0.32)	<0.0001	135	

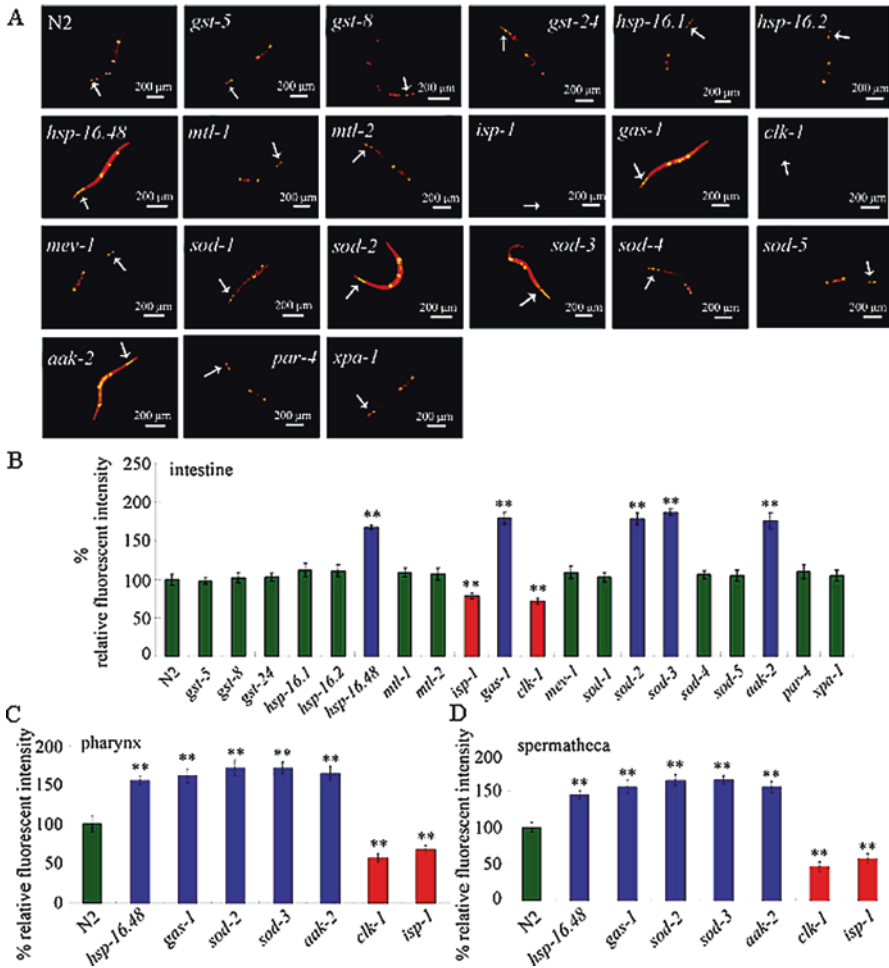


Fig. 1.5 Distributions of GO-Rho B in wild-type and mutant nematodes [39]. (a) Pictures showing the distributions of GO-Rho B in wild-type and mutant nematodes. (b) Comparison of relative fluorescence of GO-Rho B in the intestine between wild-type and mutant nematodes. (c) Comparison of relative fluorescence of GO-Rho B in the pharynx between wild-type and mutant nematodes. (d) Comparison of relative fluorescence of GO-Rho B in the spermatheca between wild-type and mutant nematodes. The arrowheads indicate the pharynx. The intestine (***) and the spermatheca (*) are also indicated. GO exposure was performed from L1-larvae to young adult. The exposure concentration of GO was 100 mg/L. Bars represent means \pm SEM. ** $P < 0.01$ vs wild type

contrast, mutation of *isp-1* or *clk-1* caused the significant suppression in the GO translocation into the body and the GO toxicity on the functions of both primary and secondary targeted organs (Fig. 1.5) [39]. Moreover, mutation of *hsp-16.48*, *gas-1*, *sod-2*, *sod-3*, or *aak-2* caused increased intestinal permeability and prolonged mean

defecation cycle length in GO-exposed nematodes; however, mutation of *isp-1* or *clk-1* resulted in decreased intestinal permeability in GO-exposed nematodes [39].

1.6 Molecular Basis for Induction of Oxidative Stress in Nematodes Exposed to Environmental Toxicants

1.6.1 Alteration in Primary Molecular Mechanism for the Control of Oxidative Stress Induced by Environmental Toxicants

With the graphene oxide (GO) as an example, prolonged exposure (from L1-larvae to adult day 1) to GO (100 mg/L) could induce the significant intestinal reactive oxygen species (ROS) production in nematodes [40]. Meanwhile, prolonged exposure to GO (100 mg/L) resulted in a significant decrease in the expression of *gas-1* and a significant increase in the expression levels of *isp-1* and *clk-1* [40].

With the thiolated GO (GO-SH) as an another example, it has been shown that prolonged exposure to GO-SH (10 mg/L) could significantly increase the expression levels of *clk-1* and *isp-1* and decrease the expression level of *gas-1* (Fig. 1.6) [41]. Very different from the expression patterns of the examined genes in nematodes exposed to GO-SH (10 mg/L), no significant alterations in expression levels of *clk-1* and *isp-1* were detected in nematodes after prolonged exposure to GO-SH (100 μ g/L) (Fig. 1.6). Among the examined genes required for the control of oxidative stress, prolonged exposure to GO-SH (100 μ g/L) could only alter the expression of *gas-1*, and the *gas-1* expression was significantly decreased by prolonged exposure to GO-SH (100 μ g/L) (Fig. 1.6) [41]. These results imply that the primary molecular

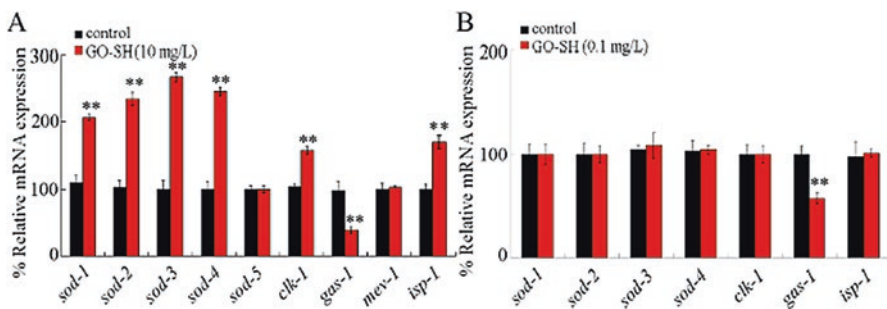


Fig. 1.6 Expression patterns of genes required for the control of oxidative stress in GO-SH-exposed nematodes [41]. (a) Expression patterns of genes required for the control of oxidative stress in 10 mg/L of GO-SH-exposed nematodes. (b) Expression patterns of genes required for the control of oxidative stress in 0.1 mg/L of GO-SH-exposed nematodes. Prolonged exposure was performed from L1-larvae to adult day 1. Bars represent means \pm SD. ** $P < 0.01$ vs control

machinery may be activated to lead to the induction of oxidative stress in nematodes exposed to environmental toxicants, such as the GO or the GO-SH.

1.6.2 Induction of Expression for Proteins with the Functions to Defend Against the Oxidative Stress Induced by Environmental Toxicants

Further with GO as an example, prolonged exposure (from L1-larvae to adult day 1) to GO (100 mg/L) could significantly increase the expression levels of *sod-1*, *sod-2*, *sod-3*, and *sod-4* [40]. Further with GO-SH as another example, prolonged exposure to GO-SH (10 mg/L) could increase the expressions of *sod-1*, *sod-2*, *sod-3*, and *sod-4* (Fig. 1.6) [41]. Besides these, prolonged exposure (from L1-larvae to young adults) to TiO₂-nanoparticles (TiO₂-NPs) with different nanosizes could also significantly increase the expression levels of *sod-2* and *sod-3* among the examined genes required for the control of oxidative stress in nematodes (Fig. 1.7) [42]. These data imply that the toxicity caused by exposure to certain environmental toxicants can further induce a protection response in nematodes, which also reflects the formation of oxidative stress in nematodes exposed to environmental toxicants. Nevertheless, the formed protection response may be not enough to counteract the oxidative damage from environmental toxicants on nematodes.

1.6.3 Suppression in Expressions of Genes Mediating the Protection Response Defending Against Oxidative Stress in Nematodes After Chronic Exposure to Certain Environmental Toxicants

Usually, a protection response will be induced in nematodes after acute or prolonged exposure to certain environmental toxicants. However, once the very severe toxicity is induced by chronic exposure to certain environmental toxicants, the expressions of genes mediating the protection response defending against the oxidative stress would be further suppressed in nematodes. With the Al₂O₃-NPs as an example, the noticeable decrease in expressions of *sod-2* and *sod-3* was detected in nematodes after chronic exposure (from young adults for 10-day) to Al₂O₃-NPs (8.1–23.1 mg/L) (Fig. 1.8) [43]. Meanwhile, the obvious decrease in expressions of *sod-2* and *sod-3* was also detected in nematodes after chronic exposure to bulk Al₂O₃ (Fig. 1.8) [43].

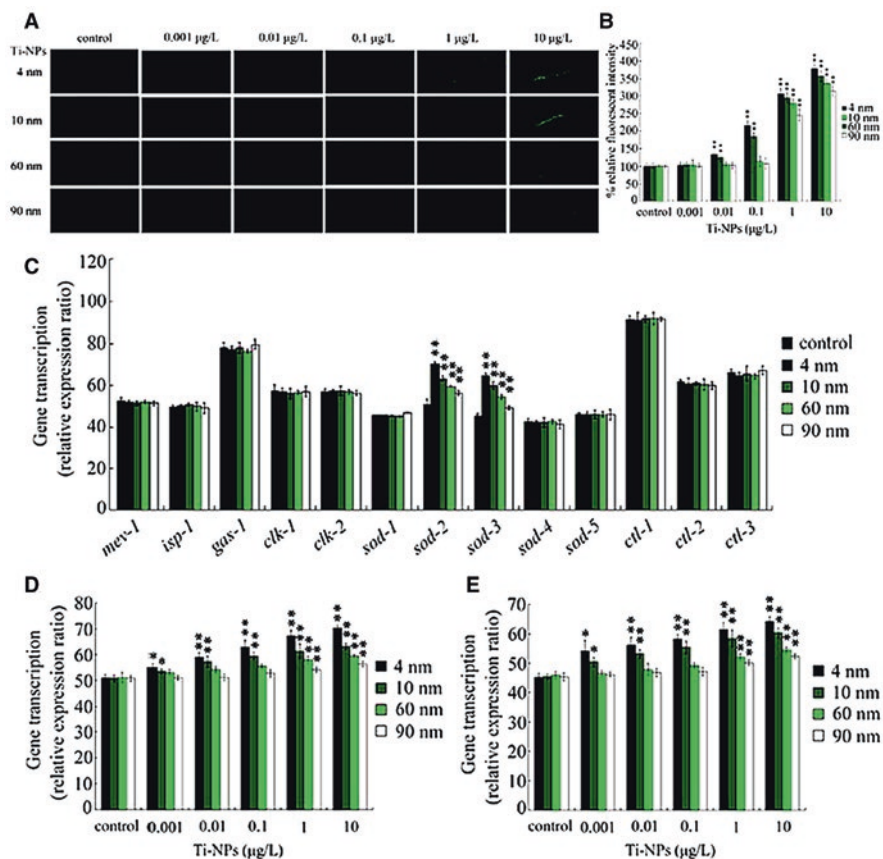


Fig. 1.7 Effects of different sizes of TiO_2 -NPs on ROS production and expression patterns of genes controlling oxidative stress in nematodes [42]. (a, b) Comparison of ROS production in nematodes exposed to different sizes of TiO_2 -NPs. (c) Expression patterns of genes controlling oxidative stress in nematodes exposed to different sizes of TiO_2 -NPs at the concentration of 10 mg/L. (d) Expression patterns of *sod-2* in nematodes exposed to different sizes of TiO_2 -NPs. (e) Expression patterns of *sod-3* in nematodes exposed to different sizes of TiO_2 -NPs. Exposure of TiO_2 -NPs was performed from L1-larvae, and the endpoints were examined when nematodes developed into the adults. Ti-NPs, TiO_2 -NPs. Bars represent mean \pm S.E.M. * $p < 0.05$, ** $p < 0.01$

1.6.4 Induction of Expression for SOD Proteins in Environmental Toxicant-Exposed Nematodes Without Obvious Activation of Oxidative Stress

Using the nematodes to perform toxicity assessment of original surface water samples collected from Three Gorges Reservoir (TGR) in the quiet season in Wanzhou, Chongqing, it was observed that the examined five original surface water samples including the sample W5 collected from the backwater area could not cause toxicity

Fig. 1.8 Expressions of *sod-2* and *sod-3* in nematodes after chronic exposure to Al₂O₃-NPs or bulk Al₂O₃ from young adults for 10 days [43]. Bars represent mean ± S.E.M. ***P* < 0.01 vs control (if not otherwise indicated)

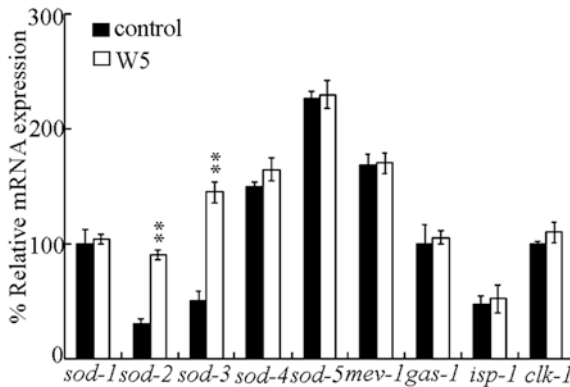
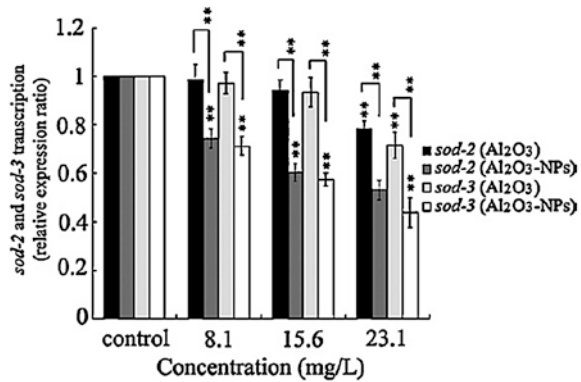


Fig. 1.9 Effect of surface water sample of W5 on transcriptional expressions of *sod-1-5*, *mev-1*, *gas-1*, *isp-1*, and *clk-1* in wild-type nematodes [44]. Relative quantification of the examined genes in comparison to reference *tba-1*. Exposures were performed from L4-larvae for 24 h. The differences between groups were analyzed using analysis of variance (ANOVA). Bars represent means ± SD. ***P* < 0.01 vs control

and induce oxidative stress in nematodes [44]. Nevertheless, the surface water sample W5 induced the significant increase in expressions of genes (*sod-2* and *sod-3*) encoding Mn-SODs in nematodes (Fig. 1.9) [44]. This observation implies one important possibility. In the nematodes exposed to the surface water sample W5, its potential toxicity could already induce a protection response mediated by the increased Mn-SODs, although its toxicity was still not enough to induce the obvious alterations in various phenotypes.

1.6.5 Molecular Signals Involved in the Regulation of Induction of Oxidative Stress in Nematodes Exposed to Environmental Toxicants

With the GO as an example, the potential molecular signals involved in the regulation of induction of oxidative stress in exposed nematodes were screened from 20 strains with mutations of genes required for stress response or oxidative stress [39]. Among these 20 mutants, mutation of *gas-1*, *sod-2*, *sod-3*, or *aak-2* could induce the greater GO translocation into the body and the greater induction of intestinal ROS production compared with those in wild-type nematodes (Fig. 1.10) [39]. In contrast, mutation of *isp-1* or *clk-1* could cause the significant decrease in both the GO translocation into the body and the induction of intestinal ROS production compared with those in wild-type nematodes (Fig. 1.10) [39]. In nematodes, *aak-2* encodes a catalytic alpha subunit of AMP-activated protein kinase.

1.7 Perspectives

In this chapter, we first systematically introduced both the molecular machinery for the activation of oxidative stress and the response signals with the functions to defend against the oxidative stress in nematodes. That is, the relatively detailed information for the molecular basis of oxidative stress activation is available in nematodes. Nevertheless, so far, most of the studies have been performed on the association of oxidative stress and longevity control. In contrast, the systematic

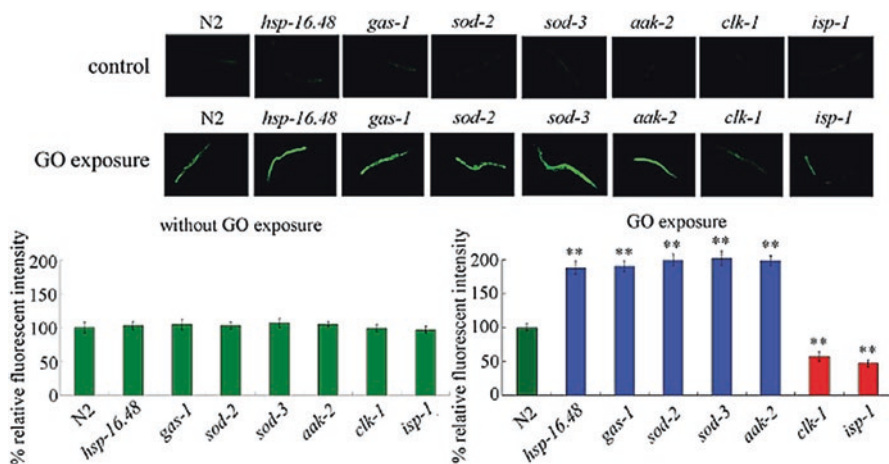


Fig. 1.10 Comparison of induction of intestinal ROS production between wild-type and mutant nematodes exposed to GO (100 mg/L) [39]. GO exposure was performed from L1-larvae to young adult. Bars represent means \pm SEM. ** $P < 0.01$ vs wild type

molecular network explaining the important role of oxidative stress in toxicity induction of different environmental toxicants or stresses is still largely unclear.

Induction of oxidative stress is very important for toxicity formation of various toxicants and stresses in nematodes [45–55]. We here further explained and discussed the known molecular basis for induction of oxidative stress in nematodes exposed to environmental toxicants. With the aim to further deeply elucidating the molecular network explaining the important role of oxidative stress in toxicity induction of different environmental toxicants or stresses, we suggest the attention and the careful consideration of effects of different exposure doses or different exposure routes of environmental toxicants or stresses on the response of nematodes and the underlying molecular mechanisms.

References

1. Liu P-D, He K-W, Li Y-X, Wu Q-L, Yang P, Wang D-Y (2012) Exposure to mercury causes formation of male-specific structural deficits by inducing oxidative damage in nematodes. *Ecotoxicol Environ Saf* 79:90–100
2. Nouara A, Wu Q-L, Li Y-X, Tang M, Wang H-F, Zhao Y-L, Wang D-Y (2013) Carboxylic acid functionalization prevents the translocation of multi-walled carbon nanotubes at predicted environmental relevant concentrations into targeted organs of nematode *Caenorhabditis elegans*. *Nanoscale* 5:6088–6096
3. Kayser EB, Morgan PG, Hoppel CL, Sedensky MM (2001) Mitochondrial expression and function of GAS-1 in *Caenorhabditis elegans*. *J Biol Chem* 276:20551–20558
4. Kayser E, Sedensky MM, Morgan PG (2004) The effects of complex I function and oxidative damage on lifespan and anesthetic sensitivity in *Caenorhabditis elegans*. *Mech Ageing Dev* 125:455–464
5. Dingley S, Polyak E, Lightfoot R, Ostrovsky J, Rao M, Greco T, Ischiropoulos H, Falk MJ (2010) Mitochondrial respiratory chain dysfunction variably increases oxidant stress in *Caenorhabditis elegans*. *Mitochondrion* 10:125–136
6. Yang W, Hekimi S (2010) A mitochondrial superoxide signal triggers increased longevity in *Caenorhabditis elegans*. *PLoS Biol* 8:e1000556
7. Ishii N, Fujii M, Hartman PS, Tsuda M, Yasuda K, Senoo-Matsuda N, Yanase S, Ayusawa D, Suzuki K (1998) A mutation in succinate dehydrogenase cytochrome b causes oxidative stress and ageing in nematodes. *Nature* 394:694–697
8. Senoo-Matsuda N, Yasuda K, Tsuda M, Ohkubo T, Yoshimura S, Nakazawa H, Hartman PS, Ishii N (2001) A defect in the cytochrome *b* large subunit in complex II causes both superoxide anion overproduction and abnormal energy metabolism in *Caenorhabditis elegans*. *J Biol Chem* 276:41553–41558
9. Feng J, Bussiere F, Hekimi S (2001) Mitochondrial electron transport is a key determinant of life span in *Caenorhabditis elegans*. *Dev Cell* 1:633–644
10. Dues DJ, Schaar CE, Johnson BK, Bowman MJ, Winn ME, Senchuk MM, Van Raamsdonk JM (2017) Uncoupling of oxidative stress resistance and lifespan in long-lived *isp-1* mitochondrial mutants in *Caenorhabditis elegans*. *Free Radic Biol Med* 108:362–373
11. Miyadera H, Amino H, Hiraishi A, Taka H, Murayama K, Miyoshi H, Sakamoto K, Ishii N, Hekimi S, Kita K (2001) Altered quinone biosynthesis in the long-lived *clk-1* mutants of *Caenorhabditis elegans*. *J Biol Chem* 276:7713–7716

12. Schaar CE, Dues DJ, Spielbauer KK, Machiela E, Cooper JF, Senchuk M, Hekimi S, Van Raamsdonk JM (2015) Mitochondrial and cytoplasmic ROS have opposing effects on lifespan. *PLoS Genet* 11:e1004972
13. Monaghan RM, Barnes RG, Fisher K, Andreou T, Rooney N, Poulin GB, Whitmarsh AJ (2015) A nuclear role for the respiratory enzyme CLK-1 in regulating mitochondrial stress responses and longevity. *Nat Cell Biol* 17:782–792
14. Anderson GL (1982) Superoxide dismutase activity in dauer larvae of *C. elegans* (Nematoda: Rhabditidae). *Can J Zool* 60:288–291
15. Yanase S, Onodera A, Tedesco P, Johnson TE, Ishii N (2009) SOD-1 deletions in *Caenorhabditis elegans* alter the localization of intracellular reactive oxygen species and show molecular compensation. *J Gerontol A Biol Sci Med Sci* 64:530–539
16. Van Raamsdonk JM, Hekimi S (2009) Deletion of the mitochondrial superoxide dismutase *sod-2* extends lifespan in *Caenorhabditis elegans*. *PLoS Genet* 5:e1000361
17. Doonan RT, McElwee JJ, Matthijssens F, Walker GA, Houthoofd KB, Back P, Matscheski A, Vanfleteren JR, Gems DH (2008) Against the oxidative damage theory of aging: superoxide dismutases protect against oxidative stress but have little or no effect on life span in *Caenorhabditis elegans*. *Genes Dev* 22:3236–3241
18. Petriv OI, Rachubinski RA (2004) Lack of peroxisomal catalase causes a progeric phenotype in *Caenorhabditis elegans*. *J Biol Chem* 279:19996–20001
19. Larsen PL (1993) Aging and resistance to oxidative damage in *Caenorhabditis elegans*. *Proc Natl Acad Sci U S A* 90:8905–8909
20. Honda Y, Honda S (1999) The *daf-2* gene network for longevity regulates oxidative stress resistance and Mn-superoxide dismutase gene expression in *Caenorhabditis elegans*. *FASEB J* 13:1385–1393
21. Kondo M, Senoo-Matsuda N, Yanase S, Ishii T, Hartman PS, Ishii N (2005) Effect of oxidative stress on translocation of DAF-16 in oxygen-sensitive mutants, *mev-1* and *gas-1* of *Caenorhabditis elegans*. *Mech Ageing Dev* 126:637–641
22. Chavez V, Mohri-Shiomi A, Maadani A, Veqa LA, Garsin DA (2007) Oxidative stress enzymes are required for DAF-16-mediated immunity due to generation of reactive oxygen species by *Caenorhabditis elegans*. *Genetics* 176:1567–1577
23. Essers MA, de Vries-Smits LM, Barker N, Polderman PE, Burgering BM, Korswagen HC (2005) Functional interaction between β -catenin and FOXO in oxidative stress signaling. *Science* 308:1181–1184
24. Khare S, Gomez T, Clarke SG (2009) Defective responses to oxidative stress in protein L-isoaspartyl repair-deficient *Caenorhabditis elegans*. *Mech Ageing Dev* 130:670–680
25. An JH, Blackwell TK (2003) SKN-1 links *C. elegans* mesendodermal specification to a conserved oxidative stress response. *Genes Dev* 17:1882–1893
26. Li H, Liu X, Wang D, Su L, Zhao T, Li Z, Lin C, Zhang Y, Huang B, Lu J, Li X (2017) O-GlcNAcylation of SKN-1 modulates the lifespan and oxidative stress resistance in *Caenorhabditis elegans*. *Sci Rep* 7:43601
27. Staab TA, Egrafov O, Knowles JA, Sieburth D (2014) Regulation of synaptic nlg-1/neuroigin abundance by the skn-1/Nrf stress response pathway protects against oxidative stress. *PLoS Genet* 10:e1004100
28. Tullet JMA, Green JW, Au C, benedetto A, Thompson MA, Clark E, Gillat AF, Young A, Schmeisser K, Gems D (2017) The SKN-1/Nrf2 transcription factor can protect against oxidative stress and increase lifespan in *C. elegans* by distinct mechanisms. *Aging Cell* 16:1191–1194
29. Inoue H, Jisamoto N, An JH, Oliveira RP, Nishida E, Blackwell TK, Matsumoto K (2005) The *C. elegans* p38 MAPK pathway regulates nuclear localization of the transcription factor SKN-1 in oxidative stress response. *Genes Dev* 19:2278–2283
30. van der Hoeven R, McCallum KC, Cruz MR, Garsin DA (2011) Ce-Duox1/BLI-3 generated reactive oxygen species trigger protective SKN-1 activity via p38 MAPK signaling during infection in *C. elegans*. *PLoS Pathog* 7:e1002453

31. Wu C-W, Deonaraine A, Przybysz A, Strange K, Choe KP (2016) The Skp1 homologs SKR-1/2 are required for the *Caenorhabditis elegans* SKN-1 antioxidant/detoxification response independently of p38 MAPK. *PLoS Genet* 12:e1006361
32. Hu Q, D'Amora DR, Macneil LT, Walhout AJM, Kubiseski TJ (2017) The oxidative stress response in *Caenorhabditis elegans* requires the GATA transcription factor ELT-3 and SKN-1/Nrf2. *Genetics* 206:1909–1922
33. An JH, Vranas K, Lucke M, Inoue H, Hisamoto N, Matsomoto K, Blackwekk TK (2005) Regulation of the *Caenorhabditis elegans* oxidative stress defense protein SKN-1 by glycogen synthase kinase-3. *Proc Natl Acad Sci USA* 102:16275–16280
34. Goh GYS, Marteli KL, Parhar KS, Kwong AWL, Wong MA, Mah A, Hou NS, Taubert S (2014) The conserved mediator subunit MDT-15 is required for oxidative stress responses in *Caenorhabditis elegans*. *Aging Cell* 13:70–79
35. Kell A, Ventura N, Kahn N, Johnson TE (2007) Activation of SKN-1 by novel kinases in *Caenorhabditis elegans*. *Free Radic Biol Med* 43:1560–1566
36. Hourihan JM, Mazzeo LEM, Fernandez-Cardenas LP, Blackwell TK (2016) Cysteine sulfenylation directs IRE-1 to activate the SKN-1/Nrf2 antioxidant response. *Mol Cell* 63:553–566
37. Rizki G, Picard CL, Pereyra C, Lee SS (2012) Host cell factor 1 inhibits SKN-1 to modulate oxidative stress responses in *Caenorhabditis elegans*. *Aging Cell* 11:717–721
38. Kim Y, Sun H (2007) Functional genomic approach to identify novel genes involved in the regulation of oxidative stress resistance and animal lifespan. *Aging Cell* 6:489–503
39. Wu Q-L, Zhao Y-L, Li Y-P, Wang D-Y (2014) Molecular signals regulating translocation and toxicity of graphene oxide in nematode *Caenorhabditis elegans*. *Nanoscale* 6:11204–11212
40. Wu Q-L, Yin L, Li X, Tang M, Zhang T, Wang D-Y (2013) Contributions of altered permeability of intestinal barrier and defecation behavior to toxicity formation from graphene oxide in nematode *Caenorhabditis elegans*. *Nanoscale* 5(20):9934–9943
41. Ding X-C, Wang J, Rui Q, Wang D-Y (2018) Long-term exposure to thiolated graphene oxide in the range of $\mu\text{g/L}$ induces toxicity in nematode *Caenorhabditis elegans*. *Sci Total Environ* 616–617:29–37
42. Li Y-X, Wang W, Wu Q-L, Li Y-P, Tang M, Ye B-P, Wang D-Y (2012) Molecular control of TiO_2 -NPs toxicity formation at predicted environmental relevant concentrations by Mn-SODs proteins. *PLoS ONE* 7(9):e44688
43. Li Y-X, Yu S-H, Wu Q-L, Tang M, Pu Y-P, Wang D-Y (2012) Chronic Al_2O_3 -nanoparticle exposure causes neurotoxic effects on locomotion behaviors by inducing severe ROS production and disruption of ROS defense mechanisms in nematode *Caenorhabditis elegans*. *J Hazard Mater* 219–220:221–230
44. Xiao G-S, Zhao L, Huang Q, Du H-H, Guo D-Q, Xia M-X, Li G-M, Chen Z-X, Wang D-Y (2018) Biosafety assessment of water samples from Wanzhou watershed of Yangtze Three Gorges Reservoir in the quiet season in *Caenorhabditis elegans*. *Sci Rep* 8:14102
45. Zhi L-T, Qu M, Ren M-X, Zhao L, Li Y-H, Wang D-Y (2017) Graphene oxide induces canonical Wnt/ β -catenin signaling-dependent toxicity in *Caenorhabditis elegans*. *Carbon* 113:122–131
46. Ren M-X, Zhao L, Lv X, Wang D-Y (2017) Antimicrobial proteins in the response to graphene oxide in *Caenorhabditis elegans*. *Nanotoxicology* 11:578–590
47. Zhao L, Rui Q, Wang D-Y (2017) Molecular basis for oxidative stress induced by simulated microgravity in nematode *Caenorhabditis elegans*. *Sci Total Environ* 607–608:1381–1390
48. Zhao Y-L, Yang J-N, Wang D-Y (2016) A microRNA-mediated insulin signaling pathway regulates the toxicity of multi-walled carbon nanotubes in nematode *Caenorhabditis elegans*. *Sci Rep* 6:23234
49. Zhi L-T, Fu W, Wang X, Wang D-Y (2016) ACS-22, a protein homologous to mammalian fatty acid transport protein 4, is essential for the control of toxicity and translocation of multi-walled carbon nanotubes in *Caenorhabditis elegans*. *RSC Adv* 6:4151–4159
50. Yang R-L, Rui Q, Kong L, Zhang N, Li Y, Wang X-Y, Tao J, Tian P-Y, Ma Y, Wei J-R, Li G-J, Wang D-Y (2016) Metallothioneins act downstream of insulin signaling to regulate toxic-

- ity of outdoor fine particulate matter (PM_{2.5}) during Spring Festival in Beijing in nematode *Caenorhabditis elegans*. *Toxicol Res* 5:1097–1105
51. Zhi L-T, Ren M-X, Qu M, Zhang H-Y, Wang D-Y (2016) Wnt ligands differentially regulate toxicity and translocation of graphene oxide through different mechanisms in *Caenorhabditis elegans*. *Sci Rep* 6:39261
 52. Xiao G-S, Zhao L, Huang Q, Yang J-N, Du H-H, Guo D-Q, Xia M-X, Li G-M, Chen Z-X, Wang D-Y (2018) Toxicity evaluation of Wanzhou watershed of Yangtze Three Gorges Reservoir in the flood season in *Caenorhabditis elegans*. *Sci Rep* 8:6734
 53. Yin J-C, Liu R, Jian Z-H, Yang D, Pu Y-P, Yin L-H, Wang D-Y (2018) Di (2-ethylhexyl) phthalate-induced reproductive toxicity involved in DNA damage-dependent oocyte apoptosis and oxidative stress in *Caenorhabditis elegans*. *Ecotoxicol Environ Saf* 163:298–306
 54. Ding X-C, Rui Q, Wang D-Y (2018) Functional disruption in epidermal barrier enhances toxicity and accumulation of graphene oxide. *Ecotoxicol Environ Saf* 163:456–464
 55. Wang D-Y (2018) *Nanotoxicology in Caenorhabditis elegans*. Springer, Singapore

Chapter 2

Molecular Basis for Reduced Lifespan Induced by Environmental Toxicants or Stresses



Abstract What's the potential basic principle for the toxicity induction on different endpoints in nematodes exposed to environmental toxicants or stresses? To answer such a question, we here focus on the endpoint of lifespan to discuss the potential basic principle for toxicity induction from environmental toxicants or stresses. In this chapter, we will discuss how the environmental toxicants or stresses reduce lifespan by affecting the molecular basis for longevity, and how the innate immune response is involved in the regulation of longevity reduction in nematodes exposed to environmental toxicants or stresses. We will further introduce the genetic identification of genes and signaling cascade in the regulation of toxicity of environmental toxicants or stresses. We will also discuss how the environmental toxicants or stresses reduce lifespan by affecting signaling pathways associated with the stress response.

Keywords Molecular basis · Lifespan reduction · Environmental exposure · *Caenorhabditis elegans*

2.1 Introduction

In nematodes, many useful sublethal endpoints have been raised and will be further raised to be used for toxicity assessment and toxicological study of various environmental toxicants and stresses. The already raised sublethal endpoints in nematodes are at least associated with development, reproduction, neuronal development and function, intestinal development and function, epidermal development, innate immune response, lifespan, metabolism, and oxidative stress [1–17]. With the concern on these valuable endpoints, we are facing upon an important scientific question. That is, what's the potential basic principle for the toxicity induction on these sublethal endpoints in nematodes exposed to environmental toxicants or stresses?

Among the widely used toxicity assessment endpoints in *C. elegans*, lifespan is an endpoint to reflect the long-term effects of certain environmental toxicants or stresses on animals [18–20]. Both lifespan and aging-related phenotypes can be

used to determine the aging process in nematodes. In this chapter, we will focus on the lifespan to discuss the potential basic principle for the toxicity induction in nematodes exposed to environmental toxicants or stresses. We first introduced the molecular basis for the longevity control, especially the important signaling pathways required for the control of longevity (insulin signaling pathway, dietary intake signaling pathway, mitochondrial respiration signaling pathway, and germline signaling pathway). After that, we discussed how the environmental toxicants or stresses reduce lifespan by affecting the molecular basis for longevity, and how the innate immune response is involved in the regulation of longevity reduction in nematodes exposed to environmental toxicants or stresses. Moreover, we introduced the genetic identification of genes and signaling cascade in the regulation of toxicity on lifespan by environmental toxicants or stresses. Finally, we tried to discuss how the environmental toxicants or stresses reduce lifespan by affecting signaling pathways associated with the stress response.

2.2 Molecular Basis for Longevity Control

Over 30 years ago, it has been found that certain genetic or environmental manipulations could result in the *C. elegans* to live over twice as long as that in wild-type nematodes [21–23]. Since this discovery, many more genes and these genes-mediated signaling pathways have been successfully identified and elucidated to explain the underlying molecular mechanisms for the aging process or longevity in *C. elegans* [24–30]. The widely described signaling pathways involved in the regulation of longevity in *C. elegans* contain insulin, dietary intake, mitochondrial respiration, and germline signaling pathways [24–30]. More importantly, these signaling pathways described in *C. elegans* can also be shared by other organisms, including the mammals [24–30], which implies that the underlying molecular mechanisms for longevity are conserved among different organisms.

2.2.1 *Insulin Signaling Pathway*

In 1997, it was reported that the lifespan extension can be achieved by mutations of *daf-2* encoding the sole insulin/IGF-1 receptor in *C. elegans* [31]. The insulin signaling pathway is the most well-described signaling pathway in the regulation of longevity in *C. elegans*.

2.2.1.1 The Basic Information for Insulin Signaling Pathway

During the control of aging process, the insulin signals activated DAF-2 can initiate a subsequent signaling cascade by activating AGE-1, a phosphatidylinositol 3-kinase (PI3K), to produce the PIP3 and the AKT family kinases in the dependent of a PDK-1 kinase [32–35]. The activated signaling cascade of AKT family kinases will phosphorylate the forkhead transcription factor DAF-16 in order to prevent the entering of DAF-16 into the nucleus to promote or inhibit the transcription of its downstream genes [36–40]. Inactivation of insulin signaling pathway occurs at least partially via the activity of DAF-18, a PIP3 phosphatase [40, 41].

2.2.1.2 Nucleus-Cytoplasmic Translocation of DAF-16

It has been widely considered that the nucleus-cytoplasmic translocation of DAF-16 plays a major role in the regulation of longevity and stress response [24–30, 42]. Nevertheless, a constitutive nuclear localization of DAF-16 did not potentially increase the lifespan of nematodes [43]. Additionally, some important regulators, such as SIR-2.1, HSF-1, LIN-14, and SMK-1, have been identified to be capable of modulating DAF-16's phenotypes once translocated into the nucleus [43–46].

2.2.1.3 Targets of DAF-16

To understand the underlying mechanisms for DAF-16 in extending the lifespan and modulating the resistance to various stressors, some groups have identified the downstream targets of DAF-16 [47–52]. Transcriptional profiling analyses by comparing wild-type, dauer, and long-lived insulin/IGF-1 signaling- *daf-2* mutant identified heat shock proteins and mitochondrial Mn-SOD protein SOD-3 as the most DAF-16-responsive downstream targets [47–50], implying the important roles of proteostasis and reactive oxygen species (ROS) detoxification in the regulation of longevity and resistance to environmental toxicants or stresses. The further more in-depth expressional profiling analysis by comparing *daf-2* and wild-type adult nematodes found that, besides the heat shock proteins, many neuropeptide-like proteins and antimicrobial proteins associated with the innate immune response could be upregulated [51]. After the profiling comparisons of *daf-2* and *age-1* mutants, or of *daf-2* gene inactivation with and without *daf-16* mutation or inactivation, totally 254 upregulated and 243 downregulated genes were identified to act as the possible targeted genes of *daf-16* [52]. Among the identified possible downstream targets for DAF-16, the potential functions of heat shock proteins (HSP-16.1, HSP-16.2, HSP-12.3, and HSP-12.6), catalases and superoxide dismutases (CTL-1, CTL-2, and SOD-3), and antimicrobial proteins (LYS, SPP, CLEC, and NLP proteins) in the regulation of longevity and stress response need to be further carefully considered [52].

2.2.2 *Dietary Intake Signaling Pathway*

In 1998, it was reported that the *eat-2* mutants can exhibit a significant increase in lifespan, which may be largely due to the result of their decreased rates of feeding [53]. Dietary restriction (DR) is defined as the reduction of particular or total nutrient intake without causing the malnutrition.

2.2.2.1 **mTOR Signaling Pathway Is a Major Effector Regulating the Dietary Restriction**

In nematodes, loss-of-function mutation of *let-363* encoding the TOR results in an increased lifespan [54, 55]. Moreover, the TOR adaptor protein rap-TOR (DAF-15) can be directly suppressed by the active DAF-16 [54, 55]. Meanwhile, loss-of-function mutation of *let-363* in combination with *daf-2* mutation could not further extend the lifespan, although the extended lifespan in *let-363* mutant could not be suppressed by *daf-16* mutation [55]. In nematodes, TOR and *daf-2* extension of longevity may share the same or similar downstream mechanisms and targets.

2.2.2.2 **Important Role of Autophagy**

In *C. elegans*, inhibition of several autophagy-related genes (*unc-51/ATG1/Ulk1*, *bec-1/ATG6/Beclin1*, *vps-34*, *atg-18/Wipi*, or *atg-7*) could effectively shorten the long lifespan phenotype of *eat-2* mutants [56–59], suggesting the potential directly link of modulation in autophagy to dietary restriction-mediated longevity. Additionally, the nematodes with the mutations of *daf-15/raptor* also require the autophagy genes for their lifespan extension [59]. Recently, it has been further observed that intestine-specific RNAi knockdown of autophagy genes *atg-18/Wipi* or *lgg-1/Atg8* in *eat-2* mutants was sufficient to shorten their extended lifespan and disrupt the improved intestinal barrier function [56].

2.2.2.3 **Transcriptional Factors Involved in the Regulation of Dietary Restriction-Mediated Lifespan Extension**

So far, at least the transcriptional factors of FOXA ortholog PHA-4, nuclear hormone receptor NHR-62, and TFEB ortholog HLH-30 have been identified to be required for dietary restriction- or mTOR-mediated lifespan extension [60, 61].

2.2.3 Mitochondrial Respiration Signaling Pathway

If the reactive oxygen species (ROS) production can be properly controlled by modulating the mitochondrial activity, the longevity is predicted to be increased. The mitochondria are primary sites producing ROS. Based on this assumption, the mitochondrial electron transport and ATP synthase have been identified as the important regulators of longevity in *C. elegans* [62–64].

2.2.3.1 Complex I (NADH:Ubiquinone Oxidoreductase)

gas-1 encodes a 49 kDa subunit of complex I. The *gas-1(fc21)* mutant has shortened lifespans and few offspring and grows slowly [65]. The increased oxidative damage onto mitochondrial protein was further observed in *gas-1* mutant nematodes [66].

nuo-1 encodes a NDUFV1 subunit of complex I. The *nuo-1* mutant cannot develop into the adulthood (arrested at the L3 stage) [67], implying that the *nuo-1* mutant can be technically considered as long-lived.

nuo-6 encodes a complex I subunit orthologous to mammalian NUDFB4 complex I subunit. The missense mutation of *nuo-6* decreased the complex I function and increased the lifespan [68].

2.2.3.2 Complex II (Succinate:Ubiquinone Oxidoreductase)

mev-1 encodes a cytochrome b large subunit of complex II [69]. The *mev-1(kn1)* mutant shows a decreased mitochondrial activity (as indicated by the reduced mitochondrial respiratory rates) and short lifespan [69–71]. In addition, the *mev-1(kn1)* mutant has a higher level of oxygen-free radicals compared with wild type [72].

2.2.3.3 Complex III

isp-1 encodes an iron–sulfur component of complex III. Mutations of *isp-1* could increase the longevity by decreasing the oxygen consumption [62, 63].

ctb-1 encodes a cytochrome b subunit of complex III. Missense mutation of *ctb-1* could suppress the slow developmental rate of *isp-1* mutant, but not the prolonged lifespan [63]. *ctb-1* mutant alone has no aging phenotype [63].

2.2.3.4 Complex IV

RNAi knockdown any of the three complex IV subunits, including the COX IV, could increase the lifespan in nematodes [64, 73].

2.2.3.5 Complex V

Loss-of-function mutation or RNAi knockdown of *atp-2* caused the extended lifespan [62, 67].

2.2.3.6 Coenzyme Q (Ubiquinone, CoQ) Synthesis

clk-1 encodes a ubiquinone biosynthesis protein COQ7. Mutation of *clk-1* could lengthen the lifespan [74]. More importantly, the long-lived phenotype of *daf-2(e1370)* mutant could be further extended by *isp-1* or *clk-1* mutation or RNAi of respiratory chain components [62–64, 74].

2.2.3.7 Mitochondrial Mn-SODs

Mitochondrial superoxide dismutases contain SOD-2 and SOD-3. SOD-2 is localized to the I:III:IV super complex.

sod-2 encodes a constitutively expressed mitochondrial dismutase. It was reported that mutation of *sod-2* could lengthen the lifespan, and the *clk-1;sod-2(ok1030)* could live longer than *clk-1* mutant, although the increased oxidative damage could be detected [75].

sod-3 encodes an inducible mitochondrial superoxide dismutase. The *sod-2;gas-1;sod-3* triple mutant is synthetically lethal [76], which implies the importance of SOD-3 for the normal survival of *sod-2;gas-1*.

2.2.4 Germline Signaling Pathway

Certain cells and tissues, such as the gonad, in the body can act as an endocrine source to regulate metabolism, behavior, development, and longevity. In nematodes, prevention of germline stem cell proliferation can induce approximately 60% extension of lifespan [77]. So far, at least steroid nuclear receptor DAF-12, FOXO transcription factor DAF-16, FOXA transcription factor PHA-4, and HNF-4-like nuclear receptor NHR-80 have been identified to be required for the control of gonadal longevity in *C. elegans* [77].

2.2.4.1 DAF-12

The longevity of nematodes lacking the germline was found to be dependent of a steroid hormone signal encoded by the nuclear hormone receptor DAF-12 [78]. After response to ligands (bile acid-like steroids or dafachronic acids (DA)), DAF-12 extends the adult lifespan when the germline stem cells are removed [78], which suggests that the DAF-12 acts as an important link between the developmental progression and the longevity. That is, when the gonad is intact, signals from the germline may impinge on the somatic gonad to inhibit the DA/DAF-12 signaling. However, when the germline is removed, the DA/DAF-12 signaling may be suppressed.

2.2.4.2 DAF-16

It has been considered that the DAF-16/FOXO can act as a central regulator of gonadal longevity [78]. Additionally, it has been shown that the *daf-2;glp-1* double mutants live four- to five-fold longer than wild-type nematodes [78]. This implies that the longevity of reduced IIS may be additive with that of gonadal longevity, and DAF-16/FOXO may respond to the germline ablation differently from the reduced IIS.

2.2.4.3 TOR Signal

Germline removal can also trigger the downregulation of TOR signal, which will in turn stimulate the PHA-4 and the autophagy to promote a healthful state through the effects on certain metabolisms (such as fats, sterols, amino acids, carbohydrates) or other stress signals [77].

2.2.4.4 NHR-80

Besides the fat metabolism, the nuclear hormone receptor NHR-80 has been found to be involved in the regulation of longevity [79]. Loss-of-function mutation of *nhr-80* could abrogate the lifespan extension of germline-less nematodes, but has little effect on the lifespan in wild-type nematodes [79]. The *nhr-80* expression could be induced upon germline ablation in a manner independent of the *daf-12* or the *daf-16* [79], which implies that this observed extended longevity may be associated with the reduced IIS, the reduced mitochondrial function, and the dietary restriction. The increase in NHR-80 expression was observed specifically within the intestine upon the germline ablation; however, loss-of-function mutation of *nhr-80* has no effect on the DAF-16/FOXO nuclear localization [79]. Additionally, RNAi knockdown of *nhr-80* could further shorten the lifespan of double mutant of *daf-16;glp-1* [79].

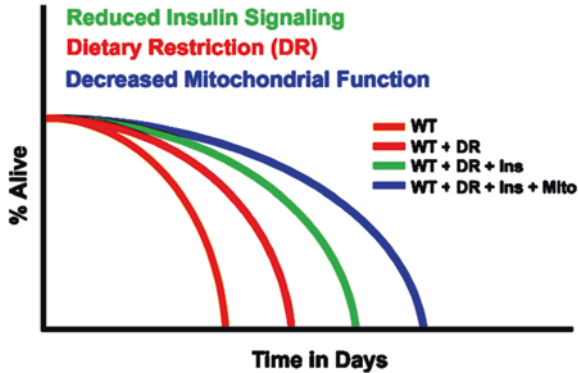


Fig. 2.1 Modulation of the three core signaling pathways that affect the aging act synergistically with each other [82]. Dietary restriction (red line), reduced insulin signaling (green line), or impairment of the mitochondrial electron transport chain (blue line) can extend the lifespan of a wild-type animal (orange line). Modulation of any two of these three pathways has an additive effect on lifespan, supporting arguments for their mechanistic autonomy. Knockdown of all three pathways should create an animal that is far longer lived than an animal with reduced function in just two of the three pathways

2.2.5 Interaction Among Different Signaling Pathways

It has been observed that the simultaneous manipulation of more than one of the signaling pathways required for the control of longevity could result in longer lifespan than that through the manipulation of a single signaling pathway [41, 53, 62, 80, 81]. Meanwhile, the combination of mutations in multiple genes downstream of IIS or of an IIS mutation in combination with the *daf-2(RNAi)* yielded the results only in the lifespan extension comparable to the single mutations or to stronger *daf-2* mutant [41, 53, 62, 80, 81]. Therefore, these synergistic effects between different signaling pathways required for the control of longevity may not be simply due to the further downregulation of insulin signaling in nematodes (Fig. 2.1).

2.3 Environmental Toxicants or Stresses Reduce Lifespan by Affecting the Molecular Basis for Longevity

2.3.1 Environmental Toxicants or Stresses Reduce Lifespan by Affecting the Insulin Signaling Pathway

Illegal or unsuitable use of weight loss agents is an important public health concern [83, 84]. Clenbuterol is a typical weight loss agent by acting as a β_2 -adrenergic agonist. It was illegally used as a feed additive to improve production performance and a carcass composition. Ractopamine is another synthetic β_2 -adrenoceptor

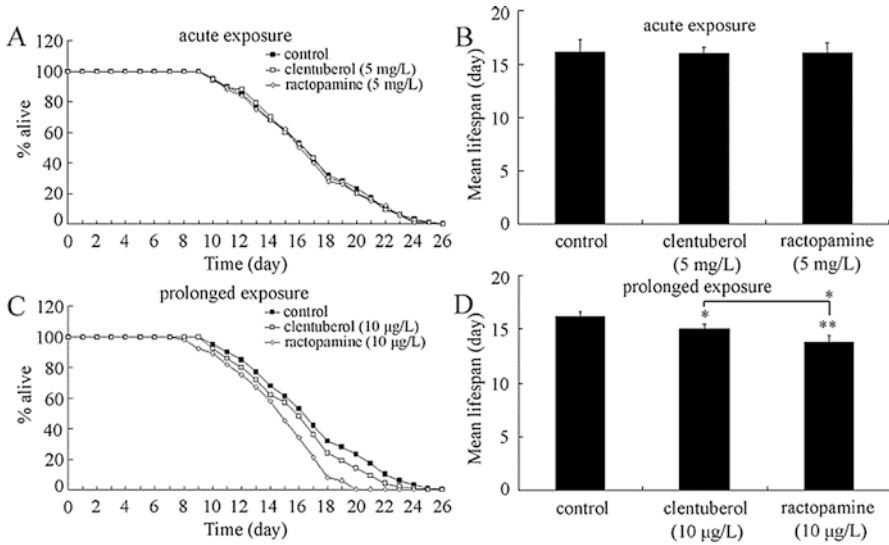


Fig. 2.2 Comparison of lifespan in nematodes exposed to clenbuterol or ractopamine [86]. (a, c) Lifespan curves of nematodes exposed to clenbuterol or ractopamine. (b, d) Comparison of mean lifespans in nematodes exposed to clenbuterol or ractopamine. Exposures were performed from the young adult for 24 h (acute exposure) or from L1-larvae to adult (prolonged exposure). Thirty nematodes were examined per treatment. Bars represent mean \pm S.E.M. * $P < 0.05$, ** $P < 0.01$

agonist and is also widely used as a feed additive to promote the reduction in body fat and to enhance the muscle growth [85]. Here, we selected the ractopamine as an example to explain the effect of certain environmental toxicants or stresses in reducing the lifespan by affecting the insulin signaling pathway in nematodes.

In nematodes, acute exposure to the ractopamine at the concentration of 5 mg/L could not significantly alter the lifespan (Fig. 2.2) [86]. In contrast, prolonged exposure to the ractopamine at the concentration of 10 mg/L could significantly reduce the lifespan (Fig. 2.2) [86]. Additionally, prolonged exposure to the ractopamine at the concentration of 10 mg/L could more severely inhibit the lifespan than that from the clenbuterol (Fig. 2.2) [86].

To determine the underlying molecular mechanism for the ractopamine to reduce the lifespan, the expression patterns of genes encoding the insulin signaling pathway were examined in the ractopamine-exposed nematodes. After prolonged exposure, ractopamine (10 mg/L) could significantly decrease the transcriptional expressions of *daf-16*, *skn-1*, and *aak-2* and increase the transcriptional expressions of *daf-2* and *age-1* [86], which implies that prolonged exposure to the ractopamine (10 mg/L) may reduce the lifespan by altering the molecular basis for insulin signaling pathway in nematodes.

To further confirm the functions of the dysregulated genes in the insulin signaling pathway in the regulation of ractopamine toxicity, the lifespans of some corresponding mutants exposed to the ractopamine were examined. It was found that the

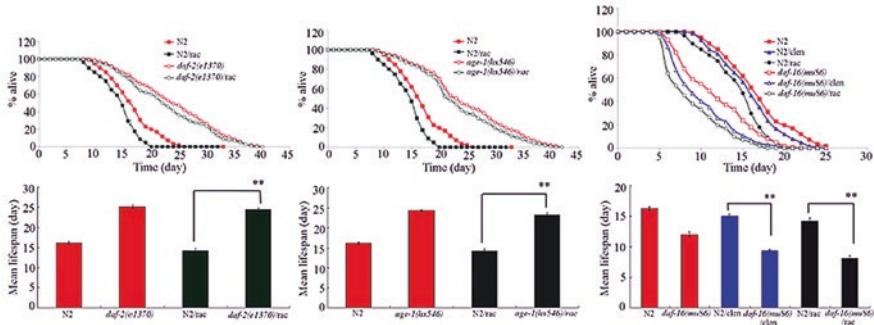


Fig. 2.3 Lifespans in wild type and mutants exposed to ractopamine [86]. Exposures were performed from L1-larvae to adult (prolonged exposure) at the concentration of 10 mg/L. Thirty nematodes were examined per treatment. rac, ractopamine. Bars represent mean \pm S.E.M. ** $P < 0.01$

daf-16(mu86) mutant nematodes showed the susceptibility to the toxicity of ractopamine (Fig. 2.3) [86]. In contrast, the *daf-2(e1370)* or the *age-1(hx546)* mutants showed the resistance to the toxicity of ractopamine (Fig. 2.3) [86]. These results further confirm the involvement of the insulin signaling pathway in the regulation of ractopamine toxicity in nematodes.

2.3.2 Environmental Toxicants or Stresses Reduce Lifespan by Affecting the Mitochondrial Respiration Signaling Pathway

Graphene oxide (GO), one of the derivatives of graphene, can be potentially applied in different areas, including drug, gene carrier, and bioimaging [87–89]. In nematodes, GO exposure could cause the toxicity on the functions of both primary targets organs (such as the intestine) and secondary targeted organs (such as the neurons and reproductive organs) [90–92]. After prolonged exposure from L1-larvae to adult day 1, it was further observed that GO at concentrations of 10–100 mg/L could significantly reduce the lifespan, although GO at concentrations of 0.1–1 mg/L did not significantly affect the lifespan (Fig. 2.4) [93]. Moreover, the aging-related properties were also affected by GO exposure in nematodes. After prolonged exposure, GO (1–100 mg/L) obviously resulted in the intestinal autofluorescence caused by lysosomal deposits of lipofuscin and the intestinal ROS production, although GO (0.1 mg/L) still could not induce the noticeable intestinal autofluorescence and intestinal ROS production (Fig. 2.4) [93]. Additionally, from adult day 4 to adult day 12, prolonged exposure to of GO (10 mg/L) could significantly decrease both the head thrash and the body bend (Fig. 2.4) [93]. Therefore, prolonged exposure to GO can not only reduce the lifespan but also alter the aging-related properties in nematodes.

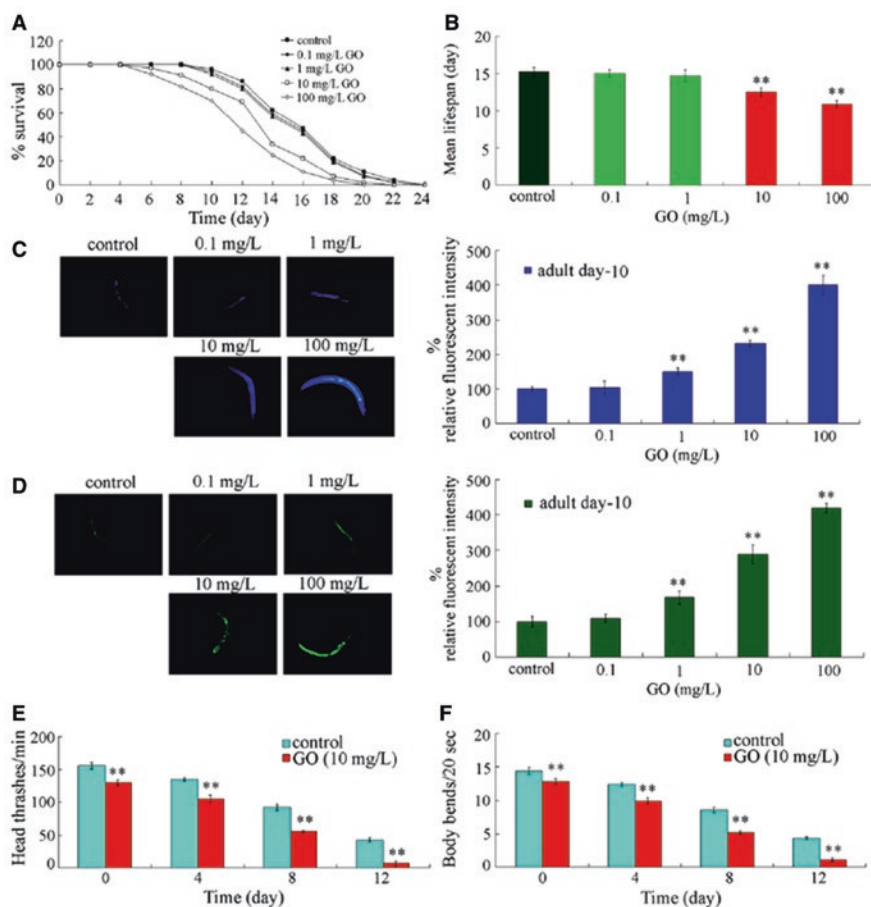


Fig. 2.4 Toxicity assessment of GO [93]. (a) Effects of GO exposure on lifespan. (b) Comparison of mean lifespans. Forty nematodes were examined per treatment. (c) Effects of GO exposure on intestinal autofluorescence. Forty nematodes were examined per treatment. (d) Effects of GO exposure on intestinal ROS production. Fifty nematodes were examined per treatment. (e–f) Effects of GO exposure on locomotion behavior as indicated by endpoints of head thrash and body bend. Thirty nematodes were examined per treatment. Bars represent mean \pm S.E.M. ** $P < 0.01$

To understand the molecular basis for the observed GO toxicity, the expression patterns of genes required for the control of oxidative stress were examined. After prolonged exposure, GO (100 mg/L) caused the significant decrease in transcriptional expression of *gas-1* and the significant increase in transcriptional expressions of *isp-1* and *clk-1* [94]. *isp-1* encodes a “Rieske” iron–sulfur protein, *gas-1* encodes a subunit of mitochondrial complex I, and *clk-1* encodes a ubiquinone biosynthesis protein COQ7. In *C. elegans*, the *gas-1(fc21)* mutant has a shortened lifespan [65], whereas mutations of *isp-1* or *clk-1* could increase the longevity [62, 63, 74].

Therefore, these results suggest that prolonged exposure to GO may reduce the lifespan by at least partially modulating the function of mitochondrial respiration signaling pathway in nematodes.

2.3.3 Environmental Toxicants or Stresses Reduce Lifespan by Affecting Certain MicroRNAs-Mediated Molecular Signals

With the aid of SOLiD sequencing, the GO-induced miRNA profiling was examined in nematodes. Total 23 upregulated and 8 downregulated miRNAs were identified in GO-exposed nematodes [93]. The upregulated miRNAs were *mir-259*, *mir-1820*, *mir-36*, *mir-82*, *mir-239*, *mir-246*, *mir-247*, *mir-392*, *mir-4806*, *mir-2217*, *mir-360*, *mir-4810*, *mir-4807*, *mir-1822*, *mir-4805*, *mir-800*, *mir-1830*, *mir-236*, *mir-244*, *mir-235*, *mir-4937*, *mir-4812*, and *mir-43*, and the downregulated miRNAs were *mir-1834*, *mir-800*, *mir-231*, *mir-5546*, *mir-42*, *mir-2214*, *mir-2210*, and *mir-73* [93]. With the aid of TargetScan database, the possible targeted genes for the dysregulated miRNAs by GO exposure we further predicted [93].

To further determine the role of dysregulated miRNAs in the regulation of GO toxicity, the available mutants for the identified dysregulated miRNAs were employed to further determine their role in regulating the lifespan in GO-exposed nematodes. After prolonged exposure, it was found that GO exposed *mir-244* or *mir-235* mutants showed the significantly decreased lifespan compared with that in GO exposed wild-type N2 (Fig. 2.5) [93]. In contrast, GO exposed *mir-247/797*, *mir-73/74*, or *mir-231* mutants exhibited the significantly increased lifespan compared with that in GO exposed wild-type N2 (Fig. 2.5) [93]. The GO exposed other miRNA mutants had the similar lifespan to that in GO exposed wild-type N2 (Fig. 2.5) [93]. These results suggest that only a limited number of miRNAs are involved in the control of GO toxicity in reducing the lifespan in nematodes.

Meanwhile, it has been shown that mutations of some miRNAs could also alter the aging-related properties in GO-exposed nematodes. GO-exposed *mir-244* or *mir-235* mutants showed the significantly increased induction of intestinal autofluorescence and intestinal ROS production compared with that in GO-exposed wild-type N2; however, GO-exposed *mir-247/797*, *mir-73/74*, or *mir-231* mutants exhibited the significantly decreased intestinal autofluorescence and intestinal ROS production compared with that in GO-exposed wild-type N2 (Fig. 2.6) [93]. Additionally, GO-exposed *mir-244* or *mir-235* mutants showed the significantly decreased locomotion behavior compared with that in GO-exposed wild-type N2, whereas GO-exposed *mir-247/797*, *mir-73/74*, or *mir-231* mutants had the significantly increased locomotion behavior compared with that in GO-exposed wild-type N2 (Fig. 2.6) [93].

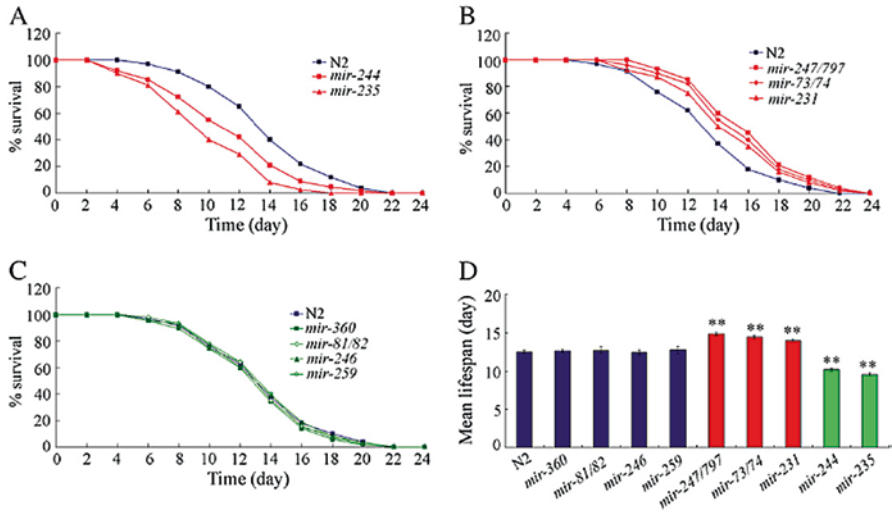


Fig. 2.5 Lifespan of mutants for some dysregulated miRNAs exposed to GO [93]. (a) Lifespan of wild-type, *mir-244*, and *mir-235* mutants exposed to GO. (b) Lifespan of wild-type, *mir-247/797*, *mir-73/74*, and *mir-231* mutants exposed to GO. (c) Lifespan of wild-type, *mir-360*, *mir-81/82*, *mir-246*, and *mir-259* mutants exposed to GO. Forty nematodes were examined per treatment. Exposure concentration was 10 mg/L. Bars represent mean \pm S.E.M. ** $P < 0.01$

To understand the underlying molecular mechanism for the candidate miRNAs in the regulation of GO toxicity in reducing lifespan, their corresponding targeted genes with function involved in the control of longevity were searched. In nematodes, *daf-16*, *daf-18*, *pdk-1*, *akt-2*, *sgk-1*, *smk-1*, *hcf-1*, *aak-2*, *unc-51*, *daf-15*, *raga-1*, *rheb-1*, *pha-4*, *daf-9*, *daf-12*, and *kri-1* were possible targeted genes for dysregulated miRNAs in GO-exposed nematodes [93], and meanwhile these genes are involved in the molecular control of longevity [30].

Moreover, based on the quantitative analysis, it was found that the expression patterns of *daf-16*, *daf-18*, *pdk-1*, *sgk-1*, *smk-1*, *daf-15*, and *kri-1* could be significantly altered in nematodes exposed to GO (10 mg/L) (Fig. 2.7) [93]. After GO (10 mg/L) exposure, transcriptional expressions of *pdk-1* and *daf-15* were significantly increased; however, transcriptional expressions of *daf-16*, *daf-18*, *sgk-1*, *smk-1*, and *kri-1* were significantly decreased (Fig. 2.7) [93]. In *C. elegans*, *daf-16*, *daf-18*, *pdk-1*, and *sgk-1* encode the insulin/IGF signaling pathway, *smk-1* encodes a DAF-16 transcriptional coregulator, *daf-15* encodes a component of TOR signaling pathway, and *kri-1* encodes a component of germline signaling pathway [30]. Therefore, a hypothesis was raised that the GO may reduce the lifespan through influencing the functions of insulin/IGF signaling, TOR signaling, and germline signaling pathways controlled by a limited number of miRNAs in nematodes.

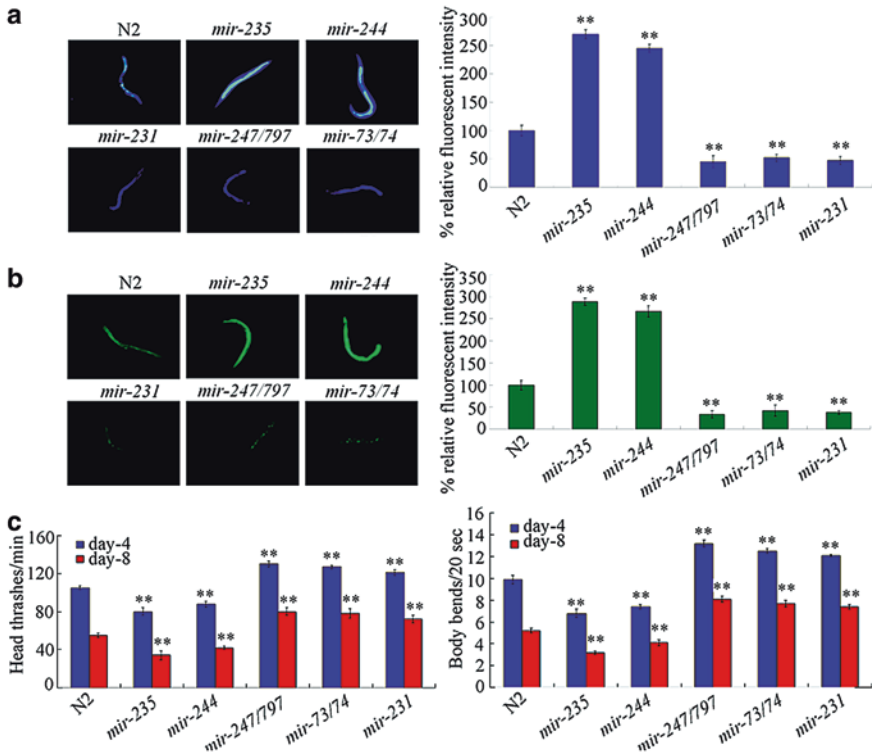
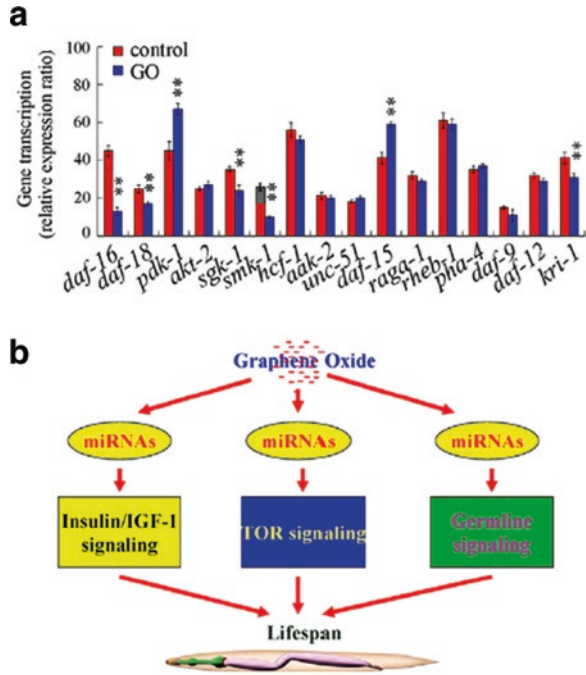


Fig. 2.6 Aging-related properties in mutants for some dysregulated miRNAs exposed to GO [93]. (a) Intestinal autofluorescence at day 10 in wild type and mutants of some dysregulated miRNAs exposed to GO. Fifty nematodes were examined per treatment. (b) Intestinal ROS productions at day 10 in wild type and mutants of some dysregulated miRNAs exposed to GO. Fifty nematodes were examined per treatment. (c) Locomotion behaviors in wild type and mutants of some dysregulated miRNAs exposed to GO. Thirty nematodes were examined per treatment. Exposure concentration was 10 mg/L. Bars represent mean \pm S.E.M. ** $P < 0.01$

2.4 Innate Immune Response Is Involved in the Regulation of Longevity Reduction in Nematodes Exposed to Environmental Toxicants or Stresses

In nematodes, the effects of chronic exposure to GO on different aspects have also been examined. Chronic exposure to GO (1 mg/L) from L1-larvae to adult day 8 induced the death of nematodes (Fig. 2.8) [95], implying the formation of lifespan reduction in GO-exposed nematodes. Moreover, although exposure to GO at the concentration of 0.001 mg/L from L1-larvae to adult day 8 could not affect the functions of both primary and secondary targeted organs, exposure to GO at concentrations of 0.01–1 mg/L from L1-larvae to adult day 8 significantly decreased the locomotion behavior and induced both the intestinal autofluorescence and the

Fig. 2.7 Expression of possible targeted genes for dysregulated miRNAs in GO-exposed nematodes [93]. **(a)** Expression patterns of targeted genes for dysregulated miRNAs in GO-exposed nematodes. Exposure concentration was 10 mg/L. Bars represent means \pm S.E.M. $**P < 0.01$. **(b)** Model for miRNAs in regulating the GO-induced lifespan reduction in nematodes. miRNAs could regulate the GO-induced lifespan reduction through influencing the insulin/insulin-like growth factor (IGF), target of rapamycin (TOR), and germline signaling pathways in nematodes



intestinal ROS production (Fig. 2.8) [95]. These results also suggest that exposure to GO from L1-larvae to adult day 8 may potentially result in the more severe toxicity on the functions of both primary and secondary targeted organs than exposure to GO from adult day 1 to adult day 8 in nematodes [95].

In *C. elegans*, the animals can survive with *E. coli* OP50 as their food source. With an increase of GO exposure duration, a severe accumulation of OP50 in the intestine was observed in nematodes at least after adult day 4 (Fig. 2.9) [95], suggesting that chronic GO exposure can induce the OP50 proliferation in the intestine of nematodes. In contrast, in day 8 adults, only a moderate accumulation of OP50 could be observed in control nematodes (Fig. 2.9) [95]. Moreover, in the day 8 adults, an obvious colocalization of GO with OP50 was observed in GO-exposed nematodes (Fig. 2.9) [95]. In the day 6 adults, this colocalization of GO with OP50 was mainly observed in the anterior region of the intestine, and the accumulation of both GO and OP50 in the tail region was seldom observed (Fig. 2.9) [95]. In the day 8 adults, this colocalization of GO with OP50 could be further formed at both the anterior region and the posterior region (Fig. 2.9) [95]. Especially, in the day 8 adults, this colocalization of GO with OP50 could be observed at the region of the defecation structure in the tail (Fig. 2.9) [95], implying the possible disrupted defecation behavior in nematodes.

In *C. elegans*, innate immune response serves as the first line of defense for animals against the infection from pathogens, including the pathogenic microbial food OP50 [96]. To further understand the results from the severe accumulation of

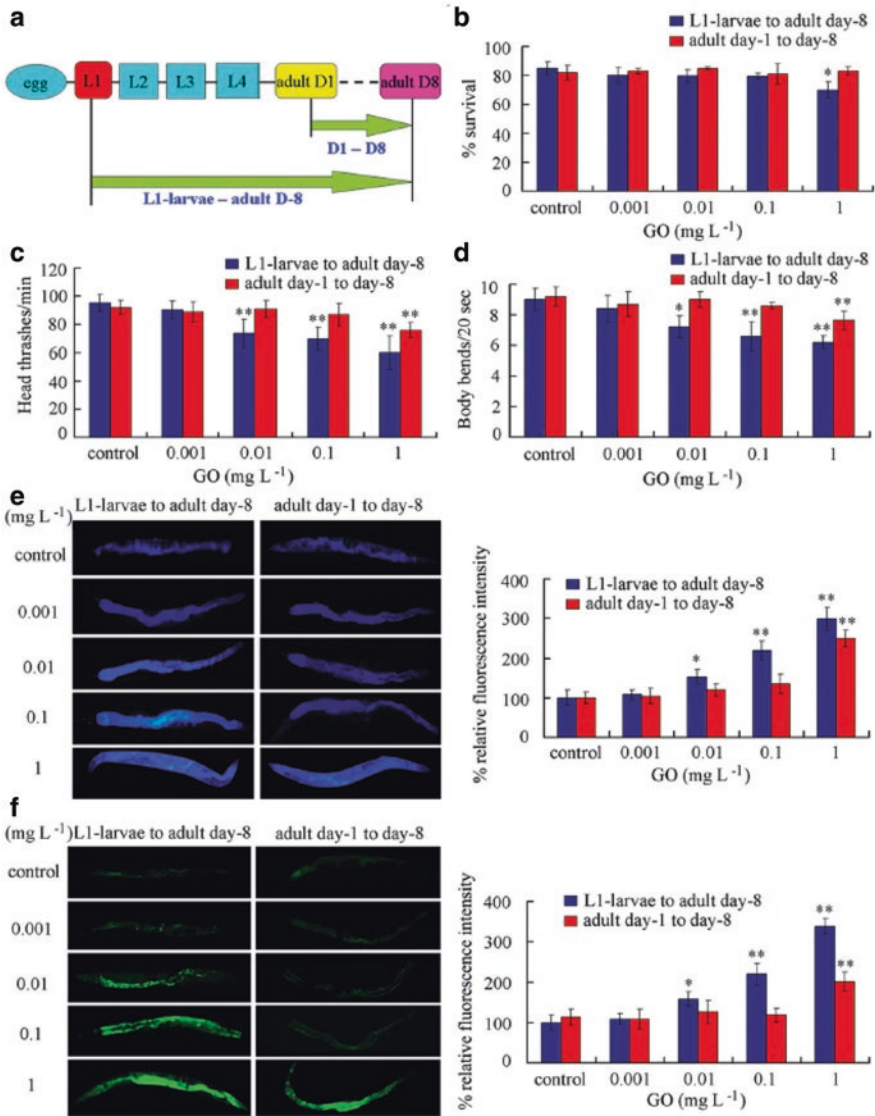


Fig. 2.8 Chronic toxicity assessment of GO using two different assay systems [95]. (a) Diagram of two assay systems for chronic GO exposure. (b) Effects of chronic GO exposure on survival of nematodes at the stage of adult day 8. (c) Effects of chronic GO exposure on head thrash. (d) Effects of GO chronic exposure on body bend. (e) Effects of chronic GO exposure on intestinal autofluorescence. (f) Effects of chronic GO exposure on intestinal ROS production. GO exposure was performed from L1-larvae to adult day 8 or from adult day 1 to adult day 8. Bars represent means \pm S.E.M. * $p < 0.05$, ** $p < 0.01$

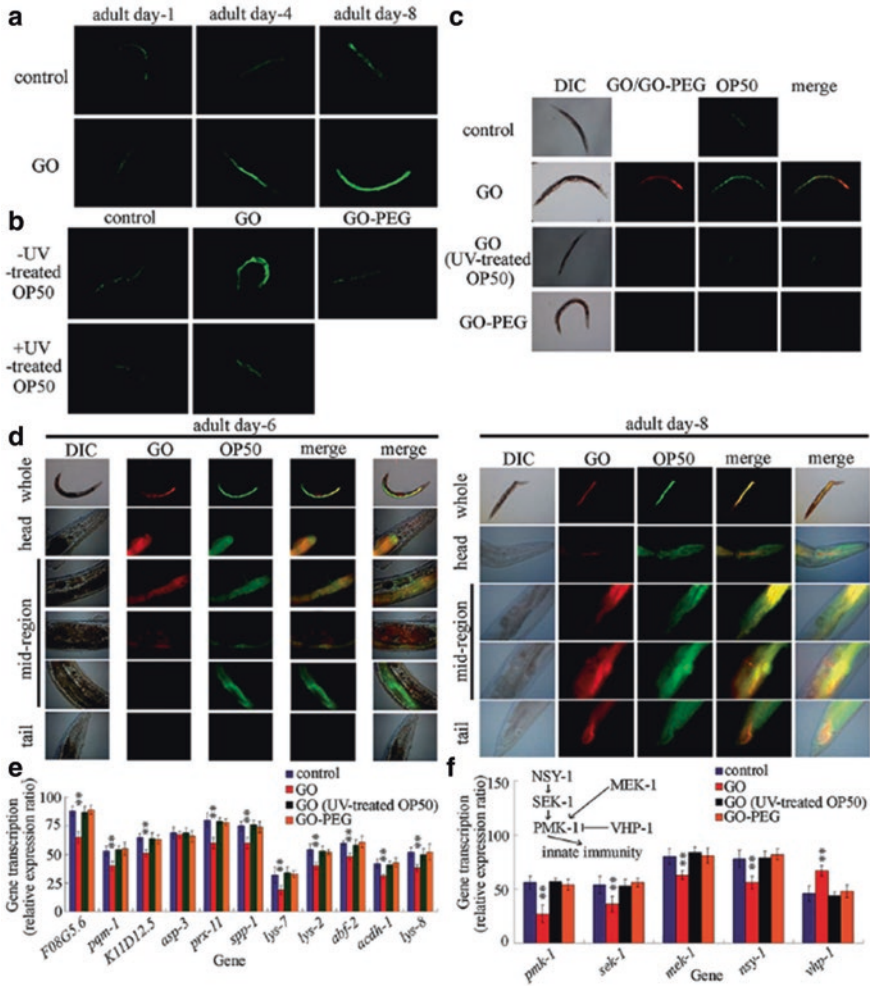


Fig. 2.9 Chronic GO exposure altered the immune response in nematodes [95]. (a) Chronic exposure to GO (1 mg/L) induced the accumulation of OP50 in the intestine. (b) Effects of UV-treated OP50 feeding or PEG surface modification on OP50 accumulation in GO (1 mg/L)-exposed nematodes. (c) Effects of UV-treated OP50 feeding or PEG surface modification on GO distribution and OP50 accumulation in the intestine of nematodes exposed to GO (1 mg/L). (d) Colocalization of GO with OP50 in GO (1 mg/L)-exposed nematodes at adult day 6 or day 8. (e) Quantitative real-time polymerase chain reaction assay showing effects of UV-treated OP50 feeding or PEG surface modification on expression patterns of genes encoding antimicrobial peptides in GO (1 mg/L)-exposed nematodes at adult day 8. (f) Quantitative real-time polymerase chain reaction assay showing effects of UV-killed OP50 feeding or PEG surface modification on expression patterns of genes encoding the p38 MAPK signaling pathway in GO (1 mg/L)-exposed nematodes at adult day 8. GO exposure at a concentration of 1 mg/L was performed from L1-larvae to adult day 8. Bars represent means \pm S.E.M. ** $p < 0.01$

OP50 in the intestine, the possible involvement of innate immunity in the control of chronic GO toxicity was further analyzed. In nematodes, *F08G5.6*, *pqm-1*, *K11D12.5*, *asp-3*, *prx-11*, *spp-1*, *lys-7*, *lys-2*, *abf-2*, *acd-1*, and *lys-8* encode antimicrobial proteins [97, 98]. Chronic GO exposure could induce a significant decrease in the transcriptional expressions of *F08G5.6*, *pqm-1*, *K11D12.5*, *prx-11*, *spp-1*, *lys-7*, *lys-2*, *abf-2*, *acd-1*, and *lys-8* (Fig. 2.9) [95]. *nlp-29* encodes another antimicrobial peptide in nematodes. The expression of *Pnlp-29::GFP* also exhibited a similar pattern in the transgenic nematodes after chronic exposure to GO [95].

In *C. elegans*, p38 MAP kinase (MAPK) pathway is one of the key signaling pathways required for the control of innate immune response to pathogen infection [97, 98]. It was further observed that chronic exposure to GO could significantly decrease the transcriptional expressions of *nsy-1*, *sek-1*, *pmk-1*, and *mek-1* and increase the transcriptional expression of *vhp-1* in the p38 MAPK signaling pathway (Fig. 2.9) [95]. Together, the innate immune response may be suppressed by chronic exposure to GO through inducing the severe accumulation of OP50 in the intestine of nematodes. That is, the suppression in certain protective response(s) may contribute greatly to the lifespan reduction in nematodes exposed to environmental toxicants or stresses.

2.5 Genetic Identification of Genes and Signaling Cascade in the Regulation of Toxicity on Lifespan by Environmental Toxicants or Stresses

Ultraviolet (UV) light is a ubiquitous environmental stress with the potential induction of DNA damage and deleterious somatic mutations by inducing pyrimidine dimers [99, 100]. UV irradiation also potentially caused the alterations in various cellular components through formation of free radicals [99, 100].

In *C. elegans*, the Age mutants were employed to test their possible involvement in the control of resistance to UV light (Uvr). It has been shown that the *age-1* (*hx546*) survived significantly longer than wild type after UV irradiation (Fig. 2.10) [101]. The mean lifespan of the other possible allele, *age-1*(*hx542*), was also longer than wild type after UV irradiation (Fig. 2.10) [101]. Meanwhile, all other Age mutants, *daf-2*, *daf-23*, *daf-28*, *spe-26*, and *clk-1*, were also UV resistant (Fig. 2.10) [101]. In contrast, in the TGF- β signaling pathway, the *daf-7* mutant was indistinguishable from wild type for UV resistance, and *daf-4* mutant was more sensitive than wild type [101].

Some evidence was further raised to prove the role of *daf-16* mutation in suppressing the resistance of Age mutant to UV irradiation. The increased UV resistance of all the recessive mutants (*age-1*, *daf-2*, *daf-23*, *spe-26*, and *clk-1*) was obviously suppressed by *daf-16* mutation (Fig. 2.11) [101]. Based on the observation above, a genetic pathway model for Age genes in the regulation of the resistance to UV irradiation and the dauer formation was provided in Fig. 2.12.

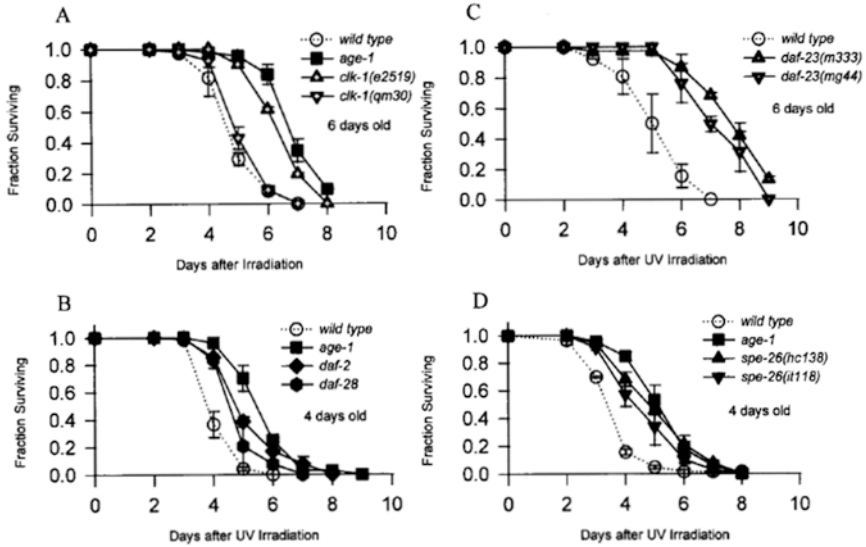


Fig. 2.10 Increased UV resistance of Age mutants in one experiment after UV irradiation [101]. Survival of the Age strains was significantly longer than wild type, N2 ($p < 0.0001$). The Uvr of the non-Age mutant, *clk-1(qm30)*, was not increased. (a) Survival of *age-1(hx546)*, *clk-1(e2519)*, and *clk-1(qm30)*. (b) Survival of *age-1(hx546)*, *daf2(e1370)*, and *daf28(sa191)*. (c) Survival of *daf23(m333)* and *daf23(mg44)*. (d) Survival of *age-1(hx546)* and the *hc138* and *it118* alleles of *spe-26*

Mean life span of various mutants and combinations

Expt	Genotype	Mean life span (days)	Ratio vs. wt*	Maximum life span (days)*	N	P vs. wt†
1	wild type	19.8 ± 4.5		26, 33	50	
	<i>daf-16(m26)</i>	19.7 ± 3.1	0.99	26, 26	59	0.678
	<i>age-1(hx546) fer-15(b26)</i>	38.3 ± 9.5	1.93	57, 57	39	<0.0001
	<i>age-1(hx546) fer-15(b26); daf-16(m26)</i>	23.0 ± 4.4	1.16	33, 33	71	<0.0001 ^d
2	wild type	21.2 ± 8.9		37, 37	53	
	<i>daf-16(m26)</i>	20.3 ± 8.0	0.95	40, 40	54	0.536
	<i>age-1(hx546)</i>	30.2 ± 11.8	1.42	50, 56	49	<0.001
	<i>age-1(hx546); daf-16(m26)</i>	20.7 ± 8.0	0.97	28, 37	41	0.652
3	wild type	19.3 ± 6.4		28, 31	47	
	<i>daf-16(m26)</i>	18.9 ± 5.9	0.98	28, 31	60	0.473
	<i>spe-26(hc138)</i>	28.0 ± 6.9	1.45	38, 38	33	<0.0001
	<i>spe-26(hc138); daf-16(m26)</i>	19.9 ± 4.6	1.03	25, 31	41	0.675
4	wild type	19.8 ± 5.0		24, 27	36	
	<i>daf-16(m26)</i>	19.2 ± 4.8	0.97	24, 24	31	0.583
	<i>daf-16(m27)</i>	20.7 ± 3.4	1.05	24, 27	36	0.705
	<i>age-1(hx542) fer-15(b26)</i>	42.0 ± 7.9	2.12	45, 45	37	<0.0001
	<i>clk-1(e2519)</i>	33.6 ± 13.0	1.70	40, 40	24	<0.001
	<i>spe-26(it118)</i>	28.9 ± 12.7	1.46	40, 40	45	0.005
	<i>age-1(hx542) fer-15(b26); daf-16(m27)</i>	22.1 ± 4.6	1.12	27, 27	43	0.019
	<i>clk-1(e2519); daf-16(m26)</i>	21.4 ± 5.2	1.08	30, 30	46	0.047
	<i>clk-1(e2519); daf-16(m27)</i>	20.7 ± 5.6	1.05	27, 30	51	0.338
	<i>spe-26(it118); daf-16(m27)</i>	16.7 ± 5.0	0.84	24, 24	39	0.008

Fig. 2.11 Mean lifespan of various mutants and combination [101]. *Daf-16* mutants represses UV resistance and life extension

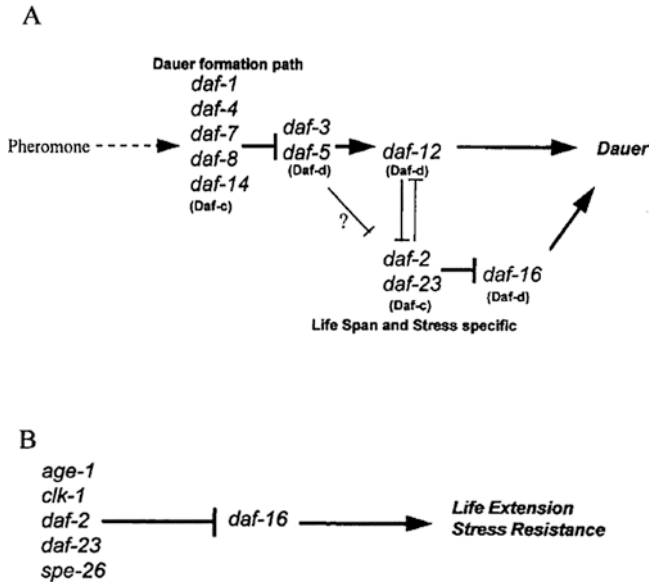


Fig. 2.12 A genetic pathway model for Age genes in the regulation of resistance to UV irradiation [101]. (a) A partial genetic pathway for dauer formation. (b) A genetic pathway for the resistance to UV irradiation

2.6 Environmental Toxicants or Stresses Reduce Lifespan by Affecting Signaling Pathways Associated with the Stress Response

In nematodes, p38 MAPK signaling pathway is at least required for the control of pathogen response and stress response [102, 103]. In the p38 MAPK signaling pathway, the core signaling pathway contains components of *pmk-1* encoded MAPK, *sek-1* encoded MAPK kinase (MAPKK), and *nsy-1* encoded MAPK kinase kinase (MAPKKK). We here selected the p38 MAPK signaling pathway to explain the important role of signaling pathways associated with the stress response in the regulation of toxicity from certain environmental toxicants or stresses in reducing the lifespan in nematodes.

In nematodes, after prolonged exposure, GO (100 mg/L) could significantly increase the transcriptional expression of *pmk-1*, *sek-1*, and *nsy-1* (Fig. 2.13) [104]. PMK-1/MAPK is predominantly expressed in the intestine. Moreover, exposure to GO (100 mg/L) could significantly increase the PMK-1::GFP expression in the intestine and the percentage of PMK-1::GFP nucleus localization in intestinal cells (Fig. 2.13) [104]. Activation of the p38 MAPK signaling pathway requires the phosphorylation of p38 MAPK/PMK-1. Exposure to GO (100 mg/L) obviously increased the expression of phosphorylated PMK-1 compared with control (Fig. 2.13) [104].

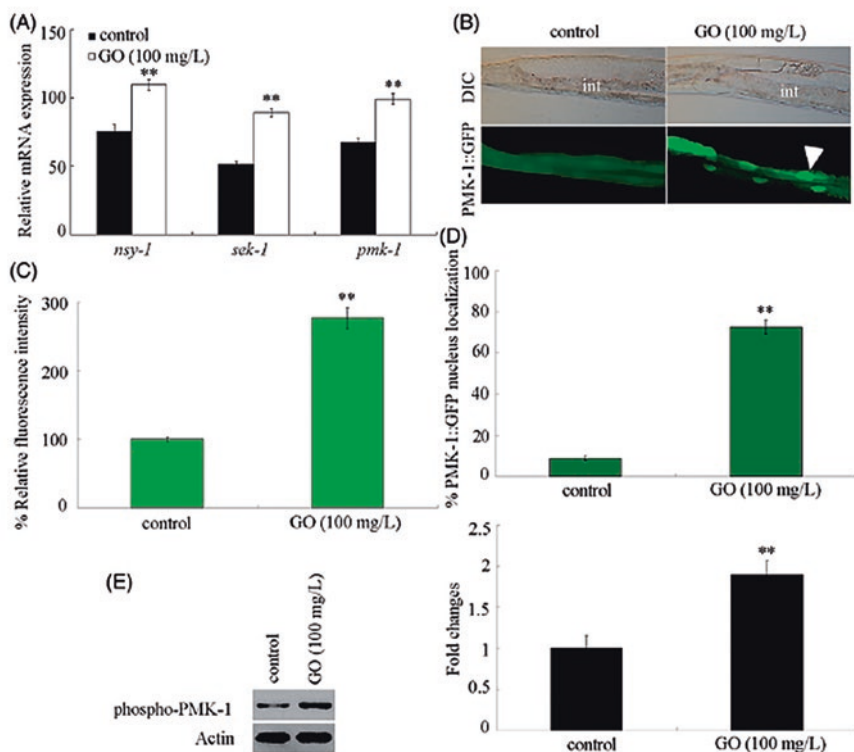


Fig. 2.13 Effects of GO exposure on expression pattern of genes encoding p38 MAPK signaling pathway in wild-type nematodes [104]. (a) GO exposure altered the transcriptional expression of genes encoding p38 MAPK signaling pathway. (b) GO exposure affected PMK-1::GFP expression in the intestine. int, intestine. Arrowhead indicates the localization of PMK-1::GFP in nucleus of intestinal cells. (c) Comparison of relative fluorescence intensity of PMK-1::GFP in the intestine. (d) GO exposure influenced nucleus translocation of PMK-1::GFP. (e) Western blotting analysis of the effect of GO exposure on expression level of phosphorylated PMK-1. Actin protein was used as the loading control. Prolonged exposure was performed from L1-larvae to young adults. Bars represent means \pm SEM. ** $p < 0.01$ vs control

More importantly, it has been recently observed that chronic exposure to GO (10 mg/L) from L1-larvae to adult day 8 could further significantly decrease the transcriptional expression of *pmk-1*, *sek-1*, and *nsy-1* (Shao and Wang, unpublished data). Therefore, GO exposure can potentially dysregulate the expression of p38 MAPK signaling pathway in nematodes.

To confirm the function of genes encoding the core p38 MAPK signaling pathway in the regulation of GO toxicity, the GO toxicity in mutants for genes encoding the core p38 MAPK signaling pathway was investigated. *pmk-1(km25)*, *sek-1(ag1)*, and *nsy-1(ag3)* mutants have the normal lifespan (Fig. 2.14) [104]. It was observed that, after prolonged exposure, GO (100 mg/L) exposure induced the more reduced

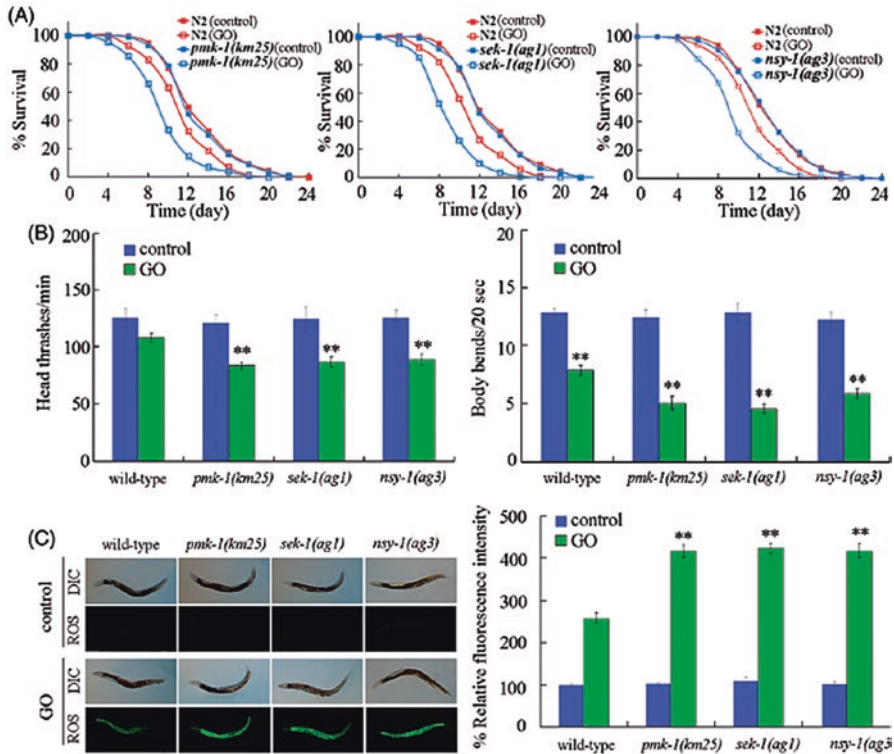


Fig. 2.14 Toxicity assessment of GO exposure on mutants of genes encoding p38 MAPK signaling pathway [104]. (a) Toxicity assessment of GO exposure on lifespan of mutants of genes encoding p38 MAPK signaling pathway. (b) Toxicity assessment of GO exposure on locomotion behavior of mutants of genes encoding p38 MAPK signaling pathway. Locomotion behavior was assessed by the endpoints of head thrash and body bend. (c) Toxicity assessment of GO exposure in inducing ROS production in mutants of genes encoding p38 MAPK signaling pathway. Prolonged exposure was performed from L1-larvae to young adults. GO exposure concentration was 100 mg/L. Bars represent means \pm SEM. ** $p < 0.01$ vs wild type

lifespan in *pmk-1(km25)*, *sek-1(ag1)*, or *nsy-1(ag3)* mutant than that in wild-type N2 nematodes (Fig. 2.14) [104]. Similarly, GO exposure at the concentration of 1 or 100 mg/L also resulted in the more decreased locomotion behavior in *pmk-1(km25)*, *sek-1(ag1)*, or *nsy-1(ag3)* mutant than that in wild-type N2 nematodes (Fig. 2.14) [104]. Additionally, GO (100 mg/L) exposure also induced a more significant induction of intestinal ROS production in *pmk-1(km25)*, *sek-1(ag1)*, or *nsy-1(ag3)* mutant than that in wild-type N2 nematodes (Fig. 2.14) [104]. Therefore, mutations of genes encoding core p38 MAPK signaling pathway may induce a susceptibility to GO toxicity, including the lifespan reduction.

As indicated above, prolonged exposure to GO (100 mg/L) could significantly increase the expression of *isp-1* and decrease the expression of *gas-1* in nematodes [94]. Moreover, after GO (100 mg/L) exposure, it was found that mutation of *pmk-1*,

sek-1, or *nsy-1* could more severely increase the expression of *isp-1* and decrease the expression of *gas-1* compared with those in wild-type nematodes [104]. These results imply that certain environmental toxicants or stresses may reduce the lifespan by affecting signaling pathways associated with stress response to dysregulate the mitochondrial respiration signaling.

2.7 Perspectives

In this chapter, we focused on the toxicity assessment endpoint of lifespan to discuss the potential basic principle for the toxicity induction on different endpoints in nematodes exposed to certain environmental toxicants or stresses. One of the important principles is that exposure to the environmental toxicants or stresses can reduce the lifespan by altering molecular basis for longevity. Another important principle is that exposure to the environmental toxicants or stresses may reduce the lifespan by suppressing protective response(s), such as the innate immune response. Besides these, exposure to the environmental toxicants or stresses can also reduce the lifespan by affecting signaling pathways associated with the stress response, such as the p38 MAPK signaling pathway, which can further dysregulate at least the mitochondrial respiration signaling. Nevertheless, with the concern on different toxicity assessment endpoints, the detailed principles may be somewhat or very different. Thus, more efforts are still needed to elucidate the detailed underlying molecular mechanisms for toxicity on other aspects in nematodes.

References

1. Zhao Y-L, Yang J-N, Wang D-Y (2016) A microRNA-mediated insulin signalling pathway regulates the toxicity of multi-walled carbon nanotubes in nematode *Caenorhabditis elegans*. *Sci Rep* 6:23234
2. Wu Q-L, Zhi L-T, Qu Y-Y, Wang D-Y (2016) Quantum dots increased fat storage in intestine of *Caenorhabditis elegans* by influencing molecular basis for fatty acid metabolism. *Nanomedicine* 12:1175–1184
3. Zhi L-T, Fu W, Wang X, Wang D-Y (2016) ACS-22, a protein homologous to mammalian fatty acid transport protein 4, is essential for the control of toxicity and translocation of multi-walled carbon nanotubes in *Caenorhabditis elegans*. *RSC Adv* 6:4151–4159
4. Shakoor S, Sun L-M, Wang D-Y (2016) Multi-walled carbon nanotubes enhanced fungal colonization and suppressed innate immune response to fungal infection in nematodes. *Toxicol Res* 5:492–499
5. Yang R-L, Rui Q, Kong L, Zhang N, Li Y, Wang X-Y, Tao J, Tian P-Y, Ma Y, Wei J-R, Li G-J, Wang D-Y (2016) Metallothioneins act downstream of insulin signaling to regulate toxicity of outdoor fine particulate matter (PM_{2.5}) during Spring Festival in Beijing in nematode *Caenorhabditis elegans*. *Toxicol Res* 5:1097–1105
6. Wu Q-L, Han X-X, Wang D, Zhao F, Wang D-Y (2017) Coal combustion related fine particulate matter (PM_{2.5}) induces toxicity in *Caenorhabditis elegans* by dysregulating microRNA expression. *Toxicol Res* 6:432–441

7. Zhi L-T, Ren M-X, Qu M, Zhang H-Y, Wang D-Y (2016) Wnt ligands differentially regulate toxicity and translocation of graphene oxide through different mechanisms in *Caenorhabditis elegans*. *Sci Rep* 6:39261
8. Zhao L, Rui Q, Wang D-Y (2017) Molecular basis for oxidative stress induced by simulated microgravity in nematode *Caenorhabditis elegans*. *Sci Total Environ* 607–608:1381–1390
9. Zhao L, Qu M, Wong G, Wang D-Y (2017) Transgenerational toxicity of nanopolystyrene particles in the range of $\mu\text{g/L}$ in nematode *Caenorhabditis elegans*. *Environ Sci Nano* 4:2356–2366
10. Xiao G-S, Zhao L, Huang Q, Yang J-N, Du H-H, Guo D-Q, Xia M-X, Li G-M, Chen Z-X, Wang D-Y (2018) Toxicity evaluation of Wanzhou watershed of Yangtze Three Gorges Reservoir in the flood season in *Caenorhabditis elegans*. *Sci Rep* 8:6734
11. Chen H, Li H-R, Wang D-Y (2017) Graphene oxide dysregulates Neuroigin/NLG-1-mediated molecular signaling in interneurons in *Caenorhabditis elegans*. *Sci Rep* 7:41655
12. Qu M, Xu K-N, Li Y-H, Wong G, Wang D-Y (2018) Using *acs-22* mutant *Caenorhabditis elegans* to detect the toxicity of nanopolystyrene particles. *Sci Total Environ* 643:119–126
13. Dong S-S, Qu M, Rui Q, Wang D-Y (2018) Combinational effect of titanium dioxide nanoparticles and nanopolystyrene particles at environmentally relevant concentrations on nematodes *Caenorhabditis elegans*. *Ecotoxicol Environ Saf* 161:444–450
14. Zhao L, Kong J-T, Krasteva N, Wang D-Y (2018) Deficit in epidermal barrier induces toxicity and translocation of PEG modified graphene oxide in nematodes. *Toxicol Res* 7(6):1061–1070. <https://doi.org/10.1039/C8TX00136G>
15. Ding X-C, Wang J, Rui Q, Wang D-Y (2018) Long-term exposure to thiolated graphene oxide in the range of $\mu\text{g/L}$ induces toxicity in nematode *Caenorhabditis elegans*. *Sci Total Environ* 616–617:29–37
16. Xiao G-S, Chen H, Krasteva N, Liu Q-Z, Wang D-Y (2018) Identification of interneurons required for the aversive response of *Caenorhabditis elegans* to graphene oxide. *J Nanbiotechnol* 16:45
17. Wang D-Y (2018) *Nanotoxicology in Caenorhabditis elegans*. Springer, Singapore
18. Li W-J, Wang D-Y, Wang D-Y (2018) Regulation of the response of *Caenorhabditis elegans* to simulated microgravity by p38 mitogen-activated protein kinase signaling. *Sci Rep* 8:857
19. Yang R-L, Ren M-X, Rui Q, Wang D-Y (2016) A *mir-231*-regulated protection mechanism against the toxicity of graphene oxide in nematode *Caenorhabditis elegans*. *Sci Rep* 6:32214
20. Zhuang Z-H, Li M, Liu H, Luo L-B, Gu W-D, Wu Q-L, Wang D-Y (2016) Function of RSKS-1-AAK-2-DAF-16 signaling cascade in enhancing toxicity of multi-walled carbon nanotubes can be suppressed by *mir-259* activation in *Caenorhabditis elegans*. *Sci Rep* 6:32409
21. Johnson TE, Wood WB (1982) Genetic analysis of life-span in *Caenorhabditis elegans*. *Proc Natl Acad Sci U S A* 79:6603–6607
22. Klass MR (1977) Aging in the nematode *Caenorhabditis elegans*: major biological and environmental factors influencing life span. *Mech Ageing Dev* 6:413–429
23. Klass MR (1983) A method for the isolation of longevity mutants in the nematode *Caenorhabditis elegans* and initial results. *Mech Ageing Dev* 22:279–286
24. Kapahi P, kaeberlein M, Hansen M (2017) Dietary restriction and lifespan: lessons from invertebrate models. *Ageing Res Rev* 39:3–14
25. Smith-Vikos T, Slack FJ (2012) MicroRNAs and their roles in aging. *J Cell Sci* 125:7–17
26. Martins R, Lithgow GJ, Link W (2016) Long live FOXO: unraveling the role of FOXO proteins in aging and longevity. *Ageing Cell* 15:196–207
27. Hekimi A, Guarente L (2003) Genetics and the specificity of the aging process. *Science* 299:1351–1354
28. Pan H, Finkel T (2017) Key proteins and pathways that regulate lifespan. *J Biol Chem* 292:6452–6460
29. Kenyon CJ (2010) The genetics of ageing. *Nature* 464:504–512
30. Lapierre LR, Hansen M (2012) Lessons from *C. elegans*: signaling pathways for longevity. *Trends Endocrinol Metab* 23:637–644

31. Kimura KD, Tissenbaum HA, Liu Y, Ruvkun G (1997) *daf-2*, an insulin receptor-like gene that regulates longevity and diapause in *Caenorhabditis elegans*. *Science* 277:942–946
32. Morris JZ, Tissenbaum HA, Ruvkun G (1996) A phosphatidylinositol-3-OH kinase family member regulating longevity and diapause in *Caenorhabditis elegans*. *Nature* 382:536–539
33. Hertweck M, Gobel C, Baumeister R (2004) *C. elegans* SGK-1 is the critical component in the Akt/PKB kinase complex to control stress response and life span. *Dev Cell* 6:577–588
34. Paradis S, Ruvkun G (1998) *Caenorhabditis elegans* Akt/PKB transduces insulin receptor-like signals from AGE-1 PI3 kinase to the DAF-16 transcription factor. *Genes Dev* 12:2488–2498
35. Paradis S, Ailion M, Toker A, Thomas JH, Ruvkun G (1999) A PDK1 homolog is necessary and sufficient to transduce AGE-1 PI3 kinase signals that regulate diapause in *Caenorhabditis elegans*. *Genes Dev* 13:1438–1452
36. Henderson ST, Johnson TE (2001) *daf-16* integrates developmental and environmental inputs to mediate aging in the nematode *Caenorhabditis elegans*. *Curr Biol* 11:1975–1980
37. Lee RY, Hench J, Ruvkun G (2001) Regulation of *C. elegans* DAF-16 and its human ortholog FKHRL1 by the *daf-2* insulin-like signaling pathway. *Curr Biol* 11:1950–1957
38. Lin K, Hsin H, Libina N, Kenyon C (2001) Regulation of the *Caenorhabditis elegans* longevity protein DAF-16 by insulin/IGF-1 and germline signaling. *Nat Genet* 28:139–145
39. Lin K, Dorman JB, Rodan A, Kenyon C (1997) *daf-16*: an HNF-3/forkhead family member that can function to double the life-span of *Caenorhabditis elegans*. *Science* 278:1319–1322
40. Ogg S, Paradis S, Gottlieb S, Patterson GI, Lee L, Tissenbaum HA, Ruvkun G (1997) The Fork head transcription factor DAF-16 transduces insulin-like metabolic and longevity signals in *C. elegans*. *Nature* 389:994–999
41. Dorman JB, Albinder B, Shroyer T, Kenyon C (1995) The *age-1* and *daf-2* genes function in a common pathway to control the lifespan of *Caenorhabditis elegans*. *Genetics* 141:1399–1406
42. Zhao Y-L, Yang R-L, Rui Q, Wang D-Y (2016) Intestinal insulin signaling encodes two different molecular mechanisms for the shortened longevity induced by graphene oxide in *Caenorhabditis elegans*. *Sci Rep* 6:24024
43. Boehm M, Slack F (2005) A developmental timing microRNA and its target regulate life span in *C. elegans*. *Science* 310:1954–1957
44. Hsu AL, Murphy CT, Kenyon C (2003) Regulation of aging and age-related disease by DAF-16 and heat-shock factor. *Science* 300:1142–1145
45. Tissenbaum HA, Guarente L (2001) Increased dosage of a *sir-2* gene extends lifespan in *Caenorhabditis elegans*. *Nature* 410:227–230
46. Wolff S, Ma H, Burch D, Maciel GA, Hunter T, Dillin A (2006) SMK-1, an essential regulator of DAF-16-mediated longevity. *Cell* 124:1039–1053
47. Shore DE, Ruvkun G (2013) A cytoprotective perspective on longevity regulation. *Trends Cell Biol* 23:409–420
48. Honda Y, Honda S (1999) The *daf-2* gene network for longevity regulates oxidative stress resistance and Mn-superoxide dismutase gene expression in *Caenorhabditis elegans*. *FASEB J* 13:1385–1478
49. Cherkasova V, Ayyadevara S, Egilmez N, Shmookler Reis R (2000) Diverse *Caenorhabditis elegans* genes that are upregulated in dauer larvae also show elevated transcript levels in long-lived, aged, or starved adults. *J Mol Biol* 300:433–481
50. Yu H, Larsen P (2001) DAF-16-dependent and independent expression targets of DAF-2 insulin receptor-like pathway in *Caenorhabditis elegans* include FKBP. *J Mol Biol* 314:1017–1045
51. Halaschek-Wiener J, Khattri JS, McKay S, Pouzyrev A, Stott JM, Yang GS, Holt RA, Jones SJ, Marra MA, Brooks-Wilson AR, Riddle DL (2005) Analysis of long-lived *C. elegans* *daf-2* mutants using serial analysis of gene expression. *Genome Res* 15:603–615
52. Murphy C, McCarroll SA, Bargmann CI, Fraser A, Kamath RS, Ahringer J, Li H, Kenyon C (2003) Genes that act downstream of DAF-16 to influence the lifespan of *Caenorhabditis elegans*. *Nature* 424:277–360

53. Lakowski B, Hekimi S (1998) The genetics of caloric restriction in *Caenorhabditis elegans*. Proc Natl Acad Sci U S A 95:13091–13096
54. Jia K, Chen D, Riddle DL (2004) The TOR pathway interacts with the insulin signaling pathway to regulate *C. elegans* larval development, metabolism and life span. Development 131:3897–3906
55. Vellai T, Takacs-Vellai K, Zhang Y, Kovacs AL, Orosz L, Muller F (2003) Genetics: influence of TOR kinase on lifespan in *C. elegans*. Nature 426:620
56. Gelino S, Chang JT, Kumsta C, She X, Davis A, Nguyen C, Panowski S, Hansen M (2016) Intestinal autophagy improves healthspan and longevity in *C. elegans* during dietary restriction. PLoS Genet 12:e1006135
57. Toth ML, Sigmond T, Borsos E, Barna J, Erdelyi P, Takacs-Vellai K, Orosz L, Kovacs AL, Csikos G, Sass M, Vellai T (2008) Longevity pathways converge on autophagy genes to regulate life span in *Caenorhabditis elegans*. Autophagy 4:330–338
58. Jia K, Levine B (2007) Autophagy is required for dietary restriction-mediated lifespan extension in *C. elegans*. Autophagy 3:597–599
59. Hansen M, Chandra A, Mitic LL, Onken B, Driscoll M, Kenyon C (2008) A role for autophagy in the extension of lifespan by dietary restriction in *C. elegans*. PLoS Genet 4:e24
60. Heestand BN, Shen Y, Liu W, Magner DB, Storm N, Meharg C, Habermann B, Antebi A (2013) Dietary restriction induced longevity is mediated by nuclear receptor NHR-62 in *Caenorhabditis elegans*. PLoS Genet 9:e1003651
61. Lapierre LR, De Magalhaes Filho CD, McQuary PR, Chu CC, Visvikis O, Chang JT, Gelino S, Ong B, Davis AE, Irazoqui JE, Dillin A, Hansen M (2013) The TFEB orthologue HLH-30 regulates autophagy and modulates longevity in *Caenorhabditis elegans*. Nat Commun 4:2267
62. Dillin A, Hsu AL, Arantes-Oliveira N, Lehrer-Graiwer J, Hsin H, Fraser AG, Kamath RS, Ahringer J, Kenyon C (2002) Rates of behavior and aging specified by mitochondrial function during development. Science 298:2398–2401
63. Feng J, Bussiere F, Hekimi S (2001) Mitochondrial electron transport is a key determinant of life span in *Caenorhabditis elegans*. Dev Cell 1:633–644
64. Lee SS, Lee RY, Fraser AG, Kamath RS, Ahringer J, Ruvkun G (2003) A systematic RNAi screen identifies a critical role for mitochondria in *C. elegans* longevity. Nat Genet 33:40–48
65. Hartman PS, Ishii N, Kayser EB, Morgan PG, Sedensky MM (2001) Mitochondrial mutations differentially affect aging, mutability and anesthetic sensitivity in *Caenorhabditis elegans*. Mech Ageing Dev 122:1187–1201
66. Kayser EB, Sedensky MM, Morgan PG (2004) The effects of complex I function and oxidative damage on lifespan and anesthetic sensitivity in *Caenorhabditis elegans*. Mech Ageing Dev 125:455–464
67. Tsang WY, Sayles LC, Grad LI, Pilgrim DB, Lemire BD (2001) Mitochondrial respiratory chain deficiency in *Caenorhabditis elegans* results in developmental arrest and increased life span. J Biol Chem 276:32240–32246
68. Yang W, Hekimi S (2010) Two modes of mitochondrial dysfunction lead independently to lifespan extension in *Caenorhabditis elegans*. Aging Cell 9:433–447
69. Ishii N, Fujii M, Hartman PS, Tsuda M, Yasuda K, Senoo-Matsuda N, Yanase S, Ayusawa D, Suzuki K (1998) A mutation in succinate dehydrogenase cytochrome b causes oxidative stress and ageing in nematodes. Nature 394:694–697
70. Ishii N, Takahashi K, Tomita S, Keino T, Honda S, Yoshino K, Suzuki K (1990) A methyl viologen-sensitive mutant of the nematode *Caenorhabditis elegans*. Mutat Res 237:165–171
71. Hosokawa H, Ishii N, Ishida H, Ichimori K, Nakazawa H, Suzuki K (1994) Rapid accumulation of fluorescent material with aging in an oxygen-sensitive mutant *mev-1* of *Caenorhabditis elegans*. Mech Ageing Dev 74:161–170
72. Senoo-Matsuda N, Yasuda K, Tsuda M, Ohkubo T, Yoshimura S, Nakazawa H, Hartman PS, Ishii N (2001) A defect in the cytochrome b large subunit in complex II causes both superox-

- ide anion overproduction and abnormal energy metabolism in *Caenorhabditis elegans*. *J Biol Chem* 276:41553–41558
73. Hamilton B, Dong Y, Shindo M, Liu W, Odell I, Ruvkun G, Lee SS (2005) A systematic RNAi screen for longevity genes in *C. elegans*. *Genes Dev* 19:1544–1555
 74. Wong A, Boutis P, Hekimi S (1995) Mutations in the *clk-1* gene of *Caenorhabditis elegans* affect developmental and behavioral timing. *Genetics* 139:1247–1259
 75. Van Raamsdonk JM, Hekimi S (2009) Deletion of the mitochondrial superoxide dismutase *sod-2* extends lifespan in *Caenorhabditis elegans*. *PLoS Genet* 5:e1000361
 76. Dancy BM, Sedensky MM, Morgan PG (2014) Effects of the mitochondrial respiratory chain on longevity in *C. elegans*. *Exp Gerontol* 56:245–255
 77. Antebi A (2013) Regulation of longevity by the reproductive system. *Exp Gerontol* 28:596–602
 78. Hsin H, Kenyon C (1999) Signals from the reproductive system regulate the lifespan of *C. elegans*. *Nature* 399:362–366
 79. Goudeau J, Bellemin S, Toselli-Mollereau E, Shamalnasab M, Chen Y, Aguilaniu H (2011) Fatty acid desaturation links germ cell loss to longevity through NHR-80/HNF4 in *C. elegans*. *PLoS Biol* 9:e1000599
 80. Arantes-Oliveira N, Berman JR, Kenyon C (2003) Healthy animals with extreme longevity. *Science* 302:611
 81. Larsen PL, Albert PS, Riddle DL (1995) Genes that regulate both development and longevity in *Caenorhabditis elegans*. *Genetics* 139:1567–1583
 82. Wolff S, Dillin A (2006) The trifecta of aging in *Caenorhabditis elegans*. *Exp Gerontol* 41:894–903
 83. Chan TY (1999) Health hazards due to clenbuterol residues in food. *J Toxicol Clin Toxicol* 37:517–519
 84. Yen M, Ewald MB (2012) Toxicity of weight loss agents. *J Med Toxicol* 8:145–152
 85. Yaeger MJ, Mullin K, Ensley SM, Ware WA, Slavin RE (2012) Myocardial toxicity in a group of greyhounds administered ractopamine. *Vet Pathol* 49:569–573
 86. Zhuang Z, Zhao Y, Wu Q, Li M, Liu H, Sun L, Gao W, Wang D (2014) Adverse effects from clenbuterol and ractopamine on nematode *Caenorhabditis elegans* and the underlying mechanism. *PLoS ONE* 9:e85482
 87. Shi X, Gong H, Li Y, Wang C, Cheng L, Liu Z (2013) Graphene-based magnetic plasmonic nanocomposite for dual imaging and photothermal therapy. *Biomaterials* 34:4786–4793
 88. Park S, Ruoff RS (2009) Chemical methods for the production of graphenes. *Nat Nanotechnol* 4:217–224
 89. Yang K, Li Y, Tan X, Peng R, Liu Z (2013) Behavior and toxicity of graphene and its functionalized derivatives in biological systems. *Small* 9:1492–1503
 90. Ren M-X, Zhao L, Ding X-C, Krasteva N, Rui Q, Wang D-Y (2018) Developmental basis for intestinal barrier against the toxicity of graphene oxide. *Particle Fibre Toxicol* 15:26
 91. Ren M-X, Zhao L, Lv X, Wang D-Y (2017) Antimicrobial proteins in the response to graphene oxide in *Caenorhabditis elegans*. *Nanotoxicology* 11:578–590
 92. Xiao G-S, Zhi L-T, Ding X-C, Rui Q, Wang D-Y (2017) Value of *mir-247* in warning graphene oxide toxicity in nematode *Caenorhabditis elegans*. *RSC Adv* 7:52694–52701
 93. Wu Q-L, Zhao Y-L, Zhao G, Wang D-Y (2014) microRNAs control of in vivo toxicity from graphene oxide in *Caenorhabditis elegans*. *Nanomedicine* 10:1401–1410
 94. Wu Q-L, Yin L, Li X, Tang M, Zhang T, Wang D-Y (2013) Contributions of altered permeability of intestinal barrier and defecation behavior to toxicity formation from graphene oxide in nematode *Caenorhabditis elegans*. *Nanoscale* 5:9934–9943
 95. Wu Q-L, Zhao Y-L, Fang J-P, Wang D-Y (2014) Immune response is required for the control of in vivo translocation and chronic toxicity of graphene oxide. *Nanoscale* 6:5894–5906
 96. Hahm J, Kim S, Paik Y (2011) GPA-9 is a novel regulator of innate immunity against *Escherichia coli* foods in adult *Caenorhabditis elegans*. *Aging Cell* 10:208–219

97. Kawli T, Tan M (2008) Neuroendocrine signals modulate the innate immunity of *Caenorhabditis elegans* through insulin signalling. *Nat Immunol* 9:1415–1424
98. Pukkila-Worley R, Ausubel FM (2012) Immune defense mechanisms in the *Caenorhabditis elegans* intestinal epithelium. *Curr Opin Immunol* 24:3–9
99. Black HS (1987) Potential involvement of free radical reactions in ultraviolet light-mediated cutaneous damage. *Photochem Photobiol* 46:213–221
100. Friedberg EC (1985) DNA repair. W.H. Freeman and Company, New York
101. Murakami S, Johnson TE (1996) A genetic pathway conferring life extension and resistance by UV stress in *Caenorhabditis elegans*. *Genetics* 143:1207–1218
102. Hayakawa T, Kato K, Jayakawa R, Hisamoto N, Katsumoto K, Takeda K, Ichijo H (2011) Regulation of anoxic death in *Caenorhabditis elegans* by mammalian apoptosis signal-regulating kinase (ASK) family proteins. *Genetics* 187:785–792
103. Kim DH, Ausubel FM (2005) Evolutionary perspectives on innate immunity from the study of *Caenorhabditis elegans*. *Curr Opin Immunol* 17:4–10
104. Zhao Y-L, Zhi L-T, Wu Q-L, Yu Y-L, Sun Q-Q, Wang D-Y (2016) p38 MAPK-SKN-1/Nrf signaling cascade is required for intestinal barrier against graphene oxide toxicity in *Caenorhabditis elegans*. *Nanotoxicology* 10:1469–1479

Chapter 3

Roles of Oxidative Stress-Related Molecular Signals in the Regulation of Toxicity of Environmental Toxicants or Stresses



Abstract In organisms, not only oxidative stress can act as a cellular contributor to toxicity induction of environmental toxicants or stress, but also oxidative stress-related molecular signals can further act as important molecular regulators for the toxicity induction of environmental toxicants or stress. We here first introduced the important roles of mitochondrial complex signals in the regulation of toxicity of environmental toxicants or stresses. Moreover, we also introduced the important roles of SOD proteins, CTL proteins, and GST proteins in the regulation of toxicity of environmental toxicants or stresses. The important roles of oxidative stress-related molecular signals in the regulation of toxicity of environmental toxicants or stresses are further discussed.

Keywords Oxidative stress-related molecular signals · Toxicity regulation · Environmental exposure · *Caenorhabditis elegans*

3.1 Introduction

In nematodes, exposure to certain environmental toxicants or stresses can lead to the toxic effects on development, reproduction, neuronal development and function, intestinal development and function, epidermal development, innate immune response, lifespan, and metabolism under normal or certain conditions [1–23]. The toxicity induction on different aspects in nematodes is under the control of different molecular signals or signaling pathways [24]. In Chap. 1, we have introduced the molecular basis for oxidative stress in nematodes exposed to environmental toxicants or stresses. Not only the oxidative stress act as a crucial cellular contributor to toxicity induction of various environmental toxicants or stress, but also the oxidative stress-related molecular signals can further act as important molecular regulators for the toxicity induction of different environmental toxicants or stresses [24–26].

We here first discussed the important roles of mitochondrial complex signals in the regulation of toxicity of environmental toxicants or stresses. Moreover, we further discussed the important roles of SOD proteins, CTL proteins, and GST proteins in the regulation of toxicity of environmental toxicants or stresses. The information

provided in this chapter highlights the importance or possibly the central role of oxidative stress-related molecular signals in the regulation of toxicity of environmental toxicants or stresses in nematodes.

3.2 Roles of Mitochondrial Complex Signals in the Regulation of Toxicity of Environmental Toxicants or Stresses

Here, we will discuss the important roles of molecular signals from mitochondrial complexes I, II, III, and IV in the regulation of toxicity of environmental toxicants or stresses. Besides these, we will also discuss the potential role of CLK-1-mediated coenzyme Q synthesis-related signal in the regulation of toxicity of environmental toxicants or stresses.

3.2.1 Complex I (NADH Ubiquinone Oxidoreductase)

3.2.1.1 GAS-1

3.2.1.1.1 Toxicity Induction of Environmental Toxicants or Stresses May Be Associated with the Decrease in *gas-1* in Nematodes

In nematodes, *gas-1* encodes a 49 kDa subunit of complex I. Both the shortened lifespan and the increased oxidative damage can be observed in *gas-1* mutant nematodes [27, 28].

The thiolated graphene oxide (GO-SH), one of the members of graphene family, can be potentially used in at least drug delivery, biosensor, perovskite solar cells, and 3-D heterostructural assembly [29–32]. In wild-type nematodes, prolonged exposure to GO-SH at concentrations more than 100 µg/L caused the significant decrease in locomotion behavior as indicated by the endpoints of head thrash and body bend and reduction in reproductive capacity as indicated by the endpoint of brood size [33], suggesting that GO-SH at concentrations more than 100 µg/L may potentially induce the toxicity on the functions of both primary and secondary targeted organs in wild-type nematodes. Additionally, prolonged exposure to GO-SH at concentrations more than 100 µg/L could result in the significant induction of intestinal reactive oxygen species (ROS) production in wild-type nematodes [33].

Meanwhile, among the examined genes required for the control of oxidative stress, prolonged exposure to GO-SH (100 µg/L) could alter the expression level of *gas-1*, and the transcriptional expression of *gas-1* was significantly decreased by GO-SH (100 µg/L) [33], which implies that the observed toxicity of GO-SH on wild-type nematodes may be closely associated with the decrease in *gas-1* expression. Moreover, among the examined genes required for the control of oxidative

stress, prolonged exposure to GO-SH (10 mg/L) could further significantly increase the transcriptional expressions of *sod-1*, *sod-2*, *sod-3*, *sod-4*, *clk-1*, and *isp-1* and decrease the transcriptional expression of *gas-1* [33].

3.2.1.1.2 Mutation of *gas-1* Induces a Susceptibility to Toxicity of Environmental Toxicants or Stresses

After prolonged exposure, the toxicity of GO-SH at the concentration of 10 $\mu\text{g/L}$ in decreasing locomotion behavior, in reducing brood size, and in inducing intestinal ROS production was observed in *gas-1* mutant nematodes, although prolonged exposure to GO-SH (10 $\mu\text{g/L}$) could not affect the locomotion behavior and brood size and induce the induction of significant intestinal ROS production in wild-type nematodes (Fig. 3.1) [33]. Moreover, the more severe decrease in locomotion behavior, reduction in brood size, and induction of intestinal ROS production could be detected in GO-SH (100 $\mu\text{g/L}$)-exposed *gas-1* mutant nematodes than those in GO-SH (100 $\mu\text{g/L}$)-exposed wild-type nematodes (Fig. 3.1) [33]. Therefore, mutation of *gas-1* may induce a susceptibility to the toxicity of environmental toxicants or stresses, such as the GO-SH. Similarly, mutation of *gas-1* also increased the sensitivity of nematodes to the volatile anesthetics, such as halothane, and the ethanol [34, 35].

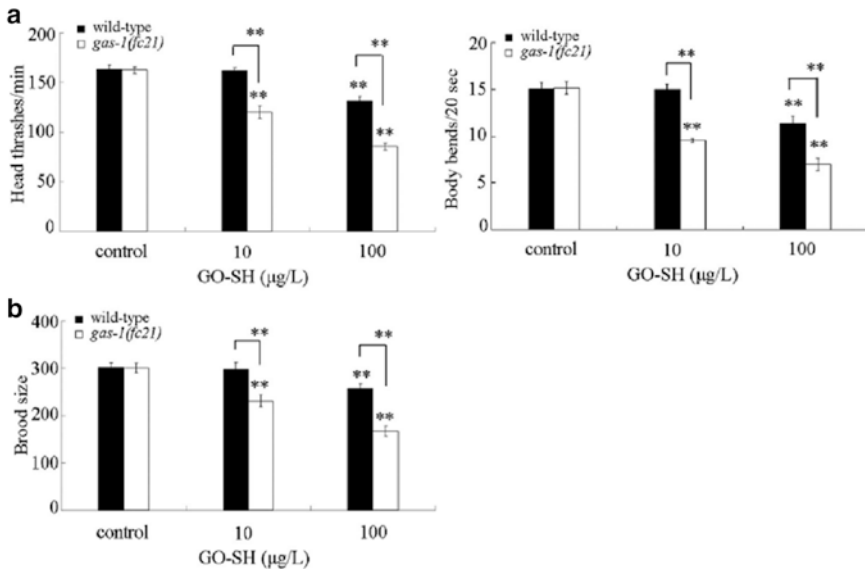


Fig. 3.1 Toxicity assessment of GO-SH in wild-type and *gas-1* mutant nematodes [33]. (a) Toxicity assessment of GO-SH in decreasing locomotion behavior in wild-type and *gas-1* mutant nematodes. (b) Toxicity assessment of GO-SH in reducing brood size in wild-type and *gas-1* mutant nematodes. Prolonged exposure was performed from L1-larvae to adult day 1. Bars represent means \pm SD. ** $P < 0.01$ vs control (if not specially indicated)

3.2.1.1.3 Cellular Basis for the Formation of Susceptibility to Toxicity of Environmental Toxicants or Stresses in *gas-1* Mutant Nematodes

The first cellular contributor for the induction of susceptibility to toxicity of environmental toxicants in *gas-1* mutant is the formation of oxidative damage induced by *gas-1* mutation [34].

Another important cellular contributor for the induction of susceptibility to toxicity of environmental toxicants in *gas-1* mutant is the formation of more severe accumulation of environmental toxicants in the body or the targeted organs in nematodes. After prolonged exposure to GO-SH/Rho B (10 $\mu\text{g/L}$), the severe accumulation of GO-SH/Rho B could be observed in the pharynx, the intestine, and the reproductive organs (such as the spermatheca) in *gas-1* mutant nematodes compared with that in wild-type nematodes (Fig. 3.2) [33]. Additionally, after prolonged exposure to GO-SH/Rho B (100 $\mu\text{g/L}$), the more severe accumulation of GO-SH/Rho B could be further detected in the spermatheca and the embryos in *gas-1* mutant nematodes compared with that in wild-type nematodes (Fig. 3.2) [33].

The third possible cellular contributor for the induction of susceptibility to toxicity of environmental toxicants in *gas-1* mutant is the enhancement in the intestinal permeability. After prolonged exposure to GO-SH (10 or 100 $\mu\text{g/L}$), the enhanced intestinal permeability was observed in *gas-1* mutant nematodes compared with that in wild-type nematodes [33], which implies that mutation of *gas-1* may enhance the intestinal permeability in GO-SH-exposed nematodes.

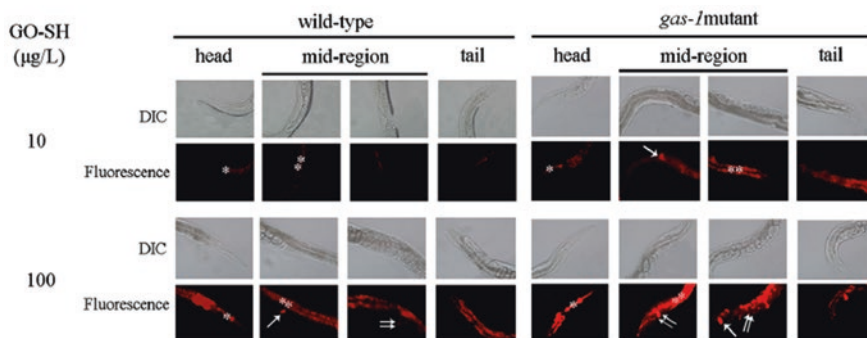


Fig. 3.2 Comparison of translocation and distribution of GO-SH/Rho B in wild-type and *gas-1* mutant nematodes [33]. The arrowheads indicate the spermatheca (single arrowheads) and the embryos (double arrowheads). The pharynx (*) and intestine (**) are also indicated. Prolonged exposure was performed from L1-larvae to adult day 1

3.2.1.1.4 Molecular Basis for the Formation of Susceptibility to Toxicity of Environmental Toxicants or Stresses in *gas-1* Mutant Nematodes

In nematodes, *daf-16* encodes a forkhead transcription factor in the insulin-signaling pathway. In wild-type animals, the DAF-16 normally resides in the cytoplasm, and its expression could be translocated to the nuclei upon activating stimuli, such as the oxidative stress [36]. However, even under the normal conditions, the DAF-16 resides constitutively in the nuclei of *gas-1* mutant nematodes [36]. Supplementation with the antioxidant (coenzyme Q10) could reverse this nuclear translocation of DAF-16 in *gas-1* mutant nematodes [36]. These observations suggest that *gas-1* mutation-mediated mitochondrial perturbations may regulate the toxicity induction of environmental toxicants or stresses by at least affecting the insulin signaling pathways [36].

3.2.1.2 NUO-1

In nematodes, *nuo-1* encodes a NDUFV1 subunit of complex I. The transgenic strains carrying the mutated *nuo-1* showed the complex I dysfunction, such as the lactic acidosis and the decreased NADH-dependent mitochondrial respiration [37]. Meanwhile, the transgenic strains carrying the mutated *nuo-1* showed the susceptibility to hyperoxia or paraquat, a generator of superoxide (Fig. 3.3) [37]. This observation has implied that the *nuo-1* mutants are hypersensitive to environmental toxicants or stresses. Moreover, it has been observed that the sensitivity of at least some transgenic strains carrying the mutated *nuo-1* to the hyperoxia or paraquat could be significantly reduced by the supplementation with sodium dichloroacetate or riboflavin (Fig. 3.3) [37]. These beneficial effects of sodium dichloroacetate and riboflavin may be largely due to their ability in stimulating the NADH oxidation and in producing a less reduction in the cellular environment [37].

3.2.1.3 NUO-6

In nematodes, *nuo-6* encodes a complex I subunit orthologous to mammalian NUDFB4 complex I subunit. The decreased function of complex I and the generation of superoxide were observed in the *nuo-6* mutant nematodes, although the overall ROS levels are not and the oxidative stress is low [38]. Moreover, it has been shown that treatment with the paraquat could not obviously affect the lifespan of long-lived *nuo-6* mutant nematodes [39], which suggests the possible resistance of *nuo-6* mutant nematodes to the oxidative stress.

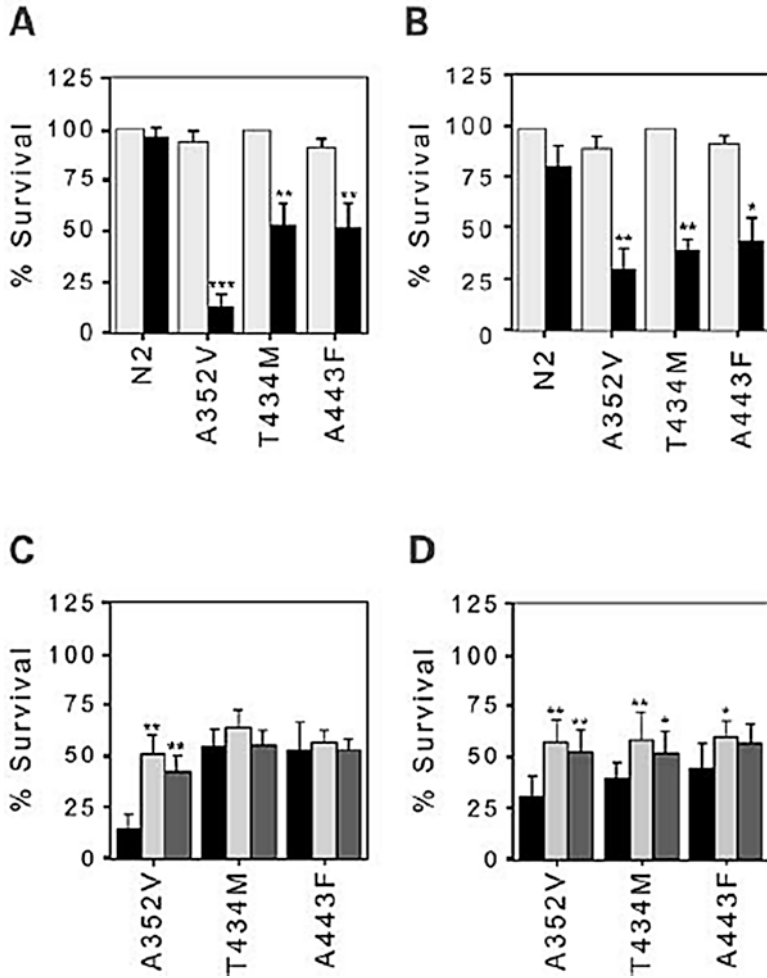


Fig. 3.3 The effects of oxidative stress on wild-type and transgenic mutant strains [37]. Survival was scored after 5 days and was defined as the percentage of L1-larvae that developed into adults. A minimum of 50 animals were scored. Each value is the mean of five trials. (a) L1-larvae were placed onto seeded NGM plates and incubated in either atmospheric (gray bars) or 100% oxygen (black bars). (b) L1-larvae were placed onto seeded NGM plates with no (gray bars) or 0.2 M paraquat (black bars). (c) L1-larvae were placed onto seeded NGM plates and incubated in 100% oxygen without added supplement (black bars), with 5 mg/ml sodium dichloroacetate (light gray bars), or with 1 mg/ml riboflavin (dark gray bars). (d) L1-larvae were placed onto seeded NGM plates with 0.2 M paraquat without added supplement (black bars), with 5 mg/ml sodium dichloroacetate (light gray bars), or with 1 mg/ml riboflavin (dark gray bars). *P* values were derived using two sample t-tests. **P* < 0.05; ***P* < 0.01; ****P* < 0.001 compared with wild type in (a) or (b) or to the non-supplemented control in (c) or (d)

In nematodes, it has been further found that the genes regulated by the FOXO transcription factor DAF-16 could be upregulated by *nuo-6* mutation [40]. Additionally, both the DAF-16 and its multiple interacting proteins (MATH-33, IMB-2, CST-1/2, and BAR-1) were required for the long-lived longevity formation in *nuo-6* mutant nematodes [40]. Therefore, NUO-6 may regulate the biological processes by affecting the function of insulin signaling pathway in nematodes.

3.2.2 Complex II (Succinate Ubiquinone Oxidoreductase)

In nematodes, *mev-1* encodes a cytochrome b large subunit of complex II. A decreased mitochondrial activity (as indicated by the reduced mitochondrial respiratory rates), short lifespan, and high level of oxygen free radicals can be detected in the *mev-1(kn1)* mutant nematodes.

3.2.2.1 Toxicity Induction of Environmental Toxicants or Stresses May Be Associated with the Decrease in *mev-1* in Nematodes

Besides the environmental radiation, microgravity is another crucial contributor to the observed physiological changes during the spaceflight. In nematodes, simulated microgravity treatment for 6, 12, or 24 h could cause the significant induction of intestinal ROS production in wild-type nematodes (Fig. 3.4) [41]. Meanwhile, the simulated microgravity treatment significantly decreased the transcriptional expressions of *mev-1* and *gas-1* and increased the transcriptional expression of *isp-1* (Fig. 3.4) [41]. These observations imply that the potential toxicity induction of simulated microgravity may be associated with the alteration in expressions of some genes required for the control of oxidative stress, including the decrease in *mev-1*, in nematodes.

3.2.2.2 Mutation of *mev-1* Induces a Susceptibility to Toxicity of Environmental Toxicants or Stresses

With the simulated microgravity as an example for the environmental stresses, it has been found that mutation of *mev-1* could strengthen the induction of intestinal ROS production in simulated microgravity-treated nematodes (Fig. 3.5) [41], which suggests that mutation of *mev-1* induces a susceptibility to toxicity of environmental toxicants or stresses, such as the microgravity.

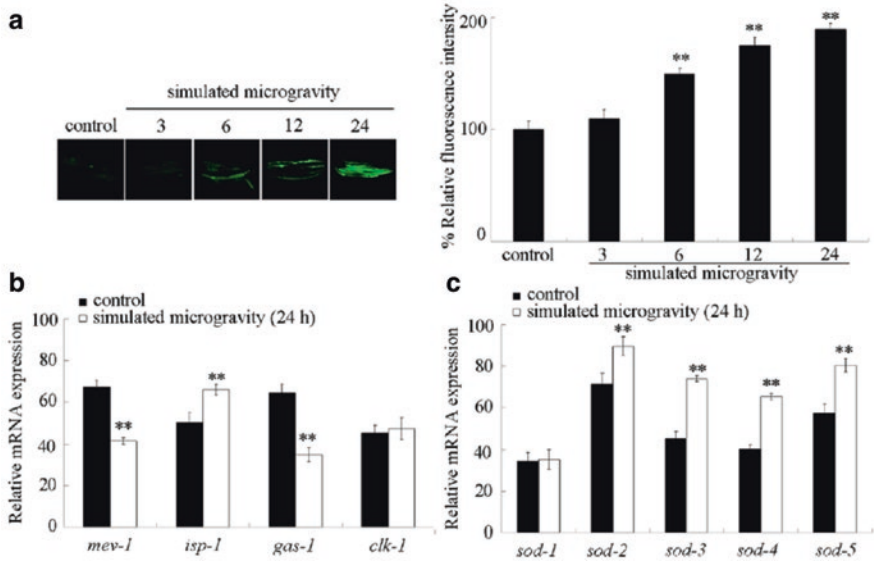


Fig. 3.4 Effect of simulated microgravity treatment in inducing ROS production in wild-type nematodes [41]. **(a)** Effect of simulated microgravity treatment in inducing ROS production in wild-type nematodes. **(b)** Effect of simulated microgravity treatment on the expressions of *mev-1*, *isp-1*, *gas-1*, and *clk-1* genes in wild-type nematodes. The relative quantification was expressed as the ratio between targeted genes and reference *tba-1* gene. **(c)** Effect of simulated microgravity treatment on the expressions of *sod* genes in wild-type nematodes. The relative quantification was expressed as the ratio between targeted genes and reference *tba-1* gene. Bars represent means \pm SD. ** $P < 0.01$ vs control

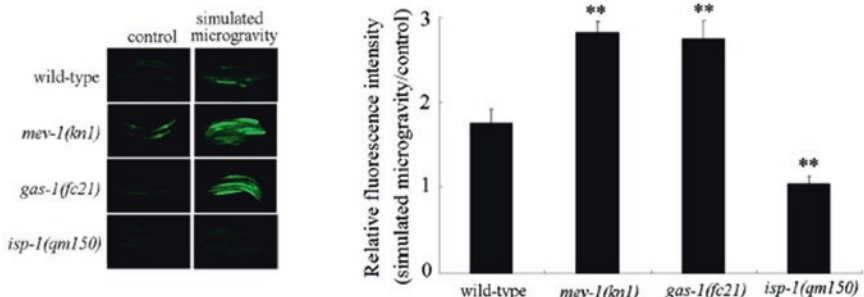


Fig. 3.5 Mutation of *mev-1*, *gas-1*, or *clk-1* affected the induction of oxidative stress in simulated microgravity-treated nematodes [41]. Bars represent means \pm SD. ** $P < 0.01$ vs wild type

3.2.2.3 Molecular Basis for the Formation of Susceptibility to Toxicity of Environmental Toxicants or Stresses in *mev-1* Mutant Nematodes

Similar to the observation in *gas-1* mutant nematodes, the DAF-16 protein can also reside constitutively in the nuclei in *mev-1* mutant nematodes under the normal conditions [36]. Meanwhile, the supplementation of coenzyme Q10 could also reverse this nuclear translocation of DAF-16 in the *mev-1* mutant nematodes [36]. Therefore, the *mev-1* mutation-mediated mitochondrial perturbations may also regulate the toxicity induction of environmental toxicants or stresses by affecting the insulin signaling pathways in nematodes.

3.2.3 Complex III

3.2.3.1 ISP-1

In nematodes, *isp-1* encodes an iron–sulfur component of complex III. The increased lifespan and the elevated generation of superoxide can be observed in *isp-1* mutant nematodes.

3.2.3.1.1 Toxicity Induction of Environmental Toxicants or Stresses May Be Associated with the Increase in *isp-1* in Nematodes

Graphene oxide (GO) is another important member of graphene family. In nematodes, prolonged exposure to GO could potentially cause the damage on the functions of both primary and secondary targeted organs [42]. For example, after prolonged exposure, GO (0.5–100 mg/L) could noticeably induce the intestinal ROS production (Fig. 3.6) [42]. Meanwhile, prolonged exposure to GO (100 mg/L) could significantly decrease the transcriptional expression of *gas-1* and increase the transcriptional expressions of *sod-1*, *sod-2*, *sod-3*, *sod-4*, *isp-1*, and *clk-1* (Fig. 3.6) [42]. Moreover, it was also found that the simulated microgravity treatment could also significantly increase the transcriptional expression of *isp-1* (Fig. 3.4) [41]. These observations suggested that the toxicity induction of environmental toxicants or stresses, such as the GO exposure or simulated microgravity treatment, may be associated with the increase in *isp-1* in nematodes.

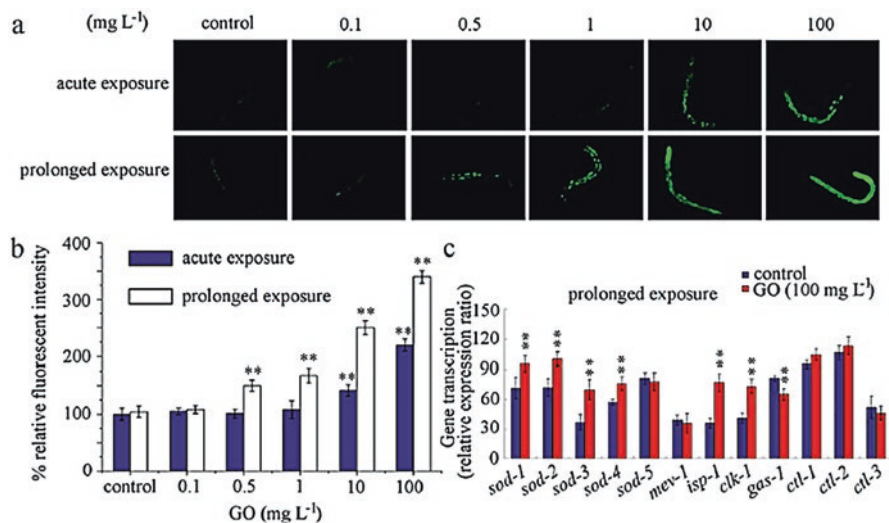


Fig. 3.6 Effects of GO exposure on intestinal ROS production in nematodes [42]. (a) Pictures showing the intestinal ROS production. (b) Comparison of intestinal ROS production in GO-exposed nematodes. (c) Expression pattern comparison of genes required for oxidative stress in GO-exposed nematodes. The final results were expressed as the relative expression ratio (between targeted gene and *tba-1* reference gene). Exposure to GO was performed from L4-larvae for 24 h (acute exposure) or from L1-larvae to adult (prolonged exposure). Bars represent means \pm SEM. ** $p < 0.01$

3.2.3.1.2 Mutation of *isp-1* Induces a Resistance to Toxicity of Environmental Toxicants or Stresses

Using locomotion behavior, brood size, and intestinal ROS production as the toxicity assessment endpoints, it was observed that mutation of *isp-1* could induce a resistance of nematodes to GO toxicity in decreasing locomotion behavior, in reducing brood size, and in inducing intestinal ROS production [43]. ISP-1 may further positively regulate the formation of transgenerational toxicity in CdTe quantum dot (QD)-exposed nematodes, and mutation or intestine-specific RNAi of *isp-1* could cause the formation of a resistance to the transgenerational toxicity of CdTe QDs and prevent the translocation of CdTe QDs from the exposed nematodes to their progeny [44]. Additionally, it was also observed that mutation of *isp-1* could result in a resistance to the oxidative stress induced by simulated microgravity treatment (Fig. 3.5) [41]. These findings suggest that mutation of *isp-1* induces a resistance to toxicity of environmental toxicants or stresses in nematodes.

3.2.3.1.3 Cellular Mechanisms for the Formation of Resistance to Toxicity of Environmental Toxicants or Stresses in *isp-1* Mutant Nematodes

Previous study has demonstrated that prolonged exposure to GO (100 mg/L) could significantly enhance the intestinal permeability as indicated by the assay of Nile Red labeling [42]. One of the raised cellular mechanisms for the formation of resistance to toxicity of environmental toxicants or stresses in *isp-1* mutant is that mutation of *isp-1* could effectively suppress this enhancement in the intestinal permeability caused by environmental toxicants or stresses, such as the GO (100 mg/L) exposure [43].

3.2.3.1.4 Molecular Mechanisms for the Formation of Resistance to Toxicity of Environmental Toxicants or Stresses in *isp-1* Mutant Nematodes

3.2.3.1.4.1 Role of DAF-16

It was found that the genes regulated by the FOXO transcription factor DAF-16 could also be upregulated by *isp-1* mutation [40]. Additionally, both the DAF-16 and its multiple interacting proteins (MATH-33, IMB-2, CST-1/2, and BAR-1) were shown to be required for the long-lived longevity phenotype of *isp-1* mutant nematodes [40]. Therefore, ISP-1 may act upstream of insulin pathway to regulate the various biological processes, including the stress response.

3.2.3.1.4.2 Elevated ROS Levels in *isp-1* Mutant May Activate Multiple Stress-Response Pathways

In nematodes, it has been found that the elevated ROS levels could help the *isp-1* mutant nematodes to activate multiple stress-response pathways [45]. The first activated stress-response pathway was the mitochondrial unfolded protein response (mt-UPR) [45]. The second activated stress-response pathway was the SKN-1-mediated stress response [45]. The third activated stress-response pathway was the antioxidant enzymes, including a marked upregulation of the inducible *sod-3*- and *sod-5*-encoding superoxide dismutases [45].

3.2.3.1.4.3 Role of Long Noncoding RNAs (lncRNAs)

In nematodes, after prolonged exposure to GO, mutation of *isp-1* could dysregulate the expressions of some lncRNAs. After prolonged exposure, the expression patterns of some dysregulated lncRNAs (*linc-37*, *linc-5*, *linc-83*, *linc-103*, *linc-68*, *anr-24*, *linc-14*, *XLOC_013642*, *XLOC_016657*, *XLOC_003625*, *XLOC_015091*,

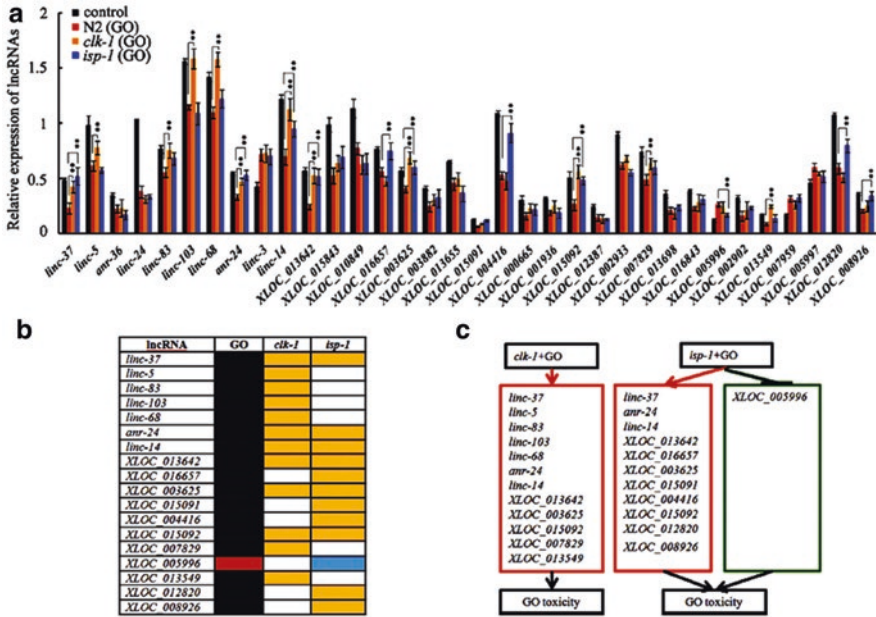


Fig. 3.7 Genetic mutation altered the expression patterns of some lncRNAs in GO-exposed wild-type nematodes [46] (a) lncRNAs' expression patterns in GO-exposed wild-type and *clk-1* or *isp-1* mutant nematodes. GO exposure concentration was 100 mg/L. Prolonged exposure to GO was performed from L1-larvae to young adults. Bars represent means \pm S.E.M. $**P < 0.01$. (b) Summary on the expression patterns of lncRNAs in GO-exposed wild-type and *clk-1* or *isp-1* mutant nematodes. Dark blue color indicates the decreased lncRNAs by GO, red color indicates the increased lncRNA by GO, yellow color indicates the increased lncRNAs by *clk-1* or *isp-1* mutation, and light blue color indicates the decreased lncRNA by *clk-1* or *isp-1* mutation. (c) Diagram for molecular mechanism of *clk-1* or *isp-1* mutation to reduce the GO toxicity through the regulation of functions of lncRNAs in nematodes

XLOC_004416, *XLOC_015092*, *XLOC_007829*, *XLOC_005996*, *XLOC_013549*, *XLOC_012820*, and *XLOC_008926*) induced by GO exposure could be reversed by the mutation of *isp-1* (Fig. 3.7) [46]. Mutation of *isp-1* could increase the expressions of *linc-37*, *anr-24*, *linc-14*, *XLOC_013642*, *XLOC_016657*, *XLOC_003625*, *XLOC_015091*, *XLOC_004416*, *XLOC_015092*, *XLOC_012820*, and *XLOC_008926* and decrease the expression of *XLOC_005996* in GO-exposed nematodes (Fig. 3.7) [46]. These results suggest that mutation of *isp-1* may reduce the GO toxicity by affecting the functions of certain lncRNAs in nematodes.

3.2.3.2 CTB-1

In nematodes, *ctb-1* encodes a cytochrome b subunit of complex III. The short-lived lifespan can be detected in *ctb-1* mutant nematodes [47]. Meanwhile, it was found that *ctb-1* mutation could suppress the nuclear-encoded complex III defect in *isp-1*

mutant nematodes [47], which implies the possibility that CTB-1 may potentially regulate the toxicity of environmental toxicants or stresses through the ISP-1 signaling in nematodes.

3.2.4 *Complex IV*

The long-lived lifespan can be observed in nematodes with RNAi knockdown any of the three complex IV subunits, including cytochrome *c* oxidase (COX) IV (*W09C5.8* and *Y37D8A.14*) [48]. In nematodes, although the overall amount of complex I was not decreased, the COX deficiencies could decrease the intrinsic complex I enzymatic activity, as well as complex I–III enzymatic activity [48]. That is, the intrinsic complex I enzymatic activity may be dependent on the presence of complex IV, and the complex IV may regulate the toxicity of environmental toxicants or stresses by affecting the activity of complex I, such as GAS-1.

3.2.5 *Coenzyme Q (Ubiquinone, CoQ) Synthesis*

In nematodes, *clk-1* encodes a ubiquinone biosynthesis protein COQ7. The long-lived lifespan phenotype can be observed in the *clk-1* mutant nematodes.

3.2.5.1 **Toxicity Induction of Environmental Toxicants or Stresses May Be Associated with the Increase in *clk-1* in Nematodes**

In nematodes, prolonged exposure to GO (100 mg/L) could significantly increase the transcriptional expression of *clk-1* (Fig. 3.6) [42]. Similarly, prolonged exposure to multiwalled carbon nanotubes (MWCNTs, 1 mg/L) could also significantly increase the transcriptional expression of *clk-1* [49]. These findings imply that the toxicity induction of environmental toxicants or stresses, such as the GO or MWCNTs exposure, may be associated with the increase in *clk-1* in nematodes.

3.2.5.2 **Mutation of *clk-1* Induces a Resistance to Toxicity of Environmental Toxicants or Stresses**

Using locomotion behavior, brood size, and intestinal ROS production as the toxicity assessment endpoints, it was observed that mutation of *clk-1* could also induce a resistance of nematodes to GO toxicity in decreasing locomotion behavior, in reducing brood size, and in inducing intestinal ROS production [43]. Mutation or intestine-specific RNAi of *clk-1* could also cause the formation of a resistance to the transgenerational toxicity of CdTe QDs and prevent the translocation of CdTe QDs

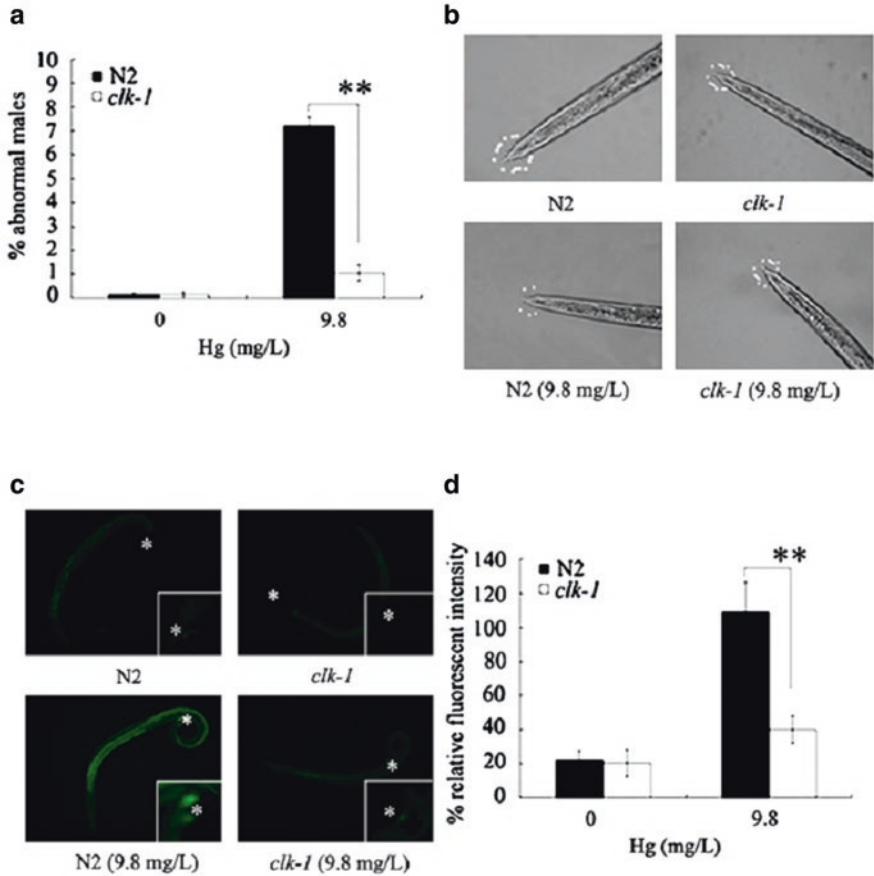


Fig. 3.8 Effects of *clk-1* mutation on the development of male-specific structures induced by Hg exposure [50]. (a) Effects of *clk-1* mutation on the formation of abnormal males induced by Hg exposure. (b) Effects of *clk-1* mutation on the development of male-specific structures induced by Hg exposure. (c) Representative images of ROS production. The asterisks indicate the position of male tails. (d) Effects of *clk-1* mutation on the ROS production induced by Hg exposure. The nematodes were treated with 9.8 mg/L Hg for 24 h at the L3-larval stage. Bars represent means \pm SEM. $**P < 0.01$

from the exposed nematodes to their progeny [44]. It was further found that mutation of *clk-1* could effectively suppress the formation of high percentage of abnormal males and severe deficits in the male-specific structures in Hg exposure-induced male nematodes (Fig. 3.8) [50]. Meanwhile, mutation of *clk-1* could further effectively suppress the formation of severe ROS production in the tails of Hg exposure-induced male nematodes (Fig. 3.8) [50]. Therefore, mutation of *clk-1* may induce a resistance to toxicity of environmental toxicants or stresses in nematodes.

3.2.5.3 Cellular Mechanisms for the Formation of Resistance to Toxicity of Environmental Toxicants or Stresses in *clk-1* Mutant Nematodes

One important cellular mechanism for the formation of resistance to toxicity of environmental toxicants or stresses in *clk-1* mutant is that mutation of *clk-1* could effectively suppress the enhancement in the intestinal permeability caused by environmental toxicants or stresses, such as the GO (100 mg/L) exposure [43].

3.2.5.4 Molecular Mechanisms for the Formation of Resistance to Toxicity of Environmental Toxicants or Stresses in *clk-1* Mutant Nematodes

3.2.5.4.1 Role of DAF-16

The genes regulated by the FOXO transcription factor DAF-16 could be further upregulated by *clk-1* mutation [40]. Moreover, both DAF-16 and its multiple interacting proteins (MATH-33, IMB-2, CST-1/2, and BAR-1) were shown to be required for the long-lived longevity phenotype of *clk-1* mutant nematodes [40]. That is, the CLK-1 may also act upstream of insulin pathway to regulate the various biological processes, including the stress response.

3.2.5.4.2 Biological Function of Nuclear CLK-1

In nematodes, the nuclear CLK-1 may mediate a retrograde signaling pathway that is conserved among different organisms and was responsive to the mitochondrial ROS, thus acting as a barometer of the oxidative metabolism [51]. A corresponding model for the regulation of ROS metabolism, UPR^{mt}, and lifespan by nuclear CLK-1 is provided in Fig. 3.9 [51].

3.2.5.4.3 Role of lncRNAs

The expression patterns of some dysregulated lncRNAs (*linc-37*, *linc-5*, *linc-83*, *linc-103*, *linc-68*, *anr-24*, *linc-14*, *XLOC_013642*, *XLOC_016657*, *XLOC_003625*, *XLOC_015091*, *XLOC_004416*, *XLOC_015092*, *XLOC_007829*, *XLOC_005996*, *XLOC_013549*, *XLOC_012820*, and *XLOC_008926*) induced by GO exposure could also be reversed by *clk-1* mutation (Fig. 3.7) [46]. Mutation of *clk-1* could increase the expressions of *linc-37*, *linc-5*, *linc-83*, *linc-103*, *linc-68*, *anr-24*,

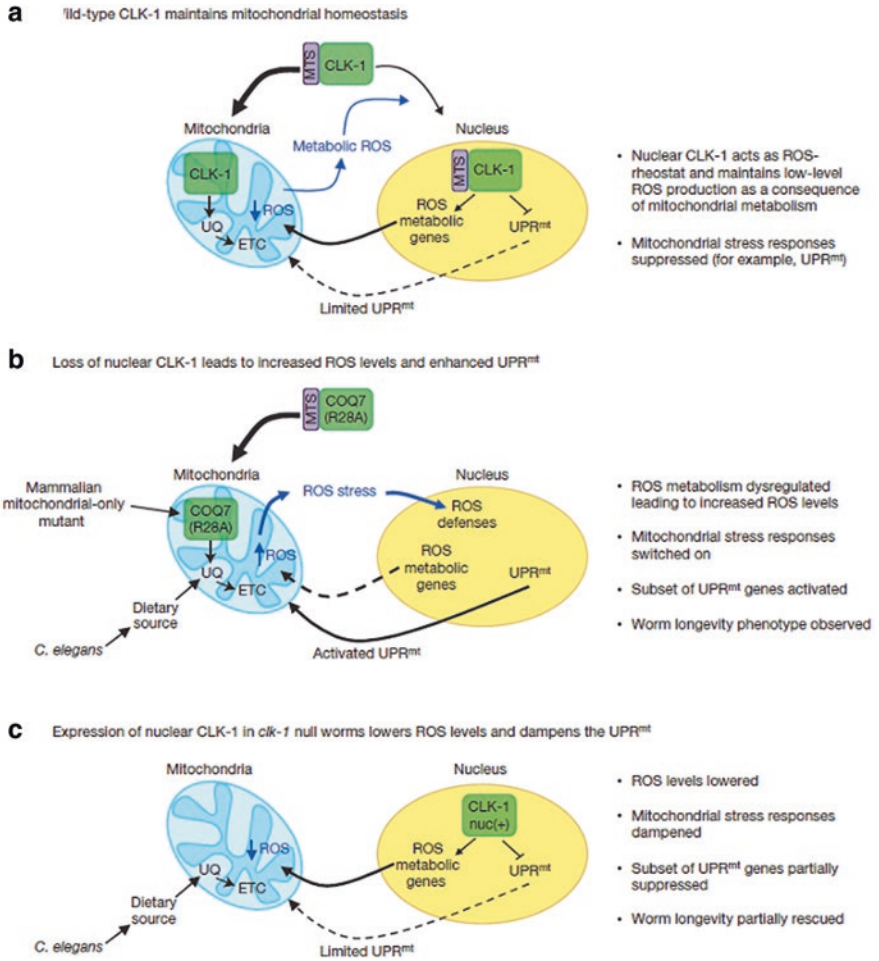


Fig. 3.9 Model for the regulation of ROS metabolism, UPR^{mt}, and lifespan by nuclear CLK-1 [51]. (a) CLK-1 regulates mitochondrial homeostasis. Most CLK-1 localizes to mitochondria by means of its mitochondrial targeting sequence (MTS), where it is required for the biosynthesis of ubiquinone (UQ), an essential cofactor in the electron transport chain (ETC). However, basal levels of ROS, produced by the mitochondria, direct a pool of CLK-1 to the nucleus where it regulates gene expression. Some CLK-1-regulated genes are directly involved in mitochondrial ROS metabolism, and, therefore, the prolonged presence of CLK-1 in the nucleus lowers ROS levels. Reduced ROS leads to CLK-1 being predominantly localized to mitochondria, and not the nucleus, so its effects on gene expression are relieved, basal ROS production returns, and homeostasis is maintained. (b) Loss of nuclear COQ7 (R28A mutant) in human cells or loss of CLK-1 in worms (that scavenge UQ from their bacterial diet) alters ROS metabolism leading to increased ROS levels, augments the UPR^{mt}, and extends the lifespan of worms. (c) The increased ROS levels, augmented UPR^{mt}, and extended lifespan in *clk-1*(-) worms were suppressed by expression of a nuclear-localized CLK-1 mutant (CLK-1^{nuc(+)}) that acts to try to maintain mitochondrial homeostasis

linc-14, *XLOC_013642*, *XLOC_003625*, *XLOC_015091*, *XLOC_007829*, *XLOC_013549*, and *XLOC_012820* in GO-exposed nematodes (Fig. 3.7) [46]. These results imply that the CLK-1 can also potentially regulate the GO toxicity by influencing the functions of certain lncRNAs in nematodes. Interestingly, it was found that both the *clk-1* mutation and the *isp-1* mutation could decrease the expressions of *linc-37*, *anr-24*, *linc-14*, *XLOC_013642*, *XLOC_003625*, and *XLOC_015092* in GO-exposed nematodes (Fig. 3.7) [46].

3.3 Roles of SODs in the Regulation of Toxicity of Environmental Toxicants or Stresses

In the organisms, the superoxide dismutases (SODs) are enzymes with the function to catalytically remove the superoxide radical ($\cdot\text{O}_2^-$) so as to protect the organisms from the oxidative damage during normal aging or after exposure to environmental toxicants or stresses [52].

3.3.1 SOD-1

3.3.1.1 Mutation of *sod-1* Induces a Susceptibility to Toxicity of Environmental Toxicants or Stresses

In nematodes, *sod-1* encodes a Cu/Zn SOD. After Cd exposure, the 24 h LC50 of Cd observed was in the order of wild-type (N2) > *sod-1(or13)* > *daf-16(mu86)* [53], which suggests the induction of susceptibility to environmental toxicants or stresses, such as the heavy metal of Cd, in *sod-1* mutant nematode.

3.3.1.2 Cellular Mechanisms for SOD-1 in the Regulation of Toxicity of Environmental Toxicants or Stresses

In *sod-1* mutant nematodes, both the cytosolic $\cdot\text{O}_2^-$ level and the mitochondrial $\cdot\text{O}_2^-$ level were obviously increased, which suggests that the activity of SOD-1 may act not only in the cytoplasm but also in the mitochondria to help the nematodes to control the detoxification of $\cdot\text{O}_2^-$ [52].

3.3.1.3 Molecular Mechanisms for SOD-1 in the Regulation of Toxicity of Environmental Toxicants or Stresses

Loss-of-function mutation of *sod-1* would cause the enhanced expression of subsets of both SKN-1 and DAF-16 targets, and a strong overexpression of *sod-1* would further induce a compensatory decrease in some of the SKN-1-regulated *gst* genes in nematodes [54].

In nematodes, it was further found the functional compensation for SOD-1 by other SODs, especially the *sod-5*, which could be induced several fold in the *sod-1* mutant nematodes [52].

3.3.2 SOD-2 and SOD-3

In nematodes, *sod-2* and *sod-3* encode the mitochondrial Mn-SODs.

3.3.2.1 Exposure to Environmental Toxicants or Stresses Dysregulates the Expressions of SOD-2 and SOD-3

Titanium dioxide nanoparticles (TiO₂-NPs), a kind of metal-oxide nanomaterials, have been widely used as pigments or additives for paints, paper, ceramics, plastics, foods, and other products, which implies the potential close contact of TiO₂-NPs with the humans. In nematodes, small sizes (4 nm and 10 nm) of TiO₂-NPs could cause the more severe toxicities than large sizes (60 nm and 90 nm) of TiO₂-NPs on animals using lethality, growth, reproduction, locomotion behavior, intestinal autofluorescence, and intestinal ROS production as the toxicity assessment endpoints [55, 56]. Meanwhile, it has been observed that, among the examined genes required for the control of oxidative stress, only the transcriptional expressions of *sod-2* and *sod-3* were significantly increased after exposure to 4 nm, 10 nm, 60 nm, or 90 nm TiO₂-NPs at 10 mg/L [55]. Additionally, the expression patterns of *sod-2* and *sod-3* in nematodes exposed to 4 nm and 10 nm TiO₂-NPs were different from those in nematodes exposed to 60 nm and 90 nm TiO₂-NPs (Fig. 3.13) [55]. Moreover, with the increases of exposure concentrations of different sizes of TiO₂-NPs, the transcriptional expressions of *sod-2* and *sod-3* also increased gradually compared with controls [55]. The transcriptional expressions of *sod-2* and *sod-3* could be significantly increased by exposure to 4 nm and 10 nm TiO₂-NPs (0.001–10 mg/L), as well as exposure to 60 nm and 90 nm TiO₂-NPs (1–10 mg/L) [55]. These observations suggest that exposure to environmental toxicants or stresses, such as TiO₂-NPs, may potentially alter the expression patterns of SOD-2 and SOD-3 in nematodes.

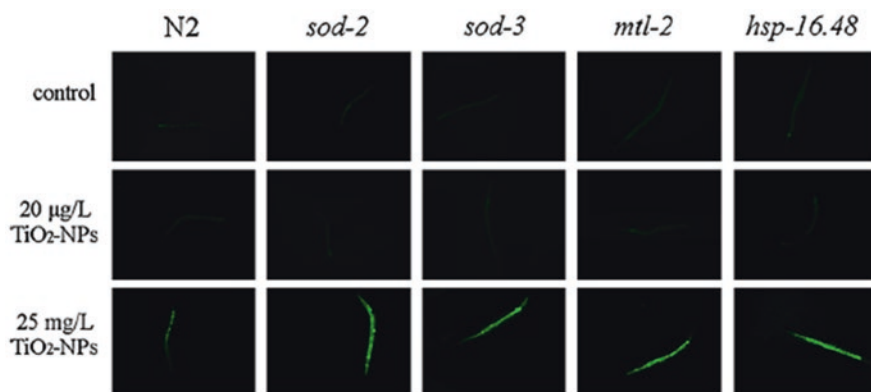


Fig. 3.10 Comparison of intestinal ROS production between wild-type and mutant nematodes acutely exposed to TiO₂-NPs [56]. Acute exposures to TiO₂-NPs were performed from young adult for 24-h in K medium of 12-well sterile tissue culture plates in the presence of food

3.3.2.2 Mutation of *sod-2* or *sod-3* Induces a Susceptibility to Toxicity of Environmental Toxicants or Stresses

With the TiO₂-NPs as an example, loss-of-function mutation of *sod-2* or *sod-3* could induce a susceptibility to TiO₂-NPs toxicity in decreasing body length, in reducing brood size, in decreasing locomotion behavior, and in inducing intestinal autofluorescence and intestinal ROS production in nematodes (Fig. 3.10) [56, 57]. The susceptibility was also observed in *sod-2* or *sod-3* mutant nematodes exposed to heavy metals, GO, Ag nanoparticles, or DMSA-coated Fe₂O₃ nanoparticles [43, 58–60]. Thus, mutation of *sod-2* or *sod-3* induces a susceptibility to toxicity of environmental toxicants or stresses in nematodes.

3.3.2.3 Cellular Mechanisms for SOD-2 and SOD-3 in the Regulation of Toxicity of Environmental Toxicants or Stresses

The first cellular contributor for the formation of susceptibility in *sod-2* or *sod-3* mutant nematodes is the enhancement in intestinal permeability in nematodes exposed to environmental toxicants or stresses. It was reported that mutation of *sod-2* or *sod-3* could significantly enhance the intestinal permeability in nematodes exposed to GO (100 mg/L) [43].

Another important contributor for the formation of susceptibility in *sod-2* or *sod-3* mutant nematodes is the extension of mean defecation cycle length in nematodes exposed to environmental toxicants or stresses. Under the normal conditions, mutation of *sod-2* or *sod-3* did not obviously affect the mean defecation cycle length

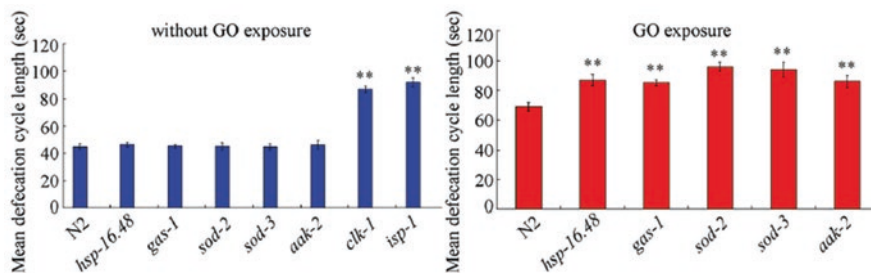


Fig. 3.11 Comparison of mean defecation cycle length between wild-type and mutant nematodes [43]. GO exposure was performed from L1-larvae to young adult. The exposure concentration of GO was 100 mg/L. Bars represent means \pm SEM. ** $P < 0.01$ vs N2

(Fig. 3.11) [43]. In contrast, after prolonged exposure to GO (100 mg/L), a greater increase in the mean defecation cycle length in *sod-2* or *sod-3* mutant nematodes was detected (Fig. 3.11) [43]. Therefore, both the intestinal permeability and the defecation behavior serve as important cellular contributors to the formation of susceptibility in *sod-2* or *sod-3* mutant nematodes.

3.3.2.4 Molecular Mechanisms for SOD-2 and SOD-3 in the Regulation of Toxicity of Environmental Toxicants or Stresses

In nematodes, loss-of-function mutation of genes encoding the Mn-SOD could increase the transcription of SKN-1-regulated genes and reduce the transcription of multiple DAF-16 targets [54]. Moreover, it has been recently found that the antimicrobial genes of *F55G11.4* and *spp-1* could act downstream of *sod-3* to regulate the GO toxicity [12]. In nematodes, SOD-3 acts downstream of intestinal DAF-16 in response to the GO exposure [61]. It was found that RNAi knockdown of *F55G11.4* or *spp-1* could significantly inhibit the resistance to GO toxicity in inducing intestinal ROS production and in decreasing locomotion behavior in transgenic strain overexpressing intestinal *sod-3* (Fig. 3.12) [12], which suggests that antimicrobial proteins of *F55G11.4* and *SPP-1* act downstream of intestinal SOD-3 in response to GO exposure in nematodes.

3.3.3 SOD-4

sod-4 encodes an extracellular Cu/Zn SOD. In nematodes, it was observed that the simulated microgravity treatment could significantly increase the transcriptional expression of *sod-4* (Fig. 3.6) [41]. Moreover, upon comparing the coal combustion-related $PM_{2.5}$ -exposed wild-type with the *smk-1* mutant nematodes, it was found that the *sod-4* expression could be further significantly decreased by *smk-1* mutation (Fig. 3.13) [8].

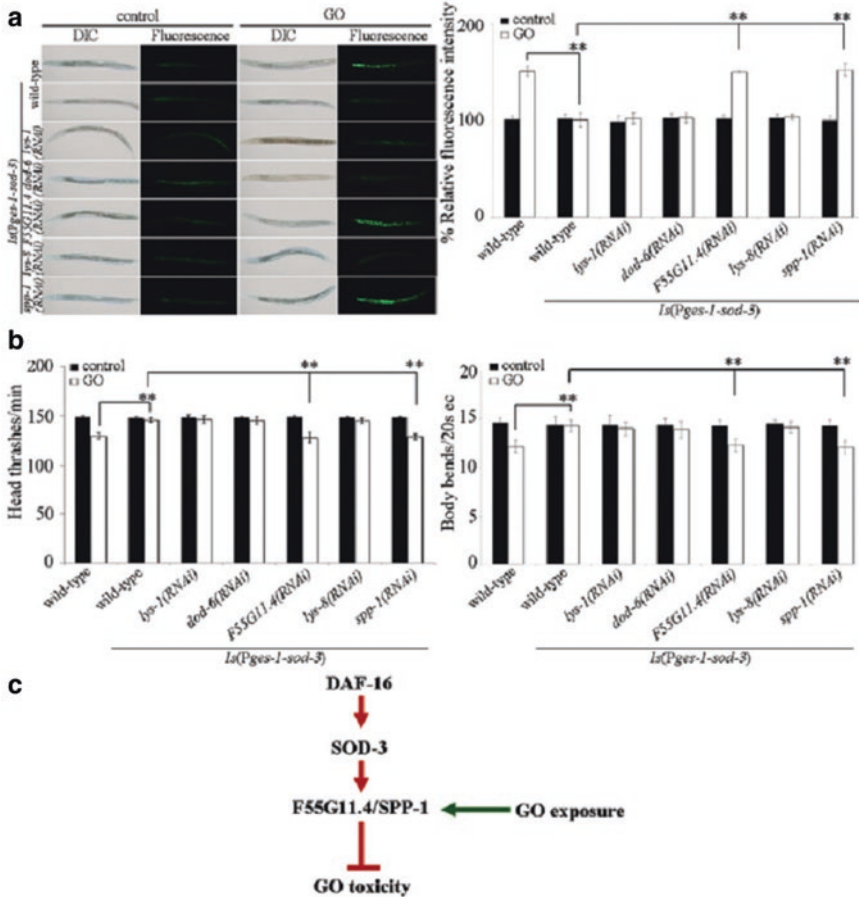


Fig. 3.12 Antimicrobial genes of *F55G11.4* and *spp-1* acted downstream of *sod-3* to regulate the GO toxicity [12]. (a) Antimicrobial genes of *F55G11.4* and *spp-1* acted downstream of *sod-3* to regulate the GO toxicity in inducing intestinal ROS production. (b) Antimicrobial genes of *F55G11.4* and *spp-1* acted downstream of *sod-3* to regulate the GO toxicity in decreasing locomotion behavior. (c) A diagram showing the interaction between SOD-3 and antimicrobial proteins of *F55G11.4* or *SPP-1* in the regulation of GO toxicity. Prolonged exposure was performed from L1-larvae to young adults. GO exposure concentration was 10 mg/L. Bars represent means \pm SD. $**p < 0.01$

In nematodes, RNAi knockdown of the *sod-4* caused the significantly higher induction of intestinal ROS production and decrease in locomotion compared in $PM_{2.5}$ -exposed nematodes compared with those in control nematodes (Fig. 3.13) [8], which suggests that mutation or RNAi knockdown of the *sod-4* may induce a susceptibility to the toxicity of environmental toxicants or stresses in nematodes.

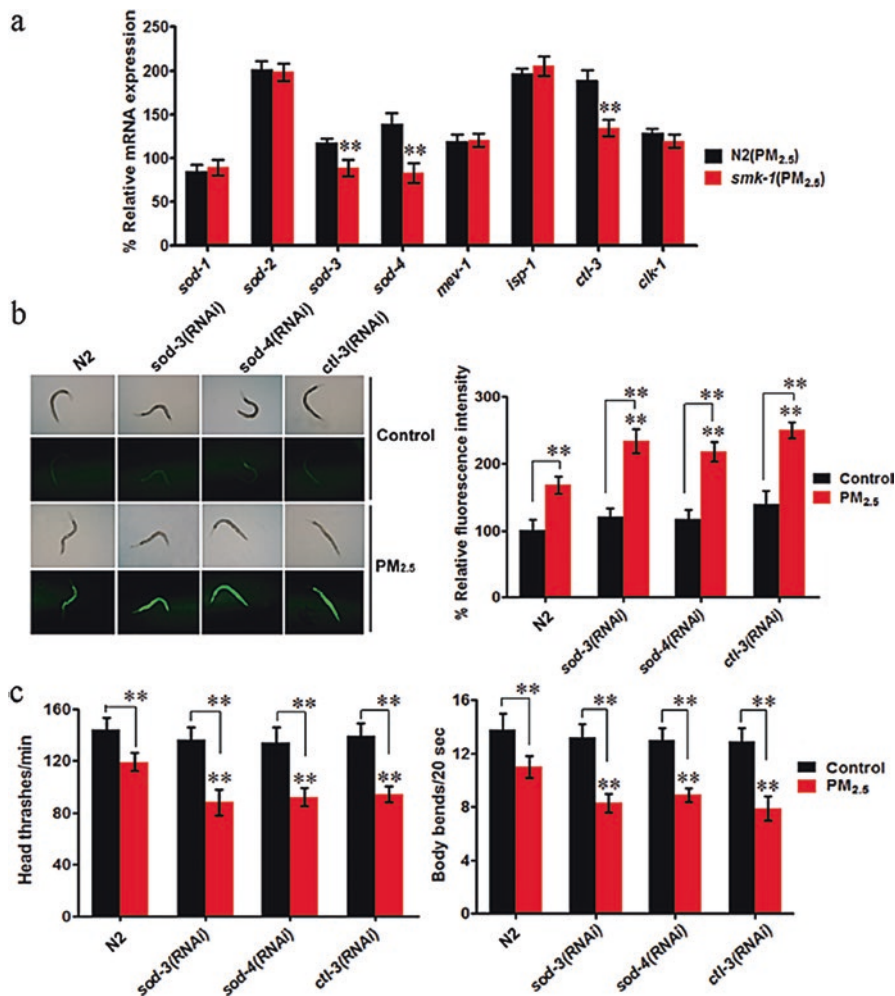


Fig. 3.13 Oxidative stress-related genes acted as downstream regulators of *smk-1* in the regulation of coal combustion-related PM_{2.5} toxicity [8]. (a) Expression pattern of genes required for the control of oxidative stress in coal combustion-related PM_{2.5}-exposed wild-type and *smk-1* mutant nematodes. (b) Effect of RNAi knockdown of *sod-3*, *sod-4*, or *ctl-3* on toxicity of coal combustion-related PM_{2.5} in inducing intestinal ROS production. (c) Effect of RNAi knockdown of *sod-3*, *sod-4*, or *ctl-3* on toxicity of coal combustion-related PM_{2.5} in decreasing locomotion behavior. The concentration of coal combustion-related PM_{2.5} was 1 mg/L. Prolonged exposure was performed from L1-larvae to young adults in the presence of food. Bars represent mean \pm SD. ** $P < 0.01$ vs N2 (if not specially indicated)

3.3.4 *SOD-5*

In nematodes, *sod-5* encodes a cytoplasmic Cu/Zn SOD. In nematodes, it was also observed that the simulated microgravity treatment could significantly increase the transcriptional expression of *sod-5* (Fig. 3.4) [41]. Additionally, exposure to original surface water sample collected from backwater area of Three Gorges Reservoir (TGR) region in the flood season in Wanzhou, Chongqing, could also increase the transcriptional expression of *sod-5* [15]. Moreover, *smk-1* mutation could further significantly decrease the transcriptional expression of *sod-5* in nematodes exposed to coal combustion-related PM_{2.5} (Fig. 3.13) [8].

In nematodes, it was further found that mutation of *sod-5* resulted in a susceptibility of nematodes to the toxicity of coal combustion-related PM_{2.5} in inducing intestinal ROS production and in decreasing locomotion compared (Fig. 3.13) [8]. Moreover, it was observed that the *sod-5* mutant nematodes were susceptible to toxicity of surface water sample collected from backwater area of Three Gorges Reservoir (TGR) region in the flood season in Wanzhou, Chongqing, in inducing intestinal ROS production, in decreasing locomotion behavior, and in reducing brood size (Fig. 3.14) [15]. Therefore, mutation or RNAi knockdown of the *sod-5* may also induce a susceptibility to the toxicity of environmental toxicants or stresses in nematodes.

3.4 Roles of CTL Proteins in the Regulation of Toxicity of Environmental Toxicants or Stresses

ctl-1, *ctl-2*, and *ctl-3* encode the catalases. In nematodes, exposure to phoxim (0.25 mM) could significantly increase the transcriptional expression of *ctl-1* [62]. Additionally, exposure to copper could increase both the activity of CAT and the transcriptional expressions of *ctl-1* and *ctl-2* (Fig. 3.15) [63]. Moreover, upon comparing the coal combustion-related PM_{2.5}-exposed wild-type with the *smk-1* mutant nematodes, the transcriptional expression of *ctl-3* could be significantly decreased by *smk-1* mutation (Fig. 3.13) [8]. These results suggest the possible association between the alteration in CTL expression and the toxicity induction of environmental toxicants or stresses in nematodes.

In nematodes, after the exposure to phoxim, the LC50 values for the *ctl-1(ok1242)* and *ctl-3(ok2042)* mutants were lower than those observed for the wild-type nematodes [62]. After the exposure to carbaryl, the LC50 values for *ctl-1(ok1242)* and *ctl-3(ok2042)* mutants were also decreased in comparison to the wild-type nematodes [62]. Additionally, the *ctl-1* mutant showed the hypersensitivity to copper tox-

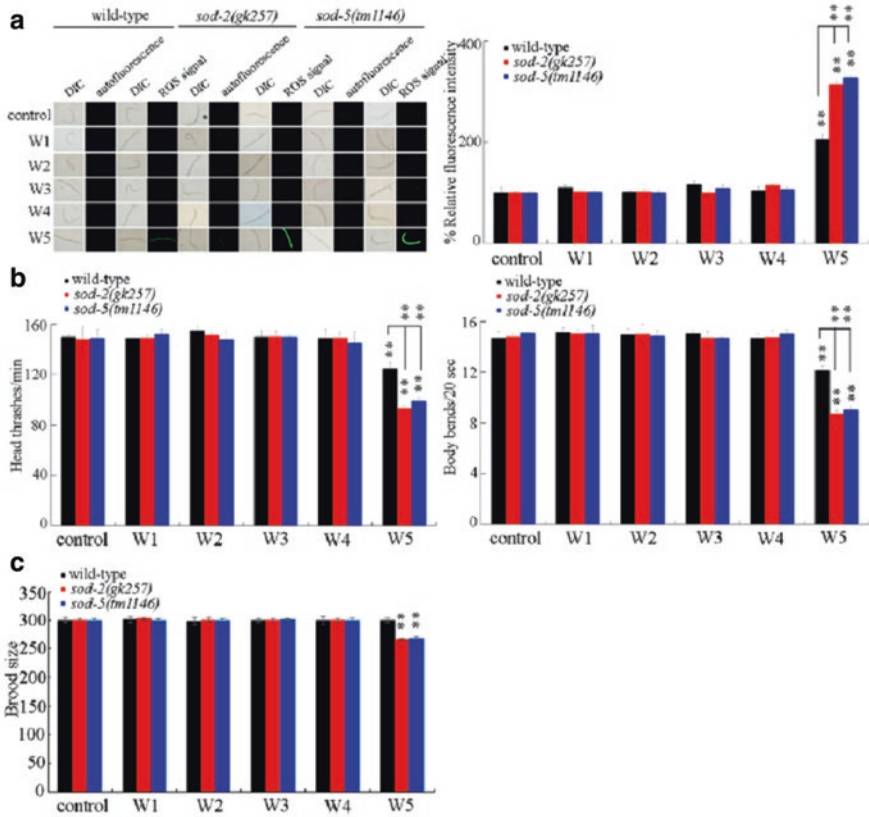


Fig. 3.14 Effect of *sod-2* or *sod-5* mutation on the induction of ROS production (a), the locomotion behavior (b), and the brood size (c) in nematodes exposed to the examined different surface water samples in the TGR region [15]. Exposures were performed from L4-larvae for 24-h. Bars represent means \pm SD. ** $P < 0.01$ vs control (if not specially indicated)

icity [63], and the *ctl-3* mutant showed the hypersensitivity to the toxicity induced by coal combustion-related PM_{2.5} toxicity in nematodes (Fig. 3.13) [8]. These data suggest the important involvement of CTL proteins in the regulation of toxicity of environmental toxicants or stresses in nematodes.

3.5 Roles of GST Proteins in the Regulation of Toxicity of Environmental Toxicants or Stresses

In nematodes, many genes encode the GST (glutathione-requiring prostaglandin D synthase) proteins. Among these genes, exposure to NaF could significantly increase the transcriptional expression of *gst-1* [64], and simulated microgravity treatment

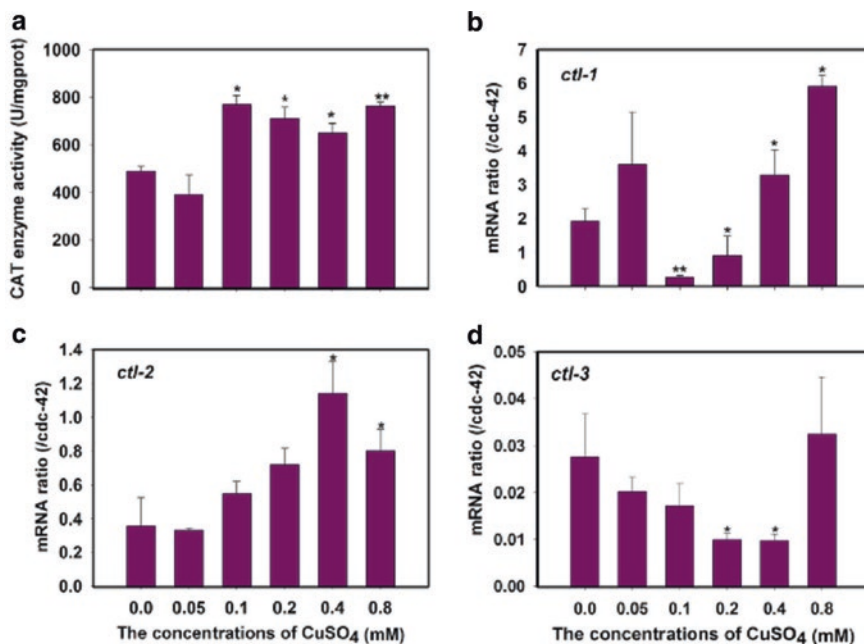


Fig. 3.15 CAT activities or mRNA expression induced by copper in *C. elegans* [63]. (a) The CAT activity and H₂O₂ content were changed during the copper stress. The gene expressions of *ctl-1* (b), *ctl-2* (c), and *ctl-3* (d) were quantified in nematode N2 under the stress of different concentrations of copper and normalized with *cdc-42*. * $P < 0.05$, ** $P < 0.01$ versus respective controls analyzed by *t*-test

could significantly increase the transcriptional expression of *gst-4* (Fig. 3.16) [41]. The response of GST-4::GFP was also observed in nematodes exposed to methylmercury (MeHg) [65].

Moreover, using the corresponding mutant, it was observed that mutation of *gst-4* could significantly enhance the induction of intestinal ROS production in simulated microgravity-treated nematodes compared with that in wild-type nematodes (Fig. 3.16) [41], suggesting that at least mutation of *gst-4* may induce a susceptibility to toxicity of environmental toxicants or stresses, such as the microgravity treatment.

3.6 Perspectives

In this chapter, we first tried to introduce and discuss the important roles of mitochondrial complex signals in the regulation of toxicity of environmental toxicants or stresses. So far, some important components of different mitochondrial complexes have been shown to be involved in the regulation of toxicity of environmental toxicants or stresses. Nevertheless, a full-scale screen for the involvement of

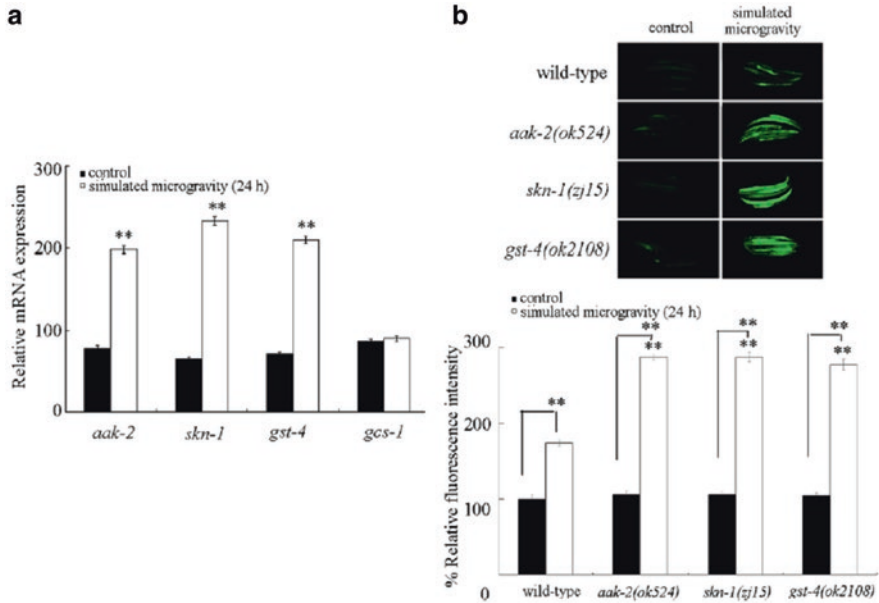


Fig. 3.16 Mutation of *akk-2*, *skn-1*, or *gst-4* enhanced the induction of oxidative stress in simulated microgravity-treated nematodes [41]. **(a)** Effect of simulated microgravity on expressions of *akk-2*, *skn-1*, *gst-4*, and *gcs-1* in wild-type nematodes. The relative quantification was expressed as the ratio between targeted genes and reference *tba-1* gene. Bars represent means \pm SD. ** $P < 0.01$ vs control. **(b)** Mutation of *akk-2*, *skn-1*, or *gst-4* enhanced the induction of oxidative stress in simulated microgravity-treated nematodes. Bars represent means \pm SD. ** $P < 0.01$ vs wild type (if not specially indicated by line connecting)

mitochondrial complex signals in the regulation of toxicity of different typical environmental toxicants or stresses is still needed based on both the alteration in expression patterns and the functional confirmation. The detailed underlying molecular mechanisms for the involvement of different mitochondrial complex signals in the regulation of toxicity of environmental toxicants or stresses are still needed to be further elucidated. Additionally, the potential interactions among different mitochondrial complex signals in the regulation of toxicity of environmental toxicants or stresses are still largely unclear.

We here also introduced and discussed the important roles of SOD proteins, CTL proteins, and GST proteins in the regulation of toxicity of environmental toxicants or stresses. So far, most of the data implies the alteration in expressions of examined SOD proteins, CTL proteins, and GST proteins may mediate a protective response for nematodes. The further examination on the alteration in expression patterns of SOD proteins, CTL proteins, and GST proteins in nematodes exposed to various environmental toxicants or stresses with different doses or exposure durations is still needed to be carefully carried out. That is, we may need to pay more attention to the possible dynamic alteration in expression patterns of SOD proteins, CTL proteins, and GST proteins in nematodes exposed to various environmental toxicants or stresses.

References

1. Yang R-L, Rui Q, Kong L, Zhang N, Li Y, Wang X-Y, Tao J, Tian P-Y, Ma Y, Wei J-R, Li G-J, Wang D-Y (2016) Metallothioneins act downstream of insulin signaling to regulate toxicity of outdoor fine particulate matter (PM_{2.5}) during Spring Festival in Beijing in nematode *Caenorhabditis elegans*. *Toxicol Res* 5:1097–1105
2. Yang R-L, Ren M-X, Rui Q, Wang D-Y (2016) A *mir-231*-regulated protection mechanism against the toxicity of graphene oxide in nematode *Caenorhabditis elegans*. *Sci Rep* 6:32214
3. Zhi L-T, Ren M-X, Qu M, Zhang H-Y, Wang D-Y (2016) Wnt ligands differentially regulate toxicity and translocation of graphene oxide through different mechanisms in *Caenorhabditis elegans*. *Sci Rep* 6:39261
4. Zhi L-T, Fu W, Wang X, Wang D-Y (2016) ACS-22, a protein homologous to mammalian fatty acid transport protein 4, is essential for the control of toxicity and translocation of multi-walled carbon nanotubes in *Caenorhabditis elegans*. *RSC Adv* 6:4151–4159
5. Shakoor S, Sun L-M, Wang D-Y (2016) Multi-walled carbon nanotubes enhanced fungal colonization and suppressed innate immune response to fungal infection in nematodes. *Toxicol Res* 5:492–499
6. Wu Q-L, Zhi L-T, Qu Y-Y, Wang D-Y (2016) Quantum dots increased fat storage in intestine of *Caenorhabditis elegans* by influencing molecular basis for fatty acid metabolism. *Nanomedicine* 12:1175–1184
7. Zhuang Z-H, Li M, Liu H, Luo L-B, Gu W-D, Wu Q-L, Wang D-Y (2016) Function of RSKS-1-AAK-2-DAF-16 signaling cascade in enhancing toxicity of multi-walled carbon nanotubes can be suppressed by *mir-259* activation in *Caenorhabditis elegans*. *Sci Rep* 6:32409
8. Wu Q-L, Han X-X, Wang D, Zhao F, Wang D-Y (2017) Coal combustion related fine particulate matter (PM_{2.5}) induces toxicity in *Caenorhabditis elegans* by dysregulating microRNA expression. *Toxicol Res* 6:432–441
9. Ding X-C, Rui Q, Wang D-Y (2018) Functional disruption in epidermal barrier enhances toxicity and accumulation of graphene oxide. *Ecotoxicol Environ Saf* 163:456–464
10. Zhao L, Qu M, Wong G, Wang D-Y (2017) Transgenerational toxicity of nanopolystyrene particles in the range of µg/L in nematode *Caenorhabditis elegans*. *Environ Sci Nano* 4:2356–2366
11. Xiao G-S, Zhi L-T, Ding X-C, Rui Q, Wang D-Y (2017) Value of *mir-247* in warning graphene oxide toxicity in nematode *Caenorhabditis elegans*. *RSC Adv* 7:52694–52701
12. Ren M-X, Zhao L, Lv X, Wang D-Y (2017) Antimicrobial proteins in the response to graphene oxide in *Caenorhabditis elegans*. *Nanotoxicology* 11:578–590
13. Qu M, Li Y-H, Wu Q-L, Xia Y-K, Wang D-Y (2017) Neuronal ERK signaling in response to graphene oxide in nematode *Caenorhabditis elegans*. *Nanotoxicology* 11:520–533
14. Chen H, Li H-R, Wang D-Y (2017) Graphene oxide dysregulates Neuroigin/NLG-1-mediated molecular signaling in interneurons in *Caenorhabditis elegans*. *Sci Rep* 7:41655
15. Xiao G-S, Zhao L, Huang Q, Yang J-N, Du H-H, Guo D-Q, Xia M-X, Li G-M, Chen Z-X, Wang D-Y (2018) Toxicity evaluation of Wanzhou watershed of Yangtze Three Gorges Reservoir in the flood season in *Caenorhabditis elegans*. *Sci Rep* 8:6734
16. Li W-J, Wang D-Y, Wang D-Y (2018) Regulation of the response of *Caenorhabditis elegans* to simulated microgravity by p38 mitogen-activated protein kinase signaling. *Sci Rep* 8:857
17. Dong S-S, Qu M, Rui Q, Wang D-Y (2018) Combinational effect of titanium dioxide nanoparticles and nanopolystyrene particles at environmentally relevant concentrations on nematodes *Caenorhabditis elegans*. *Ecotoxicol Environ Saf* 161:444–450
18. Qu M, Xu K-N, Li Y-H, Wong G, Wang D-Y (2018) Using *acs-22* mutant *Caenorhabditis elegans* to detect the toxicity of nanopolystyrene particles. *Sci Total Environ* 643:119–126
19. Zhao L, Wan H-X, Liu Q-Z, Wang D-Y (2017) Multi-walled carbon nanotubes-induced alterations in microRNA *let-7* and its targets activate a protection mechanism by conferring a developmental timing control. *Part Fibre Toxicol* 14:27

20. Zhao L, Kong J-T, Krasteva N, Wang D-Y (2018) Deficit in epidermal barrier induces toxicity and translocation of PEG modified graphene oxide in nematodes. *Toxicol Res* 7(6):1061–1070. <https://doi.org/10.1039/C8TX00136G>
21. Xiao G-S, Chen H, Krasteva N, Liu Q-Z, Wang D-Y (2018) Identification of interneurons required for the aversive response of *Caenorhabditis elegans* to graphene oxide. *J Nanbiotechnol* 16:45
22. Ren M-X, Zhao L, Ding X-C, Krasteva N, Rui Q, Wang D-Y (2018) Developmental basis for intestinal barrier against the toxicity of graphene oxide. *Part Fibre Toxicol* 15:26
23. Yin J-C, Liu R, Jian Z-H, Yang D, Pu Y-P, Yin L-H, Wang D-Y (2018) Di (2-ethylhexyl) phthalate-induced reproductive toxicity involved in DNA damage-dependent oocyte apoptosis and oxidative stress in *Caenorhabditis elegans*. *Ecotoxicol Environ Saf* 163:298–306
24. Wang D-Y (2018) *Nanotoxicology in Caenorhabditis elegans*. Springer, Singapore
25. Zhao Y-L, Wu Q-L, Li Y-P, Wang D-Y (2013) Translocation, transfer, and in vivo safety evaluation of engineered nanomaterials in the non-mammalian alternative toxicity assay model of nematode *Caenorhabditis elegans*. *RSC Adv* 3:5741–5757
26. Ruan Q-L, Qiao Y, Zhao Y-L, Xu Y, Wang M, Duan J-A, Wang D-Y. (2016) Beneficial effects of *Glycyrrhizae radix* extract in preventing oxidative damage and extending the lifespan of *Caenorhabditis elegans*. *J Ethnopharmacol* 177: 101–110
27. Pujol C, Bratic-Hench I, Sumakovic M, Hench J, Mourier A, Baumann L, Pavlenko V, Trifunovic A (2013) Succinate dehydrogenase upregulation destabilize complex I and limits the lifespan of *gas-1* mutant. *PLoS ONE* 8:e59493
28. Sedensky MM, Morgan PG (2006) Mitochondrial respiration and reactive oxygen species in *C. elegans*. *Exp Gerontol* 41:957–967
29. Cao J, Liu Y, Jing X, Yin J, Li J, Xu B, Tan Y, Zheng N (2015) Well-defined thiolated nanographene as for efficient and stable perovskite solar cells. *J Am Chem Soc* 137:10914–10917
30. Debgupta J, Pillai VK (2013) Thiolated graphene – a new platform for anchoring CdSe quantum dots for hybrid heterostructures. *Nano* 5:3615–3619
31. de Sousa IP, Büttenhauser K, Suchaoin W, Partenhauser A, Perrone M, Matuszczak B, Bernkop-Schnurch A (2016) Thiolated graphene oxide as promising mucoadhesive carrier for hydrophobic drugs. *Int J Pharm* 509:360–367
32. Wang Q, Zhou Z, Zhai Y, Zhang L, Hong W, Zhang Z, Dong S (2015) Label-free aptamer biosensor for thrombin detection based on functionalized graphene nanocomposites. *Talanta* 141:247–252
33. Ding X-C, Wang J, Rui Q, Wang D-Y (2018) Long-term exposure to thiolated graphene oxide in the range of $\mu\text{g/L}$ induces toxicity in nematode *Caenorhabditis elegans*. *Sci Total Environ* 616–617:29–37
34. Kayser E, Morgan PG, Sedensky MM (2004) Mitochondrial complex I function affects halothane sensitivity in *Caenorhabditis elegans*. *Anesthesiology* 101:365–372
35. Kayser E, Hoppel CL, Morgan PG, Sedensky MM (2003) A mutation in mitochondrial complex I increases ethanol sensitivity in *Caenorhabditis elegans*. *Alcohol Clin Exp Res* 27:584–592
36. Kondo M, Senoo-Matsuda N, Yanase S, Ishii T, Hartman PS, Ishii N (2005) Effect of oxidative stress on translocation of DAF-16 in oxygen-sensitive mutants, *mev-1* and *gas-1* of *Caenorhabditis elegans*. *Mech Ageing Dev* 126:637–641
37. Grad LI, Lemire BD (2004) Mitochondrial complex I mutations in *Caenorhabditis elegans* produce cytochrome c oxidase deficiency, oxidative stress and vitamin-responsive lactic acidosis. *Hum Mol Genet* 13:303–314
38. Yang W, Hekimi S (2010) A mitochondrial superoxide signal triggers increased longevity in *Caenorhabditis elegans*. *PLoS Biol* 8:e1000556
39. Schaar CE, Dues DJ, Spielbauer KK, Machiela E, Cooper JF, Senchuk M, Hekimi S, Van Raamsdonk JM (2015) Mitochondrial and cytoplasmic ROS have opposing effects on lifespan. *PLoS Genet* 11:e1004972
40. Senchuk MM, Dues DJ, Schaar CE, Johnson BK, Madaj ZB, Bowman MJ, Winn ME, Van Raamsdonk JM (2018) Activation of DAF-16/FOXO by reactive oxygen species contributes

- to longevity in long-lived mitochondrial mutants in *Caenorhabditis elegans*. PLoS Genet 14:e1007268
41. Zhao L, Rui Q, Wang D-Y (2017) Molecular basis for oxidative stress induced by simulated microgravity in nematode *Caenorhabditis elegans*. Sci Total Environ 607–608:1381–1390
 42. Wu Q-L, Yin L, Li X, Tang M, Zhang T, Wang D-Y (2013) Contributions of altered permeability of intestinal barrier and defecation behavior to toxicity formation from graphene oxide in nematode *Caenorhabditis elegans*. Nanoscale 5:9934–9943
 43. Wu Q-L, Zhao Y-L, Li Y-P, Wang D-Y (2014) Molecular signals regulating translocation and toxicity of graphene oxide in nematode *Caenorhabditis elegans*. Nanoscale 6:11204–11212
 44. Liu Z-F, Zhou X-F, Wu Q-L, Zhao Y-L, Wang D-Y (2015) Crucial role of intestinal barrier in the formation of transgenerational toxicity in quantum dots exposed nematodes *Caenorhabditis elegans*. RSC Adv 5:94257–94266
 45. Dues DJ, Schaar CE, Johnson BK, Bowman MJ, Winn ME, Senchuk MM, Van Raamsdonk JM (2017) Uncoupling of oxidative stress resistance and lifespan in long-lived *isp-1* mitochondrial mutants in *Caenorhabditis elegans*. Free Radic Biol Med 108:362–373
 46. Wu Q-L, Zhou X-F, Han X-X, Zhuo Y-Z, Zhu S-T, Zhao Y-L, Wang D-Y (2016) Genome-wide identification and functional analysis of long noncoding RNAs involved in the response to graphene oxide. Biomaterials 102:277–291
 47. Suthammarak W, Morgan PG, Sedensky MM (2010) Mutations in mitochondrial complex III uniquely affect complex I in *Caenorhabditis elegans*. J Biol Chem 285:40724–40731
 48. Suthammarak W, Yang Y, Morgan PG, Sedensky MM (2009) Complex I function is defective in complex IV-deficient *Caenorhabditis elegans*. J Biol Chem 284:6425–6435
 49. Wu Q-L, Li Y-X, Li Y-P, Zhao Y-L, Ge L, Wang H-F, Wang D-Y (2013) Crucial role of biological barrier at the primary targeted organs in controlling translocation and toxicity of multi-walled carbon nanotubes in nematode *Caenorhabditis elegans*. Nanoscale 5:11166–11178
 50. Liu P-D, He K-W, Li Y-X, Wu Q-L, Yang P, Wang D-Y (2012) Exposure to mercury causes formation of male-specific structural deficits by inducing oxidative damage in nematodes. Ecotoxicol Environ Saf 79:90–100
 51. Monaghan RM, Barnes RG, Fisher K, Andreou T, Rooney N, Poulin GB, Whitmarsh AJ (2015) A nuclear role for the respiratory enzyme CLK-1 in regulating mitochondrial stress responses and longevity. Nat Cell Biol 17:782–792
 52. Yanase S, Onodera A, Tedesco P, Johnson TE, Ishii N (2009) SOD-1 deletions in *Caenorhabditis elegans* alter the localization of intracellular reactive oxygen species and show molecular compensation. J Gerontol Ser A Biol Sci Med Sci A 64:530–539
 53. Roh J, Park Y, Choi J (2009) A cadmium toxicity assay using stress responsive *Caenorhabditis elegans* mutant strains. Environ Toxicol Pharmacol 28:409–413
 54. Back P, Matthijssens F, Vlaeminck C, Braeckman BP, Vanfleteren JR (2010) Effects of *sod* gene overexpression and deletion mutation on the expression profiles of reporter genes of major detoxification pathways in *Caenorhabditis elegans*. Exp Gerontol 45:603–610
 55. Li Y-X, Wang W, Wu Q-L, Li Y-P, Tang M, Ye B-P, Wang D-Y (2012) Molecular control of TiO₂-NPs toxicity formation at predicted environmental relevant concentrations by Mn-SODs proteins. PLoS ONE 7:e44688
 56. Rui Q, Zhao Y-L, Wu Q-L, Tang M, Wang D-Y (2013) Biosafety assessment of titanium dioxide nanoparticles in acutely exposed nematode *Caenorhabditis elegans* with mutations of genes stress required for oxidative stress or stress response. Chemosphere 93:2289–2296
 57. Wu Q-L, Zhao Y-L, Li Y-P, Wang D-Y (2014) Susceptible genes regulate the adverse effects of TiO₂-NPs at predicted environmental relevant concentrations on nematode *Caenorhabditis elegans*. Nanomedicine 10:1263–1271
 58. Sun L-M, Wu Q-L, Liao K, Yu P-H, Cui Q-H, Rui Q, Wang D-Y (2016) Contribution of heavy metals to toxicity of coal combustion related fine particulate matter (PM_{2.5}) in *Caenorhabditis elegans* with wild-type or susceptible genetic background. Chemosphere 144:2392–2400

59. Wu Q-L, Li Y-P, Tang M, Wang D-Y (2012) Evaluation of environmental safety concentrations of DMSA coated Fe₂O₃-NPs using different assay systems in nematode *Caenorhabditis elegans*. PLoS ONE 7:e43729
60. Roh J, Sim SJ, Yi J, Park K, Chung KH, Ryu D, Choi J (2009) Ecotoxicity of silver nanoparticles on the soil nematode *Caenorhabditis elegans* using functional ecotoxicogenomics. Environ Sci Technol 43:3933–3940
61. Zhao Y-L, Yang R-L, Rui Q, Wang D-Y (2016) Intestinal insulin signaling encodes two different molecular mechanisms for the shortened longevity induced by graphene oxide in *Caenorhabditis elegans*. Sci Rep 6:24024
62. Han Y, Song S, Wu H, Zhang J, Ma E (2017) Antioxidant enzymes and their role in phoxim and carbaryl stress in *Caenorhabditis elegans*. Pestic Biochem Physiol 138:43–50
63. Song S, Zhang X, Wu H, Han Y, Zhang J, Ma E, Guo Y (2014) Molecular basis for antioxidant enzymes in mediating copper detoxification in the nematode *Caenorhabditis elegans*. PLoS ONE 9:e107685
64. Li Q, Zhang S, Yu Y, Wang L, Guan S, Li P (2012) Toxicity of sodium fluoride to *Caenorhabditis elegans*. Biomed Environ Sci 25:216–223
65. Helmcke KJ, Aschner M (2010) Hormetic effect of methylmercury on *Caenorhabditis elegans*. Toxicol Appl Pharmacol 248:156–164

Chapter 4

Functions of MAPK Signaling Pathways in the Regulation of Toxicity of Environmental Toxicants or Stresses



Abstract In nematodes, there are three important mitogen-activated protein kinase (MAPK) signals (p38 MAPK, JNK MAPK, and ERK MAPK). It is well known for the crucial role of these three MAPK signaling pathways for organisms in response to environmental stresses by transducing the extracellular cues into the cells. In this chapter, we introduced and discussed the involvement and the contribution, as well as the underlying molecular mechanisms for the response, of these three important MAPK signaling pathways in the regulation of toxicity of environmental toxicants or stresses in nematodes.

Keywords MAPK signaling pathway · Molecular regulation · Environmental exposure · *Caenorhabditis elegans*

4.1 Introduction

Many important molecular signaling pathways required for the control of various biological processes, including the stress response, are conserved among different organisms. Based on this finding, *Caenorhabditis elegans* has been already widely used in the elucidation of underlying molecular mechanisms of toxicity induced by different environmental toxicants or stresses [1]. Among the molecular signaling pathways, the mitogen-activated protein kinase (MAPK) signals (p38 MAPK, JNK MAPK, and ERK MAPK) have well been known to be involved in the response of organisms to environmental toxicants or stresses. Additionally, the MAPK signals are considered to act as central signaling hubs in the regulation of various cellular processes by transducing the extracellular cues into the cells [2, 3].

In this chapter, we introduced the involvement of these three important MAPK signaling pathways (p38, JNK, and ERK) in the regulation of toxicity of environmental toxicants or stresses. Moreover, we discussed the possible underlying molecular mechanisms for the response of these three MAPK signals to environmental toxicants or stresses. The obtained information so far highlights the possible central role of MAPK signaling pathway for nematodes in response to various environmental toxicants or stresses.

4.2 p38 MAPK Signaling Pathway

In nematodes, the core p38 MAPK signaling pathway contains components of *pmk-1*-encoded MAPK, *sek-1*-encoded MAPK kinase (MAPKK), and *nsy-1*-encoded MAPK kinase kinase (MAPKKK).

4.2.1 *Exposure to Environmental Toxicants or Stress Dysregulates the Expression of p38 MAPK Signal*

Microgravity is a crucial contributor to the formation of adverse effects on animals and human beings during the spaceflight [4–6]. Synthecon Rotary System™ was used as a simulated microgravity assay system. With the simulated microgravity treatment as an example, it was observed that the control wild-type nematodes grown in liquid S medium showed the similar transcriptional expressions of genes (*nsy-1*, *sek-1*, and *pmk-1*) encoding the core p38 MAPK signaling pathway to those in control wild-type nematodes grown on normal NGM plates (Fig. 4.1) [7]. In contrast, after simulated microgravity treatment, the significant increase in transcriptional expressions of *nsy-1*, *sek-1*, and *pmk-1* was observed in wild-type nematodes (Fig. 4.1) [7]. Considering the fact that activation of p38 MAPK signaling usually requires the phosphorylation of p38 MAPK/PMK-1, the level of phosphorylated PMK-1 between control and simulated microgravity-treated wild-type nematodes was further examined. The control wild-type nematodes grown in liquid S medium had the similar expression of phosphorylated PMK-1 to that in control wild-type nematodes grown on normal NGM plates (Fig. 4.1) [7]. However, after simulated microgravity treatment, a significant increase in the expression of phosphorylated PMK-1 was detected in wild-type nematodes (Fig. 4.1) [7].

Graphene oxide (GO), a member of graphene family containing a two-dimensional carbon structure, can be potentially used in nanomedicine including drug delivery and bioimaging [8–10]. In nematodes, GO exposure could cause the toxicity on the functions of both primary (such as intestine) and secondary (such as neurons and reproductive organs) targeted organs [11–17]. Similarly, prolonged exposure to GO (100 mg/L) could significantly increase the transcriptional expressions of *pmk-1*, *sek-1*, and *nsy-1* and increase the expression of intestinal PMK-1::GFP [18]. Additionally, prolonged exposure to GO (100 mg/L) significantly increased the percentage of PMK-1::GFP nucleus localization in the intestinal cells [18]. Moreover, the Western blotting analysis demonstrated that prolonged exposure to GO (100 mg/L) obviously increased the expression of phosphorylated PMK-1 [18]. The decreased expression in PMK-1::GFP was further observed in GO (100 mg/L)-exposed *sek-1(ag1)* or *nsy-1(ag3)* mutant nematodes, and the decreased phosphorylation of p38 MAPK/PMK-1 was detected in GO (100 mg/L)-exposed *sek-1(ag1)* or *nsy-1(ag3)* mutant nematodes [18]. These observations suggest that the p38 MAPK signal may be upregulated by the GO exposure in nematodes. The

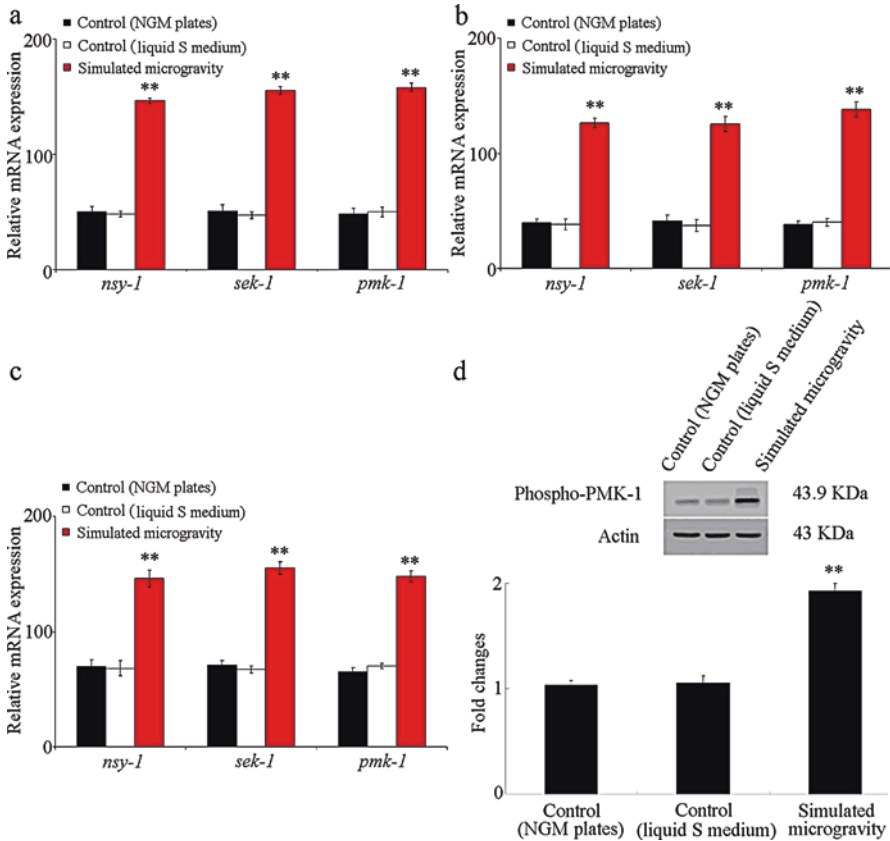


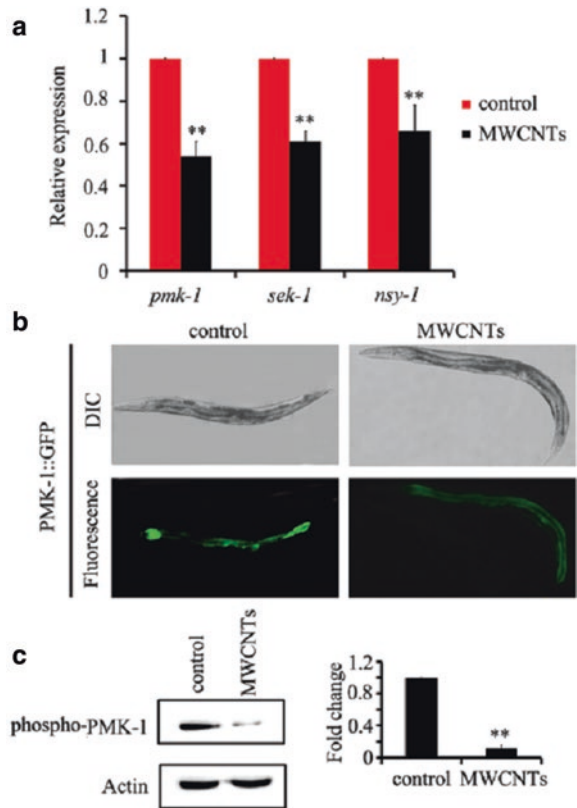
Fig. 4.1 Effect of simulated microgravity on expression of p38 MAPK signaling in wild-type nematodes [7]. (a) Effect of simulated microgravity on expression of p38 MAPK signaling in wild-type nematodes using *tba-1* as a reference gene. (b) Effect of simulated microgravity on expression of p38 MAPK signaling in wild-type nematodes using *pmp-3* as a reference gene. (c) Effect of simulated microgravity on expression of p38 MAPK signaling in wild-type nematodes using *act-1* as a reference gene. (d) Western blotting analysis of the effect of simulated microgravity on expression level of phosphorylated PMK-1. Bars represent means \pm SD. ** $P < 0.01$ vs control (NGM plates)

upregulation of p38 MAPK signal was also observed in nematodes exposed to Ag-nanoparticles [19, 20].

Multiwalled carbon nanotubes (MWCNTs) consisting of multiple concentric graphene cylinders could also cause the toxicity on the functions of both primary and secondary targeted organs in nematodes even at environmentally relevant concentrations [21–24]. The most common fungal pathogen *Candida albicans* can invade host tissues and cause life-threatening infections when the immune system of hosts is weakened (e.g., from critical illness) or the competing bacterial flora in hosts are eliminated (e.g., from broad-spectrum antibiotic use) [25–28]. *C. elegans* has also been proven to be helpful for the study of virulence of human pathogenic

fungi [29]. In nematodes, it has been observed that pre-exposure to MWCNTs (more than 100 µg/L) could enhance the adverse effect of *C. albicans* infection in reducing the lifespan [30]. Pre-exposure could enhance the colony formation of *C. albicans* in the body of nematodes and suppress the innate immune response of nematodes by decreasing the expressions of some antimicrobial genes [30]. Different from those observed in simulated microgravity-treated or GO-exposed nematodes, it was found that MWCNTs decreased the expressions of *pmk-1*, *sek-1*, and *nsy-1* and inhibited translational expression of PMK-1::GFP in the intestine and phosphorylation of PMK-1 (Fig. 4.2) [30]. Epistasis assays further suggested that MWCNTs required the involvement of the p38 MAPK signaling pathway mediated by a NSY-1-SEK-1-PMK-1 cascade to enhance the toxicity of fungal infection, to increase fungal colony formation, and to suppress innate immune response [30]. Thus, the dysregulation pattern of p38 MAPK signaling pathway may be different under different stress conditions in nematodes.

Fig. 4.2 Pre-exposure to MWCNTs altered expression patterns of genes encoding the p38 MAPK signaling pathway in wild-type nematodes [30]. (a) Effects of MWCNT exposure on transcriptional expression of *pmk-1*, *sek-1*, and *nsy-1*. (b) Effects of MWCNT exposure on expression pattern of PMK-1::GFP. (c) Western blot analysis of the effect of MWCNT exposure on expression level of phosphorylated PMK-1. Actin protein was used as the loading control. Nematodes were exposed to MWCNTs from L1-larvae to young adults in 12-well sterile tissue culture plates at 20 °C in the presence of food (OP50). MWCNT exposure concentration was 1000 µg/L. Bars represent means ± SEM ***P* < 0.01 vs control



4.2.2 p38 MAPK Signaling Pathway Regulates the Toxicity of Environmental Toxicants or Stresses

With the simulated microgravity treatment as an example, intestinal ROS production and lifespan were selected as the toxicity assessment endpoints. In wild-type nematodes, simulated microgravity did not significantly affect the longevity (Fig. 4.3) [7]. The lifespan of wild-type nematodes grown in liquid S medium was similar to that on normal NGM plates under the normal conditions, and mutation of

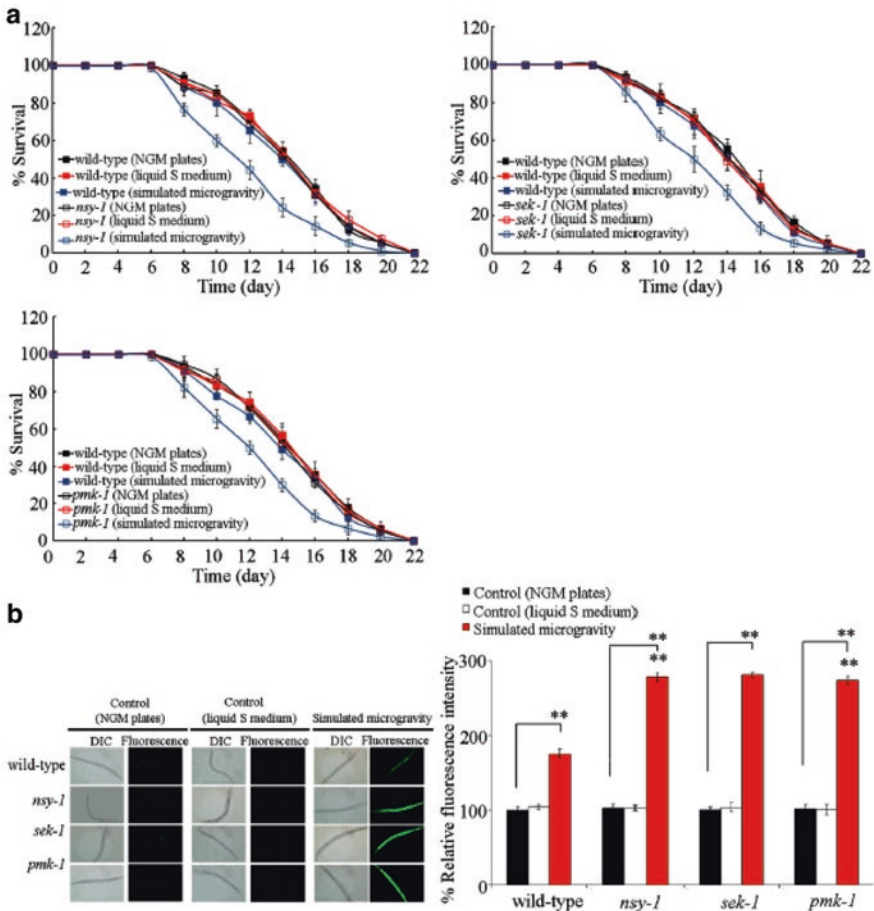


Fig. 4.3 Mutation of genes encoding p38 MAPK signaling pathway induced a susceptibility to simulated microgravity treatment in nematodes [7]. (a) Mutation of genes encoding p38 MAPK signaling pathway induced the reduced lifespan in simulated microgravity-treated nematodes. (b) Mutation of genes encoding p38 MAPK signaling pathway induced a susceptibility to simulated microgravity treatment in inducing intestinal ROS production. Bars represent means \pm SD. ** $P < 0.01$ vs wild type (if not specially indicated)

nsy-1, *sek-1*, or *pmk-1* did not alter the longevity under the normal conditions (Fig. 4.3) [7]. However, after the simulated microgravity treatment, mutation of *nsy-1*, *sek-1*, or *pmk-1* significantly reduced the lifespan (Fig. 4.3) [7]. Meanwhile, the wild-type nematodes grown in liquid S medium or on normal NGM plates did not have the significant induction of intestinal ROS production, and the *nsy-1*, *sek-1*, and *pmk-1* mutants grown in liquid S medium or grown on normal NGM plates also did not have the significant induction of intestinal ROS production under the normal conditions (Fig. 4.3) [7]. In wild-type nematodes, simulated microgravity treatment caused the significant induction of intestinal ROS production (Fig. 4.3) [7]. Moreover, after simulated microgravity treatment, mutation of *nsy-1*, *sek-1*, or *pmk-1* could induce the more severe induction of intestinal ROS production compared with wild-type nematodes (Fig. 4.3) [7].

Under the normal conditions, *pmk-1(km25)*, *sek-1(ag1)*, or *nsy-1(ag3)* mutant also has the normal locomotion behavior [18]. Similarly, prolonged exposure to GO (100 mg/L) induced the formation of more severe reduction in lifespan, decrease in locomotion behavior, and induction of intestinal ROS production in *pmk-1(km25)*, *sek-1(ag1)*, or *nsy-1(ag3)* mutant than those in wild-type nematodes [18]. Therefore, mutations of genes encoding the core p38 MAPK signaling pathway may induce a susceptibility to toxicity of environmental toxicants or stresses, such as the GO exposure and the simulated microgravity treatment. In contrast, overexpression of *pmk-1*, *sek-1*, or *nsy-1* could significantly decrease the induction of intestinal ROS production [18]. Under normal conditions, the nematodes with the overexpression of *pmk-1*, *sek-1*, or *nsy-1* do not exhibit the obvious induction of intestinal ROS production [18]. These observations imply the important role of the p38 MAPK signaling pathway in the regulation of toxicity of environmental toxicants or stresses.

4.2.3 Intestinal Signaling Cascade of p38 MAPK Signaling Pathway Regulates the Toxicity of Environmental Toxicants or Stresses

pmk-1 is broadly expressed in multiple tissues including the intestine, *sek-1* is expressed in the excretory canal, the intestine, and the neurons, and *nsy-1* is expressed in the intestine, the hypodermis, and the neurons. Under the normal conditions, the nematodes with intestinal RNAi knockdown of *pmk-1*, *sek-1*, or *nsy-1* exhibited the similar lifespan to VP303 nematodes (Fig. 4.4) [18]. With the simulated microgravity as an example, it was found that neuronal expression of *pmk-1* did not affect the lifespan and the induction of intestinal ROS production in simulated microgravity-treated *pmk-1* mutant nematodes; however, intestinal expression of *pmk-1* could significantly increase the lifespan and suppress the induction of intestinal ROS production in simulated microgravity-treated *pmk-1* mutant

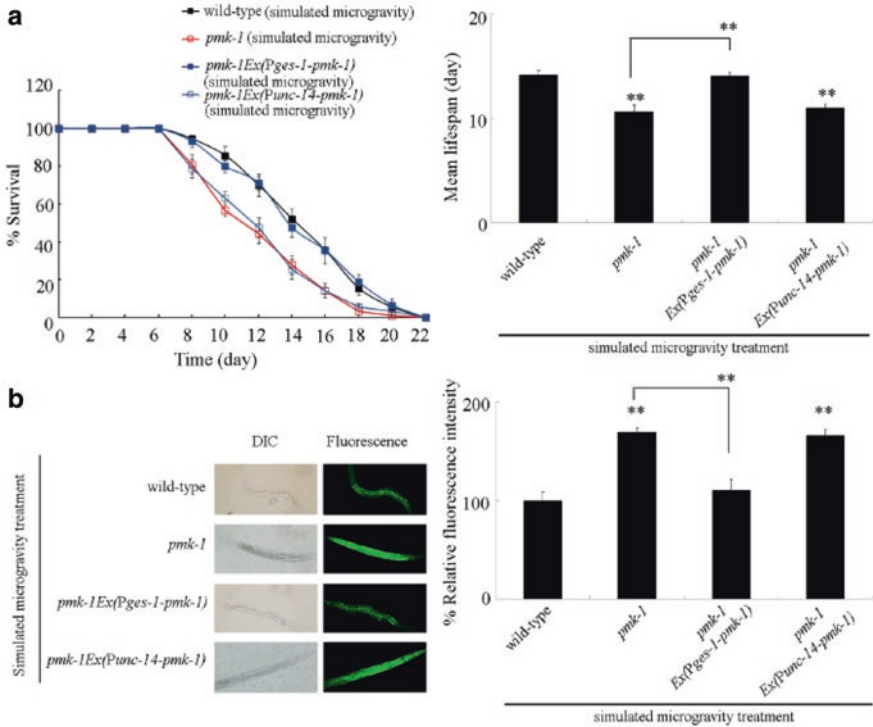


Fig. 4.4 Tissue-specific activity of PMK-1 in regulating the response of nematodes to simulated microgravity [7]. (a) Tissue-specific activity of PMK-1 in regulating lifespan in simulated microgravity-treated nematodes. (b) Tissue-specific activity of PMK-1 in regulating the induction of intestinal ROS production in simulated microgravity-treated nematodes. Bars represent means \pm SD. ** $P < 0.01$ vs wild-type (if not specially indicated)

nematodes (Fig. 4.4) [7]. Meanwhile, after simulated microgravity treatment, intestinal RNAi knockdown of *nsy-1*, *sek-1*, or *pmk-1* could reduce the lifespan and lead to the more severe induction of intestinal ROS production compared with that in VP303 strain [7]. Moreover, intestinal overexpression of PMK-1 induced a resistance to simulated microgravity treatment, since intestinal overexpression of PMK-1 significantly suppressed the induction of intestinal ROS production observed in simulated microgravity-treated wild-type nematodes [7]. Therefore, the core p38 MAPK signaling pathway may act in the intestine to regulate the toxicity of environmental toxicants or stresses in nematodes.

Similarly, with GO as an example, it has been also found that intestinal RNAi knockdown of *pmk-1*, *sek-1*, or *nsy-1* also induced a susceptibility to GO toxicity on lifespan [18], suggesting that the signaling cascade of NSY-1-SEK-1-PMK-1 can act in the intestine to regulate the GO toxicity (Fig. 4.5) [18].

Fig. 4.5 A diagram showing the intestinal p38 MAPK-SKN-1/Nrf signaling cascade involved in the control of GO toxicity in nematodes [18]

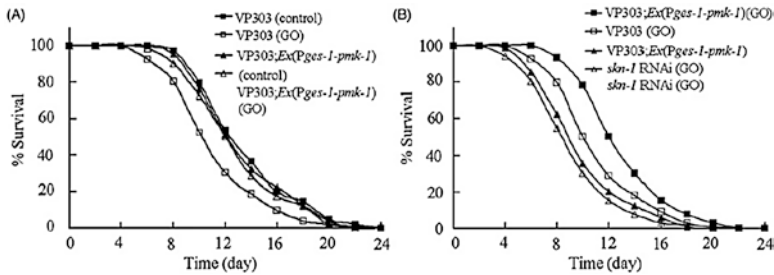
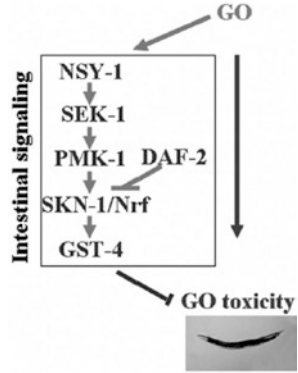


Fig. 4.6 Intestinal RNAi of *skn-1* suppressed lifespan of nematodes overexpressing *pmk-1* in intestine [18]. (a) Effect of overexpression of *pmk-1* in intestine on lifespan. (b) Effect of intestinal RNAi of *skn-1* on lifespan in nematodes overexpressing *pmk-1* in intestine. VP303 is a tool for the RNAi only in intestine. Prolonged exposure was performed from L1-larvae to young adults. GO exposure concentration was 100 mg/L.

4.2.4 SKN-1 Acts as an Important Target for Intestinal PMK-1 in Regulating the Toxicity of Environmental Toxicants or Stresses

4.2.4.1 Conformation of the Role of SKN-1 as the Target for Intestinal PMK-1 in Regulating the Toxicity of Environmental Toxicants or Stresses

SKN-1 plays a central role in the activation of oxidative stress in nematodes [31]. Intestinal RNAi knockdown of *skn-1* could cause a susceptibility to GO toxicity in reducing lifespan and in inducing intestinal ROS production [18], suggesting that SKN-1/Nrf can act in the intestine to regulate the GO toxicity. Moreover, intestinal RNAi knockdown of *skn-1* could suppress the resistance of nematodes overexpressing intestinal *pmk-1* to GO toxicity in reducing lifespan (Fig. 4.6) [18], implying that the intestinal core p38 MAPK signaling cascade may regulate the GO toxicity by acting upstream the transcriptional factor SKN-1/Nrf (Fig. 4.5) [18].

In nematodes, prolonged exposure to GO (100 mg/L) also significantly enhanced the expression of intestinal SKN-1::GFP [18]. Additionally, prolonged exposure to GO (100 mg/L) also significantly increased the percentage of SKN-1::GFP nucleus localization in intestinal cells and the expression of intestinal GST-4::GFP [18].

4.2.4.2 Identification of Downstream Targets for SKN-1 in Regulating the Toxicity of Environmental Toxicants or Stresses

One of the identified important targets for SKN-1 is the phase II detoxification protein GST-4, a glutathione-requiring prostaglandin D synthase. GST-4 is expressed in the intestine, the pharynx, and the hypodermis. Intestinal RNAi knockdown of *gst-4* could induce a susceptibility to GO toxicity in reducing lifespan and in inducing intestinal ROS production [18], suggesting that GST-4 can act in the intestine to regulate the GO toxicity. Genetic interaction analysis indicated that the SKN-1 and the GST-4 could act in the same genetic pathway to regulate the GO toxicity, since exposure to GO (100 mg/L) caused the similar toxicity on lifespan in *skn-1(RNAi); gst-4(ok2108)* to that in *skn-1(RNAi)* strain or in *gst-4(ok2108)* mutant nematodes (Fig. 4.5) [18].

Another identified important target for SKN-1 is the GCS-1, an ortholog of γ -glutamine cysteine synthetase heavy chain [32]. *Pseudomonas aeruginosa* is normally considered to be toxic and will cause a lethal intestinal infection on nematode host [33–37]. After 24 h exposure of *P. aeruginosa* PA14, both the *gcs-1* promoter activation and the GST-4 expression were significantly suppressed by feeding with *skn-1(RNAi)*, suggesting the specific requirement of SKN-1 to elicit these responses (Fig. 4.7) [32].

4.2.5 ATF-7 Acts as Another Important Target for Intestinal PMK-1 in Regulating the Toxicity of Environmental Toxicants or Stresses

In nematodes, the simulated microgravity treatment could cause the significant increase in transcriptional expression of *atf-7* encoding a bZIP transcription factor [7]. After simulated microgravity treatment, mutation of *atf-7* caused the significant decrease in relative mean lifespan (treatment/Control(NGM plates)) in nematodes (Fig. 4.8) [7]. Meanwhile, after simulated microgravity treatment, the more severe induction of intestinal ROS production was observed in *atf-7* mutant nematodes compared with wild-type nematodes (Fig. 4.8) [7]. Moreover, RNAi knockdown of *atf-7* could further dramatically suppress the induction of GST-4::GFP expression caused by simulated microgravity treatment, and *atf-7* mutation could significantly reduce the lifespan and increase the induction of intestinal ROS production in

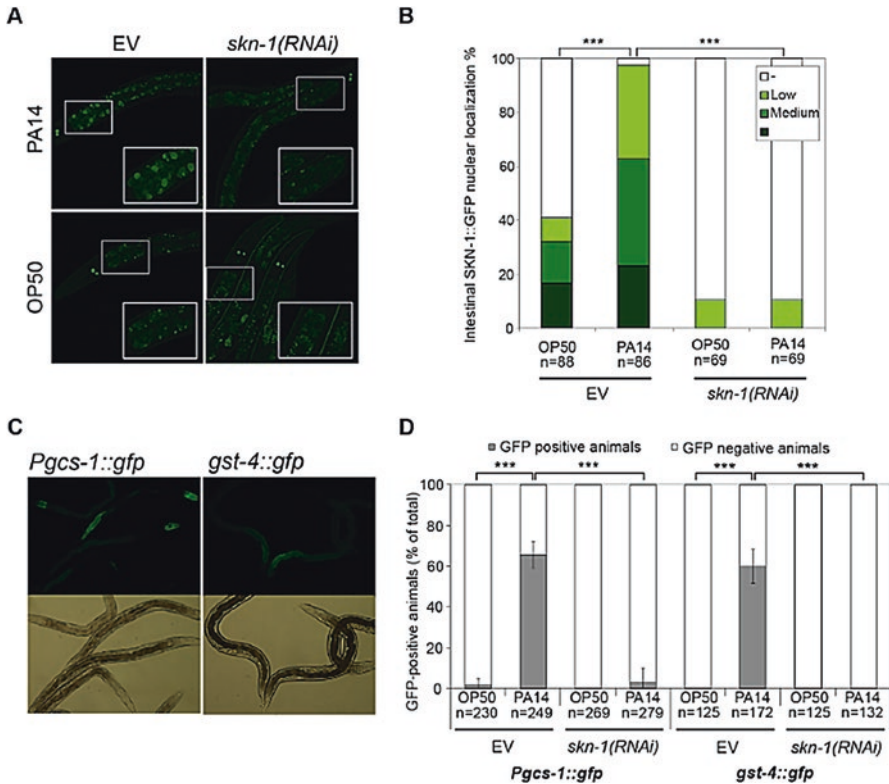


Fig. 4.7 *P. aeruginosa* infection activates SKN-1 [32]. (a) Representative epifluorescence image demonstrating the translocation of SKN-1::GFP in the *Is007*[SKN-1::GFP] strain to intestinal nuclei in L3 larvae, fed by the empty vector or *skn-1* dsRNA, upon a 5-h exposure to *P. aeruginosa* PA14. Note that the intestinal tissue displays autofluorescence, and in the ASI neurons, SKN-1::GFP is not silenced by *skn-1* RNAi treatment. (b) Quantification of SKN-1 nuclear translocation from the data shown on panel (a). “Low” refers to animals in which SKN-1::GFP was detected in less than five intestinal nuclei, while “high” indicates that SKN-1::GFP signal was present in more than 15 intestinal nuclei. (c) Representative epifluorescence microscopic image showing intestinal expression of *Pgc-1::gfp* and *gst-4::gfp* in L3 larvae upon a 24-h PA14 exposure. (d) Quantification of reporter expression demonstrating the SKN-1 dependence of the response. Data were obtained from panel (c) completed with the data of *skn-1(RNAi)* animals. Microscopic images are representatives of three independent experiments. EV: empty vector RNAi

transgenic strain overexpressing intestinal *pmk-1* in simulated microgravity- treated nematodes (Fig. 4.8) [7], which suggests the important role of ATF-7 as the important target for intestinal PMK-1 in regulating the toxicity of environmental toxicants or stresses.

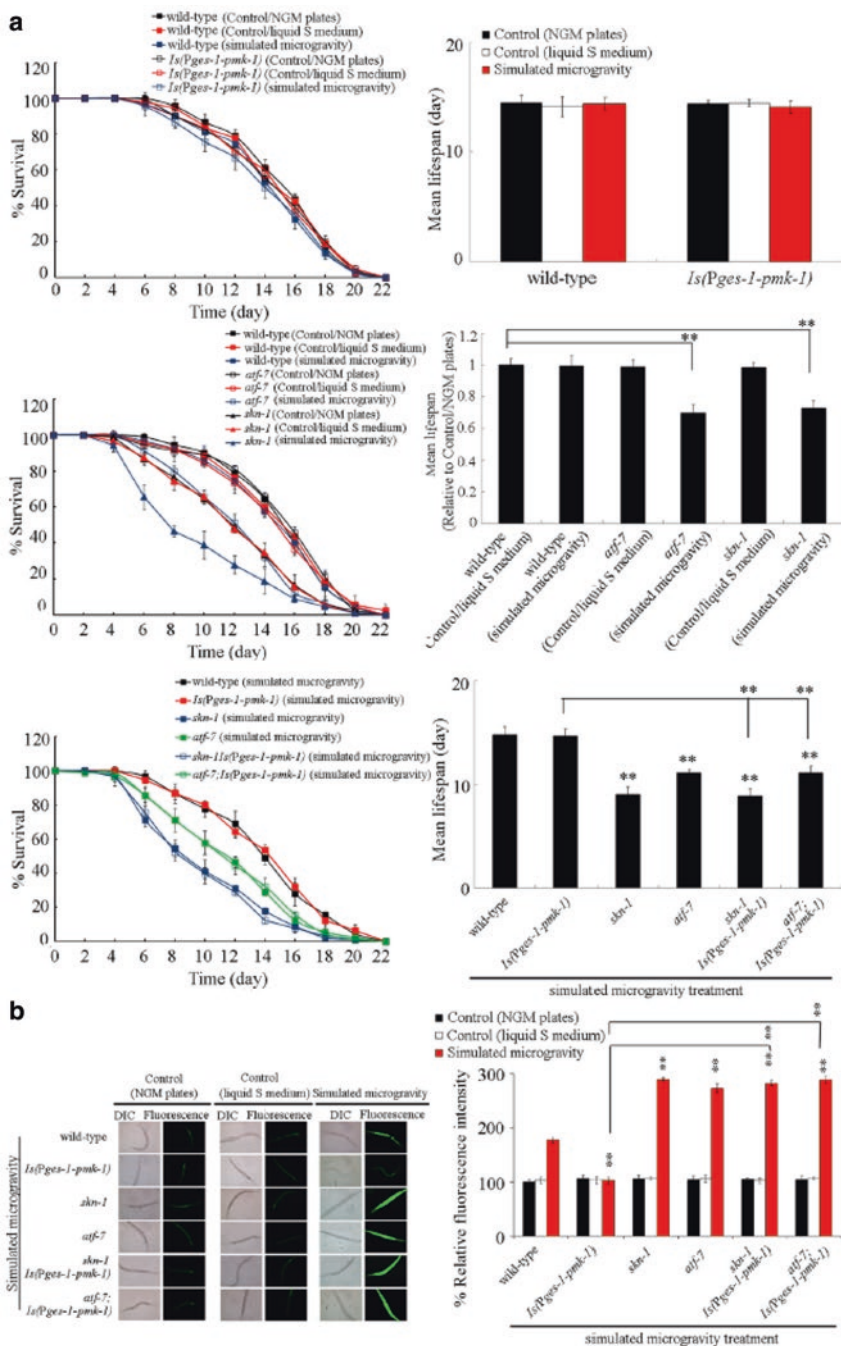


Fig. 4.8 Genetic interaction between PMK-1 and SKN-1 or ATF-7 in regulating the response of nematodes to simulated microgravity [7]. **(a)** Genetic interaction between PMK-1 and SKN-1 or ATF-7 in regulating the lifespan in simulated microgravity-treated nematodes. **(b)** Genetic interaction between PMK-1 and SKN-1 or ATF-7 in regulating the induction of intestinal ROS production in simulated microgravity treatment. Bars represent means \pm SD. $**P < 0.01$ vs wild type (if not specially indicated)

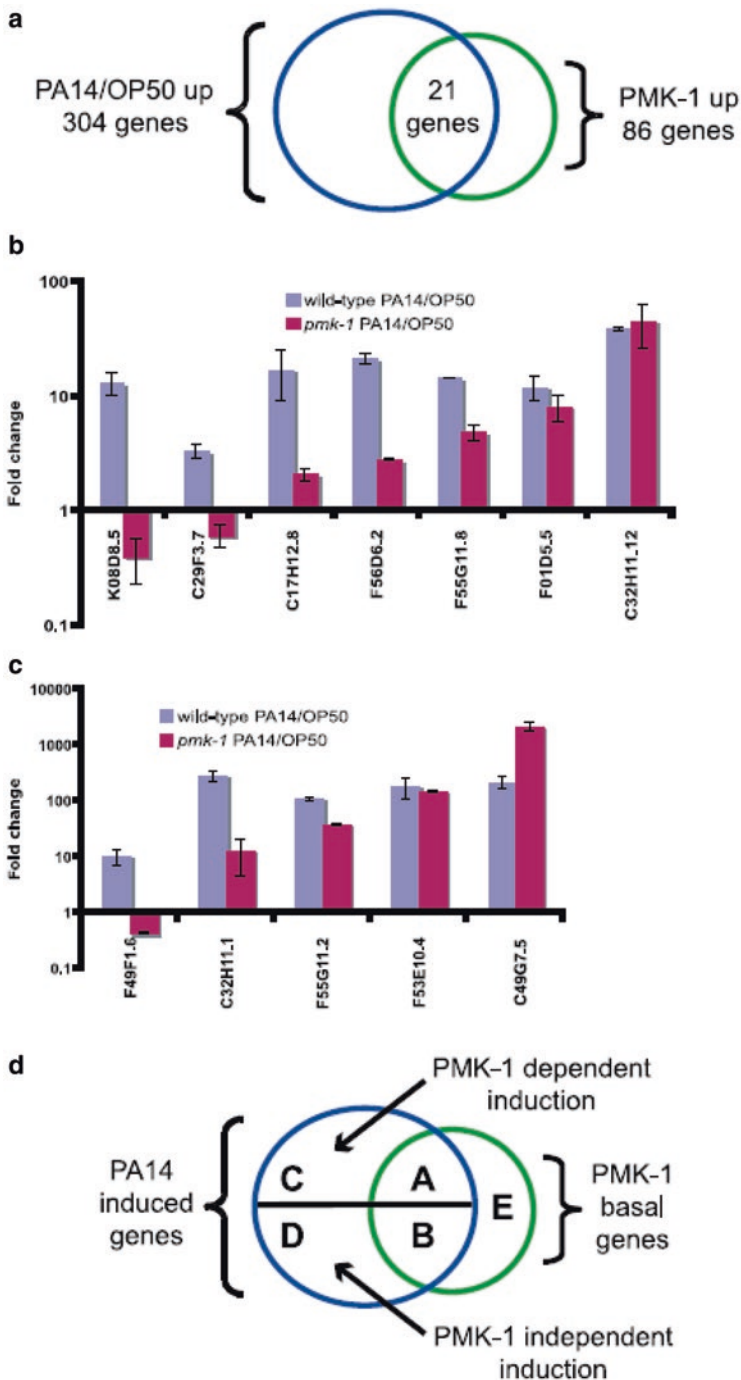


Fig. 4.9 PMK-1 regulates basal and inducible expression of *P. aeruginosa*-induced genes [38]. (a) Venn diagram of overlap between genes regulated by PMK-1 and *P. aeruginosa*. (b, c) qRT-PCR analysis of PA14-induced gene expression in wild-type animals and in *pmk-1* mutants. Results are

4.2.6 *Role of Antimicrobial Proteins as the Targets for PMK-1 in Regulating the Toxicity of Environmental Toxicants or Stresses*

In nematodes, the qRT-PCR analysis demonstrated that the basal expression of the overlap genes requires PMK-1 in animals grown on *E. coli*, and these genes could be induced by infection with *P. aeruginosa* [38]. The further examination on *P. aeruginosa*-induced gene expression in *pmk-1* mutants indicated that most of the overlap genes were not fully induced by *P. aeruginosa* in *pmk-1(km25)* mutant nematodes, suggesting that PMK-1 is required for their induction (Fig. 4.9) [38]. The microarray and qRT-PCR studies of genes regulated by PMK-1 and *P. aeruginosa* identified five classes of candidate immunity genes (Fig. 4.9) [38]. Class A genes are regulated basally by PMK-1 on *E. coli* and require PMK-1 for their induction by pathogenic *P. aeruginosa* (e.g., *K08D8.5*). Class B genes are regulated basally by PMK-1 and are induced by *P. aeruginosa*, but that induction does not require PMK-1 (e.g., *C32H11.12*). Class C genes are not regulated basally by PMK-1 based on microarray results but do require PMK-1 for induction by *P. aeruginosa* (e.g., *F49F1.6*). Class D genes are not regulated basally by PMK-1 based on microarray results and do not require PMK-1 for induction by *P. aeruginosa* (e.g., *C49G7.5*). Class E genes are regulated basally by PMK-1 but are not induced by *P. aeruginosa*.

4.2.7 *Upregulators of p38 MAPK Signaling Pathway in Response to Environmental Toxicants or Stresses*

4.2.7.1 Duox1/BLI-3

ROS can be generated during infection in the model host *C. elegans* by the dual oxidase Duox1/BLI-3 [39]. SKN-1 could be activated in the intestine upon exposure to the human bacterial pathogens, *Enterococcus faecalis* and *P. aeruginosa*, and a weakened response was observed in attenuated mutants of these pathogens [39]. The signaling cascade of NSY-1-SEK-1-PMK-1 was required for the SKN-1

←
Fig. 4.9 (continued) the average of two biological replicates, each replicate measured in duplicate and normalized to a control gene. Error bars are SEM. **(d)** Diagram of different gene classes regulated by PMK-1 and/or *P. aeruginosa*. PMK-1 is required for basal and inducible regulations of class A genes. PMK-1 is required for basal, but not inducible expression of class B genes. PMK-1 is required for inducible but not basal expression of class C genes. PMK-1 is required for neither basal nor inducible expression of class D genes. PMK-1 regulates basal expression of class E genes, but these genes are not induced by *P. aeruginosa*

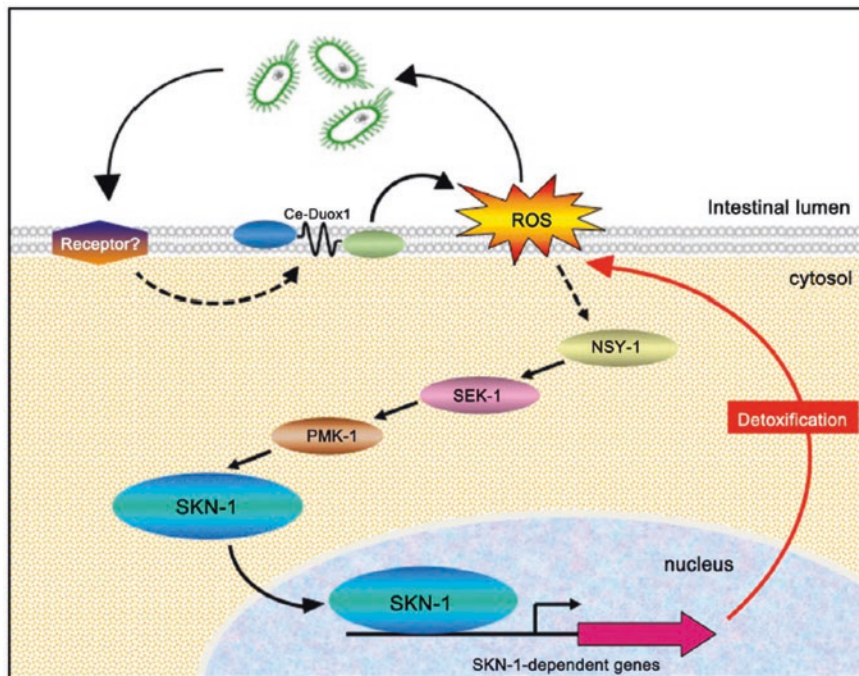


Fig. 4.10 Regulation of SKN-1 activation by Duox1/BLI-3 during infection [39]

activity during the infection [39]. Moreover, it was found that the ROS produced by Duox1/BLI-3 was just the source of SKN-1 activation via p38 MAPK signaling during the infection (Fig. 4.10) [39]. That is, the ROS generation by Duox1/BLI-3 may activate a protective SKN-1 response via p38 MAPK signaling pathway against the environmental toxicants or stresses in nematodes (Fig. 4.10) [39].

4.2.7.2 TIR-1 and VHP-1

In nematodes, silencing the *pmk-1* could entirely prevent the SKN-1-dependent activation of *gcs-1* in response to PA14 infection [32]. The PMK-1 could be inactivated by the dual specificity MAPK phosphatase VHP-1. Suppression of VHP-1 resulted in an increased PMK-1 phosphorylation and a resistance to PA14 infection, and *vhp-1(RNAi)* could significantly increase *Pgcs-1::GFP* activation upon PA14 infection (Fig. 4.11) [32]. Meanwhile, TIR-1, a conserved Toll/IL-1 resistance (TIR) domain protein, has the function to activate the p38 MAPK signaling independently of the Toll-like receptor ortholog TOL-1 during the PA14 infection. RNAi knockdown or mutation of *tir-1* could prevent the *Pgcs-1::GFP* fluorescence upon PA14 infection and prevent the nuclear translocation of SKN-1 induced by PA14 infection (Fig. 4.11) [32].

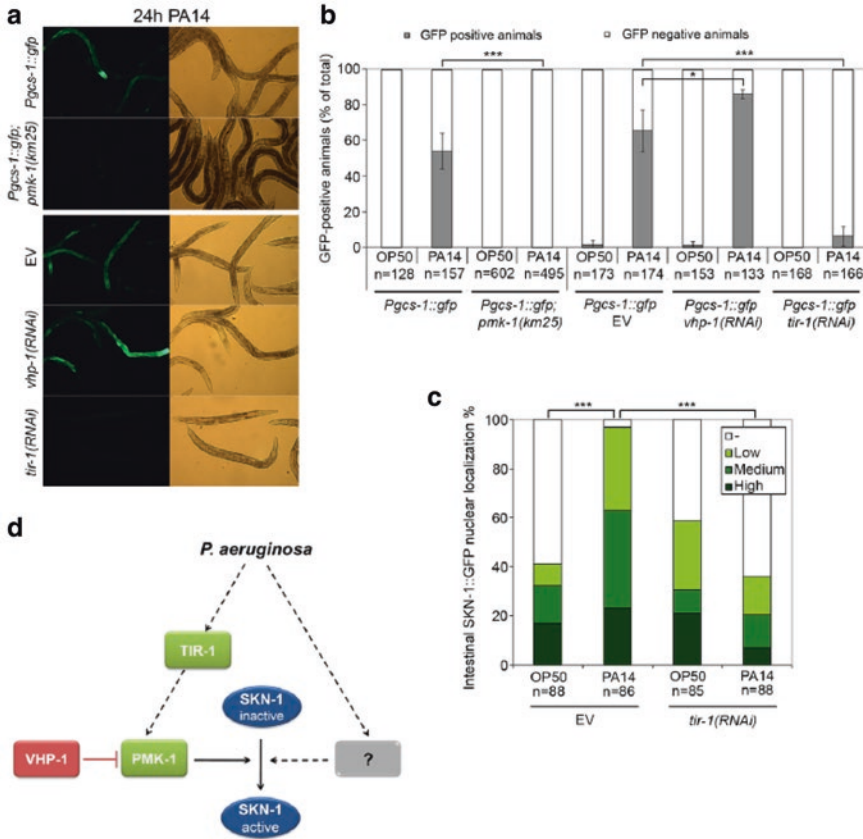


Fig. 4.11 The pathogen response-specific TIR-1 and p38 MAPK PMK-1 are required for SKN-1 activation upon *P. aeruginosa* infection [32]. (a) Representative epifluorescence microscopic images showing the expression of *Pgc-1::GFP* in *pmk-1(km25)* mutants as well as in the p38 MAPK phosphatase *vhp-1(RNAi)* and the Toll/IL-1 resistance (TIR) domain protein *tir-1(RNAi)* animals in response to *P. aeruginosa* infection. L3 larvae were exposed to PA14 for 24 h. Microscopic images are representatives from three independent experiments. (b) Quantification of reporter expression from the data shown on panel (a) completed with the data of control animals fed by OP50 for 24 h. (c) Quantification of SKN-1 nuclear translocation in *tir-1(RNAi)* L3 larvae upon 5 h PA14 exposure. (d) Suggested model of SKN-1 activation during *P. aeruginosa* infection. Upon exposure to PA14, the TIR-1/PMK-1 pathway is indispensable but insufficient to elicit SKN-1 transactivation. Solid arrows indicate a direct, while dashed arrows indicate an indirect/unknown connection. EV empty vector RNAi

4.2.7.3 MEK-1

mek-1 encodes a MAP kinase kinase (MAPKK). In nematodes, both the SEK-1 and the MEK-1 were essential for the PMK-1 activation (Fig. 4.12) [40]. Additionally, although RNAi knockdown of *pmk-1* did not affect the lifespan of *sek-1* mutant nematodes after pathogen infection, RNAi knockdown of *pmk-1* could further

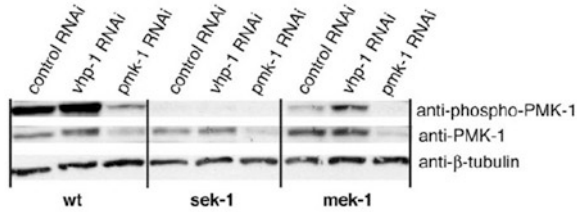


Fig. 4.12 Modulation of PMK-1 activation by MEK-1 and SEK-1 MAPKs and VHP-1 MKP: correlation of pathogen susceptibility with levels of PMK-1 activation [40]. Immunoblot analysis of lysates derived from WT and *sek-1(km4)* and *mek-1(ks54)* mutants subjected to RNAi by feeding with bacterial strains expressing double-stranded RNA corresponding to the sequence of control (L4440 vector only), *pmk-1* (pDK177), or *vhp-1* (Ahringer 44D3) genes. Activated levels of PMK-1 were detected by using an Ab (anti-phospho-p38) specific for the doubly phosphorylated form of PMK-1.

reduce the lifespan of *mek-1* mutant nematodes after pathogen infection [40]. Therefore, both the MEK-1 and the signaling cascade of NSY-1-SEK-1 can act upstream of PMK-1 to regulate the response of nematodes to environmental toxicants or stresses in nematodes.

4.2.7.4 Mitochondrial Complex I

In nematodes, downregulating complex I gene *nuo-2* or *nduf-6* could cause a significant increase in p38MAPK phosphorylation (Fig. 4.13) [41]. Meanwhile, downregulation of at least five of the six tested mitochondrial complex I genes could upregulate four of the seven ATF-7-dependent genes induced by rotenone: *C17H12.8*, *F56D6.2*, and *M02F4.7* (C-type lectins) and *F49F1.6* (*mul-1*, a mucin-like protein) (Fig. 4.13) [41]. In contrast, RNAi-mediated downregulation of the respiratory chain complex assembly factor *oxa-1*, complex III, complex IV, and complex V ATP synthase subunits did not increase the levels of phosphorylated p38 MAPK (Fig. 4.13) [41]. These observations suggest that mitochondrial complex I dysfunction can act upstream of the p38MAPK signaling pathway to regulate the stress response in nematodes.

4.3 JNK Signaling Pathway

In nematodes, the c-Jun N-terminal kinase (JNK) signaling pathway mainly contains members of MEK-1, JKK-1, and JNK-1 [42]. *mek-1* and *jkk-1* encode MAP kinase kinases, homolog of human MKK-7a, and act as an activator of JNK. *jnk-1* encodes a serine/threonine kinase, homolog of human JNK, and acts as the sole member of the JNK subgroup of MAP kinase [42].

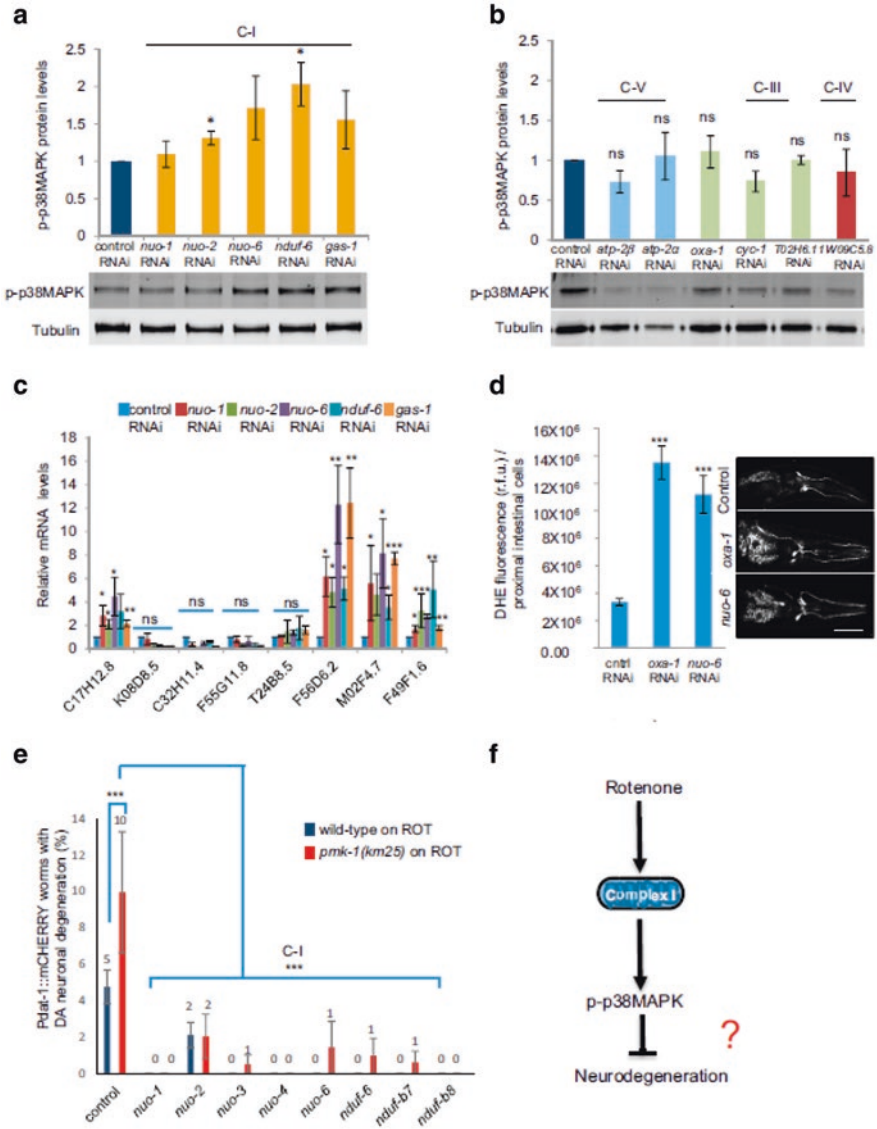


Fig. 4.13 Mitochondrial complex I dysfunction activates p38 MAPK/ATF-7 [41]. (a, b) Levels of phosphorylated p38MAPK following RNAi-mediated downregulation of complex I (C-I) subunits (a) and complex V (C-V), *oxa-1*, complex III (C-III), and complex IV (C-IV) subunits (b) relative to control RNAi-treated animals. Levels of phospho-p38MAPK (top lanes) were quantified relative to α -tubulin (bottom lanes). (c) mRNA levels of ATF-7-dependent innate immune genes in control animals and animals on complex I RNAi, determined by qRT-PCR. mRNA levels of the transcripts (x axis) were normalized to wild-type control levels. Actin is the internal control. (d) Levels of dihydroethidium (DHE) fluorescence quantitated in proximal intestinal cells of animals on control RNAi, complex I subunit *nuo-6* RNAi, and mitochondrial assembly factor *oxa-1* RNAi. Representative micrographs are of the anterior regions of animals. RFU, relative fluorescence units. Scale bar, 30 μ m

4.3.1 Exposure to Environmental Toxicants or Stress Dysregulates the Expression of JNK MAPK Signal

With the GO as an example, after prolonged exposure, the transcriptional expressions of *mek-1*, *jkk-1*, and *jnk-1* were significantly decreased by GO exposure (10 mg/L) [43], suggesting that exposure to certain environmental toxicants or stress can dysregulate the expression of JNK MAPK signal in nematodes.

4.3.2 JNK MAPK Signaling Pathway Regulates the Toxicity of Environmental Toxicants or Stresses

In nematodes, mutation of *mek-1* or *jnk-1* could induce a susceptibility to Cd or Cu toxicity in inhibiting the survival [44, 45]. Besides this, mutation of *mek-1*, *jkk-1*, or *jnk-1* could also induce a susceptibility to GO toxicity in reducing brood size, in decreasing locomotion behavior, and in inducing intestinal ROS production (Fig. 4.14) [43], which suggests the involvement of JNK MAPK signaling pathway in the regulation of toxicity of environmental toxicants or stresses, such as GO exposure.

The genetic interaction analysis further indicated that the *jnk-1(gk7);mek-1(ks54)* double mutant exhibited the similar GO toxicity in reducing brood size, in decreasing locomotion behavior, and in inducing intestinal ROS production to that in the *mek-1(ks54)* or the *jnk-1(gk7)* single mutant (Fig. 4.14) [43]. Meanwhile, the *jnk-1(gk7);jkk-1(km2)* double mutant showed the similar GO toxicity in reducing brood size, in decreasing locomotion behavior, and in inducing intestinal ROS production to that in the *jkk-1(km2)* or the *jnk-1(gk7)* single mutant (Fig. 4.14) [43]. Additionally, the activated JNK-1 was detected only in neuronal cells, and JNK-1 was found to be controlled by the MAPK JKK-1 under the heat stress [46]. These results demonstrated that the MEK-1 and the JKK-1 may act genetically in the same pathway with JNK-1 in the regulation of toxicity of environmental toxicants or stresses in nematodes.

In nematodes, the JNK MAPK signaling pathway is regulated by MLK-1 MAPK kinase kinase (MAPKKK), MEK-1 MAPK kinase (MAPKK), and KGB-1 JNK-like MAPK [47]. Moreover, loss-of-function mutation of *shc-1* encoding a homolog of Shc was defective in activation of KGB-1 and caused the hypersensitivity to heavy metals [47]. Introduction of a mutation that perturbs binding to the PTB domain or the NPXY motif could abolish the function of SHC-1 or MLK-1 and the resistance to heavy metal stress [47]. These results imply that the SHC-1 can act as a scaffold to link MLK-1/MAPKKK to MEK-1/MAPKK activation in the KGB-1/MAPK signal transduction pathway (Fig. 4.15) [47].

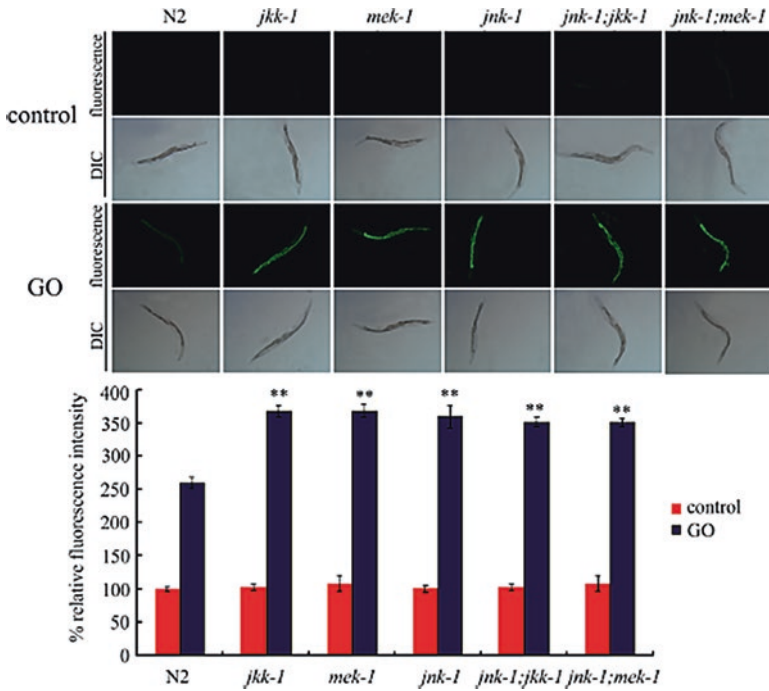
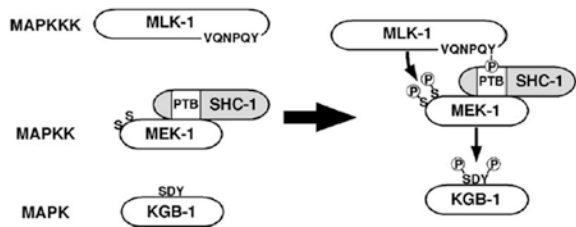


Fig. 4.14 Effects of mutations in the gene encoding JNK signaling pathways on intestinal ROS production in GO-exposed nematodes [43]. Bars represent the mean \pm SEM ** $P < 0.01$ vs wild-type N2. GO (10 mg/L) was exposed from L1-larvae to adult day 1

Fig. 4.15 Proposed model for SHC-1 function in the KGB-1 JNK signaling pathway [47]



4.4 ERK Signaling Pathway

4.4.1 Exposure to Environmental Toxicants or Stress Dysregulates the Expression of ERK MAPK Signal

In nematodes, the core ERK signaling pathway contains the *mek-2*-encoded MAPK kinase MEK and *mpk-1*-encoded ERK [48]. With GO as an example, although prolonged exposure to GO (1 mg/L) did not influence the expressions of *mpk-1* and *mek-1*, prolonged exposure to GO (10 or 100 mg/L) could significantly increase

both the transcriptional expression of *mpk-1* and the transcriptional expression of *mek-2* [49]. Therefore, exposure to environmental toxicants or stress can dysregulate the expression of ERK MAPK signal, and the increase in the expression of ERK signal may mediate a protection mechanism for nematodes in response to environmental toxicants or stresses, such as GO exposure.

4.4.2 ERK MAPK Signaling Pathway Regulates the Toxicity of Environmental Toxicants or Stresses

Using lifespan and intestinal ROS production as the toxicity assessment endpoints, mutation of *mpk-1* or *mek-2* resulted in the more severe reduction in lifespan and induction of intestinal ROS production in GO-exposed nematodes (Fig. 4.16) [49], suggesting that mutation of *mpk-1* or *mek-2* may induce a susceptibility to the toxicity of environmental toxicants or stresses.

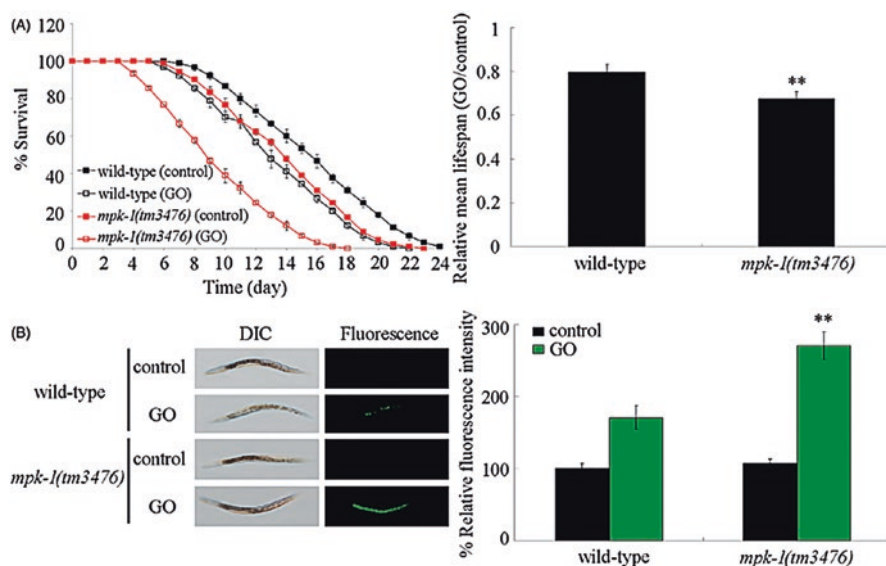


Fig. 4.16 Effects of *mpk-1* mutation on the GO toxicity [49]. (a) Effects of *mpk-1* mutation on the GO toxicity in reducing lifespan. (b) Effects of *mpk-1* mutation on the GO toxicity in inducing ROS production. Prolonged exposure was performed from L1-larvae to young adults. GO exposure concentration was 10 mg/L. Bars represent means \pm SD. ** $p < 0.01$ vs wild type

4.4.3 Signaling Cascade of ERK MAPK Signaling Pathway in the Regulation of Toxicity of Environmental Toxicants or Stresses

Genetic interaction analysis demonstrated that mutation of *mpk-1* could significantly suppress the resistance of nematodes overexpressing the neuronal *mek-2* to GO toxicity in reducing lifespan and in inducing intestinal ROS production (Fig. 4.17) [49], suggesting that the MPK-1 acts downstream of the neuronal MEK-2 to regulate the toxicity of environmental toxicants or stresses, such as GO exposure.

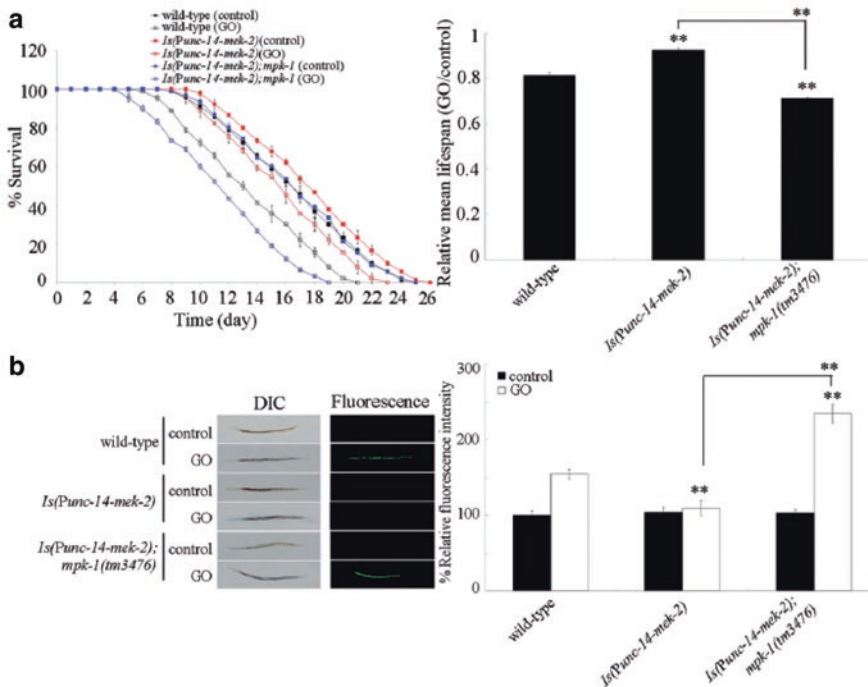


Fig. 4.17 Genetic interaction between MEK-2 and MPK-1 in the regulation of GO toxicity [49]. (a) Genetic interaction between MEK-2 and MPK-1 in the regulation of GO toxicity in reducing lifespan. (b) Genetic interaction between MEK-2 and MPK-1 in the regulation of GO toxicity in inducing ROS production. Prolonged exposure was performed from L1-larvae to young adults. GO exposure concentration was 10 mg/L. Bars represent means \pm SD. ** $p < 0.01$ versus wild-type (if not specially indicated)

4.4.4 Identification of Potential Downstream Targets for Neuronal MPK-1 in Regulating the Toxicity of Environmental Toxicants or Stresses

In nematodes, MPK-1 is expressed in both the neurons and the germline. Expression of the *mpk-1* in the neurons could suppress the susceptibility of *mpk-1(tm3476)* mutant to GO toxicity in reducing lifespan and in inducing intestinal ROS production; however, germline-specific RNAi knockdown of *mpk-1* could not significantly induce a susceptibility to GO toxicity like the phenotypes observed in the *mpk-1(tm3476)* mutant [49]. Additionally, expression of the *mek-2* in the neurons could also significantly suppress the susceptibility of *mek-2(n1989)* mutant to GO toxicity in reducing lifespan and in inducing intestinal ROS production [49]. These results suggest that the neuronal signaling cascade of MEK-2-MPK-1 may play a crucial role in regulating the response of nematodes to GO exposure.

Moreover, it was found that mutation of *skn-1* could significantly suppress the resistance of nematodes overexpressing neuronal *mpk-1* to GO toxicity in reducing lifespan and in inducing intestinal ROS production (Fig. 4.18) [49], suggesting that the SKN-1 can act as a downstream target for neuronal MPK-1 to regulate the toxicity of environmental toxicants or stresses. In nematodes, *aex-3* encodes a guanine nucleotide exchange factor. It was further observed that mutation of *aex-3* could significantly suppress the resistance of nematodes overexpressing neuronal *mpk-1* to GO toxicity in reducing lifespan and in inducing intestinal ROS production (Fig. 4.18) [49], suggesting that the AEX-3 can act as another downstream target for neuronal MPK-1 to regulate the toxicity of environmental toxicants or stresses.

In nematodes, mutation of *aex-3* could further significantly suppress the resistance of nematodes overexpressing the neuronal *skn-1b* to GO toxicity in reducing lifespan and in inducing intestinal ROS production [49], suggesting the formation of neuronal signaling cascade of MEK-1-MPK-1-SKN-1b-AEX-3 in the regulation of toxicity of environmental toxicants or stresses in nematodes.

4.4.5 Identification of Upstream Regulators for ERK MAPK Signaling Pathway in Regulating the Toxicity of Environmental Toxicants or Stresses

In nematodes, *lin-45* encodes a Raf protein in ERK signaling pathway and acts upstream of the signaling cascade of MEK-1-MPK-1. It was found that mutation of *lin-45* induced a susceptibility to GO toxicity in inducing intestinal ROS production and in decreasing locomotion behavior [50].

pkc-1 encodes a serine/threonine protein kinase C (PKC) protein. It was further observed that mutation of *lin-45* could noticeably inhibit the resistance of transgenic

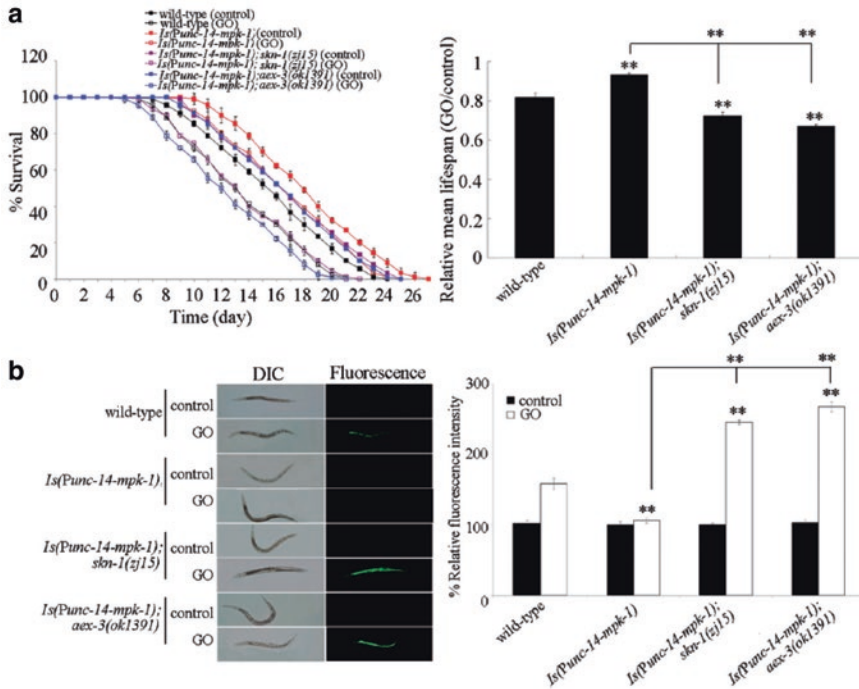
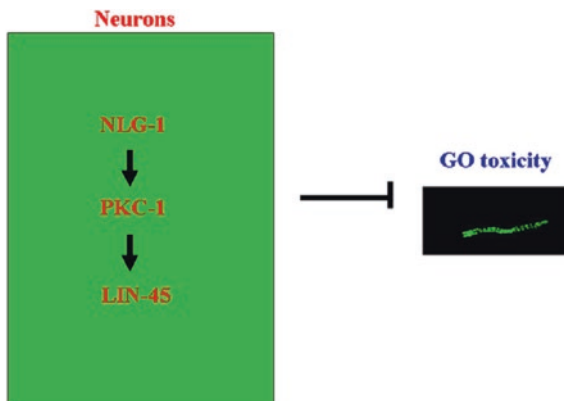


Fig. 4.18 Identification of potential downstream targets for neuronal MPK-1 in the regulation of response to GO exposure [49]. **(a)** Effect of *skn-1* or *aex-3* mutation on the resistance of nematodes overexpressing neuronal *mpk-1* to GO toxicity in reducing lifespan. **(b)** Effect of *skn-1* or *aex-3* mutation on the resistance of nematodes overexpressing neuronal *mpk-1* to GO toxicity in inducing ROS production. Prolonged exposure was performed from L1-larvae to young adults. GO exposure concentration was 10 mg/L. Bars represent means \pm SD. ** $p < 0.01$ vs wild type (if not specially indicated)

nematodes overexpressing neuronal PKC-1 to GO toxicity in inducing intestinal ROS production and in decreasing locomotion behavior [50], suggesting LIN-45 acts downstream of neuronal PKC-1 to regulate the response to GO exposure.

In nematodes, *nlg-1* gene encodes a neuroligin, a postsynaptic cell adhesion protein. After GO (1 mg/L) exposure, mutation of *nlg-1* could significantly decrease the expression of *pkc-1* [50]. Moreover, mutation of *pkc-1* could obviously suppress the resistance of transgenic nematodes overexpressing neuronal NLG-1 to GO toxicity in inducing intestinal ROS production and in decreasing locomotion behavior [50], suggesting that PKC-1 can further act downstream of neuronal NLG-1 to regulate the response to GO exposure. Therefore, a signaling cascade of NLG-1-PKC-1-LIN-45 was identified to act upstream of ERK MAPK signaling pathway to regulate the toxicity of environmental toxicants or stresses in nematodes (Fig. 4.19) [50].

Fig. 4.19 A diagram showing the role of neuronal NLG-1-PKC-1-LIN-45 signaling cascade in the induction of GO toxicity in nematodes [50]



4.5 Perspectives

In this chapter, we introduced and discussed the involvement and contribution of three important MAPK signaling pathways (p38 MAPK, JNK MAPK, and ERK MAPK) in regulating the toxicity of environmental toxicants or stresses in nematodes. The introduced information here can largely reflect the crucial role of these three MAPK signaling pathways in the regulation of toxicity of environmental toxicants or stresses. So far, many more information for the involvement and the underlying molecular mechanisms of p38 MAPK signaling pathway in regulating the toxicity of environmental toxicants or stresses is available in nematodes. In contrast to this, the available information for the involvement and the underlying molecular mechanisms of JNK MAPK or ERK MAPK signaling pathway in regulating the toxicity of environmental toxicants or stresses is relatively limited.

Moreover, there are at least two critical questions needed to be further clarified and elucidated. First of all, how these three MAPK signaling pathways transduce the extracellular cues into the cells through the intestinal barrier is still largely unknown. Additionally, the interactions among these three MAPK signaling pathways in different tissues to regulate the toxicity of environmental toxicants or stresses are still largely unclear. That is, what network may be formed among these three MAPK signaling pathways in the regulation of toxicity of environmental toxicants or stresses in nematodes?

References

1. Wang D-Y (2018) Nanotoxicology in *Caenorhabditis elegans*. Springer, Singapore
2. Matsukawa J, Matsuzawa A, Takeda K, Ichijo H (2004) The ASK1-MAP kinase cascades in mammalian stress response. *J Biochem* 136:261–265
3. Roux PP, Blenis J (2004) ERK and p38 MAPK-activated protein kinases: a family of protein kinases with diverse biological functions. *Microbiol Mol Biol Rev* 68:320–344

4. Altman PL, Talbot JM (1987) Nutrition and metabolism in spaceflight. *J Nutr* 117:421–427
5. Smith SM, Zwart SR, Block G, Rice BL, Davis-Street JE (2005) The nutritional status of astronauts is altered after long-term space flight aboard the international Space Station. *J Nutr* 135:437–443
6. Zhao L, Rui Q, Wang D-Y (2017) Molecular basis for oxidative stress induced by simulated microgravity in nematode *Caenorhabditis elegans*. *Sci Total Environ* 607–608:1381–1390
7. Li W-J, Wang D-Y, Wang D-Y (2018) Regulation of the response of *Caenorhabditis elegans* to simulated microgravity by p38 mitogen-activated protein kinase signaling. *Sci Rep* 8:857
8. Geim AK (2009) Graphene: status and prospects. *Science* 324:1530–1534
9. Bitounis D, Ali-Boucetta H, Hong BH, Min D, Kostarelos K (2013) Prospects and challenges of graphene in biomedical applications. *Adv Mater* 25:2258–2268
10. Yang K, Li Y, Tan X, Peng R, Liu Z (2013) Behavior and toxicity of graphene and its functionalized derivatives in biological systems. *Small* 9:1492–14503
11. Yang R-L, Ren M-X, Rui Q, Wang D-Y (2016) A *mir-231*-regulated protection mechanism against the toxicity of graphene oxide in nematode *Caenorhabditis elegans*. *Sci Rep* 6:32214
12. Zhi L-T, Ren M-X, Qu M, Zhang H-Y, Wang D-Y (2016) Wnt ligands differentially regulate toxicity and translocation of graphene oxide through different mechanisms in *Caenorhabditis elegans*. *Sci Rep* 6:39261
13. Xiao G-S, Zhi L-T, Ding X-C, Rui Q, Wang D-Y (2017) Value of *mir-247* in warning graphene oxide toxicity in nematode *Caenorhabditis elegans*. *RSC Adv* 7:52694–52701
14. Ren M-X, Zhao L, Lv X, Wang D-Y (2017) Antimicrobial proteins in the response to graphene oxide in *Caenorhabditis elegans*. *Nanotoxicology* 11:578–590
15. Xiao G-S, Chen H, Krasteva N, Liu Q-Z, Wang D-Y (2018) Identification of interneurons required for the aversive response of *Caenorhabditis elegans* to graphene oxide. *J Nanbiotechnol* 16:45
16. Ren M-X, Zhao L, Ding X-C, Krasteva N, Rui Q, Wang D-Y (2018) Developmental basis for intestinal barrier against the toxicity of graphene oxide. *Part Fibre Toxicol* 15:26
17. Zhao L, Kong J-T, Krasteva N, Wang D-Y (2018) Deficit in epidermal barrier induces toxicity and translocation of PEG modified graphene oxide in nematodes. *Toxicol Res* 7(6):1061–1070. <https://doi.org/10.1039/C8TX00136G>
18. Zhao Y-L, Zhi L-T, Wu Q-L, Yu Y-L, Sun Q-Q, Wang D-Y (2016) p38 MAPK-SKN-1/Nrf signaling cascade is required for intestinal barrier against graphene oxide toxicity in *Caenorhabditis elegans*. *Nanotoxicology* 10:1469–1479
19. Lim D, Roh JY, Eom HJ, Choi JY, Hyun J, Choi J (2012) Oxidative stress-related PMK-1 P38 MAPK activation as a mechanism for toxicity of silver nanoparticles to reproduction in the nematode *Caenorhabditis elegans*. *Environ Toxicol Chem* 31:585–592
20. Chatterjee N, Eom HJ, Choi J (2014) Effects of silver nanoparticles on oxidative DNA damage-repair as a function of p38 MAPK status: a comparative approach using human Jurkat T cells and the nematode *Caenorhabditis elegans*. *Environ Mol Mutagen* 55:122–133
21. Nouara A, Wu Q-L, Li Y-X, Tang M, Wang H-F, Zhao Y-L, Wang D-Y (2013) Carboxylic acid functionalization prevents the translocation of multi-walled carbon nanotubes at predicted environmental relevant concentrations into targeted organs of nematode *Caenorhabditis elegans*. *Nanoscale* 5:6088–6096
22. Wu Q-L, Li Y-X, Li Y-P, Zhao Y-L, Ge L, Wang H-F, Wang D-Y (2013) Crucial role of biological barrier at the primary targeted organs in controlling translocation and toxicity of multi-walled carbon nanotubes in nematode *Caenorhabditis elegans*. *Nanoscale* 5:11166–11178
23. Zhuang Z-H, Li M, Liu H, Luo L-B, Gu W-D, Wu Q-L, Wang D-Y (2016) Function of RSKS-1-AAK-2-DAF-16 signaling cascade in enhancing toxicity of multi-walled carbon nanotubes can be suppressed by *mir-259* activation in *Caenorhabditis elegans*. *Sci Rep* 6:32409
24. Zhao L, Wan H-X, Liu Q-Z, Wang D-Y (2017) Multi-walled carbon nanotubes-induced alterations in microRNA *let-7* and its targets activate a protection mechanism by conferring a developmental timing control. *Part Fibre Toxicol* 14:27

25. Sun L-M, Liao K, Hong C-C, Wang D-Y (2017) Honokiol induces reactive oxygen species-mediated apoptosis in *Candida albicans* through mitochondrial dysfunction. *PLoS ONE* 12:e0172228
26. Sun L-M, Liao K, Wang D-Y (2017) Honokiol induces superoxide production by targeting mitochondrial respiratory chain complex I in *Candida albicans*. *PLoS ONE* 12:e0184003
27. Sun L-M, Liao K, Li Y-P, Zhao L, Liang S, Guo D, Hu J, Wang D-Y (2016) Synergy between PVP-coated silver nanoparticles and azole antifungal against drug-resistant *Candida albicans*. *J Nanosci Nanotechnol* 16:2325–2335
28. Sun L-M, Liao K, Liang S, Yu P-H, Wang D-Y (2015) Synergistic activity of magnolol with azoles and its possible antifungal mechanism against *Candida albicans*. *J Appl Microbiol* 118:826–838
29. Sun L-M, Zhi L-T, Shakoor S, Liao K, Wang D-Y (2016) microRNAs involved in the control of innate immunity in *Candida* infected *Caenorhabditis elegans*. *Sci Rep* 6:36036
30. Shakoor S, Sun L-M, Wang D-Y (2016) Multi-walled carbon nanotubes enhanced fungal colonization and suppressed innate immune response to fungal infection in nematodes. *Toxicol Res* 5:492–499
31. Blackwell TK, Steinbaugh MJ, Hourihan JM, Ewald CY (2015) SKN-1/Nrf, stress responses, and aging in *Caenorhabditis elegans*. *Free Radic Biol Med* 88:290–301
32. Papp D, Csermely P, Soti C (2012) A role for SKN-1/Nrf in pathogen resistance and immunosenescence in *Caenorhabditis elegans*. *PLoS Pathog* 8:e1002673
33. Yu Y-L, Sun L-M, Wu Q-L, Jing L-N, Wang D-Y (2018) NPR-9 regulates innate immune response in *Caenorhabditis elegans* by antagonizing activity of AIB interneurons. *Cell Mol Immunol* 15:27–37
34. Zhi L-T, Yu Y-L, Li X-Y, Wang D-Y, Wang D-Y (2017) Molecular control of innate immune response to *Pseudomonas aeruginosa* infection by intestinal *let-7* in *Caenorhabditis elegans*. *PLoS Pathog* 13:e1006152
35. Zhi L-T, Yu Y-L, Jiang Z-X, Wang D-Y (2017) *mir-355* functions as an important link between p38 MAPK signaling and insulin signaling in the regulation of innate immunity. *Sci Rep* 7:14560
36. Yu Y-L, Zhi L-T, Guan X-M, Wang D-Y, Wang D-Y (2016) FLP-4 neuropeptide and its receptor in a neuronal circuit regulate preference choice through functions of ASH-2 trithorax complex in *Caenorhabditis elegans*. *Sci Rep* 6:21485
37. Wu Q-L, Cao X-O, Yan D, Wang D-Y, Aballay A (2015) Genetic screen reveals link between maternal-effect sterile gene *mes-1* and *P. aeruginosa*-induced neurodegeneration in *C. elegans*. *J Biol Chem* 290:29231–29239
38. Troemel ER, Chu SW, Reinke V, Lee SS, Ausubel FM, Kim DH (2006) p38 MAPK regulates expression of immune response genes and contributes to longevity in *C. elegans*. *PLoS Genet* 2:e183
39. van der Hoeven R, McCallum KC, Cruz MR, Garsin DA (2011) Ce-Duox1/BLI-3 generated reactive oxygen species trigger protective SKN-1 activity via p38 MAPK signaling during infection in *C. elegans*. *PLoS Pathog* 7:e1002453
40. Kim DH, Liberati NT, Mizuno T, Inoue H, Hisamoto N, Matsumoto K, Ausubel FM (2004) Integration of *Caenorhabditis elegans* MAPK pathways mediating immunity and stress resistance by MEK-1 MAPK kinase and VHP-1 MAPK phosphatase. *Proc Natl Acad Sci USA* 101:10990–10994
41. Chikka MR, Anbalagan C, Dvorak K, Dombeck K, Prahlad V (2016) The mitochondria-regulated immune pathway activated in the *C. elegans* intestine is neuroprotective. *Cell Rep* 16:2399–2414
42. Koga M, Zwaal R, Guan KL, Avery L, Ohshima Y (2000) A *Caenorhabditis elegans* MAP kinase kinase, MEK-1, is involved in stress responses. *EMBO J* 19:5148–5156
43. Zhao Y-L, Wu Q-L, Wang D-Y (2015) A microRNAs-mRNAs network involved in the control of graphene oxide toxicity in *Caenorhabditis elegans*. *RSC Adv* 5:92394–92405

44. Villanueva A, Lozano J, Morales A, Lin X, Deng X, Hengartner MO, Kolesnick RN (2001) *jkk-1* and *mek-1* regulate body movement coordination and response to heavy metals through *jnk-1* in *Caenorhabditis elegans*. *EMBO J* 20:5114–5128
45. Koga M, Zwaal R, Guan K, Avery L, Ohshima Y (2000) A *Caenorhabditis elegans* MAP kinase kinase, MEK-1, is involved in stress responses. *EMBO J* 19:5148–5156
46. Wolf M, Nunes F, Henkel A, Heinick A, Paul RJ (2018) The MAP kinase JNK-1 of *Caenorhabditis elegans*: location, activation, and influences over temperature-dependent insulin-like signaling, stress responses, and fitness. *J Cell Physiol* 214:721–729
47. Mizuno T, Fujiki K, Sasakawa A, Hisamoto N, Matsumoto K (2008) Role of the *Caenorhabditis elegans* Shc adaptor protein in the c-Jun N-terminal kinase signaling pathway. *Mol Cell Biol* 28:7041–7049
48. Okuyama T, Inoue H, Ookuma S, Satoh T, Kano K, Honjoh S, Hisamoto N, Matsumoto K, Nishida E (2010) The ERK-MAPK pathway regulates longevity through SKN-1 and insulin-like signaling in *Caenorhabditis elegans*. *J Biol Chem* 285:30274–30281
49. Qu M, Li Y-H, Wu Q-L, Xia Y-K, Wang D-Y (2017) Neuronal ERK signaling in response to graphene oxide in nematode *Caenorhabditis elegans*. *Nanotoxicology* 11:520–533
50. Chen H, Li H-R, Wang D-Y (2017) Graphene oxide dysregulates Neuroigin/NLG-1-mediated molecular signaling in interneurons in *Caenorhabditis elegans*. *Sci Rep* 7:41655

Chapter 5

Functions of Insulin and the Related Signaling Pathways in the Regulation of Toxicity of Environmental Toxicants or Stresses



Abstract In nematodes, the insulin signaling pathway can potentially participate in the regulation of various biological processes. In this chapter, we further discussed the involvement and possible pivotal function of core insulin signaling pathway in the regulation of toxicity of environmental toxicants or stresses. Moreover, we introduced the related information on the potential targets for DAF-16 and the possible upregulators for the insulin signaling pathway in regulating the toxicity of environmental toxicants or stresses. The possible formation of a large physical interaction surrounding the DAF-16 in regulating the toxicity of environmental toxicants or stresses needs to be paid more attention in nematodes.

Keywords Insulin and the related signaling pathways · Molecular regulation · Environmental exposure · *Caenorhabditis elegans*

5.1 Introduction

The nematode *Caenorhabditis elegans* has been successfully used in both the toxicity assessment and the toxicological study of various toxicants or stresses [1]. In nematodes, it has been shown that exposure to environmental toxicants or stresses can lead to the toxicity on many aspects of animals as reflected by a series of toxicity assessment endpoints [2–10]. Meanwhile, the insulin signaling pathway has been widely proven to participate in the regulation of various biological processes in organisms [11–18]. More and more data have implied the possible or even the potential pivotal role of insulin signaling pathway in the regulation of stress response in nematodes exposed to environmental toxicants or stresses.

In *C. elegans*, in the core insulin signaling pathway, insulin ligands bind to DAF-2/IGF-1 receptor (InR) to activate tyrosine kinase activity, which will allow to initiate the cascade of several kinases (AGE-1/phosphatidylinositol 3-kinase (PI3K), PDK-1/3-phosphoinositide-dependent kinase 1, AKT-1/2/serine/threonine kinase Akt/PKB, and SGK-1/serine or threonine-protein kinase). AKT and the SGK-1 will further phosphorylate and inactivate the transcription factor DAF-16/FOXO, which thereby blocks the transcription of its multiple target genes to regulate various biological processes

[19, 20]. We here first introduced the involvement of core insulin signaling pathway in the regulation of toxicity of environmental toxicants or stresses. We also introduced and discussed the potential targets for DAF-16 in the insulin signaling pathway in the regulation of toxicity of environmental toxicants or stresses. Moreover, we further introduced and discussed the possible upregulators for insulin signaling pathway in the regulation of toxicity of environmental toxicants or stresses. So far, the obtained data imply the possible formation of a large physical interaction surrounding the DAF-16 in the regulation of toxicity of environmental toxicants or stresses in nematodes.

5.2 Environmental Toxicants or Stresses Dysregulate the Expression of Insulin Signaling Pathway

Graphene oxide (GO), an important carbon-based engineered nanomaterials, can cause several aspects of toxicity, including adverse effects on the function of both primary (such as the intestine) and secondary (such as the neurons and the reproductive organs) targeted organs, on nematodes [21–27]. With the GO as an example, prolonged exposure to GO (100 mg/L) could result in a significant increase in the expression levels of *daf-2*, *age-1*, *akt-1*, and *akt-2* and decrease in the expression levels of *daf-18* and *daf-16* in wild-type nematodes [28]. Additionally, a significant increase in DAF-16::GFP expression in the nuclei of GO-exposed (100 mg/L) nematodes was also observed [28], which suggests that long-term exposure to GO not only affects the transcriptional activities of genes encoding the core insulin signaling pathway but also influences the nucleus-cytoplasm translocation of DAF-16. The induction of nucleus-cytoplasm translocation of DAF-16 and/or decrease in *daf-16* expression could also be observed in nematodes exposed to heavy metals (such as Mn or As) or traffic-related PM_{2.5} [29–32]. Therefore, exposure to certain environmental toxicants or stresses may potentially dysregulate the expression of insulin signaling pathway in nematodes (Fig. 5.1).

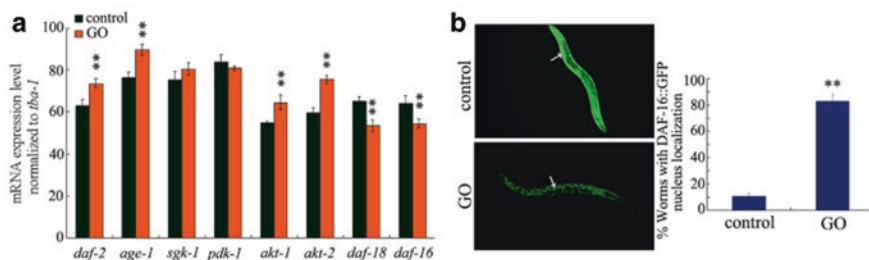


Fig. 5.1 Effects of GO exposure on the expression patterns of genes encoding insulin signaling pathway in wild-type nematodes [28]. **(a)** GO exposure altered expression levels of some genes encoding insulin signaling pathway in wild-type nematodes. **(b)** GO exposure influenced the nucleus translocation of DAF-16::GFP. Arrowheads indicate the DAF-16 expression in the intestine. GO exposure concentration was 100 mg/L. Prolonged exposure was performed from L1-larvae to young adults. Bars represent means \pm SEM. ** $P < 0.01$ vs control

5.3 The Insulin Signaling Pathway Regulates the Toxicity of Environmental Toxicants or Stresses

Further with GO as an example, it has been shown that mutation of *daf-16* or *daf-18* could induce a susceptibility to GO toxicity in decreasing locomotion behavior and in reducing lifespan, whereas mutation of *daf-2*, *age-1*, *akt-1*, or *akt-2* could induce a resistance to GO toxicity in decreasing locomotion behavior and in reducing lifespan (Fig. 5.2) [28]. In nematodes, mutation of *daf-16* could also induce a susceptibility to the toxicity of heavy metals or traffic-related PM_{2.5} in inducing intestinal ROS production [31, 33–36]. Additionally, mutation of *daf-2* or *age-1* could also suppress the toxicity of Hg in inducing deficits in development of male-specific structures, of heavy metals (Cd or Ca) or hypoxic stress in reducing lifespan, or of traffic-related PM_{2.5} in inducing intestinal ROS production [31, 33–36]. These studies performed on different environmental toxicants or stresses demonstrate the important function of insulin signaling pathway in regulating the toxicity of environmental toxicants or stresses in nematodes.

5.4 Genetic Interactions of Genes in the Insulin Signaling Pathway in Regulating the Toxicity of Environmental Toxicants or Stresses

In nematodes, genetic interaction analysis demonstrated that DAF-16 acted downstream of DAF-2, AGE-1, AKT-1, or AKT-2 to regulate the GO toxicity in reducing the longevity, because mutation of *daf-16* could effectively decrease the lifespan in *daf-2(e1370)*, *age-1(hx546)*, *akt-1(ok525)*, or *akt-2(ok393)* mutant nematodes exposed to GO (Fig. 5.3) [28]. Therefore, a signaling cascade of DAF-2-AGE-1-AKT-1/2-DAF-16 in the insulin signaling pathway was identified to be involved in the control of GO toxicity. Meanwhile, it was found that mutation of *daf-18* could effectively reduce the lifespan in *age(hx546)* mutant exposed to GO (Fig. 5.3) [28], which suggests the suppressor role of DAF-18 on the function of AGE-1 in the regulation of GO toxicity. The raised signaling cascade in the insulin signaling in regulating toxicity of environmental toxicants or stresses was further supported or confirmed by other toxicological studies performed in nematodes. It was also observed that mutation of *daf-16* could suppress the resistance of *daf-2* mutant nematodes to the traffic-related PM_{2.5} toxicity in inducing intestinal ROS production or enhancing intestinal permeability, to the combined Ca/Cd toxicity in reducing the lifespan, or to the As toxicity in inducing ROS production [31, 32, 35].

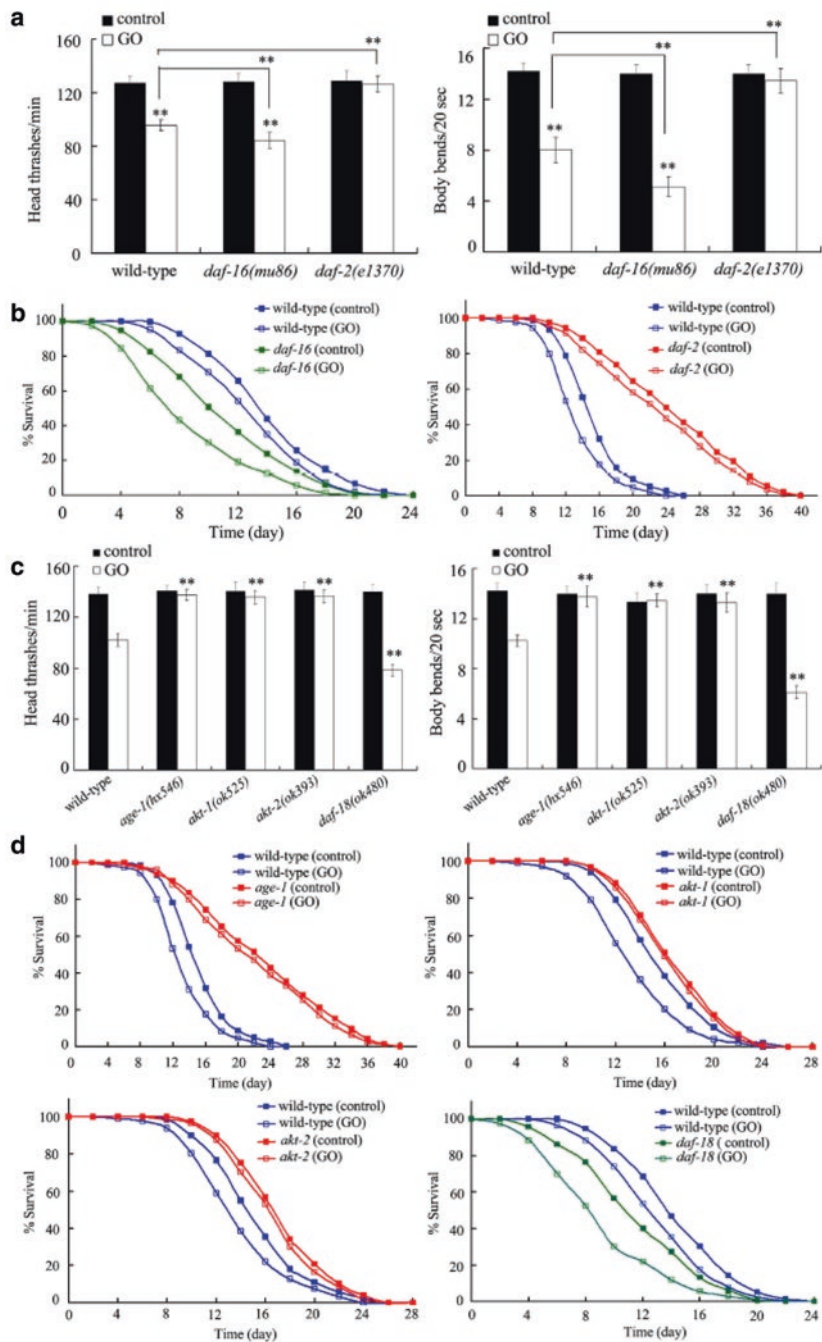


Fig. 5.2 Effects of *daf-16*, *daf-2*, *age-1*, *akt-1*, *akt-2*, or *daf-18* mutation on nematodes exposed to GO [28]. **(a)** Effects of *daf-16* or *daf-2* mutation on locomotion behavior in nematodes exposed to GO. **(b)** Effects of *daf-16* or *daf-2* mutation on lifespan in nematodes exposed to GO. **(c)** Mutations of *age-1*, *akt-1*, *akt-2*, or *daf-18* affected GO toxicity on locomotion behavior in nematodes. **(d)** Mutations of *age-1*, *akt-1*, *akt-2*, or *daf-18* affected GO toxicity on lifespan in nematodes. GO exposure concentration was 100 mg/L. Prolonged exposure was performed from L1-larvae to young adults. Bars represent means \pm SEM. ** $P < 0.01$ vs control (if not specially indicated)

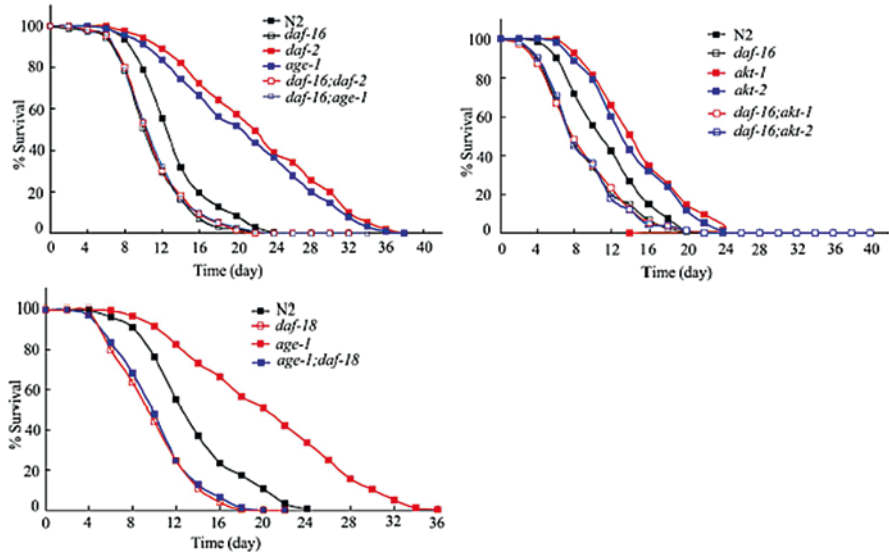


Fig. 5.3 Genetic interactions of genes in the insulin signaling pathway in regulating the GO toxicity on lifespan in nematodes [28]. GO exposure concentration was 100 mg/L. Prolonged exposure was performed from L1-larvae to young adults

5.5 Targets of DAF-16 in Regulating the Toxicity of Environmental Toxicants or Stresses

5.5.1 SOD-3

In *C. elegans*, *daf-16* is expressed in almost all tissues, including the intestine, the neurons, the muscle, and the pharynx. Nevertheless, expression of the *daf-16* in neurons, muscle, or pharynx could not significantly affect the GO toxicity in decreasing locomotion behavior and in reducing lifespan in *daf-16(mu86)* mutant nematodes [28]. In contrast, intestinal expression of *daf-16* could effectively augment the decreased locomotion behavior or reduced lifespan in GO-exposed *daf-16(mu96)* mutant nematodes [28], which demonstrating that the DAF-16 acts primarily in the intestine to regulate the toxicity of environmental toxicants or stresses. Actually, the core insulin signaling pathway can act in the intestine to regulate the GO toxicity in nematodes [28].

SOD-3, a mitochondrial iron/manganese superoxide dismutase, is expressed in the pharynx in the head, the intestine, the muscle, the vulva, and the tail. Intestinal RNAi knockdown of *sod-3* could induce a susceptibility to GO toxicity in reducing lifespan [28]. Genetic interaction analysis suggested that DAF-16 acted upstream of SOD-3 to regulate the GO toxicity, because the resistance of transgenic strain of *Ex(Pges-1-daf-16)* overexpressing intestinal DAF-16 to GO toxicity in reducing lifespan and in inducing intestinal ROS production could be inhibited by *sod-3*

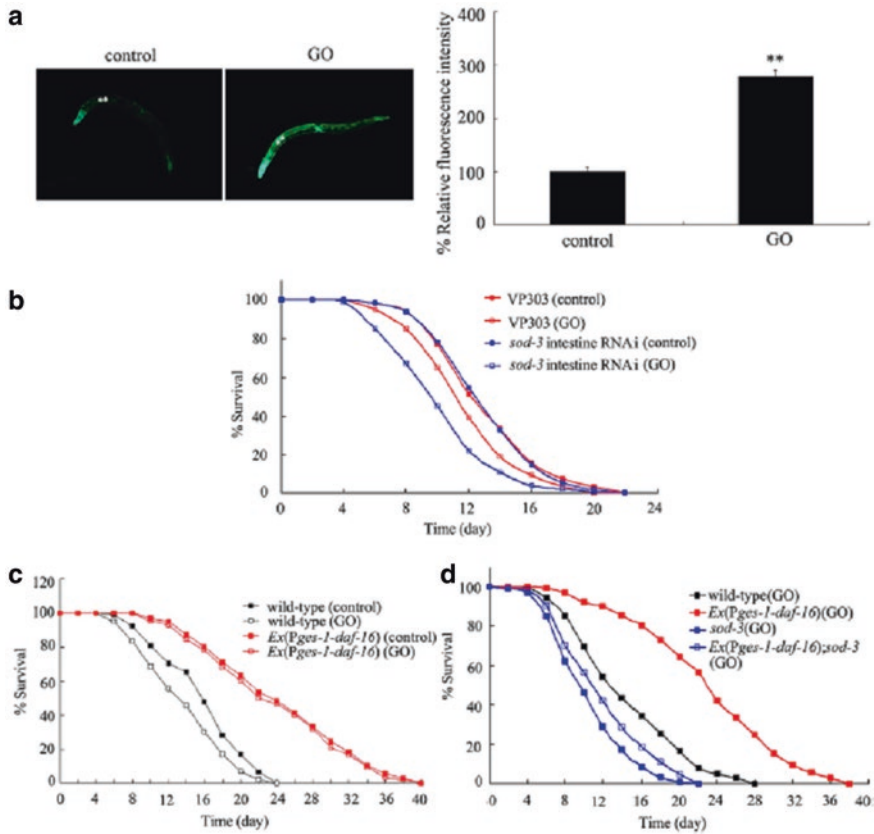


Fig. 5.4 Role of SOD-3 in regulating the GO toxicity in nematodes [28]. **(a)** Effects of GO exposure on SOD-3::GFP expression. The left shows images for SOD-3::GFP expression, and the right shows comparison of relative fluorescence intensity of SOD-3::GFP in the intestine of nematodes. Asterisks indicate the intestine of nematodes. **(b)** Effects of intestine-specific RNAi of *sod-3* gene on lifespan in GO-exposed nematodes. **(c)** Effects of intestinal overexpression of *daf-16* gene on GO toxicity on lifespan in nematodes. **(d)** Effects of *sod-3* mutation on lifespan in GO-exposed nematodes overexpressing *daf-16* gene in the intestine in nematodes. GO exposure concentration was 100 mg/L. Prolonged exposure was performed from L1-larvae to young adults. Bars represent means \pm SEM. ** $P < 0.01$ vs wild type

mutation (Fig. 5.4) [28]. This observation also implies that prolonged exposure to GO could inhibit the function of DAF-16 within the insulin signaling and, thereby, result in the further suppression of the function of SOD-3, which plays an important role in defense against oxidative stress in nematodes [28].

5.5.2 Antimicrobial Proteins

In nematodes, among the candidate targeted genes for DAF-16, some genes (*lys-1*, *lys-7*, *lys-8*, *dod-6*, *F55G11.4*, *spp-1*, *spp-12*, and *dod-22*) encoding potential antimicrobial proteins have also been identified to act as the targeted genes for *daf-16* in regulating the toxicity of GO toxicity [37–40]. Among these genes encoding potential antimicrobial proteins, RNAi knockdown of *lys-1*, *dod-6*, *F55G11.4*, *lys-8*, or *spp-1* could significantly suppress the resistance of nematodes overexpressing intestinal *daf-16* to GO toxicity in inducing intestinal ROS production and in decreasing locomotion behavior (Fig. 5.5) [41], suggesting that LYS-1, DOD-6,

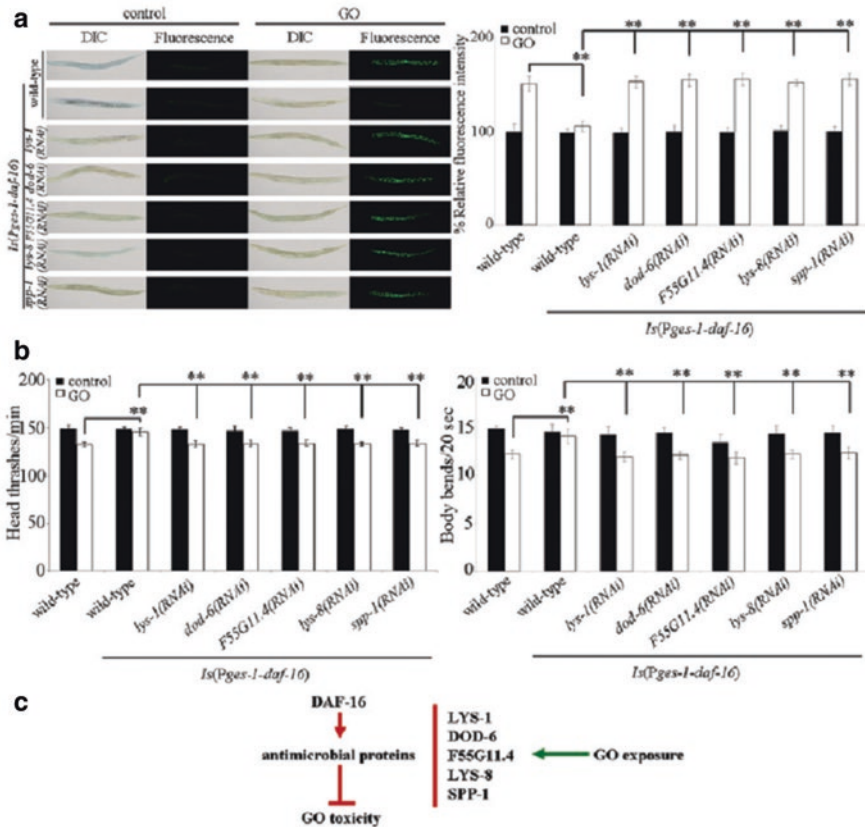


Fig. 5.5 Antimicrobial genes acted downstream of *daf-16* to regulate the GO toxicity [41]. (a) Antimicrobial genes acted downstream of *daf-16* to regulate the GO toxicity in inducing intestinal ROS production. (b) Antimicrobial genes acted downstream of *daf-16* to regulate the GO toxicity in decreasing locomotion behavior. (c) A diagram showing the interaction between DAF-16 and antimicrobial proteins in the regulation of GO toxicity. Prolonged exposure was performed from L1-larvae to young adults. GO exposure concentration was 10 mg/L. Bars represent means \pm SD. $**p < 0.01$

F55G11.4, LYS-8, and SPP-1 act as downstream targets for intestinal DAF-16 in regulating the toxicity of environmental toxicants or stresses.

Among LYS-1, DOD-6, F55G11.4, LYS-8, and SPP-1, F55G11.4 and SPP-1 acted further downstream of SOD-3 in the regulation of GO toxicity, because RNAi knockdown of *F55G11.4* or *spp-1* could significantly suppress the resistance of nematodes overexpressing intestinal *sod-3* to GO toxicity in inducing intestinal ROS production and in decreasing locomotion behavior [41]. The antimicrobial proteins of F55G11.4 and SPP-1 affected the expression of *gas-1* encoding a subunit of mitochondrial complex I that is required for the oxidative phosphorylation in GO-exposed nematodes [41], implying the important effect of F55G11.4 and SPP-1 on GAS-1-mediated molecular basis for oxidative stress in GO-exposed nematodes.

5.5.3 MTL-1 and MTL-2

In nematodes, *mtl-1* and *mtl-2* encode metallothioneins and can be expressed in the intestine. Exposure to the outdoor PM_{2.5} could induce the significant expression of MTL-1 and MTL-2 [42]. Meanwhile, mutation of the *mtl-1* or *mtl-2* resulted in a susceptibility to the outdoor PM_{2.5} toxicity [42], because a more severe decrease in locomotion behavior and a more significant induction of intestinal ROS production were observed in *mtl-1(tm1770)* or *mtl-2(gk125)* mutants exposed to outdoor PM_{2.5} (10 mg/L) compared with those in wild-type nematodes [42]. After PM_{2.5} exposure, the head thrash and body bend in the double mutant of *daf-16(mu86);mtl-1(RNAi)* were similar to those in *daf-16(mu86)* or *mtl-1(RNAi)* nematodes, and the head thrash and body bend in the double mutant of *daf-16(mu86);mtl-2(RNAi)* were similar to those in *daf-16(mu86)* or *mtl-2(RNAi)* nematodes (Fig. 5.6) [42]. These observations suggest that MTL-1 or MTL-2 acted in the same genetic pathway with DAF-16 in regulating the toxicity of environmental toxicants or stresses. Moreover, it was observed that the outdoor PM_{2.5} exposed *daf-2(e1370);mtl-1(RNAi)* mutant exhibited a similar head thrash and body bend to those in outdoor PM_{2.5} exposed *mtl-1(RNAi)* nematodes, and the outdoor PM_{2.5} exposed *daf-2(e1370);mtl-2(RNAi)* mutant exhibited a similar head thrash and body bend to those in outdoor PM_{2.5} exposed *mtl-2(RNAi)* nematodes (Fig. 5.6) [42]. That is, MTL-1 and MTL-2 may act further downstream of the DAF-16 to regulate the toxicity of environmental toxicants or stresses in nematodes.

5.5.4 NATC-1

In nematodes, *natc-1* encodes an evolutionarily conserved subunit of the N-terminal acetyltransferase C (NAT) complex, and the N-terminal acetylation is a useful modification for eukaryotic proteins. NATC-1 is expressed in many cells and tissues

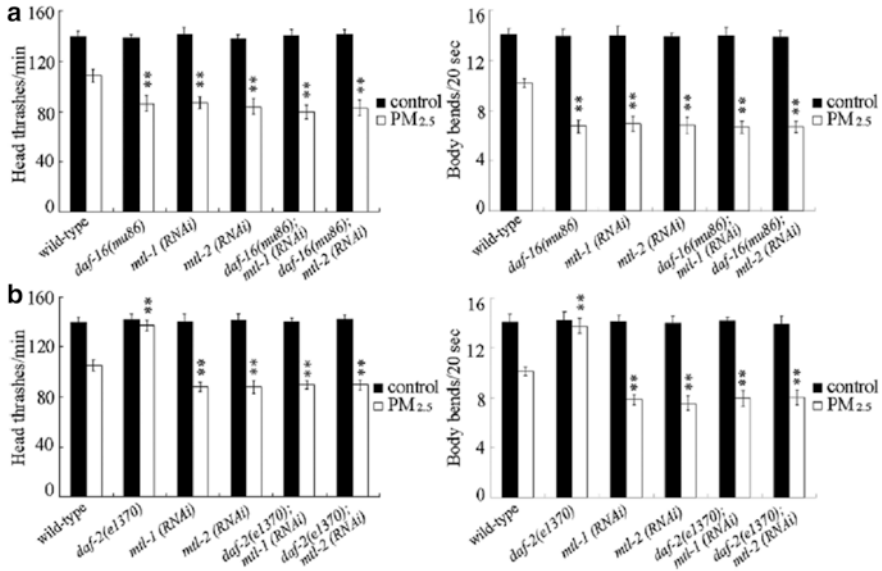


Fig. 5.6 Genetic interaction between *daf-16* or *daf-2* and genes encoding metallothioneins in regulating outdoor PM_{2.5} toxicity on locomotion behavior [42]. (a) Genetic interaction between *daf-16* and *mtl-1* or *mtl-2* in regulating outdoor PM_{2.5} toxicity on locomotion behavior. (b) Genetic interaction between *daf-2* and *mtl-1* or *mtl-2* in regulating outdoor PM_{2.5} toxicity on locomotion behavior. Exposure concentration of outdoor PM_{2.5} was 10 mg/L. Acute exposure was performed from young adults for 24 h. Bars represent mean \pm SEM. ** $P < 0.01$ vs wild type

and localizes to the cytoplasm [43]. Loss-of-function mutation of *natc-1* caused a resistance to a broad-spectrum of physiologic stressors, including multiple metals (such as Zn), heat stress, and oxidation stress [43]. DAF-16 was predicted to directly bind the *natc-1* promoter, and *natc-1* mRNA levels were repressed by DAF-16 activity, indicating the role of *natc-1* as a physiological target of DAF-16 (Fig. 5.7) [43]. Additionally, the *daf-2* mutants displayed a twofold decrease in *natc-1* expression compared to wild-type nematodes [43]. Genetic interaction analysis demonstrated that *natc-1(am138)* could enhance the dauer formation in *daf-2(e1370)* mutant nematodes, and the *daf-2(e1370);natc-1(am138)* double mutant nematodes displayed enhanced stress resistance compared to either single mutant animal (Fig. 5.7) [43]. Moreover, the *daf-16(mu86);natc-1(am138)* double mutant animals displayed heat stress resistance similar to *natc-1* single mutant animals, although the *daf-16(mu86)* mutant displayed a mild sensitivity to the heat stress (Fig. 5.7) [43]. Therefore, NATC-1 functions downstream of DAF-16 to mediate the resistance of nematodes to environmental toxicants or stresses.

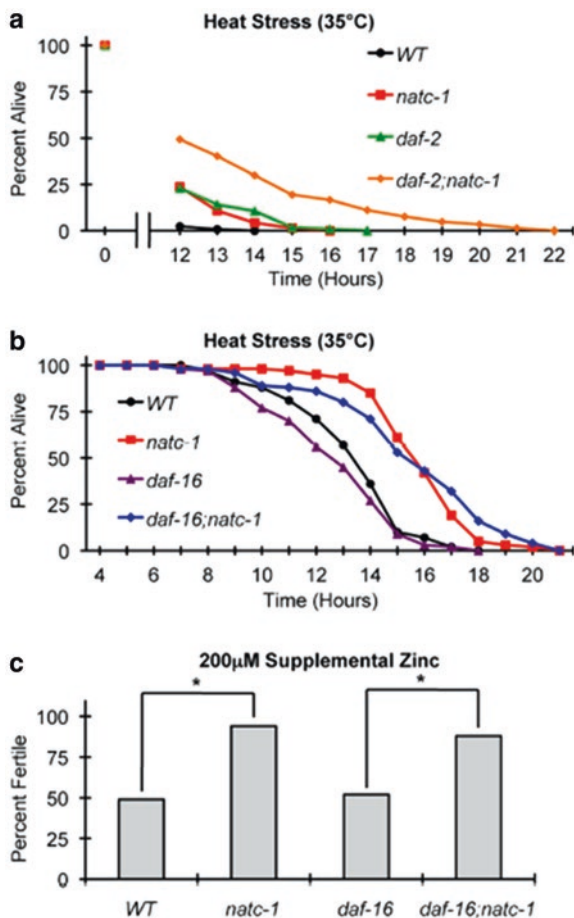


Fig. 5.7 *natc-1* is epistatic to *daf-16* in resistance to heat and zinc stress [43]. (a) Wild-type (WT), *natc-1(am138)*, *daf-2(e1370)*, and *daf-2(e1370);natc-1(am138)* animals were cultured at 15 °C on NGM, shifted to 35 °C as day 1 adults, and assayed for survival hourly beginning at 12 h ($N = 39-61$). (b) Wild-type (WT), *natc-1(am138)*, *daf-16(mu86)*, and *daf-16(mu86);natc-1(am138)* animals were cultured at 15 °C on NGM, shifted to 35 °C as day 1 adults, and assayed for survival hourly. (c) Embryos were cultured on NAMM with 200 mM supplemental zinc. Bars indicate the percentage of embryos that generated fertile adults. Genotypes were wild type (WT), *natc-1(am138)*, *daf-16(mu86)*, and *daf-16(mu86);natc-1(am138)* ($N = 49-54$). *daf-16(mu86)* animals were similar to wild-type animals, and *natc-1(am138)* caused significant zinc resistance in wild-type and *daf-16(mu86)* mutant animals

5.5.5 HSF-1

Pseudomonas aeruginosa is a commonly considered bacterial pathogen for human beings [44–47]. In nematodes, both the *daf-2(e1370)* mutant nematodes and the nematodes carrying additional *daf-16* gene copies were resistant to *P. aeruginosa*

and showed higher levels of HSP90 than wild-type animals (Fig. 5.8) [48], suggesting that a higher activity of HSF-1 may be in part responsible for the increased resistance of nematodes to *P. aeruginosa*. In contrast, this enhanced resistance of *daf-2(e1370)* and *daf-16::gfp* animals to *P. aeruginosa* was reduced by the RNAi knockdown of *hsf-1* (Fig. 5.8) [48]. Additionally, the heat-shock protection was not detected in *daf-16* RNAi nematodes (Fig. 5.8) [48]. Therefore, the HSF-1-regulated proteins may be effectors for the signaling cascade of DAF-2-DAF-16 required for the pathogen resistance in nematodes.

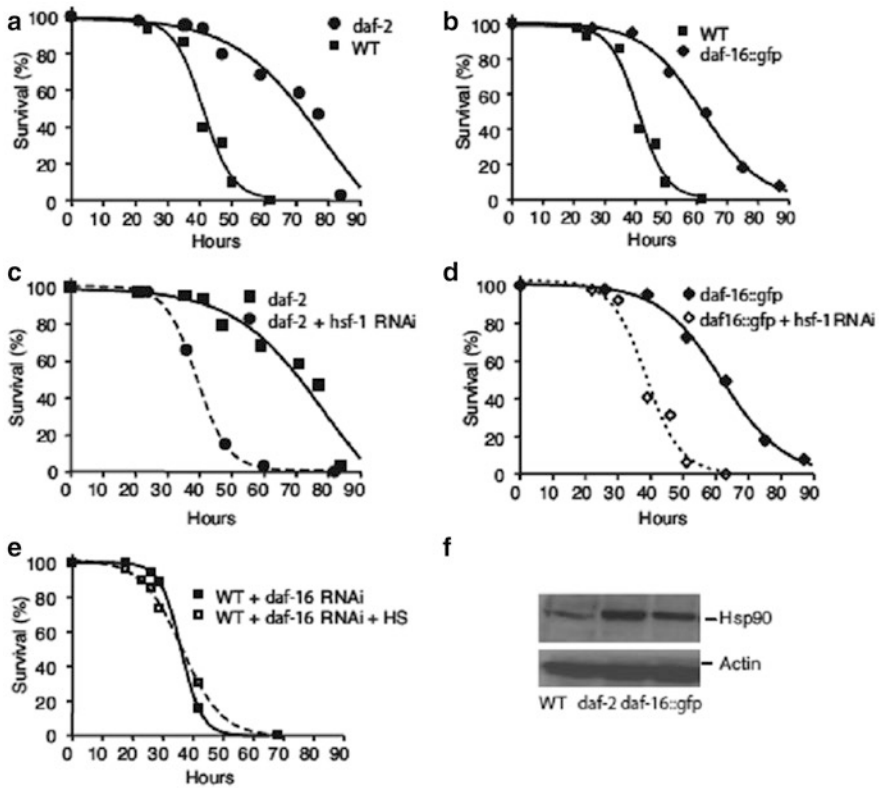


Fig. 5.8 The enhanced resistance phenotype of *daf-2(e1370)* and *daf-16::gfp* animals to *P. aeruginosa* requires HSF-1 activity [48]. (a, b) Wild-type, *daf-2(e1370)*, and *daf-16::gfp* animals were exposed to *P. aeruginosa*. (c) *daf-2(e1370)* grown on *E. coli* carrying a vector control or expressing *hsf-1* double-stranded RNA were exposed to *P. aeruginosa*. (d) *daf-16::gfp* grown on *E. coli* carrying a vector control or expressing *hsf-1* double-stranded RNA were exposed to *P. aeruginosa*. (e) Wild-type animals grown on *E. coli* expressing *daf-16* double-stranded RNA were untreated or HS-treated and exposed to *P. aeruginosa*. For each condition, 80–100 animals were used. (f) Immunological detection of Hsp90 in WT, *daf-2(e1370)*, and *daf-16::gfp* animals

5.5.6 Genetic Interaction Between SOD-3 and Antimicrobial Proteins in the Regulation of Toxicity of Environmental Toxicants or Stresses

In nematodes, it has been further observed that RNAi knockdown of *sod-3* could not affect the resistance of nematodes overexpressing intestinal *lys-1* or *lys-8* to GO toxicity in inducing intestinal ROS production and in decreasing locomotion behavior, although RNAi knockdown of *sod-3* could suppress the resistance of nematodes overexpressing intestinal *dod-6* to GO toxicity in inducing intestinal ROS production and in decreasing locomotion behavior (Fig. 5.9) [41]. These results imply that LYS-1 and LYS-8 acted in a different genetic pathway from the DAF-16-SOD-3 signaling cascade, and DOD-6 acted upstream of SOD-3 to regulate the toxicity of environmental toxicants or stresses.

LYS-1 and LYS-8 are two members of the lysozyme family. Genetic interaction analysis demonstrated that LYS-1 and LYS-8 functioned redundantly in the regulation of GO toxicity, because the GO-exposed double mutant of *lys-8(ok3504);lys-1(ok2445)* exhibited the more severe induction of intestinal ROS production and decrease in locomotion behavior than that in GO-exposed *lys-1(ok2445)* mutant or in GO-exposed *lys-8(ok3504)* mutant [41]. Meanwhile, after GO (10 mg/L) exposure, mutation of *lys-1* or *lys-8* did not influence the expressions of *clk-1*, *gas-1*, and *isp-1*, which are required for the control of oxidative stress [41].

Moreover, it was found that mutation of *lys-1* significantly decreased the transcriptional expression of *tub-2* in GO (10 mg/L) exposed nematodes, and intestine-specific RNAi of *tub-2* significantly suppressed the resistance of nematodes overexpressing intestinal LYS-1 to GO toxicity in inducing ROS production and in decreasing locomotion behavior (Fig. 5.10) [41]. *tub-2* encodes an ortholog of human tubby like protein 4, and intestine-specific RNAi of *tub-2* could cause a susceptibility to GO toxicity [41]. Besides this, it was also observed that loss-of-function mutation of *lys-8* significantly decreased the transcriptional expression of *daf-8* and increased the transcriptional expression of *daf-5* in GO (10 mg/L) exposed nematodes [41]. In nematodes, *daf-5* encodes a transcriptional factor, and *daf-8* encodes a R-Smad protein in the TGF- β signaling pathway. Intestine-specific RNAi of *daf-8* could cause a susceptibility to GO toxicity in inducing ROS production, whereas intestine-specific RNAi of *daf-5* caused a resistance to GO toxicity in inducing ROS production [41]. Furthermore, intestine-specific RNAi of *daf-8* could significantly inhibit the resistance of transgenic strain overexpressing intestinal *lys-8* to GO toxicity in inducing ROS production and in decreasing locomotion behavior (Fig. 5.10) [41]. Therefore, these results suggest the formation of signaling cascades of DAF-16-LYS-1-TUB-2 and DAF-16-LYS-8-DAF-8-DAF-5 in regulating the toxicity of environmental toxicants or stresses in nematodes.

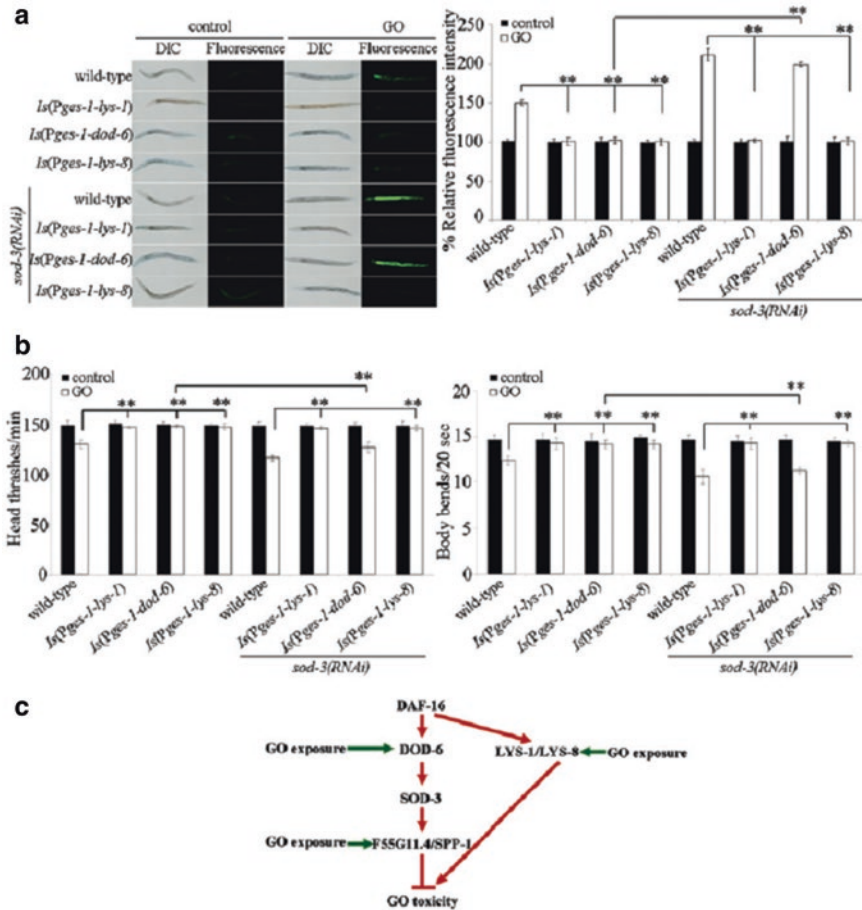


Fig. 5.9 Genetic interaction between SOD-3 and LYS-1, DOD-6, or LYS-8 in the regulation of GO toxicity [41]. **(a)** Genetic interaction between SOD-3 and LYS-1, DOD-6, or LYS-8 in the regulation of GO toxicity in inducing intestinal ROS production. **(b)** Genetic interaction between SOD-3 and LYS-1, DOD-6, or LYS-8 in the regulation of GO toxicity in decreasing locomotion behavior. **(c)** A diagram showing the unique role of LYS-1 and LYS-8 in the regulation of GO toxicity. Prolonged exposure was performed from L1-larvae to young adults. GO exposure concentration was 10 mg/L. Bars represent means ± SD. ***p* < 0.01

5.6 Upregulators of Insulin Signaling Pathway in Regulating the Toxicity of Environmental Toxicants or Stresses

So far, many upregulators of insulin signaling pathway in regulating the biological processes, especially the longevity, have been raised. However, only limited upregulators of insulin signaling pathway in regulating the toxicity of environmental toxicants or stresses have been identified.

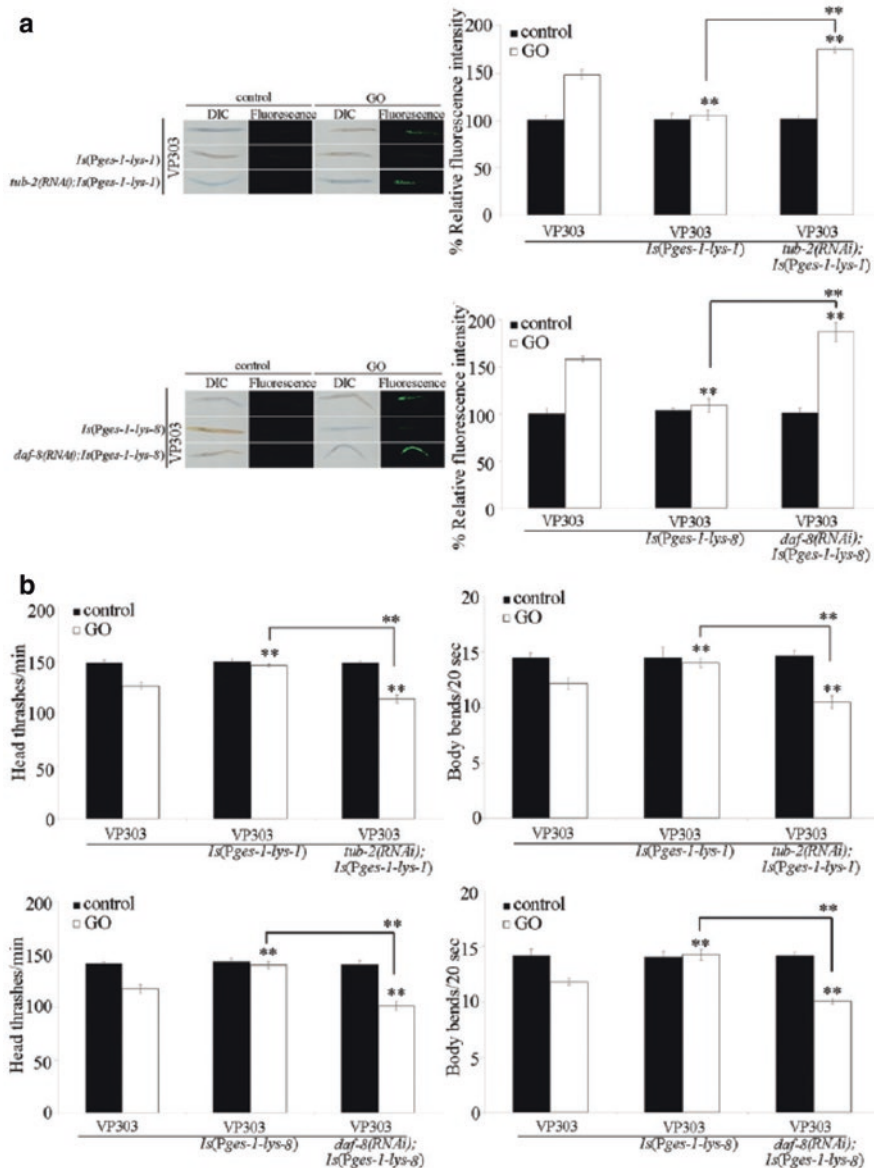


Fig. 5.10 Genetic interaction assays between LYS-1 or LYS-8 and their target(s) in the regulation of GO toxicity [41]. (a) Genetic interaction assays between LYS-1 or LYS-8 and their target(s) in the regulation of GO toxicity in inducing intestinal ROS production. (b) Genetic interaction assays between LYS-1 or LYS-8 and their target(s) in the regulation of GO toxicity in decreasing locomotion behavior. Prolonged exposure was performed from L1-larvae to young adults. GO exposure concentration was 10 mg/L. Bars represent means \pm SD. ** $p < 0.01$ vs VP303 (if not specially indicated)

5.6.1 *SMK-1*

In nematodes, *smk-1* encodes a homolog to mammalian SMEK. Under the normal conditions, the *smk-1(mn156)* mutant nematodes have a reduced lifespan, normal locomotion behavior, and no significant induction of intestinal ROS production [49]. After prolonged exposure to GO (100 mg/L), the *smk-1(mn156)* mutant showed the more severe reduction in lifespan, decrease in locomotion behavior, and induction of intestinal ROS production than wild-type nematodes [49]. Similarly, the *smk-1(mn156)* mutant also exhibited the susceptibility to the toxicity of coal combustion-related fine particulate matter (PM_{2.5}) in inducing intestinal ROS production and in decreasing locomotion behavior [50]. These results suggest the potential susceptibility of *smk-1(mn156)* mutant nematodes to the toxicity of environmental toxicants or stresses.

In nematodes, *smk-1* is expressed in the intestine, pharynx, neurons, muscle, and hypodermis. The tissue-restricted expression of *smk-1* in the pharynx, the neurons, the muscle, or the hypodermis did not affect the GO toxicity in reducing lifespan and in decreasing locomotion behavior in *smk-1(mn156)* mutant nematodes; however, expression of *smk-1* in the intestine could significantly suppress the GO toxicity in reducing lifespan and in decreasing locomotion behavior in *smk-1(mn156)* mutant nematodes [49]. That is, SMK-1 acted in the intestine to regulate the GO toxicity. Moreover, it was observed that the transgenic strain of *Is(Pges-1-smk-1)* overexpressing intestinal *smk-1* had a resistance to the GO toxicity in reducing lifespan and in decreasing locomotion behavior [49], which further confirmed the tissue-specific activity of SMK-1 in the intestine in the regulation of GO toxicity.

Moreover, it has been shown that the lifespan and the locomotion behavior in GO (100 mg/L) exposed double mutant of *daf-16(RNAi);smk-1(mn156)* were similar to those in GO (100 mg/L) exposed single mutant of *smk-1(mn156)* or *daf-16(RNAi)* nematodes [49], suggesting that SMK-1 and DAF-16 may act in the same genetic pathway to regulate the toxicity of environmental toxicants or stresses. More importantly, it was found that RNAi knockdown of *daf-16* could significantly suppress the protective effects of *smk-1* overexpression on both the lifespan and the locomotion behavior in GO-exposed nematodes (Fig. 5.11) [49], which demonstrates that SMK-1 acts upstream of DAF-16 to regulate the toxicity of environmental toxicants or stresses in nematodes.

In nematodes, it has been further found that the expressions of *sod-3*, *sod-4*, and *ctl-3* were significantly decreased in *smk-1* mutant nematodes compared to wild-type N2 after coal combustion-related PM_{2.5} exposure (Fig. 5.12) [50]. SOD-3 (an iron/manganese superoxide dismutase), SOD-4 (an extracellular Cu²⁺/Zn²⁺ superoxide dismutase), and CTL-3 (a catalase) are considered as the possible downstream targets of DAF-16. After exposure to coal combustion-related PM_{2.5}, *sod-3(RNAi)*, *sod-4(RNAi)*, or *ctl-3(RNAi)* nematodes had a significantly higher induction of intestinal ROS production and decrease in locomotion compared to the wild-type N2 (Fig. 5.12) [50], suggesting the susceptibility of *sod-3(RNAi)*, *sod-4(RNAi)*, or *ctl-3(RNAi)* nematodes to the toxicity of coal combustion-related

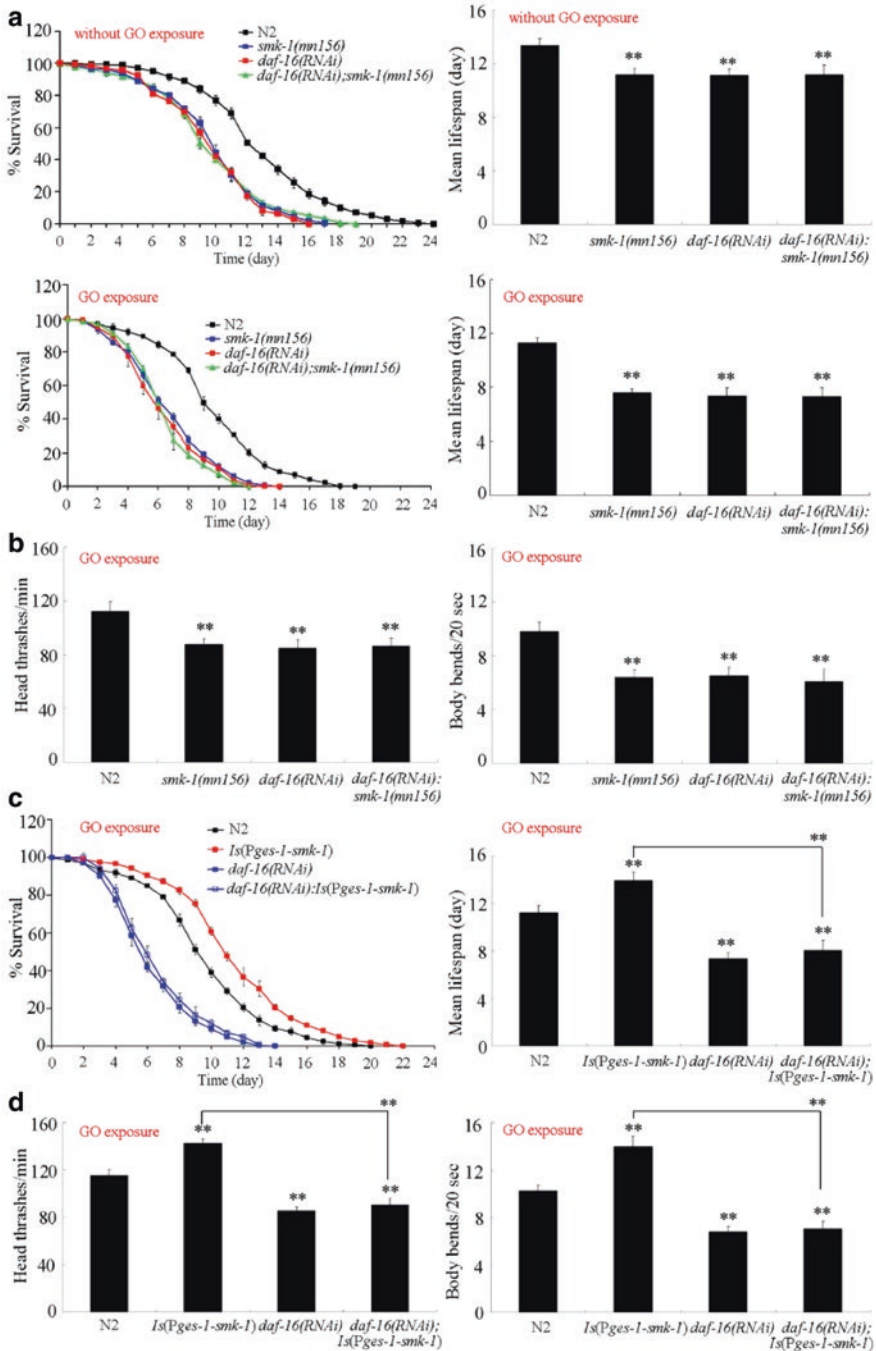


Fig. 5.11 Genetic interaction between *smk-1* and *daf-16* in regulating GO toxicity in nematodes [49]. **(a)** Genetic interaction between *smk-1* and *daf-16* in regulating GO toxicity in reducing lifespan in nematodes. **(b)** Genetic interaction between *smk-1* and *daf-16* in regulating GO toxicity in decreasing locomotion behavior in nematodes. **(c)** Effect of RNAi knockdown of *daf-16* gene on

PM_{2.5}. These results imply that the possible signaling cascade of SMK-1-DAF-16-SOD-3/SOD-4/CTL-3 may exist in regulating the toxicity of environmental toxicants or stresses in nematodes.

5.6.2 AAK-2

In nematodes, *aak-2* encodes a catalytic alpha subunit of AMP-activated protein kinases (AMPKs). Multi-walled carbon nanotubes (MWCNTs) is another important carbon-based nanomaterials widely used in different fields [51–54]. Previous study has indicated that AAK-2 may function upstream of DAF-16 in insulin signaling pathway to regulate the longevity [19]. In nematodes, mutation of *aak-2* induced a susceptibility to the toxicity of both MWCNTs and GO [51, 55]. Moreover, it was observed that the lifespan and the locomotion behavior at adult day-8 in MWCNTs (1 mg/L) exposed double mutant of *daf-16(mu86);aak-2(om524)* were similar to those in MWCNTs (1 mg/L) exposed single mutant of *aak-2(om524)* or *daf-16(mu86)* nematodes (Fig. 5.13) [51], implying that AAK-2 can further act together with DAF-16 in the same genetic pathway to form a signaling cascade of AAK-2-DAF-16 to regulate the toxicity of environmental toxicants or stresses in nematodes.

5.6.3 JNK-1

JNK-1 is a core component in the JNK signaling pathway. We have introduced the related detailed information in the Chap. 4. It was further observed that the loss-of-function mutation of *jnk-1* could significantly suppress the nuclear translocation of DAF-16 caused by heat stress or ROS stress (induced by H₂O₂) (Fig. 5.14) [56]. The degree of nuclear translocation of DAF-16::GFP was generally and statistically significantly lower in the *jnk-1* mutant than in the wild type after exposure to heat stress or ROS stress (Fig. 5.14) [56]. Moreover, loss-of-function mutation of *jnk-1* could further significantly inhibit the increase in SOD-3::GFP (a direct target of DAF-16) induced by heat stress [56]. Therefore, JNK-1 may modulate the environmental toxicant- or stress-induced translocation of DAF-16 from the cytosol into the cell nucleus in nematodes.



Fig. 5.11 (continued) lifespan in GO-exposed transgenic nematodes overexpressing *smk-1* in the intestine. **(d)** Effect of RNAi knockdown of *daf-16* gene on locomotion behavior in GO-exposed transgenic nematodes overexpressing *smk-1* in the intestine. GO exposure concentration was 100 mg/L. Prolonged exposure was performed from L1-larvae to young adults. Bars represent means \pm SD. ** $P < 0.01$ vs N2 (if not specially indicated)

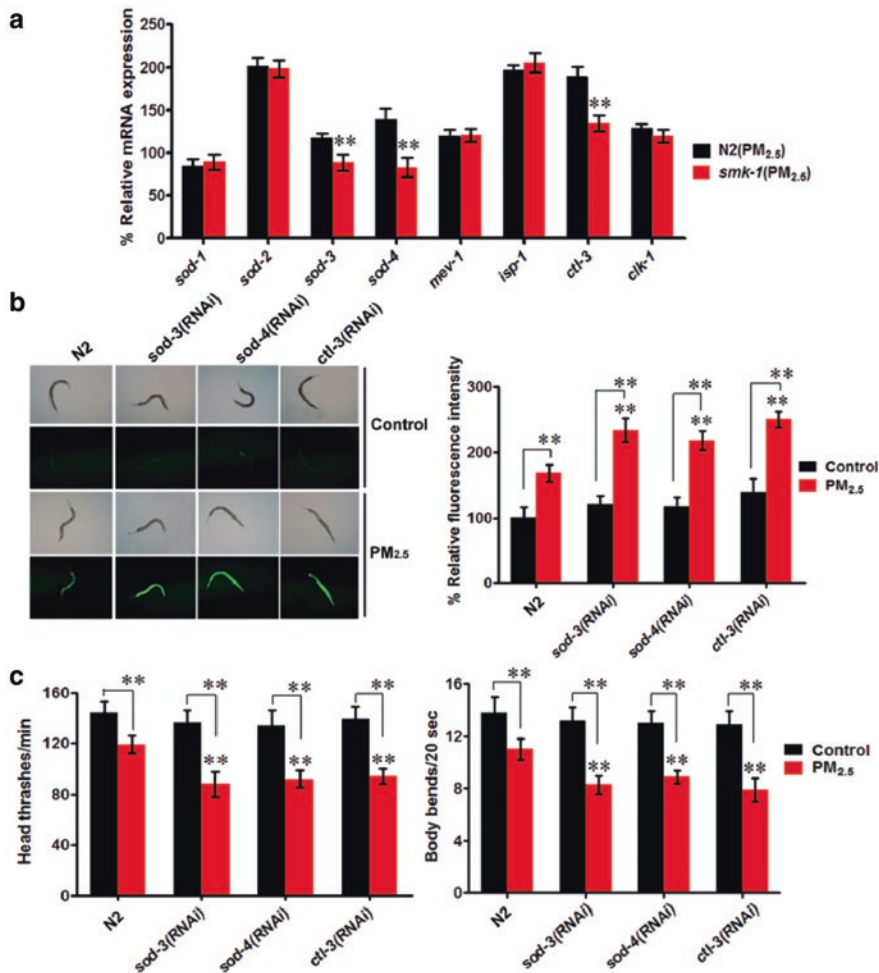
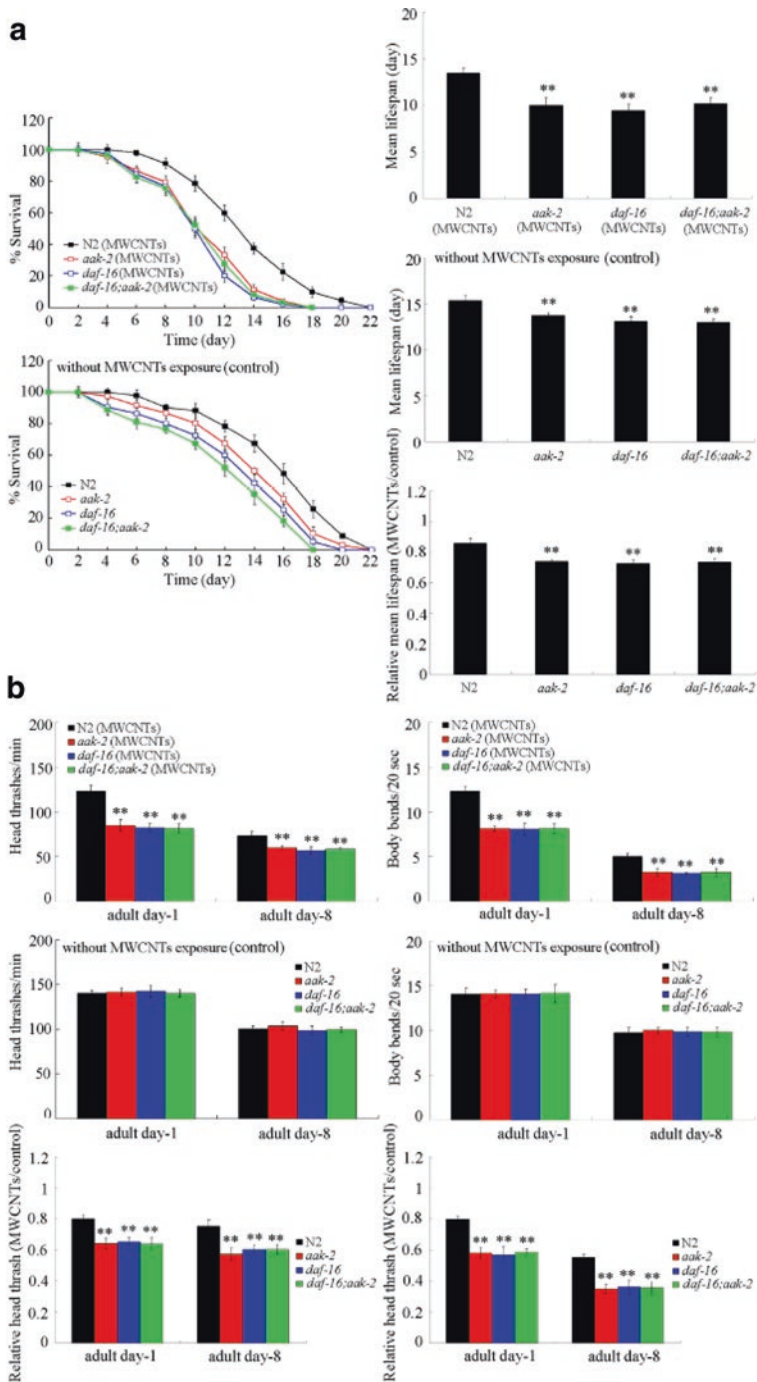


Fig. 5.12 Oxidative stress-related genes acted as downstream regulators of *smk-1* in the regulation of coal combustion-related PM_{2.5} toxicity [50]. (a) Expression pattern of genes required for the control of oxidative stress in coal combustion-related PM_{2.5} exposed wild-type and *smk-1* mutant nematodes. (b) Effect of RNAi knockdown of *sod-3*, *sod-4*, or *ctl-3* on toxicity of coal combustion-related PM_{2.5} in inducing intestinal ROS production. (c) Effect of RNAi knockdown of *sod-3*, *sod-4*, or *ctl-3* on toxicity of coal combustion-related PM_{2.5} in decreasing locomotion behavior. The concentration of coal combustion-related PM_{2.5} was 1 mg/L. Prolonged exposure was performed from L1-larvae to young adults at 20 °C in the presence of food. Bars represent mean ± SD. ***P* < 0.01 vs N2 (if not specially indicated)



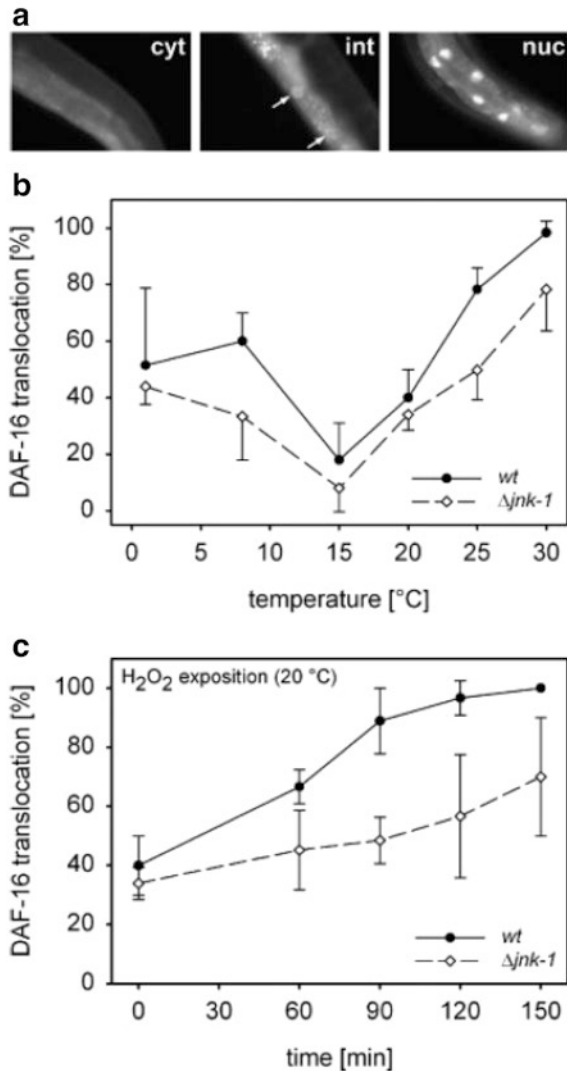


Fig. 5.14 The temperature- and H₂O₂-induced nuclear translocation of DAF-16 within intestinal cells of *C. elegans* is lower in a *jnk-1* deletion mutant than in the wild-type nematodes [56]. **(a)** Depending on the degree of nuclear GFP fluorescence, three different states of translocation of DAF-16::GFP from the cytoplasm into the cell nuclei of intestinal cells can be distinguished: cytoplasmic location (cyt; no nuclear GFP fluorescence), intermediate location (int; weak nuclear GFP fluorescence), and nuclear location (nuc; strong nuclear GFP fluorescence). **(b)** After incubation at different ambient temperatures, the degree of nuclear DAF-16 translocation within intestinal cells was minimal at 15 °C and increased toward lower and higher temperatures both in wild-type and mutant worms. In the mutant, however, DAF-16 translocation was significantly reduced in comparison to the wild type. **(c)** The degree of nuclear DAF-16 translocation also increased with the incubation period (0–150 min) on NGM plates containing 1 mM H₂O₂. Again, this cellular response was significantly lower in the mutant than in the wild type

5.6.4 HCF-1

In nematodes, *hcf-1* encodes a conserved homolog of host cell factor 1. The *hcf-1(pk924)* mutant nematodes showed the resistant to the paraquat treatment compared to wild-type nematodes at multiple time points (Fig. 5.15) [57]. Moreover, it has been found that this paraquat resistance of the *hcf-1(pk924)* mutants was dependent on *daf-16*, as the *daf-16(mgDf47);hcf-1(pk924)* double mutant was sensitive to paraquat, similar to that of the *daf-16(mgDf47)* single mutant (Fig. 5.15) [57]. Similarly, the *hcf-1(pk924)* mutant nematodes were resistant to the cadmium exposure compared to wild-type nematodes at multiple time points, and the cadmium resistance of the *hcf-1(pk924)* mutant was also *daf-16*-dependent (Fig. 5.15) [57]. It has been found that the RNA levels of *sod-3*, *mtl-1*, and *F21F3.3* encoding a farnesyl cysteine carboxyl methyltransferase were significantly elevated in both the

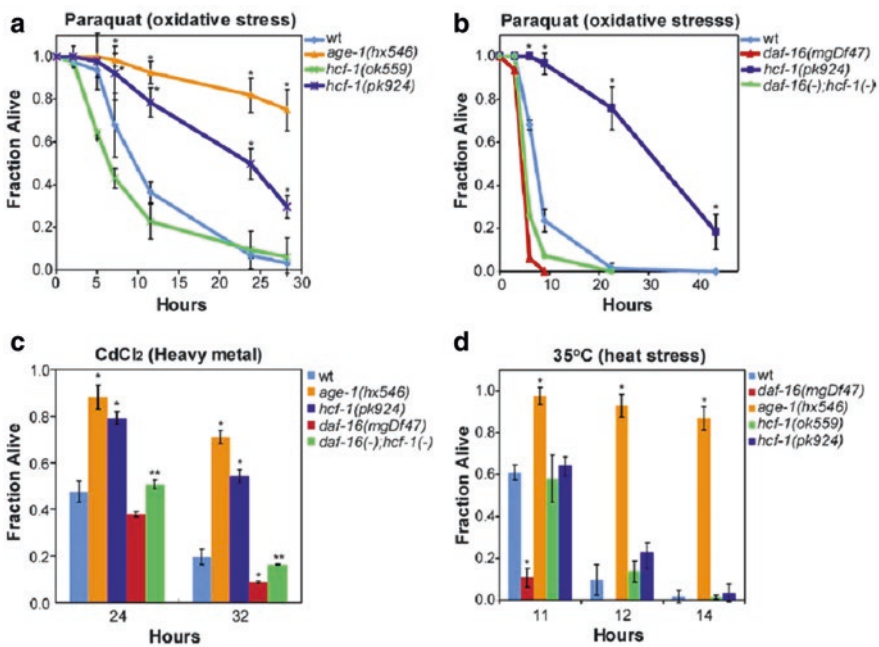


Fig. 5.15 Loss of *hcf-1* results in heightened resistance to specific environmental stresses [57]. (a) The *hcf-1(pk924)* mutant worms exhibited increased survival in 200 mM paraquat compared to wild-type worms. (b) The enhanced paraquat resistance of *hcf-1(pk924)* was dependent on *daf-16*. (c) The *hcf-1(pk924)* mutant worms showed increased survival in CdCl₂ (18 mM) that was *daf-16* dependent. (d) The *hcf-1(pk924)* and *hcf-1(ok559)* mutants and wild-type worms showed similar survival kinetics when cultured at 35 °C. For the stress assays, duplicate to quadruplicate samples were examined for each strain. Mean fraction alive indicates the average survival among the multiplicates and error bars represent the standard deviation of the multiplicates. *p*-Value was calculated using Student's *t*-test. **p* < 0.05 when compared to wild type (wt). ***p* < 0.05 when compared to *hcf-1(pk924)*. Each of the stress assays was repeated at least two independent times with similar results, and the data of representative experiments are shown

hcf-1(ok559) and the *hcf-1(pk924)* mutants as compared to wild-type nematodes [57]. This elevated expression of *sod-3*, *mtl-1*, and *F21F3.3* in the *hcf-1* mutant nematodes was also dependent on *daf-16*, since the levels of *sod-3*, *mtl-1*, and *F21F3.3* in the *daf-16(mgDf47);hcf-1(ok559)* double mutant remained low and was similar to that seen in the *daf-16(mgDf47)* single mutant nematodes [57]. Meanwhile, among the DAF-16-repressed genes, the expression level of *C32H11.4* showed a greater than twofold downregulation in *hcf-1* mutant nematodes compared to wild-type nematodes, and this repressed expression of *C32H11.4* could also be partially dependent on *daf-16* [57]. Therefore, HCF-1 may act upstream of DAF-16 and suppress the function of DAF-16 to regulate the toxicity of environmental toxicants or stresses in nematodes.

5.6.5 SIR-2.1/SIRT1

In nematodes, overexpressing *sir-2.1* can confer a lifespan extension phenotype that is dependent on the DAF-16 [19]. Under the paraquat or t-BOOH exposure conditions, the *sir-2.1(ok434)* mutant nematodes were sensitive, and the *hcf-1(pk924)* mutant nematodes were resistant to the treatments (Fig. 5.16) [58]. It has been further observed that, under the paraquat or t-BOOH exposure conditions, mutation of *hcf-1* could suppress the susceptibility of *sir-2.1(ok434)* mutant nematodes to the toxicity of paraquat or t-BOOH (Fig. 5.16) [58]. These observations imply that SIR-2.1 can act upstream of the insulin signaling pathway to regulate the toxicity of environmental toxicants or stresses by suppressing the function of HCF-1 in nematodes.

In nematodes, it was further found that the DAF-16 and the SIR-2.1 can interact even under the stress condition, and this interaction depended on the 14-3-3 proteins as the SIR-2.1 binding partners (Fig. 5.17) [59]. The 14-3-3 proteins were also required for the SIR-2.1-induced transcriptional activation of DAF-16 and the stress resistance [59]. Following the heat stress, SIR-2.1 will bind DAF-16 in a 14-3-3-dependent manner (Fig. 5.17) [59]. In contrast, the low insulin-like signaling did not promote the SIR-2.1/DAF-16 interaction, and thereby *sir-2.1* and the 14-3-3 were not required for the regulation of lifespan by the insulin-like signaling pathway [59]. Therefore, very large physical interactions surrounding the DAF-16 may be formed during the regulation of toxicity of environmental toxicants or stresses in nematodes.

5.6.6 PRDX-2

In nematodes, PRDX-2 is a single cytosolic 2-Cys Prx. Loss-of-function mutation of *prdx-2* increased the arsenite resistance by increasing both SKN-1 and DAF-16 activities [60]. Under the normal conditions, there was a significant increase in the

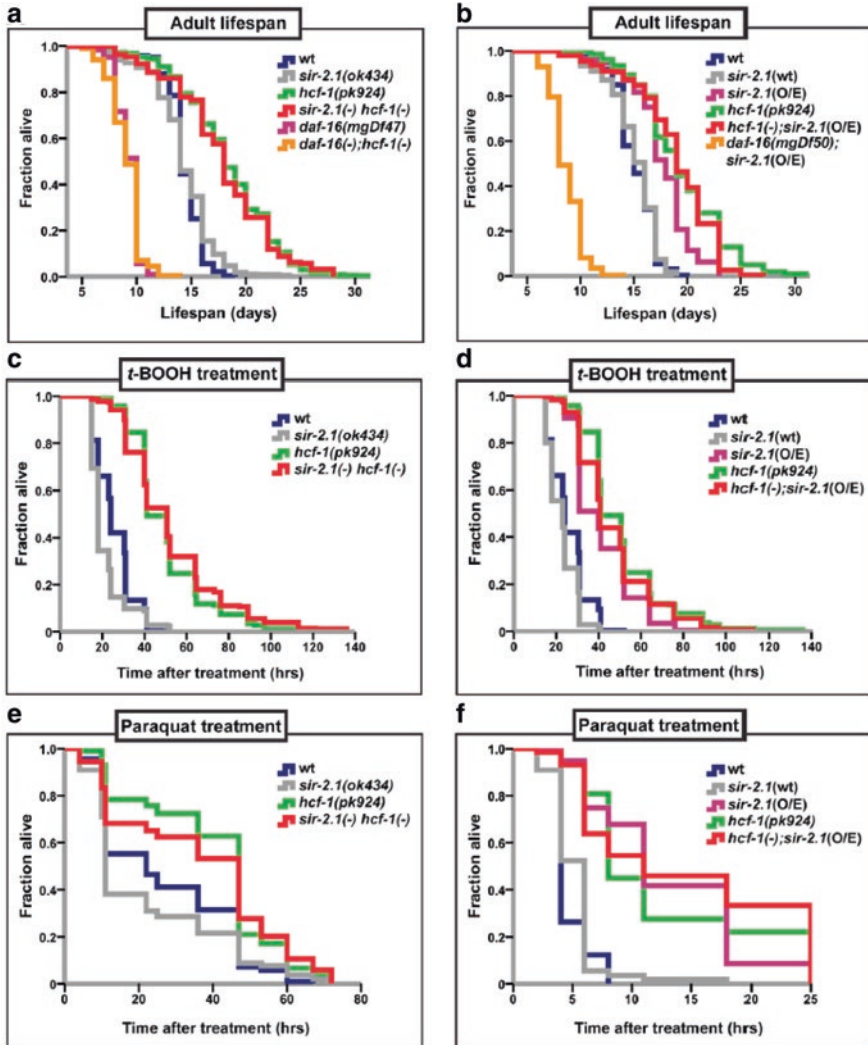


Fig. 5.16 *hcf-1* acts downstream of *sir-2.1* to modulate lifespan and oxidative stress response [58]. (a, b) Lifespans of synchronized adult populations of indicated genotypes. (a) Data pooled from four independent experiments are plotted. (b) Pooled data from three independent experiments are displayed. (c–f) Oxidative stress response of adult worms. (c, d) Day 1 adult worms were exposed to 6 mM t-BOOH on plates and their survival monitored through time. The survival curves represent pooled data from two independent experiments. (e, f) Day 2 adult worms were exposed to 150 mM (e) or 200 mM (f) paraquat in M9 buffer and their survival monitored through time. Survival curves are generated using pooled data from two independent experiments (e) or data from one of two representative experiments (f)

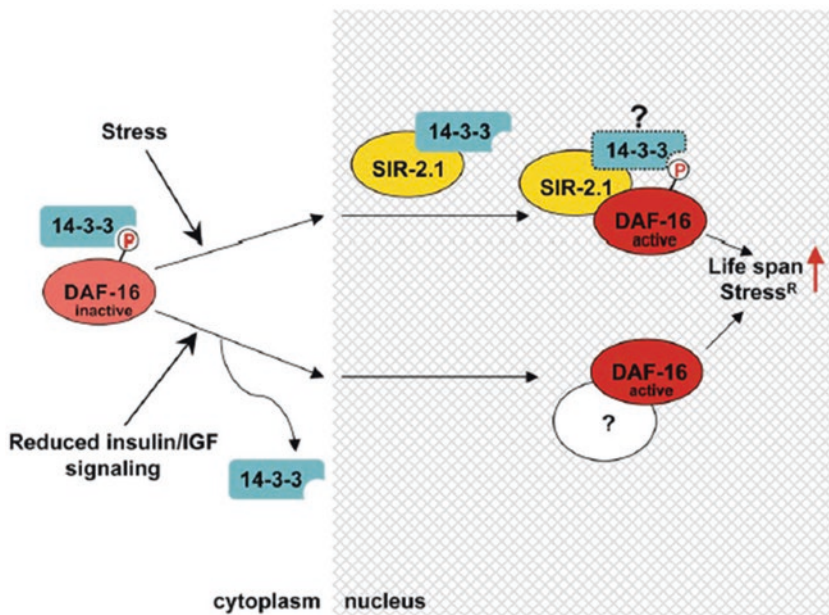


Fig. 5.17 A model for the roles of SIR-2.1 and 14-3-3 in DAF-16 regulation of stress resistance and lifespan [59]. It is proposed that, following the stress, SIR-2.1 binds DAF-16 in the nucleus in a 14-3-3-dependent manner, and the resulting complex participates in transcriptional activation of DAF-16 target genes. 14-3-3 may promote the interaction between SIR-2.1 and DAF-16 either by scaffolding the complex or through a modification of DAF-16 or SIR-2.1 following stress. Under the low insulin-like signaling conditions, DAF-16 is not phosphorylated at the Akt sites, becomes dissociated from 14-3-3, and accumulates in the nucleus. Nuclear DAF-16 produced by low insulin-like signaling does not bind SIR-2.1 and does not require *sir-2.1* and 14-3-3 function for activation

nuclear localization of DAF-16::GFP in *prdx-2* mutant nematodes (Fig. 5.18) [60]. Meanwhile, the expressions of several DAF-16-activated genes (*mtl-1*, *sod-3*, *gst-7*), as well as the expression of *sod-3p::gfp*, were also increased in *prdx-2* mutant nematodes (Fig. 5.18) [60]. More importantly, it was observed that mutation of *daf-16* or *skn-1* could suppress the resistance of *prdx-2(RNAi)* nematodes to the toxicity of arsenite in reducing the lifespan (Fig. 5.18) [60], which suggests that PRDX-2 acts upstream of both the DAF-16 and the SKN-1 to regulate the toxicity of environmental toxicants or stresses in nematodes.

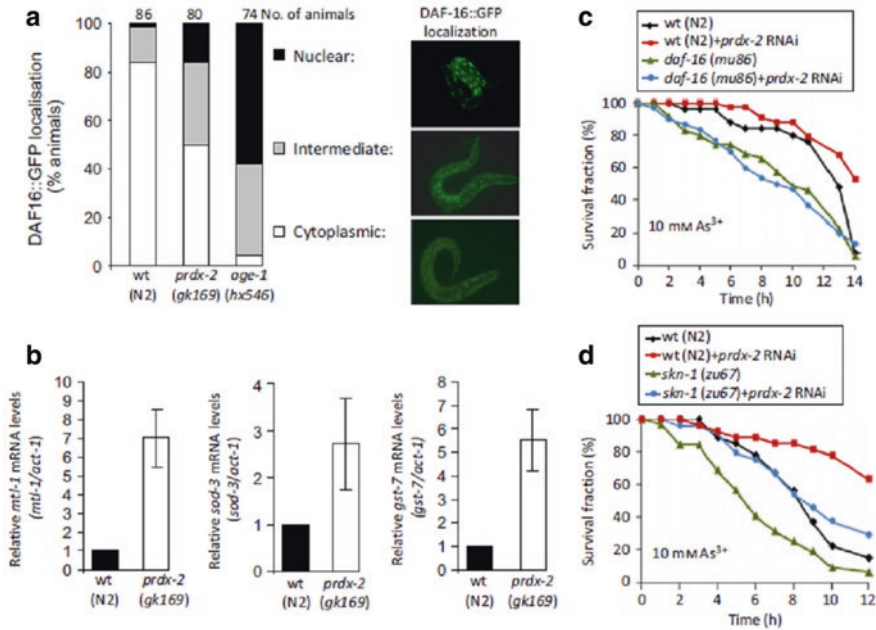


Fig. 5.18 Loss of PRDX-2 increases arsenite resistance by increasing both SKN-1 and DAF-16 activities [60]. **(a)** Loss of *prdx-2* causes nuclear accumulation of DAF-16. The localization of a DAF-16::GFP fusion protein was assessed in L2/L3 larval stage wild-type and *prdx-2* (*gk169*) and *age-1* (*hx584*) mutant animals expressing *daf-16a::GFP*. PRDX-2 deficiency caused nuclear accumulation of *daf-16a::GFP* in the intestinal nuclei. n refers to the number of worms examined in each group in the representative experiment shown. **(b)** *prdx-2* mutant animals contain increased levels of mRNA for *mtl-1*, *sod-3*, and *gst-7* compared with wild-type (N2) animals. mRNA levels were calculated relative to control (*act-1*) mRNA in at least six independently prepared RNA samples. Each panel depicts the levels of a particular mRNA in *prdx-2* mutant normalized to wild type (N2). Error bars represent the SEM. **(c, d)** The survival of L4 larval stage wild-type (N2) and *daf-16*(*mu86*) and *skn-1*(*zu67*) mutant animals microinjected with *prdx-2* dsRNA was monitored on NGM-L plates containing 10 mM sodium arsenite at indicated time points. **(c)** Loss of *prdx-2* significantly increased the arsenite resistance of wild-type but not *daf-16*(*mu86*) mutant animals. **(d)** *prdx-2* RNAi produces a greater increase in the arsenite resistance of wild-type than *skn-1*(*zu67*) mutant animals

5.7 Genetic Interaction Between SKN-1 and DAF-16 or DAF-2 in Regaling the Toxicity of Environmental Toxicants or Stresses

In nematodes, both the FOXO transcriptional factor DAF-16 and the FOXO transcriptional factor SKN-1/Nrf can act downstream of the insulin receptor DAF-2 in the insulin signaling pathway to regulate various biological processes, such as the stress response [28, 61]. Using intestinal ROS production as the toxicity assessment endpoint, it has been shown that the GO toxicity in inducing intestinal ROS

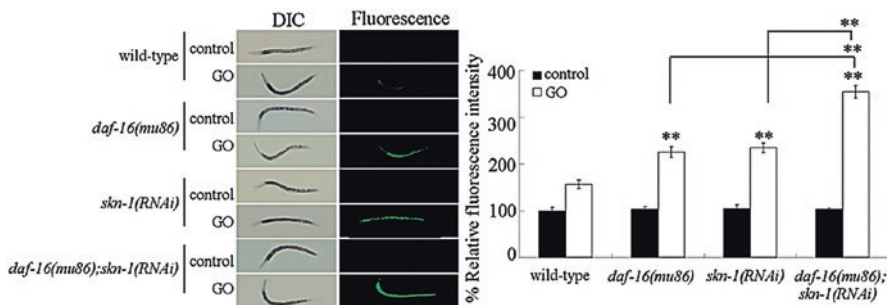


Fig. 5.19 Genetic interaction between DAF-16 and SKN-1 in the regulation of response to GO exposure [22]. Prolonged exposure was performed from L1-larvae to young adults. GO exposure concentration was 10 mg/L. Bars represent means \pm SD. ** $p < 0.01$ versus wild type (if not specially indicated)

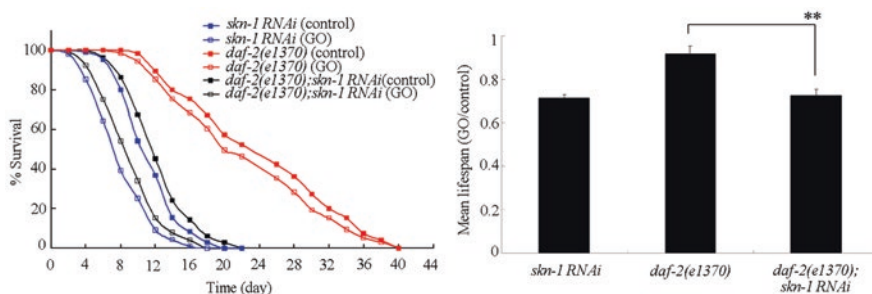


Fig. 5.20 Genetic interaction between DAF-2 and SKN-1 in regulating GO toxicity in nematodes [61]. Prolonged exposure was performed from L1-larvae to young adults. GO exposure concentration was 100 mg/L. Bars represent means \pm SEM. ** $P < 0.01$

production in *daf-16(mu86);skn-1(RNAi)* was more severe than that in *daf-16(mu86)* or in *skn-1(RNAi)* (Fig. 5.19) [22], suggesting that the SKN-1 and the DAF-16 may act in parallel signaling pathways to regulate the toxicity of environmental toxicants or stresses in nematodes.

Besides this, the genetic interaction between DAF-2 in insulin signaling pathway and SKN-1 in p38 MAPK signaling pathway in regulating GO toxicity was also examined. Prolonged exposure to GO (100 mg/L) could cause the similar toxicity on lifespan in double mutant of *daf-2(e1370);skn-1(RNAi)* to that in *skn-1(RNAi)* nematodes (Fig. 5.20) [61], suggesting that RNAi knockdown of *skn-1* may potentially suppress the resistance of *daf-2* mutant to the GO toxicity. Therefore, both the core signaling cascade of p38 MAPK signaling pathway and the insulin receptor DAF-2 in the insulin signaling pathway can act upstream of SKN-1 to regulate the toxicity of environmental toxicants or stresses in nematodes.

5.8 Perspectives

So far, a large amount of data has highlighted the possible pivotal function or role of the core insulin signaling pathway in the regulation of environmental toxicants or stresses in nematodes. Nevertheless, the detailed insulin signaling pathway involved in the control of toxicity from different environmental toxicants or stresses may be different. At least for the kinase cascade in the insulin signaling pathway, different environmental toxicants or stresses may affect different components. More importantly, among the large amount of targeted genes (predicted) for *daf-16*, only several genes have been proven to act as the downstream targeted genes for *daf-16* in regulating the toxicity of environmental toxicants or stresses. That is, it is still unclear whether the rest of predicted genes can also act as the targeted genes for *daf-16* in the regulation of toxicity of environmental toxicants or stresses.

As introduced above, the obtained data so far may imply the formation of a large physical interaction surrounding the DAF-16 in regulating the toxicity of environmental toxicants or stresses. The identification of exact scaffold molecules in this large complex may provide an important basis for further screen of related components and the thorough elucidation of the underlying mechanism for insulin signaling pathway in regulating the toxicity of environmental toxicants or stresses in nematodes.

References

1. Wang D-Y (2018) Nanotoxicology in *Caenorhabditis elegans*. Springer, Singapore
2. Wu Q-L, Zhi L-T, Qu Y-Y, Wang D-Y (2016) Quantum dots increased fat storage in intestine of *Caenorhabditis elegans* by influencing molecular basis for fatty acid metabolism. *Nanomedicine* 12:1175–1184
3. Shakoor S, Sun L-M, Wang D-Y (2016) Multi-walled carbon nanotubes enhanced fungal colonization and suppressed innate immune response to fungal infection in nematodes. *Toxicol Res* 5:492–499
4. Zhao L, Wan H-X, Liu Q-Z, Wang D-Y (2017) Multi-walled carbon nanotubes-induced alterations in microRNA *let-7* and its targets activate a protection mechanism by conferring a developmental timing control. *Part Fibre Toxicol* 14:27
5. Zhao L, Qu M, Wong G, Wang D-Y (2017) Transgenerational toxicity of nanopolystyrene particles in the range of $\mu\text{g/L}$ in nematode *Caenorhabditis elegans*. *Environ Sci Nano* 4:2356–2366
6. Zhao L, Rui Q, Wang D-Y (2017) Molecular basis for oxidative stress induced by simulated microgravity in nematode *Caenorhabditis elegans*. *Sci Total Environ* 607–608:1381–1390
7. Yin J-C, Liu R, Jian Z-H, Yang D, Pu Y-P, Yin L-H, Wang D-Y (2018) Di (2-ethylhexyl) phthalate-induced reproductive toxicity involved in DNA damage-dependent oocyte apoptosis and oxidative stress in *Caenorhabditis elegans*. *Ecotoxicol Environ Saf* 163:298–306
8. Xiao G-S, Zhao L, Huang Q, Yang J-N, Du H-H, Guo D-Q, Xia M-X, Li G-M, Chen Z-X, Wang D-Y (2018) Toxicity evaluation of Wanzhou watershed of Yangtze Three Gorges Reservoir in the flood season in *Caenorhabditis elegans*. *Sci Rep* 8:6734

9. Ding X-C, Wang J, Rui Q, Wang D-Y (2018) Long-term exposure to thiolated graphene oxide in the range of $\mu\text{g/L}$ induces toxicity in nematode *Caenorhabditis elegans*. *Sci Total Environ* 616–617:29–37
10. Li W-J, Wang D-Y, Wang D-Y (2018) Regulation of the response of *Caenorhabditis elegans* to simulated microgravity by p38 mitogen-activated protein kinase signaling. *Sci Rep* 8:857
11. Christopoulos PF, Corthay A, Koutsilieris M (2018) Aiming for the insulin-like growth factor-1 system in breast cancer therapeutics. *Cancer Treat Rev* 63:79–95
12. Haeusler RA, McGraw TE, Accili D (2018) Biochemical and cellular properties of insulin receptor signalling. *Nat Rev Mol Cell Biol* 19:31–44
13. Bryan MR, Bowman AB (2017) Manganese and the insulin-IGF signaling network in Huntington's disease and other neurodegenerative disorders. *Adv Neurobiol* 18:113–142
14. Guo CA, Guo S (2017) Insulin receptor substrate signaling controls cardiac energy metabolism and heart failure. *J Endocrinol* 233:R131–R143
15. Das D, Arur S (2017) Conserved insulin signaling in the regulation of oocyte growth, development, and maturation. *Mol Reprod Dev* 84:444–459
16. Stanley M, Macauley SL, Holtzman DM (2016) Changes in insulin and insulin signaling in Alzheimer's disease: cause or consequence? *J Exp Med* 213:1375–1385
17. Riera CE, Merkwirth C, De Magalhaes Filho CD, Dillin A (2016) Signaling networks determining life span. *Annu Rev Biochem* 85:35–64
18. Soultoukis GA, Partridge L (2016) Dietary protein, metabolism, and aging. *Annu Rev Biochem* 85:5–34
19. Kenyon C (2010) The genetics of ageing. *Nature* 464:504–512
20. Lapierre LR, Hansen M (2012) Lessons from *C. elegans*: signaling pathways for longevity. *Trends Endocrinol Metab* 23:637–644
21. Xiao G-S, Zhi L-T, Ding X-C, Rui Q, Wang D-Y (2017) Value of *mir-247* in warning graphene oxide toxicity in nematode *Caenorhabditis elegans*. *RSC Adv* 7:52694–52701
22. Qu M, Li Y-H, Wu Q-L, Xia Y-K, Wang D-Y (2017) Neuronal ERK signaling in response to graphene oxide in nematode *Caenorhabditis elegans*. *Nanotoxicology* 11:520–533
23. Chen H, Li H-R, Wang D-Y (2017) Graphene oxide dysregulates Neuroligin/NLG-1-mediated molecular signaling in interneurons in *Caenorhabditis elegans*. *Sci Rep* 7:41655
24. Xiao G-S, Chen H, Krasteva N, Liu Q-Z, Wang D-Y (2018) Identification of interneurons required for the aversive response of *Caenorhabditis elegans* to graphene oxide. *J Nanobiotechnol* 16:45
25. Zhao L, Kong J-T, Krasteva N, Wang D-Y (2018) Deficit in epidermal barrier induces toxicity and translocation of PEG modified graphene oxide in nematodes. *Toxicol Res* 7(6):1061–1070. <https://doi.org/10.1039/C8TX00136G>
26. Ding X-C, Rui Q, Wang D-Y (2018) Functional disruption in epidermal barrier enhances toxicity and accumulation of graphene oxide. *Ecotoxicol Environ Saf* 163:456–464
27. Ren M-X, Zhao L, Ding X-C, Krasteva N, Rui Q, Wang D-Y (2018) Developmental basis for intestinal barrier against the toxicity of graphene oxide. *Part Fibre Toxicol* 15:26
28. Zhao Y-L, Yang R-L, Rui Q, Wang D-Y (2016) Intestinal insulin signaling encodes two different molecular mechanisms for the shortened longevity induced by graphene oxide in *Caenorhabditis elegans*. *Sci Rep* 6:24024
29. Gubert P, Puntel B, Lehmen T, Bornhorst J, Avila DS, Aschner M, Soares FAA (2016) Reversible reprotoxic effects of manganese through DAF-16 transcription factor activation and vitellogenin downregulation in *Caenorhabditis elegans*. *Life Sci* 151:218–223
30. Avila DS, Somlyai G, Somlyai I, Aschner M (2012) Anti-aging effects of deuterium depletion on Mn-induced toxicity in a *C. elegans* model. *Toxicol Lett* 211:319–324
31. Yang R-L, Zhao Y-L, Yu X-M, Lin Z-Q, Xi Z-G, Rui Q, Wang D-Y (2015) Insulin signaling regulates toxicity of traffic-related $\text{PM}_{2.5}$ on intestinal development and function in nematode *Caenorhabditis elegans*. *Toxicol Res* 4:333–343

32. Wang S, Teng X, Wang Y, Yu H, Luo X, Xu A, Wu L (2014) Molecular control of arsenite-induced apoptosis in *Caenorhabditis elegans*: roles of insulin-like growth factor-1 signaling pathway. *Chemosphere* 112:248–255
33. Barsyte D, Lovejoy DA, Lithgow GJ (2001) Longevity and heavy metal resistance in *daf-2* and *age-1* long-lived mutants of *Caenorhabditis elegans*. *FASEB J* 15:627–634
34. Liu P-D, He K-W, Li Y-X, Wu Q-L, Yang P, Wang D-Y (2012) Exposure to mercury causes formation of male-specific structural deficits by inducing oxidative damage in nematodes. *Ecotoxicol Environ Saf* 79:90–100
35. Wang D-Y, Liu P-D, Yang Y-C, Shen L-L (2010) Formation of combined Ca/Cd toxicity on lifespan of nematode *Caenorhabditis elegans*. *Ecotoxicol Environ Saf* 73:1221–1230
36. Scott BA, Avidan MS, Crowder MC (2002) Regulation of hypoxic death in *C. elegans* by the insulin/IGF receptor homolog DAF-2. *Science* 296:2388–2391
37. Jensen VL, Simonsen KT, Lee Y-H, Park D, Riddle DL (2010) RNAi screen of DAF-16/FOXO target genes in *C. elegans* links pathogenesis and dauer formation. *PLoS ONE* 5:e15902
38. McElwee J, Bubb K, Thomas JH (2003) Transcriptional outputs of the *Caenorhabditis elegans* forkhead protein DAF-16. *Aging Cell* 2:111–121
39. Murphy CT, McGarroll SA, Bargmann CI, Fraser A, Kamath RS, Ahringer J, Kenyon C (2003) Genes that act downstream of DAF-16 to influence the lifespan of *Caenorhabditis elegans*. *Nature* 424:277–284
40. Tepper RG, Ashraf J, Kaletsky R, Kleemann G, Murphy CT, Bussemaker HJ (2013) PQM-1 complements DAF-16 as a key transcriptional regulator of DAF-2-mediated development and longevity. *Cell* 154:676–690
41. Ren M-X, Zhao L, Lv X, Wang D-Y (2017) Antimicrobial proteins in the response to graphene oxide in *Caenorhabditis elegans*. *Nanotoxicology* 11:578–590
42. Yang R-L, Rui Q, Kong L, Zhang N, Li Y, Wang X-Y, Tao J, Tian P-Y, Ma Y, Wei J-R, Li G-J, Wang D-Y (2016) Metallothioneins act downstream of insulin signaling to regulate toxicity of outdoor fine particulate matter (PM_{2.5}) during Spring Festival in Beijing in nematode *Caenorhabditis elegans*. *Toxicol Res* 5:1097–1105
43. Warnhoff K, Murphy JT, Kumar S, Schneider DL, Peterson M, Hsu S, Guthrie J, Robertson JD, Kornfeld K (2014) The DAF-16 FOXO transcription factor regulates *natc-1* to modulate stress resistance in *Caenorhabditis elegans*, linking insulin/IGF-1 signaling to protein N-terminal acetylation. *PLoS Genet* 10:e1004703
44. Yu Y-L, Zhi L-T, Wu Q-L, Jing L-N, Wang D-Y (2018) NPR-9 regulates innate immune response in *Caenorhabditis elegans* by antagonizing activity of AIB interneurons. *Cell Mol Immunol* 15:27–37
45. Zhi L-T, Yu Y-L, Li X-Y, Wang D-Y, Wang D-Y (2017) Molecular control of innate immune response to *Pseudomonas aeruginosa* infection by intestinal *let-7* in *Caenorhabditis elegans*. *PLoS Pathog* 13:e1006152. (9)
46. Zhi L-T, Yu Y-L, Jiang Z-X, Wang D-Y (2017) *mir-355* functions as an important link between p38 MAPK signaling and insulin signaling in the regulation of innate immunity. *Sci Rep* 7:14560
47. Yu Y-L, Zhi L-T, Guan X-M, Wang D-Y, Wang D-Y (2016) FLP-4 neuropeptide and its receptor in a neuronal circuit regulate preference choice through functions of ASH-2 trithorax complex in *Caenorhabditis elegans*. *Sci Rep* 6:21485
48. Singh V, Aballay A (2006) Heat-shock transcription factor (HSF)-1 pathway required for *Caenorhabditis elegans* immunity. *Proc Natl Acad Sci U S A* 103:13092–13097
49. Yang R-L, Ren M-X, Rui Q, Wang D-Y (2016) A *mir-231*-regulated protection mechanism against the toxicity of graphene oxide in nematode *Caenorhabditis elegans*. *Sci Rep* 6:32214
50. Wu Q-L, Han X-X, Wang D, Zhao F, Wang D-Y (2017) Coal combustion related fine particulate matter (PM_{2.5}) induces toxicity in *Caenorhabditis elegans* by dysregulating microRNA expression. *Toxicol Res* 6:432–441

51. Zhuang Z-H, Li M, Liu H, Luo L-B, Gu W-D, Wu Q-L, Wang D-Y (2016) Function of RSKS-1-AAK-2-DAF-16 signaling cascade in enhancing toxicity of multi-walled carbon nanotubes can be suppressed by *mir-259* activation in *Caenorhabditis elegans*. *Sci Rep* 6:32409
52. Zhao Y-L, Wu Q-L, Li Y-P, Nouara A, Jia R-H, Wang D-Y (2014) In vivo translocation and toxicity of multi-walled carbon nanotubes are regulated by microRNAs. *Nanoscale* 6:4275–4284
53. Nouara A, Wu Q-L, Li Y-X, Tang M, Wang H-F, Zhao Y-L, Wang D-Y (2013) Carboxylic acid functionalization prevents the translocation of multi-walled carbon nanotubes at predicted environmental relevant concentrations into targeted organs of nematode *Caenorhabditis elegans*. *Nanoscale* 5:6088–6096
54. Wu Q-L, Li Y-X, Li Y-P, Zhao Y-L, Ge L, Wang H-F, Wang D-Y (2013) Crucial role of biological barrier at the primary targeted organs in controlling translocation and toxicity of multi-walled carbon nanotubes in nematode *Caenorhabditis elegans*. *Nanoscale* 5:11166–11178
55. Wu Q-L, Zhao Y-L, Li Y-P, Wang D-Y (2014) Molecular signals regulating translocation and toxicity of graphene oxide in nematode *Caenorhabditis elegans*. *Nanoscale* 6:11204–11212
56. Wolf M, Nunes F, Henkel A, Heinick A, Paul RJ (2008) The MAP kinase JNK-1 of *Caenorhabditis elegans*: location, activation, and influences over temperature-dependent insulin-like signaling, stress responses, and fitness. *J Cell Physiol* 214:721–729
57. Li J, Ebata A, Dong Y, Rizki G, Iwata T, Lee SS (2008) *Caenorhabditis elegans* HCF-1 functions in longevity maintenance as a DAF-16 regulator. *PLoS Biol* 6:e233
58. Rizki G, Iwata TN, Li J, Riedel CG, Picard CL, Jan M, Murphy CT, Lee SS (2011) The evolutionarily conserved longevity determinants HCF-1 and SIR-2.1/SIRT1 collaborate to regulate DAF-16/FOXO. *PLoS Genet* 7:e1002235
59. Berdichevsky A, Viswanathan M, Horvitz HR, Guarente L (2006) *C. elegans* SIR-2.1 interacts with 14-3-3 proteins to activate DAF-16 and extend life span. *Cell* 125:1165–1177
60. Olahova M, Veal EA (2015) A peroxiredoxin, PRDX-2, is required for insulin secretion and insulin/IIS-dependent regulation of stress resistance and longevity. *Aging Cell* 14:558–568
61. Zhao Y-L, Zhi L-T, Wu Q-L, Yu Y-L, Sun Q-Q, Wang D-Y (2016) p38 MAPK-SKN-1/Nrf signaling cascade is required for intestinal barrier against graphene oxide toxicity in *Caenorhabditis elegans*. *Nanotoxicology* 10:1469–1479

Chapter 6

Functions of Development-Related Signaling Pathways in the Regulation of Toxicity of Environmental Toxicants or Stresses



Abstract Although the development-related signaling pathways are normally considered to be required for certain aspects of development, some development-related signaling pathways may participate in regulating the toxicity of environmental toxicants or stresses under certain conditions. In this chapter, we introduced and discussed the involvement of Wnt, TGF- β , Notch, and developmental timing control-related signaling pathways in the regulation of toxicity of environmental toxicants or stresses and the underlying mechanisms in nematodes. The information introduced here further confirms the potential dual roles of some developmental related signals in the toxicity induction of environmental toxicants or stresses.

Keywords Development-related signaling pathways · Molecular regulation · Environmental exposure · *Caenorhabditis elegans*

6.1 Introduction

In Chaps. 3, 4, and 5, we have introduced and discussed the value of *C. elegans* in toxicological study and the important functions or roles of oxidative stress, MAPK, and insulin signaling pathways in the regulation of toxicity of environmental toxicants or stresses [1–14]. Among the molecular signaling pathways involved in the regulation of toxicity of environmental toxicants or stresses, the development-related signaling pathways are relatively specific. Normally, these development-related signaling pathways are required for certain aspects of development. Nevertheless, under certain conditions, some development-related signaling pathways may also participate in the regulation of toxicity of environmental toxicants or stresses in nematodes. That is, at least some development-related signaling pathways may have dual roles in organisms.

In this chapter, we first introduced and discussed the involvement of Wnt, TGF- β , and Notch signaling pathways in the regulation of toxicity of environmental toxicants or stresses and the underlying mechanisms. Moreover, we introduced and discussed the important function of developmental timing control-related signals, especially the *let-7*-mediated developmental related signals in the regulation of

toxicity of environmental toxicants or stresses in nematodes. The information introduced here implies the dual roles of developmental related signals in the toxicity induction of environmental toxicants or stresses. That is, on the one hand, environmental exposure to certain toxicants or stresses may induce the developmental toxicity by dysregulating developmental related signals. On the other hand, the dysregulation of certain developmental related signals may itself regulate the toxicity induction of environmental toxicants or stresses.

6.2 Wnt Signaling Pathway

6.2.1 *Involvement of Certain Wnt Ligands in Regulating the Toxicity of Environmental Toxicants or Stresses*

In nematodes, five Wnt ligands have been identified in the Wnt signaling pathway, and they are LIN-44, EGL-20, MOM-2, CWN-1, and CWN-2. Graphene and its derivatives, such as graphene oxide (GO), can be used in many industrial and medical fields, and meanwhile some of the members may potentially cause the toxicity on several aspects in nematodes [15–22]. With the GO as an example, among these Wnt ligands, it has been found that mutation of *mom-2* or *egl-20* could not affect the formation of GO toxicity in inducing intestinal ROS production and in decreasing locomotion behavior (Fig. 6.1) [23]. In contrast, mutation of *cwn-1* or *lin-44* induced a resistance to GO toxicity in inducing intestinal ROS production and in decreasing locomotion behavior; however, mutation of *cwn-2* induced a susceptibility to GO toxicity in inducing intestinal ROS production and in decreasing locomotion behavior (Fig. 6.1) [23]. Therefore, the Wnt ligands of CWN-1, CWN-2, and LIN-44 play an important role in regulating the toxicity of environmental toxicants or stresses.

Moreover, mutation of *cwn-2* enhanced the intestinal permeability in GO-exposed nematodes, and mutation of *cwn-1* inhibited the intestinal permeability in GO-exposed nematodes as indicated by the analysis on Nile Red signal [23]. Furthermore, *lin-44* mutation suppressed mean defecation cycle length in GO-exposed nematodes [23]. Therefore, Wnt ligands may regulate the toxicity of environmental toxicants or stresses through different underlying cellular mechanisms.

6.2.2 *Genetic Interactions of Wnt Ligands in Regulating the Toxicity of Environmental Toxicants or Stresses*

Genetic interaction analysis demonstrated that mutation of *cwn-1* or *lin-44* could inhibit the susceptibility of *cwn-2(ok895)* mutant to GO toxicity in inducing intestinal ROS production and in decreasing locomotion behavior (Fig. 6.2) [23].

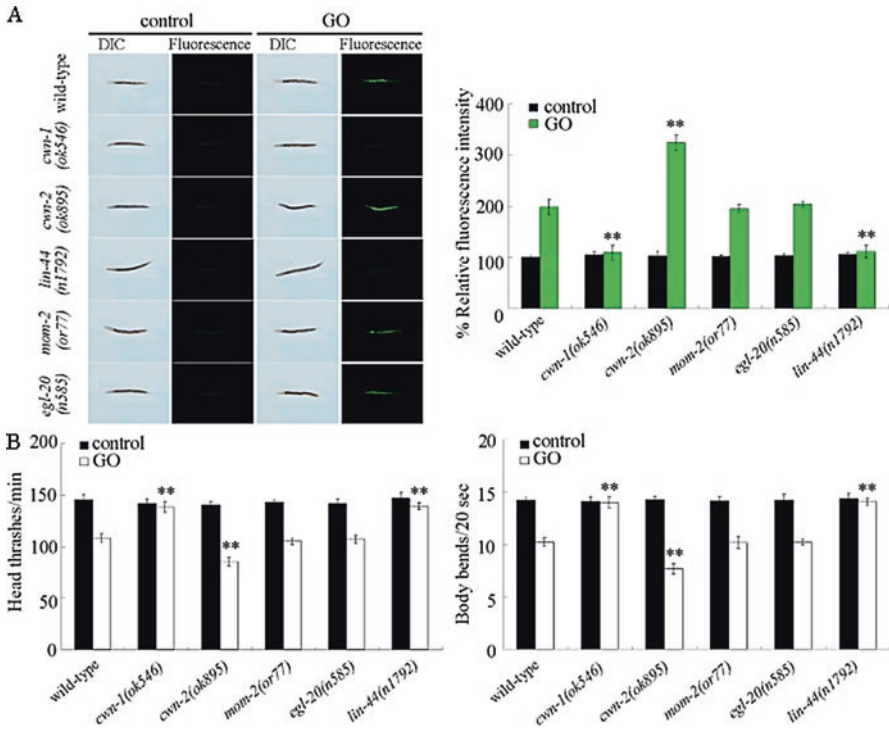


Fig. 6.1 Effects of *cwn-1*, *cwn-2*, *mom-2*, *egl-20*, or *lin-44* mutation on GO toxicity in nematodes [23]. (a) Effects of *cwn-1*, *cwn-2*, *mom-2*, *egl-20*, or *lin-44* mutation on GO toxicity in inducing intestinal ROS production. (b) Effects of *cwn-1*, *cwn-2*, *mom-2*, *egl-20*, or *lin-44* mutation on GO toxicity in decreasing locomotion behavior. GO exposure concentration was 100 mg/L. Prolonged exposure was performed from L1-larvae to young adults. Bars represent means \pm SD. ** $P < 0.01$ vs wild type

Additionally, CWN-1 and LIN-44 functioned in the same genetic pathway to regulate the GO toxicity in inducing intestinal ROS production and in decreasing locomotion behavior (Fig. 6.2) [23]. Moreover, the *lin-44(n1792); cwn-1(ok546); cwn-2(ok895)* triple mutant nematodes showed the similar induction of intestinal ROS production and locomotion behavior to those in *cwn-1(ok546); cwn-2(ok895)*, *lin-44(n1792); cwn-1(ok546)*, or *lin-44(n1792); cwn-2(ok895)* double mutant nematodes (Fig. 6.2) [23], which implies that these Wnt ligand signals may, as a whole, positively regulate the toxicity of environmental toxicants or stresses in nematodes.

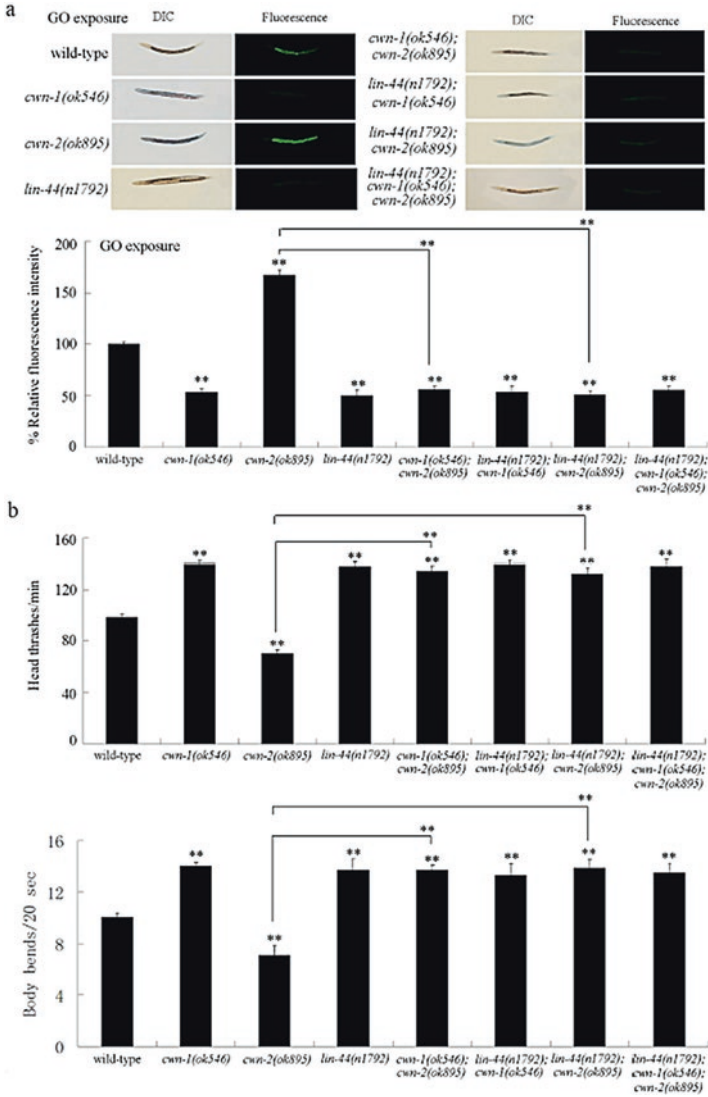


Fig. 6.2 Genetic interactions of Wnt ligands in regulating GO toxicity in nematodes [23]. **(a)** Genetic interactions of Wnt ligands in regulating GO toxicity in inducing intestinal ROS production in nematodes. **(b)** Genetic interactions of Wnt ligands in regulating GO toxicity in decreasing locomotion behavior in nematodes. GO exposure concentration was 100 mg/L. Prolonged exposure was performed from L1-larvae to young adults. Bars represent means \pm SD. ** $P < 0.01$ vs wild type (if not specially indicated)

6.2.3 *Involvement of Canonical Wnt/ β -Catenin Signaling Pathway in Regulating the Toxicity of Environmental Toxicants or Stresses*

In nematodes, *bar-1* encodes β -catenin in canonical Wnt signaling pathway. Wnt ligand(s) binds to Frizzled receptors (LIN-17, MOM-5, MIG-1, or CFZ-2), and then activates Dishevelled proteins (MIG-5, DSH-1, and/or DSH-2) [24]. The Dishevelled proteins further suppress the activity of APC complex (containing APR-1/Axin, PRY-1/CK1a, KIN-19, and GSK-3) in order to stabilize the activity of BAR-1 [24].

In nematodes, mutation of *bar-1* induced a susceptibility to some aspects of GO toxicity, such as induction of ROS production and decrease in locomotion behavior (Fig. 6.3) [25]. After prolonged exposure, GO (1 mg/L) could significantly decrease the *bar-1* expression in wild-type nematodes (Fig. 6.3) [25], implying that long-term exposure to GO may potentially suppress the *bar-1* expression.

GO (1 mg/L) exposure increased the expressions of *apr-1* and *gsk-3* encoding components of APC complex [25]. Mutation of *apr-1* or *gsk-3* induced a resistance to some aspects of GO toxicity, such as induction of ROS production and decrease in locomotion behavior [25]. More importantly, RNAi knockdown of *bar-1* inhibited the resistance of *apr-1* or *gsk-3* mutants to GO toxicity [25], suggesting that APR-1 and GSK-3 act upstream of BAR-1 in regulating the toxicity of environmental toxicants or stresses.

Among the genes encoding the Dishevelled proteins, prolonged exposure to GO (1 mg/L) could significantly decrease the expressions of *dsh-1* and *dsh-2* [25]. Meanwhile, mutation of *dsh-1* or *dsh-2* induced a susceptibility to GO toxicity in inducing intestinal ROS production and in decreasing locomotion behavior [25]. Moreover, it was found that RNAi knockdown of *apr-1* or *gsk-3* could significantly suppress the susceptibility of *dsh-1* or *dsh-2* mutant nematodes to GO toxicity in inducing intestinal ROS production and in decreasing locomotion behavior [25], which suggests that DSH-1 and DSH-2 act upstream of APR-1 or GSK-3 in regulating the toxicity of environmental toxicants or stresses.

Among the genes encoding the Frizzled receptors, prolonged exposure to GO (1 mg/L) could significantly decrease the expressions of *mom-5* and *cfz-2* (Fig. 6.4) [25]. Meanwhile, mutation of *mom-5* or *cfz-2* induced a susceptibility to GO toxicity in inducing intestinal ROS production and in decreasing locomotion behavior (Fig. 6.4) [25]. Moreover, it was found that Frizzled receptors of MOM-5 and CFZ-2 act in the same genetic pathway with DSH-1 or DSH-2 to regulate the toxicity of environmental toxicants or stresses in nematodes (Fig. 6.4) [25].

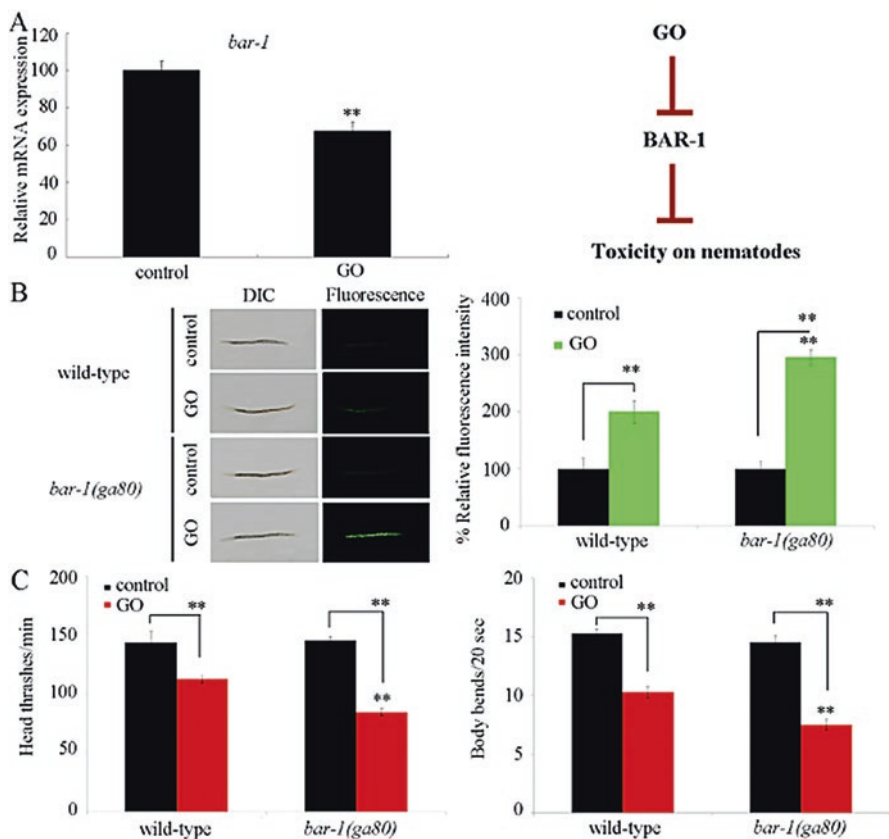


Fig. 6.3 BAR-1 regulated GO toxicity in nematodes [25]. (a) Effect of GO exposure on *bar-1* expression in wild-type nematodes. Bars represent means \pm SD. ** $P < 0.01$ vs control. (b) BAR-1 regulated GO toxicity in inducing intestinal ROS production. Bars represent means \pm SD. ** $P < 0.01$ vs wild type (if not specially indicated). (c) BAR-1 regulated GO toxicity in decreasing locomotion behavior. Bars represent means \pm SD. ** $P < 0.01$ vs wild type (if not specially indicated). Prolonged exposure was performed from L1-larvae to young adults. GO exposure concentration was 1 mg/L.

6.2.4 Role of HMP-2 in the Regulation of Toxicity of Environmental Toxicants or Stresses

In nematodes, HMP-2 is another β -catenin protein. HMP-2 is required for the control of development of intestinal apical junctions, especially the tissue integrity of intestinal tube [26]. VP303 strain is a tool for intestine-specific RNAi of certain genes in nematodes [27]. VP303 was used as an intestine-specific RNAi knockdown tool, and intestinal ROS production was used as an endpoint to assess the potential toxicity of GO exposure on intestinal function. Under the normal conditions, intestine-specific RNAi knockdown of *hmp-2* cannot result in the induction of significant

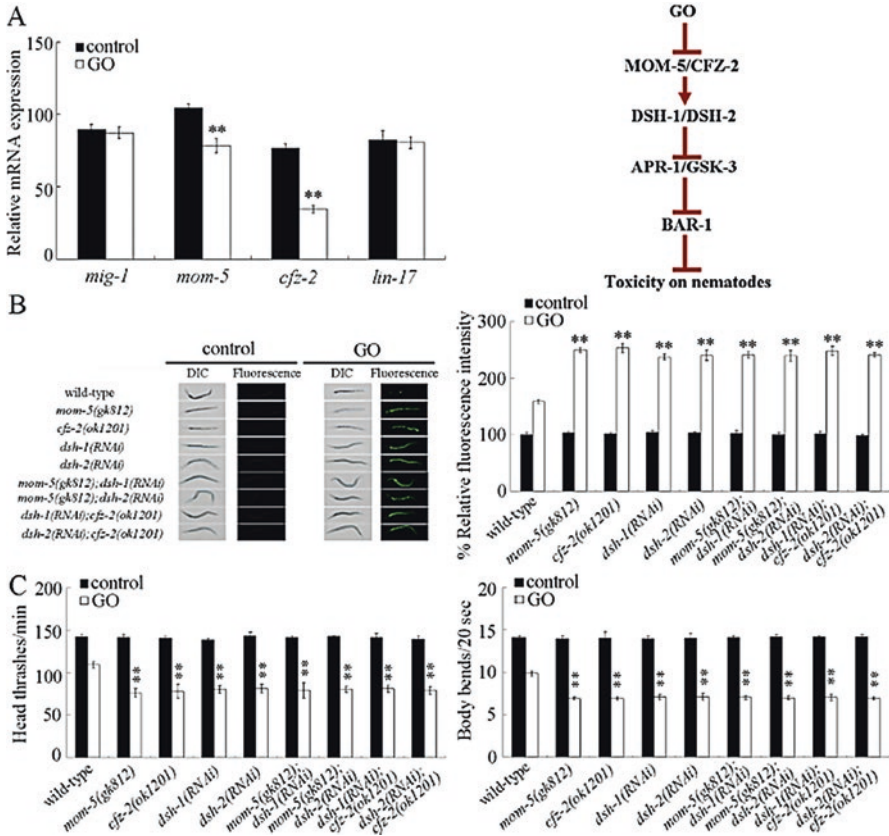


Fig. 6.4 Role of Frizzled receptors in the regulation of GO toxicity in nematodes [25]. (a) Effect of GO exposure on expression of genes encoding Frizzled receptors in wild-type nematodes. Bars represent means ± SD. ***P* < 0.01 vs control. (b) Role of Frizzled receptors in the regulation of GO toxicity in inducing intestinal ROS production. Bars represent means ± SD. ***P* < 0.01 vs wild type. (c) Role of Frizzled receptors in the regulation of GO toxicity in decreasing locomotion behavior. Bars represent means ± SD. ***P* < 0.01 vs wild type. Prolonged exposure was performed from L1-larvae to young adults. GO exposure concentration was 1 mg/L

intestinal ROS production (Fig. 6.5) [28]. After acute exposure to GO, among the examined genes required for the control of development of intestinal apical junctions, although intestine-specific RNAi knockdown of *dlg-1*, *ajm-1*, *egl-8*, *lin-7*, *hmp-1*, or *hmr-1* did not significantly influence the induction of intestinal ROS production, intestine-specific RNAi knockdown of *hmp-2* caused the enhanced induction of intestinal ROS production (Fig. 6.5) [28]. Additionally, intestine-specific RNAi knockdown of *hmp-2* significantly enhanced the accumulation of GO/Rho B in the body of nematodes [28]. These results demonstrate the important role of HMP-2 in regulating the toxicity of environmental toxicants or stresses.

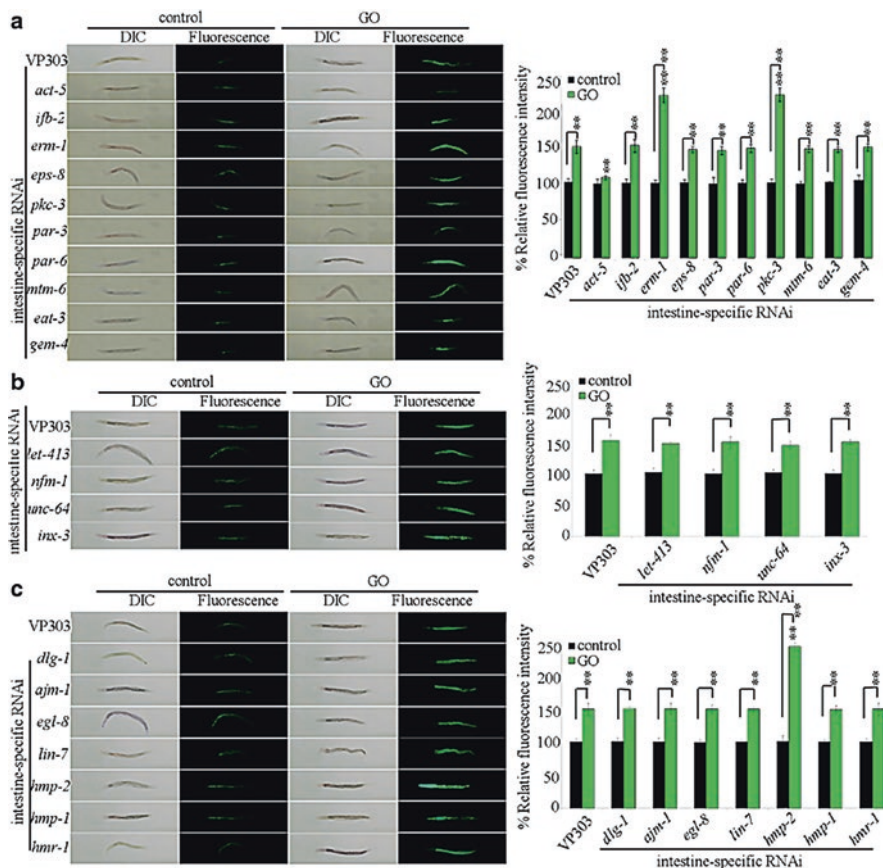


Fig. 6.5 Effects of intestine-specific RNAi knockdown of intestine-developmental related genes on GO toxicity [28]. (a) Effects of intestine-specific RNAi knockdown of genes required for the control of development of intestinal apical domain on GO toxicity in inducing intestinal ROS production. (b) Effects of intestine-specific RNAi knockdown of genes required for the control of development of intestinal basolateral domain on GO toxicity in inducing intestinal ROS production. (c) Effects of intestine-specific RNAi knockdown of genes required for the control of development of intestinal apical junctions on GO toxicity in inducing intestinal ROS production. Acute exposure was performed from L4-larvae for 24 h. GO exposure concentration was 10 mg/L. Bars represent means \pm SD. $**P < 0.01$ vs VP303 (if not specially indicated)

6.2.5 Identification of Downstream Targets for β -Catenin *BAR-1* in Regulating the Toxicity of Environmental Toxicants or Stresses

Among the potential targets (LIN-39, MAB-5, and EGL-5) of *BAR-1*, GO (1 mg/L) exposure suppressed *egl-5* expression, and *egl-5* mutation induced a susceptibility to GO toxicity (Fig. 6.6) [25]. Moreover, it was found that *BAR-1* and *EGL-5*

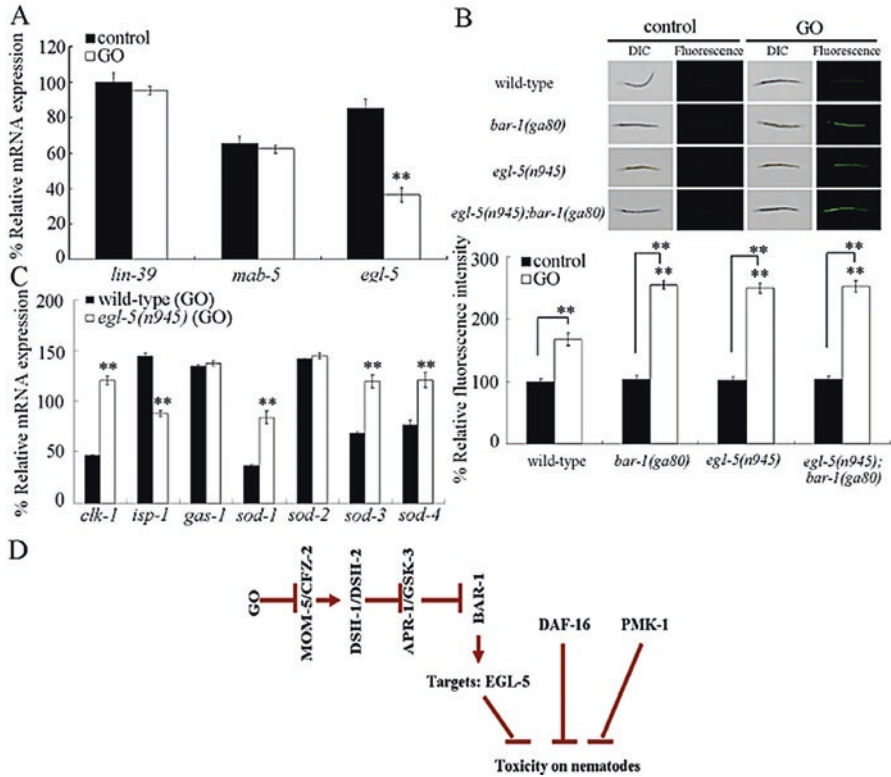


Fig. 6.6 Role of EGL-5 in the regulation of GO toxicity in nematodes [25]. (a) Effect of GO exposure on expression of genes encoding downstream mediators of BAR-1 in nematodes. Bars represent means \pm SD. $**P < 0.01$ vs control. (b) Genetic interaction between BAR-1 and EGL-5 in the regulation of GO toxicity in inducing intestinal ROS production. Bars represent means \pm SD. $**P < 0.01$ vs wild type (if not specially indicated). (c) Effect of *egl-5* mutation on expression of genes required for the control of oxidative stress after GO exposure. Bars represent means \pm SD. $**P < 0.01$ vs wild type (GO). Prolonged exposure was performed from L1-larvae to young adults. GO exposure concentration was 1 mg/L. (d) A diagram showing the signaling cascade of canonical Wnt/ β -catenin signaling in the regulation of GO toxicity in nematodes

function in the same pathway to regulate the GO toxicity (Fig. 6.6) [25]. EGL-5 is a homeodomain transcription factor. Similarly, after the infection with *Staphylococcus aureus*, transcriptional profiling and reverse genetic analysis suggested that mutation of *bar-1* or its downstream homeobox gene *egl-5* resulted in a defective response and hypersensitivity to *S. aureus* infection [29].

Additionally, mutation of *egl-5* could significantly increase the expression of *clk-1*, *sod-1*, *sod-3*, and *sod-4* and decrease the expression of *gas-1* in GO-exposed nematodes (Fig. 6.6) [25]. Thus, a signaling cascade of MOM-5/CFZ-2-DSH-1/DSH-2-APR-1/GSK-3-BAR-1-EGL-5 in the canonical Wnt/ β -catenin signaling pathway has been raised for the control of toxicity of environmental toxicants or stresses, such as GO exposure.

6.2.6 Genetic Interactions Between β -Catenin BAR-1 and Other Signaling Pathways in Regulating the Toxicity of Environmental Toxicants or Stresses

Genetic analysis has indicated that a synergistic effect between BAR-1 and DAF-16 was formed during the control of GO toxicity (Fig. 6.7) [25]. Additionally, a synergistic effect between BAR-1 and PMK-1 was also formed during the control of GO toxicity (Fig. 6.7) [25]. That is, Wnt/ β -catenin signaling can function in parallel with p38 MAPK signaling or insulin signaling in regulating the toxicity of environmental toxicants or stresses in nematodes.

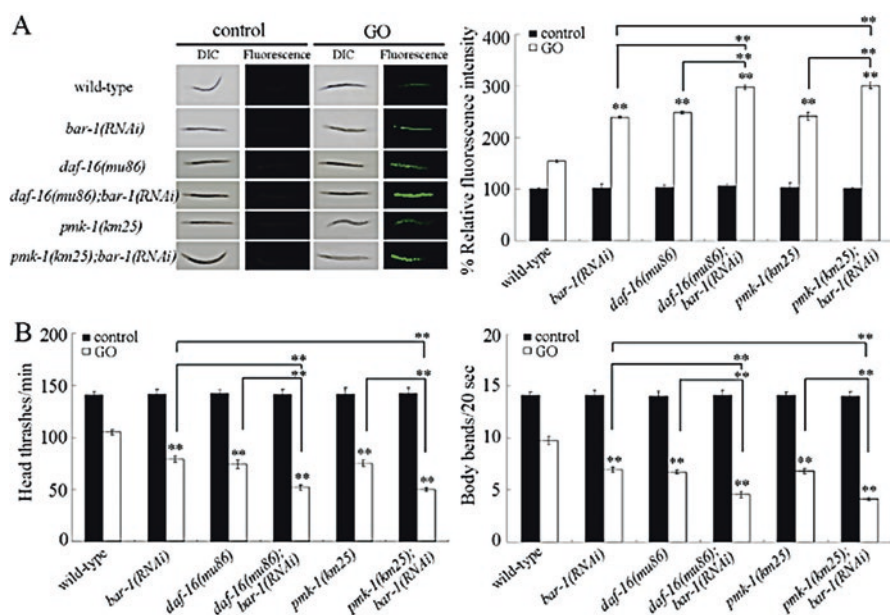


Fig. 6.7 Genetic interaction between BAR-1 with DAF-16 or p38 MAPK/PMK-1 in the regulation of GO toxicity in nematodes [25]. (a) Genetic interaction between BAR-1 with DAF-16 or p38 MAPK/PMK-1 in the regulation of GO toxicity in inducing intestinal ROS production. Bars represent means \pm SD. ** $P < 0.01$ vs wild type (if not specially indicated). (b) Genetic interaction between BAR-1 with DAF-16 or p38 MAPK/PMK-1 in the regulation of GO toxicity in decreasing locomotion behavior. Bars represent means \pm SD. ** $P < 0.01$ vs wild type (if not specially indicated). Prolonged exposure was performed from L1-larvae to young adults. GO exposure concentration was 1 mg/L

6.3 TGF- β Signaling Pathway

The basic information for the TGF- β signaling pathway in nematodes has been well described in the review (Fig. 6.8) [30].

6.3.1 DBL-1-Mediated TGF- β Signaling Pathway

6.3.1.1 Involvement of DBL-1 in the Regulation of Toxicity of Environmental Toxicants or Stresses

Both bacterial and fungal pathogens are toxic for animals, and the nematodes can respond to the invading pathogens [31–37]. The *dbl-1* mutants exhibited a dramatically reduced lifespan in the presence of *S. marcescens* Db11 or *S. marcescens* Db1140 relative to wild-type nematodes (Fig. 6.9) [38]. Meanwhile, although they

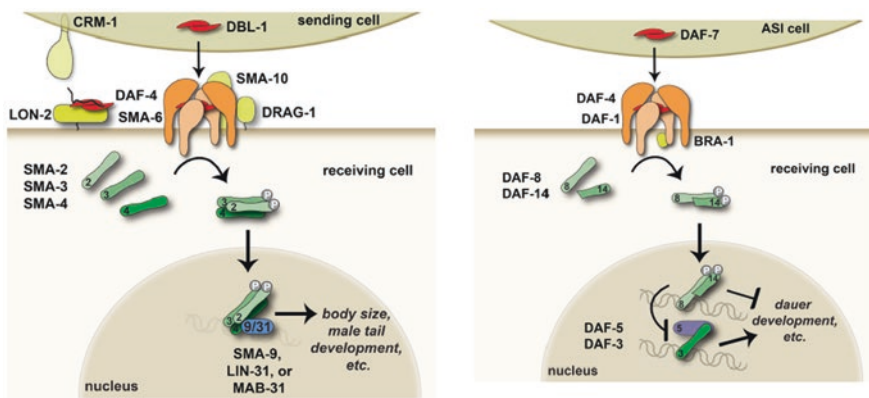


Fig. 6.8 TGF- β signaling pathway [30]. The left image shows the Sma/Mab TGF- β -related pathway. In this pathway, DBL-1 signal (red) is received by a heterotetrameric receptor composed of two SMA-6 type I receptor and two DAF-4 type II receptor subunits (light and dark orange, respectively). Extracellular regulators (yellows) of DBL-1 signaling include CRM-1, which acts at the sending cell membrane or in the extracellular space to promote DBL-1 signaling, SMA-10 and DRAG-1, which promote DBL-1 signaling at the membrane of the receiving cell, and LON-2/glypican, which inhibits DBL-1 signaling at the receiving cell. The DBL-1 signal is transduced by SMA-2, SMA-3, and SMA-4 Smads (greens). Transcription factors (blue) that act with Smads to carry out DBL-1-mediated responses include SMA-9/Schnurri, LIN-31/forkhead, and MAB-31. The right image shows the dauer TGF- β related pathway. In this pathway, DAF-7 promotes continuous, non-dauer development. The DAF-7 signal (red) is received by a heterotetrameric receptor composed of two DAF-1 type I receptor and two DAF-4 type II receptor subunits (light and dark orange, respectively). BRA-1/BMP receptor-associated protein (BRAM) (yellow) is a negative intracellular regulator of DAF-1. The DAF-7 signal is transduced by DAF-8 and DAF-14 Smads (light greens). These components, when activated, inhibit the functions of DAF-3/Co-Smad (dark green) and DAF-5/Sno/Ski (indigo), which promote dauer development. The Smad/Ski model shown is not definitive

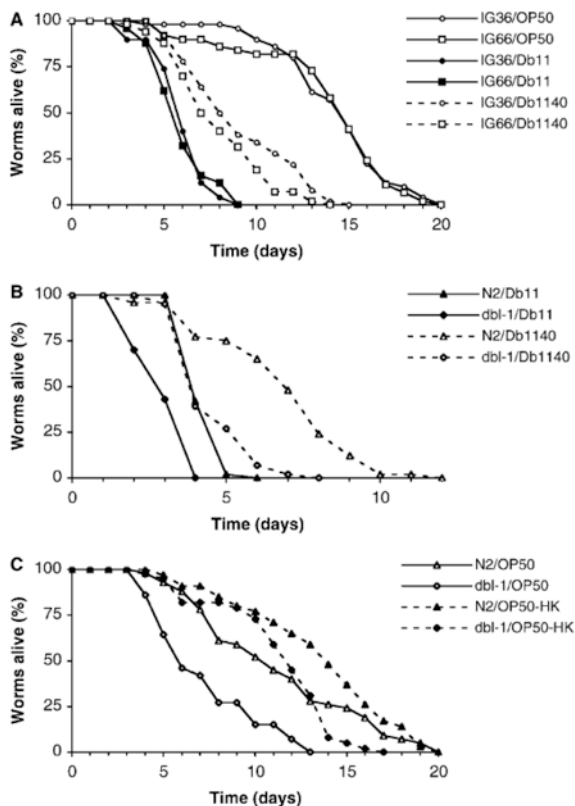


Fig. 6.9 Modulation of the resistance of *C. elegans* to infection [38]. (a) Transgenic worms expressing *lys-1::GFP* resist infection by *S. marcescens*. Representative time courses of the survival of control worms (IG66; squares) or worms expressing *lys-1::GFP* (IG36; circles) in the presence of *E. coli* OP50 (open symbols) and *S. marcescens* strains Db11 (closed symbols) and Db1140 (open symbols, dashed lines). The increase in the survival of IG36 relative to IG66 on Db1140 is very significant. (b, c) *dbl-1* mutants are vulnerable to infection. Representative time courses of the survival of wild-type N2 worms (triangles) and *dbl-1(nk3)* mutants (diamonds) in the presence of (b) *S. marcescens* Db11 (closed symbols) and Db1140 (open symbols, dashed lines) and (c) *E. coli* OP50 (open symbols) or heat-killed OP50 (closed symbols, dashed lines). While the difference between the survival of wild-type worms on OP50 and on heat-killed OP50 is not extremely significant, that for *dbl-1* mutants is. All tests were repeated at least three times, starting with 50 worms under each condition per test

showed a reduced lifespan when grown on living OP50, the *dbl-1* mutants were more susceptible to infection by OP50 than wild-type nematodes (Fig. 6.9) [38]. Additionally, the *dbl-1* mutants were visibly sick when grown on live OP50, but not when grown on the heat-killed [38]. Therefore, the TGF- β ligand DBL-1 is involved in the regulation of toxicity of environmental toxicants or stresses in nematodes.

6.3.1.2 Involvement of Signaling Cascade of SMA-6-SMA-2/SMA-3/SMA-4 in the Regulation of Toxicity of Environmental Toxicants or Stresses

The small body size phenotype (Sma) and male tail abnormal phenotype (Mab) of *daf-4* led to genetic identification of *sma-2*, *sma-3*, and *sma-4* genes. In nematodes, SMA-6, SMA-3, SMA-2, and SMA-4 were found to be involved in the control of innate immune response to pathogen infection [39, 40]. On the pathogen infection, some of the highest induced targets of the Sma/Mab pathway are at least lectins and lysozymes [40]. Additionally, some of the genes whose regulation changes on bacterial infection overlap with known downstream targets of the Sma/Mab pathway [40]. Therefore, the signaling cascade of SMA-6-SMA-2/SMA-3/SMA-4 is involved in the regulation of toxicity of environmental toxicants or stresses in nematodes.

6.3.2 DAF-7-Mediated TGF- β Signaling Pathway

6.3.2.1 Involvement of DAF-7 in the Regulation of Toxicity of Environmental Toxicants or Stresses

In nematodes, the UV-activated TiO₂NPs could lead to the significant reproductive toxicity [41]. Meanwhile, an increased expression of *daf-7* was observed in nematodes exposed to UV + TiO₂NPs (Fig. 6.10) [41]. This suggests the involvement of DAF-7-mediated TGF- β signaling pathways in the reproductive failure induced

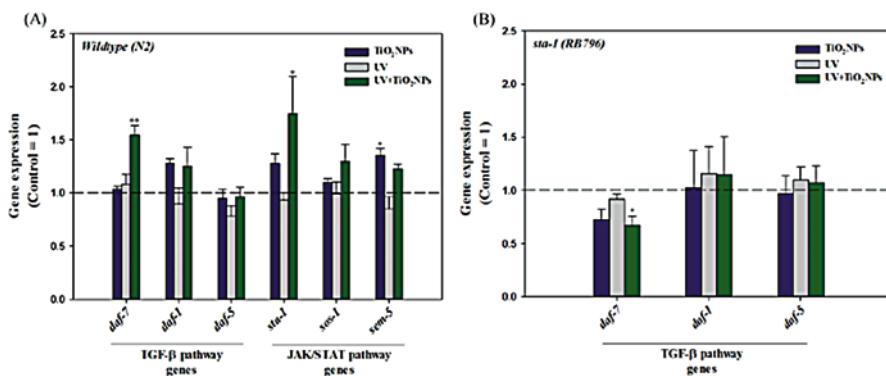


Fig. 6.10 The expression of TGF- β pathway genes (*daf-7*, *daf-1*, and *daf-5*) and JAK/STAT pathway genes (*sta-1*, *sos-1*, and *sem-5*) in wild type (a) and TGF- β pathway genes (*daf-7*, *daf-1*, and *daf-5*) in *sta-1* mutant (b) [41]. Wild-type and *sta-1* mutant *C. elegans* were exposed to TiO₂NPs, UV, and UV + TiO₂NPs, and gene expression was analyzed using qRT-PCR. The results were expressed as the mean value compared to Control (Control = 1, $n = 3$; mean standard error of the mean; two-tailed t-test, * $p < 0.05$; ** $p < 0.01$)

by UV-activated TiO₂NPs. Additionally, it was observed that mutation of *daf-7* could strengthen the reproductive toxicity induced by UV + TiO₂NPs [41]. Therefore, DAF-7 may be involved in the regulation of toxicity of environmental toxicants or stresses in nematodes.

6.3.2.2 Involvement of Signaling Cascade of DAF-8-DAF-5 in the Regulation of Toxicity of Environmental Toxicants or Stresses

In *C. elegans*, intestine-specific RNAi knockdown or mutation of *daf-8* induced in a susceptibility to GO toxicity in inducing intestinal ROS production, whereas intestine-specific RNAi knockdown or mutation of *daf-5* induced a resistance to GO toxicity in inducing intestinal ROS production (Fig. 6.11) [42]. *daf-5* encodes a transcriptional factor, and *daf-8* encodes a R-Smad protein. Genetic interaction analysis further indicated that double mutations of *daf-8* and *daf-5* induced a resistance to GO toxicity in inducing intestinal ROS production and in decreasing locomotion behavior (Fig. 6.11) [42]. That is, mutation of *daf-5* could suppress the

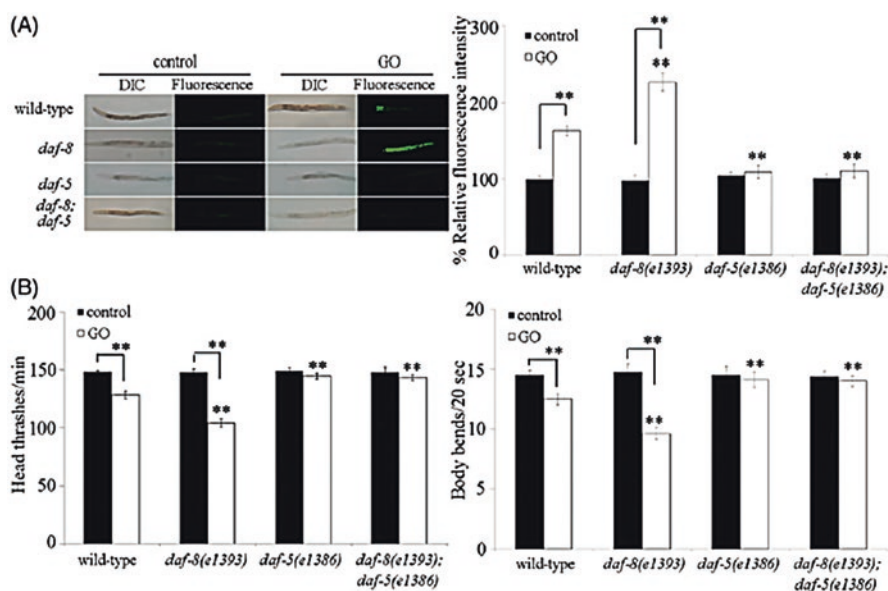


Fig. 6.11 Genetic interaction between DAF-8 and DAF-5 in the regulation of GO toxicity [42]. (a) Genetic interaction between DAF-8 and DAF-5 in the regulation of GO toxicity in inducing intestinal ROS production. (b) Genetic interaction between DAF-8 and DAF-5 in the regulation of GO toxicity in decreasing locomotion behavior. (c) A diagram showing the mechanisms for the function of antimicrobial proteins in the regulation of GO toxicity. Prolonged exposure was performed from L1-larvae to young adults. GO exposure concentration was 10 mg/L. Bars represent means \pm SD. ** $p < 0.01$ vs wild type (if not specially indicated)

susceptibility of *daf-8(e1393)* mutant to GO toxicity. Therefore, a signaling cascade of DAF-8-DAF-5 can be formed during the regulation of toxicity of environmental toxicants or stresses in nematodes.

In nematodes, *lys-8* mutation inhibited the *daf-8* expression and increased the *daf-5* expression after GO exposure [42]. Intestine-specific *daf-8* RNAi knockdown suppressed the resistance of animals with intestinal *lys-8* overexpression to GO toxicity [42]. Therefore, DAF-16-LYS-8 in the insulin signaling pathway can act upstream the signaling cascade of DAF-8-DAF-5 in the TGF- β signaling pathway to regulate the toxicity of environmental toxicants or stresses in nematodes.

6.3.2.3 DAF-7-Mediated TGF- β Signaling Pathway Is Involved in the Control of Stress-Induced Sleep

In organisms, the stress-induced sleep (SIS) is characterized by the cessation of motor activity and the rapidly reversible reduction in sensory responsiveness, which appears to be beneficial, conferring a survival advantage compared to sleepless animals under the same conditions. Mutations in *daf-7*, but not *daf-2*, interfered with SIS (Fig. 6.12) [43], indicating that the TGF- β was required. An SIS defect could also be observed in an *rf* mutation in the TGF- β type-1 coreceptor, encoded by *daf-1*, and the disruption of SIS in *daf-7* mutants was greater for locomotor quiescence (Fig. 6.12) [43].

The *daf-5* and *daf-3* mutants for SIS were similar to the wild-type nematodes (Fig. 6.12) [43]. The sleep of *daf-3;daf-7* double mutants were similar to *daf-3* single mutant nematodes (Fig. 6.12) [43], suggesting that the DAF-7 promotes SIS by antagonizing the DAF-3 activity. Moreover, after the use of multiple transgenic lines of *daf-1(rf)* to target expression of DAF-1 to all neurons or specifically to the RIM/RIC interneurons, DAF-1 expression exclusively in the RIM/RIC was sufficient to rescue the *daf-1* SIS defect (Fig. 6.12) [43], indicating the important role of possible signaling cascade of DAF-1-DAF-3/DAF-5 in the RIM/RIC interneurons to regulate the SIS in nematodes.

6.4 Notch Signaling Pathway

6.4.1 Role of GLP-1 in the Regulation of Toxicity of Environmental Toxicants or Stresses

glp-1 encodes an N-glycosylated transmembrane receptor of LIN-12/Notch signal. In nematodes, *Pseudomonas aeruginosa* infection could cause a number of neural changes that are hallmarks of the neurodegeneration [44]. Using the germline-deficient mutant of *glp-1(e2141)*, it was observed that the *glp-1(e2141)* mutant nematodes displayed reduced levels of neurodegeneration following the *P.*

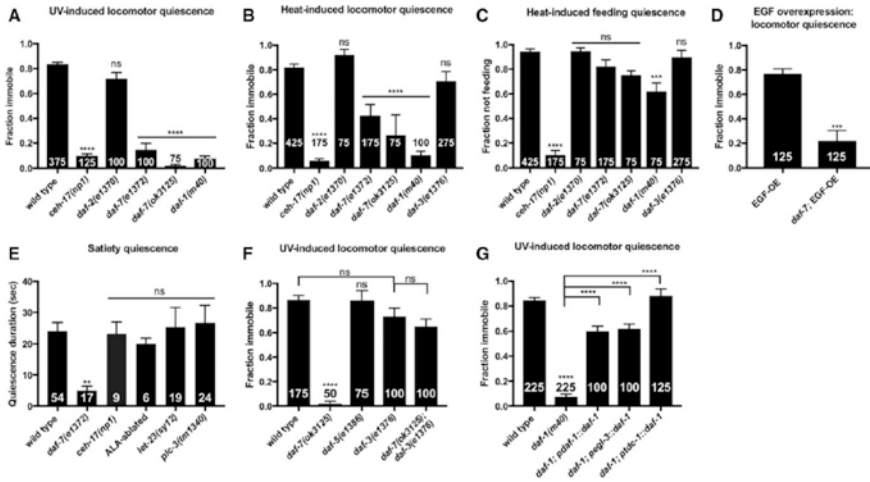


Fig. 6.12 TGF- β signaling is required in the RIM/RIC interneurons to promote SIS [43]. (a) *daf-2(rf)* mutants exhibit normal UV-induced sleep, while *daf-7(rf)* and *daf-1(rf)* mutants are severely impaired. (b) *rf* mutations in *daf-2/insulin* signaling display wild-type, heat-induced locomotor quiescence, while *rf* mutations in *daf-7* and *daf-1*, components of TGF- β signaling, are severely impaired for locomotor quiescence during SIS. *daf-3/Co-SMAD(rf)* mutants do not show a significant SIS defect. (c) Only *daf-1(rf)* mutants show a significant defect in heat-induced feeding quiescence. (d) *daf-7* is required downstream of ALA activation for EGF-induced sleep. Mild heat exposure was used to induce EGF-OE and 2 h later animals were examined for immobility as a measure of EGF-induced sleep. (e) Satiety quiescence is not mediated by components of the SIS pathway. Animals lacking a functional ALA neuron (*ceh-17* mutants and ALA laser-ablated animals) show wild-type satiety quiescence, as do *let-23/EGFR(rf)* and *plc-3/PLC-g* null mutant animals. (f) *daf-3(e1376)* fully suppresses the SIS defect of *daf-7(ok3125)*. (g) *daf-1* expression under the endogenous *daf-1*, pan-neuronal *egl-3*, and RIM/RIC-specific *tdc-1* promoters rescues the SIS defect of *daf-1(m40)* mutants. Cessation of locomotion and feeding were examined as measures of SIS after a 45 s exposure to UV light or an 11 min, heat shock as indicated above each graph. The total number of animals examined is indicated at the bottom of each bar. Error bars represent SEM. One-way ANOVA with Dunnett's (a–c, e), Tukey's (f, g), or Student's *t*-test (d). ** $P \# 0.001$, *** $P \# 0.001$, **** $P \# 0.0001$. *ns* not significant vs wild type (unless otherwise indicated by connecting bars on graph)

aeruginosa infection (Fig. 6.13) [44], confirming that the sterility induced by *glp-1* mutation may confer protective effects to neurons in response to pathogen infection in nematodes.

Besides this, it was further found that the *glp-1* mutant nematodes exhibit an enhanced resistance to a wide array of pathogens, including the Gram-negative bacteria *P. aeruginosa* and *S. enterica*, the Gram-positive bacterium *E. faecalis*, and the fungal pathogen *C. neoformans* (Fig. 6.14) [45]. Therefore, GLP-1 plays an important function in regulating the toxicity of environmental toxicants or stresses in nematodes.

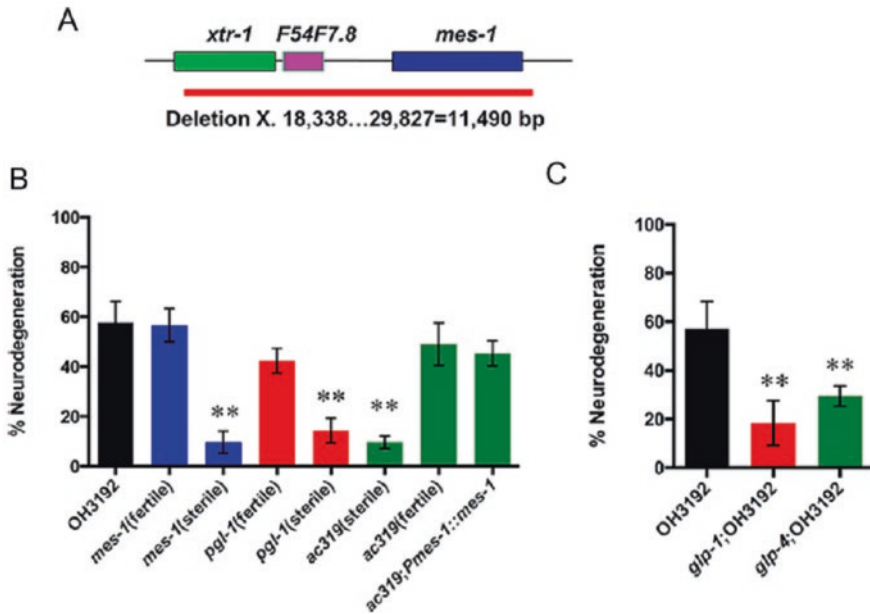


Fig. 6.13 Germline-deficient animals are resistant to neurodegeneration induced by *P. aeruginosa* [44]. (a) Location of the mutation in both fertile and sterile *ac319* animals. A deletion of 11,490 bp on chromosome X from 18,338 to 29,827 was identified. (b) Neurodegeneration rates in *pgl-1*(*bn101*), *mes-1*(*bn7*), *ac319*, and *ac319;Pmes-1::mes-1* young animals crossed with strain OH3192. (c) Neurodegeneration rate in *glp-1*(*e2141*) and *glp-4*(*bn2*) animals crossed with strain OH3192. Young adult nematodes were cultured on full lawn plates of *P. aeruginosa* for 30 h at 25 °C. Asterisks indicate significant differences (*, $p < 0.05$; **, $p < 0.01$). The graph represents the combined results of three independent experiments ($n = 30$ –60 animals). Bars, mean \pm S.E. (error bars)

6.4.2 Genetic Interaction Between GLP-1 and Insulin Signal in the Regulation of Toxicity of Environmental Toxicants or Stresses

In nematodes, genetic analysis demonstrated that RNAi knockdown of *daf-16* in the insulin signaling pathway could suppress the resistance of *glp-1*(*e2141*) mutant nematodes to the pathogen-induced neurodegeneration (Fig. 6.15) [44], suggesting that the DAF-16 is required for the resistance to the pathogen-induced neurodegeneration of *glp-1*(*e2141*) mutant nematodes. Nevertheless, *daf-16* RNAi did not fully suppress the enhanced resistance to *P. aeruginosa*-induced neurodegeneration of *glp-1*(*e2141*) mutant nematodes (Fig. 6.15) [44], implying that some other signals might be also involved in this process.

Similarly, it was observed that *daf-16* RNAi inhibited the enhanced resistance to *C. neoformans* of *glp-1* mutant nematodes, although *daf-16* RNAi had no effect on the resistance to *C. neoformans* of wild-type nematodes (Fig. 6.16) [45]. Additionally,

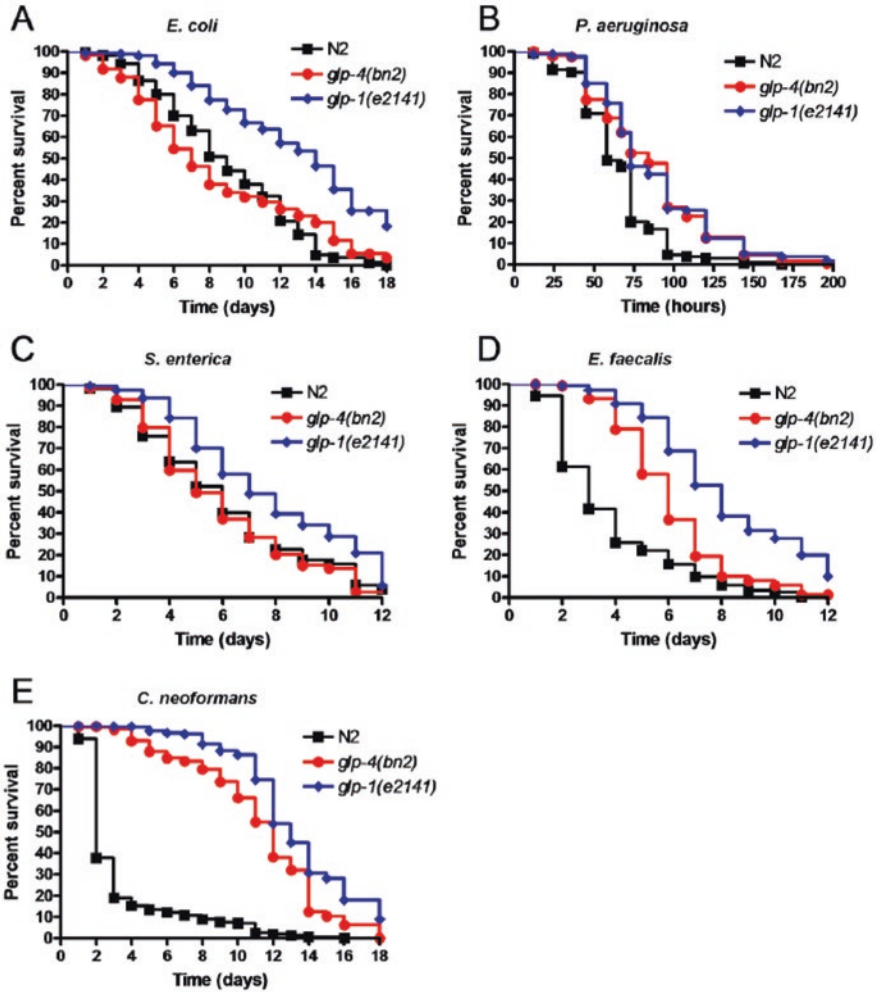


Fig. 6.14 Germline-deficient mutants exhibit different responses to pathogens [45]. Wild-type, *glp-4(bn2)* mutant, and *glp-1(e2141)* mutant nematodes were exposed to (a) *E. coli*, (b) *P. aeruginosa*, (c) *S. enterica*, (d) *E. faecalis*, and (e) *C. neoformans*. Significant differences were found when wild-type nematodes were compared to *glp-1(e2141)* mutants on all five pathogens. Significant differences were also found when wild-type nematodes were compared to *glp-4(bn2)* mutants on *P. aeruginosa*, *E. faecalis*, and *C. neoformans* but not on *E. coli* nor *S. enterica*. 160–300 nematodes were used for each condition

daf-16 RNAi also shortened the lifespan of *glp-1* mutant nematodes grown on lawns of both live and killed *E. coli* (Fig. 6.16) [45].

In nematodes, infection with the *C. neoformans* decreased the DAF-16 nuclear location (Fig. 6.17) [45]. Moreover, it was further found that *glp-1* mutation significantly increased the DAF-16 nuclear location in nematodes after infection with the

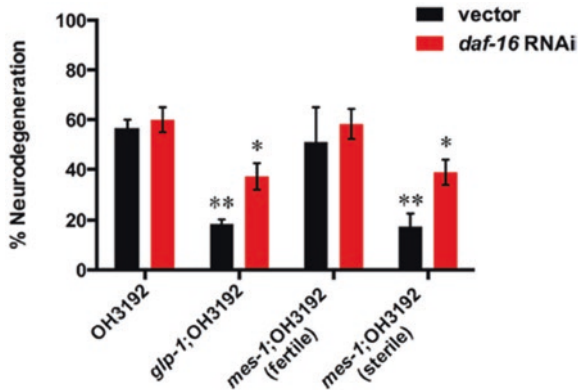


Fig. 6.15 DAF-16 is required for the resistance to *P. aeruginosa*-induced neurodegeneration of germline-deficient animals [44]. Shown are neurodegeneration rates in *glp-1(e2141)* and *mes-1(bn7)* animals crossed with strain OH3192. The animals were grown on control or *daf-16* RNAi plates until the young adult stage and then cultured on full lawn plates of *P. aeruginosa* for 30 h at 25 °C. The graph represents the combined results of three independent experiments ($n = 30$ animals). Bars, mean \pm S.E. (error bars)

C. neoformans (Fig. 6.17) [45]. Under the normal conditions, the *glp-1* mutation also significantly increased the DAF-16 nuclear location (Fig. 6.17) [45]. These results suggest that GLP-1 acts upstream of DAF-16 in the insulin signaling pathway to regulate the toxicity of environmental toxicants or stresses in nematodes.

6.5 Developmental Timing Control-Related Signals

6.5.1 Involvement of *let-7* in Regulating the Toxicity of Environmental Toxicants or Stresses

let-7 is one of the founding members of the miRNA family firstly identified with the function in regulating the timing of larval and adult transition [46, 47]. In nematodes, prolonged exposure to MWCNTs (10 μ g/L) or *P. aeruginosa* PA14 infection could cause the significant decrease in the expression of *let-7::GFP* (Fig. 6.18) [48, 49]. Moreover, mutation of *let-7* induced a resistance to MWCNTs toxicity in inducing intestinal ROS production and in decreasing locomotion behavior or to *P. aeruginosa* PA14 infection in increasing colony of *P. aeruginosa* PA14 and in reducing lifespan [48]. These results suggest the important function of *let-7* in the regulation of environmental toxicants or stresses in nematodes.

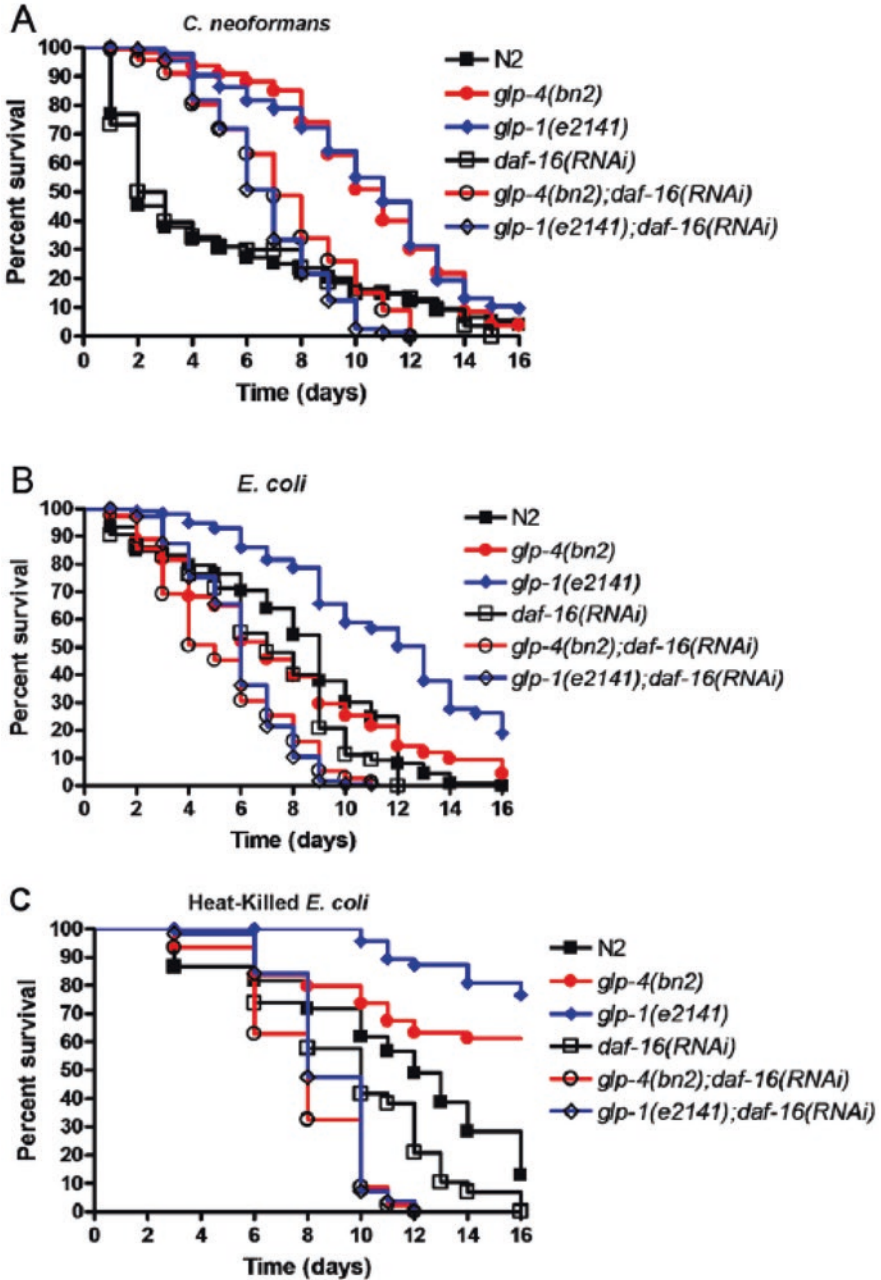


Fig. 6.16 Increased resistance and longevity in germline-deficient mutants requires DAF-16 [45]. Wild-type, *glp-4(bn2)* mutant, and *glp-1(e2141)* mutant nematodes grown on *E. coli* carrying a vector control plasmid or expressing *daf-16* dsRNA were exposed to (a) *C. neoformans*, (b) *E. coli*, or (c) heat-killed *E. coli*. Significant differences were found when *glp-4(bn2); daf-16(RNAi)*

6.5.2 *Tissue-Specific Activity of let-7 in the Regulation of Toxicity of Environmental Toxicants or Stresses*

After *P. aeruginosa* PA14 infection, expression of *let-7* in the pharynx, the muscle, or the hypodermis did not significantly affect the survival and the CFU of *P. aeruginosa* PA14 in *let-7(mg279)* mutant nematodes (Fig. 6.19) [49]. In contrast, after *P. aeruginosa* PA14 infection, expression of *let-7* in the intestine or the neurons significantly reduced the survival, increased the CFU of *P. aeruginosa* PA14, and decreased the expressions of antimicrobial genes (*lys-1*, *dod-22*, *K08D8.5*, *F55G11.7*, and *F55G11.4*) in *let-7(mg279)* mutant nematodes (Fig. 6.19) [49]. The survival, CFU of *P. aeruginosa* PA14, or expression patterns of antimicrobial genes (*lys-1*, *dod-22*, *K08D8.5*, *F55G11.7*, and *F55G11.4*) in *P. aeruginosa* PA14-infected transgenic strain of *let-7(mg279)Ex(Pges-1-let-7)* or *let-7(mg279)Ex(Punc-14-let-7)* were similar to those in *P. aeruginosa* PA14-infected wild-type nematodes (Fig. 6.19) [49]. Additionally, the nematodes overexpressing *let-7* in the intestine or the neurons were susceptible to *P. aeruginosa* PA14 infection [49]. Therefore, *let-7* can act in the intestine or the neurons to regulate the toxicity of environmental toxicants or stresses in nematodes.

6.5.3 *Downstream Targets of let-7 in the Regulation of Toxicity of Environmental Toxicants or Stresses*

6.5.3.1 HBL-1 and LIN-41

HBL-1 and LIN-41 are the normally considered direct targets for *let-7* during the regulation of timing of larval and adult transition [46, 47]. In nematodes, prolonged exposure to MWCNTs (10 µg/L) could significantly increase the expressions of both *hbl-1* and *lin-41* [48]. In MWCNTs exposed nematodes, *let-7* mutation could significantly increase the expressions of both the *hbl-1* and the *lin-41* [48]. Different from the phenotype in *let-7* mutant, mutation of *hbl-1* or *lin-41* induced a susceptibility to MWCNTs toxicity in inducing intestinal ROS production and in decreasing locomotion behavior (Fig. 6.20) [48]. Moreover, genetic interaction analysis demonstrated that mutation of *hbl-1* or *lin-41* could suppress the resistance of *let-7(mg279)* mutant to MWCNTs toxicity in inducing intestinal ROS production and in decreasing locomotion behavior (Fig. 6.20) [48]. These data suggests that

←

Fig. 6.16 (continued) worms were compared to vector control-treated *glp-4(bn2)* nematodes on *C. neoformans*, *E. coli*, and heat-killed *E. coli*. Likewise, significant differences were found when *glp-1(e2141);daf-16(RNAi)* nematodes were compared to vector control-treated *glp-1(e2141)* nematodes on *C. neoformans*, *E. coli*, and heat-killed *E. coli*. When wild-type nematodes were compared to *daf-16(RNAi)* animals, significant differences were seen on *E. coli* and heat-killed *E. coli* but not on *C. neoformans*. 60–300 nematodes were used for each condition

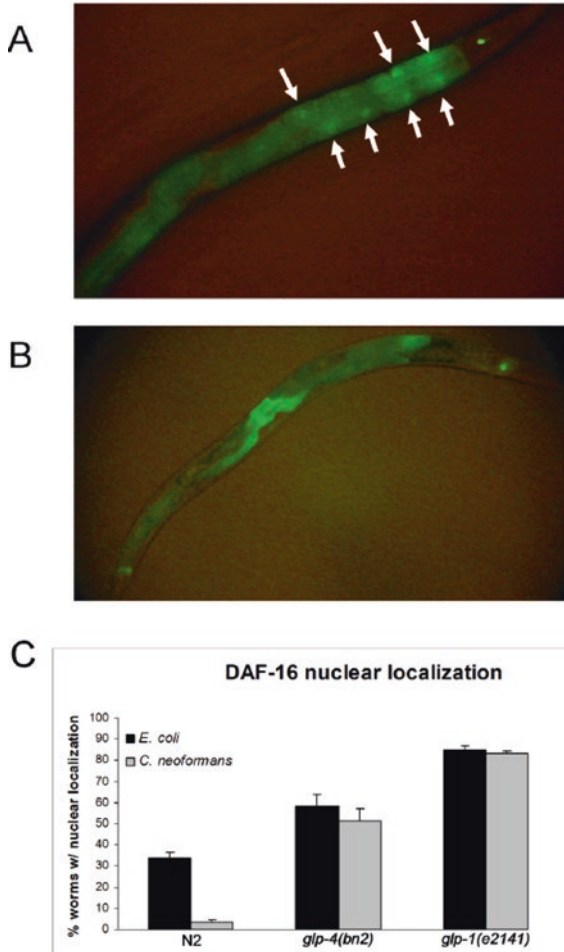


Fig. 6.17 The germline-deficient mutants of *glp-1* and *glp-4* have higher levels of DAF-16 activation than wild-type animals regardless of pathogen exposure [45]. (a) A *glp-1(e2141)* mutant nematode expressing a *daf-16:gfp* transgene under control of *Pgly-19* after exposure to *E. coli*. (b) A wild-type nematode expressing a *daf-16:gfp* transgene under control of *Pgly-19* after exposure to *E. coli*. (c) Wild-type, *glp-4(bn2)* mutant, and *glp-1(e2141)* nematodes expressing transgenic DAF-16::GFP under control of *Pgly-19* were exposed to either *E. coli* or *C. neoformans* and categorized as predominately nuclear or cytoplasmic. Significant differences were found when *glp-4(bn2)* mutants were compared to wild type on both *E. coli* and *C. neoformans*. Likewise, significant differences were also found when *glp-1(e2141)* mutants were compared to wild type on both *E. coli* and *C. neoformans*. No significant differences were found when comparing the two *glp-4(bn2)* groups nor with the two *glp-1(e2141)* groups, but there were significant differences in DAF-16 localization between the wild-type nematodes on *E. coli* and *C. neoformans*

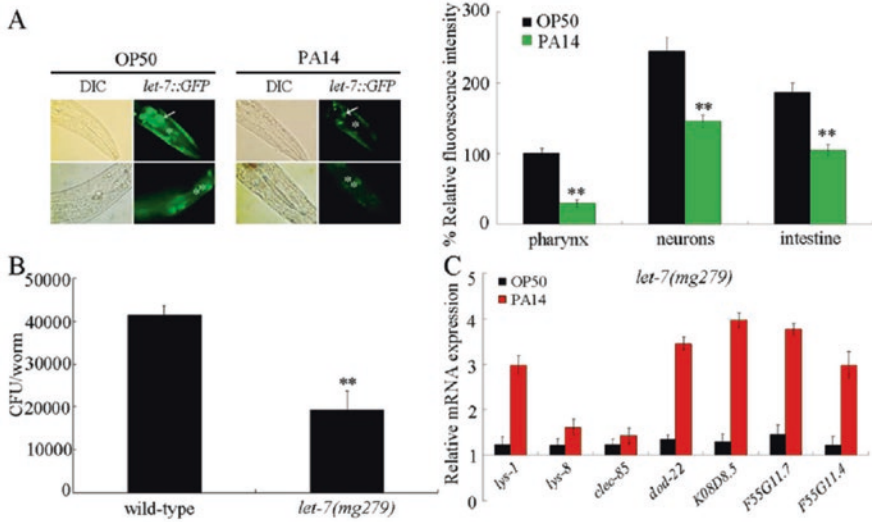


Fig. 6.18 Response of *let-7* to *P. aeruginosa* PA14 infection [49]. (a) Effect of *P. aeruginosa* PA14 infection on *let-7::GFP* expression. Arrowheads indicate the neurons. Pharynx (*) and intestine (**) were also indicated. Nematodes were infected with *P. aeruginosa* PA14 for 24 h. Thirty animals were examined. Bars represent mean \pm SD. ** $P < 0.01$ vs OP50. (b) Comparison of *P. aeruginosa* PA14 CFU between wild-type N2 and *let-7(mg279)* mutants infected with *P. aeruginosa* PA14. Bars represent mean \pm SD. ** $P < 0.01$ vs wild type. (c) Quantitative real-time PCR analysis of expression patterns of the antimicrobial peptide genes in *let-7(mg279)* mutant infected with *P. aeruginosa* PA14. Normalized expression is presented relative to wild-type expression. Bars represent mean \pm SD

HBL-1 and LIN-41 act as the targets for *let-7* in the regulation of toxicity of environmental toxicants or stresses in nematodes.

6.5.3.2 SDZ-24

SDZ-24 is a SKN-1-dependent zygotic protein. After *P. aeruginosa* PA14 infection, RNAi knockdown of *sdz-24* significantly reduced the survival, enhanced the colony formation of *P. aeruginosa* PA14 in the body, and decreased expression in antimicrobial genes (*lys-1*, *dod-22*, *K08D8.5*, and *F55G11.7*) [49]. Moreover, it was found that mutation of *sdz-24* significantly reduced the survival, increased the CFU of *P. aeruginosa* PA14 in the body, and decreased the expression of antimicrobial genes (*lys-1*, *dod-22*, *K08D8.5*, and *F55G11.7*) in *let-7(mg279)* mutant [49]. SDZ-24::GFP is primarily expressed in the posterior of the intestine and could be significantly increased by *P. aeruginosa* PA14 infection [49]. Loss-of-function mutation of *let-7* significantly increased the SDZ-24::GFP expression under both the *E. coli* OP50 exposure condition and the *P. aeruginosa* PA14 exposure condition [49].

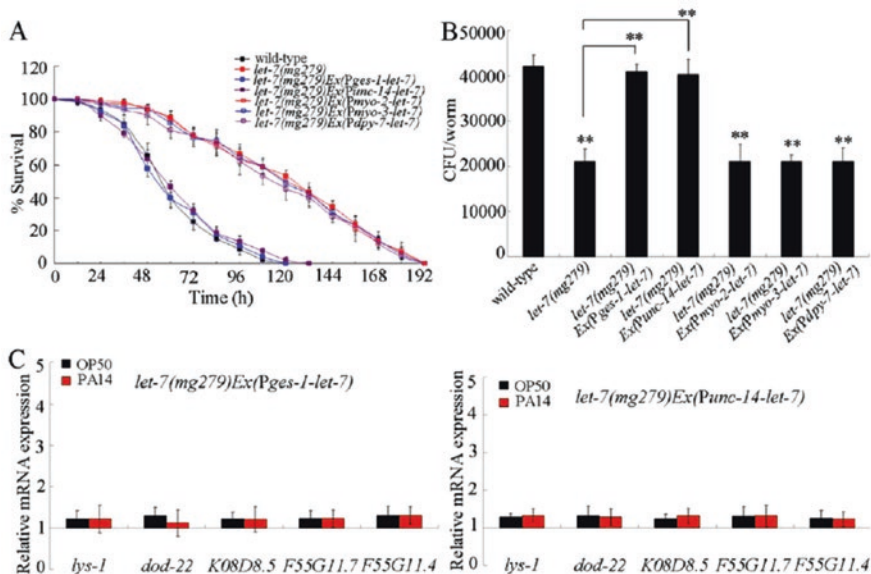


Fig. 6.19 Tissue-specific activity of *let-7* in the regulation of innate immunity [49]. (a) Tissue-specific activity of *let-7* in the regulation of survival in *P. aeruginosa* PA14-infected nematodes. Statistical comparisons of the survival plots indicate that, after *P. aeruginosa* PA14 infection, the survival of *let-7(mg279)Ex(Pges-1-let-7)* ($P < 0.0001$) or *let-7(mg279)Ex(Punc-14-let-7)* ($P < 0.0001$) was significantly different from that of *let-7(mg279)*, and the survival of *let-7(mg279)Ex(Pmyo-2-let-7)* ($P = 0.9643$), *let-7(mg279)Ex(Pmyo-3-let-7)* ($P = 0.9234$), or *let-7(mg279)Ex(Pdpy-7-let-7)* ($P = 0.9545$) was not significantly different from that of *let-7(mg279)*. (b) Tissue-specific activity of *let-7* in the regulation of *P. aeruginosa* PA14 CFU in the body of nematodes. (c) Tissue-specific activity of *let-7* in the regulation of expression patterns of antimicrobial genes in *P. aeruginosa* PA14-infected nematodes. Normalized expression is presented relative to wild-type expression. Bars represent mean \pm SD. ** $P < 0.01$ vs wild type (if not specially indicated)

More importantly, after *P. aeruginosa* PA14 infection, the transgenic strain of *Ex(Pges-1-sdz-24-3'-UTR);Is(Pges-1-let-7)* exhibited the similar survival, CFU of *P. aeruginosa* PA14, and expression patterns of antimicrobial genes (*lys-1*, *dod-22*, *K08D8.5*, and *F55G11.7*) to those in the transgenic strain of *Ex(Pges-1-sdz-24-3'-UTR)* (nematodes overexpressing intestinal SDZ-24 without its 3'-UTR) (Fig. 6.21) [49], suggesting that the overexpression of *sdz-24* gene lacking 3'-UTR in the intestine may not be able to be affected by the intestinal *let-7*. Very different from these, intestinal overexpression of *let-7* could significantly reduce the survival, enhance the CFU of *P. aeruginosa* PA14, and decrease the expressions of antimicrobial genes (*lys-1*, *dod-22*, *K08D8.5*, and *F55G11.7*) in *P. aeruginosa* PA14-infected transgenic strain of *Ex(Pges-1-sdz-24+3'-UTR);Is(Pges-1-let-7)* (*Ex(Pges-1-sdz-24+3'-UTR)*), nematodes overexpressing intestinal SDZ-24 containing its 3'-UTR) (Fig. 6.21) [49], suggesting the effects of intestinal expression of *let-7*. The in vivo 3'-UTR binding assay of *sdz-24* further confirmed that *let-7* may suppress the function of SDZ-24 through binding to its 3'-UTR and inhibiting its translation in *P. aeruginosa* PA14-

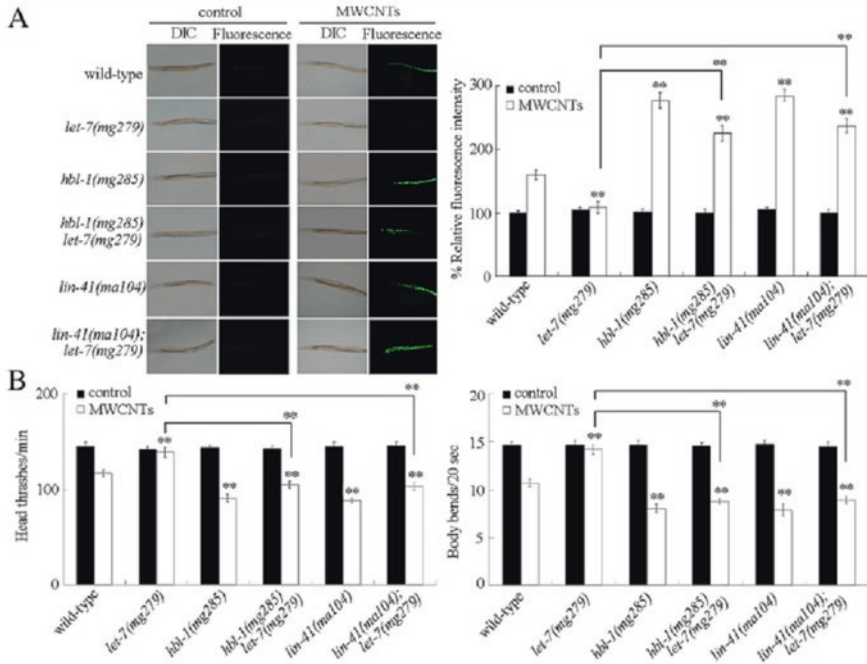


Fig. 6.20 Genetic interaction between *let-7* and *hbl-1* or *lin-41* in the regulation of MWCNTs toxicity [48]. (a) Genetic interaction between *let-7* and *hbl-1* or *lin-41* in the regulation of MWCNTs toxicity in inducing intestinal ROS production. Sixty nematodes were examined per treatment. (b) Genetic interaction between *let-7* and *hbl-1* or *lin-41* in the regulation of MWCNTs toxicity in decreasing locomotion behavior. Sixty nematodes were examined per treatment. Prolonged exposure was performed from L1-larvae to young adults. Exposure concentration of MWCNTs was 10 µg/L. Bars represent means ± SD. ***P* < 0.01 vs wild type (if not specially indicated)

infected nematodes. These results demonstrate that the SDZ-24 can act as another direct target for *let-7* in the regulation of environmental toxicants or stresses in nematodes.

6.5.4 Identification of Downstream Targets for HBL-1 in Regulating the Toxicity of Environmental Toxicants or Stresses

In nematodes, totally 13 genes (*T01D3.6*, *F13B12.4*, *ugt-18*, *cpt-4*, *clec-60*, *F28H1.1*, *W04G3.3*, *K12B6.3*, *nurf-1*, *sym-1*, *tir-1*, *nhx-3*, and *zig-4*) could be significantly increased (more than 2.5-fold changes) by *hbl-1* overexpression [50]. *hbl-1* mutation suppressed expressions of *tir-1*, *sym-1*, and *lpr-4* in nematodes exposed to MWCNTs (10 µg/L) [48]. *tir-1* or *sym-1* mutation could induce a

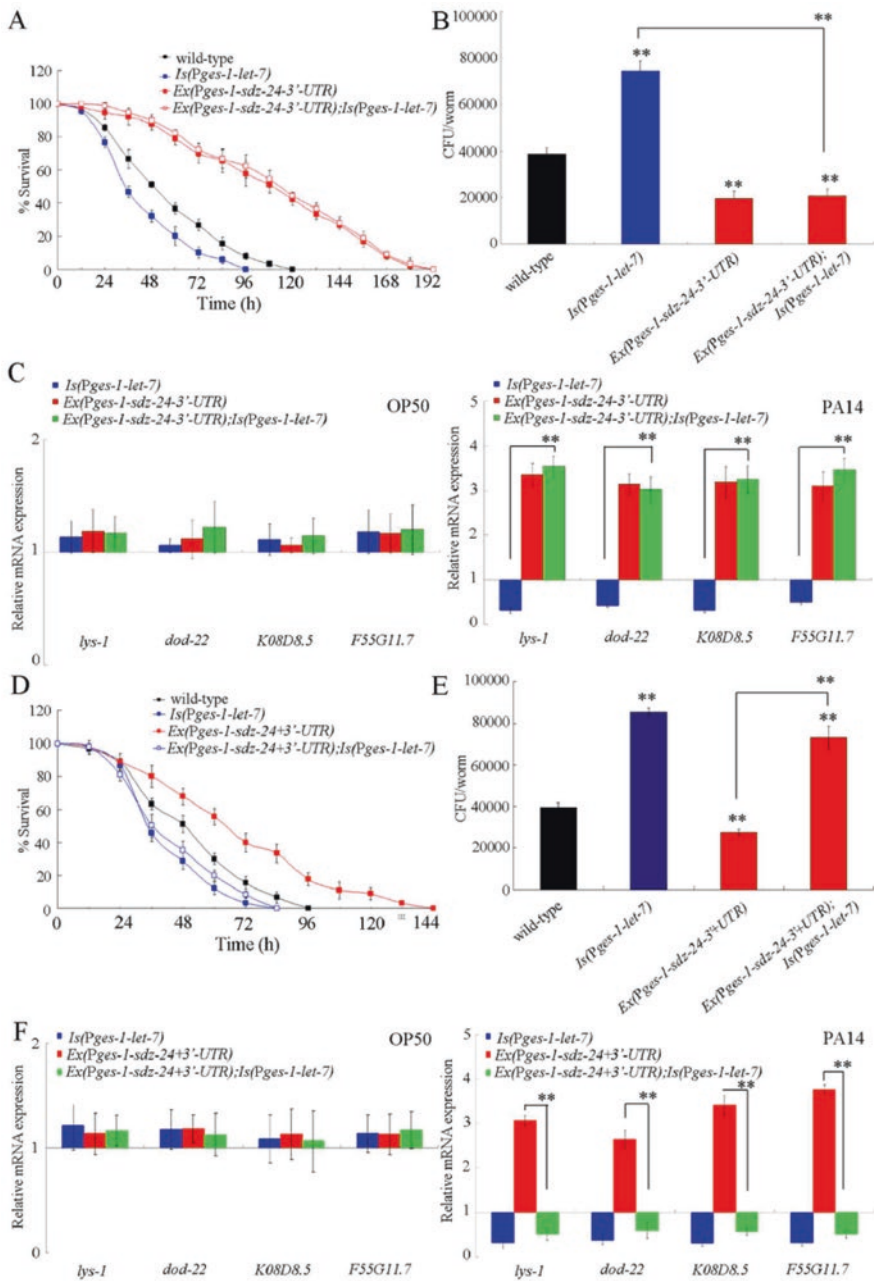


Fig. 6.21 Effects of intestinal overexpression of *sdz-24* lacking 3'-UTR or containing 3'-UTR on innate immune response to *P. aeruginosa* PA14 infection in nematodes overexpressing intestinal *let-7* [49]. (a) Effects of intestinal overexpression of *sdz-24* lacking 3'-UTR on survival in *P. aeruginosa* PA14-infected nematodes overexpressing intestinal *let-7*. Statistical comparisons of the survival plots indicate that, after *P. aeruginosa* PA14 infection, the survival of transgenic strain of *Ex(Pges-1-sdz-24-3'-UTR);Is(Pges-1-let-7)* was significantly different from that of transgenic strain of *Is(Pges-1-let-7)* ($P < 0.0001$). (b) Effects of intestinal overexpression of *sdz-24* lacking 3'-UTR on CFU of *P. aeruginosa* PA14 in *P. aeruginosa* PA14-infected nematodes overexpressing

susceptibility to MWCNTs toxicity; however, *lpr-4* mutation did not influence the MWCNTs toxicity (Fig. 6.22) [48].

tir-1 encodes a Toll-interleukin 1 receptor (TIR) domain adaptor protein, and *sym-1* encodes a protein containing 15 contiguous leucine-rich repeats (LRRs). Genetic interaction analysis demonstrated that mutation of *tir-1* or *sym-1* could significantly suppress the resistance of nematodes overexpressing HBL-1 to MWCNTs toxicity in inducing intestinal ROS production and in decreasing locomotion behavior (Fig. 6.22) [48], which suggest the formation of a signaling cascade of *let-7*-HBL-1-TIR-1/SYM-1 in the regulation of toxicity of environmental toxicants or stresses in nematodes.

6.5.5 Genetic Interaction Between LIN-41 and ALG-1 or ALG-2 in Regulating the Toxicity of Environmental Toxicants or Stresses

ALG-1 and ALG-2 are RDE-1 proteins. *lin-41* mutation can suppress *alg-1/alg-2(RNAi)*-induced retarded heterochronic phenotypes [51]. Genetic analysis has indicated that the ALG-1 or the ALG-2 acts upstream of the LIN-41 in the regulation of toxicity of environmental toxicants or stresses in nematodes (Fig. 6.23) [48].

6.5.6 Feedback Loop Formed by let-7 and Its Direct Targets During the Control of ENMs Toxicity

hbl-1 or *lin-41* mutation increased *let-7::GFP* expression in MWCNTs exposed nematodes (Fig. 6.24) [48], implying the formation of a feedback loop by *let-7* and its direct targets during the control of toxicity from environmental toxicants or stresses in nematodes.

←

Fig. 6.21 (continued) intestinal *let-7*. (c) Effects of intestinal overexpression of *sdz-24* lacking 3'-UTR on expression patterns of antimicrobial genes in *P. aeruginosa* PA14-infected nematodes overexpressing intestinal *let-7*. Normalized expression is presented relative to wild-type expression. (d) Effects of intestinal overexpression of *sdz-24* containing 3'-UTR on survival in *P. aeruginosa* PA14-infected nematodes overexpressing intestinal *let-7*. Statistical comparisons of the survival plots indicate that, after *P. aeruginosa* PA14 infection, the survival of transgenic strain of *Ex(Pges-1-sdz-24+3'-UTR);Is(Pges-1-let-7)* was significantly different from that of transgenic strain of *Ex(Pges-1-sdz-24+3'-UTR)* ($P < 0.0001$). (e) Effects of intestinal overexpression of *sdz-24* containing 3'-UTR on CFU of *P. aeruginosa* PA14 in *P. aeruginosa* PA14-infected nematodes overexpressing intestinal *let-7*. (f) Effects of intestinal overexpression of *sdz-24* containing 3'-UTR on expression patterns of antimicrobial genes in *P. aeruginosa* PA14-infected nematodes overexpressing intestinal *let-7*. Normalized expression is presented relative to wild-type expression. –, lacking 3'-UTR; +, containing 3'-UTR. Bars represent mean \pm SD. ** $P < 0.01$ vs wild type (if not specially indicated)

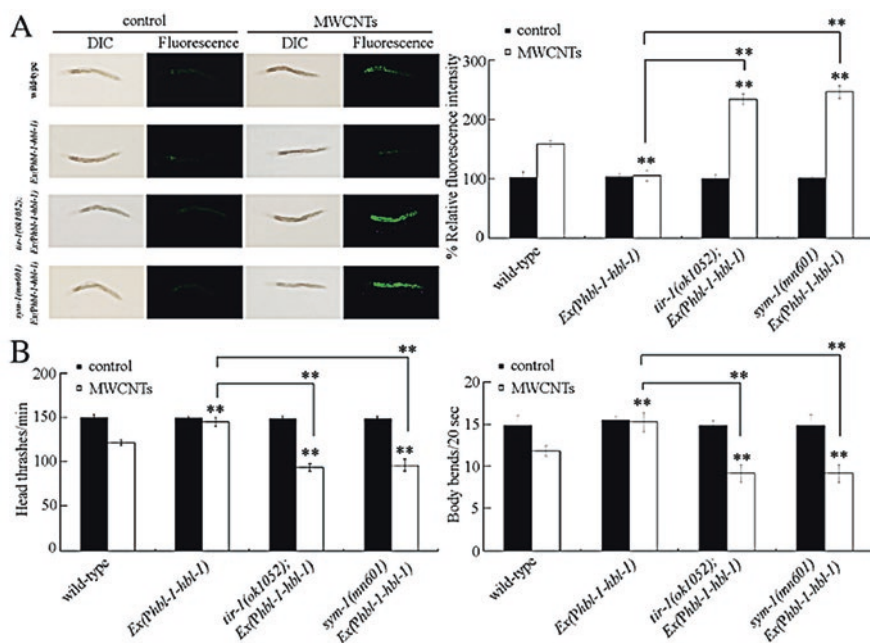


Fig. 6.22 Genetic interaction between HBL-1 and TIR-1 or SYM-1 in the regulation of MWCNTs toxicity [48]. (a) Genetic interaction between HBL-1 and TIR-1 or SYM-1 in the regulation of MWCNTs toxicity in inducing intestinal ROS production. Sixty nematodes were examined per treatment. (b) Genetic interaction between HBL-1 and TIR-1 or SYM-1 in the regulation of MWCNTs toxicity in decreasing locomotion behavior. Sixty nematodes were examined per treatment. WT wild type. Prolonged exposure was performed from L1-larvae to young adults. Exposure concentration of MWCNTs was 10 $\mu\text{g/L}$. Bars represent means \pm SD. ** $P < 0.01$ vs wild type (if not specially indicated)

6.6 Perspectives

In contrast to the functions of oxidative stress, MAPK, and insulin signaling pathways in the regulation of toxicity of environmental toxicants or stresses, the association between developmental related signals and toxicity induction of environmental toxicants or stresses has received only limited attention. In this chapter, we have introduced and discussed the important functions of Wnt, TGF- β , and Notch signaling pathways in the regulation of toxicity of environmental toxicants or stresses. Actually, besides these three signaling pathways, there are still many other developmental related signals in nematodes or mammals. The possible association between those developmental related signals and toxicity induction of environmental toxicants or stresses is still largely unknown.

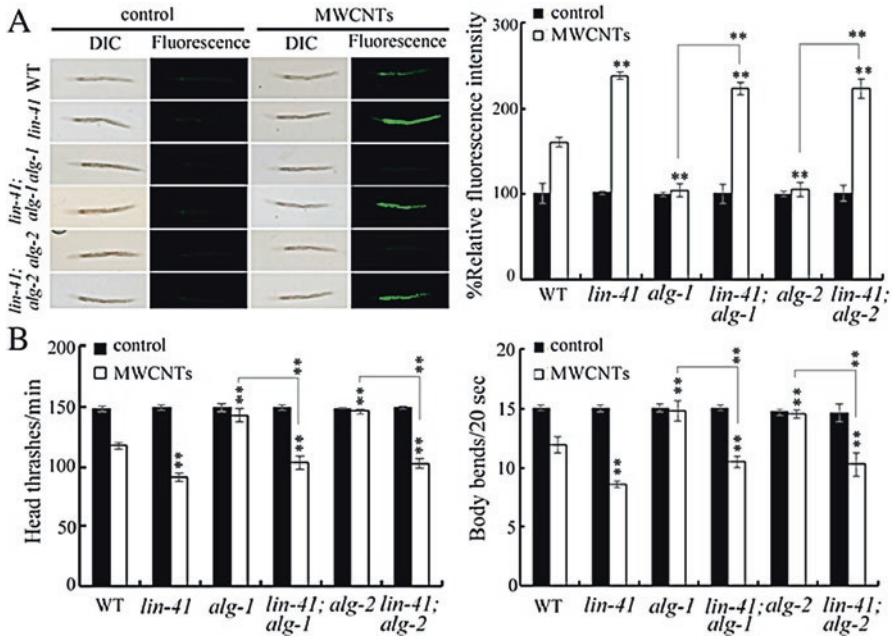


Fig. 6.23 Genetic interaction between LIN-41 and ALG-1 or ALG-2 in the regulation of MWCNTs toxicity [48]. (a) Genetic interaction between LIN-41 and ALG-1 or ALG-2 in the regulation of MWCNTs toxicity in inducing intestinal ROS production. Sixty nematodes were examined per treatment. (b) Genetic interaction between LIN-41 and ALG-1 or ALG-2 in the regulation of MWCNTs toxicity in decreasing locomotion behavior. Sixty nematodes were examined per treatment. *WT* wild type. Prolonged exposure was performed from L1-larvae to young adults. Exposure concentration of MWCNTs was 10 µg/L. Bars represent means ± SD. ***P* < 0.01 vs wild type (if not specially indicated)

In this chapter, we also introduced and discussed the important role of *let-7*-mediated developmental timing control-related signal in the regulation of toxicity of environmental toxicants or stresses. Nevertheless, it is still needed to further elucidate at least these two possibilities. One possibility is that *let-7* may regulate the toxicity of environmental toxicants or stresses by altering the molecular basis of certain aspects of development. Another possibility is that, besides the molecular basis of development, *let-7* may regulate the toxicity of environmental toxicants or stresses by further modulating the molecular basis for oxidative stress or stress response. Moreover, besides the *let-7*, the potential role of *lin-4*-mediated developmental timing control-related signal in the regulation of toxicity of environmental toxicants or stresses is still unclear. In nematodes, *lin-4* and its targets are involved in the longevity regulation by acting as an upstream regulator of DAF-16.

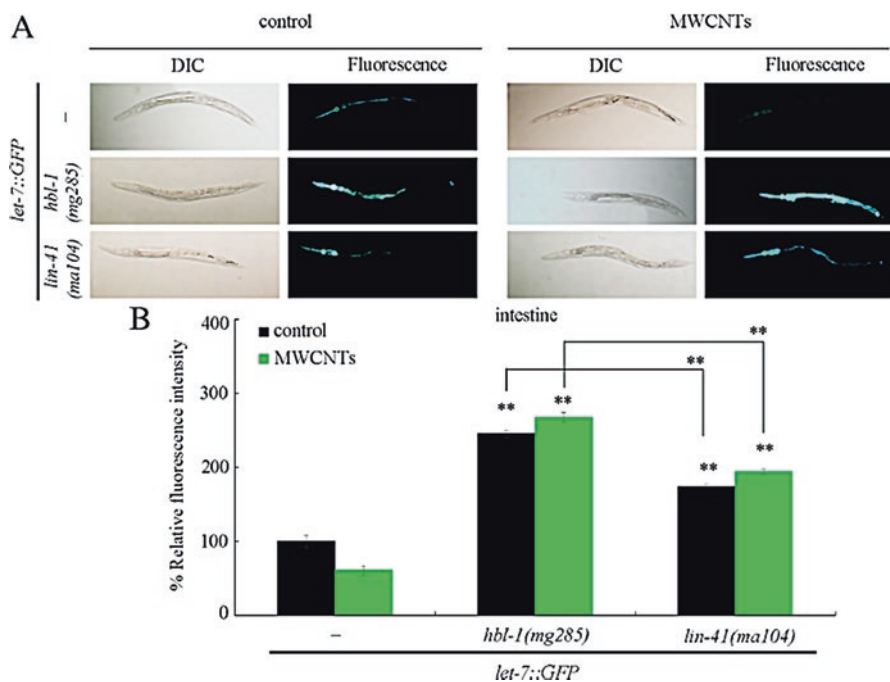


Fig. 6.24 Effect of mutation of *hbl-1* or *lin-41* on *let-7::GFP* expression in MWCNTs exposed nematodes [48]. (a) Comparison of *let-7::GFP* expression. (b) Comparison of intestinal *let-7::GFP* expression. “-” nematodes without mutation of *hbl-1* or *lin-41*. Prolonged exposure was performed from L1-larvae to young adults. Exposure concentration of MWCNTs was 10 $\mu\text{g/L}$. Bars represent means \pm SD. ** $P < 0.01$ vs nematodes without mutation of *hbl-1* or *lin-41* (if not specially indicated)

References

1. Wang D-Y (2018) Nanotoxicology in *Caenorhabditis elegans*. Springer, Singapore
2. Dong S-S, Qu M, Rui Q, Wang D-Y (2018) Combinational effect of titanium dioxide nanoparticles and nanopolystyrene particles at environmentally relevant concentrations on nematodes *Caenorhabditis elegans*. *Ecotoxicol Environ Saf* 161:444–450
3. Qu M, Xu K-N, Li Y-H, Wong G, Wang D-Y (2018) Using *acs-22* mutant *Caenorhabditis elegans* to detect the toxicity of nanopolystyrene particles. *Sci Total Environ* 643:119–126
4. Xiao G-S, Zhao L, Huang Q, Yang J-N, Du H-H, Guo D-Q, Xia M-X, Li G-M, Chen Z-X, Wang D-Y (2018) Toxicity evaluation of Wanzhou watershed of Yangtze Three Gorges Reservoir in the flood season in *Caenorhabditis elegans*. *Sci Rep* 8:6734
5. Zhao L, Rui Q, Wang D-Y (2017) Molecular basis for oxidative stress induced by simulated microgravity in nematode *Caenorhabditis elegans*. *Sci Total Environ* 607–608:1381–1390
6. Wu Q-L, Han X-X, Wang D, Zhao F, Wang D-Y (2017) Coal combustion related fine particulate matter (PM_{2.5}) induces toxicity in *Caenorhabditis elegans* by dysregulating microRNA expression. *Toxicol Res* 6:432–441
7. Li W-J, Wang D-Y, Wang D-Y (2018) Regulation of the response of *Caenorhabditis elegans* to simulated microgravity by p38 mitogen-activated protein kinase signaling. *Sci Rep* 8:857

8. Zhi L-T, Yu Y-L, Jiang Z-X, Wang D-Y (2017) *mir-355* functions as an important link between p38 MAPK signaling and insulin signaling in the regulation of innate immunity. *Sci Rep* 7:14560
9. Yin J-C, Liu R, Jian Z-H, Yang D, Pu Y-P, Yin L-H, Wang D-Y (2018) Di (2-ethylhexyl) phthalate-induced reproductive toxicity involved in DNA damage-dependent oocyte apoptosis and oxidative stress in *Caenorhabditis elegans*. *Ecotoxicol Environ Saf* 163:298–306
10. Shakoor S, Sun L-M, Wang D-Y (2016) Multi-walled carbon nanotubes enhanced fungal colonization and suppressed innate immune response to fungal infection in nematodes. *Toxicol Res* 5:492–499
11. Wu Q-L, Zhi L-T, Qu Y-Y, Wang D-Y (2016) Quantum dots increased fat storage in intestine of *Caenorhabditis elegans* by influencing molecular basis for fatty acid metabolism. *Nanomedicine* 12:1175–1184
12. Zhuang Z-H, Li M, Liu H, Luo L-B, Guo W-D, Wu Q-L, Wang D-Y (2016) Function of RSKS-1-AAK-2-DAF-16 signaling cascade in enhancing toxicity of multi-walled carbon nanotubes can be suppressed by *mir-259* activation in *Caenorhabditis elegans*. *Sci Rep* 6:32409
13. Zhao L, Qu M, Wong G, Wang D-Y (2017) Transgenerational toxicity of nanopolystyrene particles in the range of $\mu\text{g/L}$ in nematode *Caenorhabditis elegans*. *Environ Sci Nano* 4:2356–2366
14. Yang R-L, Rui Q, Kong L, Zhang N, Li Y, Wang X-Y, Tao J, Tian P-Y, Ma Y, Wei J-R, Li G-J, Wang D-Y (2016) Metallothioneins act downstream of insulin signaling to regulate toxicity of outdoor fine particulate matter ($\text{PM}_{2.5}$) during Spring Festival in Beijing in nematode *Caenorhabditis elegans*. *Toxicol Res* 5:1097–1105
15. Xiao G-S, Zhi L-T, Ding X-C, Rui Q, Wang D-Y (2017) Value of *mir-247* in warning graphene oxide toxicity in nematode *Caenorhabditis elegans*. *RSC Adv* 7:52694–52701
16. Qu M, Li Y-H, Wu Q-L, Xia Y-K, Wang D-Y (2017) Neuronal ERK signaling in response to graphene oxide in nematode *Caenorhabditis elegans*. *Nanotoxicology* 11:520–533
17. Chen H, Li H-R, Wang D-Y (2017) Graphene oxide dysregulates neuroigin/NLG-1-mediated molecular signaling in interneurons in *Caenorhabditis elegans*. *Sci Rep* 7:41655
18. Xiao G-S, Chen H, Krasteva N, Liu Q-Z, Wang D-Y (2018) Identification of interneurons required for the aversive response of *Caenorhabditis elegans* to graphene oxide. *J Nanobiotechnol* 16:45
19. Zhao L, Kong J-T, Krasteva N, Wang D-Y (2018) Deficit in epidermal barrier induces toxicity and translocation of PEG modified graphene oxide in nematodes. *Toxicol Res* 7(6):1061–1070. <https://doi.org/10.1039/C8TX00136G>
20. Ding X-C, Rui Q, Wang D-Y (2018) Functional disruption in epidermal barrier enhances toxicity and accumulation of graphene oxide. *Ecotoxicol Environ Saf* 163:456–464
21. Ding X-C, Wang J, Rui Q, Wang D-Y (2018) Long-term exposure to thiolated graphene oxide in the range of $\mu\text{g/L}$ induces toxicity in nematode *Caenorhabditis elegans*. *Sci Total Environ* 616–617:29–37
22. Yang R-L, Ren M-X, Rui Q, Wang D-Y (2016) A *mir-231*-regulated protection mechanism against the toxicity of graphene oxide in nematode *Caenorhabditis elegans*. *Sci Rep* 6:32214
23. Zhi L-T, Ren M-X, Qu M, Zhang H-Y, Wang D-Y (2016) Wnt ligands differentially regulate toxicity and translocation of graphene oxide through different mechanisms in *Caenorhabditis elegans*. *Sci Rep* 6:39261
24. Eisenmann DM (2005) Wnt signaling. In: *WormBook*. <https://doi.org/10.1895/wormbook.1.7.1>
25. Zhi L-T, Qu M, Ren M-X, Zhao L, Li Y-H, Wang D-Y (2017) Graphene oxide induces canonical Wnt/ β -catenin signaling-dependent toxicity in *Caenorhabditis elegans*. *Carbon* 113:122–131
26. Segbert C, Johnson K, Theres C, van Furden D, Bossinger O (2004) Molecular and functional analysis of apical junction formation in the gut epithelium of *Caenorhabditis elegans*. *Dev Biol* 266:17–26
27. Espelt MV, Estevez AY, Yin X, Strange K (2005) Oscillatory Ca^{2+} signaling in the isolated *Caenorhabditis elegans* intestine: role of the inositol-1,4,5- trisphosphate receptor and phospholipases C β and γ . *J Gen Physiol* 126:379–392

28. Ren M-X, Zhao L, Ding X-C, Krasteva N, Rui Q, Wang D-Y (2018) Developmental basis for intestinal barrier against the toxicity of graphene oxide. *Part Fibre Toxicol* 15:26
29. Irazoqui JE, Ng A, Xavier RJ, Ausubel FM (2008) Role for β -catenin and HOX transcription factors in *Caenorhabditis elegans* and mammalian host epithelial-pathogen interactions. *Proc Natl Acad Sci U S A* 105:17469–17474
30. Gumienny TL, Savage-Dunn C (2013) TGF- β signaling in *C. elegans*. In: *WormBook*. <https://doi.org/10.1895/wormbook.1.22.2>
31. Sun L-M, Liao K, Liang S, Yu P-H, Wang D-Y (2015) Synergistic activity of magnolol with azoles and its possible antifungal mechanism against *Candida albicans*. *J Appl Microbiol* 118:826–838
32. Sun L-M, Liao K, Li Y-P, Zhao L, Liang S, Guo D, Hu J, Wang D-Y (2016) Synergy between PVP-coated silver nanoparticles and azole antifungal against drug-resistant *Candida albicans*. *J Nanosci Nanotechnol* 16:2325–2335
33. Sun L-M, Zhi L-T, Shakoov S, Liao K, Wang D-Y (2016) microRNAs involved in the control of innate immunity in *Candida* infected *Caenorhabditis elegans*. *Sci Rep* 6:36036
34. Yu Y-L, Zhi L-T, Guan X-M, Wang D-Y, Wang D-Y (2016) FLP-4 neuropeptide and its receptor in a neuronal circuit regulate preference choice through functions of ASH-2 trithorax complex in *Caenorhabditis elegans*. *Sci Rep* 6:21485
35. Sun L-M, Liao K, Hong C-C, Wang D-Y (2017) Honokiol induces reactive oxygen species-mediated apoptosis in *Candida albicans* through mitochondrial dysfunction. *PLoS ONE* 12:e0172228
36. Sun L-M, Liao K, Wang D-Y (2017) Honokiol induces superoxide production by targeting mitochondrial respiratory chain complex I in *Candida albicans*. *PLoS ONE* 12:e0184003
37. Yu Y-L, Zhi L-T, Wu Q-L, Jing L-N, Wang D-Y (2018) NPR-9 regulates innate immune response in *Caenorhabditis elegans* by antagonizing activity of AIB interneurons. *Cell Mol Immunol* 15:27–37
38. Mallo GV, Kurz CL, Couillaud C, Pujol N, Granjeaud S, Kohara Y, Ewbank JJ (2002) Inducible antibacterial defense system in *C. elegans*. *Curr Biol* 12:1209–1214
39. Partridge FA, Gravato-Nobre MJ, Hodgkin J (2010) Signal transduction pathways that function in both development and innate immunity. *Dev Dyn* 239:1330–1336
40. Savage-Dunn C, Padgett RW (2017) The TGF- β family in *Caenorhabditis elegans*. *Cold Spring Harb Perspect Biol*. <https://doi.org/10.1101/cshperspect.a022178>
41. Kim H, Jeong J, Chatterjee N, Roca CP, Yoon D, Kim S, Kim Y, Choi J (2017) JAK/STAT and TGF- β activation as potential adverse outcome pathway of TiO₂NPs phototoxicity in *Caenorhabditis elegans*. *Sci Rep* 7:17833
42. Ren M-X, Zhao L, Lv X, Wang D-Y (2017) Antimicrobial proteins in the response to graphene oxide in *Caenorhabditis elegans*. *Nanotoxicology* 11:578–590
43. Goetting DL, Soto R, Van Buskirk C (2018) Food-dependent plasticity in *Caenorhabditis elegans* stress-induced sleep is mediated by TOR–FOXA and TGF- β signaling. *Genetics* 209:1183–1195
44. Wu Q-L, Cao X-O, Yan D, Wang D-Y, Aballay A (2015) Genetic screen reveals link between maternal-effect sterile gene *mes-1* and *P. aeruginosa*-induced neurodegeneration in *C. elegans*. *J Biol Chem* 290:29231–29239
45. TeKippe M, Aballay A (2010) *C. elegans* germline-deficient mutants respond to pathogen infection using shared and distinct mechanisms. *PLoS ONE* 5:e11777
46. Sokol NS (2012) Small temporal RNAs in animal development. *Curr Opin Genet Dev* 22:368–373
47. Reinhart B, Slack F, Basson M, Pasquinelli AE, Bettinger JC, Rougvie AE, Horvitz HR, Ruvkun G (2000) The 21 nucleotide *let-7* RNA regulates *C. elegans* developmental timing. *Nature* 403:901–906

48. Zhao L, Wan H-X, Liu Q-Z, Wang D-Y (2017) Multi-walled carbon nanotubes-induced alterations in microRNA *let-7* and its targets activate a protection mechanism by conferring a developmental timing control. *Part Fibre Toxicol* 14:27
49. Zhi L-T, Yu Y-L, Li X-Y, Wang D-Y, Wang D-Y (2017) Molecular control of innate immune response to *Pseudomonas aeruginosa* infection by intestinal *let-7* in *Caenorhabditis elegans*. *PLoS Pathog* 13:e1006152
50. Fuhrman LE, Goel AK, Smith J, Shianna KV, Aballay A (2009) Nucleolar proteins suppress *Caenorhabditis elegans* innate immunity by inhibiting p53/CEP-1. *PLoS Genet* 5:e1000657
51. Cogoni C, Macino G (2000) Post-transcriptional gene silencing across kingdoms. *Curr Opin Genet* 6:638–643

Chapter 7

Functions of Cell Death and DNA Damage-Related Signaling Pathways in the Regulation of Toxicity of Environmental Toxicants or Stresses



Abstract Cell death and DNA damage are central biological events in organisms. Meanwhile, they also have another important role in regulating the toxicity formation in nematodes exposed to various toxicants or stresses. We here introduced and discussed the role of cell death and DNA damage-related signaling pathway in the regulation of toxicity of environmental toxicants or stresses and the underlying mechanisms. The involvement of DNA replication stress-related signal and telomere-related signal in regulating toxicity of environmental toxicants or stresses was also introduced and discussed.

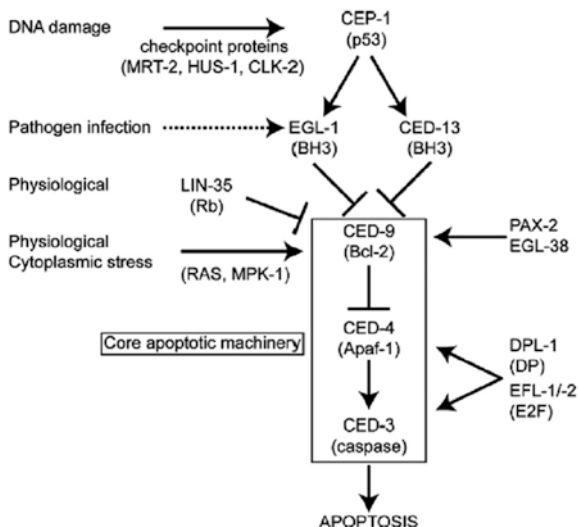
Keywords Cell death and DNA damage-related signaling pathways · Molecular regulation · Environmental exposure · *Caenorhabditis elegans*

7.1 Introduction

Caenorhabditis elegans is a wonderful animal model for the elucidation of molecular mechanisms for the observed toxicity of various toxicants or stresses [1–6]. Among the observed different aspects of toxicity induced by various toxicants or stresses, germ cell death and DNA damage have gradually received the attention [1, 7]. Similar to the development-related signals introduced in Chap. 6, the cell death and DNA damage-related signals also have dual roles in the toxicity formation in nematodes exposed to various toxicants or stresses.

The basic information on the involvement of cell death and DNA damage-related signals in the regulation of germ cell apoptosis has been well-described in the review [8]. In this chapter, we first introduced and discussed the role of cell death-related signaling pathway in the regulation of toxicity of environmental toxicants or stresses and the underlying mechanisms. After that, we further introduced and discussed the function of DNA damage-related signaling pathway in the regulation of toxicity of environmental toxicants or stresses and the underlying mechanisms. We also tried to introduce the involvement of DNA replication stress-related signal and telomere-related signal in the regulation of toxicity of environmental toxicants or stresses (Fig. 7.1).

Fig. 7.1 Regulation of germ cell apoptosis [8]



At least two distinct pathways of germ cell apoptosis function in *C. elegans*. Physiological apoptosis is *cep-1*-independent and a normal feature of oogenesis. The frequency of *cep-1*-independent germ cell apoptosis increases in response to various cytoplasmic stresses (oxidative, heat, osmotic, starvation). It is not clear whether this increase involves the same triggering mechanism as physiological apoptosis. In each case, these apoptotic events depend upon Ras/MAP-kinase signaling. CEP-1-dependent apoptosis is induced by a DNA damage or chromosomal integrity checkpoint. Rb and E2F transcription factor subunits promote physiological cell death and appear to function downstream of or in parallel to CEP-1 in the DNA damage response. Pathogen-induced germ cell apoptosis is arbitrarily shown as acting directly on EGL-1, because it has not been determined whether CEP-1 is involved. Physiological and DNA damage germ cell apoptosis pathways are suppressed by the PAX-2 and EGL-38 Pax-family proteins, which increase transcription of the antiapoptotic protein CED-9.

7.2 Apoptosis Signaling Pathway

7.2.1 Involvement of Core Apoptosis Signaling Pathway in the Control of Toxicity of Environmental Toxicants or Stresses

Some members of carbon-based engineered nanomaterials, such as graphene oxide (GO), can cause toxic effects on the functions of both primary and secondary targeted organs in nematodes [9–16]. It was further observed that prolonged

exposure to 10–100 mg/L of GO could cause the production of more germ cell corpses compared with control based on AO staining results [17]. *ced-1* encoding a single-pass transmembrane protein is a component of apoptotic pathway and functions to initiate the signaling pathway in phagocytic cells in promoting cell corpse engulfment, phagosome maturation, and, ultimately, apoptotic cell degradation [18]. Additionally, using the CED-1::GFP transgenic strain, it was found that prolonged exposure to GO (10 mg/L) could also induce the production of more apoptotic cells in pachytene region of gonad in nematodes compared with control [17]. The core signaling pathway of *C. elegans* apoptosis is constituted by CED-3, CED-4, and CED-9 [8, 19]. CED-3, a cysteine aspartate protease, is required for the execution of apoptosis and acts in a conserved genetic pathway with the CED-4 [19]. CED-9 is the sole homolog of mammalian cell death inhibitor Bcl-2 and negatively regulates the CED-4 activity to prevent the cells from undergoing apoptosis [19]. Prolonged exposure to GO (10 mg/L) could further significantly increase the expressions of *ced-3* and *ced-4* and decrease the expression of *ced-9* (Fig. 7.2) [17]. Therefore, long-term exposure to GO can induce the germ cell apoptosis by altering the core molecular basis of apoptosis in nematodes.

Meanwhile, it was found that mutation of *ced-3* or *ced-4* inhibited the germ cell apoptosis induced by GO exposure and mutation of *ced-9* also altered the germ cell apoptosis induced by GO exposure (Fig. 7.2) [17]. These results suggest the potential involvement of this core signaling pathway of apoptosis constituted by CED-3, CED-4, and CED-9 in regulating the reproductive toxicity of environmental toxicants or stresses.

Similarly, mutation of core pro-apoptotic regulator genes, *ced-3* and *ced-4*, could suppress the hydroxylated fullerene nanoparticle-induced cell death [20]. Mutation of *ced-3* or *ced-4* could abrogate both copper-induced and physiological germline apoptosis [21]. Microcystin-LR or tributyltin (TBT)-induced germline apoptosis was also absent in *ced-3* or *ced-4* loss-of-function mutant nematodes [22, 23].

7.2.2 Upregulators of Core Apoptosis Signaling Pathway in Regulating the Toxicity of Environmental Toxicants or Stresses

Both bacterial and fungal pathogens can cause different aspects of toxic effects on organisms, including the nematodes [24–33]. In nematodes, the enhanced level of gonadal apoptosis could be observed when fed on *Salmonella*, which could be observed in *sek-1* or *nsy-1* mutant nematodes or in nematodes in which *pmk-1* has been inactivated by RNAi (Fig. 7.3) [34]. These results suggest that the enhanced level of germ cell apoptosis by *Salmonella* feeding is PMK-1 dependent. Nevertheless, the “basal” level of apoptosis observed when feeding on *E. coli* is PMK-1 independent [34].

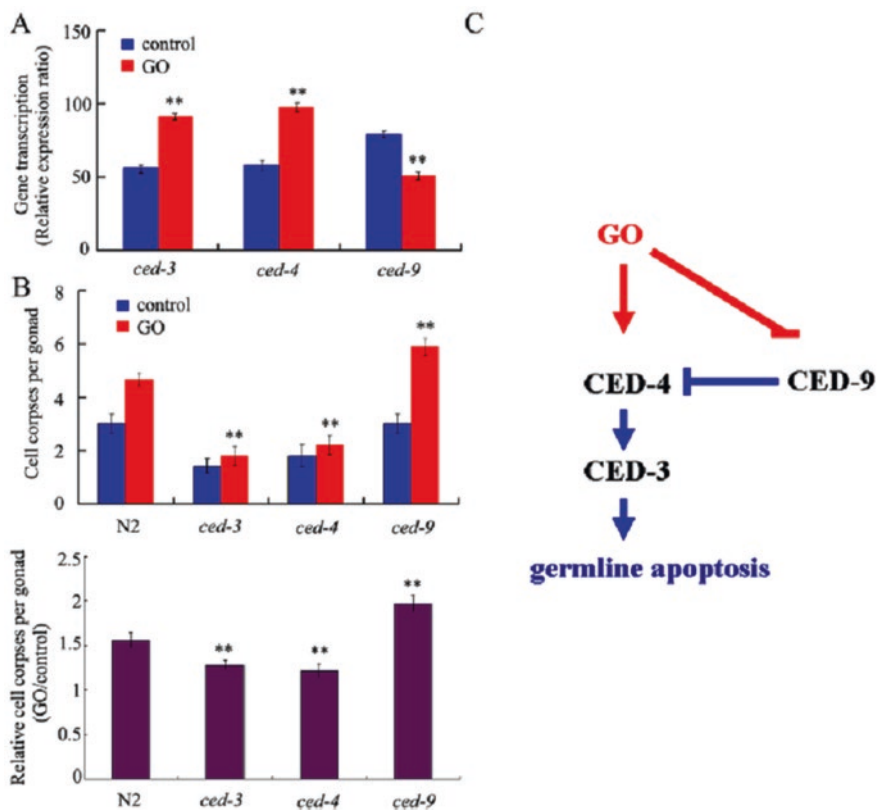
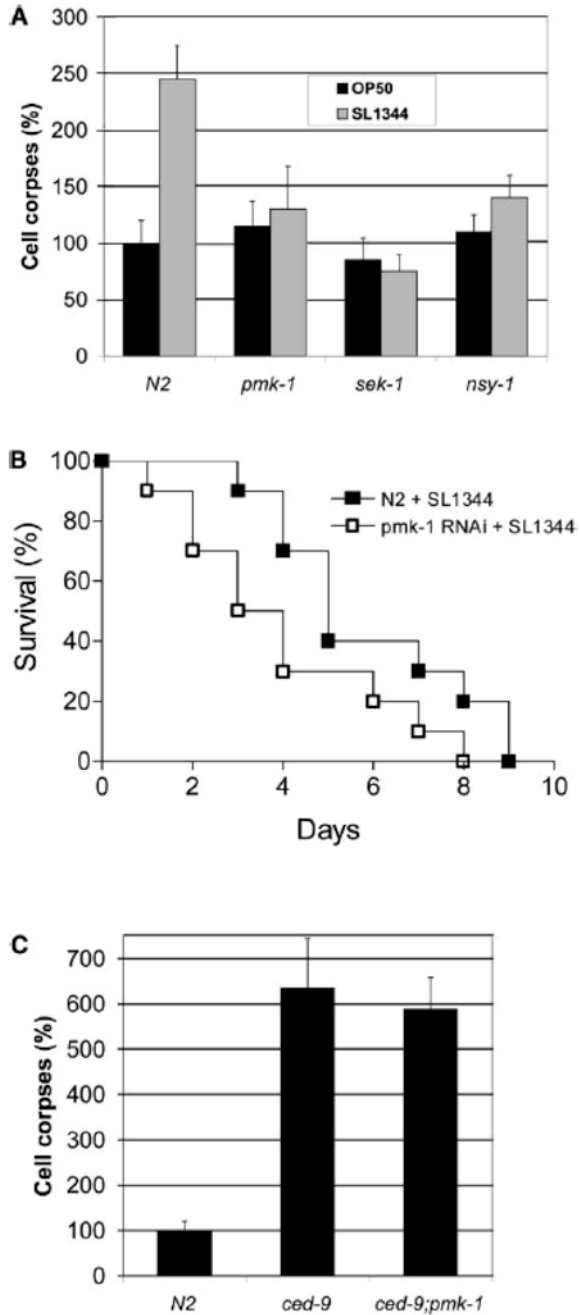


Fig. 7.2 Role of the core apoptosis signaling pathway in the control of GO toxicity in inducing germline apoptosis [17]. (a) GO exposure altered expression patterns of genes encoding the core apoptosis signaling pathway. Bars represent means \pm SEM ** $P < 0.01$ vs control. (b) Mutations of genes encoding the core apoptosis signaling pathway affected the germline apoptosis in nematodes exposed to GO. The used strains were wild-type N2, *ced-3*(n717), *ced-4*(n1162), and *ced-9*(n1950). Bars represent means \pm SEM ** $P < 0.01$. (c) A model for the core apoptosis signaling pathway in the control of GO toxicity in inducing germline apoptosis. GO exposure concentration was 10 mg/L. Prolonged exposure to GO was performed from L1-larvae to young adults

Moreover, it was observed that the PMK-1 inhibition by RNAi in *ced-9* mutant nematodes could not reduce the high level of spontaneous gonadal apoptosis observed when fed on *E. coli* OP50 (Fig. 7.3) [34]. Additionally, in *ced-9* gain-of-function mutant nematodes, *Salmonella*-induced apoptosis could be completely blocked [34]. Therefore, the observed *Salmonella*-elicited apoptosis is CED-9 dependent, and the *Salmonella*-elicited CED cell death signaling pathway may lie downstream of PMK-1. That is, PMK-1 in the p38 MAPK signaling pathway can act as an upstream regulator for core apoptosis signaling pathway in regulating the toxicity of environmental toxicants or stresses.

Fig. 7.3 *S. enterica* elicits a PMK-1-dependent CED cell death pathway in *C. elegans* [34]. (a) N2, *nsy-1*, *sek-1*, or *pmk-1* RNAi young adult animals were exposed to *E. coli* OP50 or *S. enterica* SL1344, and cell corpses were counted 24 h after the initial exposure. Data (mean \pm SD) were from two independent experiments, and more than 15 animals were scored in each case. (b) *C. elegans* N2 or *pmk-1* RNAi young adult animals were exposed to *S. enterica* SL1344. A total of 20 animals were used in each case. Nematode survival was plotted with the PRISM computer program. A p value that was <0.05 was considered significant. (c) N2, *ced-9*, or *ced-9* RNAi *pmk-1* young adult animals were exposed to *S. enterica* SL1344, and cell corpses were counted 24 h after the initial exposure. Data (mean \pm SD) were from two independent experiments, and more than 15 animals were scored in each case



7.2.3 Targets of Core Apoptosis Signaling Pathway in Regulating the Toxicity of Environmental Toxicants or Stresses

SIR-2.1 is a member of the sirtuin family related to *Saccharomyces cerevisiae* Sir2p. In nematodes, *sir-2.1* was required for induction germ cell apoptosis caused by ionizing radiation-induced DNA damage [35]. *sir-2.1* mutation did not affect the DNA damage response pathway upstream of CEP-1 [35]. The cell cycle arrest following the DNA damage was not affected by the *sir-2.1* deletion [35]. SIR-2.1 was also not required for the CEP-1-dependent transcriptional induction of *egl-1* and *ced-13* [35]. After the ionizing radiation, the SIR-2.1 would be translocated from the nucleus to the cytoplasm of dying cells [35]. In contrast, mutation of *cep-1* or *ced-3* affected this translocation from the nucleus to the cytoplasm in dying cells (Fig. 7.4) [35]. Moreover, it was observed that the SIR-2.1 colocalized with the CED-4 in germ cells in nematodes exposed to the ionizing irradiation (Fig. 7.5) [35]. These results suggest that SIR-2.1 can act as an important downstream target of core apoptosis signaling pathway in regulating the toxicity of environmental toxicants or stresses in nematodes.

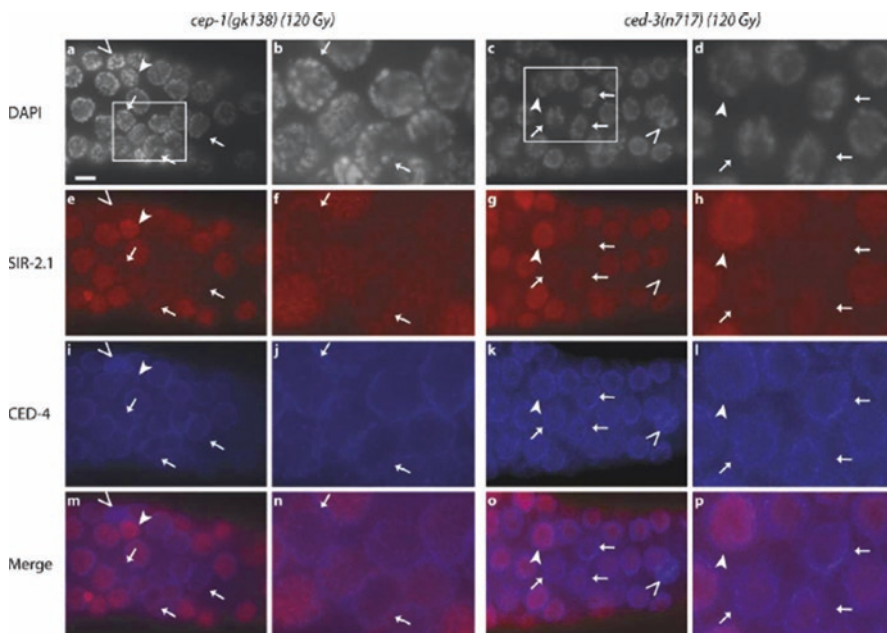


Fig. 7.4 SIR-2.1 translocation is independent of *cep-1* and *ced-3* [35]. Arrows indicate nuclei that have lost SIR-2.1 but where the nucleus is still intact. Arrowheads indicate nuclei with strong SIR-2.1 staining. Empty arrowheads indicate cells in the late stages of apoptosis. Germlines were stained with goat anti-SIR-2.1 (126.3) and rabbit anti-CED-4 (9103.1) antibodies

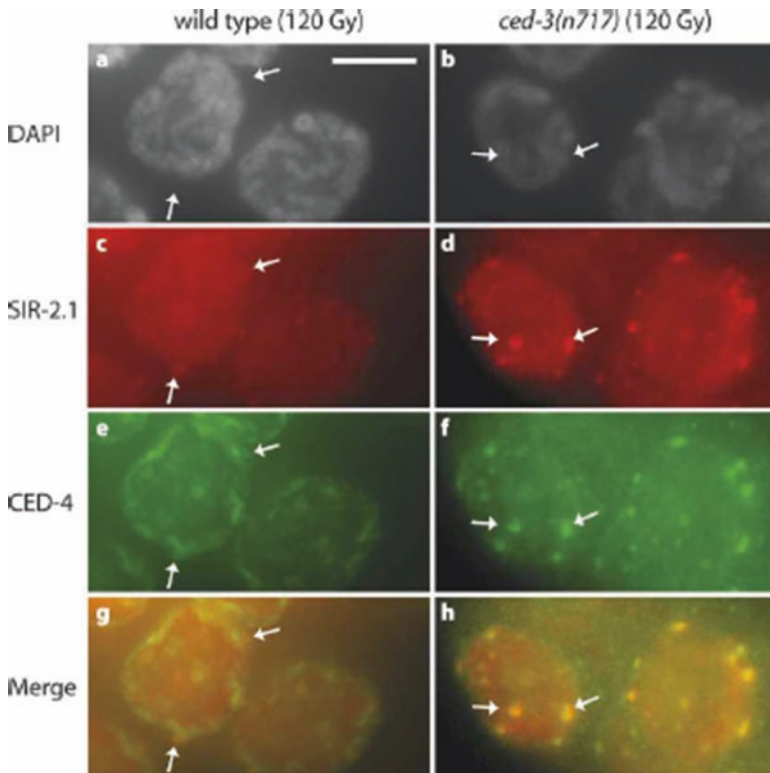


Fig. 7.5 SIR-2.1 colocalizes with CED-4 in germ cells after Irradiation [35]. The apparent weak intranuclear CED-4 staining is nonspecific. Bar, 5 μ m. Germlines were stained with rabbit anti-SIR-2.1 (1434.3) and goat anti-CED-4 (10147.1)

7.3 DNA Damage Signaling Pathway

7.3.1 *Involvement of Core DNA Damage Signaling Pathway in the Control of Toxicity of Environmental Toxicants or Stresses*

In the DNA damage-related signaling pathway, EGL-1, a protein containing a region similar to BH3 domain of mammalian cell death activators, functions as an upstream activator in the core apoptosis signaling pathway and as a DNA damage checkpoint [36–38]. CEP-1, an ortholog of human tumor suppressor p53, functions in promoting the DNA damage-induced apoptosis by activating EGL-1 [36–38]. CLK-2, an ortholog of telomere length-regulating protein Tel2p, and HUS-1 are required for the function of CEP-1 in activating DNA damage-induced apoptosis [36–38]. With GO as an example, prolonged exposure to GO (10 mg/L) could induce the DNA damage and reduced the number of mitotic cells in gonad of

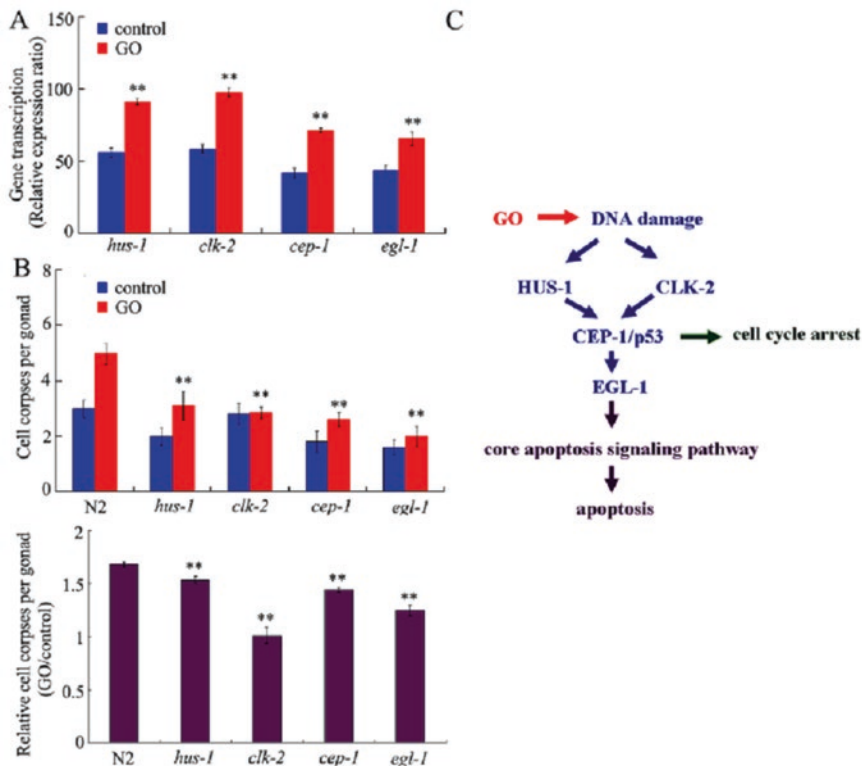


Fig. 7.6 Role of the signaling pathway for DNA damage checkpoints in the control of GO toxicity in inducing germline apoptosis [17]. (a) GO exposure altered expression patterns of genes encoding the signaling pathway for DNA damage checkpoints. Bars represent means \pm SEM ** $P < 0.01$ vs control. (b) Mutations of genes encoding the signaling pathway for DNA damage checkpoints affected the germline apoptosis in nematodes exposed to GO. The used strains were wild-type N2, *egl-1(n1084n3082)*, *hus-1(op241)*, *cep-1(gk138)*, and *clk-2(mn159)*. Bars represent means \pm SEM ** $P < 0.01$. (c) A model for the signaling pathway for DNA damage checkpoints in the control of GO toxicity in inducing germline apoptosis. GO exposure concentration was 10 mg/L. Prolonged exposure to GO was performed from L1-larvae to young adults

nematodes [17]. Meanwhile, prolonged exposure to GO (10 mg/L) significantly increased the expressions of *hus-1*, *clk-2*, *cep-1*, and *egl-1* (Fig. 7.6) [17], suggesting that long-term exposure to GO can induce the germ DNA damage by altering the core molecular basis of DNA damage in nematodes.

Moreover, it was observed that mutation of *hus-1*, *clk-2*, *cep-1*, or *egl-1* could noticeably suppress the germline apoptosis induced by GO exposure (Fig. 7.6) [17], suggesting the further involvement of signaling pathway for DNA damage checkpoints in the control of reproductive toxicity of GO. Therefore, the core signaling pathway of DNA damage checkpoints can potentially also participate in regulation of toxicity of environmental toxicants or stresses in nematodes.

In nematodes, it was further found that the DNA damage-related signaling pathway was involved in the induction of reproductive toxicity of heavy metal (Cd and Cu), microcystin-LR, TBT, or tributyltin chloride [21–23, 39, 40].

7.3.2 *Upregulators of Core DNA Damage-Related Signaling Pathway in Regulating the Toxicity of Environmental Toxicants or Stresses*

7.3.2.1 *mir-360*

In nematodes, some corresponding miRNAs for *ced-3*, *ced-4*, and *ced-9* encoding the core apoptosis signaling pathway and for *hus-1*, *clk-2*, *cep-1*, and *elg-1* encoding the signaling pathway for DNA damage checkpoints were identified in GO-exposed nematodes based on bioinformatics analysis [17]. Among the dysregulated miRNAs induced by GO, *mir-2210*, *mir-4810*, *mir-4805*, *mir-259*, *mir-82*, *mir-360*, and *mir-4807* might be involved in the control of reproductive toxicity in inducing germline apoptosis in GO-exposed nematodes [17]. Among these miRNAs, mutation of *mir-360* significantly enhanced the reproductive toxicity of GO in inducing germline apoptosis, whereas *mir-360* overexpression significantly suppressed the reproductive toxicity of GO in inducing germline apoptosis in nematodes (Fig. 7.7) [17].

For the underlying molecular mechanism of *mir-360* in regulating the reproductive toxicity of GO in inducing germline apoptosis, CEP-1 was identified as a molecular target for *mir-360*. The double mutant of *cep-1(RNAi);mir-360(n4635)* exposed to GO (10 mg/L) showed the similar phenotype of germline apoptosis to that in *cep-1(RNAi)* nematodes exposed to GO (10 mg/L) (Fig. 7.7) [17], implying the role of CEP-1 as the potential target for *mir-360* in regulating the reproductive toxicity of GO in inducing germline apoptosis. In nematodes, GO exposure increased the expression of *mir-360* [41]. This implies that the increased *mir-360* may mediate a protection response or function for nematodes against the reproductive toxicity of GO by suppressing the function of CEP-1 in the DNA damage checkpoints signaling pathway. Therefore, *mir-360* can act as an upstream regulator of core DNA damage-related signaling pathway in regulating the toxicity of environmental toxicants or stresses in nematodes.

7.3.2.2 *ABL-1*

c-Abl is a conserved nonreceptor tyrosine kinase with the function to integrate the genotoxic stress responses by acting as a transducer of both pro- and antiapoptotic effector pathways. In nematodes, loss-of-function mutation of *abl-1* encoding the c-Abl caused the hypersensitivity to radiation-induced apoptosis in the germline (Fig. 7.8) [42], implying the possible role in the regulation of DNA damage in the germ cells of nematodes.

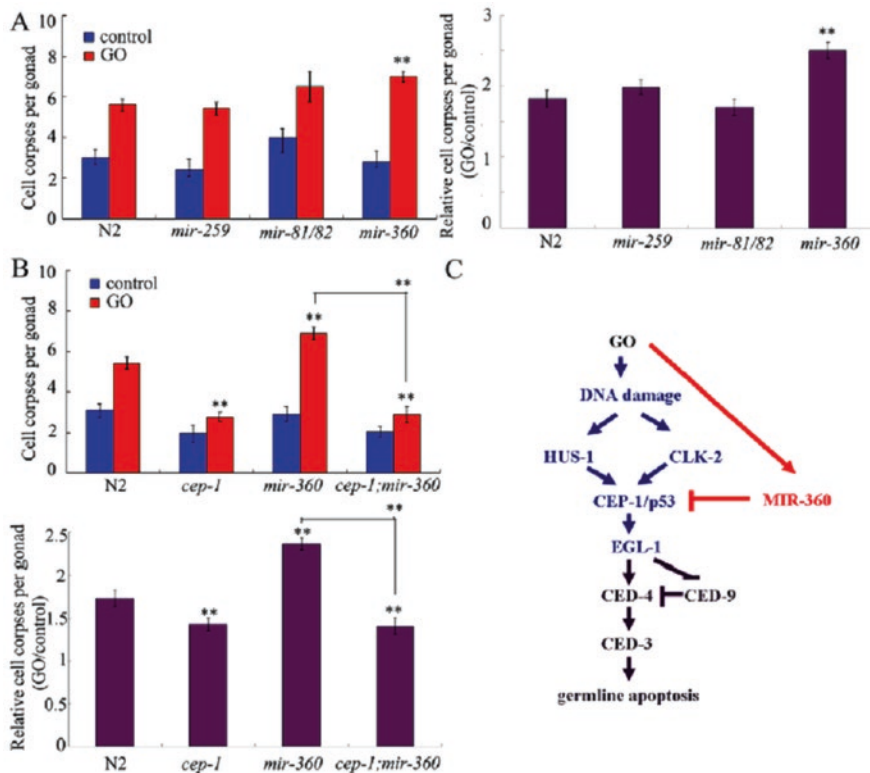


Fig. 7.7 *mir-360* negatively regulated the functions of signaling pathways of DNA damage checkpoints and apoptosis in the control of reproductive toxicity in GO-exposed nematodes [17]. (a) Germline apoptosis in *mir-259*, *mir-81/82*, or *mir-360* mutant exposed to GO. The used mutants were wild-type N2, *mir-360*(n4635), *mir-259*(n4106), and *mir-81&82*(nDf54). (b) Genetic interaction of *mir-360* with *cep-1* in regulating germline apoptosis in nematodes exposed to GO. The used strains were wild-type N2, *mir-360*(n4635), *cep-1*(RNAi), and *cep-1*(RNAi);*mir-360*(n4635). (c) A summary model for the molecular control of reproductive toxicity of GO in inducing germline apoptosis in nematodes. GO exposure concentration was 10 mg/L. Prolonged exposure to GO was performed from L1-larvae to young adults. Bars represent means \pm SEM ** $P < 0.01$

The further findings implies the role of ABL-1 in antagonizing the apoptotic pathway, and this process required the sequentially cell cycle checkpoint genes *clk-2*, *hus-1*, and *mrt-2*; the p53 homolog, *cep-1*; and the genes encoding the components of the conserved apoptotic machinery, *ced-3*, *ced-9* and *egl-1* (Fig. 7.9) [42]. It was observed that mutation of DNA damage checkpoint and p53 could prevent the germ cell apoptosis in *abl-1*(ok171) mutant nematodes (Fig. 7.9) [42]. That is, ABL-1 serves an antiapoptotic purpose in the germline, since it can act as a negative regulator of the p53 homolog CEP-1 and the checkpoint pathway and thereby constrain the conserved apoptosis machinery. Therefore, ABL-1 is another important upstream regulator of core DNA damage-related signaling pathway in regulating the toxicity of environmental toxicants or stresses in nematodes.

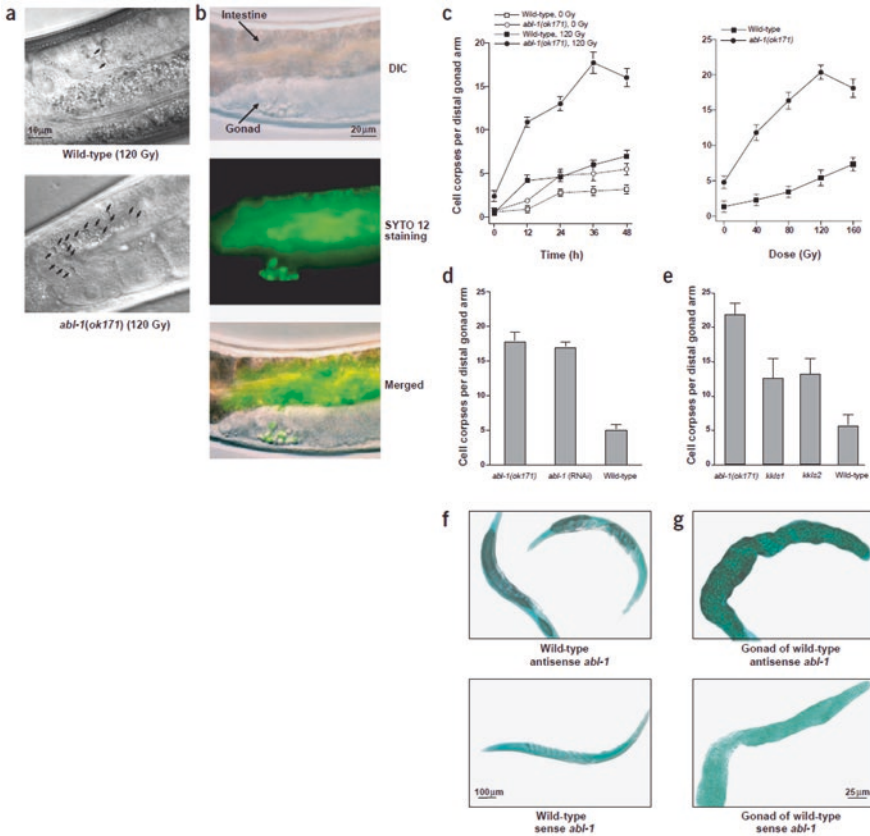


Fig. 7.8 The *abl-1(ok171)* mutant is hypersensitive to radiation-induced germ cell apoptosis [42] (a–c) Wild-type and mutant worms were synchronized at 20 °C and treated as young adults (24 h after L4 stage) with the indicated doses of radiation. The distal arm of one side of the gonad was scored for cell corpses under Nomarski optics. Error bars indicate SEM from 15 to 20 worms per group. (a) Germ cell corpses were scored 36 h after exposure to 120 Gy. Apoptotic cells are indicated by arrowheads in a single focal plane. (b) Increased germ cell apoptosis in *abl-1(ok171)* was confirmed by SYTO 12 staining. Nonspecific staining can be observed in the intestine, located above the gonad. (c) Germ cell apoptosis was scored at the indicated times (left panel) after exposure to 120 Gy or at 36 h after the indicated doses of radiation (right panel). Error bars indicate SEM from 10–15 worms per group. (d) *abl-1* dsRNA was introduced into wild-type adult worms by microinjection. Germ cell corpses were scored in F1 young adult worms 36 h after exposure to 120 Gy. Error bars indicate SEM from 10 to 15 worms per group. (e) Two independent transgenes, *kkIs1* and *kkIs2*, with cosmid M79 stably integrated in the background of *abl-1(ok171)*, were generated to rescue the *abl-1(ok171)* phenotype. Germ cell corpses were counted in adult transgenic worms 36 h after exposure to 120 Gy. Error bars indicate SEM from 10–15 worms per group. (f,g) Adult wild-type worms were hybridized with antisense or sense *abl-1* probes. Expression of *abl-1* was viewed under bright-field microscopy. Dark blue represents positive staining; light green represents background staining. (f) Intact wild-type worms. (g) Gonadal tissue dissected from wild-type worms

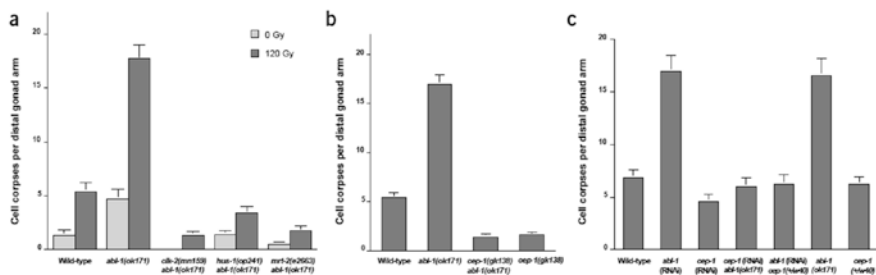


Fig. 7.9 DNA damage checkpoint and p53 mutations prevent germ cell apoptosis in *abl-1(ok171)* worms [42] (a) Young adult *abl-1(ok171)* and double mutants *clk-2(mn159) abl-1(ok171)*, *hus-1(op241) abl-1(ok171)* and *mrt-2(e2663) abl-1(ok171)* were irradiated with 120 Gy, and germ cell corpses were counted after 36 h. Error bars represent SEM from 15 worms per group. (b) *abl-1(ok171)* was crossed with the deletion allele *cep-1(gk138)*, and individual progeny with the double-mutant genotype *cep-1(gk138) abl-1(ok171)* were isolated. The strain with the genotype *abl-1(ok171)* worms was selected as a control. Germ cell corpses were scored in adult worms 24 h after exposure to 120 Gy. Error bars represent SEM from 10 to 15 worms per group. (c) RNAi of *abl-1* and *cep-1*. *abl-1* dsRNA was introduced into *cep-1(w40)* worms, and *cep-1* dsRNA was introduced into *abl-1(ok171)* worms by microinjection. Germ cell corpses were counted in adult F1 progeny 24 h after exposure to 120 Gy. Error bars represent SEM from 25 to 35 worms per group

7.3.2.3 NOL-6

nol-6 encodes a nucleolar RNA-associated protein (NRAP) that is involved in the early stages of ribosome biogenesis. Inhibition of Pol-I by actinomycin D, an inhibitor of ribosome biogenesis, caused an enhanced resistance to *S. enterica*-mediated killing in wild-type nematodes; however, actinomycin D treatment in *nol-6* mutant nematodes had no such effect (Fig. 7.10) [43]. Additionally, 5 days after the infection, only 30% of control nematodes remained alive, while 72–98% of nematodes in which individual *rps* genes were depleted by RNAi could remain alive (Fig. 7.10) [43]. That is, the ribosome can act as a negative regulator of innate immunity, and the reduced ribosomal function by mutation or RNAi can boost the innate immunity.

Moreover, it was observed that mutation of *cep-1* could suppress not only the enhanced resistance to *S. enterica*-mediated killing of *nol-6* RNAi nematodes but also that of *rps* RNAi nematodes (Fig. 7.10) [43], suggesting that the derepression of CEP-1 transcriptional activity by *nol-6* or *rps* RNAi may activate the innate immunity against *S. enterica*.

The expression analysis further demonstrated that the CEP-1-regulated genes were upregulated in *nol-6* RNAi nematodes and the CEP-1 target, *egl-1*, was also upregulated in *nol-6* RNAi nematodes compared to vector control wild-type nematodes (Fig. 7.11) [43]. This suggests that higher CEP-1 activity is responsible for the enhanced resistance to *S. enterica*-mediated killing in animals with impaired

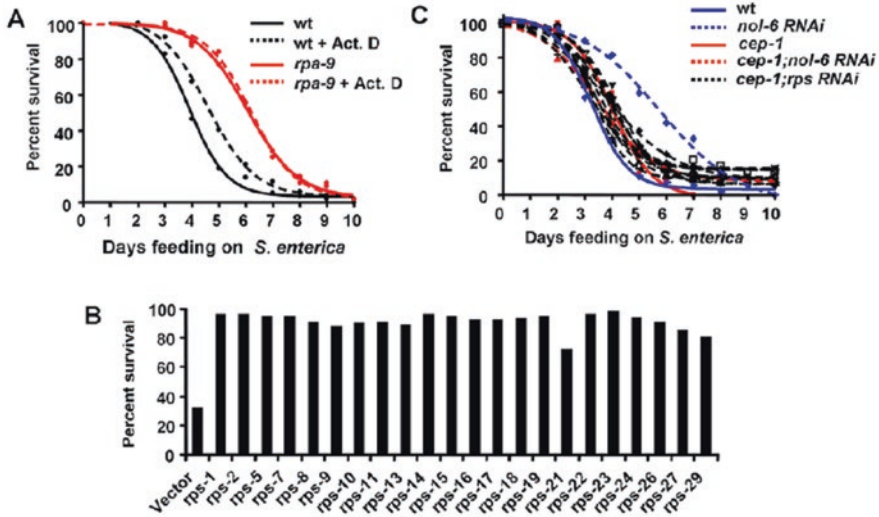


Fig. 7.10 Nucleolar protein knockdown activates immunity against *S. enterica* in a p53/*cep-1*-dependent manner [43]. (a) Wild-type and *rpa-9* nematodes were fed *S. enterica* on plates containing either 0.005 mg/mL actinomycin D or buffer. Wild-type vs wild-type+Act. D: $p = 0.0261$. (b) Wild-type nematodes were grown on dsRNA for vector control or dsRNA for *rps* genes, and the number of living nematodes was scored after 5 days of feeding on *S. enterica*. Differences between vector and *rps* RNAi was statistically significant in all cases. (c) Wild-type and *cep-1(gk138)* nematodes were grown on dsRNA for vector control, dsRNA for *nol-6*, or dsRNA for *rps* genes, and the number of live vs dead animals was scored over time. Wild type vs *nol-6* RNAi. Wild type vs *cep-1(gk138);nol-6* RNAi. Since *cep-1(gk138)* nematodes exhibit an Egl phenotype, the animals that die from matricide were censored. For each condition, 57–61 animals were used

ribosomal function due to mutation or RNAi of *nol-6*. Therefore, NUL-6 can also act as an upstream regulator of core DNA damage-related signaling pathway in regulating the toxicity of environmental toxicants or stresses in nematodes.

7.4 DNA Replication Stress-Related Signal

Cells can face upon the DNA replication stress when the progress of DNA polymerases on the template strand is hindered by DNA damage, tightly bound proteins, nucleotide exhaustion, or tri-nucleotide repeats [44]. The ATR protein kinase ATL-1 is the master regulator of the response to DNA replication stress [45]. The DNA replication stress can be induced either by HU treatment or UV-C (254 nm) light. One critical ATR substrate is the CHK1/CHK-1 protein kinase. WRN-1, ortholog of the human Werner syndrome helicase, acts upstream of ATR during the DNA replication stress response [46].

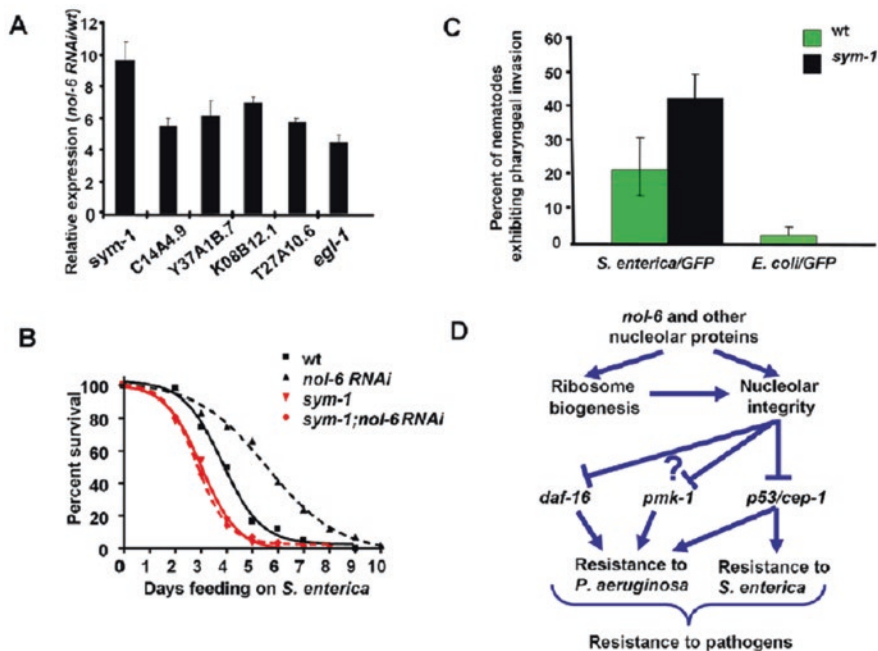
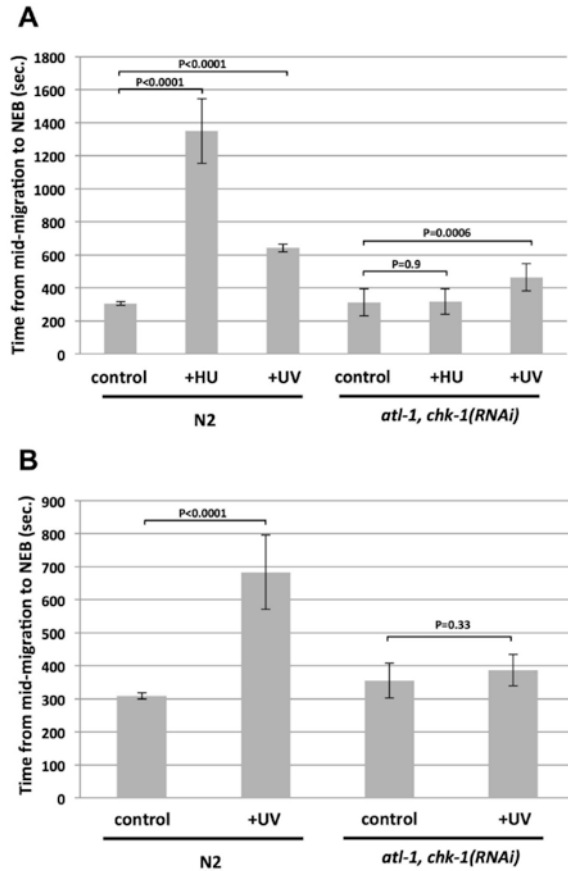


Fig. 7.11 Derepression of CEP-1 transcriptional activity by *nol-6* RNAi activates immunity against *S. enterica* [43]. (a) Quantitative RT-PCR analysis of 7 *cep-1*-dependent genes in nematodes grown on dsRNA for vector control or dsRNA for *nol-6*. Data were analyzed by normalization to pan-actin (*act-1*, *act-3*, *act-4*) and relative quantification using the comparative-cycle threshold method. Student's exact *t*-test indicates that differences among the groups are significantly different; bar graphs correspond to mean \pm SEM ($n = 3$). (b) Wild-type and *sym-1(mn601)* nematodes grown on dsRNA for vector control or dsRNA for *nol-6* were fed *S. enterica*, and the number of live vs dead animals was scored over time. Vector vs *sym-1(mn601)*. For each condition, 60 animals were used. This experiment was performed in duplicate. (c) Wild-type and *sym-1(mn601)* nematodes were fed *S. enterica*/GFP or *S. enterica*/GFP for 48 h, and the percentages of worms exhibiting pharyngeal invasion of *S. enterica* were quantified. Wild type vs *sym-1(mn601)* *S. enterica*/GFP. For each condition, approximately 100 animals were used. (d) Mechanism by which disruption of the nucleolus may lead to enhanced resistance to pathogen through the activation of CEP-1. Inhibition of *nol-6* and other nucleolar proteins via RNAi or mutation disrupts nucleolar integrity leading to an upregulation of CEP-1-dependent transcription and an increase in resistance to both *S. enterica* and *P. aeruginosa*. Disruption of the nucleolus may also lead to enhanced resistance to *P. aeruginosa* through the activity of PMK-1 and DAF-16

7.4.1 Involvement of ATR Signaling Pathway in the Regulation of DNA Replication Stress Induced by Environmental Toxicants or Stresses

Under the normal conditions, embryos required ~ 300 s to progress from mid-migration to nuclear envelop breakdown (NEB). This process was increased by HU to nearly 1400 s and by UV-C to ~ 600 s [47]. In contrast, for *atl-1,chk-1(RNAi)*

Fig. 7.12 The ATR pathway controls cell cycle delay after HU- or UV-C-mediated replication stress in one cell embryos [47]. (a) Either wild-type (N2) or *atl-1,chk-1(RNAi)* embryos were optionally treated with either HU or UV-C, as indicated. The time required for embryos to progress from the mid-migration to the NEB stage was then recorded. For each data point, ten embryos were timed over two independent biological replicates (5/replicate), and the values were then averaged and plotted. (b) Same as (a) except HU treatment was omitted and five embryos were timed per data point over one biological replicate



embryos, HU could not significantly extend the cell cycle, while UV-C did but only modestly (Fig. 7.12) [47]. These observations suggest that some components of cell cycle delay after UV-C might occur independently of the ATR pathway, since UV-C delay was not absolutely reduced by *atl-1,chk-1* RNAi. Actually, it was observed that *atl-1,chk-1* RNAi could significantly reverse the UV-C-induced delay (Fig. 7.12) [47]. Therefore, the ATR signaling pathway is involved in the control of cell cycle delay under the DNA replication stress induced by environmental toxicants or stresses.

In nematodes, both RPA-1 and WRN-1 belong to the ATR docking factors [47]. RPA-1 functions in recruiting ATL-1 to the sites of DNA replication stress and can physically interact with the WRN-1. Under the normal conditions, both *rpa-1(RNAi)* and *wrn-1(RNAi)* embryos were modestly slower than wild-type nematodes [47]. Under the DNA replication stress, although the wild-type embryos showed typical patterns of cell cycle delay, the *rpa-1(RNAi)* embryos could not be significantly delayed by either HU or UV-C [47]. Additionally, under the DNA replication stress, *wrn-1* depletion prevented the HU-imposed cell cycle delay; however, UV-C could

still impose a cell cycle delay [47]. Therefore, both the RPA-1 and the WRN-1 are required for the ATR pathway function in the early embryo when the DNA replication is stressed.

In nematodes, the ATR activators contain MUS-101 (TOPBP1) and HPR-17 (RAD17). Under the normal condition, the *mus-101(RNAi)* or *hpr-17(RNAi)* embryos displayed a slower first cell cycle [47]. Under the DNA replication stress induced by HU, although the control embryos showed a robust delay, the cell cycle delay was not observed in *mus-101(RNAi)* or *hpr-17(RNAi)* nematodes [47]. In contrast, under the DNA replication stress, UV induced the cell cycle arrest for *mus-101(RNAi)* or *hpr-17(RNAi)* nematodes [47].

7.4.2 Cell-Type-Specific Responses to DNA Replication Stress Induced by Environmental Toxicants or Stresses

To the time P0, the animals we irradiated, and then newly fertilized embryos were identified [47]. For the AB and the P1, the animals were irradiated and then immediately dissected out the embryos. After HU irradiation, the P1 response was closer to its sister AB than its mother P0, suggesting that the DNA replication stress response is remodeled after cell division in the early embryo [47]. Therefore, the DNA replication stress response will vary between cell types in the early embryo. That is, the DNA replication stress response is under the developmental control (Fig. 7.13).

7.5 Telomere-Related Signal

Telomerase is a reverse transcriptase with the function in maintaining the telomere in dividing cells and in protecting from oxidative stress and DNA damage. During this process, two subunits are involved, and they are the enzyme TERT (telomerase reverse transcriptase) and the RNA component TERC (telomerase RNA component). In nematodes, *trt-1* is the catalytic subunit of telomerase [48].

Heavy metal of Mn represents an environmental risk factor for Parkinson's disease (PD). After acute Mn treatment of 1 h at the first larval (L1) stage, it was observed that the *trt-1* mutant nematodes were less sensitive to Mn-induced lethality compared to wild-type nematodes (Fig. 7.14) [49]. That is, Mn could induce the DAergic degeneration in wild-type nematodes, but not in *trt-1* mutant nematodes [49]. This observation implies the involvement of telomere-related signal in the regulation of toxicity of environmental toxicants or stresses in nematodes.

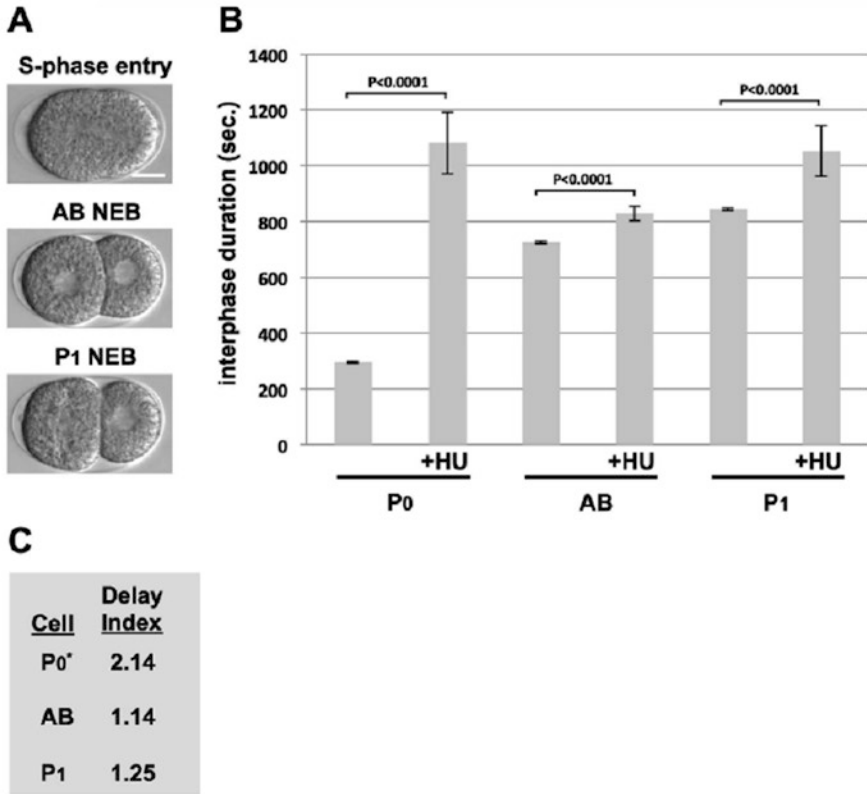


Fig. 7.13 Comparing the HU response between the P0, AB, and P1 blastomeres [47]. (a) Images depicting when cell cycle timing was started (top panel) and when it was terminated for AB (middle panel) or P1 (bottom panel). Bar = 10 μ M. (b) N2 animals were optionally treated with HU, and interphase duration for a given cell type was plotted. Each data point represents the average of ten embryos obtained over two biological replicates (5/replicate). (c) The delay indices (DI) for the given cell types are depicted. Please see the main text for how the DIs were calculated

7.6 Perspectives

Cell death and DNA damage-related signaling pathways are essential for the normal development of nematodes. Moreover, the increasing evidence has highlighted their crucial function in regulating the toxicity of environmental toxicants or stresses in nematodes. During the regulation of toxicity of environmental toxicants or stresses, an important question needed to be further elucidated is the detailed interactions between the cell death and DNA damage-related or development-related signaling pathways and the oxidative stress or stress response-related signaling pathways, such as MAPK and insulin signaling pathways.

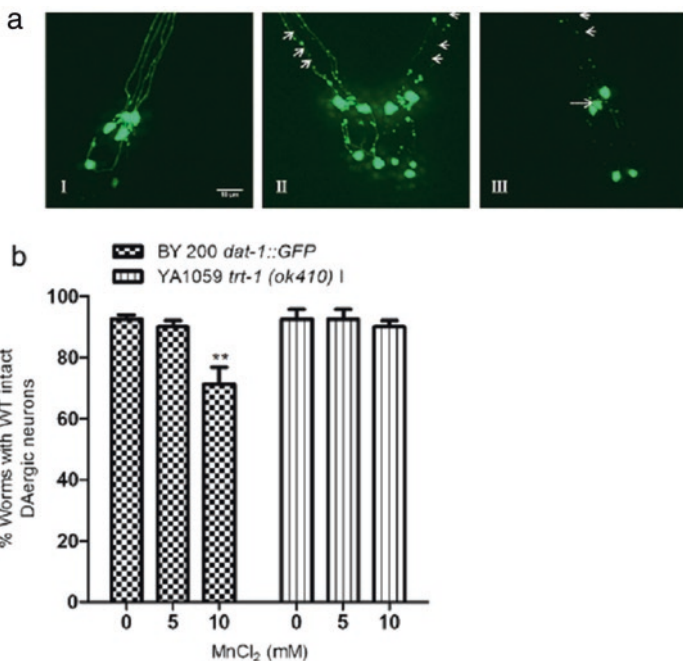


Fig. 7.14 Mn induces DAergic degeneration in wt worms but not in *trt-1* mutants [49]. BY200 (*dat-1::GFP*) worms express green fluorescent protein (GFP) in DAergic neurons. Male *dat-1::GFP* worms were crossed with hermaphrodites of *trt-1* worms. Twenty worms were observed and scored for DAergic degeneration of CEP neurons. Representative confocal images of cephalic (CEP) neurons in head of worms are shown (a). I show intact neurons in worm head; II and III show degenerating neurons in worms. Morphological features of degeneration include dendritic puncta (arrows), shrunken soma (dashed arrow), and loss of dendrites or soma. Worms with intact or degenerating neurons were counted. Data are expressed as percentage of worms with intact neurons (b). Two-way ANOVA; ** $P < 0.01$

In this chapter, we also introduced the involvement of DNA replication stress-related signal and telomere-related signal in regulating the toxicity of environmental toxicants or stresses. Actually, all the signaling pathways introduced in this chapter are essential for the normal development. Under the normal conditions, mutation of these genes during the embryo or early larvae stages will cause the developmental defects or arrest. So far, most of the obtained data for these signaling pathways are based on the exposure from the embryo or larvae stage. Then, an important question needed to be further determined is the exact role of these signaling pathways in regulating the toxicity of environmental toxicants or stresses at the adult stage or during the aging process. To understand such a role for these signaling pathways, the expression alterations for the related genes should be carefully examined at the adult stage or during the aging process after exposure to certain environmental toxicants or stresses.

References

1. Wang DY (2018) Nanotoxicology in *Caenorhabditis elegans*. Springer, Singapore
2. Qu M, Xu K-N, Li Y-H, Wong G, Wang D-Y (2018) Using *acs-22* mutant *Caenorhabditis elegans* to detect the toxicity of nanopolystyrene particles. *Sci Total Environ* 643:119–126
3. Li W-J, Wang D-Y, Wang D-Y (2018) Regulation of the response of *Caenorhabditis elegans* to simulated microgravity by p38 mitogen-activated protein kinase signaling. *Sci Rep* 8:857
4. Dong S-S, Qu M, Rui Q, Wang D-Y (2018) Combinational effect of titanium dioxide nanoparticles and nanopolystyrene particles at environmentally relevant concentrations on nematodes *Caenorhabditis elegans*. *Ecotoxicol Environ Saf* 161:444–450
5. Zhao L, Rui Q, Wang D-Y (2017) Molecular basis for oxidative stress induced by simulated microgravity in nematode *Caenorhabditis elegans*. *Sci Total Environ* 607–608:1381–1390
6. Wu Q-L, Han X-X, Wang D, Zhao F, Wang D-Y (2017) Coal combustion related fine particulate matter (PM_{2.5}) induces toxicity in *Caenorhabditis elegans* by dysregulating microRNA expression. *Toxicol Res* 6:432–441
7. Yin J-C, Liu R, Jian Z-H, Yang D, Pu Y-P, Yin L-H, Wang D-Y (2018) Di (2-ethylhexyl) phthalate-induced reproductive toxicity involved in DNA damage-dependent oocyte apoptosis and oxidative stress in *Caenorhabditis elegans*. *Ecotoxicol Environ Saf* 163:298–306
8. Gartner A, Boag PR, Blackwell TK (2008) Germline survival and apoptosis. *WormBook*. <https://doi.org/10.1895/wormbook.1.145.1>
9. Ren M-X, Zhao L, Ding X-C, Krasteva N, Rui Q, Wang D-Y (2018) Developmental basis for intestinal barrier against the toxicity of graphene oxide. *Part Fibre Toxicol* 15:26
10. Xiao G-S, Chen H, Krasteva N, Liu Q-Z, Wang D-Y (2018) Identification of interneurons required for the aversive response of *Caenorhabditis elegans* to graphene oxide. *J Nanbiotechnol* 16:45
11. Ding X-C, Rui Q, Wang D-Y (2018) Functional disruption in epidermal barrier enhances toxicity and accumulation of graphene oxide. *Ecotoxicol Environ Saf* 163:456–464
12. Ding X-C, Wang J, Rui Q, Wang D-Y (2018) Long-term exposure to thiolated graphene oxide in the range of µg/L induces toxicity in nematode *Caenorhabditis elegans*. *Sci Total Environ* 616–617:29–37
13. Zhao L, Kong J-T, Krasteva N, Wang D-Y (2018) Deficit in epidermal barrier induces toxicity and translocation of PEG modified graphene oxide in nematodes. *Toxicol Res* 7(6):1061–1070. <https://doi.org/10.1039/C8TX00136G>
14. Xiao G-S, Zhi L-T, Ding X-C, Rui Q, Wang D-Y (2017) Value of *mir-247* in warning graphene oxide toxicity in nematode *Caenorhabditis elegans*. *RSC Adv* 7:52694–52701
15. Zhao L, Wan H-X, Liu Q-Z, Wang D-Y (2017) Multi-walled carbon nanotubes-induced alterations in microRNA *let-7* and its targets activate a protection mechanism by conferring a developmental timing control. *Part Fibre Toxicol* 14:27
16. Zhuang Z-H, Li M, Liu H, Luo L-B, Gu W-D, Wu Q-L, Wang D-Y (2016) Function of RSKS-1-AAK-2-DAF-16 signaling cascade in enhancing toxicity of multi-walled carbon nanotubes can be suppressed by *mir-259* activation in *Caenorhabditis elegans*. *Sci Rep* 6:32409
17. Zhao Y-L, Wu Q-L, Wang D-Y (2016) An epigenetic signal encoded protection mechanism is activated by graphene oxide to inhibit its induced reproductive toxicity in *Caenorhabditis elegans*. *Biomaterials* 79:15–24
18. Zhou Z, Hartweg E, Horvitz HR (2001) CED-1 is a transmembrane receptor that mediates cell corpse engulfment in *C. elegans*. *Cell* 104:43–56
19. Lettre G, Hengartner MO (2006) Developmental apoptosis in *C. elegans*: a complex CEDnario. *Annu Rev Mol Cell Biol* 7:97–108
20. Cha YJ, Lee J, Choi SS (2012) Apoptosis-mediated *in vivo* toxicity of hydroxylated fullerene nanoparticles in soil nematode *Caenorhabditis elegans*. *Chemosphere* 87:49–54
21. Wang S, Wu L, Wang Y, Luo X, Lu Y (2009) Copper-induced germline apoptosis in *Caenorhabditis elegans*: the independent roles of DNA damage response signaling and the dependent roles of MAPK cascades. *Chem Biol Interact* 180:151–157

22. Wang S, Geng Z, Wang Y, Tong Z, Yu H (2012) Essential roles of p53 and MAPK cascades in microcystin-LR-induced germline apoptosis in *Caenorhabditis elegans*. *Environ Sci Technol* 46:3442–3448
23. Wang Y, Wang S, Luo X, Yang Y, Jian F, Wang X, Xie L (2014) The roles of DNA damage-dependent signals and MAPK cascades in tributyltin-induced germline apoptosis in *Caenorhabditis elegans*. *Chemosphere* 108:231–238
24. Yu Y-L, Zhi L-T, Wu Q-L, Jing L-N, Wang D-Y (2018) NPR-9 regulates innate immune response in *Caenorhabditis elegans* by antagonizing activity of AIB interneurons. *Cell Mol Immunol* 15:27–37
25. Zhi L-T, Yu Y-L, Li X-Y, Wang D-Y, Wang D-Y (2017) Molecular control of innate immune response to *Pseudomonas aeruginosa* infection by intestinal *let-7* in *Caenorhabditis elegans*. *PLoS Pathog* 13:e1006152
26. Zhi L-T, Yu Y-L, Jiang Z-X, Wang D-Y (2017) *mir-355* functions as an important link between p38 MAPK signaling and insulin signaling in the regulation of innate immunity. *Sci Rep* 7:14560
27. Sun L-M, Liao K, Hong C-C, Wang D-Y (2017) Honokiol induces reactive oxygen species-mediated apoptosis in *Candida albicans* through mitochondrial dysfunction. *PLoS One* 12:e0172228
28. Sun L-M, Liao K, Wang D-Y (2017) Honokiol induces superoxide production by targeting mitochondrial respiratory chain complex I in *Candida albicans*. *PLoS One* 12:e0184003
29. Yu Y-L, Zhi L-T, Guan X-M, Wang D-Y, Wang D-Y (2016) FLP-4 neuropeptide and its receptor in a neuronal circuit regulate preference choice through functions of ASH-2 trithorax complex in *Caenorhabditis elegans*. *Sci Rep* 6:21485
30. Sun L-M, Zhi L-T, Shakoor S, Liao K, Wang D-Y (2016) microRNAs involved in the control of innate immunity in *Candida* infected *Caenorhabditis elegans*. *Sci Rep* 6:36036
31. Sun L-M, Liao K, Li Y-P, Zhao L, Liang S, Guo D, Hu J, Wang D-Y (2016) Synergy between PVP-coated silver nanoparticles and azole antifungal against drug-resistant *Candida albicans*. *J Nanosci Nanotechnol* 16:2325–2335
32. Sun L-M, Liao K, Liang S, Yu P-H, Wang D-Y (2015) Synergistic activity of magnolol with azoles and its possible antifungal mechanism against *Candida albicans*. *J Appl Microbiol* 118:826–838
33. Wu Q-L, Cao X-O, Yan D, Wang D-Y, Aballay A (2015) Genetic screen reveals link between maternal-effect sterile gene *mes-1* and *P. aeruginosa*-induced neurodegeneration in *C. elegans*. *J Biol Chem* 290:29231–29239
34. Aballay A, Drenkard E, Hilbun LR, Ausubel FM (2003) *Caenorhabditis elegans* innate immune response triggered by *Salmonella enterica* requires intact LPS and is mediated by a MAPK signaling pathway. *Curr Biol* 13:47–52
35. Greiss S, Hall J, Ahmed S, Gartner A (2008) *C. elegans* SIR-2.1 translocation is linked to a proapoptotic pathway parallel to *cep-1*/p53 during DNA damage-induced apoptosis. *Genes Dev* 22:2831–2842
36. O’Neil N, Rose A (2006) DNA repair. *WormBook*. <https://doi.org/10.1895/wormbook.1.54.1>
37. Hofmann ER, Milstein S, Boulton SJ, Ye M, Hofmann JJ, Stergiou L, Gartner A, Vidal M, Hengartner MO (2002) *Caenorhabditis elegans* HUS-1 is a DNA damage checkpoint protein required for genome stability and EGL-1-mediated apoptosis. *Curr Biol* 12:1908–1918
38. Kamath RK, Martinez-Campos M, Zipperlen P, Fraser AG, Ahringer J (2001) Effectiveness of specific RNA-mediated interference through ingested double stranded RNA in *C. elegans*. *Genome Biol* 2:1–10
39. Wang S, Tang M, Pei B, Xiao X, Wang J, Hang H, Wu L (2008) Cadmium-induced germline apoptosis in *Caenorhabditis elegans*: the roles of HUS1, p53, and MAPK signaling pathways. *Toxicol Sci* 102:345–351
40. Cheng Z, Tian H, Chu H, Wu J, Li Y, Wang Y (2014) The effect of tributyltin chloride on *Caenorhabditis elegans* germline is mediated by a conserved DNA damage checkpoint pathway. *Toxicol Lett* 225:413–421

41. Wu Q-L, Zhao Y-L, Zhao G, Wang D-Y (2014) microRNAs control of *in vivo* toxicity from graphene oxide in *Caenorhabditis elegans*. *Nanomedicine* 10:1401–1410
42. Deng X, Hofmann ER, Villanueva A, Hobert O, Capodiceci P, Veach DR, Yin X, Campodonico L, Glekas A, Cordon-Cardo C, Clarkson B, Bornmann WG, Fuks Z, Hengartner MO, Kolesnick R (2004) *Caenorhabditis elegans* ABL-1 antagonizes p53-mediated germline apoptosis after ionizing irradiation. *Nat Genet* 36:906–912
43. Fuhrman LE, Goel AK, Smith J, Shianna KV, Aballay A (2009) Nucleolar proteins suppress *Caenorhabditis elegans* innate immunity by inhibiting p53/CEP-1. *PLoS Genet* 5:e1000657
44. Zeman MK, Cimprich KA (2014) Causes and consequences of replication stress. *Nat Cell Biol* 16:2–9
45. Flynn RL, Zou L (2011) ATR: a master conductor of cellular responses to DNA replication stress. *Trends Biochem Sci* 36:133–140
46. Lee SJ, Gartner A, Hyun M, Ahn B, Koo HS (2010) The *Caenorhabditis elegans* Werner syndrome protein functions upstream of ATR and ATM in response to DNA replication inhibition and double-strand DNA breaks. *PLoS Genet* 6:e1000801
47. Stevens H, Williams AB, Michael WM (2016) Cell-type specific responses to DNA replication stress in early *C. elegans* embryos. *PLoS One* 11:e0164601
48. Meier B, Clejan I, Liu Y, Lowden M, Gartner A, Jonathan H, Shawn A (2006) *trt-1* is the *Caenorhabditis elegans* catalytic subunit of telomerase. *PLoS Genet* 2:e18
49. Ijomone OM, Miah MR, Peres TV, Nwoha PU, Aschner M (2016) Null allele mutants of *trt-1*, the catalytic subunit of telomerase in *Caenorhabditis elegans*, are less sensitive to Mn-induced toxicity and DAergic degeneration. *Neurotoxicology* 57:54–60

Chapter 8

Functions of Metabolism-Related Signaling Pathways in the Regulation of Toxicity of Environmental Toxicants or Stresses



Abstract We here selected the fat metabolism as an example to discuss the potential involvement of metabolism-related signaling pathways in the regulation of toxicity of environmental toxicants or stresses. We first introduced and discussed the functions of fat metabolic sensors (SBP-1, NHR-49, MDT-15, and NHR-80) and related signaling pathways in regulating the toxicity of environmental toxicants or stresses. Moreover, we discussed the roles of different components of the fat metabolic pathways during the regulation of toxicity of environmental toxicants or stresses. We also discussed the important function of fatty acid transport protein ACS-22 in regulating the toxicity of environmental toxicants or stresses. The described information in this chapter will help us to establish a connection between certain metabolism(s) and toxicity induction of environmental toxicants and stresses in nematodes.

Keywords Metabolism-related signaling pathway · Fatty acid metabolism · Molecular regulation · Environmental exposure · *Caenorhabditis elegans*

8.1 Introduction

Exposure to certain environmental toxicants or stresses can lead to many aspects of toxicity in nematodes [1]. For example, engineered nanomaterial exposure could cause the toxicity on the functions of both primary (such as the intestine) and secondary (such as the neurons and reproductive organs) targeted organs in nematodes [2–9]. Moreover, it has been found that exposure to environmental toxicants or stresses can affect certain aspects of metabolisms in nematodes. For example, exposure to CdTe quantum dots (QDs) could induce an increase in fat storage in the intestine, and this was partially due to prolonged defecation cycle length in CdTe QD-exposed nematodes (Fig. 8.1) [10]. Moreover, CdTe QDs altered the molecular basis of both synthesis and degradation of fatty acid (Fig. 8.2) [10]. Exposure to CdTe QDs could increase the expression of *fasn-1* and *pod-2* encoding enzymes required for the fatty acid synthesis and decrease the expression of *acs-2* and *ech-1* encoding enzymes required for fatty acid β -oxidation (Fig. 8.2) [10].

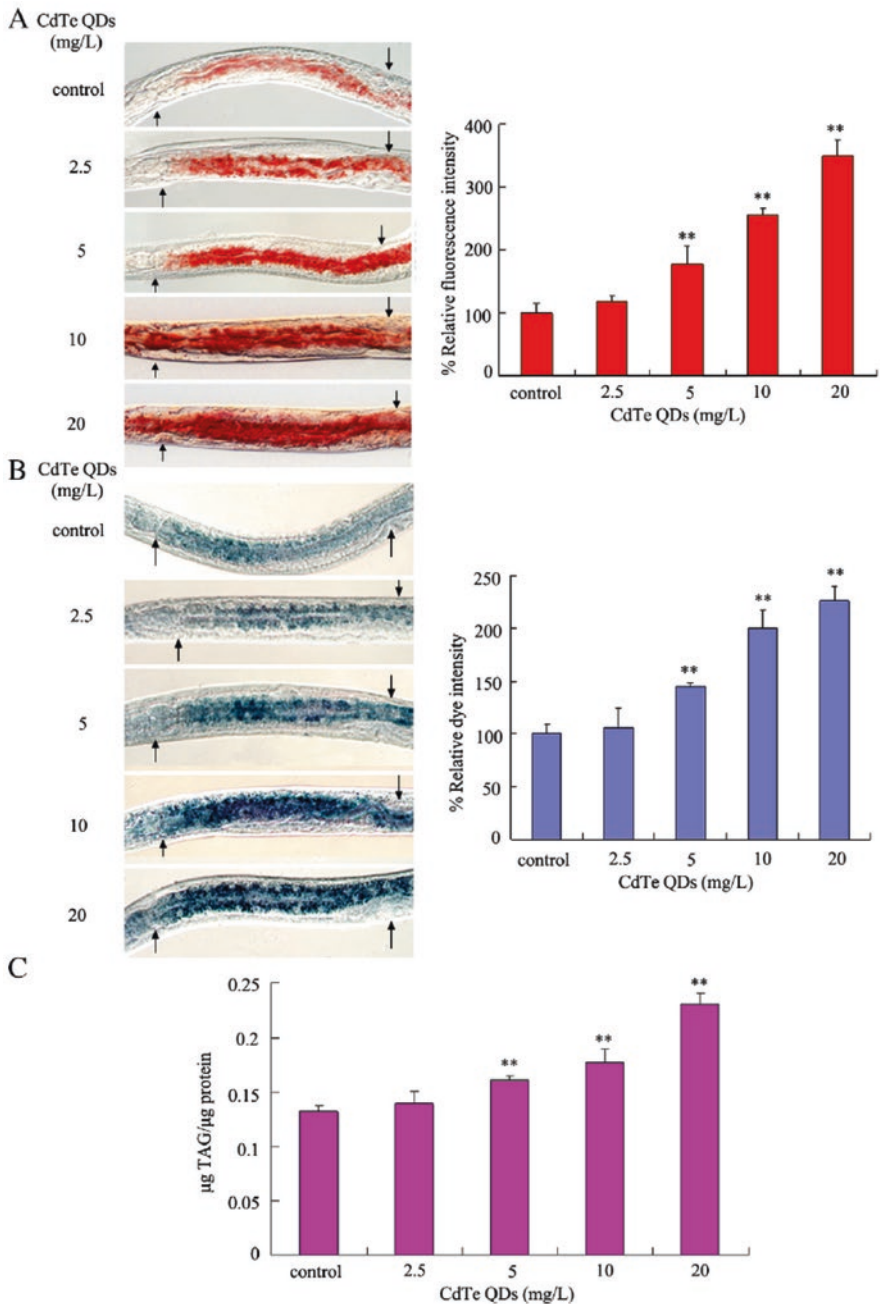


Fig. 8.1 Comparison of fat storage in CdTe QD-exposed nematodes [10]. (a) Comparison of intestinal fat storage in CdTe QD-exposed nematodes based on oil red staining. (b) Comparison of intestinal fat storage in CdTe QD-exposed nematodes based on Sudan Black staining. (c) Comparison of triglyceride amount in CdTe QD-exposed nematodes. Arrowheads indicate the anterior part of the intestine. CdTe QDs' exposure was performed from L1-larvae to young adult in 12-well sterile tissue culture plates at 20 °C in the presence of food (OP50). Bars represent means \pm SEM ** $P < 0.01$ vs control

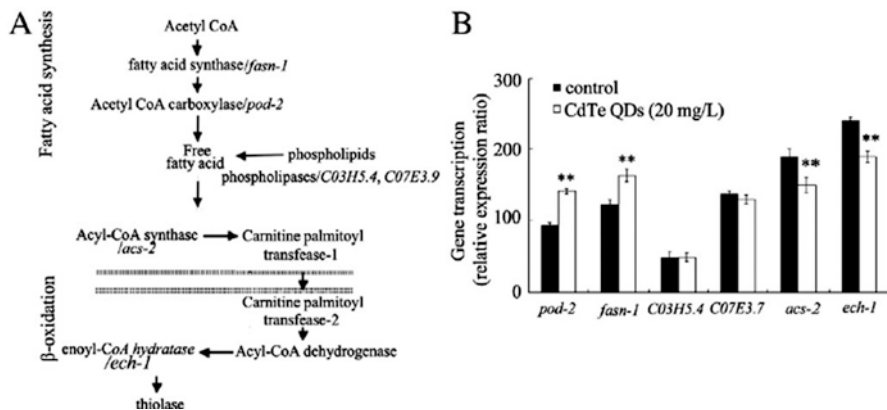


Fig. 8.2 CdTe QDs' exposure altered the molecular basis for both synthesis and degradation of fatty acid in nematodes [10]. (a) Putative *C. elegans* fatty acid metabolism pathways. (b) qRT-PCR assay of genes encoding the enzymes required for the synthesis or degradation of fatty acid in nematodes. Prolonged exposure was performed from L1-larvae to young adult in 12-well sterile tissue culture plates at 20 °C in the presence of food (OP50). Bars represent means \pm SEM ** $P < 0.01$ vs control

In this chapter, we selected the fat metabolism as an example to introduce the involvement of metabolism-related signaling pathways in the regulation of toxicity of environmental toxicants or stresses. The related information on molecular regulation of fat metabolism has been well-described in the review [11]. We here first introduced and discussed the functions of fat metabolic sensors (SBP-1, NHR-49, MDT-15, and NHR-80) in the regulation of toxicity of environmental toxicants or stresses. We also introduced the involvement of signaling pathways, such as the AMPK signaling pathway, in regulating the toxicity of environmental toxicants or stresses. Moreover, we introduced and discussed the roles of different components of the fat metabolic pathways in the regulation of toxicity of environmental toxicants or stresses. Finally, we also discussed the role of fatty acid transport protein ACS-22 in the regulation of toxicity of environmental toxicants or stresses.

8.2 Functions of Fat Metabolic Sensors in the Regulation of Toxicity of Environmental Toxicants or Stresses

In organisms, the fat metabolic sensing mechanisms are thought to have the potential in coordinating the responses to the changing nutritional status [11].

8.2.1 *SBP-1*

In nematodes, *sbp-1* encodes a sterol response element binding protein (SREBP), a transcriptional regulator of fat and sterol synthesis [11].

8.2.1.1 Involvement of SBP-1 in the Regulation of Toxicity of Environmental Toxicants or Stresses

It was observed that the *sbp-1* RNAi or mutation substantially reduced the lifespan under the glucose-fed conditions (Fig. 8.3) [12]. Meanwhile, knockdown of *sbp-1* further dramatically accelerated age-dependent declines in movement and feeding capacities under the glucose-fed conditions (Fig. 8.3) [12]. Therefore, SBP-1 functions in protecting against the toxicity of environmental toxicants or stresses in nematodes.

8.2.1.2 Tissue-Specific Activity of SBP-1 in the Regulation of Toxicity of Environmental Toxicants or Stresses

Intestine-specific *sbp-1* RNAi knockdown could decrease the short lifespan of glucose-fed worms, whereas hypodermis-specific or body wall muscle-specific *sbp-1* RNAi knockdown did not (Fig. 8.3) [12], suggesting that SBP-1 acts in the intestine to regulate the toxicity of environmental toxicants or stresses.

8.2.1.3 Upregulators of SBP-1 in the Regulation of Toxicity of Environmental Toxicants or Stresses

In nematodes, mutations in the *S*-adenosyl methionine synthetase gene (*sams-1*) could increase the activity of SBP-1. Under the glucose-fed conditions, the long-lived lifespan in *sams-1* mutant nematodes could be suppressed by RNAi knockdown of *sbp-1* (Fig. 8.4) [12], suggesting that SAMS-1 acts upstream of SBP-1 to regulate the toxicity of environmental toxicants or stresses.

8.2.2 *NHR-49*

In nematodes, *nhr-49* encodes a nuclear hormone receptor and is the homology to mammalian peroxisome proliferator-activated receptor (PPAR α). NHR-49 functions as a metabolic sensor and master regulator of energy balance [11].

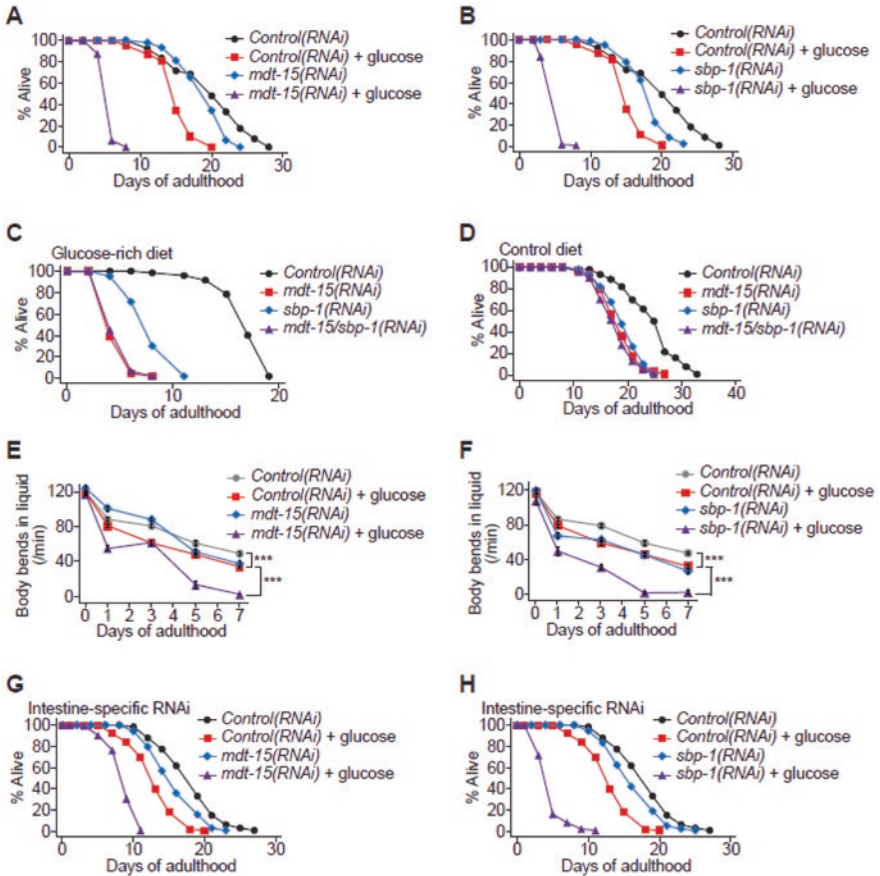


Fig. 8.3 MDT-15 and SBP-1 are required for protecting worms from living too short upon glucose treatment [12]. (a and b) Genetic inhibition of *mdt-15* (a) or *sbp-1* (b) by RNAi further shortened lifespan upon glucose treatment. (c and d) Shown are lifespan curves of worms treated with *mdt-15/sbp-1* double RNAi on a glucose-rich diet (c) and a control diet (d). *sbp-1* RNAi treatment did not further shorten the lifespan of *mdt-15* RNAi-treated worms. Note that *mdt-15*(RNAi) worms may have lived too short upon glucose feeding to display further decreases in lifespan. (e and f) Knockdown of *mdt-15* (e) or *sbp-1* (f) enhanced age-dependent declines in motility (body bends in liquid) on a glucose-rich diet. (***) $P < 0.001$; P -values were calculated by using two-way ANOVA test. Error bars represent SEM. $n = 15$. (g and h) *mdt-15* RNAi (g) or *sbp-1* RNAi (h) specifically in the intestine by using an *nhx-2* promoter-driven *rde-1* in an RNAi-defective *rde-1(ne219)* mutant background further decreased the short lifespan of glucose-fed worms. For the lifespan and motility assays, worms were treated with *mdt-15* RNAi only during adulthood and were treated with *sbp-1* RNAi for their whole lives

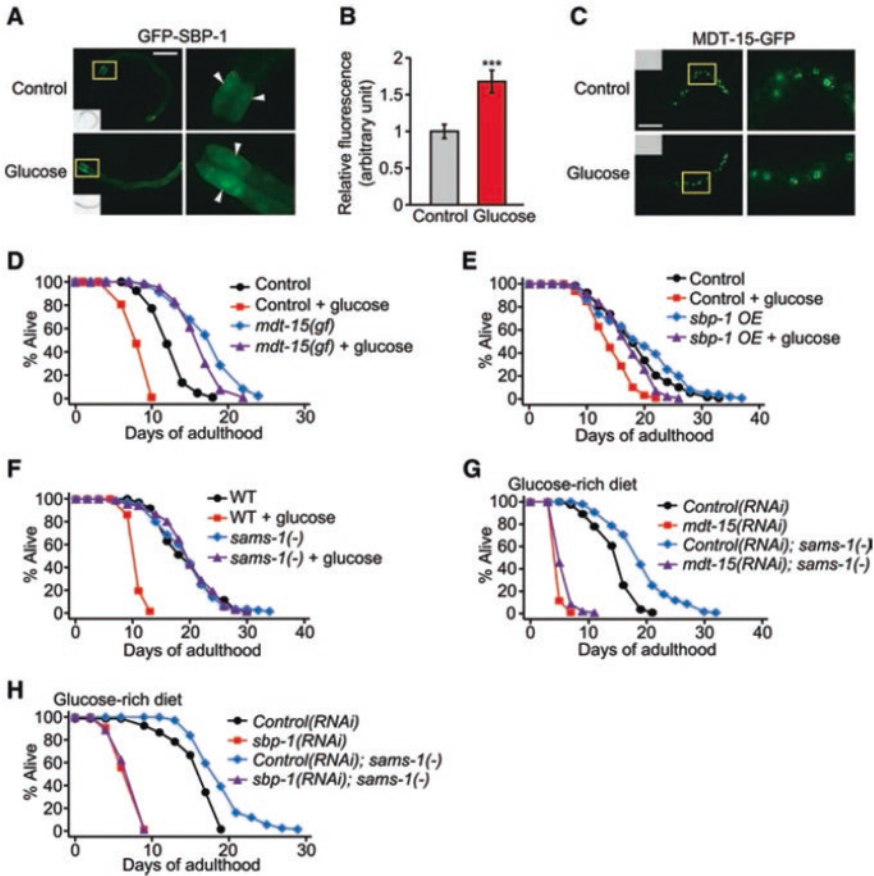


Fig. 8.4 SBP-1 and MDT-15 are sufficient for detoxifying the effects of glucose on lifespan [12]. (a) Glucose-rich diet feeding increased the fluorescence intensity of GFP-SBP-1 proteins in the intestinal cells of IJ1208 *sbp-1p::GFP::sbp-1* animals (L4-larvae). Arrowheads indicate the intestinal nuclei. Bar, 100 μ m. Yellow boxes indicate the enlarged regions in A and C. (b) Quantification of GFP-SBP-1 levels in A. $n \geq 21$ from three independent experiments. (c) Glucose feeding did not affect the expression pattern of MDT-15-GFP proteins in *mdt-15p::mdt-15::GFP* animals (L2-larvae). Bar, 50 μ m. (d) The *mdt-15* (*et14*) gain-of-function (*gf*) mutation suppressed the shortened lifespan of worms fed with a glucose-rich diet. Please note that all animals that were used for the lifespan assay in D contained *paqr-2(tm3410)* mutations because the *mdt-15(et14)* mutation is very closely linked (0.33 cM) to *paqr-2(tm3410)* mutations. (e) *sbp-1* overexpression (*sbp-1* OE; *sbp-1p::GFP::sbp-1*) largely restored normal lifespan in glucose-rich conditions. Injection marker (roller) transgenic worms (CF1290) were used as a control. (f) *sams-1* (*ok3033*) [*sams-1(-)*] mutation suppressed short lifespan caused by glucose-rich diet feeding. *mdt-15(gf)*, *sbp-1* overexpression, and *sams-1(-)* also suppressed the lifespan-shortening effect of 0.2% dietary glucose. (g and h) Knockdown of *mdt-15* (g) or *sbp-1* (h) suppressed the restored lifespan by *sams-1* mutation upon glucose-rich diet feeding

8.2.2.1 Involvement of NHR-49 in the Regulation of Toxicity of Environmental Toxicants or Stresses

In the environment, both bacterial and fungal pathogens have the potential to cause toxic effects on human health and animals, including the nematodes [13–21]. After *Enterococcus faecalis* infection, RNAi knockdown of *nhr-49* could significantly reduce the lifespan compared with control (Fig. 8.5) [22]. Similarly, mutation of *nhr-49* was susceptible to the toxicity of tBOOH (6 mM) in reducing lifespan (Fig. 8.6) [23], and RNAi knockdown of *nhr-49* was susceptible to paraquat (10 mM) in decreasing the viability [24]. In contrast, overexpression of NHR-49 caused the resistance to the toxicity of tBOOH (6 mM) in reducing lifespan (Fig. 8.6) [23]. Therefore, NHR-49 is involved in the regulation of toxicity of environmental toxicants or stresses in nematodes.

8.2.2.2 Upregulators of NHR-49 in the Regulation of Toxicity of Environmental Toxicants or Stresses

As introduced in Chap. 6, the *glp-1* mutant nematodes are resistant to the toxicity of environmental toxicants or stresses in nematodes. After exposure to tBOOH (6 mM), it was observed that the resistance of *glp-1* mutant nematodes to tBOOH toxicity in reducing lifespan was significantly inhibited by *nhr-49* mutation (Fig. 8.6) [23], which suggests that GLP-1 can act as an upstream regulator of NHR-49 in the regulation of toxicity of environmental toxicants or stresses in nematodes.

8.2.2.3 Targets of NHR-49 in the Regulation of Toxicity of Environmental Toxicants or Stresses

After short-term food withdrawal (fasting), the induction of three mitochondrial fatty acid β -oxidation genes, *acs-2*, *acs-11*, and *hacd-1*, was virtually eliminated by *nhr-49* mutation (Fig. 8.7) [25]. Additionally, the stimulation of the glyoxylate pathway gene *gei-7* was also partially abrogated by *nhr-49* mutation (Fig. 8.7) [25]. That is, at least some of the genes controlling the mitochondrial fatty acid β -oxidation process can act as the targeted genes for *nhr-49* in the regulation of toxicity of environmental toxicants or stresses in nematodes. That is, under the stress conditions, the activated NHR-49 may mediate the fatty acid degradation.

8.2.3 MDT-15

In nematodes, *mdt-15* encodes a homolog of mammalian PGC-1 and acts as co-activator for both NHR-49/PPAR α and SBP-1/SREBP [11].

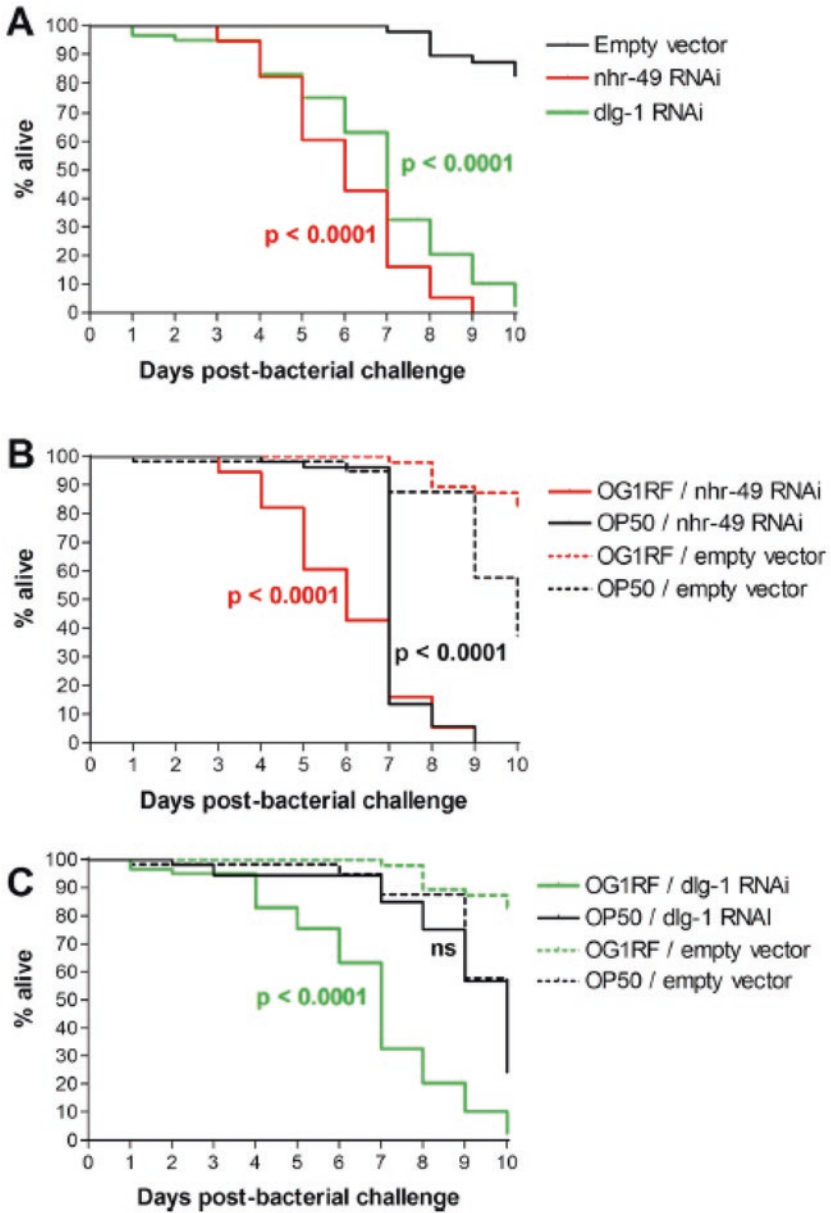


Fig. 8.5 Effect of gene knockdown on *C. elegans* lifespan upon challenge with OG1RF [22]. (a) Kaplan–Meier survival curves showing the effect of *nhr-49* and *dlg-1* knockdown upon challenge with OG1RF. (b and c) Data from (a) shown alongside survival curves for *nhr-49* and *dlg-1* knockdown upon challenge with OP50; OG1RF and OP50 survival assays were performed on separate occasions. Data represent three biological replicates with 20–30 nematodes each; *p*-values indicate comparisons between gene knockdown and empty vector for the same bacteria

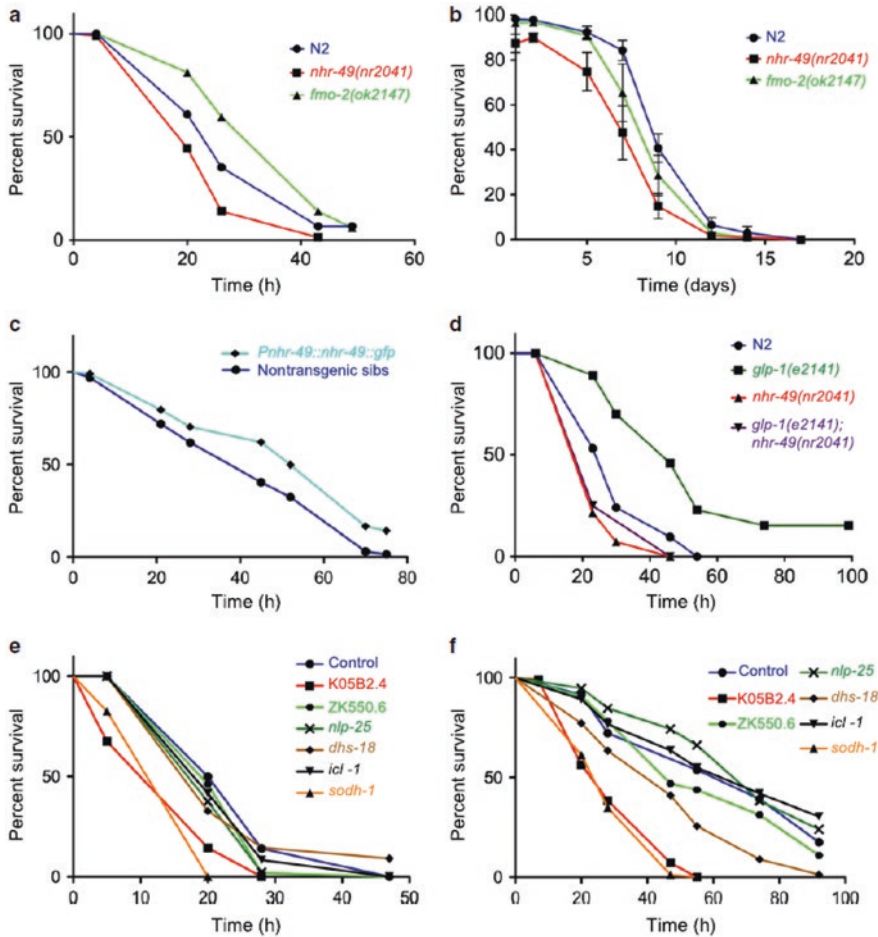


Fig. 8.6 *nhr-49* is required and sufficient for stress resistance [23]. (a) Survival plots of wild-type N2, *nhr-49(nr2041)*, and *fmo-2(ok2147)* worms on 6 mM tBOOH. (b) Survival of wild-type N2, *nhr-49(nr2041)*, and *fmo-2(ok2147)* worms after L1 fasting over time ($p < 0.05$ vs N2 for both genotypes, determined by calculating area under the curve). (c) Survival plots of NHR-49 overexpressing worms (*Pnhr-49::nhr-49::gfp*) and nontransgenic siblings, on 6 mM tBOOH. (d) Survival plots of wild-type N2, *glp-1(e2141)*, *nhr-49(nr2041)*, and *nhr-49(nr2041); glp-1(e2141)* worms on 6 mM tBOOH. (e and f) Survival plots of wild-type (e) and *glp-1(e2141)* (f) worms grown on control RNAi or RNAi clones targeting six different NHR-49-regulated genes while exposed to 6 mM tBOOH

8.2.3.1 Involvement of MDT-15 in the Regulation of Toxicity of Environmental Toxicants or Stresses

It was observed that the *mdt-15* RNAi or mutation substantially reduced the lifespan under the glucose-fed conditions (Fig. 8.3) [12]. Knockdown of *mdt-15* also dramatically accelerated age-dependent declines in movement and feeding capacities under the glucose-fed conditions (Fig. 8.3) [12].

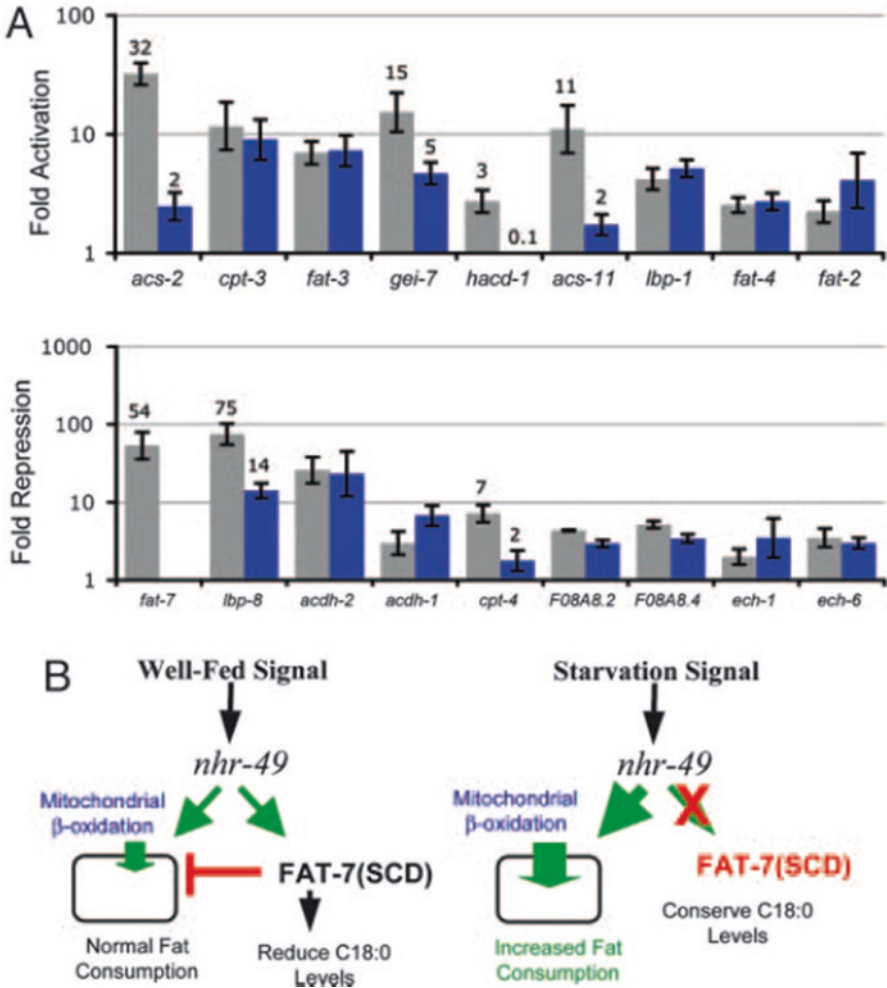


Fig. 8.7 The effect of *nhr-49* deletion on the fasting response [25]. (a) Fasting-dependent activation or repression of each fasting response gene in L4 WT (gray bars) and L4 *nhr-49(nr2041)* (blue bars). Error bars represent standard error of measurement. For *nhr-49*-dependent genes, the fold activation or repression values are displayed in the graph, above the corresponding bars. (b) Model demonstrating the putative role of *nhr-49* in regulating fat expenditure and composition in response to changing food availability

Besides these, MDT-15 was further found to be involved in the regulation of innate immunity of nematodes to pathogens. F08G5.6 is an immune effector containing a CUB-like domain and can be transcriptionally induced by several bacterial pathogens. RNAi knockdown of genes in p38 MAPK signaling pathway (*tir-1*, *pmk-1*, and *atf-7*) could abrogate the induction of pF08G5.6::GFP induced by RPW-24, a small molecule protecting the host during the bacterial infection (Fig. 8.8) [26]. Similarly, RNAi knockdown of *mdt-15* also eliminated the visible expression of pF08G5.6::GFP induced by RPW-24 (Fig. 8.8) [26].

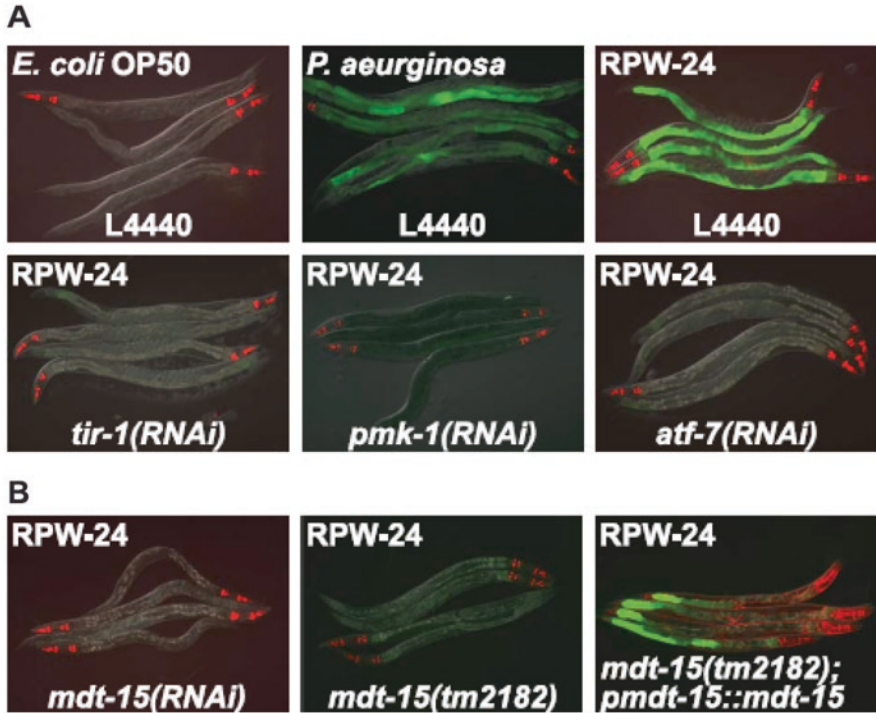


Fig. 8.8 RNAi screen identifies a role for the *C. elegans* mediator subunit MDT-15 in regulating the induction of the p38 MAP kinase PMK-1-dependent immune reporter pF08G5.6::GFP [26]. (a) *C. elegans* carrying the pF08G5.6::GFP immune reporter were exposed to the vector control (L4440) or the indicated RNAi strain and then transferred at the L4 stage to either *E. coli* OP50 food, *P. aeruginosa*, or *E. coli* OP50 supplemented with RPW-24 for 18 h. Photographs were acquired using the same imaging conditions. (b) *C. elegans mdt-15(RNAi)* and *mdt-15(tm2182)* animals carrying the pF08G5.6::GFP immune reporter with or without *agEx114* (*pmdt-15::mdt-15*) were exposed to RPW-24 as described above. In all animals shown in this figure, red pharyngeal expression is the *pmyo-2::mCherry* co-injection marker, which confirms the presence of the pF08G5.6::GFP transgene. In the *mdt-15(tm2182)* animals carrying the *agEx114* array, the presence of the *pmdt-15::mdt-15* transgene is confirmed by the *pmyo-3::mCherry* co-injection marker which is expressed in the body wall muscle

The *mdt-15(tm2182)* mutant nematodes were further shown to be susceptible to the toxicity of inorganic arsenite or organic peroxide tBOOH in reducing lifespan [27]. Moreover, RNAi knockdown of *mdt-15* suppressed the increase in genes (*gst-4*, *gcs-1*, and *ptps-1*) induced by arsenite (Fig. 8.9) [27]. Additionally, after arsenite exposure, the induction of intestinal *gcs-1p::gfp* or *gst-4p::gfp* was severely inhibited by RNAi knockdown of *mdt-15* (Fig. 8.9) [27]. These observations suggest the important role of MDT-15 in the regulation of toxicity of environmental toxicants or stresses in nematodes.

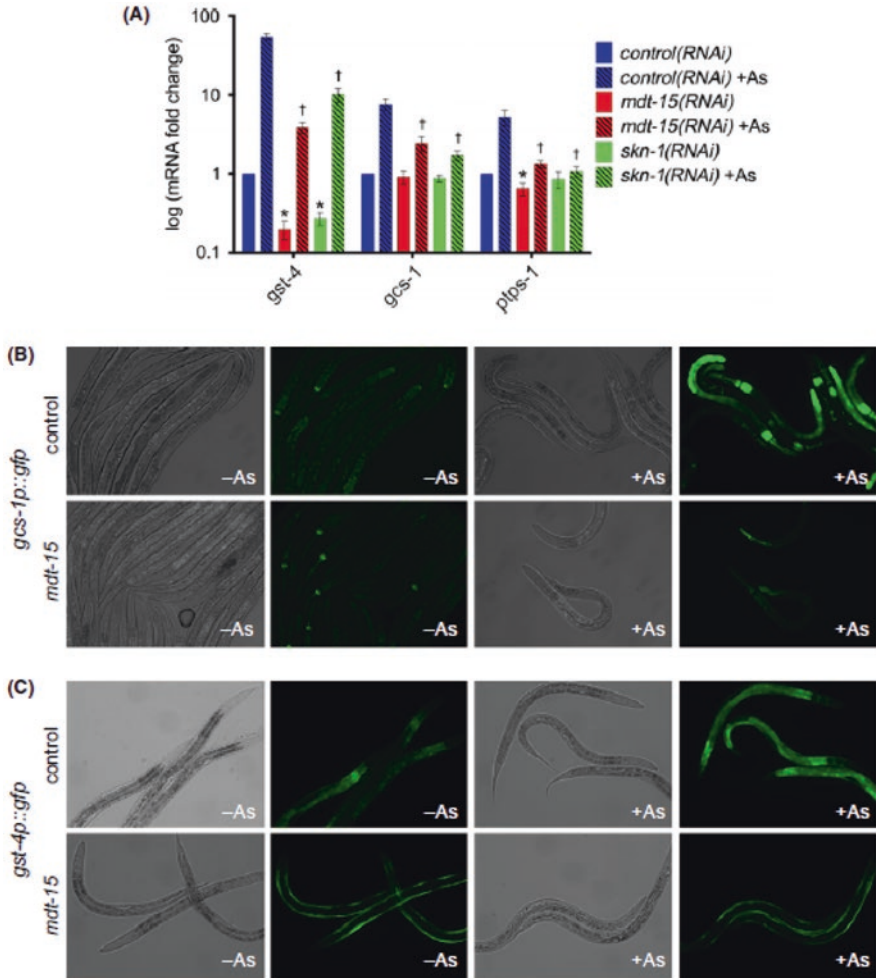


Fig. 8.9 *mdt-15* is required for the transcriptional response to arsenite [27]. (a) Fold changes of mRNA levels (relative to untreated control(RNAi)) in L4 wild-type worms grown on control, *mdt-15*, or *skn-1* RNAi and treated with 5 mM sodium arsenite for 4 h ($n = 5$). mRNA levels were normalized to *act-1*, *ama-1*, *cdc-42*, and *tba-1*; error bars represent SEM. Untreated *mdt-15*(RNAi) or *skn-1*(RNAi) worms differ significantly from control (RNAi) worms. Treated *mdt-15*(RNAi) or *skn-1*(RNAi) worms differ significantly from control (RNAi) worms. (b) DIC and fluorescence micrographs show *gcs-1p::gfp* worms grown on control or *mdt-15* RNAi after 4 h on 5 mM sodium arsenite. One of three repeats is shown. (c) Same as (b), except with *gst-4p::gfp* worms

8.2.3.2 Tissue-Specific Activity of MDT-15 in the Regulation of Toxicity of Environmental Toxicants or Stresses

RNAi knockdown against *mdt-15* in the intestine, hypodermis, or neurons could significantly shorten the lifespan of glucose-treated animals; *mdt-15* RNAi knockdown in body wall muscle did not (Fig. 8.3) [12], suggesting that MDT-15 acts in

the intestine, the hypodermis, or the neurons to regulate the toxicity of environmental toxicants or stresses.

8.2.3.3 Targets of MDT-15 in the Regulation of Toxicity of Environmental Toxicants or Stresses

8.2.3.3.1 SBP-1

Genetic inhibition of *sbp-1* did not decrease the short lifespan of *mdt-15(RNAi)* nematodes on a glucose-rich diet (Fig. 8.3) [12], which supports the idea that SBP-1 and MDT-15 act together as a complex to regulate the toxicity of environmental toxicants or stresses.

8.2.3.3.2 SKN-1c

The yeast two-hybrid assay indicated that the MDT-15 can physically associate with the SKN-1c via its non-KIX-domain [27], suggesting the role of SKN-1c as the direct target for MDT-15 in the regulation of toxicity of environmental toxicants or stresses.

8.2.3.4 Upregulators of MDT-15 in the Regulation of Toxicity of Environmental Toxicants or Stresses

8.2.3.4.1 SAMS-1

Under the glucose-fed conditions, the long-lived lifespan in *sams-1* mutant nematodes could be suppressed by RNAi knockdown of *mdt-15* (Fig. 8.4) [12], suggesting that SAMS-1 acts upstream of MDT-15 to regulate the toxicity of environmental toxicants or stresses.

8.2.3.4.2 p38 MAPK Signaling Pathway

In nematodes, MAP kinase phosphatase VHP-1 is a negative regulator of the p38 MAP kinase PMK-1. After *P. aeruginosa* infection, RNAi knockdown of *vhp-1* caused an increased induction of F08G5.6::GFP, and this induction of F08G5.6::GFP was entirely suppressed in the *mdt-15(tm2182)* mutant nematodes (Fig. 8.10) [26]. qRT-PCR further confirmed this observation, and a requirement for MDT-15 in the *vhp-1(RNAi)*-mediated induction of *F08G5.6* and *F35E12.5* was observed during the *P. aeruginosa* infection (Fig. 8.10) [26]. These data imply that MDT-15 acts downstream of the p38 MAPK signaling pathway to regulate the toxicity of environmental toxicants or stresses.

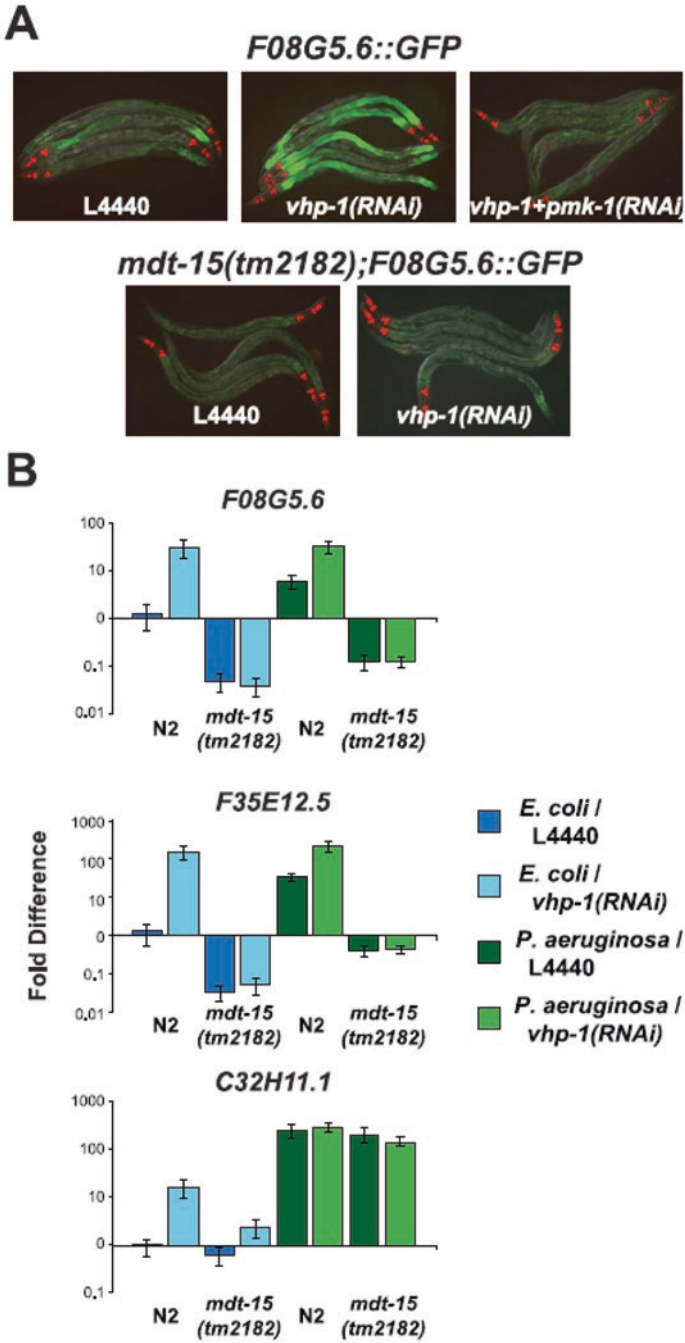


Fig. 8.10 The mediator subunit MDT-15 acts downstream of the p38 MAP kinase PMK-1 to regulate the induction of *F08G5.6* and *F35E12.5* [26]. (a) Wild-type or *mdt-15(tm2182)* mutant

8.2.4 *NHR-80*

In nematodes, *nhr-80* encodes an intestinal nuclear hormone receptor to regulate the expression of delta-9 desaturases FAT-5, FAT-6, and FAT-7 [11]. It was found that some of the key genes, such as the *nhr-80*, was required for the increase in lifespan upon the removal of germline precursor cells, because the germline ablations in *nhr-80* mutant nematodes resulted in a significant decrease in survival when fed *X. nematophila* as compared to germline-ablated wild-type nematodes (Fig. 8.11) [28], suggesting the potential role of NHR-80 in the regulation of toxicity of environmental toxicants or stresses.

8.3 AMPK Signaling Pathway

Insulin and TGF- β signaling pathways play important roles in regulating the fat storage in nematodes [11]. The functions of these two signaling pathways in regulating the toxicity of environmental toxicants or stresses and the underlying mechanisms have been introduced and discussed in Chaps. 5 and 6. AMP-activated kinase (AMPK), a major cellular fuel gauge, is responsive to the cellular AMP:ATP ratio and the upstream kinase cascades [11]. We here further introduced the involvement of AMPK in the regulation of toxicity of environmental toxicants or stresses in nematodes.

aak-2 encodes the homolog of the catalytic subunit of mammalian AMPK [29]. It was observed that the *aak-2* mutant nematodes showed a hypersensitivity to heat or oxidative stress [30]. Mild electrical stimulation (MES) at 0.1 ms pulse can increase the stress resistance in wild-type nematodes. MES could not extend the survival rate of *aak-2(gt33)* or *aak-2(ok524)* mutant nematodes under heat stress or oxidative stress conditions (Fig. 8.12) [31]. Meanwhile, the expressions of anti-heat stress genes (*hsps*) and anti-oxidative stress genes (*sods*) in *aak-2(gt33)* or *aak-2(ok524)* mutant nematodes were also not induced by the MES (Fig. 8.12) [31]. These results suggest that AAK-2 plays an important role in MES-induced stress resistance in nematodes.

←
Fig. 8.10 (continued) synchronized L1 animals containing the pF08G5.6::*GFP* immune reporter were grown on vector control (L4440), *vhp-1(RNAi)*, or a combination of *vhp-1(RNAi)* and *pmk-1(RNAi)* bacteria and then transferred as L4 animals to PA14 for 18 h. Animals were photographed under the same imaging conditions. (b) qRT-PCR was used to examine the expression levels of *F08G5.6*, *F35E12.5*, and *C32H11.1* in wild-type N2 and *mdt-15(tm2182)* mutant animals exposed to *vhp-1(RNAi)* or the vector control (L4440) under basal conditions (as described above) and 8 h after exposure to *P. aeruginosa*. Knockdown of *vhp-1* caused significant induction of *F08G5.6* and *F35E12.5* in wild-type N2 animals, but not in *mdt-15(tm2182)* animals, under baseline (*E. coli*) and pathogen-induced conditions. The expression of *C32H11.1* was significantly induced by *vhp-1(RNAi)* in an *mdt-15*-dependent manner under baseline conditions, but not following exposure to *P. aeruginosa*. Data are the average of two biological replicates each normalized to a control gene with error bars representing SEM and are presented as the value relative to the average expression of the indicated gene in the baseline condition (L4440 animals exposed to *E. coli*)

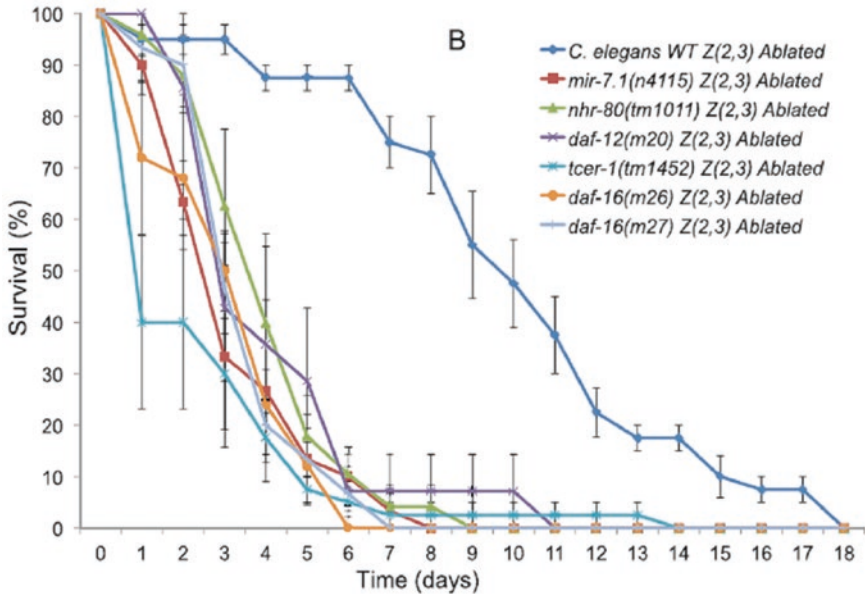


Fig. 8.11 Survival of germline-ablated Z(2,3) *C. elegans* wild type (dark blue) $n = 78$ (8), Z(2,3)-ablated *daf-16(mu26)* (turquoise) $n = 35$ (4), Z(2,3)-ablated *daf-16(mu27)* (orange) $n = 29$ (3), Z(2,3)-ablated *daf-16(mu86)* (light blue) $n = 10$ (1), Z(2,3)-ablated *daf-12(m20)* (pink) $n = 14$ (2), Z(2,3)-ablated *tcer-1(tm1452)* (purple) $n = 15$ (2), Z(2,3)-ablated *mir-7.1(n4115)* (green) $n = 25$ (3), and Z(2,3)-ablated *nhr-80(tm1011)* (red) $n = 30$ (3) when exposed to *X. nematophila* [28]

AAK-2 can be activated by the LKB1 homolog PAR-4 [30]. The *par-4* mutant nematodes also exhibited hypersensitivity to heat or oxidative stress (Fig. 8.13) [31]. MES also could not extend the survival rate of *par-4(it47)* or *par-4(it57)* mutant nematodes under heat stress or oxidative stress conditions (Fig. 8.13) [31]. Additionally, MES could not induce the expression of anti-heat stress genes (*hsps*) and anti-oxidative stress genes (*sods*) in *par-4(it47)* or *par-4(it57)* mutant nematodes (Fig. 8.13) [31]. Therefore, a signaling cascade of PAR-4-AAK-2 was raised to be required for the regulation of toxicity of environmental toxicants or stresses in nematodes.

8.4 ACC and FAS

In nematodes, ACC (POD-2) controls the synthesis of malonyl CoA from the acetyl CoA, and FAS (FASN-1) controls the synthesis of saturated fatty acyl CoAs from the malonyl CoA [11]. Under the glucose-fed conditions, RNAi knockdown of ACC (*pod-2* RNAi) or FAS (*fasn-1* RNAi) caused the reduced lifespan (Fig. 8.14) [12], suggesting the potential involvement of ACC (POD-2) and FAS (FASN-1) in the regulation of toxicity of environmental toxicants or stresses in nematodes.

8.5 FAT-6 and FAT-7

In nematodes, FAT-5, FAT-6, and FAT-7 control the change from the saturated fatty acyl CoAs to the monounsaturated fatty acyl CoAs [11]. It was observed that RNAi knockdown of *fat-6* or *fat-7* could enhance the toxicity of paraquat (10 mM) in decreasing the viability, whereas RNAi knockdown of *fat-5* did not affect the toxicity of paraquat (10 mM) in decreasing the viability (Fig. 8.15) [24]. These observations suggest that at least FAT-6 and FAT-7 are involved in the regulation of toxicity of environmental toxicants or stresses.

It was further observed that the *fat-6(tm331);fat-7(wa36)* double mutant nematodes had the dramatically reduced lifespan under the cold stress condition (Fig. 8.16) [32]. Moreover, it was found that the *fat-6(tm331);fat-7(wa36)* double mutation could suppress the resistance of *age-1(hx546)* mutant nematodes to cold stress in reducing the lifespan (Fig. 8.16) [32]. Therefore, FAT-6 and FAT-7 may act downstream of the insulin signaling pathway to regulate the toxicity of environmental toxicants or stresses in nematodes.

8.6 Role of ELO Proteins in the Regulation of Toxicity of Environmental Toxicants or Stresses

In nematodes, ELO proteins (such as ELO-2, ELO-5, and ELO-6) control the synthesis of polyunsaturated fatty acyl CoAs from the monounsaturated fatty acyl CoAs [11]. It was observed that RNAi knockdown of *elo-2* could enhance the toxicity of paraquat (10 mM) in decreasing the viability (Fig. 8.15) [24], suggesting the possible role of ELO proteins in regulating the toxicity of environmental toxicants or stresses.

8.7 Role of Fatty Acid Transport Protein ACS-22 in the Regulation of Toxicity of Environmental Toxicants or Stresses

8.7.1 ACS-22 Regulate the Intestinal Barrier in Nematodes

Using the blue food dye of erioglaucline disodium (5.0% wt/vol in water), it was observed that mutation of *acs-22* caused the obvious dye leakage from the intestinal lumen into the intestinal cells and even the body cavity under the normal conditions (Fig. 8.17) [33]. In control or nanopolystyrene particle (1 µg/L)-exposed wild-type nematodes, the dye was mainly accumulated within the intestinal lumen (Fig. 8.17) [33]. Moreover, the more severe dye leakage from the intestinal lumen into the intestinal cells and the body cavity was observed in *acs-22* mutant nematodes exposed to nanopolystyrene particles (1 µg/L) compared with that in *acs-22* mutant nematodes under the normal conditions (Fig. 8.17) [33].

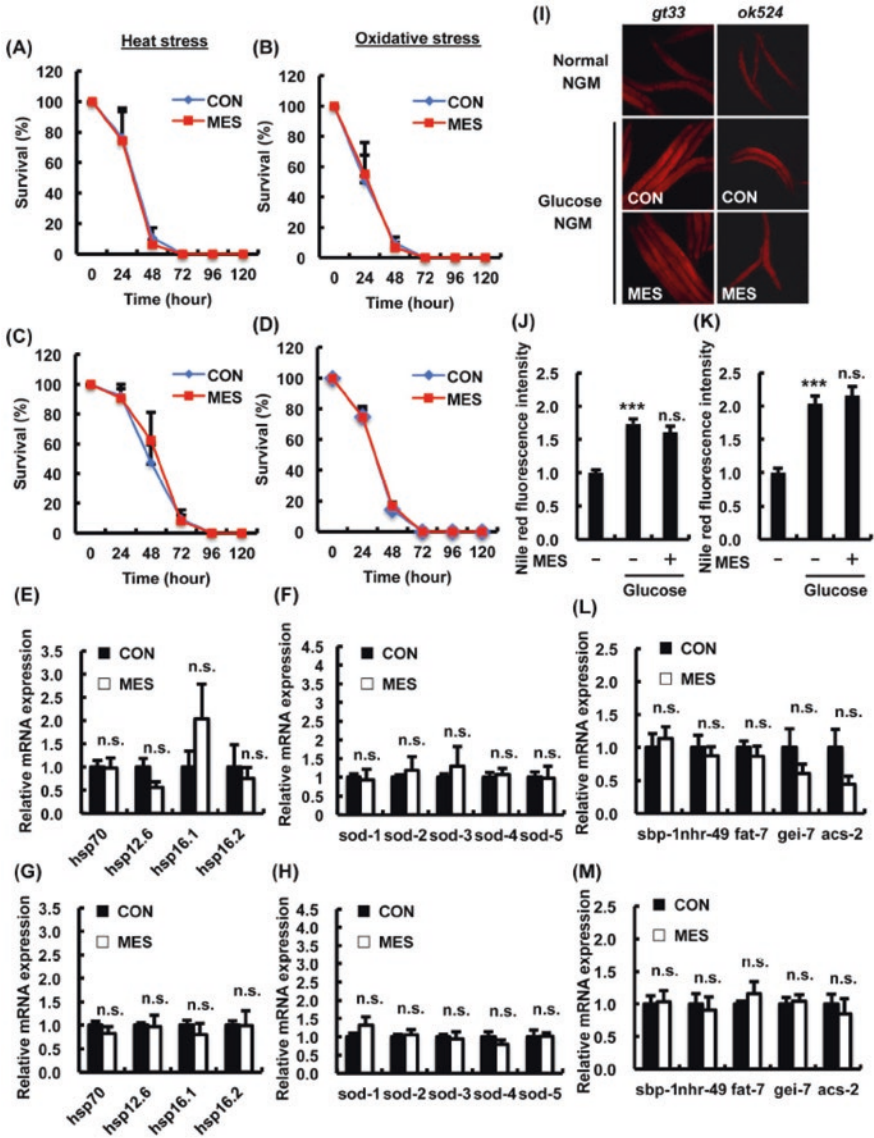


Fig. 8.12 MES-induced phenotypes are not observed in AMPK homolog *aak-2* mutant worms [31]. (a–d) *aak-2* mutant worms (a and b: *gt33*; c and d: *ok524*) were treated once a day with MES (0.1 ms, 2 V/cm, 55 pps) for 20 min at larval stage. After the last treatment, worms were incubated under (a and c) heat stress (30 °C) or (b and d) oxidative stress (4 mM paraquat) condition. Worms’ survival was checked every 24 h. Each time point is the average of three independent experiments using 80–100 animals per group. (e–h) *aak-2* mutant worms (e and f: *gt33*; g and h: *ok524*) were bred on NGM plates and treated once a day with MES for 20 min at larval stage. After the last treatment, total RNA was extracted and subjected to quantitative real-time PCR. The mRNA levels were normalized to the level of β -actin (internal control). Data are presented as mean \pm SE. n.s. versus control, assessed by unpaired Student’s t-test. (i) *aak-2(gt33, ok524)* worms were bred on

8.7.2 *Mutation of *acs-22* Causes a Susceptibility to the Toxicity of Environmental Toxicants of Stresses*

In nematodes, the toxicity in inducing intestinal ROS production and in decreasing locomotion behavior could be observed in *acs-22* mutant nematodes exposed to nanopolystyrene particles at concentrations $\geq 1 \mu\text{g/L}$ (Fig. 8.18) [33]. Additionally, the more severe toxicity of nanopolystyrene particles ($10 \mu\text{g/L}$) in inducing intestinal ROS production and in decreasing locomotion behavior was observed in *acs-22* mutant nematodes compared with that in wild-type nematodes (Fig. 8.18) [33]. Similarly, the susceptibility to the toxicity of multiwalled carbon nanotubes (MWCNTs) in decreasing locomotion behavior, in reducing brood size, and in inducing intestinal ROS production was also found in *acs-22(tm3236)* mutant nematodes [34].

Moreover, it was observed that mutation of the *acs-22* strengthened the distribution of MWCNTs in both the primary targeted organs, such as the pharynx and intestine, and the secondary targeted organs, such as spermatheca (Fig. 8.19) [34]. In contrast, overexpression of *acs-22* could reduce the distribution of MWCNTs in the body of exposed nematodes (Fig. 8.19) [34].

8.7.3 *Mutation of *acs-22* Disrupts the Beneficial Function of LAB in Preventing the Toxicity of Environmental Toxicants or Stresses*

In nematodes, the lactic acid bacteria (LAB) can prevent the graphene oxide (GO) toxicity on the functions of both primary and secondary targeted organs in wild-type nematodes [35]. Nevertheless, after the LAB administration, the significant induction of intestinal ROS production and decrease in locomotion behavior could still be detected in GO exposed *acs-22* mutant nematodes [35]. These observations suggest that the beneficial effect of LAB administration in maintaining the normal intestinal permeability is dependent on the normal function of ACS-22.

←

Fig. 8.12 (continued) NGM plates and treated once a day with MES for 20 min at larval stage. After the last treatment, worms were stained with Nile red and observed using a fluorescent microscope. (j and k) Relative fluorescence intensity of Nile red for (j) *gt33* and (k) *ok524* was quantified. Data are representative of two independent experiments using 40–50 animals per group. Data are presented as mean \pm SE. *** $P < 0.001$ versus control without D-glucose, n.s. versus control with D-glucose, assessed by one-way ANOVA. (l and m) *aaak-2* mutant worms (l: *gt33*; m: *ok524*) were bred on NGM plates containing D-glucose (10 mM) and treated once a day with MES for 20 min at larval stage. After the last treatment, total RNA was extracted and subjected to quantitative real-time PCR. The mRNA levels were normalized to the level of β -actin (internal control). Data are presented as mean \pm SE. n.s. versus control, assessed by unpaired *t*-test. n.s. not significant. For mRNA analysis (e–h and l–m), data shown are representative of two independent experiments using approximately 200 animals per group

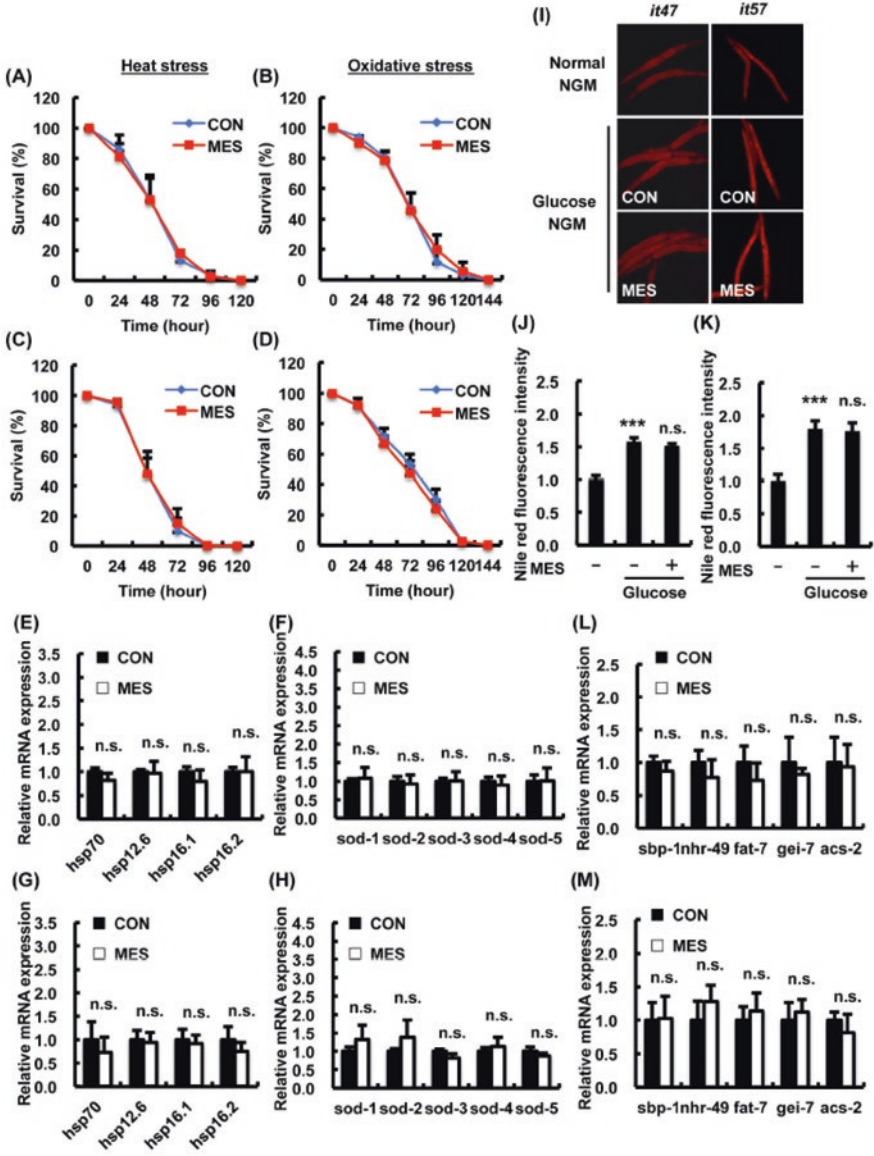


Fig. 8.13 MES-induced phenotypes are not observed in AMPK-kinase LKB1 homolog *par-4* mutant worms [31]. (a–d) *par-4* mutant worms (a and b: *it47*; c and d: *it57*) were treated once a day with MES (0.1 ms, 2 V/cm, 55 pps) for 20 min at larval stage. After the last treatment, worms were incubated under (a and c) heat stress (30 °C) or (b and d) oxidative stress (4 mM paraquat) condition. Worm survival was checked every 24 h. Each time point is the average of three independent experiments using 80–100 animals per group. (e–h) *par-4* mutant worms (E, F: *it47*; G, H: *it57*) were bred on NGM plates and treated once a day with MES for 20 min at larval stage. After the last treatment, total RNA was extracted and subjected to quantitative real-time PCR. The mRNA levels were normalized to the level of β -actin (internal control). Data are presented

8.8 Perspectives

In this chapter, we only selected the fat metabolism as an example to discuss the potential involvement of metabolism-related signaling pathways in the regulation of toxicity of environmental toxicants or stresses. With the increasing attention on the study of molecular basis for different metabolisms in nematodes, the possible association of toxicity induction of environmental toxicants or stresses with different metabolisms will be gradually elucidated. During the elucidation of the association of toxicity induction of environmental toxicants or stresses with different metabolisms, the potential connections between metabolism-related signaling pathways and the known oxidative stress or stress response-related signaling pathways in different tissues, especially in the intestine, are suggested to be carefully determined.

To elucidate the association of toxicity induction of environmental toxicants or stresses with different metabolisms, the related genetic and molecular basis should be clarified. Besides these, it may be more important to determine the related chemical basis for the formation of certain association of toxicity induction of environmental toxicants or stresses with different metabolisms. That is, at least for environmental toxicants, what are their possible roles in the development and even in the metabolisms under certain genetic mutation backgrounds?

Fig. 8.13 (continued) as mean \pm SE. n.s. versus control, assessed by unpaired *t*-test. (I) *par-4(it47, it57)* worms were bred on NGM plates containing D-glucose (10 mM) and treated once a day with MES for 20 min at larval stage. After the last treatment, worms were stained with Nile red and observed using a fluorescent microscope. (j and k) Relative fluorescence intensity of Nile red for (j) *it47* and (k) *it57* was quantified. Data are representative of two independent experiments using 40–50 animals per group. Data are presented as mean \pm SE. ****P* < 0.001 versus control without D-glucose, n.s. versus control with D-glucose, assessed by one-way ANOVA. (l and m) *par-4* mutant worms (l: *it47*; m: *it57*) were bred on NGM plates containing D-glucose (10 mM) and treated once a day with MES for 20 min at larval stage. After the last treatment, total RNA was extracted and subjected to quantitative real-time PCR. The mRNA levels were normalized to the level of β -actin (internal control). Data are presented as mean \pm SE. n.s. versus control, assessed by unpaired *t*-test. n.s. not significant. For mRNA analysis (e–h and l–m), data shown are representative of two independent experiments using approximately 200 animals per group

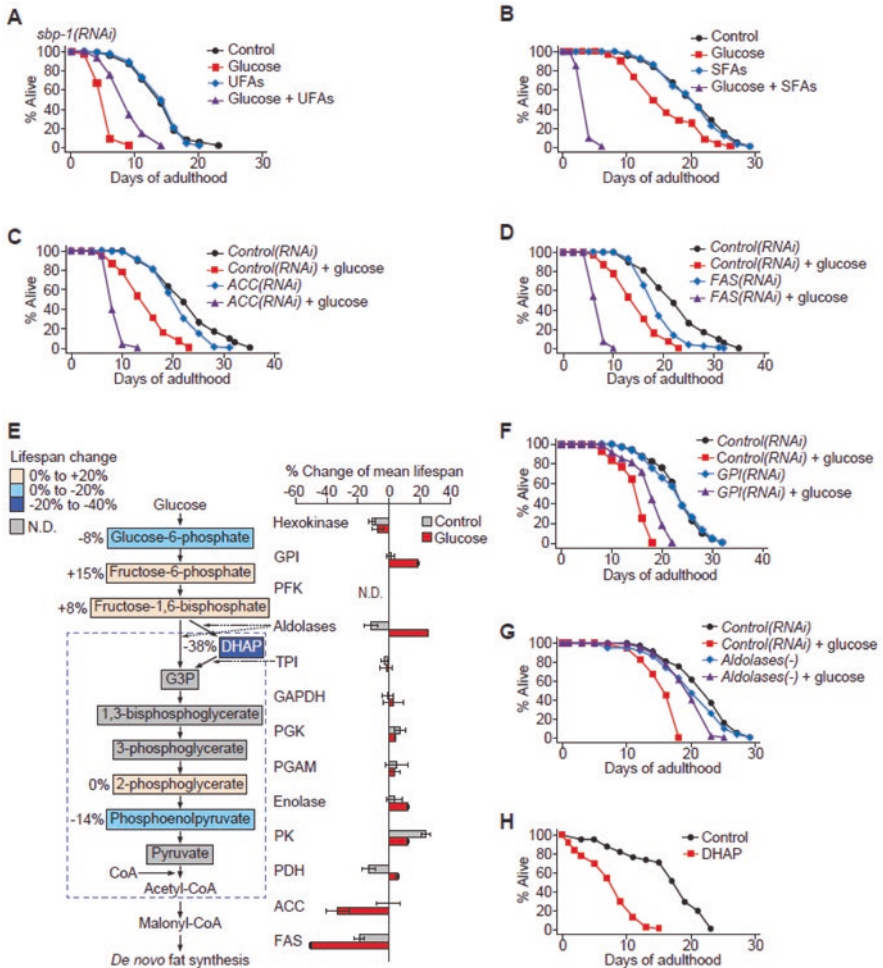


Fig. 8.14 Accumulation of intermediate metabolites from glucose to FA synthesis causes short lifespan [12]. (a) UFA mixture (600 μ M C18:1n-9, C18:1n-7, and C18:2n-6) feeding partly suppressed the short lifespan of the worms treated with *sbp-1* RNAi on a glucose-enriched diet. (b) SFA mixture (600 μ M C14:0 and C16:0) greatly shortened the lifespan of wild-type animals on a glucose-rich diet. NP-40 (0.1%) was added to all experimental conditions in A and B. (c and d) Knockdown of ACC (*pod-2* RNAi) (c) or FAS (*fasn-1* RNAi) (d) caused very short lifespan upon glucose-rich diet feeding. Worms were treated with *pod-2* RNAi or *fasn-1* RNAi only during adulthood. (e) Simplified glycolysis and FA synthesis pathways and percent changes of mean lifespan upon genetically inhibiting enzymes in the pathways. DHAP dihydroxyacetonephosphate, G3P glyceraldehyde-3-phosphate, GPI glucose-6-phosphate isomerase, PFK phosphofruktokinase TPI triosephosphate isomerase, GAPDH glyceraldehyde-3-phosphate dehydrogenase, PGK phosphoglycerate kinase, PGAM phosphoglycerate mutase, PK pyruvate kinase, PDH pyruvate dehydrogenase. Error bars represent SEM of mean lifespans from two independent experiments. Colored boxes for metabolites indicate percent changes in mean lifespan upon treatment with the respective metabolites. (N.D.) Not determined. (f) Knockdown of GPI (*gpi-1* RNAi) partly suppressed the short lifespan of glucose-treated animals. (g) Aldolases(-) [*aldo-1(tm5782)* mutation with *aldo-2* RNAi treatment] largely suppressed the glucose toxicity on lifespan. Lifespan curves in (c, d, f, and g) are representative data of those shown in (e). (h) DHAP treatment greatly reduced lifespan

Fig. 8.15 Fatty acid metabolism affected the stress (paraquat)-resistance mechanisms [24]. Worms were cultured on RNAi media for 72 h and treated with 0.5 mg/ml FUDR for 24 h. Worms were transferred to RNAi plates containing 10 mM paraquat (PQ), and the survival rate was calculated after 6 days ($N = 6$). The error bar indicates the standard error (SEM)

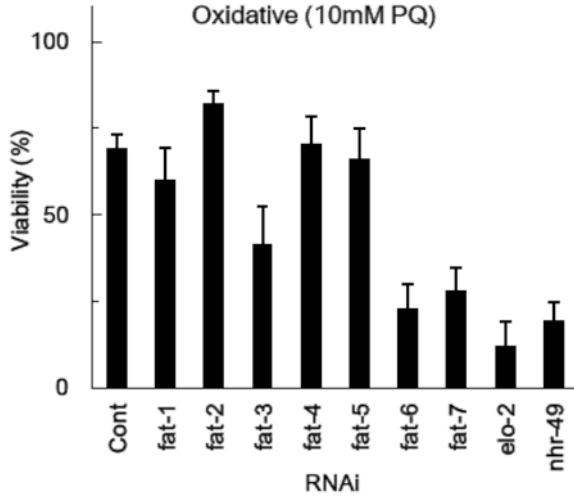


Fig. 8.16 Survival curves wild type (N2), *age-1(hx546)* mutants, *fat-6(tm331); fat-7(wa36)* double mutants, and *age-1(hx546); fat-6(tm331); fat-7(wa36)* triple mutants ($n = 90-100$ per genotype) under the cold stress condition [32]

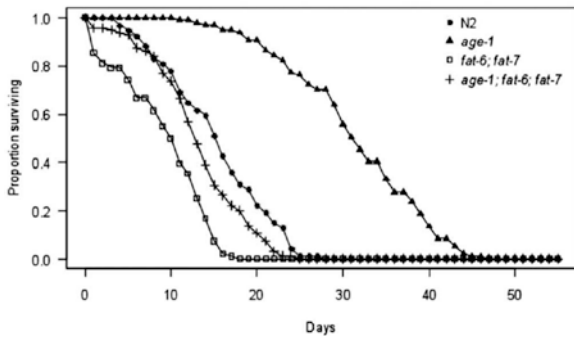
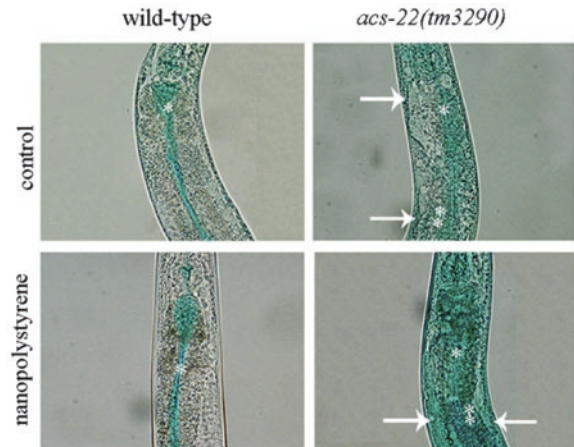


Fig. 8.17 Effect of *acs-22* mutation on intestinal permeability [33]. Arrowheads indicate the dye leakage from the intestinal lumen into the body cavity. The intestinal lumen (*) and the intestinal cells (***) were indicated by asterisks. Prolonged exposure to nanopolystyrene particles was performed from L1-larvae to adult day 1. Exposure concentration of nanopolystyrene particles was 1 $\mu\text{g/L}$.



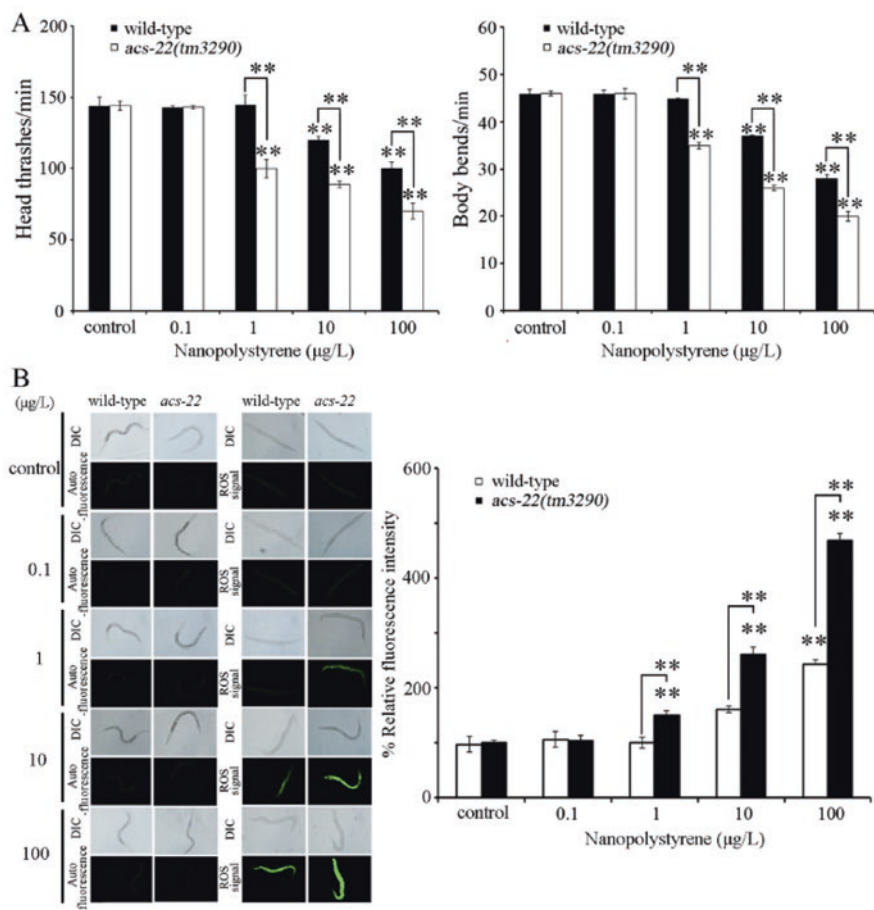


Fig. 8.18 Effect of *acs-22* mutation on toxicity of nanoplastyrene particles in nematodes after prolonged exposure [33]. **(a)** Effect of *acs-22* mutation on toxicity of nanoplastyrene particles in decreasing locomotion behavior. **(b)** Effect of *acs-22* mutation on toxicity of nanoplastyrene particles in inducing intestinal ROS production. Two-way ANOVA was performed for the comparison between wild-type and *acs-22* mutant. Prolonged exposure to nanoplastyrene particles was performed from L1-larvae to adult day 1. Bars represent means \pm SD. $**P < 0.01$ vs control (if not specially indicated)

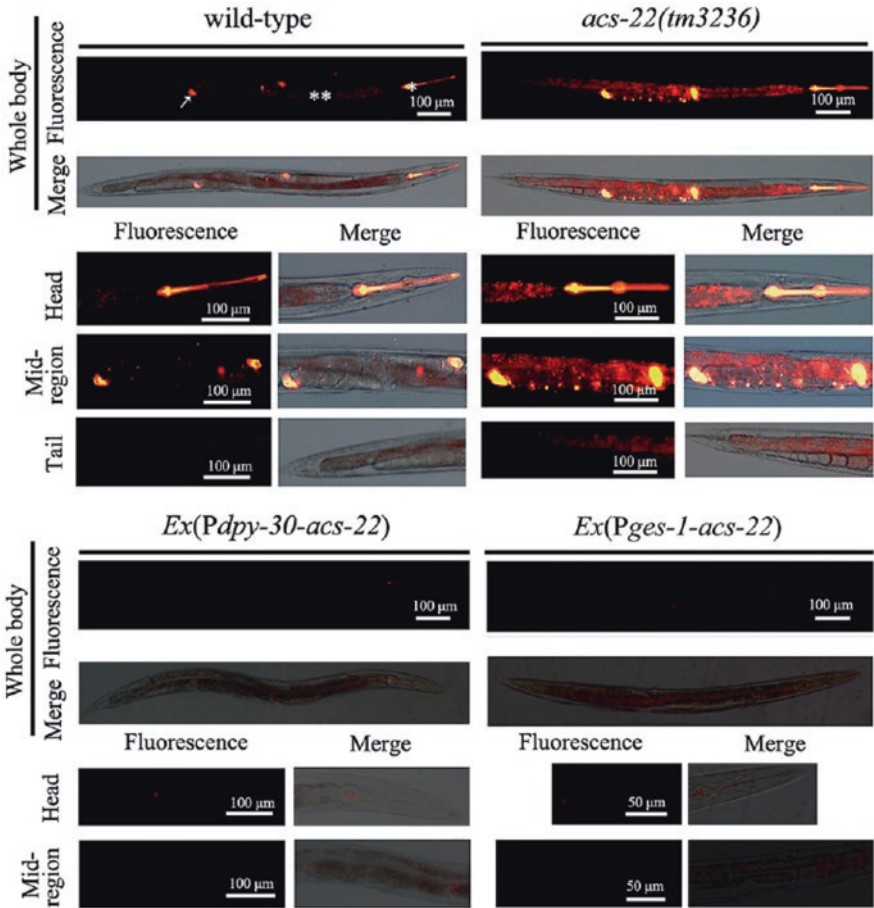


Fig. 8.19 Distribution of MWCNTs/Rho B in wild type, *acs-22* mutant, and nematodes overexpressing the *acs-22* gene [34]. The merged images were obtained by splitting multichannel images in an Image J system. The merged images can tell us the possible localization position of fluorescence signals in nematodes. MWCNTs/Rho B exposure was performed during development from L1-larvae to young adults in 12-well sterile tissue culture plates in the presence of food (OP50). Exposure concentration of MWCNTs/Rho B was 1 mg/L. Arrowhead indicates the spermatheca. The pharynx (*) and intestine (**) are also indicated

References

1. Wang D-Y (2018) Nanotoxicology in *Caenorhabditis elegans*. Springer, Singapore
2. Ren M-X, Zhao L, Ding X-C, Krasteva N, Rui Q, Wang D-Y (2018) Developmental basis for intestinal barrier against the toxicity of graphene oxide. *Part Fibre Toxicol* 15:26
3. Xiao G-S, Chen H, Krasteva N, Liu Q-Z, Wang D-Y (2018) Identification of interneurons required for the aversive response of *Caenorhabditis elegans* to graphene oxide. *J Nanbiotechnol* 16:45
4. Ding X-C, Rui Q, Wang D-Y (2018) Functional disruption in epidermal barrier enhances toxicity and accumulation of graphene oxide. *Ecotoxicol Environ Saf* 163:456–464
5. Zhao L, Kong J-T, Krasteva N, Wang D-Y (2018) Deficit in epidermal barrier induces toxicity and translocation of PEG modified graphene oxide in nematodes. *Toxicol Res* 7(6):1061–1070. <https://doi.org/10.1039/C8TX00136G>
6. Dong S-S, Qu M, Rui Q, Wang D-Y (2018) Combinational effect of titanium dioxide nanoparticles and nanopolystyrene particles at environmentally relevant concentrations on nematodes *Caenorhabditis elegans*. *Ecotoxicol Environ Saf* 161:444–450
7. Xiao G-S, Zhi L-T, Ding X-C, Rui Q, Wang D-Y (2017) Value of *mir-247* in warning graphene oxide toxicity in nematode *Caenorhabditis elegans*. *RSC Adv* 7:52694–52701
8. Zhao L, Wan H-X, Liu Q-Z, Wang D-Y (2017) Multi-walled carbon nanotubes-induced alterations in microRNA *let-7* and its targets activate a protection mechanism by conferring a developmental timing control. *Part Fibre Toxicol* 14:27
9. Zhao L, Qu M, Wong G, Wang D-Y (2017) Transgenerational toxicity of nanopolystyrene particles in the range of $\mu\text{g/L}$ in nematode *Caenorhabditis elegans*. *Environ Sci Nano* 4:2356–2366
10. Wu Q-L, Zhi L-T, Qu Y-Y, Wang D-Y (2016) Quantum dots increased fat storage in intestine of *Caenorhabditis elegans* by influencing molecular basis for fatty acid metabolism. *Nanomedicine* 12:1175–1184
11. Ashrafi K (2007) Obesity and the regulation of fat metabolism. *WormBook*. <https://doi.org/10.1895/wormbook.1.130.1>
12. Lee D, Jeong D, Son HG, Yamaoka Y, Kim H, Seo K, Khan AA, Roh T, Moon DW, Lee Y, Lee SV (2015) SREBP and MDT-15 protect *C. elegans* from glucose-induced accelerated aging by preventing accumulation of saturated fat. *Genes Dev* 29:2490–2503
13. Yu Y-L, Zhi L-T, Wu Q-L, Jing L-N, Wang D-Y (2018) NPR-9 regulates innate immune response in *Caenorhabditis elegans* by antagonizing activity of AIB interneurons. *Cell Mol Immunol* 15:27–37
14. Zhi L-T, Yu Y-L, Li X-Y, Wang D-Y, Wang D-Y (2017) Molecular control of innate immune response to *Pseudomonas aeruginosa* infection by intestinal *let-7* in *Caenorhabditis elegans*. *PLoS Pathog* 13:e1006152
15. Zhi L-T, Yu Y-L, Jiang Z-X, Wang D-Y (2017) *mir-355* functions as an important link between p38 MAPK signaling and insulin signaling in the regulation of innate immunity. *Sci Rep* 7:14560
16. Sun L-M, Liao K, Hong C-C, Wang D-Y (2017) Honokiol induces reactive oxygen species-mediated apoptosis in *Candida albicans* through mitochondrial dysfunction. *PLoS One* 12:e0172228
17. Sun L-M, Liao K, Wang D-Y (2017) Honokiol induces superoxide production by targeting mitochondrial respiratory chain complex I in *Candida albicans*. *PLoS One* 12:e0184003
18. Yu Y-L, Zhi L-T, Guan X-M, Wang D-Y, Wang D-Y (2016) FLP-4 neuropeptide and its receptor in a neuronal circuit regulate preference choice through functions of ASH-2 trithorax complex in *Caenorhabditis elegans*. *Sci Rep* 6:21485
19. Sun L-M, Zhi L-T, Shakoos S, Liao K, Wang D-Y (2016) microRNAs involved in the control of innate immunity in *Candida* infected *Caenorhabditis elegans*. *Sci Rep* 6:36036

20. Sun L-M, Liao K, Li Y-P, Zhao L, Liang S, Guo D, Hu J, Wang D-Y (2016) Synergy between PVP-coated silver nanoparticles and azole antifungal against drug-resistant *Candida albicans*. *J Nanosci Nanotechnol* 16:2325–2335
21. Wu Q-L, Cao X-O, Yan D, Wang D-Y, Aballay A (2015) Genetic screen reveals link between maternal-effect sterile gene *mes-1* and *P. aeruginosa*-induced neurodegeneration in *C. elegans*. *J Biol Chem* 290:29231–29239
22. Sim S, Hibberd ML (2016) *Caenorhabditis elegans* susceptibility to gut *Enterococcus faecalis* infection is associated with fat metabolism and epithelial junction integrity. *BMC Microbiol* 16:6
23. Goh GYS, Winter JJ, Bhanshali F, Doering KRS, Lai R, Lee K, Veal EA, Taubert S (2018) NHR-49/HNF4 integrates regulation of fatty acid metabolism with a protective transcriptional response to oxidative stress and fasting. *Aging Cell* 17:e12743
24. Horikawa M, Sakamoto K (2009) Fatty acid metabolism is involved in stress resistance mechanisms of *Caenorhabditis elegans*. *Biochem Biophys Res Commun* 390:1402–1407
25. Gilst MR, Hadjivassiliou H, Yamamoto KR (2005) A *Caenorhabditis elegans* nutrient response system partially dependent on nuclear receptor NHR-49. *Proc Natl Acad Sci U S A* 102:13496–13501
26. Pukkila-Worley R, Feinbaum RL, McEwan DL, Conery AL, Ausubel FM (2014) The evolutionarily conserved mediator subunit MDT-15/MED15 links protective innate immune responses and xenobiotic detoxification. *PLoS Pathog* 10:e1004143
27. Goh GYS, Martelli KL, Parhar KS, Kwong AWL, Wong MA, Mah A, Hou NS, Taubert S (2014) The conserved mediator subunit MDT-15 is required for oxidative stress responses in *Caenorhabditis elegans*. *Aging Cell* 13:70–79
28. Sinha A, Rae R (2014) A functional genomic screen for evolutionarily conserved genes required for lifespan and immunity in germline-deficient *C. elegans*. *PLoS One* 9:e101970
29. Apfeld J, O'Connor G, McDonagh T, DiStefano PS, Curtis R (2004) The AMP-activated protein kinase AAK-2 links energy levels and insulin-like signals to lifespan in *C. elegans*. *Genes Dev* 18:3004–3009
30. Lee H, Cho JS, Lambacher N, Lee J, Lee SJ, Lee TH, Gartner A, Koo HS (2008) The *Caenorhabditis elegans* AMP-activated protein kinase AAK-2 is phosphorylated by LKB1 and is required for resistance to oxidative stress and for normal motility and foraging behavior. *J Biol Chem* 283:14988–14993
31. Matsuyama S, Moriuchi M, Suico MA, Yano S, Morino-Koga S, Shuto T, Yamanaka K, Kondo T, Araki E, Kai H (2014) Mild electrical stimulation increases stress resistance and suppresses fat accumulation via activation of LKB1-AMPK signaling pathway in *C. elegans*. *PLoS One* 9:e114690
32. Savory FR, Sait SM, Hope IA (2011) DAF-16 and $\Delta 9$ desaturase genes promote cold tolerance in long-lived *Caenorhabditis elegans* *age-1* mutants. *PLoS One* 6:e24550
33. Qu M, Xu K-N, Li Y-H, Wong G, Wang D-Y (2018) Using *acs-22* mutant *Caenorhabditis elegans* to detect the toxicity of nanopolystyrene particles. *Sci Total Environ* 643:119–126
34. Zhi L-T, Fu W, Wang X, Wang D-Y (2016) ACS-22, a protein homologous to mammalian fatty acid transport protein 4, is essential for the control of toxicity and translocation of multi-walled carbon nanotubes in *Caenorhabditis elegans*. *RSC Adv* 6:4151–4159
35. Zhao Y-L, Yu X-M, Jia R-H, Yang R-L, Rui Q, Wang D-Y (2015) Lactic acid bacteria protects *Caenorhabditis elegans* from toxicity of graphene oxide by maintaining normal intestinal permeability under different genetic backgrounds. *Sci Rep* 5:17233

Chapter 9

Functions of Protective Response-Related Signaling Pathways in the Regulation of Toxicity of Environmental Toxicants or Stresses



Abstract In nematodes, there are many forms of protective response potentially activated by environmental toxicants or stresses. We here focused on the introduction and discussion of important protection functions of neurotransmitters, antimicrobial proteins, mitochondrial UPR, endoplasmic reticulum UPR, and autophagy for nematodes in response to environmental toxicants or stresses. The underlying molecular mechanisms for the formation of these protective responses in nematodes exposed to environmental toxicants or stresses were also carefully discussed.

Keywords Protective response signals · Neurotransmitter · Mitochondrial UPR · Endoplasmic reticulum UPR · Autophagy · Environmental exposure · *Caenorhabditis elegans*

9.1 Introduction

In nematode *Caenorhabditis elegans*, long-term exposure to environmental toxicants or stresses or short-term exposure to high doses of environmental toxicants or stresses can cause the severe toxicity at multiple aspects [1–5]. Meanwhile, it has been assumed that environmental toxicants or stresses at low doses or after short-term exposure may activate different forms of protective response of nematodes against the potential toxic effects. For example, the antioxidation defense response introduced in Chaps. 1 and 3 belongs to such a protective response of nematodes against the toxicity of environmental toxicants or stresses. Examination and elucidation of the detailed mechanisms for protective responses of nematodes to environmental toxicants or stresses will be helpful for our understanding of the molecular basis of toxicity induction and designing strategies to prevent the toxicity in nematodes exposed to certain environmental toxicants or stresses.

In this chapter, we focused on five aspects of protective responses of nematodes to environmental toxicants or stresses. These five protective responses are neurotransmitters, antimicrobial proteins, mitochondrial unfolded protein response

(UPR), endoplasmic reticulum UPR, and autophagy. Moreover, we discussed the underlying molecular mechanisms for the formation of these protective responses in nematodes exposed to environmental toxicants or stresses.

9.2 Neurotransmitters

The nematodes contain some classic neurotransmitters found in the vertebrates, such as acetylcholine, glutamate, gamma-aminobutyric acid (GABA), serotonin, dopamine, tyramine, and octopamine.

9.2.1 *Involvement of Neurotransmitter Signals in the Regulation of Toxicity of Environmental Toxicants or Stresses*

Some engineered nanomaterials have been shown to potentially cause the toxicity at different aspects on organisms, including the nematodes [1, 6–12]. *bas-1* encodes an aromatic acid decarboxylase required for serotonin and dopamine synthesis, *eat-4* encodes a glutamate transporter, and *tdc-1* encodes an aromatic-L-amino-acid/L-histidine decarboxylase required for making tyramine and octopamine. With the Al₂O₃-nanoparticles (NPs) (60 nm) as an example, after acute exposure for 6 or 12 h, mutations of *bas-1* or *eat-4* could significantly suppress the Al₂O₃-NP toxicity in decreasing locomotion behavior; however, mutation of *tdc-1* could not affect the Al₂O₃-NP toxicity in decreasing locomotion behavior (Fig. 9.1) [13], which implies that glutamate, serotonin, and/or dopamine may regulate the toxicity formation of environmental toxicants or stresses in nematodes.

cat-2 encodes a tyrosine hydroxylase essential for dopamine synthesis, *dat-1* encodes a dopamine transporter, *tph-1* encodes a tryptophan hydroxylase required for serotonin synthesis, and *mod-5* encodes a serotonin transporter. Moreover, after acute exposure for 6 or 12 h, mutation of *cat-2* or *tph-1* could significantly suppress the Al₂O₃-NP toxicity in decreasing locomotion behavior (Fig. 9.1) [13], suggesting that both the dopamine and the serotonin may be required for the formation of Al₂O₃-NP toxicity in nematodes. Meanwhile, after acute exposure for 6 or 12 h, mutation of *dat-1* or *mod-5* could also significantly suppress the Al₂O₃-NP toxicity in decreasing locomotion behavior (Fig. 9.1) [13]. These results suggest the crucial functions of at least dopamine and serotonin transporters in the toxicity formation of environmental toxicants or stresses in nematodes.

Moreover, it was observed that the octopamine administration could enhance the resistance to the oxidative stress induced by paraquat in nematodes (Fig. 9.2) [14]. RNAi knockdown of *daf-16* encoding the FOXO transcriptional factor in the insulin signaling pathway, but not the *skn-1* encodes the Nrf protein required for the control

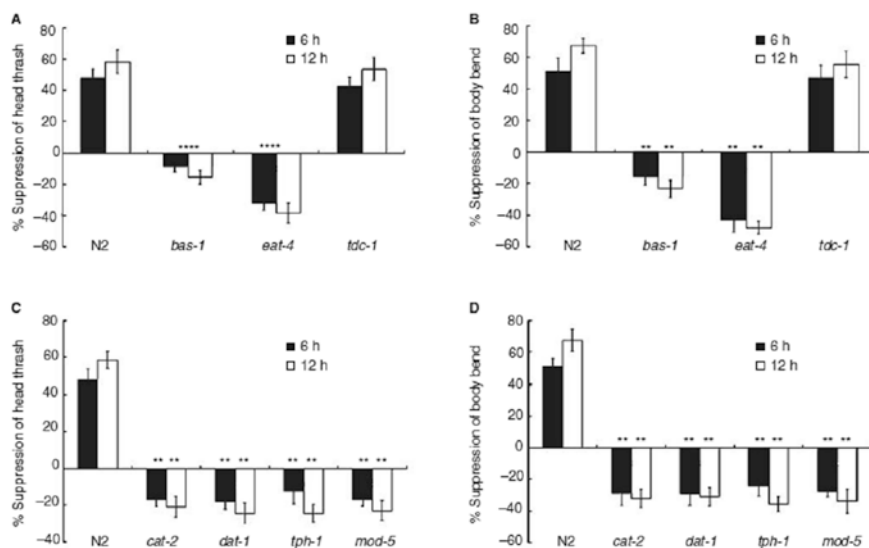


Fig. 9.1 Formation of adverse effects on locomotion behavior in Al_2O_3 -NP-exposed nematodes requires glutamate, dopamine, and serotonin [13]. (a) The head thrashes in Al_2O_3 -NP-exposed wild-type N2, *bas-1*, *eat-4*, and *tdc-1* mutant nematodes. (b) Body bends in Al_2O_3 -NP-exposed wild-type N2, *bas-1*, *eat-4*, and *tdc-1* mutant nematodes. (c) Head thrashes in Al_2O_3 -NP-exposed wild-type N2, *cat-2*, *dat-1*, *tph-1*, and *mod-5* mutant nematodes. (d) Body bends in Al_2O_3 -NP-exposed wild-type N2, *cat-2*, *dat-1*, *tph-1*, and *mod-5* mutant nematodes. Al_2O_3 -NP exposure at the concentration of 25 mg/L was performed at the L4 larval stage. Data are quantified as percentage suppression of locomotion behavior between naïve and Al_2O_3 -NP-exposed conditions for each genotype. % suppression = (locomotion behavior under the naïve condition – locomotion behavior under the Al_2O_3 -NP-exposed condition)/locomotion behavior under the naïve condition. Bars represent mean \pm SEM *** $p < 0.01$

of oxidative stress, could suppress the formation of this resistance from octopamine administration to oxidative stress induced by paraquat (Fig. 9.2) [14]. It was further found that the octopamine administration induced the DAF-16 nuclear accumulation in a dose-dependent manner [14]. Therefore, the octopamine is involved in the regulation of toxicity of environmental toxicants or stresses by inducing DAF-16 nuclear accumulation, and its function is dependent on the DAF-16 in nematodes.

9.2.2 Genetic Interactions of Neurotransmitter Signals in the Regulation of Toxicity of Environmental Toxicants or Stresses

Genetic interaction analysis demonstrated that the more severe Al_2O_3 -NP toxicity in decreasing locomotion behavior was formed in the *bas-1eat-4* double mutant compared with that in *bas-1* or in *eat-4* single mutant (Fig. 9.3) [13], implying that

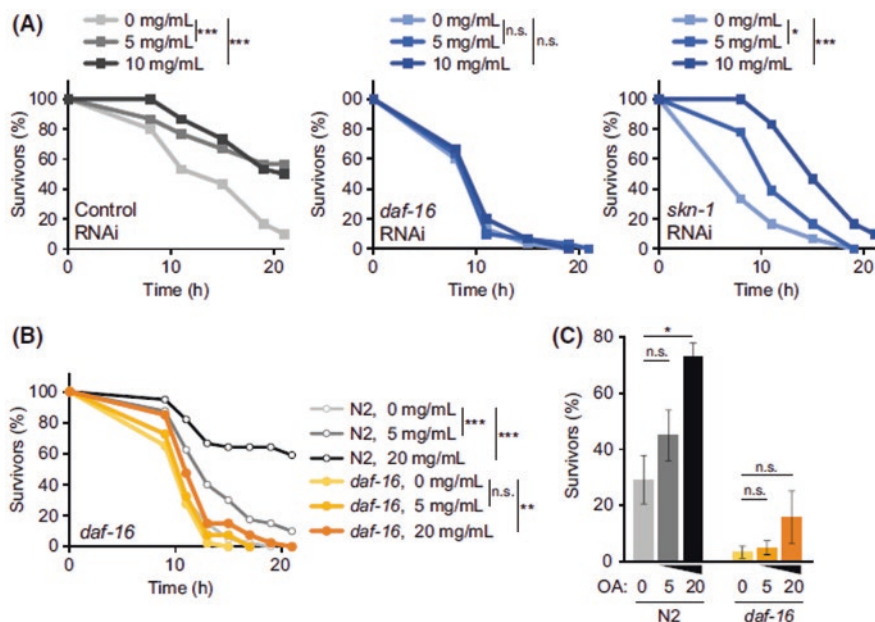


Fig. 9.2 Octopamine-enhanced oxidative stress resistance requires DAF-16 [14]. (a) Survival curves of the indicated RNAi-treated worms after 2 days of octopamine (OA) treatment at the indicated doses are shown. [Control RNAi-treated worms, $n = 30$ (0, 5 and 10 mg/mL); *daf-16* RNAi-treated worms, $n = 30$ (0, 5 and 10 mg/mL); *skn-1* RNAi-treated worms, $n = 30$ (0 and 10 mg/mL), 18 (5 mg/mL)]. $*P < 0.05$, $***P < 0.001$, log-rank (Mantel–Cox) test. (b) Survival curves of indicated worms after 2 days of OA treatment at the indicated doses are shown. [N2 worms, $n = 40$ (0 and 5 mg/mL), 39 (20 mg/mL); *daf-16* worms, $n = 40$ (0, 5 and 20 mg/mL)]. $**P < 0.01$, $***P < 0.001$, log-rank (Mantel–Cox) test. (c) The mean survival rate of at least three independent experiments after 13 h of paraquat treatment. The error bars represent SE. $*P < 0.05$, t -test

glutamate signal may function in the parallel pathways with dopamine signal or serotonin signal in the regulation of toxicity of environmental toxicants. Additionally, the more severe Al_2O_3 -NP toxicity in decreasing locomotion behavior was detected in the *tph-1cat-2* double mutant compared with that in *tph-1* or in *cat-2* single mutant, and the more severe Al_2O_3 -NP toxicity in decreasing locomotion behavior was observed in the *mod-5;dat-1* double mutant compared with that in *mod-5* or in *dat-1* single mutant (Fig. 9.3) [13], suggesting that dopamine signal and the serotonin signal may further function in the parallel pathways in the regulation of toxicity of environmental toxicants.

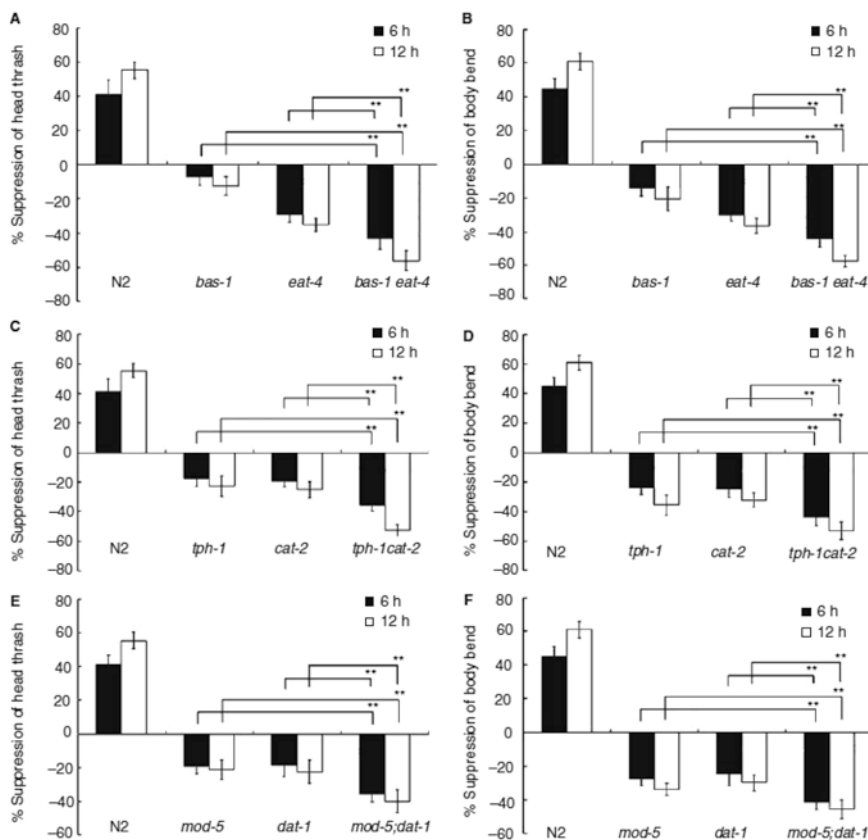


Fig. 9.3 Genetic interactions of glutamate, dopamine, and serotonin in regulating the formation of adverse effects on locomotion behavior in Al_2O_3 -NP-exposed nematodes [13]. (a and b) Genetic interactions of *bas-1* and *eat-4* genes in regulating the formation of adverse effects on locomotion behavior in Al_2O_3 -NP-exposed nematodes. (c and d) Genetic interactions of *tph-1* and *cat-2* genes in regulating the formation of adverse effects on locomotion behavior in Al_2O_3 -NP-exposed nematodes. (e and f) Genetic interactions of *mod-5* and *dat-1* genes in regulating the formation of adverse effects on locomotion behavior in Al_2O_3 -NP-exposed nematodes. Al_2O_3 -NP exposure at the concentration of 25 mg/L was performed at the L4 larval stage. Data are quantified as percentage suppression of locomotion behavior between naïve and Al_2O_3 -NP-exposed conditions for each genotype. % suppression = (locomotion behavior under the naïve condition – locomotion behavior under the Al_2O_3 -NP-exposed condition)/locomotion behavior under the naïve condition. Bars represent mean \pm SEM ** $p < 0.01$

9.2.3 Serotonin Response to Environmental Toxicants or Stresses

The environmental pathogens can potentially result in toxic effects at many aspects on human beings and animals, including the nematodes [15–22]. In nematodes, *tph-1* encodes a rate-limiting serotonin (5-HT) biosynthesis enzyme tryptophan hydroxylase. With the *Pseudomonas aeruginosa* PA14 as an example, PA14 infection significantly increased the TPH-1 expression (Fig. 9.4) [23], suggesting the serotonin response to pathogen infection.

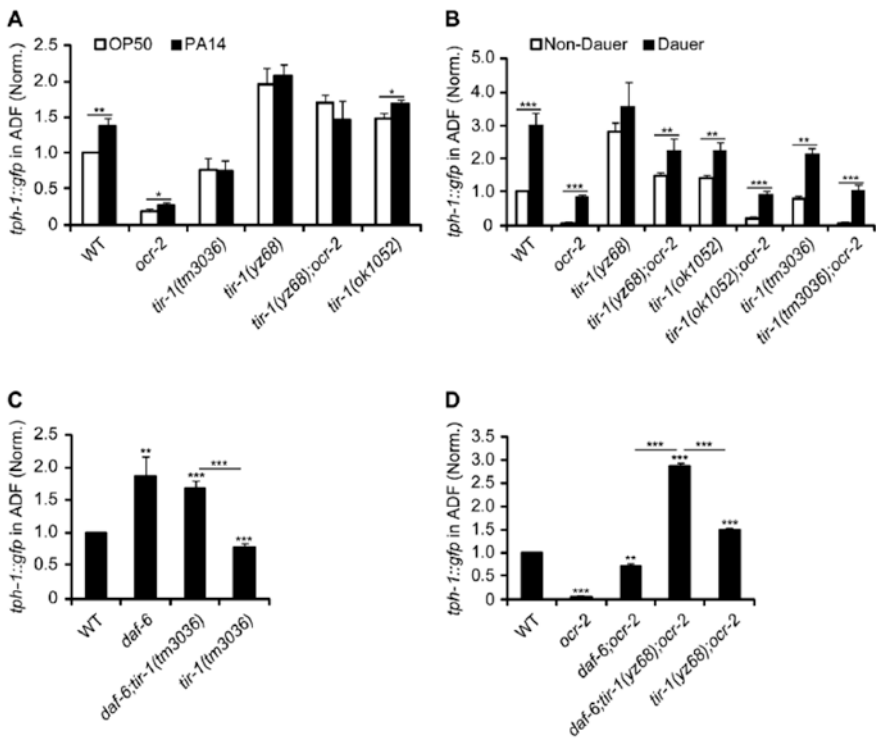


Fig. 9.4 TIR-1 signaling selectively regulates *tph-1::gfp* response to pathogenic bacterial food [23]. (a) PA14-induced ADF *tph-1::gfp* upregulation was impaired in *tir-1(tm3036lf)* and *tir-1(yz68gf)* mutants. (b) *tir-1(tm3036lf)* and *tir-1(yz68gf)* mutations did not block *tph-1::gfp* upregulation during dauer formation. (c) TIR-1 is not required for *tph-1::gfp* upregulation caused by changes in ciliary morphology. Mutations in *daf-6*/Patched alter the morphology of dendritic cilia of all chemosensory neurons including ADF and cause ADF *tph-1::gfp* upregulation on its own as well as in *tir-1(lf)* background. (d) *tir-1(yz68gf)* and *daf-6* mutations confer additive upregulation of *tph-1::gfp* in the ADF neurons. Data represent the average of three trials each with at least 20 animals per strain per condition \pm SEM. The value of ADF GFP fluorescence in WT animals under a stress paradigm and that of mutants is normalized to the value of WT animals under optimal conditions. * $p < 0.05$, ** $p < 0.01$, *** $p < 0.001$

Moreover, it was observed that this TPH-1 increase induced by PA14 infection could be suppressed by *tir-1* mutation (Fig. 9.4) [23]. In nematodes, it has been proven that the TIR-1 selectively regulates the serotonergic response to the toxicity of environmental toxicants or stresses.

9.2.4 Neurotransmitter Receptors

9.2.4.1 Dopamine Receptors

The neurotransmitters exert their functions by acting on certain corresponding receptors. In nematodes, after acute exposure for 6 or 12 h, mutation of *dop-1* significantly suppressed the Al₂O₃-NP toxicity in decreasing locomotion behavior; however, mutation of *dop-2*, *dop-3*, or *dop-4* did not obviously affect the Al₂O₃-NP toxicity in decreasing locomotion behavior (Fig. 9.5) [13], suggesting the involvement of D1-like dopamine receptor DOP-1 in the regulation of toxicity of environmental toxicants in nematodes.

Moreover, among the examine dopamine receptor mutants, only the *dop-4(tm1392)* mutant nematodes showed an enhanced resistance to *P. aeruginosa* infection compared with wild-type nematodes (Fig. 9.6) [24]. The *dop-4(tm1392)* mutant nematodes did not show a significant lifespan extension on heat-killed bacteria compared to wild-type nematodes (Fig. 9.6) [24], indicating that DOP-4 may modulate immunity without affecting longevity. The conserved p38/PMK-1 MAP kinase pathway was further proven to be required for the enhanced resistance to *P. aeruginosa* infection of *dop-4* mutant nematodes [24]. Furthermore, the dopaminergic CEP neurons were identified in controlling the immunity through DOP-4 expressed in ASG neurons [24].

9.2.4.2 Serotonin Receptors

After acute exposure for 6 or 12 h, mutation of *mod-1* significantly suppressed the Al₂O₃-NP toxicity in decreasing locomotion behavior; however, mutation of *ser-1*, *ser-4*, or *ser-7* did not obviously influence the Al₂O₃-NP toxicity in decreasing locomotion behavior (Fig. 9.5) [13], suggesting that the ionotropic serotonin receptor MOD-1 is required for the regulation of toxicity of environmental toxicants in nematodes.

9.2.4.3 Glutamate Receptors

After acute exposure for 6 or 12 h, mutation of *glr-2* or *glr-6* significantly suppressed the Al₂O₃-NP toxicity in decreasing locomotion behavior; however, mutation of *glr-1*, *glr-3*, *glr-4*, *glr-5*, *glr-7*, *glr-8*, *nmr-1*, or *nmr-2* did not obviously affect the Al₂O₃-NP toxicity in decreasing locomotion behavior (Fig. 9.5) [13], suggesting the involvement of non-NMDA receptors of GLR-2 and GLR-6 in the regulation of toxicity of environmental toxicants or stresses in nematodes.

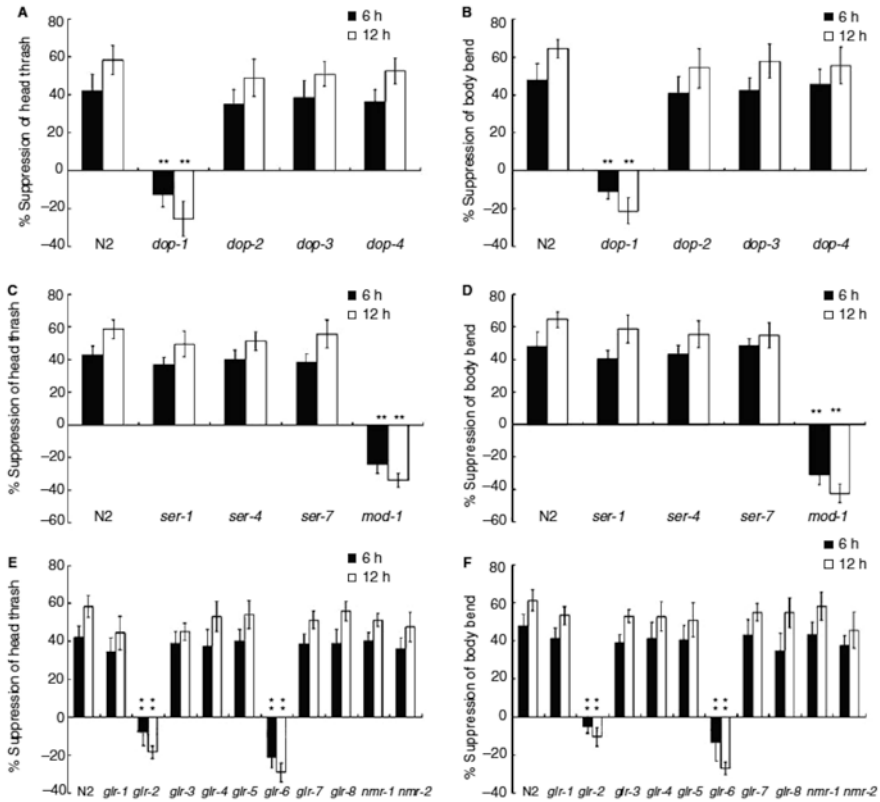


Fig. 9.5 Formation of adverse effects on locomotion behavior in Al₂O₃-NP-exposed nematodes requires dopamine receptor DOP-1, serotonin receptor MOD-1, and glutamate receptors GLR-2 and GLR-6 [13]. (a) Head thrashes in Al₂O₃-NP-exposed wild-type N2, *dop-1*, *dop-2*, *dop-3*, and *dop-4* mutant nematodes. (b) Body bends in Al₂O₃-NP-exposed wild-type N2, *dop-1*, *dop-2*, *dop-3*, and *dop-4* mutant nematodes. (c) Head thrashes in Al₂O₃-NP-exposed wild-type N2, *ser-1*, *ser-4*, *ser-7*, and *mod-1* mutant nematodes. (d) Body bends in Al₂O₃-NP-exposed wild-type N2, *ser-1*, *ser-4*, *ser-7*, and *mod-1* mutant nematodes. (e) Head thrashes in Al₂O₃-NP-exposed wild-type N2, *glr-1*, *glr-2*, *glr-3*, *glr-4*, *glr-5*, *glr-6*, *glr-7*, *glr-8*, *nmr-1*, and *nmr-2* mutant nematodes. (f) Body bends in Al₂O₃-NP-exposed wild-type N2, *glr-1*, *glr-2*, *glr-3*, *glr-4*, *glr-5*, *glr-6*, *glr-7*, *glr-8*, *nmr-1*, and *nmr-2* mutant nematodes. Al₂O₃-NP exposure at the concentration of 25 mg/L was performed at the L4 larval stage. Data are quantified as percentage suppression of locomotion behavior between naïve and Al₂O₃-NP-exposed conditions for each genotype. % suppression = (locomotion behavior under the naïve condition – locomotion behavior under the Al₂O₃-NP-exposed condition)/locomotion behavior under the naïve condition. Bars represent mean ± SEM ***p* < 0.01

9.2.4.4 Octopamine Receptors

In nematodes, OCTR-1, SER-3, and SER-6 are octopamine receptors. It was found that only deletion mutation of *ser-3* or *ser-6* suppressed the octopamine-induced enhancement in the resistance to oxidative stress induced by paraquat (Fig. 9.7) [14]. Moreover, the double mutation of *ser-3* and *ser-6* could more substantially

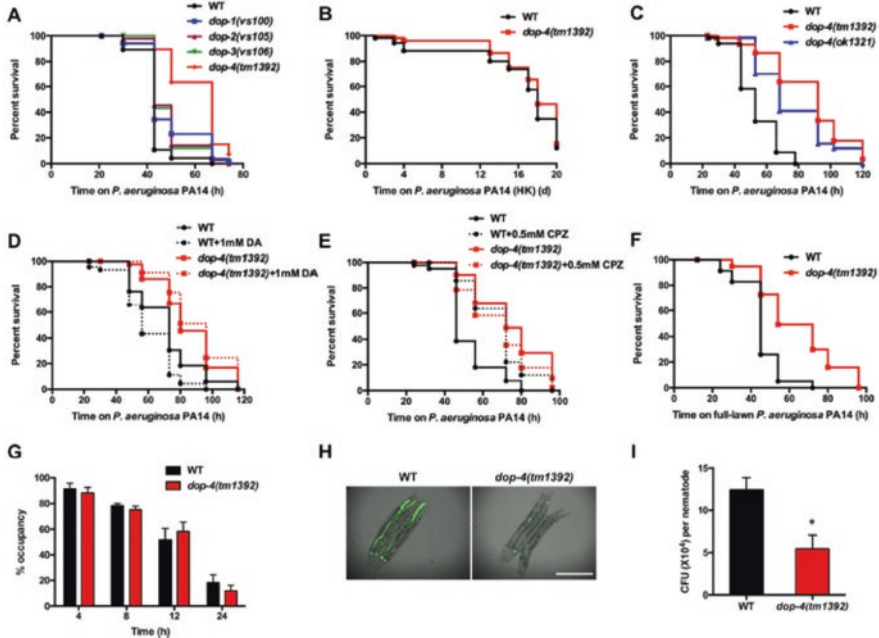


Fig. 9.6 The D1-like dopamine receptor DOP-4 controls immunity against *P. aeruginosa* infection [24]. (a) Wild-type animals and dopamine receptor mutants were exposed to *P. aeruginosa* PA14 and scored for survival. WT vs *dop-4(tm1392)*: $p < 0.0001$. (b) Wild-type and *dop-4(tm1392)* animals were exposed to heat-killed *P. aeruginosa* PA14 and scored for survival. WT vs *dop-4(tm1392)*: $p > 0.1$. (c) Wild-type, *dop-4(tm1392)*, and *dop-4(ok1321)* animals were exposed to *P. aeruginosa* PA14 and scored for survival. WT vs *dop-4(tm1392)*: $p < 0.001$; WT vs *dop-4(ok1321)*: $p < 0.001$. (d) Wild-type and *dop-4(tm1392)* animals were exposed to *P. aeruginosa* PA14 in the presence or absence of dopamine and scored for survival. WT vs WT+DA: $p < 0.01$; *dop-4(tm1392)* vs *dop-4(tm1392)*+DA: $p > 0.1$. (e) Wild-type and *dop-4(tm1392)* animals were exposed to *P. aeruginosa* PA14 in the presence or absence of chlorpromazine and scored for survival. WT vs WT+CPZ: $p < 0.001$; *dop-4(tm1392)* vs *dop-4(tm1392)*+CPZ: $p > 0.1$. (f) Wild-type and *dop-4(tm1392)* animals were exposed to a full lawn of *P. aeruginosa* PA14 and scored for survival. WT vs *dop-4(tm1392)*: $p < 0.001$. (g) Wild-type and *dop-4(tm1392)* animals were cultured on partial pathogen lawns, and the percentage of animals on the pathogen lawn was calculated for each time point. (h) Wild-type and *dop-4(tm1392)* animals were exposed to *P. aeruginosa* PA14-GFP for 30 h and visualized using a Leica M165 FC fluorescence stereomicroscope. Scale bar = 0.5 mm. (i) Wild-type and *dop-4(tm1392)* animals were exposed to *P. aeruginosa* PA14-GFP for 30 h, and the colony-forming units (CFU) were counted. Ten animals were used for each condition. All bars represent means \pm SEM; * $p < 0.05$

suppress the octopamine-enhanced resistance to oxidative stress than single mutation of *ser-3* or *ser-6* (Fig. 9.7) [14], suggesting that SER-3 and SER-6 act in the parallel pathway to regulate this resistance enhancement. These results suggest the involvement of octopamine receptors of SER-3 and SER-6 in the regulation of toxicity of environmental toxicants or stresses in nematodes.

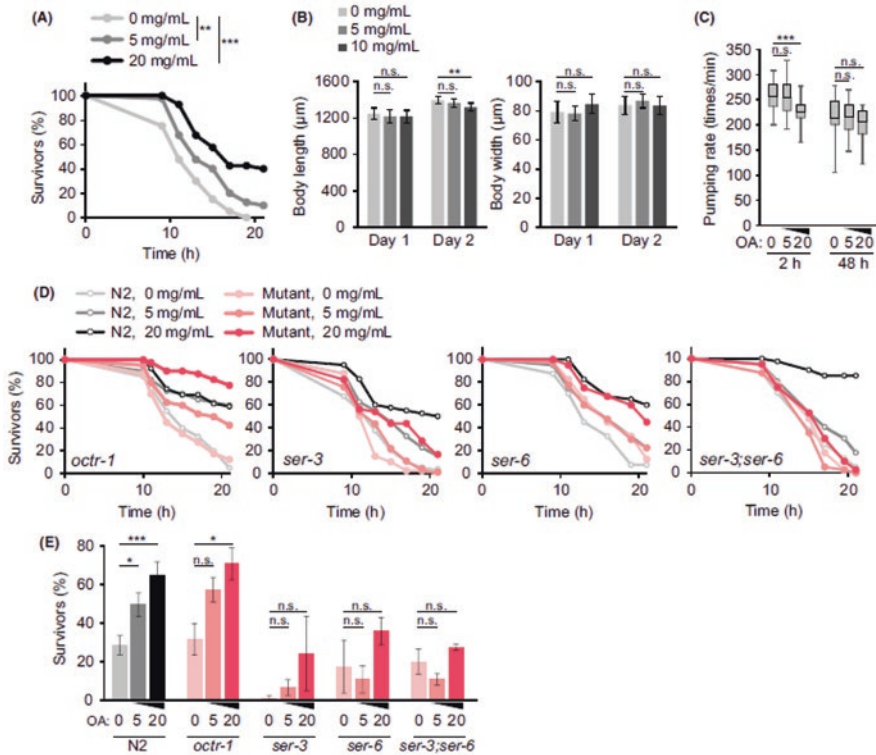


Fig. 9.7 Octopamine administration enhances oxidative stress resistance in a SER-3- and SER-6-dependent manner [14]. (a) Survival curves of N2 worms after 2 days of octopamine (OA) treatment at the indicated dose, which were exposed to 300 mM paraquat, are shown. [n = 40 (0, 5 and 20 mg/mL)]. **P < 0.01, ***P < 0.001, log-rank (Mantel–Cox) test. (b) The mean body length (left) and width (right) of N2 worms after 1 or 2 days of OA treatment at indicated doses are shown. [n = 7 (0, 5 and 10 mg/mL)]. The error bars represent SD. **P < 0.01, t-test. (c) Box plot of the pumping rates of worms after 2 h or 2 days of OA treatment at the indicated doses is shown. Boxes denote median and 25–75 percentile, and whiskers denote minimum/maximum values of the data set. [n = 30 (0, 5 and 20 mg/mL for 2 h); n = 20 (0, 5 and 20 mg/mL for 2 days)]. ***P < 0.001, t-test. (d) Survival curves of indicated worms exposed to 300 mM paraquat after 2 days of OA treatment at the indicated dose are shown. [n = 40 in the cases unmentioned below. n = 39 (20 mg/mL in N2 compared to *octr-1*), 37 (5 mg/mL in *ser-3*), and 39 (20 mg/mL in *ser-3*)]. (e) The mean survival rate of at least three independent experiments after 17 h of paraquat treatment. The error bars represent SE

9.2.5 Function of Neurotransmission in the Regulation of Toxicity of Environmental Toxicants or Stresses

aex-3 encoding a guanine exchange factor for GTPase is required for neuronal vesicle trafficking and synaptic vesicle release [25, 26]. Mutation of *aex-3* enhanced both the induction of intestinal ROS production and the intestinal permeability in

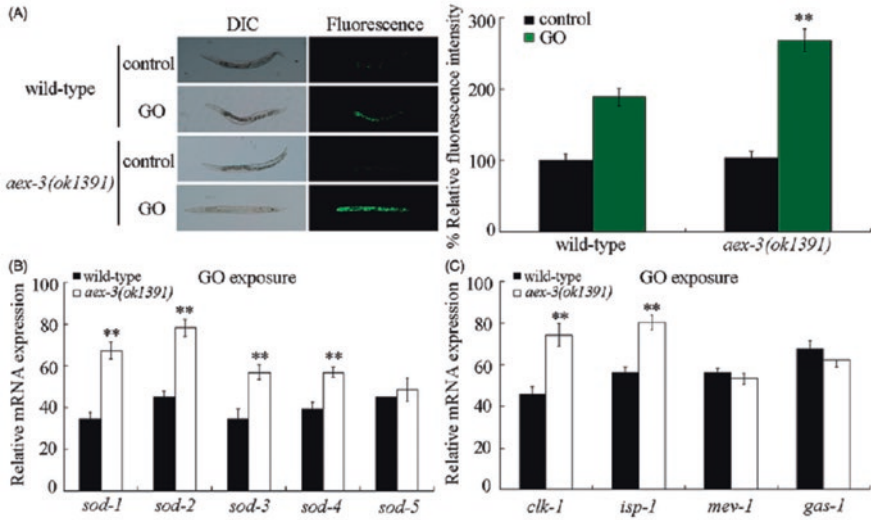


Fig. 9.8 Effect of *aex-3* mutation on the induction of oxidative stress in nematodes [27]. (a) Effect of *aex-3* mutation on the induction of oxidative stress. (b) Effect of *aex-3* mutation on the expressions of *sod* genes. (c) Effect of *aex-3* mutation on the expression of *clk-1*, *isp-1*, *mev-1*, and *gas-1*. Prolonged exposure was performed from L1-larvae to young adults. GO exposure concentration was 10 mg/L. Bars represent means \pm SD. ** $p < 0.01$ versus wild type

nematodes exposed to graphene oxide (GO), a carbon-based nanomaterial (Fig. 9.8) [27]. Exposure to GO (10 mg/L) could further significantly increase the transcriptional expressions of *sod-1*, *sod-2*, *sod-3*, and *sod-4* in *aex-3* mutant compared with those in wild-type nematodes (Fig. 9.8) [27]. Meanwhile, exposure to GO (10 mg/L) could significantly increase the transcriptional expressions of *clk-1* and *isp-1* in *aex-3* mutant compared with those in wild-type nematodes (Fig. 9.8) [27]. Thus, the molecular basis for neurotransmission may be involved in the response to or the regulation of toxicity of environmental toxicants or stresses.

9.3 Antimicrobial Proteins

9.3.1 Response of Antimicrobial Proteins to the Toxicity of Environmental Toxicants or Stresses

The bacterial or fungal pathogens can induce the innate immune response in nematodes by activating the expression of antimicrobial proteins, although the antimicrobial function for most of these proteins has not been confirmed. With *P. aeruginosa* PA14 infection as an example, PA14 infection could induce the activation of a series of antimicrobial proteins (Fig. 9.9) [28]. In contrast, under the normal conditions

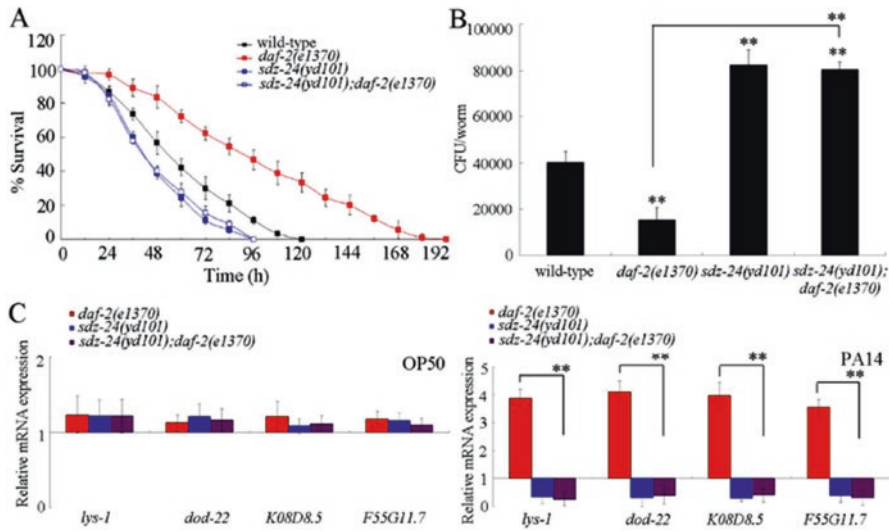


Fig. 9.9 Genetic interaction between *sdz-24* and *daf-2* in the regulation of innate immune response to *P. aeruginosa* PA14 infection [28]. (a) Genetic interaction between *sdz-24* and *daf-2* in the regulation of survival in *P. aeruginosa* PA14-infected nematodes. Statistical comparisons of the survival plots indicate that, after *P. aeruginosa* PA14 infection, the survival of *sdz-24(yd101);daf-2(e1370)* was not significantly different from that of *sdz-24(RNAi)* ($P = 0.9218$), and the survival of *sdz-24(yd101);daf-2(e1370)* was significantly different from that of *daf-2(e1370)* ($P < 0.0001$). (b) Genetic interaction between *sdz-24* and *daf-2* in the regulation of CFU of *P. aeruginosa* PA14 in the body of nematodes. (c) Genetic interaction between *sdz-24* and *daf-2* in the regulation of expression patterns of antimicrobial genes in *P. aeruginosa* PA14-infected nematodes. Normalized expression is presented relative to wild-type expression. Bars represent mean \pm SD. ** $P < 0.01$ vs wild type (if not specially indicated)

(fed on *E. coli* OP50), these antimicrobial proteins would not be activated (Fig. 9.9) [28]. The activation of these antimicrobial proteins was regulated by some signaling pathways, such as the insulin signaling pathway (Fig. 9.9) [28]. The molecular basis for the induction of innate immune response has been well-described in some reviews [29–34]. The signaling pathways involved in the control of innate immunity in nematodes contain MAPK signaling pathways, insulin and related signaling pathways, development-related signaling pathways, and cell death and DNA damage-related signaling pathways. The involvement of these signaling pathways in the regulation of toxicity of environmental toxicants or stresses has been introduced and discussed in Chaps. 4, 5, 6, and 7.

With GO as the example, it was further observed that acute exposure to GO (10 mg/L) could induce the significant increase in expressions of *lys-1*, *dod-6*, *F55G11.4*, *lys-8*, and *spp-1* in nematodes (Fig. 9.10) [35]. *lys-1* and *lys-8* encode lysozymes, *dod-6* encodes a protein downstream of DAF-16, *F55G11.4* encodes a

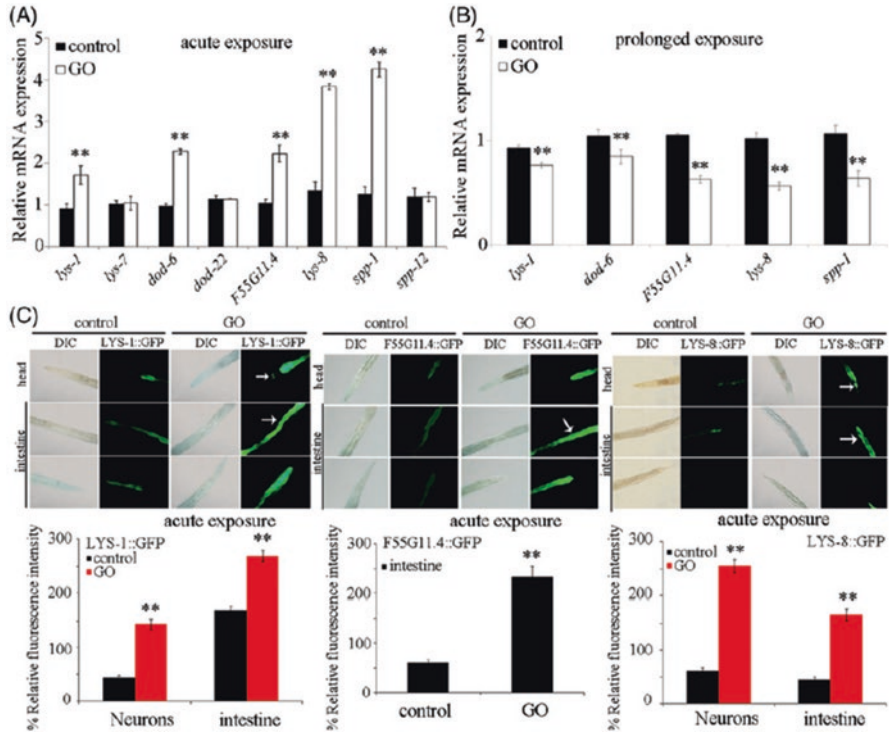


Fig. 9.10 Response of antimicrobial proteins to GO exposure [35]. (a) Effect of acute exposure to GO on the expressions of antimicrobial genes. (b) Effect of prolonged exposure to GO on the expressions of antimicrobial genes. (c) Effect of acute exposure to GO on the expressions of *LYS-1::GFP*, *F55G11.4::GFP*, and *LYS-8::GFP*. Arrowheads indicate the neurons in the head and the intestine, respectively. Acute exposure to GO was performed from young adult for 24 h. Prolonged exposure was performed from L1-larvae to young adults. GO exposure concentration was 10 mg/L. Bars represent means \pm SD. ** $p < 0.01$ vs control

protein containing a CUB-like domain, and *spp-1* encodes a caenopore. *LYS-1* is expressed in the neurons and the intestine, *F55G11.4* is expressed in the intestine, and *LYS-8* is expressed in the neurons and the intestine. Acute exposure to GO (10 mg/L) could further significantly increase the expression of *LYS-1::GFP* in both the neurons and the intestine, the intestinal expression of *F55G11.4::GFP*, and the expression of *LYS-8::GFP* in both the neurons and the intestine (Fig. 9.10) [35]. These results suggest that the expression of some antimicrobial protein-mediated innate immune response may be activated for nematodes against the toxicity of environmental toxicants or stresses.

9.3.2 *Molecular Control of Toxicity of Environmental Toxicants or Stresses by Antimicrobial Proteins*

In nematodes, it has been observed that mutation of *lys-1*, *lys-8*, or *spp-1* induced a susceptibility to GO toxicity in inducing intestinal ROS production and in decreasing locomotion behavior (Fig. 9.11) [35]. Additionally, RNAi knockdown of *dod-6* or *F55G11.4* also induced a susceptibility to GO toxicity in inducing intestinal ROS production and in decreasing locomotion behavior (Fig. 9.11) [35]. These results suggest that these antimicrobial proteins may negatively regulate the toxicity of environmental toxicants or stresses in nematodes.

Meanwhile, it has been found that intestine-specific RNAi knockdown of the antimicrobial gene of *lys-1*, *dod-6*, *F55G11.4*, *lys-8*, or *spp-1* also caused a susceptibility to GO toxicity in nematodes using the transgenic strain of VP303 as an intestine-specific RNAi knockdown tool [35], which implies that these antimicrobial proteins can at least act in the intestine in response to environmental toxicants or stresses.

9.4 Mitochondrial UPR

Recently, the induction and the molecular control of mitochondrial UPR have been introduced and discussed in some reviews [36].

9.4.1 *Induction of Mitochondrial UPR in Nematodes Exposed to Environmental Toxicants or Stresses*

HSP-6::GFP and HSP-60::GFP can be employed as the markers for mitochondrial UPR [36]. In nematodes, a screen was performed from a chemical library containing 1200 compounds to identify the compounds that specifically activated the mitochondrial UPR [37]. The testing concentration for the compounds was 100 mM, and HSP-60::GFP was used as a marker of mitochondrial UPR [37]. The oxidative agent paraquat was used as a positive control during the screen [37]. After the screen, eight compounds were identified, and only four of the eight compounds might specifically cause the activation of the mitochondrial UPR without meanwhile activating the ER UPR as indicated by the maker of HSP-4::GFP (Fig. 9.12) [37]. The identified four compounds were minocycline hydrochloride, methacycline hydrochloride, chlorprothixene hydrochloride, and auranofin [37].

Additionally, infection with the *P. aeruginosa* PA14 could also induce the mitochondrial UPR as indicated by the increase in both HSP-60 and HSP-6 (Fig. 9.13) [38]. Moreover, it was observed that induction of mitochondrial UPR might be reg-

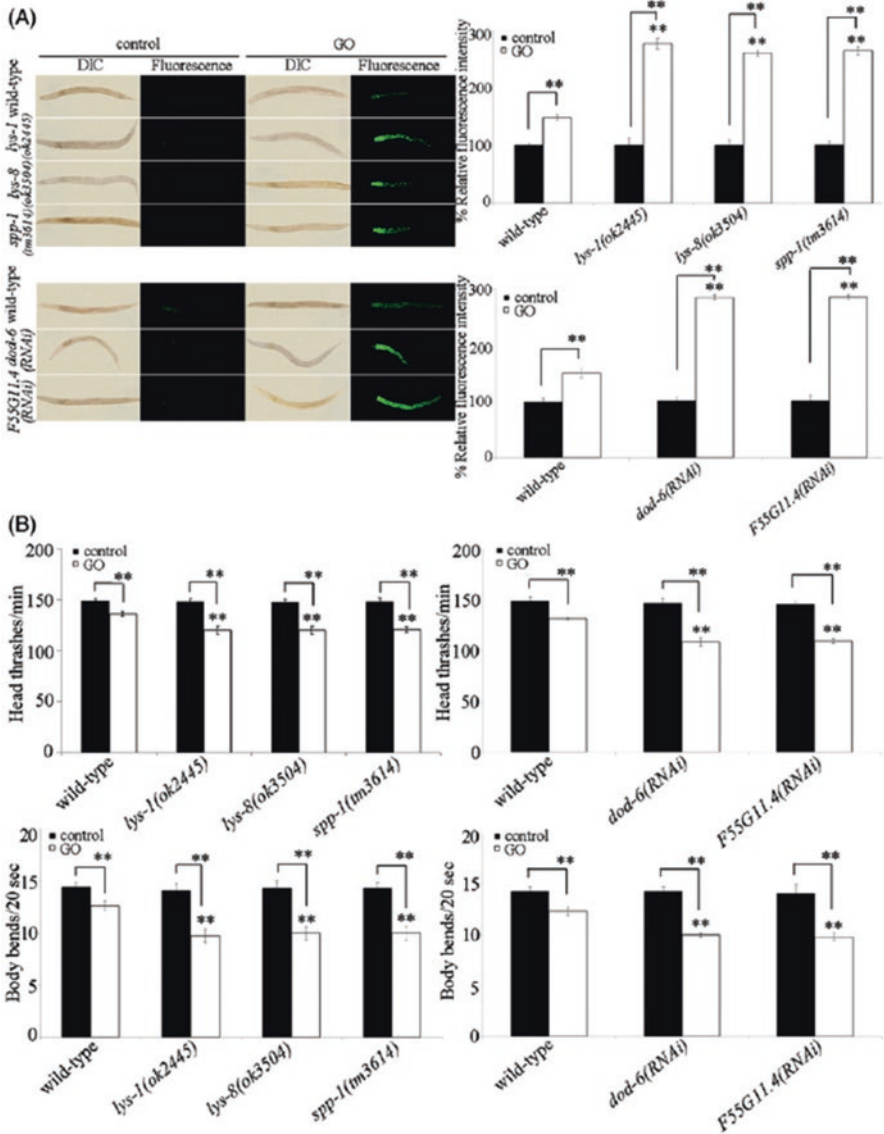


Fig. 9.11 Mutation or RNAi knockdown of antimicrobial genes induced an enhanced susceptibility to GO toxicity [35]. **(a)** Mutation or RNAi knockdown of antimicrobial genes induced an enhanced susceptibility to GO toxicity in inducing intestinal ROS production. **(b)** Mutation or RNAi knockdown of antimicrobial genes induced an enhanced susceptibility to GO toxicity in decreasing locomotion behavior. Prolonged exposure was performed from L1-larvae to young adults. GO exposure concentration was 10 mg/L. Bars represent means \pm SD. ** $p < 0.01$ vs wild type (if not specially indicated)

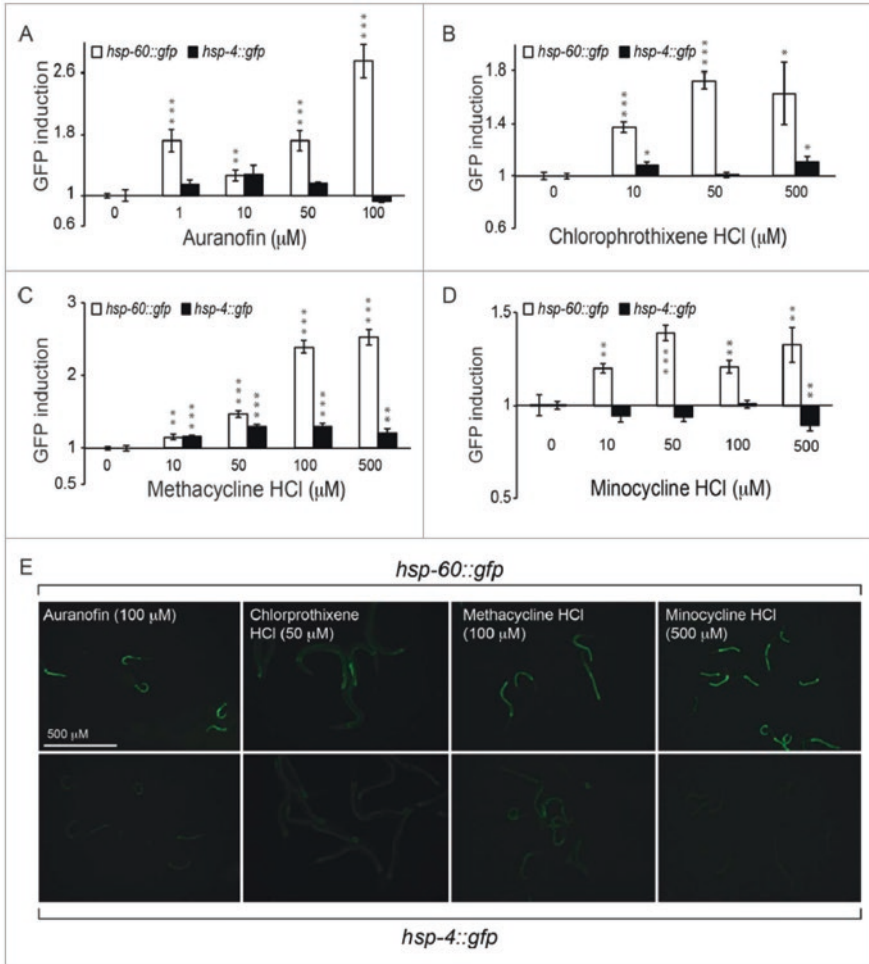


Fig. 9.12 Four drugs specifically activate the UPR^{mt} [37]. Treatment of four drugs specifically activates UPR^{mt} reporters (*hsp60::GFP*) but not the UPR^{cr} reporter (*hsp4::GFP*). (a–d) GFP induction of UPR^{mt} reporters and UPR^{cr} reporters on various doses of drugs. (e) shows corresponding images. The bars show the average ± SEM ($n > 20$). * $p < 0.05$; ** $p < 0.01$; *** $p < 0.001$ in paired Student’s t -test

ulated by multiple *P. aeruginosa* virulence factors (Fig. 9.13) [38]. Infection with *P. aeruginosa* strains lacking individual siderophore, pyocyanin, or cyanide toxin genes caused the less mitochondrial UPR activation than wild-type *P. aeruginosa* (Fig. 9.3) [38]. That is, multiple pathogen toxins will target the mitochondrial function, which will then result in the mitochondrial UPR activation.

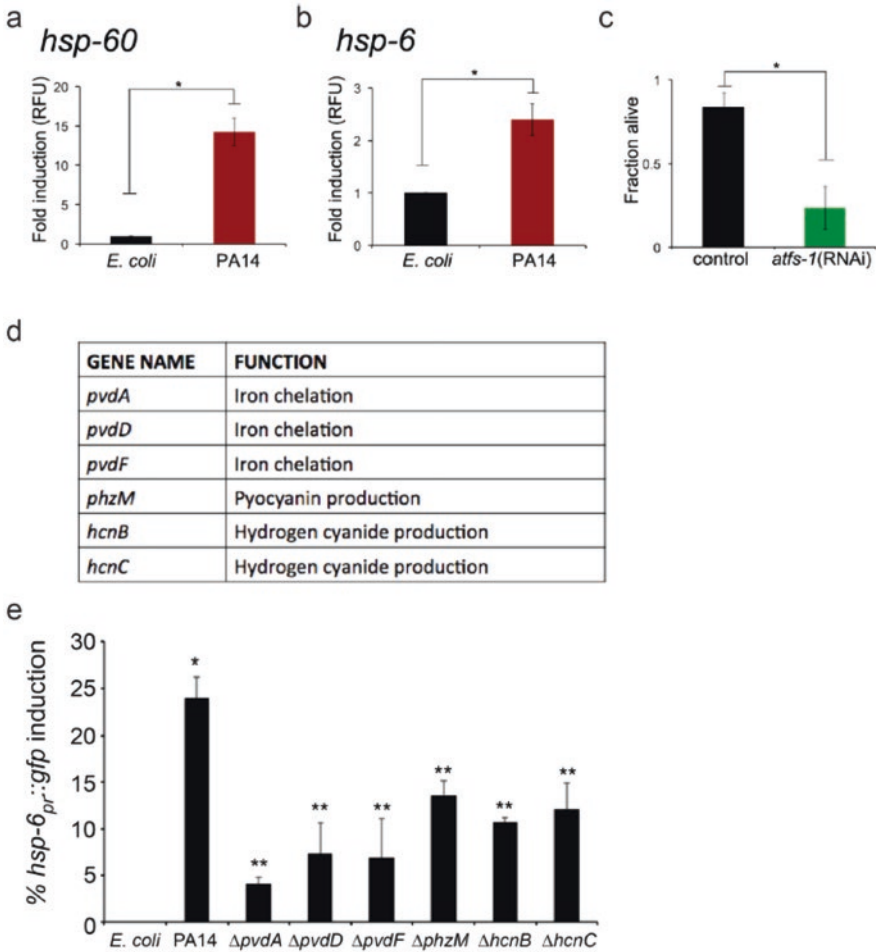


Fig. 9.13 Multiple *P. aeruginosa* virulence genes contribute to UPR^{mt} activation [38]. **(a and b)** Expression of *hsp-60* and *hsp-6* mRNA for *glp-4(bn2)* worms exposed to *E. coli* or *P. aeruginosa* liquid-killing using qRT-PCR ($N = 3$, \pm SD). Fold inductions are normalized to wild-type *E. coli* test group, $*p < 0.05$ (Student's *t*-test). **(c)** Quantitation of survival for *glp-4(bn2)* worms raised on control or *affs-1*(RNAi) and exposed to *P. aeruginosa* liquid-killing, $*p < 0.0001$ (Student's *t*-test). **(d)** List of *P. aeruginosa* toxin mutants. **(e)** Quantitation of the proportion of worms showing increased *hsp-6_{pr}::gfp* expression in the intestine under slow-killing conditions. Exposure to *P. aeruginosa* caused *hsp-6_{pr}::gfp* induction ($N = 3$, \pm SE), $*p < 0.05$ (Student's *t*-test). However, exposure to *P. aeruginosa* with mutations in the *pvdA*, *pvdD*, *pvdF*, *phzM*, *hcnB*, or *hcnC* toxin genes resulted in relatively less UPR^{mt} activation ($N = 3$, \pm SE), $**p < 0.05$ (Student's *t*-test)

9.4.2 *Molecular Basis for Mitochondrial UPR Induced by Environmental Toxicants or Stresses*

9.4.2.1 ATFS-1

atfs-1 encodes a leucine zipper (bZIP) transcription factor containing both a mitochondrial targeting sequence (MTS) and a nuclear localization sequence (NLS). The mitochondrial UPR is regulated by the ATFS-1 [36, 38]. Besides the expression pattern of ATFS-1, the presence of dual subcellular localization sequences enables ATFS-1 to mediate a mitochondrial-to-nuclear communication (Fig. 9.14) [36]. That is, under the homeostatic conditions, ATFS-1 is efficiently imported into the mitochondrial matrix, in which it will be degraded by the protease LON (Fig. 9.14) [36]. However, under the mitochondrial UPR conditions, the mitochondrial import of ATFS-1 will be reduced, which will then cause its accumulation in the cytosol and further traffic to the nucleus to activate the transcriptional response (Fig. 9.14) [36]. It is supposed that the cells may use the mitochondrial import efficiency as an indicator of mitochondrial function, and employ the ATFS-1 as both a sensor and a mitochondria-to-nucleus signaling mechanism [36].

ATFS-1 not only induced the mitochondrial protective genes but also regulated the innate immunity in nematodes [38]. The survival of *atfs-1*(RNAi) nematodes was significantly reduced when exposed to *P. aeruginosa*, but not *E. coli* (Fig. 9.15) [38], suggesting that ATFS-1 activation may mediate a protective transcriptional response to environmental toxicants or stresses. Moreover, it was found that mitochondrial UPR pre-activation by allowing the nematodes to develop on *spg-7*(RNAi) for 2 days prior to pathogen exposure could dramatically reduce the intestinal accumulation of *P. aeruginosa* and prolong the survival of nematodes challenged with *P. aeruginosa*, which required the *atfs-1* (Fig. 9.15) [38], suggesting that mitochondrial UPR activation can promote the pathogen clearance. Similarly, the *atfs-1* gain-of-function mutant *atfs-1(et18)*, which constitutively activates mitochondrial UPR, accumulated less *P. aeruginosa*-GFP in the intestine and survived longer than wild-type nematodes (Fig. 9.15) [38].

Furthermore, it was observed that the increase in mitochondrial chaperone reporter (*hsp-6* and *hsp-60pr::gfp*) activation in the intestine by *P. aeruginosa* exposure required the *atfs-1* and was correlated with the increased nuclear accumulation of ATFS-1::GFP and the NLS in ATFS-1 (Fig. 9.16) [38], implying that the nuclear accumulation of ATFS-1 is required for mitochondrial UPR activation in nematodes exposed to environmental toxicants or stresses.

haf-1 encodes a mitochondria-localized ATP-binding cassette protein. The defect in the mitochondrial UPR signaling in *haf-1* deleted nematodes was associated with the failure of ATFS-1 to localize to nuclei in nematodes with perturbed mitochondrial protein folding [39]. During the mitochondrial stress, more ATFS-1 accumulated within mitochondria was observed in *haf-1(ok705)* mutant nematodes (Fig. 9.17)

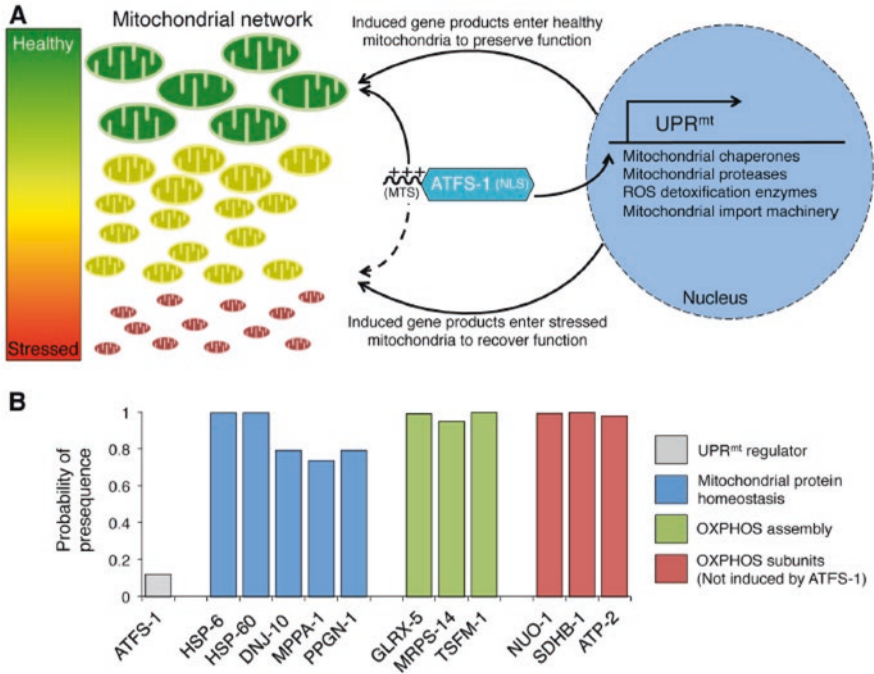


Fig. 9.14 Model by which mitochondrial import efficiency of ATFS-1 and gene products induced by ATFS-1 promote mitochondrial network recovery [36]. (a) The transcription factor ATFS-1 harbors both a mitochondrial targeting sequence (MTS) and a nuclear localization sequence (NLS). ATFS-1 is efficiently imported into healthy mitochondria (green); however, import efficiency is reduced by OXPHOS or mitochondrial proteostasis perturbations that cause mitochondrial dysfunction (yellow, red). If ATFS-1 fails to be imported into mitochondria, it is trafficked to the nucleus where it induces transcription of mitochondrial protective genes including mitochondrial chaperones and proteases, antioxidants as well as mitochondrial protein import components. In turn, mitochondrial import of the protective gene products promotes organelle stabilization and recovery. (b) Relative to the proteins induced during the UPR^{mt}, the program MitoFates predicts that ATFS-1 has a substantially weaker mitochondrial signal sequence. It was hypothesized that a weak MTS allows ATFS-1 to be sensitive to modest mitochondrial dysfunction and translocate to the nucleus. In turn, the strong MTSs in those proteins induced by ATFS-1 can still enter dysfunctional mitochondria with reduced import efficiency to recover function. HSP-6, HSP-60, and DNJ-10 are mitochondrial chaperones, MPPA-1 is a subunit of the mitochondrial presequence processing protease, PPGN-1 is a matrix-localized protease, GLRX-5 is a glutaredoxin that functions in mitochondrial iron–sulfur cluster biogenesis, MRPS-14 is a subunit of the mitochondrial ribosome, and TSFM-1 is a mitochondrial translational elongation factor, all of which are induced during mitochondrial dysfunction by ATFS-1. NUO-1, SDHB-1, and ATP-2 are all subunits of the OXPHOS complexes, none of which are activated by the UPR^{mt} (complexes I, II, and V, respectively)

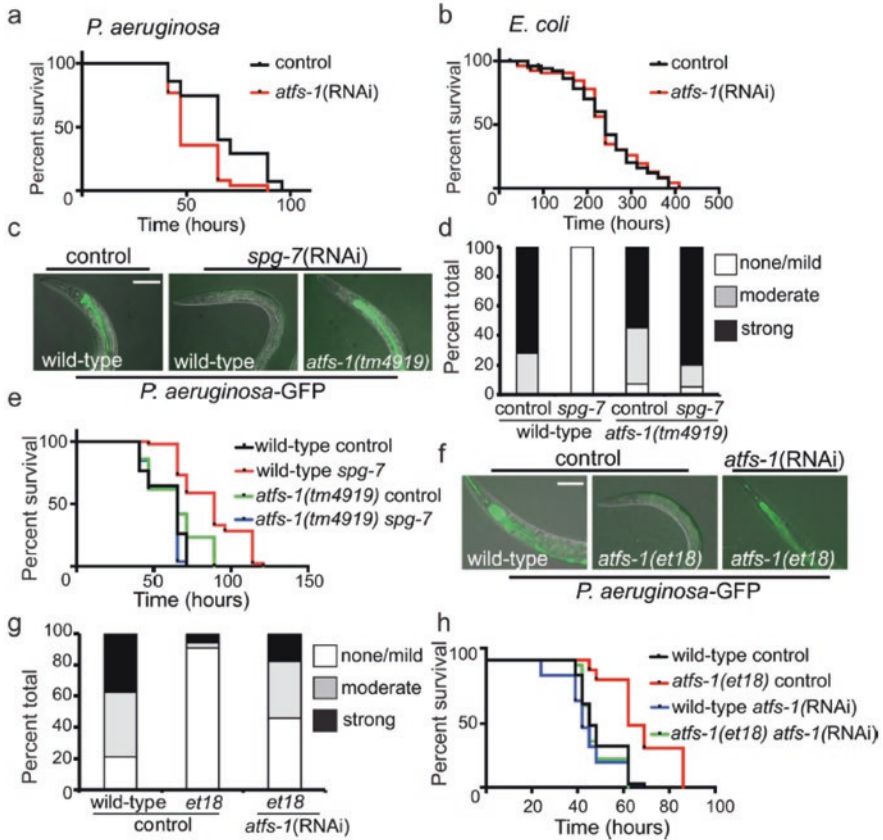


Fig. 9.15 UPR^{mt} activation provides resistance to *P. aeruginosa* [38]. (a and b) Survival of worms on control or *atfs-1*(RNAi) exposed to *P. aeruginosa* or *E. coli*. (c and d) Images and quantitation of *P. aeruginosa*-GFP in wild-type or *atfs-1(tm4919)* worms on control or *spg-7*(RNAi). Scale bar, 0.1 mm. (*N* = 35 each treatment). (e) Survival of wild-type and *atfs-1(tm4919)* worms on control or *spg-7*(RNAi) exposed to *P. aeruginosa*. (f and g) Images and quantitation of *P. aeruginosa*-GFP in wild-type and *atfs-1(et18)* worms on control or *atfs-1*(RNAi) (*N* = 35 each treatment). Scale bar, 0.1 mm. (h) Survival of wild-type and *atfs-1(et18)* worms on control or *atfs-1*(RNAi) exposed to *P. aeruginosa*

[40]. Import into the mitochondrial matrix requires the TOM complex, the TIM23 complex, the electron transport chain (ETC), and the matrix-localized molecular chaperone HSP70. It was found that *tim-23(RNAi)* caused the ATFS-1::GFP to accumulate within the nuclei and strong induction of *hsp-60_{pr}::gfp* expression, and impairment of HSP-70 or the ETC by the *isp-1(qm150)* mutation or *cco-1(RNAi)* activated the mitochondrial UPR (Fig. 9.17) [40]. Meanwhile, the *haf-1(ok705)* mutant nematodes were unable to induce *hsp-60_{pr}::gfp* expression caused by the *clk-1(qm30)* mutation or 30 μg/ml EtBr (Fig. 9.17) [40]. Nevertheless, the mitochondrial UPR activation caused by the conditions that directly inhibited mitochon-

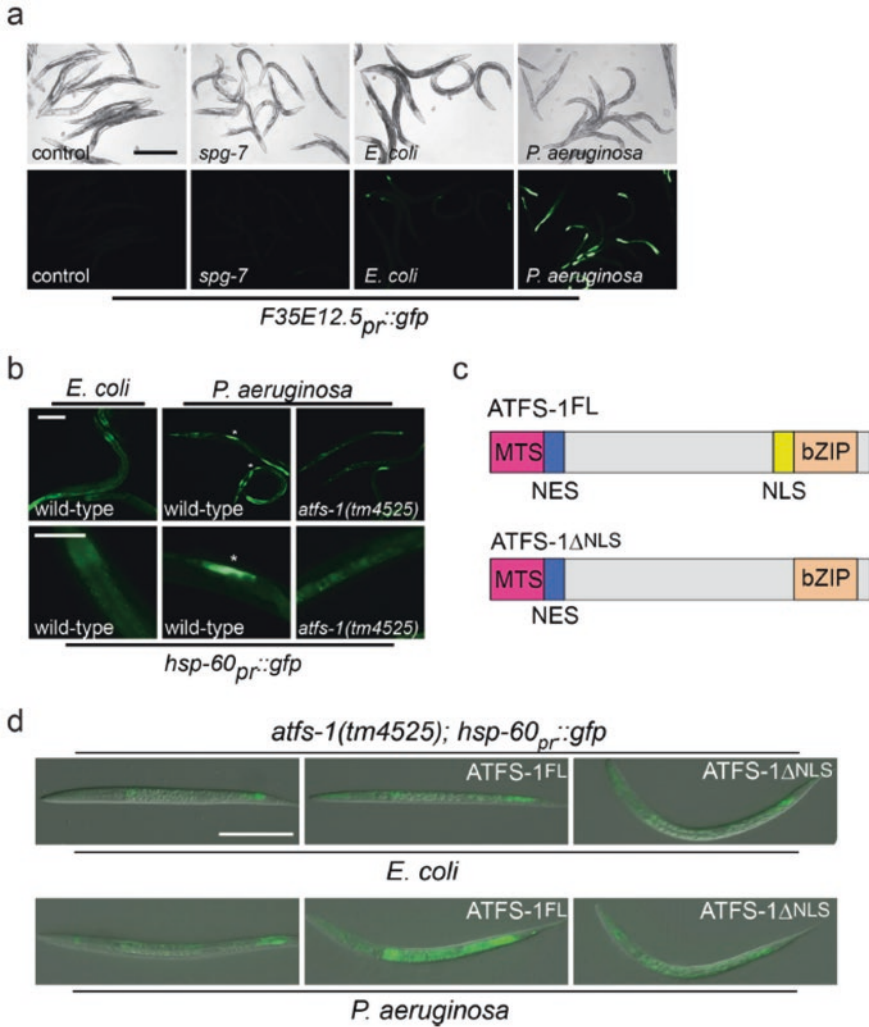


Fig. 9.16 Nuclear accumulation of ATFS-1 is required for UPR^{mt} activation during *P. aeruginosa* exposure [38]. **(a)** Representative photomicrographs of *F35E12.5_{pr}::gfp* transgenic worms raised on control or *spg-7*(RNAi). No detectable increase in expression was observed following *spg-7*(RNAi) treatment. In contrast, strong expression of *F35E12.5_{pr}::gfp* was observed following exposure to *P. aeruginosa* compared to *E. coli* controls. Scale bar, 0.5 mm. **(b)** Wild-type or *atfs-1(tm4525);hsp-60_{pr}::gfp* worms on *E. coli* or *P. aeruginosa*. Lower panels are magnified views of the intestine showing enhanced expression of *hsp-60_{pr}::gfp* (asterisks). Scale bars, 0.05 mm. **(c)** Diagrams of wild-type ATFS-1 (ATFS-1^{FL}) and ATFS-1 with a mutated nuclear localization signal (ATFS-1^{ΔNLS}). **(d)** Photomicrographs of *atfs-1(tm4525);hsp-60_{pr}::gfp* worms expressing ATFS-1^{FL} or ATFS-1^{ΔNLS} via the *hsp-16* promoter exposed to *E. coli* or *P. aeruginosa*. Scale bar, 0.1 mm

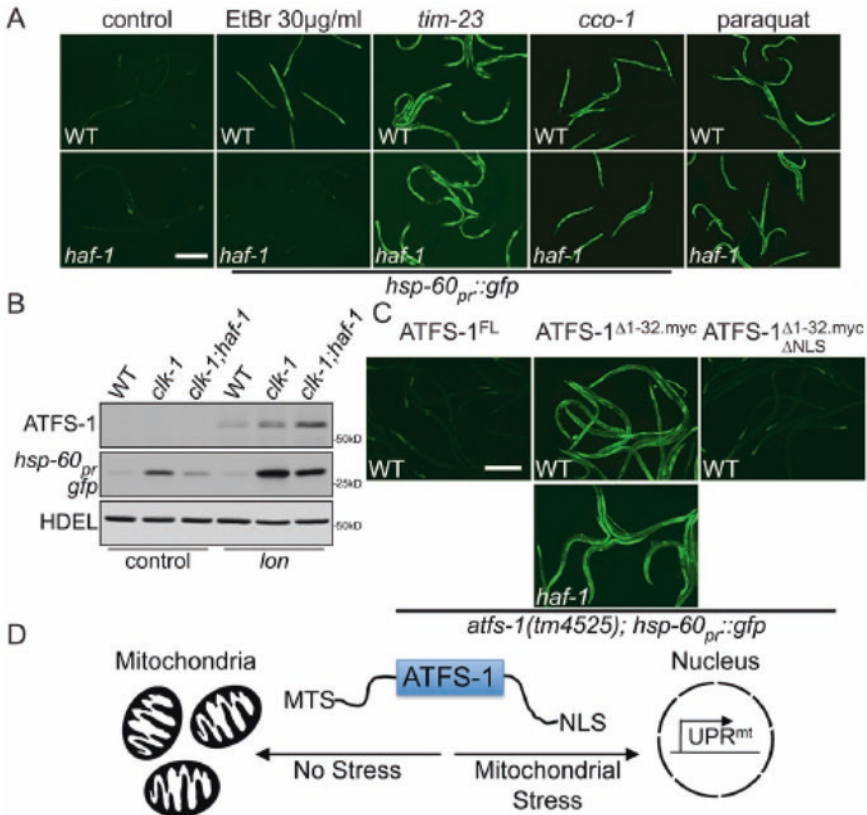


Fig. 9.17 HAF-1 modulates UPR^{mt} signaling by slowing mitochondrial import of ATFS-1 [40]. (a) Photomicrographs of wild-type and *haf-1(ok705); hsp-60^{pr}::gfp* worms raised on control, *tim-23*, *cco-1(RNAi)*, EtBr, or 0.5 mM paraquat. Scale bar, 0.5 mm. The images for *cco-1(RNAi)* and paraquat were exposed longer because of smaller worm size. (b) Immunoblots of wild-type, *clk-1(qm30)* or *clk-1(qm30); haf-1(ok705)* worms raised on control or *lon(RNAi)*. (c) Photomicrographs of *atfs-1(tm4525); hsp-60^{pr}::gfp* worms expressing wild-type (^{FL}) ATFS-1, ATFS-1^{Δ1-32.myc}, or ATFS-1^{Δ1-32.myc.ΔNLS} raised on control(RNAi). The lower panel harbors the *haf-1(ok705)* allele. Scale bar, 0.5 mm. (d) Schematic illustrating ATFS-1 regulation

drial import, such as *tomm-40(RNAi)*, *tim-23(RNAi)*, *cco-1(RNAi)*, or paraquat, did not require the *haf-1* (Fig. 9.17) [40], suggesting that HAF-1 affects the mitochondrial UPR signaling by modulating the mitochondrial import of ATFS-1. Mutating the NLS in ATFS-1 lacking the MTS could prevent HSP-60::GFP expression (Fig. 9.17) [40], indicating that when ATFS-1 cannot be imported into mitochondria, ATFS-1 requires the NLS for further mitochondrial UPR activation.

9.4.2.2 Chromatin Remodeling

It was further observed that the chromatin can be specifically remodeled during mitochondrial dysfunction to promote the mitochondrial UPR activation [36]. During this process, histone methyltransferase MET-2 in concert with LIN-65, along with two jumonji domain histone demethylases, JMJD-3.1 and JMJD-1.2, was required for mitochondrial UPR activation [36].

In nematodes, both the homeodomain-containing transcription factor DVE-1 and the small ubiquitin-like protein UBL-5 were required for the activation of mitochondrial UPR [41]. The activation of the mitochondrial UPR was also correlated temporally and spatially with nuclear redistribution of DVE-1 and the enhanced binding to the promoters of mitochondrial chaperone genes [41]. Moreover, the chromatin state could be stabilized by the DVE-1 and the UBL-5 [36].

9.4.2.3 NDUF-7

In nematodes, NDUF-7 is a component of complex I in the mitochondrial electron transport chain. The loss-of-function *nduf-7(et19)* mutant nematodes exhibit constitutive and ATFS-1-dependent activation of mitochondrial UPR and prolonged lifespan, and these phenotypes were mediated by the ROS production (Fig. 9.18) [42]. Additionally, the lifespan extension of *nduf-7(et19)* mutant nematodes was dependent on pro-apoptotic gene *ced-4* (Fig. 9.18) [42]. These data imply the important role of NDUF-7-mediated molecular basis for ROS in activating ATFS-1 and mitochondrial UPR in nematodes exposed to environmental toxicants or stresses.

9.4.3 *Targets of Mitochondrial UPR Signaling Pathway in Nematodes Exposed to Environmental Toxicants or Stresses*

9.4.3.1 Mitochondrial Components Required for the Control of Mitochondrial Function

In nematodes, HSP-6, HSP-60, and DNJ-10 (mitochondrial chaperones), MPPA-1 (a subunit of the mitochondrial presequence processing protease), PPGN-1 (a matrix-localized protease), GLRX-5 (a glutaredoxin that functions in mitochondrial iron–sulfur cluster biogenesis), MRPS-14 (a subunit of the mitochondrial ribosome), and TSFM-1 (a mitochondrial translational elongation factor) could be induced during mitochondrial dysfunction by ATFS-1 (Fig. 9.19) [36, 40]. The detailed information was discussed in the review [36].

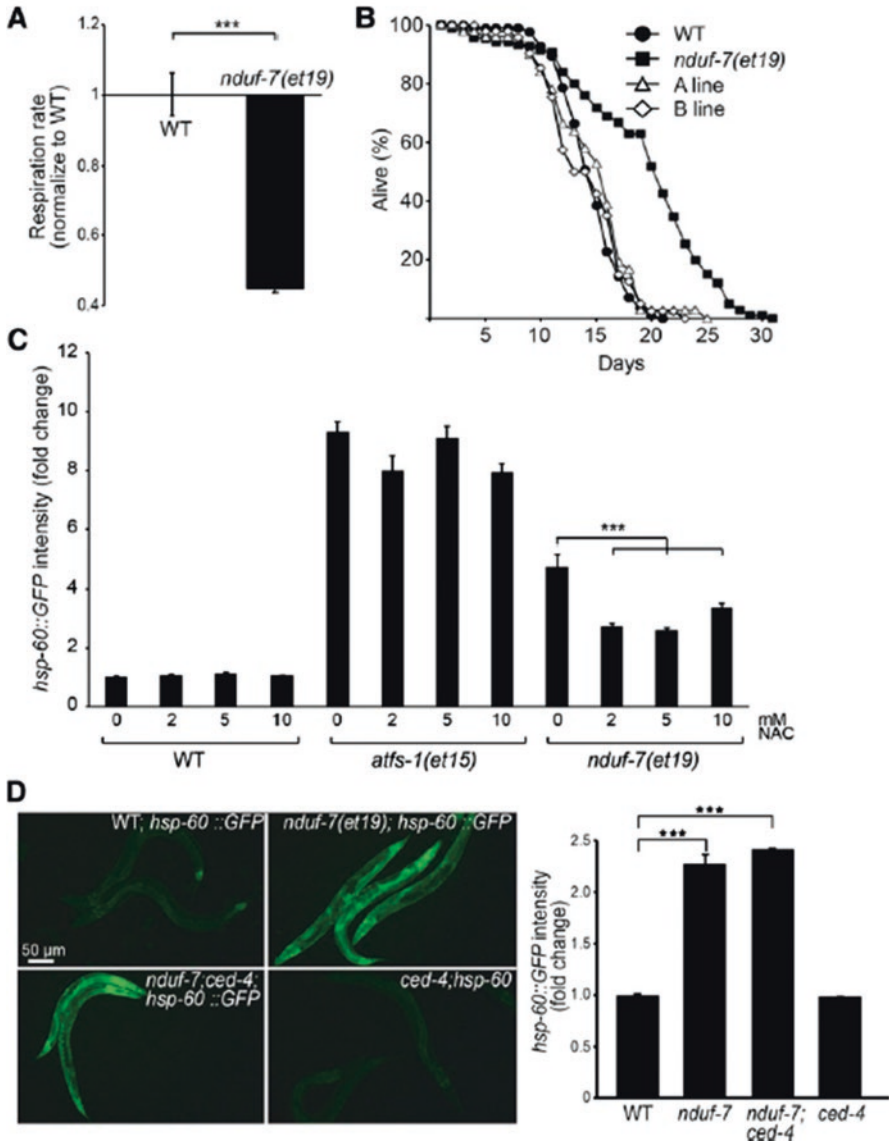


Fig. 9.18 The *nduf-7(et19)* mutant has defective respiration and extended lifespan and requires ROS but not *ced-4* for UPR^{mt} activation [42]. (a) *nduf-7(et19)* mutant worms have reduced respiration rate. (b) *nduf-7(et19)* mutant worms have an extended lifespan that is suppressed when these worms carry wild-type *nduf-7* as a transgene (a and b lines). (c) Constitutive *hsp-60::GFP* expression is suppressed by nicotinic acid (NAC) in *nduf-7(et19)* mutant but not in *atfs-1(et15)* mutant worms. ****P* < 0.001 using Student's *t*-test. (d) The *ced-4(n1162)* mutation has no effect on its own or on the constitutive expression of *hsp-60::GFP* in the *nduf-7(et19)* mutant

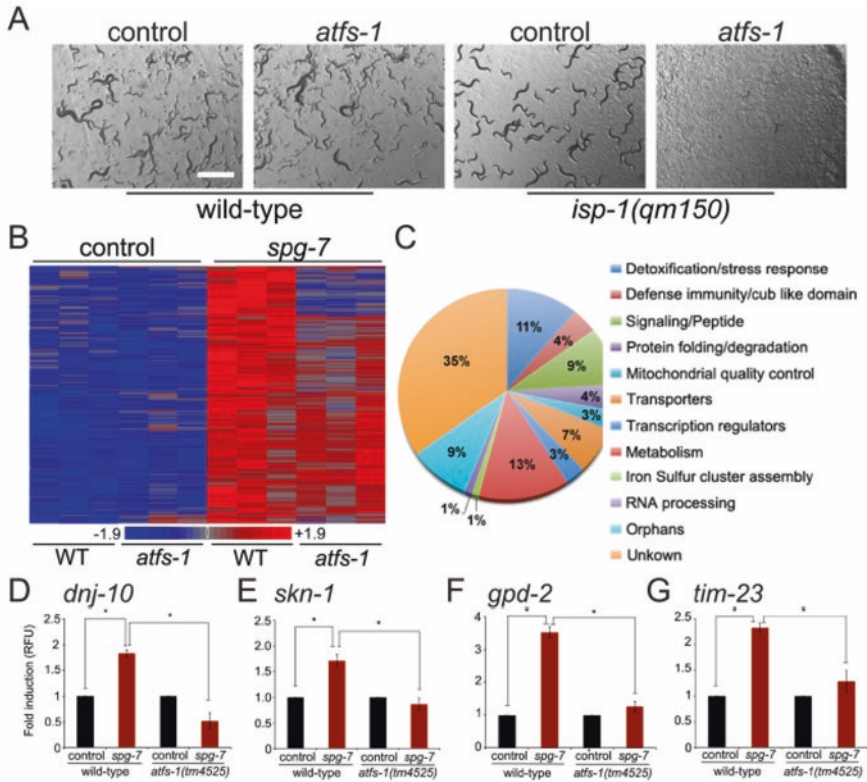


Fig. 9.19 ATFS-1 mediates a broad and protective transcriptional program [40]. (a) Representative photomicrographs of wild-type or *isp-1(qm150)* worms raised on control or *atfs-1(RNAi)*. Scale bar, 1 mm. (b) Heat map comparing gene expression patterns of wild-type or *atfs-1(tm4525)* worms raised on control or *spg-7(RNAi)*. (c) Functional categories of the 391 ATFS-1-dependent genes identified by hierarchical clustering. (d–g) Expression levels of *dnj-10*, *skn-1*, *gpd-2*, and *tim-23* mRNA in wild-type or *atfs-1(tm4525)* worms raised on control or *spg-7(RNAi)* determined by qRT-PCR ($N = 3$, \pm SD, p^* (Student’s t -test) < 0.05)

9.4.3.2 Antimicrobial Proteins

In nematodes, the antimicrobial peptide *abf-2*, secreted lysozyme *lys-2*, and two C-type lectins could be induced during the mitochondrial stress (Fig. 9.20) [38]. Meanwhile, it was found that the induction of innate immune genes by *spg-7(RNAi)* required the ATFS-1 (Fig. 9.20) [38], suggesting that ATFS-1 transcriptionally upregulated the innate immune genes during the mitochondrial stress.

In nematodes, *P. aeruginosa* also generates the exotoxin A, which impairs the protein synthesis and leads to induction of the innate immune gene (*irg-1*) via transcription factor ZIP-22. The induction of *irg-1pr::gfp* by mitochondrial stress was

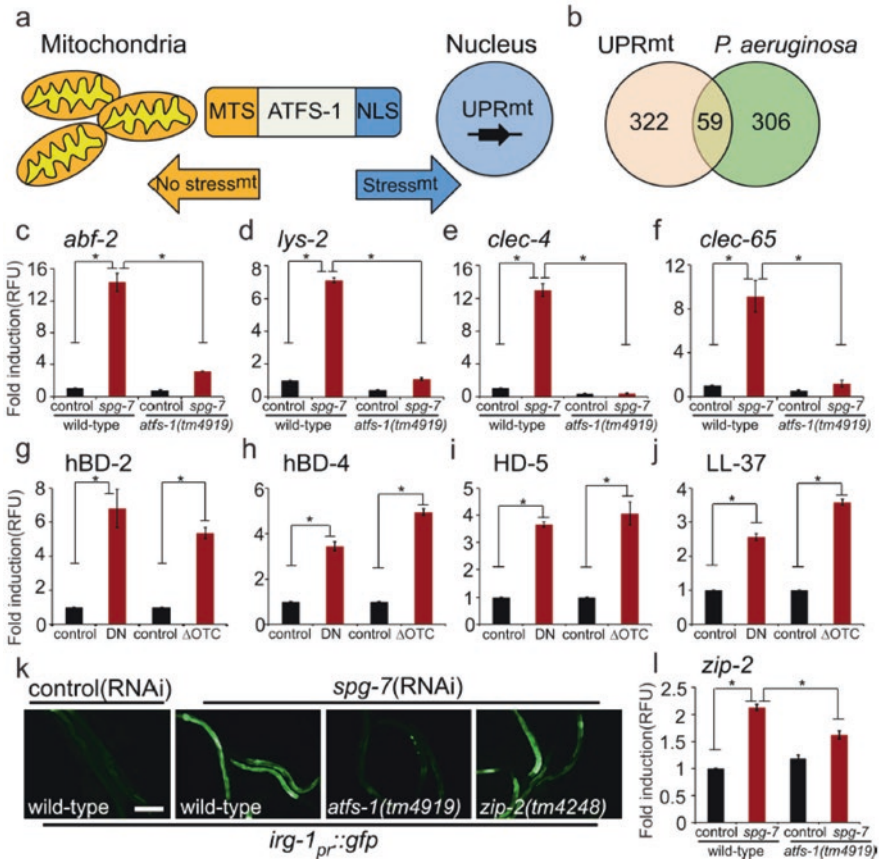


Fig. 9.20 ATFS-1 induces innate immunity genes during mitochondrial dysfunction [38]. (a) UPR^{mt} regulation. (b) ATFS-1-dependent UPR^{mt} genes in common with genes induced by *P. aeruginosa*. (c–f) *abf-2*, *lys-2*, *clec-4*, and *clec-65* transcripts in wild-type or *atfs-1(tm4919)* worms on control versus *spg-7(RNAi)* ($N = 3$, \pm SD), $*p < 0.05$ (Student’s *t*-test). (g–j) Antimicrobial peptide transcripts in mammalian cells during mitochondrial stress caused by expression of dominant-negative AFG3L2 (DN), or misfolded ornithine transcarbamylase (Δ OTC) ($N = 3$, \pm SD), $*p < 0.05$ (Student’s *t*-test). (k) *irg-1_{pr}::gfp* in wild-type, *atfs-1(tm4919)* or *zip-2(tm4248)* worms on control versus *spg-7(RNAi)*. Scale bar, 0.15 mm. (l) *zip-2* transcripts in wild-type or *atfs-1(tm4919)* worms on control or *spg-7(RNAi)* ($N = 3$, \pm SD), $*p < 0.05$ (Student’s *t*-test)

also blocked in *atfs-1(tm4919)* and partially in *zip-2(tm4248)* mutant nematodes (Fig. 9.20) [38]. Additionally, the ZIP-22 induction during the mitochondrial stress also required the *atfs-1* (Fig. 9.20) [38]. Therefore, ATFS-1 regulates a subset of innate immune genes during the mitochondrial stress in nematodes exposed to environmental toxicants or stresses.

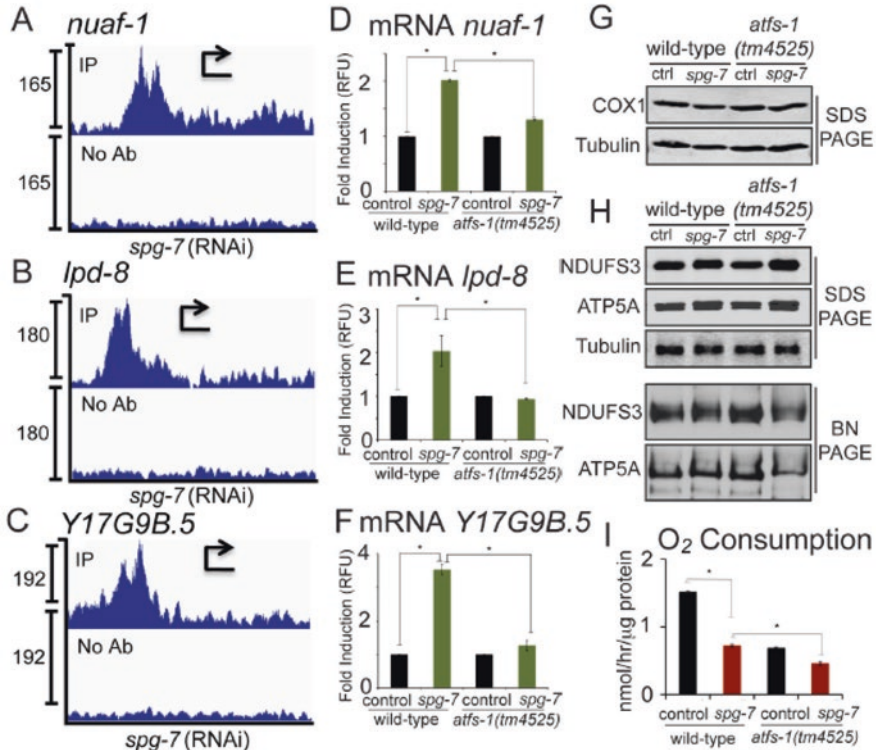


Fig. 9.21 ATFS-1 promotes OXPHOS complex assembly during mitochondrial dysfunction [43]. (a–c) ChIP-seq profiles of *nuaf-1*, *lpd-8*, and *Y17G9B.5* of wild-type worms raised on *spg-7*(RNAi), using ATFS-1 antibody or no antibody. The y-axis is the number of sequence reads, and the x-axis is approximately 2.5 kilobases with the start codon marked with an arrowhead. (d–f) Expression levels of *nuaf-1*, *lpd-8*, and *Y17G9B.5* mRNA in wild-type or *atfs-1(tm4525)* worms raised on control or *spg-7*(RNAi) determined by qRT-PCR ($N = 3$, \pm SD, p^* (Student’s t -test) <0.05) (right panels). (g) SDS-PAGE immunoblots of extracts from wild-type and *atfs-1(tm4525)* worms raised on control or *spg-7*(RNAi). COX1 is a component of the cytochrome c oxidase complex (IV), and tubulin was used as a loading control. (h) SDS-PAGE immunoblots of extracts from wild-type and *atfs-1(tm4525)* worms raised on control or *spg-7*(RNAi) (upper three panels). The lower two panels are blue-native PAGE immunoblots of the same extracts. NDUFS3 is a component of the NADH ubiquinone oxidoreductase complex, ATP5A is an ATP synthase component, and tubulin was used as a loading control. (i) Oxygen consumption in wild-type or *atfs-1(tm4525)* worms raised on control or *spg-7*(RNAi) ($N = 3$, \pm SD, p^* (Student’s t -test) <0.05)

9.4.3.3 Oxidative Phosphorylation Machinery (OXPHOS) Complex

ATFS-1 also bound the promoters of OXPHOS complex assembly factors and iron–sulfur biogenesis components. For example, ATFS-1 bound promoters of *nuaf-1* and *Y17G9B.5* (*ECSIT*), two NADH ubiquinone oxidoreductase assembly factors, and *lpd-8* (*NFU1*), a Fe–S cluster biogenesis component, and these genes could be induced during mitochondrial stress in an *atfs-1*-dependent manner (Fig. 9.21) [43].

atfs-1(tm4525) mutant nematodes expressed higher levels of NDUFS3 (complex I) and ATP5A (complex V) when raised on *spg-7(RNAi)* (Fig. 9.21) [43], suggesting that *atfs-1* limits the OXPHOS mRNA accumulation. Additionally, assembly of complexes I and V was reduced in *atfs-1*-deletion nematodes (Fig. 9.21) [43], suggesting that ATFS-1 promotes the OXPHOS process in nematodes.

9.5 Endoplasmic Reticulum (ER) UPR

9.5.1 Induction of ER UPR in Nematodes Exposed to Environmental Toxicants or Stresses

9.5.1.1 Induction of ER UPR by Environmental Toxicants or Stresses

With the pore-forming toxin (PFT) of Cry5B as an example and *hsp-4::GFP* (the *ire-1* regulated gene) and *xbp-1* expression as the markers of ER UPR, feeding the *Escherichia coli* expressing Cry5B induced the increase in both *xbp-1* expression and intestinal *hsp-4::GFP* expression (Fig. 9.22) [44], suggesting the induction of ER UPR and the activation of IRE-1 pathway in nematodes exposed to environmental toxicants or stresses.

9.5.1.2 Alteration in ER UPR Induction During the Aging Process

In nematodes, the *hsp-4p::GFP* could also be induced by tunicamycin, an inhibitor of N-linked glycosylation, and this induction was dependent upon *xbp-1* and *ire-1* (Fig. 9.23) [45]. The induction of *hsp-4p::GFP* was robust at days 1–2 of adulthood, but reduced sharply by days 3–4 (Fig. 9.23) [45]. Moreover, the induction of *hsp-4p::GFP* was nonexistent by days 7–10 of adulthood during the aging process (Fig. 9.23) [45]. The similar performance was also observed for the *xbp-1* expression (Fig. 9.23) [45]. Moreover, the transcriptional upregulation of UPR^{ER} target genes (*hsp-4*, *crt-1*, *T14G8.3*, and *Y41C4A.11*) was also significantly reduced by day 5 (Fig. 9.23) [45]. That is, both the *xbp-1* splicing and the UPR^{ER}-induced transcriptional changes can be abrogated with the aging process in nematodes.

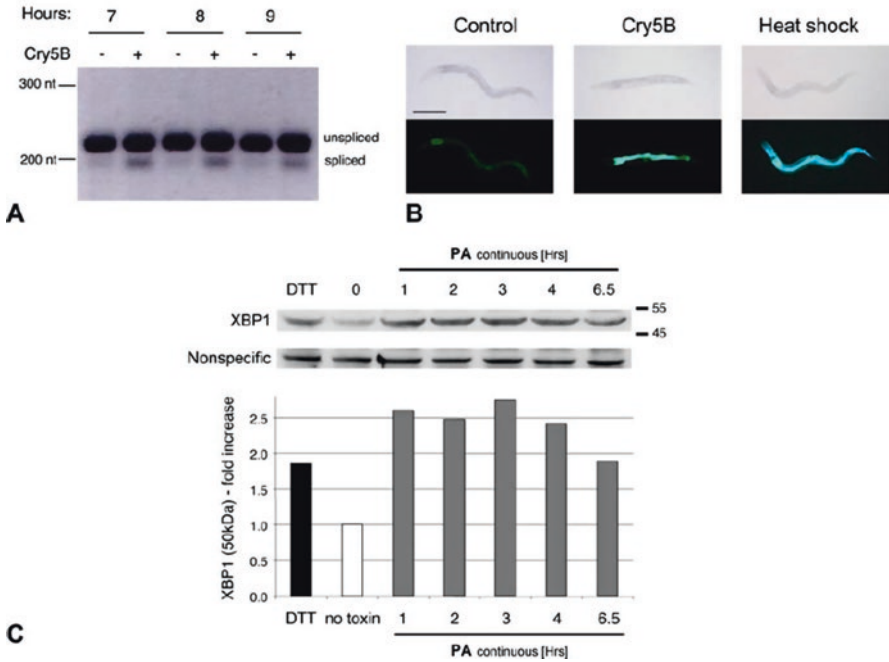


Fig. 9.22 The IRE-1 UPR is activated in response to PFTs [44]. (a) *xbp-1* mRNA splicing is induced in wild-type *C. elegans* fed *E. coli* expressing Cry5B compared to control *E. coli* not expressing Cry5B. The time the worms were allowed to feed on the *E. coli* before total RNA was prepared for RT-PCR is indicated at the top, and the positions of the nucleotide size markers are indicated at the left. (b) Compared to worms fed control non-Cry5B-expressing *E. coli*, in vivo activation of *hsp-4::GFP* occurs specifically in the intestines of worms fed Cry5B-expressing *E. coli* for 8 h. As a comparison for GFP induction, separate worms on control bacteria were heat shocked at 30 °C for 8 h to induce the ER stress response by causing unfolded proteins. The heat shock worms have a strong increase in GFP throughout the body including the head, intestine, and hypodermis. Thus, although the entire worm is capable of activating the *ire-1-xbp-1* pathway as judged by *hsp-4* induction, activation in Cry5B-fed animals is occurring only in those cells targeted by the PFT. Images taken by light microscopy are compared to images with fluorescence microscopy. Scale bar is 0.2 mm. The experiment was performed three times, and representative worms are shown. (c) Aerolysin induces activation of IRE1 in mammalian cells. Exposure of HeLa cells to proaerolysin (2 ng/mL) leads to increased production of spliced XBP1 protein as shown on this immunoblot (upper) and quantitated relative to no toxin control (lower). DTT (10 mg/mL for 2 h) was used as a positive control. Positions of molecular weight markers (kDa) are indicated on the right side of the figure. A nonspecific antibody-reacting band was used as a loading control and normalization of the XBP1 signal in each lane

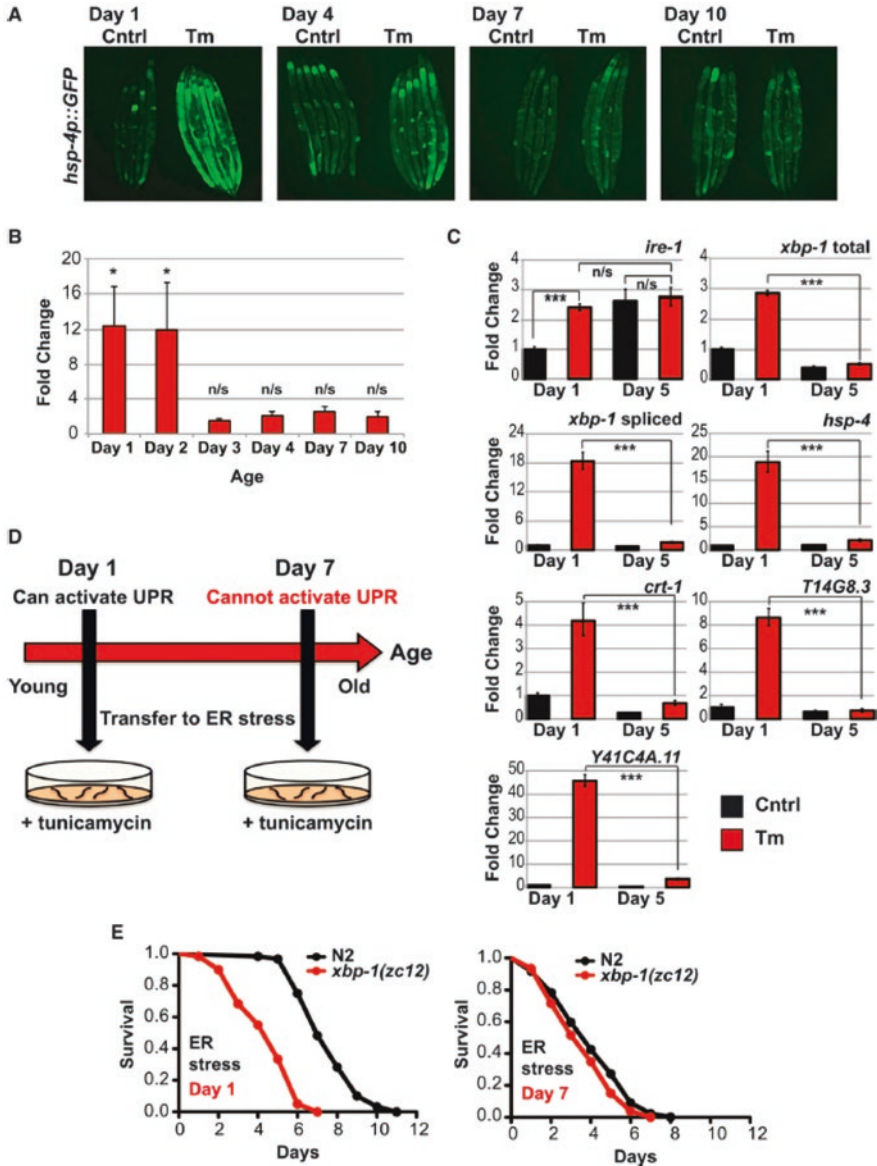


Fig. 9.23 The ability to activate the UPR^{ER} declines with age [45]. (a) *hsp-4p::GFP* UPRER reporter worms were treated at days 1, 4, 7, and 10 of adulthood with 25 ng/μl tunicamycin in M9 buffer, or buffer only, for 4 h, and GFP fluorescence assessed. (b) *hsp-4p::GFP* UPRER reporter worms were treated as above at days 1, 2, 3, 4, 7, and 10 of adulthood, and GFP expression was measured by fluorimetry. Fold inductions relative to untreated animals are shown, with error bars indicating mean ± standard error of the mean (SEM) ($n = 3$). A Student's *t*-test was used to assess statistical significance of induction at each age: * $p < 0.05$, *n/s* = not significant. (c) N2 animals were treated as above at day 1 and day 5 of adulthood. Transcript levels of UPR regulators and targets in tunicamycin-treated (red) and untreated (black) animals were measured by quantitative

9.5.2 Molecular Basis for ER UPR Induced by Environmental Toxicants or Stresses

9.5.2.1 ER UPR Transducers (IRE-1, PEK-1, and ATF-6)

In nematodes, *ire-1* encodes a transmembrane serine/threonine protein kinase, *pek-1* encodes a transmembrane protein kinase, and *atf-6* encodes an ortholog of mammalian transmembrane ATF6 α . IRE-1, PEK-1, and ATF-6 are three important ER UPR transducers in nematodes. Under the normal conditions, among the examined *atf-6(ok551)*, *pek-1(ok275)*, and *ire-1(v33)* mutant nematodes, the *ire-1(v33)* mutant nematodes are clearly smaller than the other strains [44]. Among these genes, the severe susceptibility to the toxicity was observed only in *ire-1(v33)* mutant or *ire-1(RNAi)* nematodes exposed to the PFT toxin of Cry5B at the low moderate levels (Fig. 9.24) [44]. Additionally, the moderate susceptibility to the toxicity was also observed in the *atf-6(ok551)* mutant nematodes exposed to the PFT toxin of Cry5B at the low moderate levels (Fig. 9.24) [44]. No susceptibility to the toxicity was observed in the *pek-1(ok275)* mutant nematodes exposed to the PFT toxin of Cry5B at the low moderate levels (Fig. 9.24) [44]. Therefore, both ATF-6 and IRE-1 are involved in the regulation of toxicity of environmental toxicants or stresses in nematodes.

9.5.2.2 XBP-1

xbp-1 encodes a bZIP transcriptional factor. The XBP-1 protein encoded by the processed murine *xbp-1* mRNA accumulated during the ER UPR, whereas the protein encoded by unprocessed *xbp-1* mRNA did not [47]. In nematodes, it has been shown that *xbp-1* mRNA is an IRE-1 substrate or a direct target required for the IRE-1 signaling [46, 47]. Activation of the ER UPR caused the IRE-1-dependent splicing of a small intron from *xbp-1* mRNA [47]. In nematodes, mutations in either *ire-1* or *xbp-1* could abolish the ER UPR induction [47].

Among the examined *atf-6(ok551)*, *pek-1(ok275)*, *ire-1(v33)*, and *xbp-1(zc12)* mutant nematodes, the susceptibility was observed only in the *ire-1(v33)* and the *xbp-1(zc12)* mutant nematodes exposed to the PFT toxin of Cry5B at the low moderate levels (Fig. 9.24) [44]. Meanwhile, expression of *xbp-1s* under the *sur-5p* promoter constitutively could activate the ER UPR and prevent the decline in ER stress resistance [45].

←
Fig. 9.23 (continued) RT-PCR, with error bars indicating mean \pm standard deviation (SD). A Student's *t*-test was used to assess significance: *** $p < 0.005$, *n/s* = not significant. **(d)** Schematic describing the measurement of age-dependent ER stress resistance. Animals are transferred to plates containing tunicamycin at either day 1 or day 7 of adulthood. **(e)** N2 (black) and *xbp-1(zc12)* (red) animals were transferred at day 1 and day 7 of adulthood to plates containing 50 $\mu\text{g/ml}$ tunicamycin, and survival was monitored (N2 day 1, median lifespan 7 days; *xbp-1(zc12)* day 1, median lifespan 5 days; $p < 0.0001$. N2 day 7, median lifespan 4 days; *xbp-1(zc12)* day 7, median lifespan 4 days; $p = 0.9211$)

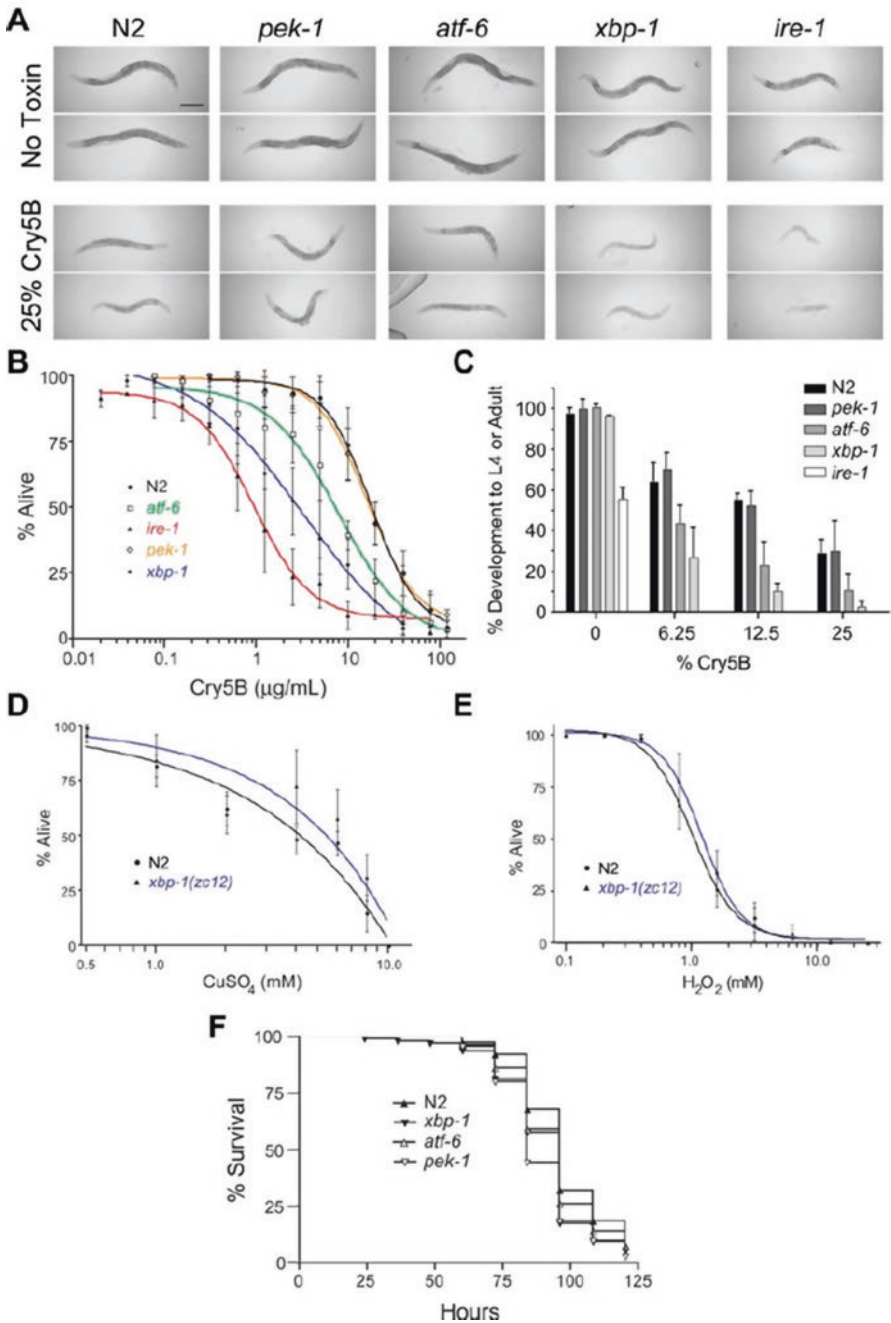


Fig. 9.24 Loss of specific UPR pathways causes hypersensitivity to PFT but not other toxins or pathogenic bacteria [44]. (a) Comparison of ER stress response mutants to wild-type N2 on 25% Cry5B-expressing *E. coli* plates indicates *ire-1(v33)* and *xbp-1(zc12)* are hypersensitive to Cry5B

In nematodes, neuronal *xbp-1s* expression could induce a cell-nonautonomous activation of the ER UPR [45]. Additionally, it was observed that the expression of intestinal XBP-1 was required for the protection of nematodes against the Cry5B PFT toxicity [44]. Therefore, both neuronal and intestinal activities of XBP-1 are necessary for XBP-1 in regulating the ER UPR in nematodes exposed to environmental toxicants or stresses. Upon the ER stress, activation of *hsp-4p::GFP* expression was dependent on the presence of functional IRE-1 and XBP-1 [45]. After expression of *rab-3p::xbp-1s* in *hsp-4p::GFP* animals that had an *ire-1(v33)* mutant background, it was further found that the *ire-1(v33)* mutation prevented ER UPR activation in the intestine of *rab-3p::xbp-1s* animals expressing neuronal XBP-1, whereas the neuronal ER UPR activation was still significantly upregulated (Fig. 9.25) [45]. Meanwhile, after feeding with *xbp-1* RNAi, ER UPR in neurons was significantly activated by neuronally expressed *xbp-1s*; however, the distal ER UPR induction was abolished by *rab-3p::xbp-1s* (Fig. 9.25) [45]. That is, endogenous IRE-1 signaling regulates the cell-nonautonomous ER UPR activation in distal cells, and the endogenous XBP-1 is required for the perception of this signal.

In addition, the increase in both IRE-1 and PEK-1 activities in XBP-1 deficiency in the absence of exogenous compounds to impose the ER stress implies that the ER UPR signaling maintains ER homeostasis in response to the extremes of ER stress, and the negative feedback loops involving the activation of IRE-1-XBP-1 and PEK-1 pathways may be formed in nematodes [48].

←

Fig. 9.24 (continued) intoxication. Two representative worms are shown for each strain 48 h after feeding either on *E. coli* without Cry5B or on *E. coli* of which 25% expressed Cry5B. Scale bar is 0.2 mm. **(b)** A lethal concentration assay was performed using purified Cry5B toxin to quantitatively compare sensitivities of wild-type N2 and the ER stress mutants. Lethality was determined after 8 days. This semi-log graph represents three independent experiments, and each data point is the mean and standard deviations of the experiments. **(c)** A Cry5B developmental inhibition assay was performed beginning with synchronized worms at the first larval stage. Worms were grown on plates containing different percentages of Cry5B-expressing *E. coli* (% Cry5B as indicated under the figure), and the percent of worms reaching the L4 stage or adulthood 72 h later is indicated. *ire-1(v33)* was included only on the plates with 0% Cry5B. Data are presented as mean and standard deviation. **(d)** A lethal concentration assay comparing sensitivity to CuSO₄ revealed *xbp-1(zc12)* is not hypersensitive compared to wild-type N2. Lethality was determined after 8 days of CuSO₄ exposure, the same time frame as the Cry5B lethality assay. Data, plotted semi-log, are the mean and standard deviation of three independent experiments. **(e)** A lethal concentration assay comparing sensitivity to H₂O₂ revealed *xbp-1(zc12)* is not hypersensitive compared to wild-type N2. Lethality was determined after 4 h of H₂O₂ exposure. Data, plotted semi-log, are the mean and standard deviation of three independent experiments. **(f)** A lifespan assay was used to compare the ER stress mutants to slow killing by *P. aeruginosa* PA14. This graph represents combined data from three experiments

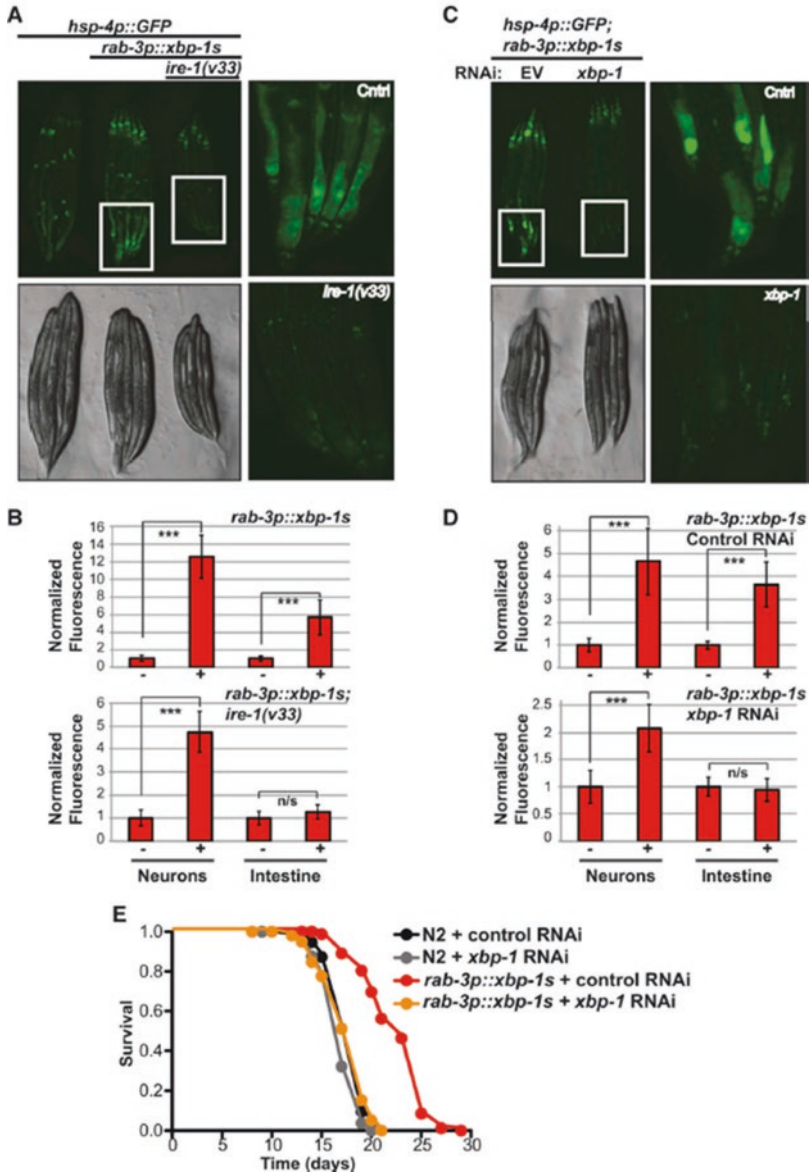


Fig. 9.25 Cell-nonautonomous activation of the UPR^{ER} requires *ire-1* and *xbp-1* [45]. (a) Fluorescent micrograph of *hsp-4p::GFP* and *hsp-4p::GFP*; *ire-1(v33)* worms expressing *rab-3p::xbp-1s* at day 1 of adulthood. (b) Using a COPAS Biosort, fluorescence in the nerve ring and intestine was approximated by measuring GFP fluorescence in equidistant sections through the proximal 25% (nerve ring) and distal 75% (intestine) of *hsp-4p::GFP* (-) and *hsp-4p::GFP*; *rab-3p::xbp-1s* or *hsp-4p::GFP*; *rab-3p::xbp-1s*; *ire-1(v33)* (+) worms. Total fluorescence in each region was divided by number of sections to give average fluorescence per section, which was then averaged among animals and normalized to control *hsp-4p::GFP* worms. Error bars indicate

9.5.2.3 HPL-2

hpl-2 encodes the homolog of heterochromatin protein 1 (HP1). In nematodes, it has been shown that HPL-2 downregulates the intestinal ER UPR [49]. Inactivation of HPL-2 caused an enhanced resistance to ER stress, and this was dependent on the XBP-1 and the induction of autophagy as reflected by the expressions of LGG-1 and LGG-2 (Fig. 9.26) [49]. The increased resistance to ER stress in *hpl-2* mutant nematodes was associated with the increased basal levels of XBP-1 activation and ER chaperone expression under the physiological conditions [49]. The activities of both intestinal and neuronal HPL-2 were required for its function in influencing the ER stress response, and the intestinal HPL-2 expression was sufficient to rescue the stress resistance [49]. For the underlying mechanism, it was raised that the retinoblastoma protein homolog LIN-35 and the LIN-13 zinc finger protein acted in the same pathway with HPL-2 to limit the ER stress response [49]. The LIN-13 can physically interact with and recruit the HPL-2 to the nuclear foci. That is, HPL-2 may regulate the ER UPR response in nematodes exposed to environmental toxicants or stresses by affecting the functions of these two retinoblastoma proteins.

9.5.2.4 Components for mRNA Surveillance

Based on the RNAi screen of mutants exhibiting synthetic growth and intestinal defects with the *ire-1(v33)* mutant nematodes, genes (*exos-3* and *F48E8.6*) encoding subunits of the exosome complex that functions in mRNA surveillance were identified for the induction of ER UPR response [50]. RNAi knockdown of these genes caused the ER stress [50]. Additionally, as indicated by the alterations in HSP-4::GFP and *hsp-4* expression, the ER UPR could be activated in nematodes with the mutations of *smg-1* or *smg-6* encoding the products required for nonsense-mediated mRNA decay (NMD) [50], suggesting the involvement of NMD-mediated mRNA quality in controlling the ER UPR response. Although the ER stress could not activate the mRNA surveillance complex assembly, these observations imply the potential interaction between mRNA surveillance control and induction of ER UPR response in nematodes exposed to environmental toxicants or stresses.

←
Fig. 9.25 (continued) mean ± SD. A Student's *t*-test was used to assess significance: ****p* < 0.005, *n/s* = not significant. (c) Fluorescent micrograph of *hsp-4p::GFP; rab-3p::xbp-1s* worms grown on empty vector and *xbp-1* RNAi. (d) Fluorescence in the nerve ring and intestine was approximated as above in *hsp-4p::GFP* animals on control empty vector RNAi (–) and *hsp-4p::GFP; rab-3p::xbp-1s* animals on control or *xbp-1* RNAi (+). Error bars indicate mean ± SD. A Student's *t*-test was used to assess significance: ****p* < 0.005, *n/s* = not significant. (e) Survival of *rab-3p::xbp-1s* and N2 worms grown on empty vector control or *xbp-1* RNAi (*rab-3p::xbp-1s* on *xbp-1* [red], median lifespan 18 days; *rab-3p::xbp-1s* on empty vector [orange], median lifespan 22 days; *p* < 0.0001)

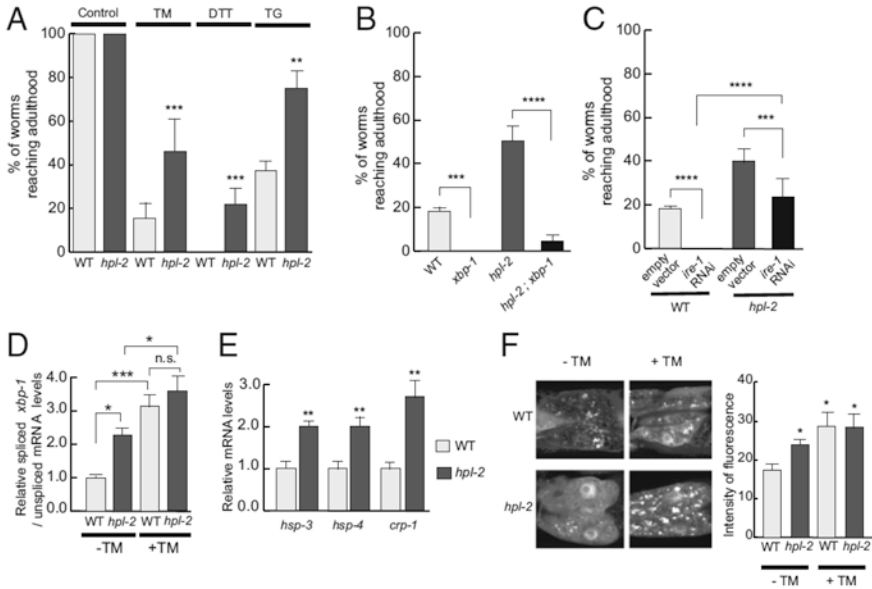


Fig. 9.26 Loss of HPL-2 increases ER stress resistance and activates the UPR [49]. (a) Survival assay showing the proportion of wild-type (WT) or *hpl-2* animals reaching adulthood after 72 h of development from eggs laid on plates containing 3 μg/mL tunicamycin (TM), 5 mM DTT, or 10 μM thapsigargin (TG) at 20 °C. Two-way ANOVA with factors “genotype” (WT, *hpl-2*) and “treatment” (control, TM, DTT, and TG) was used for statistical analysis. (b) and (c) HPL-2 acts through XBP-1 and IRE-1 to influence the ER stress response. (b) Survival assay of mutant animals treated as in A (3 μg/mL TM). One-way ANOVA with factor genotype (WT, *xbp-1*, *hpl-2*, *xbp-1;hpl-2*). (c) Survival assay on RNAi animals treated as in A (3 μg/mL TM). Two-way ANOVA with factors genotype (WT, *hpl-2*) and “presence or absence of *ire-1* RNAi.” (d) Quantitative real-time PCR (qPCR) analysis of total and spliced *xbp-1* mRNA in *hpl-2* relative to WT young adults grown on plates with or without TM (5 μg/mL) for 6 h. Two-way ANOVA with factors genotype (WT, *hpl-2*) and specific treatment” (nontreated control, TM) (*n.s.*, not significant). (e) qPCR analysis of UPR targets in *hpl-2* mutant relative to WT young adults. (f) Quantification of *hsp-4::mCherry* expression in the intestine of WT and *hpl-2* animals grown on plates with or without TM (5 μg/mL, 8 h at 20 °C). For E and F, an unpaired Student’s *t*-test was performed. For all tests, **P* ≤ 0.05, ***P* ≤ 0.01, ****P* ≤ 0.005, *****P* ≤ 0.0001. ANOVA was performed using Graphpad Prism version 6.0 for Macintosh GraphPad software, followed by Holm–Sidak for all pairwise multiple comparisons. Results represent the mean of at least three independent experiments

9.5.3 Targets of ER UPR Signaling Pathway in Nematodes Exposed to Environmental Toxicants or Stresses

9.5.3.1 ABU Proteins

The ABU (activated in blocked UPR) family proteins were identified to be potentially induced in ER-stressed *xbp-1* mutant nematodes compared with those in ER-stressed wild-type nematodes [51]. Among these genes, RNAi knockdown of *abu-1* activated the ER stress marker *hsp-4::gfp* in otherwise normal animals and killed 50% of ER-stressed *ire-1* and *xbp-1* mutant nematodes [51].

More importantly, RNAi knockdown of *abu-1* enhanced the effect of RNAi knockdown of *sel-1* encoding a protein functioning in ER-associated protein degradation [51], suggesting that the ABU proteins may interact with abnormal ER client proteins to induce an impaired UPR in nematodes.

9.5.3.2 Immune Response Genes

Mutation or RNAi knockdown of *vit-1*, *vit-2*, *vit-4*, or *vit-5* suppressed the enhanced ER UPR [52]. The more severe susceptibility to pathogen infection was observed in *vit-1*, *vit-2*, *vit-4*, or *vit-5* mutant nematodes with the RNAi knockdown of *xbp-1* or *ire-1* compared with the *xbp-1(RNAi)* or *ire-1(RNAi)* [52], suggesting that VIT proteins act in parallel pathways with IRE-1-XBP-1 signaling in the regulation of ER UPR response in nematodes exposed to environmental toxicants or stresses.

During the control of innate immunity, it was further observed that a subset of downregulated genes associated with defense responses to Gram-negative and Gram-positive bacteria were enriched in *vit-2* mutant nematodes, and these downregulated genes included lysozymes, saposin-like proteins (*spp* genes), and C-type lectins (Fig. 9.27) [52], suggesting that VIT proteins may regulate the innate immune response by activating the antimicrobial proteins in nematodes.

9.5.4 Upregulators of ER UPR Signaling Pathway in Nematodes Exposed to Environmental Toxicants or Stresses

9.5.4.1 p38 MAPK Signal Pathway

The p38 MAPK signaling activation and the upregulation of *ttm-2*, a downstream transcriptional target of the p38 MAPK pathway, could occur normally in the *xbp-1(zc12)* mutant nematodes [44], suggesting that the ER UPR is not required for the activation of p38 MAPK signaling pathway in response to environmental toxicants or stresses in nematodes. It was further found that the activation of *ire-1-xbp-1* pathway and HSP-4::GFP in response to PFT was dependent on the p38 MAPK signaling pathway [44], implying that the p38 MAPK signaling pathway is required for the activation of the *ire-1-xbp-1* pathway in nematodes exposed to environmental toxicants or stresses.

9.5.4.2 CDC-48-RUVB-2 Signaling Cascade

In organisms, ER accumulation of misfolded proteins activates the ER UPR response in order to restore the ER homeostasis. In nematodes, AAA⁺ ATPase p97/CDC-48 plays a key role in the ER stress by promoting both ER protein degradation and

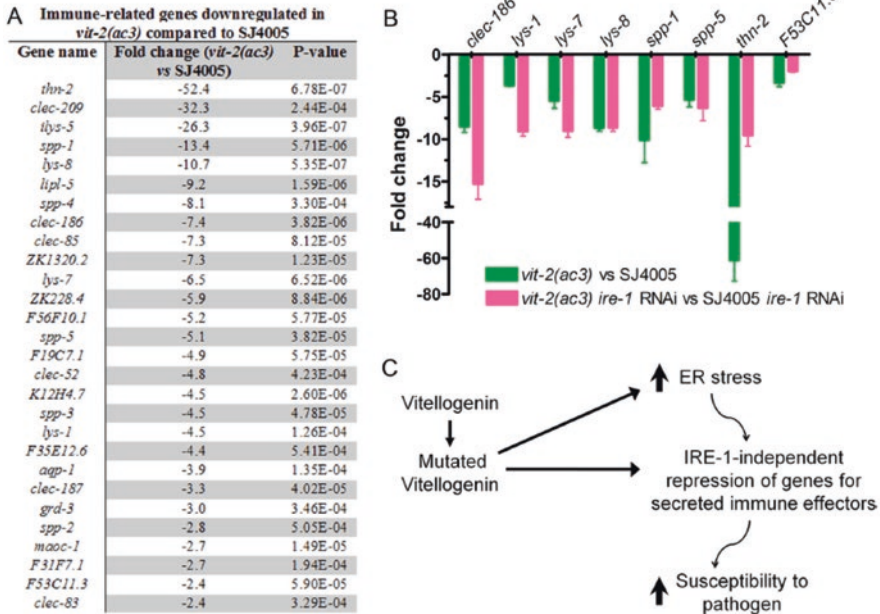


Fig. 9.27 *vit-2(ac3)* animals exhibit reduced expression of immune genes [52]. (a) List of immune-related genes that are downregulated in *vit-2(ac3)* animals compared to SJ4005 animals. (b) qRT-PCR for selected immune genes. The bar graph shows the means plus SD for three independent experiments. Comparing the values of all genes in *vit-2(ac3)* animals versus SJ4005 animals, $P < 0.0001$. (c) Model for the effects of mutations in vitellogenin proteins on innate immunity. Mutations in vitellogenin proteins lead to enhanced ER stress. Accumulation of mutated vitellogenin proteins and/or enhanced ER stress leads to suppression of secreted immune effectors in an IRE-1-independent manner, resulting in an enhanced susceptibility to pathogen infection

transcription of ER UPR response genes [53]. Based on the reporter-based genome-wide RNAi screen, at least RUVB-2, a AAA⁺ ATPase, was identified as the repressor of ER UPR response genes, and the degradation of RUVB-2 by CDC-48 enhanced the expression of ER UPR response genes through an XBP1-dependent mechanism (Fig. 9.28) [53], which suggests the important role of protein degradation in regulating the expression of ER UPR response genes in nematodes exposed to environmental toxicants or stresses.

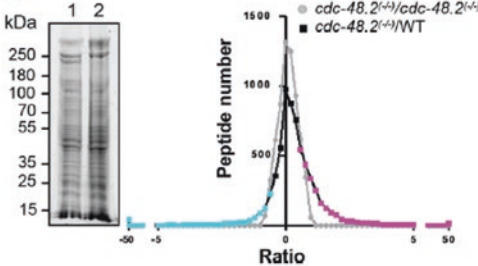
9.5.4.3 CED-1

In nematodes, PQN (prion-like glutamine[Q]/asparagine[N]-rich domain-bearing protein)/ABU (activated in blocked unfolded protein response) proteins represent a noncanonical UPR response [54]. Based on a full-genome microarray analysis,

A

Process	Sequence Name	Gene Name	Brief description of gene product
Metabolism (lipid)	C24A11.9	<i>coq-1</i>	putative hexaprenyl pyrophosphate synthetase
Metabolism (lipid)	C49D10.4	<i>oac-10</i>	O-acyltransferase homolog
Metabolism (lipid)	Y42G9A.4	<i>mvk-1</i>	orthologous to the human gene MEVALONATE KINASE
Metabolism (lipid)	C52B9.1	<i>cka-2</i>	isoform of choline kinase
Metabolism (redox)	C29E4.7	<i>gstl-1</i>	thiol oxidoreductase and dehydroascorbate reductase
Metabolism (redox)	F56F10.3	<i>cdo-1</i>	cysteine dioxygenase
Metabolism (RNA)	F25H5.6	<i>mrpl-54</i>	mitochondrial ribosomal protein, large
Metabolism (RNA)	R74.5	<i>asd-1</i>	alternative Splicing Defective
Metabolism (protein)	Y87D9C.5	<i>eef-1</i>	Hect E3 ubiquitin ligase 1
Metabolism (protein)	F59A3.3	<i>mrpl-24</i>	Mitochondrial Ribosomal Protein, Large
Metabolism (protein)	K07C5.7	<i>ttl-15</i>	putative tubulin polyaminoacid ligase
Metabolism (protein)	M01F1.1	<i>gly-14</i>	N-acetylglucosaminyltransferase I (GlnT1)
Metabolism (protein)	F26D10.10	<i>gln-5</i>	glutamine synthetase (glutamate-ammonia ligase)
Signaling	Y47D3B.2	<i>nlp-21</i>	neuropeptide-like proteins
Signaling	T02D1.3	<i>srp-15</i>	Serpentine receptor, class U
Signaling	T22B7.5	<i>srp-7</i>	serpentine receptor, class V
Signaling	ZC204.11	<i>btb-13</i>	BTB (Broad/complex/Tramtrack/Bric a brac) domain protein
Signaling	M01G12.1	<i>sri-14</i>	serpentine receptor, class I
Signaling	F45C12.10	<i>math-29</i>	MATH (mephrin-associated Traf homology) domain containing
Signaling	F55A12.3	<i>ppk-1</i>	phosphatidylinositol-4-phosphate 5' kinase
Signaling	K07C5.8	<i>cash-1</i>	orthologous to Drosophila CKA and the human striatins
Signaling	C04E12.11	<i>arrd-20</i>	ARRRestin Domain protein
Signaling	F14F3.2	<i>glt-1</i>	homologous to mammalian G protein-coupled receptor kinase InTeractor 1
Traffic/transport	Y48G1A.3	<i>daf-25</i>	<i>C. elegans</i> ortholog of mammalian Ankyrmy2
Traffic/transport	C06G3.2	<i>ktp-18</i>	kinesin motor protein
Traffic/transport	C54G10.3	<i>pmp-3</i>	putative ABC transporter orthologous to human ABCD4
Traffic/transport	M03F8.2	<i>pst-1</i>	orthologous to the PAPST1 transporter
Transcription	K08A2.5	<i>nhr-88</i>	nuclear Hormone Receptor family
Transcription	T22D1.10	<i>ruv-2</i>	RUVB (recombination protein) homolog

B



C

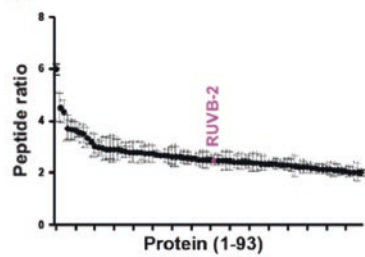


Fig. 9.28 Identification of RUVB2 as a candidate CDC-48 target [53]. (a) List of RNAi clones suppressing the *cdc-48.2(-/-)* phenotype. (b) Graph representing identified peptide number identified in function of peptide quantity ratio. *cdc-48.2(-/-); ckb-2::gfp* and *ccb-2::gfp* synchronized L1 larvae were grown to the L4 stage and exposed to tunicamycin (5 µg/ml) for 16 h on plates. Proteins (60 µg) were separated on a 10% SDS gel. A coomassie blue staining image representative of the SDS gel is shown on the left (1: *cdc-48.2(-/-); ckb-2::gfp*, 2: *ccb-2::gfp*). Gel lanes were cut into slices before proteins were in-gel-digested. Peptides were then identified and quantified by label-free LC-MS/MS mass spectrometry. Peptides that were more (magenta) or less (cyan) abundant in the *cdc-48.2(-/-); ckb-2::gfp* than in *ccb-2::gfp* worms were defined as those having a ratio above 1.5 or below 0.5, respectively. *N* = 3. (c) Graph representing peptide quantity ratio ((*cdc-48.2(-/-); ckb-2::gfp*)/(*ccb-2::gfp*)) for the 93 proteins that are more abundant in *cdc-48.2(-/-)* mutant background compared to WT background

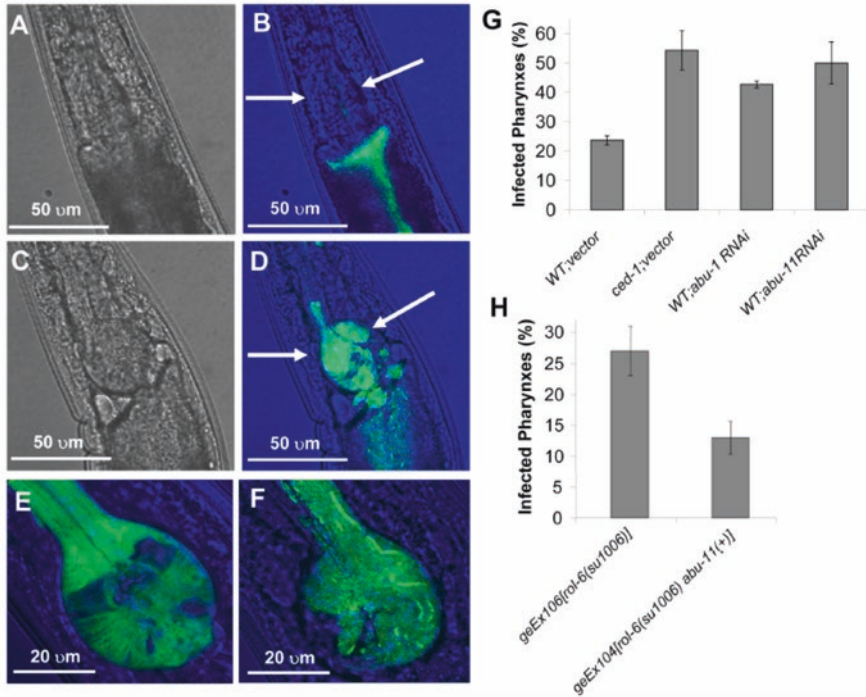


Fig. 9.29 *pqn/abu* genes expressed in a CED-1-dependent manner are required for *C. elegans* defense to pharyngeal invasion by *S. enterica* [54]. (a–d) Confocal images show the pharynx of wild-type (a and b) and *ced-1(e1735)* (c and d) animals infected for 48 h with *S. enterica* expressing GFP. In the merged images (b and d), the terminal bulb of the pharynx is indicated with arrows. (e) Confocal image of the terminal bulb of an *abu-1::gfp(zcEx8)* animal showing pharyngeal expression of ABU-1::GFP. (f) Confocal image of the infected terminal bulb of a *ced-1(e1735)* animal fed *S. enterica* expressing GFP for 48 h. (g) The percentage of nematodes with infected pharynxes when fed *S. enterica* expressing GFP for 48 h was determined for wild-type and *ced-1(e1735)* animals exposed to dsRNA targeting *abu-1* and *abu-11*. (h) The percentage of nematodes with infected pharynxes when fed *S. enterica* expressing GFP for 48 h was determined for *geEx106[rol-6(su1006)]* and *geEx104[rol-6(su1006)abu-11(+)]* animals. Bars correspond to mean \pm SD.

CED-1, a phagocytic receptor recognizing the cell corpses and initiating their engulfment, was identified to have the function in activating the expression of *pqn/abu* genes, and *abu-1* and *pqn-54* were downregulated 3.3- and 2.6-fold, respectively, in *ced-1(e1735)* mutant nematodes [54]. The *pqn/abu* genes expressed in a CED-1-dependent manner were required for innate immunity to live bacterial pathogen (*S. enterica*), and overexpression of *pqn/abu* genes conferred a protection for nematodes to pathogen-mediated killing [54]. Moreover, *pqn/abu* genes expressed in a CED-1-dependent manner were further found to be required for the defense to pharyngeal invasion by *S. enterica* in nematodes (Fig. 9.29) [54]. Therefore, the CED-1 may regulate the noncanonical UPR response genes during the control of toxicity of environmental toxicants or stresses in nematodes.

9.5.4.4 SKN-1/Nrf

SKN-1/Nrf, an important transcriptional factor for the control of oxidative stress, was further found to be required for the response of nematodes to ER UPR [55]. SKN-1 was regulated by the ER UPR and UPR factors (Fig. 9.30) [55]. Meanwhile, SKN-1 also regulated the ER UPR signaling and transcription factors, such as IRE-1, and binded to common downstream targets with XBP-1 and ATF-6 (Fig. 9.30) [55]. Moreover, SKN-1 was essential for resistance of nematodes to the ER stress, and SKN-1-mediated responses to the oxidative stress also depended upon signaling from the ER (Fig. 9.30) [55]. Therefore, a feedback mechanism may be formed during the regulation of ER UPR response in nematodes exposed to environmental toxicants or stresses.

9.5.4.5 MDT-15

As indicated by the alterations in expressions of *hsp-4* and spliced *xbp-1* (*xbp-1s*), mutation of *mdt-15* resulted in ER UPR activation (Fig. 9.31) [56]. Similarly, *hsp-4p::GFP* was strongly upregulated in *mdt-15(RNAi)* and *mdt-15(tm2182)* nematodes (Fig. 9.31) [56]. Additionally, activation of UPR^{ER} PERK arm attenuated protein translation by phosphorylating and inhibiting translation initiation factor eIF2 α , and RNAi knockdown of *mdt-15* increased the levels of phosphorylated eIF2 α (Fig. 9.31) [56]. That is, loss-of-function mutation of *mdt-15* may perturb the ER homeostasis and activate at least two branches of canonical ER UPR in nematodes.

Meanwhile, it was observed that uptake and incorporation of the supplemented FAs were effective in both control(RNAi) and *mdt-15(RNAi)* nematodes (Fig. 9.31) [56]. Additionally, the small reduction observed in the PC level of *mdt-15(RNAi)* nematodes could also be suppressed by FA supplementation (Fig. 9.31) [56], implying that the disrupted ER homeostasis in *mdt-15* mutant nematodes may be the consequence of reduced membrane PL polyunsaturation.

In nematodes, MDT-15 is not part of the ER UPR and not required for the mitochondrial protein homeostasis. In contrast, *mdt-15* mutation or depletion of the lipid metabolism enzymes stearoyl-CoA-desaturases (SCD) and S-adenosyl methionine synthetase (*sams-1*) could activate the ER UPR without promoting the misfolded protein aggregates [56]. These observations suggest that the constitutively activated ER UPR in *mdt-15*, *SCD*, and *sams-1* mutant nematodes may be not the consequence of proteotoxic stress, but likely is the direct result of changes in ER membrane fluidity and composition in nematodes. It was further observed that the defects in membrane PL composition or synthesis could activate the ER UPR without compromising ER protein folding [56].

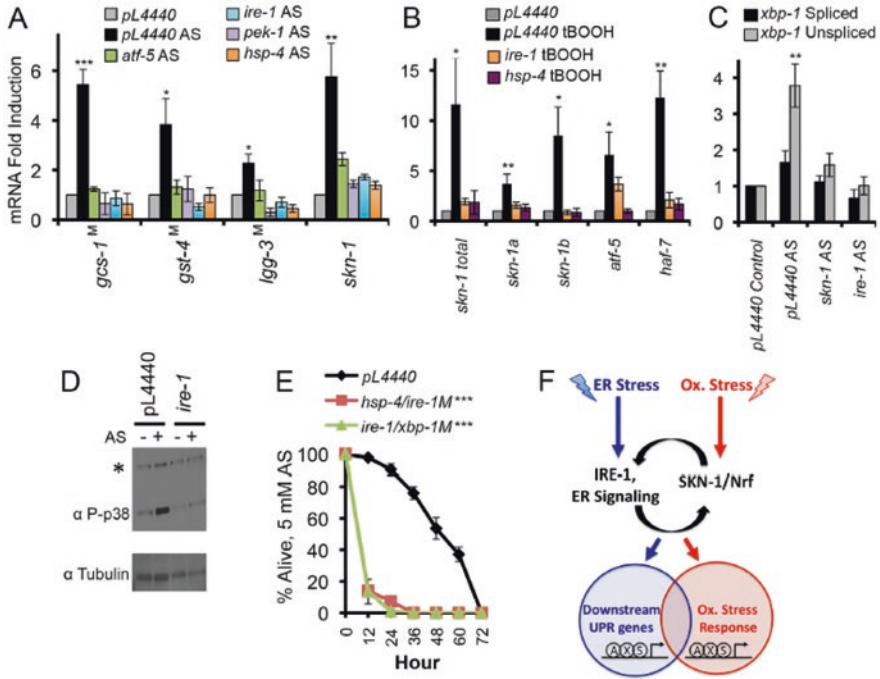


Fig. 9.30 Dependence of oxidative stress responses on UPR components [55]. (a and b) Importance of core UPR genes for SKN-1-mediated oxidative stress responses. Induction of *skn-1* and *skn-1* target gene transcription by AS (a) or t-BOOH (b) was impaired by RNAi against core UPR genes or in core UPR factor mutants (indicated by M). qRT-PCR was performed after treatment with 5 mM AS for 1 h or 12 mM t-BOOH for 1 h. (c) Accumulation of *xbp-1* mRNA in response to AS-induced oxidative stress. Note the predominant increase in the unspliced form. (d) Dependence of AS-induced p38 phosphorylation on *ire-1*. Phosphorylated (active) p38 was assayed by phospho-specific antibody, and *ire-1* expression was knocked down by RNAi. *background signal. (e) UPR factors are required for oxidative stress defense. Survival of AS treatment (5 mM) was scored in RNAi Control, *hsp-4(RNAi)/ire-1(zc14)*, and *ire-1(RNAi)/xbp-1(SJ17)* animals (M indicates mutant). Error bars represent SEM, and * $p < 0.05$, ** $p < 0.01$, *** $p < 0.001$, relative to pL4440 Control calculated using Student's *t*-test. (f) Functional integration of the ER and oxidative stress responses through SKN-1 and canonical UPR components. SKN-1 is essential for the UPR because it directly controls transcription of most UPR signaling and transcription factors. These UPR factors in turn regulate SKN-1 expression and function in concert with SKN-1 at downstream targets. This is shown arbitrarily as SKN-1 (S) binding to target promoters together with XBP-1 (X) and ATF- 6 (a). SKN-1 and mammalian Nrf proteins are present in the ER, suggesting a possible signaling role. UPR factors are required not only for SKN-1 to function in the context of the UPR, but also for SKN-1 to mobilize distinct oxidative stress responses.

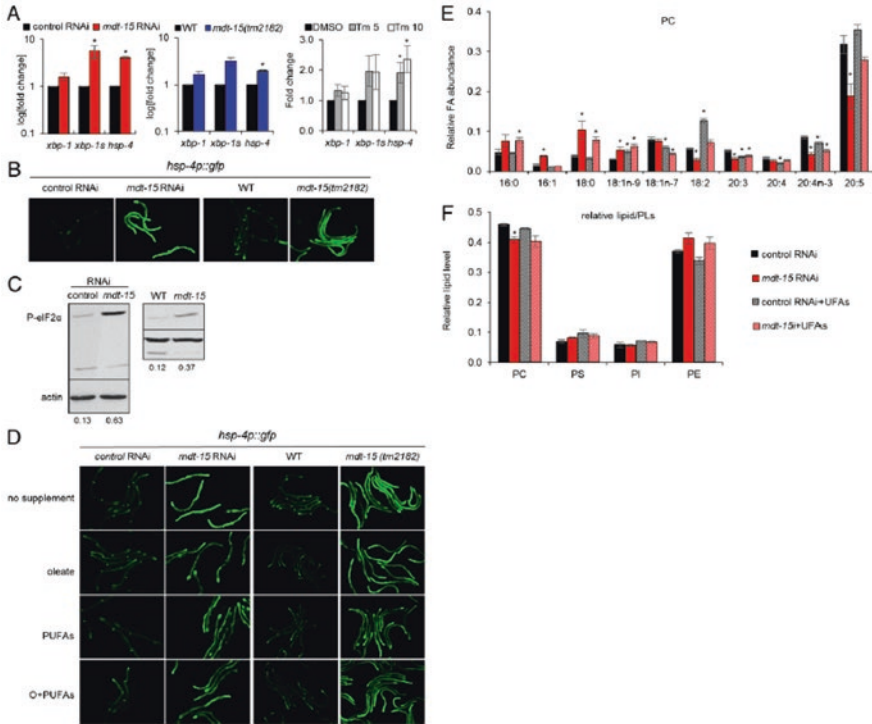


Fig. 9.31 *mdt-15* inactivation alters membrane lipid composition and induces the UPR^{ER} [56]. (a) Bar graphs represent the average fold change of *xbp-1*, spliced *xbp-1* (*xbp-1s*), and *hsp-4* mRNA levels in control(RNAi) and *mdt-15*(RNAi) worms ($P = 0.098, 0.049, \text{ and } 0.00049$, respectively) (left), WT and *mdt-15(tm2182)* worms ($P = 0.19, 0.063, \text{ and } 0.0064$, respectively) (center), or control(RNAi) worms treated with DMSO, 5 $\mu\text{g}/\text{mL}$ tunicamycin (Tm 5; $P = 0.16, 0.13, 0.04$, respectively), or 10 $\mu\text{g}/\text{mL}$ tunicamycin (Tm 10; $P = 0.31, 0.18, 0.03$, respectively) (right). $n = 3$ for all experiments; error bars represent SEM; $*P < 0.05$ (two-tailed Student's *t*-test). (b) Micrographs depict control(RNAi) and *mdt-15*(RNAi) worms or WT and *mdt-15(tm2182)* worms expressing the *hsp-4p::GFP* transcriptional reporter; one of four independent experiments is shown. (c) Immunoblots depict the levels of phospho-Ser51 eIF2 α (P-eIF2 α) and actin protein levels in control(RNAi), *mdt-15*(RNAi), WT, and *mdt-15(tm2182)* worms. The numbers represent the intensity of the P-eIF2 α bands relative to corresponding actin bands. One of four independent experiments is shown. (d) Micrographs show control(RNAi) and *mdt-15*(RNAi) worms or WT and *mdt-15(tm2182)* worms expressing the *hsp-4p::GFP* transcriptional reporter grown without dietary supplements (no supplement), with 300 μM C18:1n-9 (oleate), with 150 μM C18:2 and 150 μM C20:5 (PUFAs), or with 150 μM C18:1n-9 and 300 μM PUFAs (O+PUFAs). (e) Bars represent the relative abundance of individual FAs in PC. (f) Bars represent the average levels of individual lipid species relative to total PLs. For E and F, lipids were extracted from L4-stage control(RNAi) or *mdt-15*(RNAi) worms raised in the absence or presence of dietary unsaturated FAs (UFAs; C18:1n-9, C18:2, and C20:5). $n = 3$; error bars represent SEM; $*P < 0.05$ as determined by two-tailed Student's *t*-test

9.6 Autophagy

The related information for autophagy in *C. elegans* has been well-summarized in the reviews (Figs. 9.32 and 9.33) [57, 58].

9.6.1 Induction of Autophagy in Nematodes Exposed to Environmental Toxicants or Stresses

Using GFP::LGG-1 as a marker for autophagy induction, it was observed that infection with the *P. aeruginosa* PA14 could markedly increase the GFP::LGG-1 puncta in both seam cells and intestine (Fig. 9.34) [59]. The ratio of phosphatidylethanolamine (PE)-conjugated LGG-1 (PE-LGG-1::GFP) to LGG-1 by using Western blotting further confirmed this autophagy induction (Fig. 9.34) [59]. Meanwhile, the autophagy was also detected in nematodes on a lawn of PA14 mixed with the relatively nonpathogenic food source *Escherichia coli* OP50 [59], suggesting the non-involvement of nutrient deprivation. The autophagy genes induced by pathogen infection were further summarized in Fig. 9.35 [58]. Besides the environmental pathogen infection, environmental metabolite extracted from *Streptomyces venezuelae* also induced the increase in mCherry::LGG-1, and this autophagy induction was dependent of PINK-1, a PARK9 homolog [60]. Therefore, environmental exposure to toxicants or stresses may potentially induce the autophagy induction in nematodes.

9.6.2 Molecular Control of Autophagy in Nematodes Exposed to Environmental Toxicants or Stresses

9.6.2.1 BEC-1

bec-1 encodes an ortholog of yeast and mammalian autophagy protein ATG6/VPS30/beclin1. Nematodes subjected to *bec-1* RNAi were susceptible to *P. aeruginosa* PA14 infection (Fig. 9.34) [59], suggesting its involvement in the control of host defense against pathogen infection. Nevertheless, it was found that *bec-1* RNAi had no impact on colony-forming units (CFU) of *P. aeruginosa* PA14 in the body of nematodes, and the accumulation of *P. aeruginosa* expressing GFP in the body subjected to *bec-1* RNAi was also comparable to that observed in control nematodes (Fig. 9.34) [59], which implies that the protective role of BEC-1-mediated autophagy induction in *C. elegans* survival is unlikely the result of direct elimination of *P. aeruginosa*.

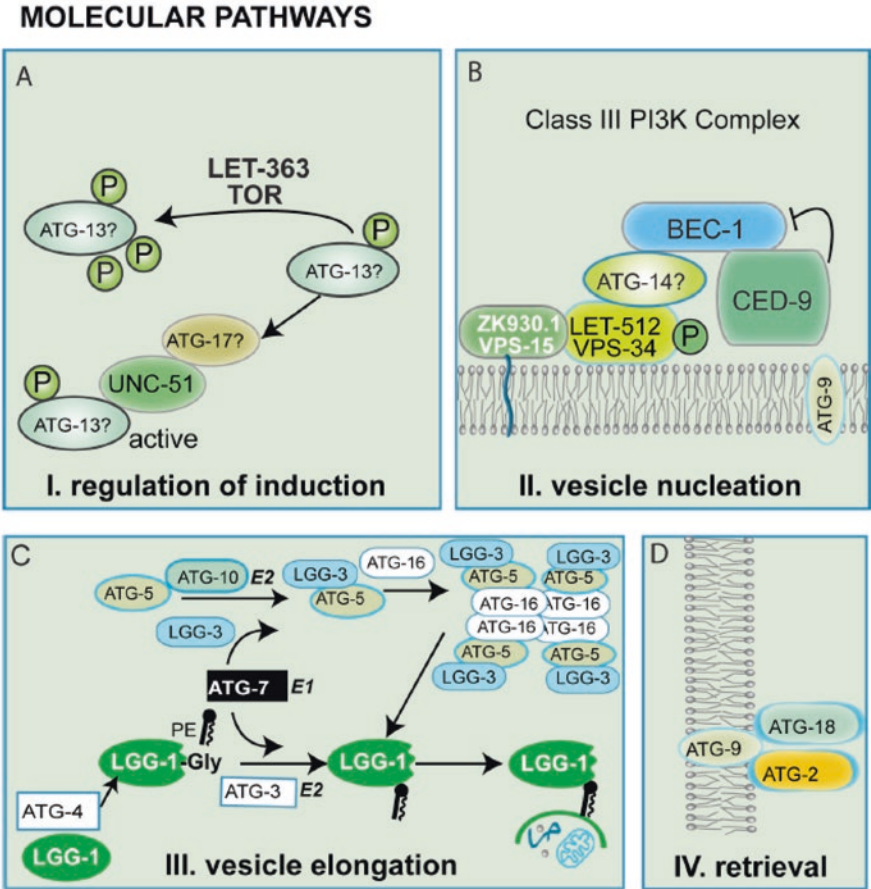


Fig. 9.32 Schematic diagram of the presumed role for *C. elegans* autophagy proteins involved in the formation of an autophagosome [57]. (a) Regulation of induction: In yeast, the Tor kinase and its effectors regulate the induction of autophagy. UNC-51 is the *C. elegans* Atg1 ortholog. (b) Vesicle nucleation requires a lipid kinase complex, which includes the class III phosphatidylinositol 3-kinase (PI3K), Vps34 (in *C. elegans* LET-512). In yeast, Vps34 activation depends on its binding partners, Atg6, Atg14, and Vps15. In *C. elegans*, the ATG6 ortholog is *bec-1*. The interaction between the antiapoptotic protein CED-9 and BEC-1 is conserved in *C. elegans*. A similar interaction between the mammalian proteins Bcl-2 and Beclin 1 inhibits autophagy. (c) Two novel ubiquitin-like conjugation pathways the Atg12 conjugation system (Atg5, Atg12, and Atg16) and the Atg8 lipidation system (Atg8, Atg3, and Atg7) mediate vesicle expansion and vesicle completion. Orthologs to all the members of these two complexes have been found in *C. elegans*, where they are named ATG-3, ATG-4, ATG-5, ATG-7, ATG-16, LGG-1/Atg8, and LGG-3/Atg12. In yeast, Atg8 undergoes two posttranslational processing events resulting in conjugation to phosphatidylethanolamine (PE) and recruitment to the PAS membrane. ATG-7 is an E1 ubiquitin activating enzyme required for the activation of LGG-1. LGG-3-ATG-5 oligomerize with ATG-16 to allow for the formation of the multimeric complex. ATG-3 and ATG-10 are E2-like ubiquitin conjugating enzymes and ATG-4 is a cysteine protease. As for its yeast ortholog, LGG-1 appears to remain in the completed autophagosome and thus is an excellent marker for early and late autophagosomal structures. (d) The retrieval of the integral membrane protein ATG-9 from the phagophore assembly site (PAS) involves ATG-2 and ATG-18, two interacting peripheral proteins

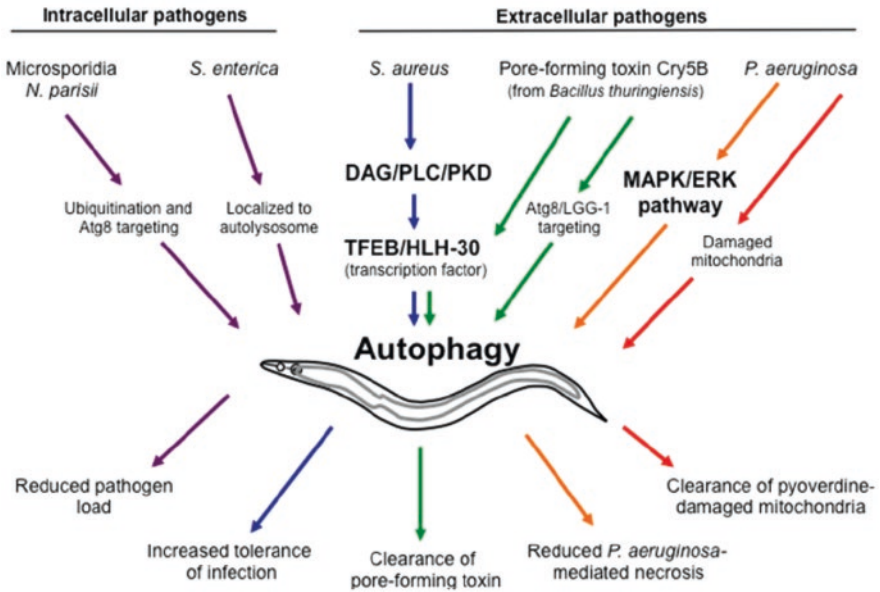


Fig. 9.33 Pathogen responses linked to autophagy in *Caenorhabditis elegans* [58]. Autophagy plays crucial roles in the defense against both intracellular and extracellular pathogens in the nematode *C. elegans*. The microsporidian pathogen *Nematocida parisii* is targeted for ubiquitination and recruitment of Atg8/LGG-1, which likely results in xenophagy. Replication of *Salmonella enterica* is restricted by localization to lysosomes. *Staphylococcus aureus* and the *Bacillus thuringiensis* pore-forming toxin Cry5B both induce transcription of autophagy-related genes via TFEB/HLH-30. *Pseudomonas aeruginosa*-induced necrosis of *C. elegans* is reduced by activation of autophagy through the MAPK/ERK signaling pathway. Autophagy (mitophagy) also clears mitochondria damaged by the *P. aeruginosa* virulence factor pyoverdine, thereby reducing mortality

Moreover, it was found that the induced hypoxia hypersensitive phenotype by *bec-1(RNAi)* could be blocked by loss-of-function mutations in either the apoptosis (CED-3, a canonical caspase) or necrosis (CTR-1, a calreticulin) pathway [61], suggesting that BEC-1 may act upstream of both CED-3 and CTR-1 to regulate the autophagy induction in nematodes exposed to environmental toxicants or stresses.

9.6.2.2 LGG-1, LGG-2, and UNC-51

It was observed that, besides mutation or RNAi knockdown of *bec-1*, RNAi knockdown of *lgg-1* or *lgg-2* encoding LC3/Atg8 or mutation of *unc-51* encoding Atg1 could decrease the *C. elegans* survival after a severe hypoxic stress (Fig. 9.36) [61]. Therefore, the autophagy genes of *bec-1*, *lgg-1*, *lgg-2*, and *unc-51* can promote the *C. elegans* survival after exposure to environmental toxicants or stresses.

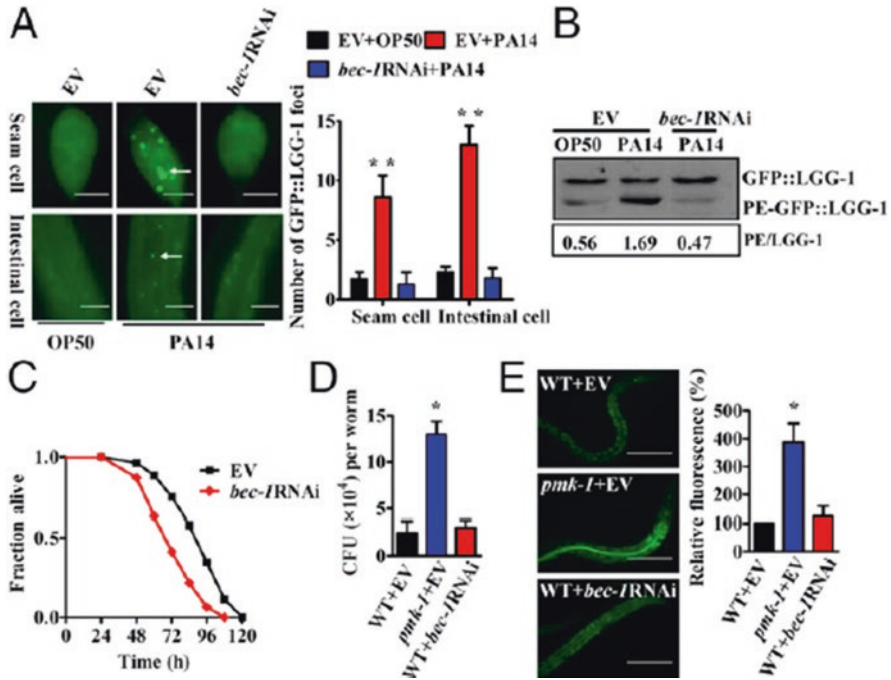


Fig. 9.34 Autophagy mediates host defense against *P. aeruginosa* in *C. elegans* [59]. (a) Representative images of autophagosomes (GFP::LGG-1 puncta) in the seam cells and intestinal cells of worms exposed to *P. aeruginosa* PA14 for 12 h. The numbers of GFP::LGG-1 puncta in the seam cells and intestinal cells were counted (right). These results are mean \pm SD of three independent experiments performed in triplicate. $**P < 0.01$ versus OP50+empty vector (EV). The arrow denotes a representative autophagosome. (Scale bars: seam cells, 10 μ m; intestinal cells, 20 μ m.) (b) The levels of PE-conjugated LGG-1–GFP and LGG-1–GFP were measured by Western blotting. The blot shown here is typical of three independent experiments. $P < 0.05$, PA14 versus OP50; $P < 0.01$, PA14+bec-1 RNAi versus PA14+EV. (c) *bec-1* RNAi significantly reduced survival of worms exposed to PA14. $P < 0.01$ versus EV. (d) Numbers of colony-forming units of PA14 were measured in worms subjected to *bec-1* RNAi. These results are mean \pm SD of three independent experiments performed in triplicate. $*P < 0.05$ versus WT+EV. (e) Fluorescence of worms exposed to *P. aeruginosa* PA14 expressing GFP for 24 h. The image is representative of three independent experiments. Right shows quantification of GFP levels. $*P < 0.05$ versus WT+EV. (Scale bars: 50 μ m)

9.6.2.3 HLH-30/TFEB

HLH-30/TFEB is the sole *C. elegans* MiT transcription factor. In nematodes, HLH-30 could be activated shortly after *Staphylococcus aureus* infection [62]. HLH-30 is expressed in the intestine, rectal epithelial cells, vulval epithelial cells, spermatheca, and pharynx [62]. Under the normal conditions, the HLH-30::GFP signals were equally distributed between nucleus and cytoplasm [62]. After pathogen infection, the HLH-30::GFP signals were dramatically concentrated in the nucleus after just 30 min of infection [62].

<i>D. melanogaster</i>	<i>S. cerevisiae/H. sapiens</i>	Pathogen
<i>Atg1</i>	<i>Atg1/ULK1</i>	<i>Wolbachia</i> , VSV
<i>Atg6</i>	<i>VPS30/BECN1</i>	VSV
<i>Atg2</i>	<i>ATG2</i>	VSV
<i>Atg18</i>	<i>WIPI2</i>	VSV
<i>Atg9</i>	<i>ATG9</i>	VSV
<i>Atg12</i>	<i>ATG12</i>	<i>E. coli</i> , VSV
<i>Atg7</i>	<i>ATG7</i>	<i>E. coli</i> , VSV
<i>Atg4</i>	<i>ATG4</i>	VSV
<i>Atg5</i>	<i>ATG5</i>	<i>L. monocytogenes</i> , <i>E. coli</i>
<i>Atg8</i>	<i>MAP1LC3</i>	VSV
<i>Park</i>	<i>PRKN</i>	<i>M. marinum</i> , <i>S. enterica</i>

<i>C. elegans</i>	<i>S. cerevisiae/H. sapiens</i>	Pathogen
<i>unc-51</i>	<i>Atg1/ULK1</i>	<i>S. aureus</i>
<i>atg-13</i>	<i>ATG13</i>	<i>S. aureus</i>
<i>bec-1</i>	<i>Vps30/BECN1</i>	<i>S. enterica</i> , <i>P. aeruginosa</i> , Cry5B
<i>vps-34</i>	<i>Vps34/PIK3C3</i>	<i>S. aureus</i>
<i>atg-2</i>	<i>ATG2</i>	<i>S. aureus</i>
<i>atg-18</i>	<i>WIPI2</i>	<i>N. parisii</i> , Cry5B
<i>lgg-3</i>	<i>ATG12</i>	Cry5B
<i>atg-7</i>	<i>ATG7</i>	<i>S. enterica</i>
<i>atg-16.2</i>	<i>ATG16L1</i>	<i>S. aureus</i>
<i>atg-4.1/2</i>	<i>ATG4</i>	Cry5B
<i>lgg-1</i>	<i>MAP1LC3</i>	<i>S. aureus</i> , <i>S. enterica</i> , <i>P. aeruginosa</i> , <i>N. parisii</i> , Cry5B
<i>lgg-2</i>	<i>MAP1LC3</i>	<i>S. aureus</i>
<i>sqst-1</i>	<i>SQSTM1</i>	<i>N. parisii</i>

Fig. 9.35 Autophagy-related genes linked to immunity in *D. melanogaster* and *C. elegans* [58]

In nematodes, HLH-30 drove the expression of antimicrobial genes, such as *lys-5* and *ilys-2* [62]. Additionally, the *hlh-30*-dependent induction of *kbg-1* (human JNK homolog), *nsy-1* (homologous to human ASK1), *mdl-1* (MAD-like bHLH transcription factor), *ins-11* (insulin), *sgk-1* (SGK), and *dct-1* (target of DAF-16/FOXO) was also observed in nematodes after pathogen infection [62]. Meanwhile, it was further found that the induction of autophagy genes *lgg-1* and *lgg-2*, *unc-51*, and *atg-2*, *atg-13*, and *atg-16.2* (homologous to human *ATG2*, *ATG13*, and *ATG16L1*, respectively) was also *hlh-30*-dependent in nematodes after pathogen infection (Fig. 9.37) [62], suggesting that the pathogen infection can result in the induction of autophagy genes in order to enhance the defense against infection in nematodes.

Moreover, the infection-induced expression was abrogated by deletion of *hlh-30*, and the GFP::LGG-1 expression was markedly reduced in *hlh-30* mutant nematodes (Fig. 9.37) [62]. In contrast, these genes were increased by overexpression of HLH-30::GFP (Fig. 9.37) [62], suggesting that HLH-30 is necessary for the cytoprotec-

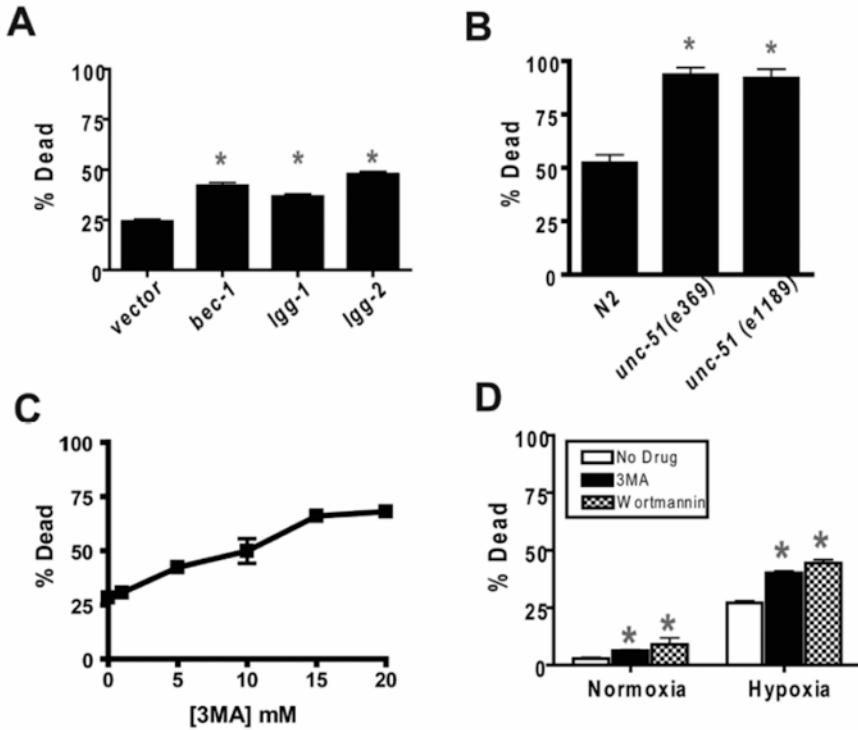


Fig. 9.36 Inhibition of autophagy increases hypoxic sensitivity [61]. (a) Hypoxic sensitivity of animals treated with RNAi against *bec-1*, *lgg-1*, and *lgg-2* autophagy genes compared to empty vector control. Second-generation RNAi-treated adult animals were scored as alive or dead after a 24 h recovery from a 12 h hypoxic incubation. Error bars are mean \pm SEM of 5 trials. * $p < 0.01$ vs vector control, two-tailed *t*-test. (b) Hypoxic sensitivity of loss-of-function mutants of *unc-51*. % dead following recovery from a 12 h hypoxic incubation. The N2 control animals were scored contemporaneously with the *unc-51* mutants. * $p < 0.01$ vs N2, two-tailed *t*-test. (c) Concentration/response curve for the effect of 3-methyladenine (3MA) on hypoxic sensitivity. Adult animals were transferred into M9 buffer containing the indicated concentrations of 3-MA, then immediately placed into the hypoxia chamber for 12 h, recovered on agar plates without 3MA for 24 h, and then scored as alive or dead. Error bars are mean \pm SEM of 5 trials. (d) Effect of 3MA (10 mM) and wortmannin (100 μ M) on death after normoxic or hypoxic incubation. Wortmannin experiments are otherwise identical to that described for 3MA. Bars are mean \pm SEM of nine trials for 3MA and three trials for wortmannin. * $p < 0.01$ vs no drug, two-tailed *t*-test

tive gene induction. Meanwhile, RNAi knockdown of autophagy genes (*lgg-1*, *unc-51*, or *vps-34*) did not affect the susceptibility of *hlh-30* mutant nematodes to pathogen infection, nor their longevity (Fig. 9.37) [62]. Furthermore, it has been shown that HLH-30-mediated autophagy functioned in a cell-autonomous manner for epithelium intrinsic cellular defense against bacterial pore-forming toxin [63], which suggests a connection between HLH-30-mediated autophagy and epithelium intrinsic cellular defense against environmental toxicants or stresses. These results suggest the key role of transcriptional factor HLH-30 in regulating autophagy induction in nematodes exposed to environmental toxicants or stresses.

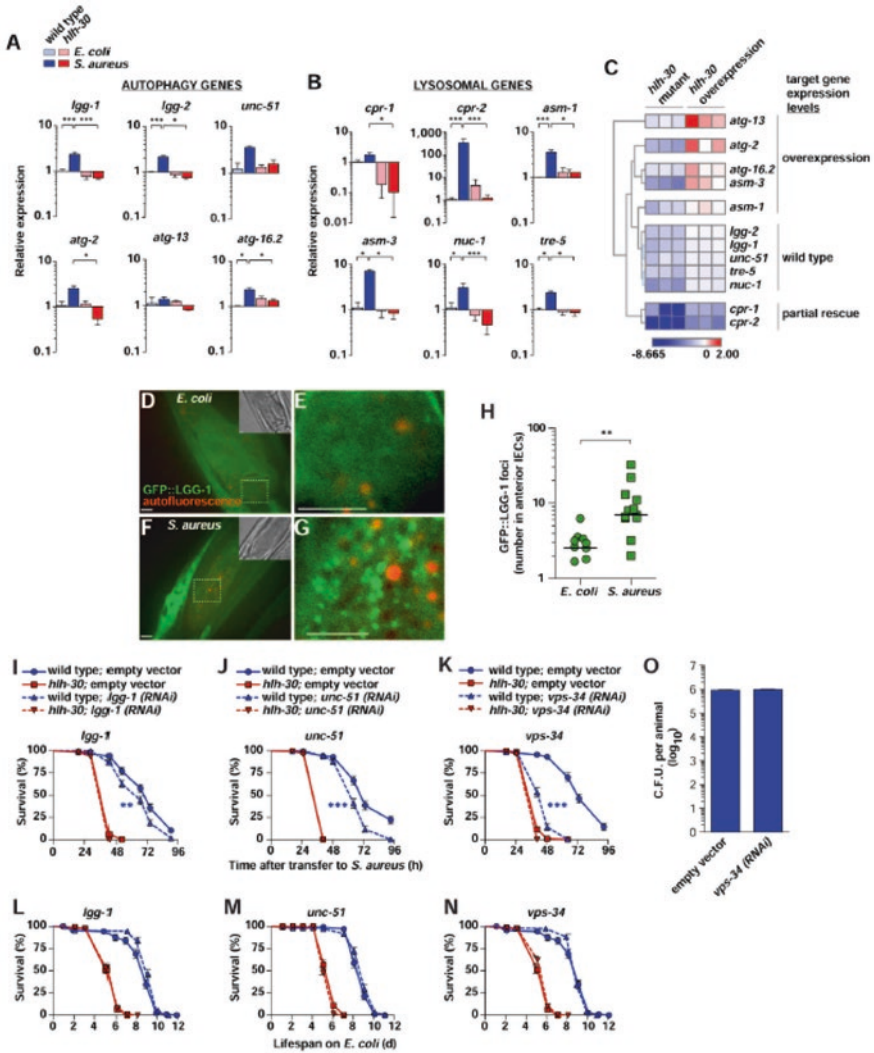


Fig. 9.37 HLH-30-regulated autophagy genes are required for defense [62]. (a and b) qRT-PCR of HLH-30-dependent autophagy and lysosomal genes, of animals exposed to *S. aureus* or control *E. coli* (8 h). (c) Unsupervised hierarchical clustering of HLH-30-dependent gene expression (qRT-PCR). (d–g) Confocal micrographs of anterior intestinal cells containing GFP::LGG-1 puncta in animals fed nonpathogenic *E. coli* (d and e) or infected 8 h with *S. aureus* (f and g). Insets are Nomarski micrographs of the same field. Red puncta indicate autofluorescent gut granules. (e and g): higher magnification of areas indicated in (d and f), respectively. Bar = 6 μm . (h) Quantification of GFP::LGG-1 puncta. Data are mean \pm SEM, $N = 13$ animals each. ** $p < 0.01$ (two-sample *t*-test). (i–n) Survival of wild-type and *hlh-30* animals, empty vector or *lgg-1* (i and l), *unc-51* (j, m) and *vps-34* RNAi-treated (k and n), and subsequently infected with *S. aureus* (i–k) or maintained on RNAi bacteria (l and m). Experiments are representative of at least two independent trials. ** $p < 0.01$; *** $p < 0.0001$ (log-rank test). (o) *S. aureus* accumulation in RNAi-treated animals after 27 h of infection, expressed as C.F.U./animal. Representative experiment of two independent trials. Data are mean \pm SEM ($N = 3$ replicates). Differences between groups were not significant (two-sample *t*-test)

9.6.2.4 Target of Rapamycin Complex 1 (TORC1)

In *C. elegans*, *hpk-1* encodes a Hipk homolog. HPK-1 was required for the maintenance of proteostasis and the protection against the formation of polyglutamine (Q35::YFP) protein aggregates and locomotory toxicity [64]. More importantly, HPK-1 regulated the induction of autophagy and was necessary for induction of autophagosome formation and autophagy gene expression in response to dietary restriction (DR) or inactivation of TORC1. The autophagy-stimulating transcription factors *pha-4/FoxA* and *mxl-2/MLx*, but not *hlh-30/TFEB* and nuclear hormone receptor *nhr-62*, were necessary for the observed extended longevity induced by HPK-1 overexpression [64].

9.6.2.5 PKA/KIN-1

kin-1 encodes a protein kinase A (PKA). In nematodes, KIN-1 regulated the expression of a set of antimicrobial effectors in the non-neuron tissues, and the neuronal KIN-1 contributed to resistance against *Salmonella enterica* infection [65]. Moreover, during the *S. enterica* infection, KIN-1 regulated the expression of lysosomal genes [65]. These results suggest that KIN-1-mediated lysosomal signaling molecules are involved in the autophagy by controlling the autophagic flux, rather than the formation of autophagosomes in nematodes.

9.6.2.6 HSF-1

Hormetic heat shock induced the autophagy as indicated by the alterations in LGG-1::GFP and autophagy genes (phosphoinositide-binding protein *atg-18*, SQSTM1/p62 ortholog *sqst-1*, and *atg-16.2*) [66]. These autophagy genes were required for heat shock-mediated survival, and overexpression of HSF-1 was sufficient to induce the autophagy [66]. In addition, the heat shock and HSF-1 improved the proteostasis via autophagy [66]. Moreover, it was found that RNAi silencing of autophagy genes could reduce the enhanced stress tolerance and longevity in nematodes overexpressing HSF-1 (Fig. 9.38) [66], suggesting that the autophagy genes are essential for resistance to thermal stress and lifespan extension in nematodes overexpressing HSF-1.

9.6.2.7 Tumor Suppressor FLCN

Tumor suppressor FLCN is an AMPK-binding partner. In nematodes, loss-of-function mutation of *flcn-1* encoding FLCN conferred a resistance to oxidative stress, and this resistance to oxidative stress was dependent of *aak-2* encoding AMPK, but not the classical ROS detoxification pathways (insulin signaling, *sod* genes, and *ctl* genes) [67], suggesting that FLCN-1 is a negative regulator of AAK-2. Moreover, the increased autophagy upon loss-of-function mutation of *flcn-1*

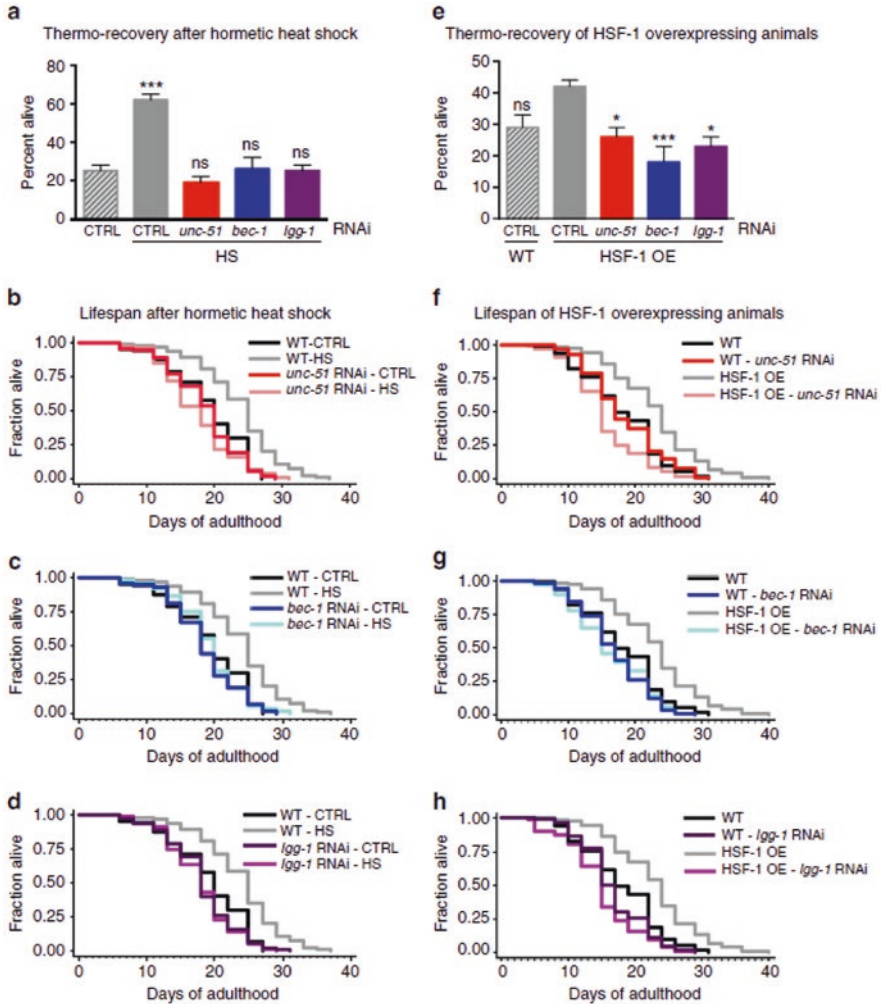


Fig. 9.38 Autophagy genes are required for heat shock- and HSF-1-mediated survival [66]. **(a)** Survival of wild-type (WT) animals subjected to hormetic heat shock on day 1 of adulthood and then incubated for 8 h at heat stress on day 4 of adulthood. Animals were fed from day 1 of adulthood with control bacteria (empty vector, CTRL) or bacteria expressing dsRNA targeting the autophagy genes *unc-51*/ATG1, *bec-1*/ATG6, and *lgg-1*/ATG8 ($N = 65-90$ animals, $n = 4$ plates). **(b-d)** Lifespan analysis of animals subjected to hormetic heat shock with RNAi-mediated autophagy gene reduction from day 1 of adulthood. WT-CTRL animals (19.2 days, $N = 104$) compared with WT-HS animals (23.7 days, $N = 94$): $P < 0.0001$, **(b)** *unc-51*/ATG1 RNAi-CTRL (18.5 days, $N = 110$) compared with *unc-51*/ATG1 RNAi-HS (17.5 days, $N = 107$): $P = 0.04$, **(c)** *bec-1*/ATG6 RNAi-CTRL (19.2 days, $N = 116$) compared with *bec-1*/ATG6 RNAi-HS (18.4 days, $N = 112$): $P = 0.3$, **(d)** *lgg-1*/ATG8 RNAi-CTRL (18.1 days, $N = 108$) compared with *lgg-1*/ATG8 RNAi-HS (17.9 days, $N = 79$): $P = 0.7$. **(e)** Survival of WT or HSF-1-overexpressing (HSF-1 OE) animals incubated for 8 h at heat stress on day 3 of adulthood. Animals were fed from day 1 of adulthood with control bacteria (empty vector, CTRL) or bacteria expressing dsRNA targeting the indicated autophagy genes Error bars indicate SEM ns: $P > 0.05$, $*P < 0.05$ and $***P < 0.001$ by

conferred a resistance to oxidative stress, and RNAi knockdown of essential autophagy genes (*atg-7* and *bec-1*) abolished the resistance of *flcn-1(ok975)* mutant nematodes to PQ toxicity (Fig. 9.39) [67]. Therefore, loss of FLCN may result in a constitutive activation of AMPK, which further induces the autophagy and inhibits the toxicity of environmental toxicants or stresses in nematodes.

9.6.2.8 Insulin Signaling

daf-2 encodes an insulin receptor, and *daf-16* encodes a FOXO transcriptional factor in the insulin signaling pathway. RNAi knockdown of autophagy genes (*bec-1* or *lgg-1*) could abrogate the pathogen resistance conferred by a loss-of-function mutation of *daf-2* (Fig. 9.40) [68]. In addition, RNAi knockdown of autophagy genes (*bec-1* or *lgg-1*) could also abrogate the pathogen resistance conferred by overexpression of the DAF-16 [68]. Therefore, the insulin signaling may regulate the toxicity of environmental toxicants or stresses by influencing the autophagy induction in nematodes.

9.6.2.9 ERK Signaling

It was found that the active role of autophagy in innate immune responses to *P. aeruginosa* PA14 in *C. elegans* could be suppressed by RNAi knockdown of *mpk-1*, but not *pmk-1*, *dkf-2*, *egl-30*, *daf-16*, and *fshr-1*, as indicated by the reduction in the number of GFP::LGG-1 puncta in seam cells and intestine in *mpk-1(n2521)* mutant nematodes after *P. aeruginosa* PA14 infection (Fig. 9.41) [58]. This suggests the important role of ERK signaling in the regulation of autophagy induction in nematodes exposed to environmental toxicants or stresses. Among the other core components of ERK signaling (small G protein LET-60 RAS, MAPK kinase kinase LIN-45 RAF, MAPK kinase MEK-2, and MPK-1), mutations in *let-60(n1700)*, *lin-45(sy96)*, or *mek-2(n1989)* also caused a decrease in the number of GFP::LGG-1 puncta in seam cells and intestine (Fig. 9.41) [58]. Meanwhile, the mutations in *let-60(n1700)*, *lin-45(sy96)*, *mek-2(n1989)*, or *mpk-1(n2521)* enhanced the susceptibility of nematodes to *P. aeruginosa* PA14 infection, and a gain-of-function mutation *let-60(n1046)* resulted in the enhanced resistance to the killing by PA14

Fig. 9.38 (continued) one-way ANOVA. (f–h) Lifespan analysis of WT and HSF-1 OE animals subjected to RNAi-mediated autophagy gene reduction from day 1 of adulthood. WT animals (18.1 days, $N = 113$) compared with HSF-1 OE animals (23.0 days, $N = 121$): $P < 0.0001$, (f) WT: CTRL compared with *unc-51/ATG1* RNAi (18.3 days, $N = 128$): $P = 0.9$, HSF-1 OE: CTRL compared with *unc-51/ATG1* RNAi (15.4 days, $N = 133$): $P < 0.0001$, (g) WT: CTRL compared with *bec-1/ATG6* RNAi (16.7 days, $N = 123$): $P = 0.02$, HSF-1 OE: CTRL compared with *bec-1/ATG6* RNAi (16.3 days, $N = 140$): $P < 0.0001$, (h) WT: CTRL compared with *lgg-1/ATG8* RNAi (16.7 days, $N = 109$): $P = 0.02$, HSF-1 OE: CTRL compared with *lgg-1/ATG8* RNAi (14.9 days, $N = 147$): $P < 0.0001$, by log-rank test

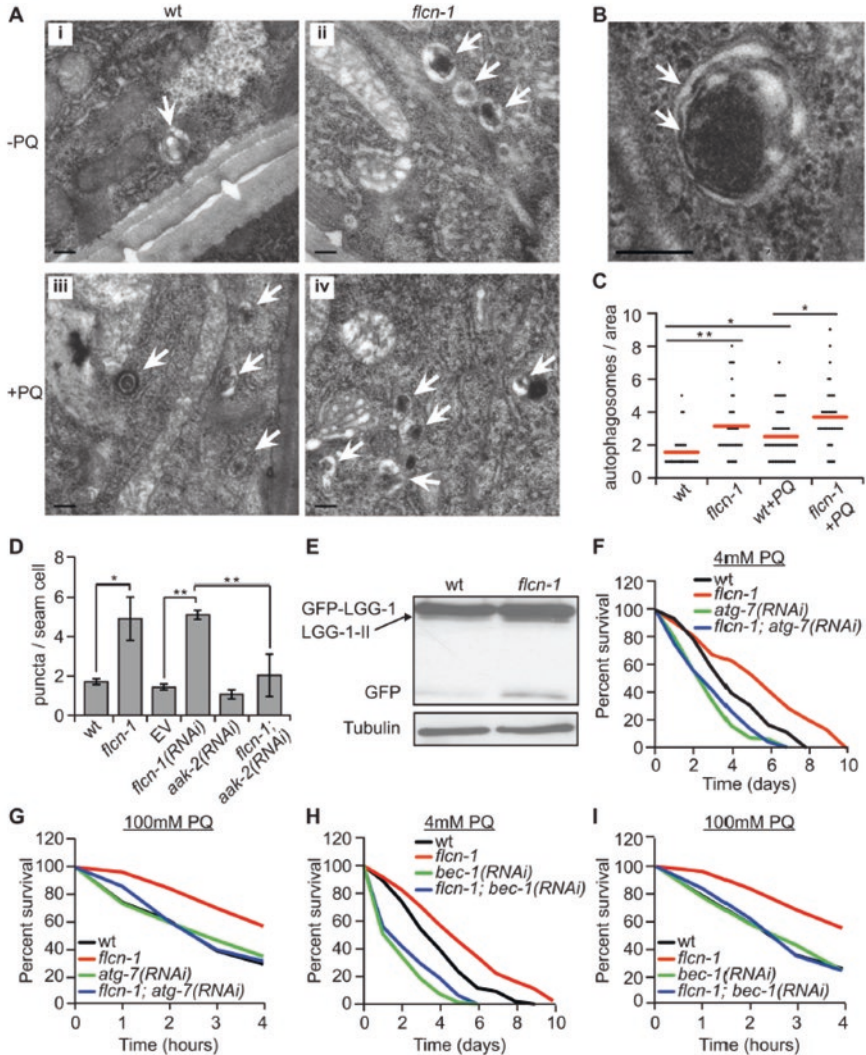


Fig. 9.39 Loss of *flcn-1* activates autophagy resulting in oxidative stress resistance in *C. elegans* [67]. (a and b) Representative electron micrographs from longitudinal sections of the hypodermis in indicated nematode strains. Arrows represent autophagic vacuoles (a) and autophagosomal membranes (b). Scale bars: 0.2 μ m (a and b). (c) Quantification of the autophagic events observed in defined surface area of 4.25 μ m² of electron micrographs taken from at least five animals. Red lines represent the mean of autophagosome numbers per area indicated strains and treatment condition. (d) Number of GFP::LGG-1 positive autophagosome puncta in the seam cells of the indicated worm strains. (e) Western blot analysis of the GFP::LGG-1 cleavage profile (LGG-1-II, GFP) in worm protein extracts. (f–i) Percent survival of indicated strains upon 4 mM (f and h) or 100 mM (g and i) PQ. Data represent the means \pm SEM, $n \geq 3$

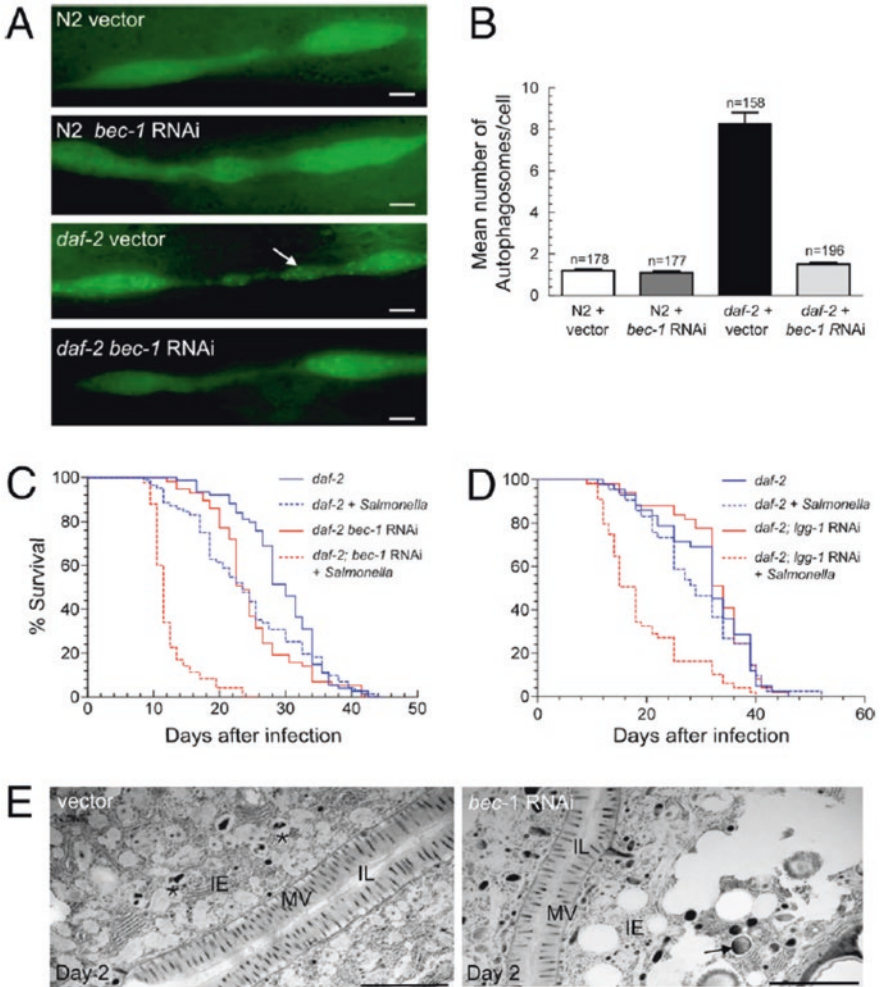


Fig. 9.40 *Atg* genes mediate insulin signaling-regulated resistance against *Salmonella* in *C. elegans* [68]. (a) Representative images of autophagosomes (GFP::LGG-1 dots) in seam cells of N2 wild-type and *daf-2*-mutant animals treated either with RNAi control vector or *bec-1* RNAi. The arrow denotes a representative autophagosome. (Scale bars, 2 μ M.) (b) Quantification of autophagosomes per seam cell (mean \pm SEM) for each genotype. *n* = number of seam cells per group in 20 animals. Similar results were obtained in two independent experiments. (c and d) Survival curves of *daf-2*(*e1370*)-mutant animals treated with either control or indicated *atg* gene-RNAi feeding plasmids following a 2-day exposure to *S. typhimurium* or normal food at 20 °C. (e) Representative EMs of *Salmonella*-infected control and *bec-1*-RNAi *daf-2*(*e1370*) animals 2 days after a 2-day *Salmonella* ingestion period. The asterisk denotes a representative autolysosome containing partially degraded bacteria. The arrow denotes representative SCV

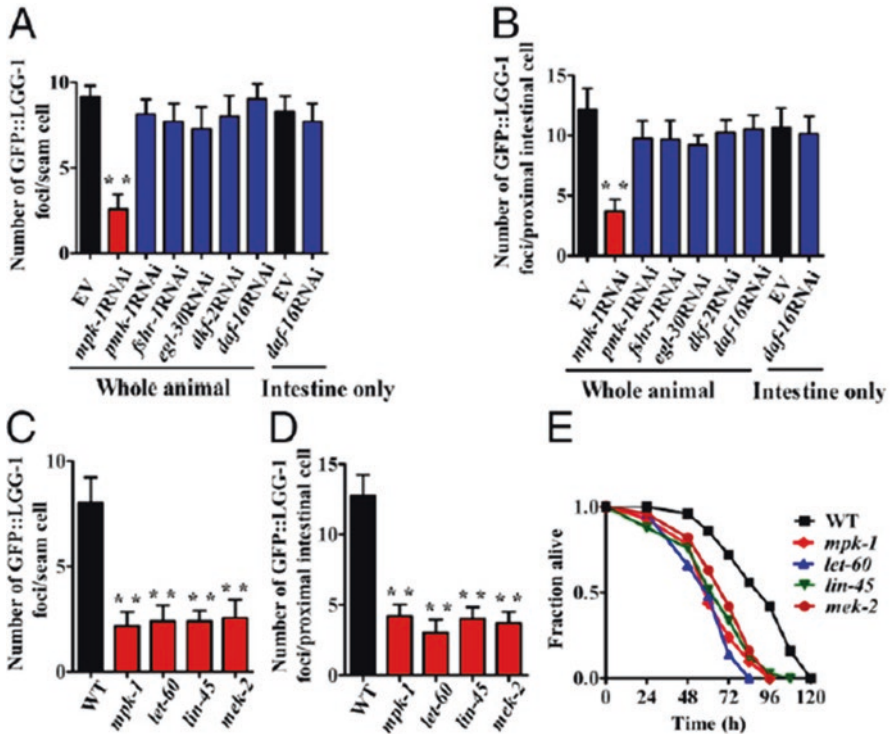


Fig. 9.41 The ERK pathway is required for autophagy during *P. aeruginosa* infection [58]. (a and b) The numbers of GFP::LGG-1 puncta were counted in the seam cells (a) and intestinal cells (b) of worms exposed to *P. aeruginosa* PA14. (c and d) Mutations in the components of the ERK pathway suppressed autophagy in the seam cells (c) and intestinal cells (d) of worms exposed to PA14. These results are mean \pm SD of three independent experiments performed in triplicate. ** $P < 0.01$ versus control (EV or WT). (e) Mutations in the components of the ERK pathway reduced survival of worms exposed to PA14. $P < 0.01$ versus WT

(Fig. 9.41) [58]. KSR proteins and LIP-1 are regulators of ERK signaling pathway. The *ksr-1*(*ku68*), but not *ksr-2*(*dx27*), mutant nematodes exhibited an enhanced susceptibility to *P. aeruginosa*-mediated killing, and the *lip-1*(*zh15*) mutants exhibited an enhanced resistance to *P. aeruginosa* PA14 infection [58]. Meanwhile, the numbers of GFP::LGG-1 puncta in seam cells and intestine could be reduced in *ksr-1*(*ku68*) mutants and increased in *lip-1*(*zh15*) mutants [58]. In nematodes, *P. aeruginosa* infection could activate the ERK signaling [58]. Therefore, ERK signaling can act as an upregulator for the molecular signaling of autophagy in nematodes exposed to environmental toxicants or stresses. Moreover, it was found that the CDC-48.2 functioned downstream of the ERK signaling to promote the autophagy induction in nematodes infected with pathogen [58].

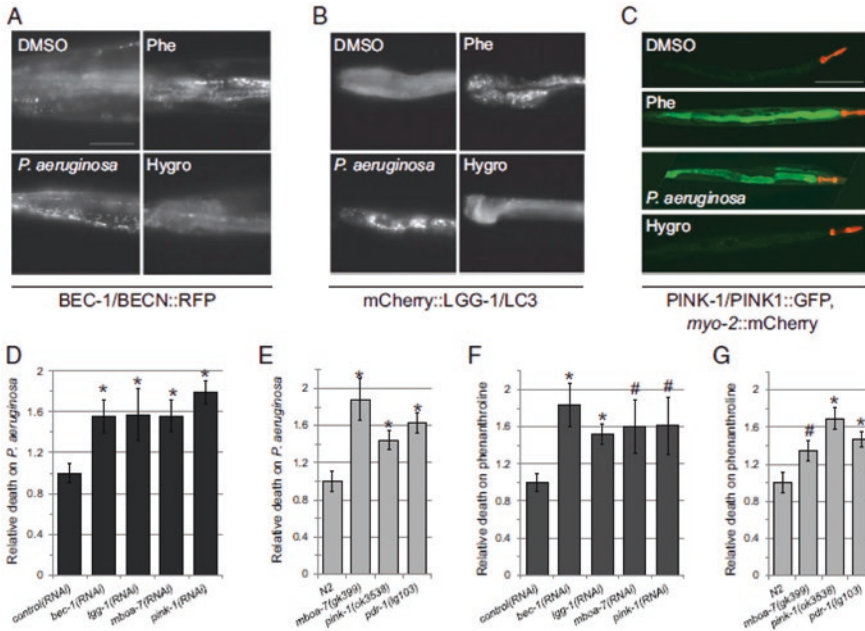


Fig. 9.42 Mitophagy confers resistance to *P. aeruginosa* [69]. (a–c) Fluorescence microscopy of (a) BEC-1/BECN::RFP, (b) mCherry::LGG-1/LC3, or (c) myo-2::mCherry;PINK-1/PINK1::GFP worms treated with DMSO, Phe (1 mM), *P. aeruginosa*, or hygromycin (80 µg/mL). (d and e) Pyoverdine-mediated killing by *P. aeruginosa* and (f and g) Phe toxicity are enhanced by RNAi knockdown (d and f) or mutation (e and g) of autophagy pathway genes *bec-1*/BECN1, *lgg-1*/LC3, and *mboa-7*/MBOAT7 or the mitophagic regulators *pink-1*/PINK1 and *pdr-1*/PARK2. Survival was normalized to empty plasmid (d and f) or wild-type (e and g) controls. Three biological replicates were used for each experiment; $n = 850$ (d and e), $n = 360$ (f and g) per replicate. Error bars represent SEM. * $P < 0.01$, # $P < 0.05$ (Student’s *t*-test). (Scale bars: a, B, 50 µm; c, 200 µm)

9.6.2.10 Mitophagy

Mitophagy shares the biological events with generalized autophagy, including development of an isolation membrane and maturation of autophagosome. Using BEC-1/Beclin1 and LGG-1/LC3 to monitor the related intracellular events, treatment with phenanthroline or *P. aeruginosa* triggered coalescence of the constitutively expressed BEC-1/BECN1::RFP and mCherry::LGG-1/LC3 from a diffuse, cytoplasmic pattern into discrete punctae representing the autophagosomes (Fig. 9.42) [69]. This mitophagy induction required at least two specific regulators (PINK-1/PINK1 and PDR-1/Parkin) to target the mitochondria for recycling, and phenanthroline or *P. aeruginosa* inhibited the mitochondrial import and degradation of PINK-1/PINK1::GFP (Fig. 9.42) [69].

In nematodes, disruption of the autophagy genes (*bec-1/BECN1*, *lgg-1/LC3*, *mboa-7/MBOAT7*) or mitophagic regulators (*pink-1/PINK1* and *pdr-1/PARK2*) increased the lethality of nematodes treated with *P. aeruginosa* or phenanthroline (Fig. 9.42) [69], suggesting the important role of mitophagy in promoting survival in the face of *P. aeruginosa* exposure or phenanthroline treatment. Therefore, the mitophagy is involved in the regulation of toxicity of environmental toxicants or stresses in nematodes.

9.7 Perspectives

Besides the protective responses introduced in some previous chapters, we here only focused on five possible protective response-related signaling pathways to introduce their involvement in the control of toxicity of environmental toxicants or stresses in nematodes. Undoubtedly, more protective response-related signaling pathways will be identified to be involved in the control of toxicity of environmental toxicants or stresses or to replace the importance of already identified protective response-related signaling pathway(s). In addition, some new protective responses may be further formed during the evolution.

During the identification of protective response-related signaling pathways, such as mitochondrial UPR and ER UPR, an important question needed to be further clarified is the specificity of raised signaling pathways for certain protective response. Actually, the chemicals (such as paraquat) used to activate certain protective response normally also have the function to induce the other forms of responses in nematodes. Therefore, at least some raised signaling pathways for certain protective response might be not the directly associated.

At least surrounding the protective responses introduced in this chapter, an assumption can be further raised. That is, some commonly shared molecular signals may exist for these protective responses for nematodes against the environmental toxicants or stresses. The detailed crosstalk events in subcellular compartments or certain tissues, as well as their possible communication between different cells or tissues, still need to be further elucidated.

In this chapter, we mainly introduced and discussed the beneficial roles of these five responses and the underlying molecular mechanisms. Besides these, it is also necessary to pay attention to the potential effects of excessive induction or activation of these responses on nematodes. At least the excessive induction or activation of autophagy may be toxic for organisms. In nematodes, the related information seldom receives the attention so far.

In nematodes, many environmental toxicants or stresses have been shown to potentially cause the toxic effects on different aspects of animals [70–76]. Now, the protective responses to only very limited toxicants or stresses have been examined. The systematic examination of these protective response-related signaling pathways in nematodes exposed to different typical toxicants or stresses are suggested to be performed under different conditions.

References

1. Wang D-Y (2018) *Nanotoxicology in Caenorhabditis elegans*. Springer, Singapore
2. Dong S-S, Qu M, Rui Q, Wang D-Y (2018) Combinational effect of titanium dioxide nanoparticles and nanopolystyrene particles at environmentally relevant concentrations on nematodes *Caenorhabditis elegans*. *Ecotoxicol Environ Saf* 161:444–450
3. Zhao L, Qu M, Wong G, Wang D-Y (2017) Transgenerational toxicity of nanopolystyrene particles in the range of $\mu\text{g/L}$ in nematode *Caenorhabditis elegans*. *Environ Sci Nano* 4:2356–2366
4. Qu M, Xu K-N, Li Y-H, Wong G, Wang D-Y (2018) Using *acs-22* mutant *Caenorhabditis elegans* to detect the toxicity of nanopolystyrene particles. *Sci Total Environ* 643:119–126
5. Zhao Y-L, Wu Q-L, Li Y-P, Wang D-Y (2013) Translocation, transfer, and in vivo safety evaluation of engineered nanomaterials in the non-mammalian alternative toxicity assay model of nematode *Caenorhabditis elegans*. *RSC Adv* 3:5741–5757
6. Ren M-X, Zhao L, Ding X-C, Krasteva N, Rui Q, Wang D-Y (2018) Developmental basis for intestinal barrier against the toxicity of graphene oxide. *Part Fibre Toxicol* 15:26
7. Xiao G-S, Chen H, Krasteva N, Liu Q-Z, Wang D-Y (2018) Identification of interneurons required for the aversive response of *Caenorhabditis elegans* to graphene oxide. *J Nanobiotechnol* 16:45
8. Ding X-C, Rui Q, Wang D-Y (2018) Functional disruption in epidermal barrier enhances toxicity and accumulation of graphene oxide. *Ecotoxicol Environ Saf* 163:456–464
9. Zhao L, Kong J-T, Krasteva N, Wang D-Y (2018) Deficit in epidermal barrier induces toxicity and translocation of PEG modified graphene oxide in nematodes. *Toxicol Res* 7(6):1061–1070. <https://doi.org/10.1039/C8TX00136G>
10. Xiao G-S, Zhi L-T, Ding X-C, Rui Q, Wang D-Y (2017) Value of *mir-247* in warning graphene oxide toxicity in nematode *Caenorhabditis elegans*. *RSC Adv* 7:52694–52701
11. Zhao L, Wan H-X, Liu Q-Z, Wang D-Y (2017) Multi-walled carbon nanotubes-induced alterations in microRNA *let-7* and its targets activate a protection mechanism by conferring a developmental timing control. *Part Fibre Toxicol* 14:27
12. Wang Q-Q, Zhao S-Q, Zhao Y-L, Rui Q, Wang D-Y (2014) Toxicity and translocation of graphene oxide in *Arabidopsis* plants under stress conditions. *RSC Adv* 4:60891–60901
13. Li Y-X, Yu S-H, Wu Q-L, Tang M, Wang D-Y (2013) Transmissions of serotonin, dopamine and glutamate are required for the formation of neurotoxicity from Al_2O_3 -NPs in nematode *Caenorhabditis elegans*. *Nanotoxicology* 7:1004–1013
14. Hoshikawa H, Uno M, Honjoh S, Nishida E (2017) Octopamine enhances oxidative stress resistance through the fasting-responsive transcription factor DAF-16/FOXO in *C. elegans*. *Genes Cells* 22:210–219
15. Yu Y-L, Zhi L-T, Wu Q-L, Jing L-N, Wang D-Y (2018) NPR-9 regulates innate immune response in *Caenorhabditis elegans* by antagonizing activity of AIB interneurons. *Cell Mol Immunol* 15:27–37
16. Zhi L-T, Yu Y-L, Jiang Z-X, Wang D-Y (2017) *mir-355* functions as an important link between p38 MAPK signaling and insulin signaling in the regulation of innate immunity. *Sci Rep* 7:14560
17. Sun L-M, Liao K, Hong C-C, Wang D-Y (2017) Honokiol induces reactive oxygen species-mediated apoptosis in *Candida albicans* through mitochondrial dysfunction. *PLoS One* 12:e0172228
18. Sun L-M, Liao K, Wang D-Y (2017) Honokiol induces superoxide production by targeting mitochondrial respiratory chain complex I in *Candida albicans*. *PLoS One* 12:e0184003
19. Yu Y-L, Zhi L-T, Guan X-M, Wang D-Y, Wang D-Y (2016) FLP-4 neuropeptide and its receptor in a neuronal circuit regulate preference choice through functions of ASH-2 trithorax complex in *Caenorhabditis elegans*. *Sci Rep* 6:21485
20. Sun L-M, Zhi L-T, Shakoos S, Liao K, Wang D-Y (2016) microRNAs involved in the control of innate immunity in *Candida* infected *Caenorhabditis elegans*. *Sci Rep* 6:36036

21. Sun L-M, Liao K, Li Y-P, Zhao L, Liang S, Guo D, Hu J, Wang D-Y (2016) Synergy between PVP-coated silver nanoparticles and azole antifungal against drug-resistant *Candida albicans*. *J Nanosci Nanotechnol* 16:2325–2335
22. Wu Q-L, Cao X-O, Yan D, Wang D-Y, Aballay A (2015) Genetic screen reveals link between maternal-effect sterile gene *mes-1* and *P. aeruginosa*-induced neurodegeneration in *C. elegans*. *J Biol Chem* 290:29231–29239
23. Xie Y, Moussaif M, Choi S, Xu L, Sze JY (2013) RFX transcription factor DAF-19 regulates 5-HT and innate immune responses to pathogenic bacteria in *Caenorhabditis elegans*. *PLoS Genet* 9:e1003324
24. Cao X, Aballay A (2016) Neural inhibition of dopaminergic signaling enhances immunity in a cell non-autonomous manner. *Curr Biol* 26:2329–2334
25. Iwasaki K, Staunton J, Saifee O, Nonet ML, Thomas JH (1997) *aex-3* encodes a novel regulator of presynaptic activity in *C. elegans*. *Neuron* 18:613–622
26. Iwasaki K, Toyonaga R (2000) The Rab3 GDP/GTP exchange factor homolog AEX-3 has a dual function in synaptic transmission. *EMBO J* 19:4806–4816
27. Qu M, Li Y-H, Wu Q-L, Xia Y-K, Wang D-Y (2017) Neuronal ERK signaling in response to graphene oxide in nematode *Caenorhabditis elegans*. *Nanotoxicology* 11:520–533
28. Zhi L-T, Yu Y-L, Li X-Y, Wang D-Y, Wang D-Y (2017) Molecular control of innate immune response to *Pseudomonas aeruginosa* infection by intestinal *let-7* in *Caenorhabditis elegans*. *PLoS Pathog* 13:e1006152
29. Kim DH, Ewbank JJ (2018) Signaling in the innate immune response. *WormBook*. <https://doi.org/10.1895/wormbook.1.83.2>
30. Ewbank JJ, Pujol N (2016) Local and long-range activation of innate immunity by infection and damage in *C. elegans*. *Curr Opin Immunol* 38:1–7
31. Kim DH (2013) Bacteria and the aging and longevity of *Caenorhabditis elegans*. *Annu Rev Genet* 47:233–246
32. Pukkila-Worley R, Ausubel FM (2012) Immune defense mechanisms in the *Caenorhabditis elegans* intestinal epithelium. *Curr Opin Immunol* 24:3–9
33. Irazoqui JE, Urbach JM, Ausubel FM (2010) Evolution of host innate defence: insights from *Caenorhabditis elegans* and primitive invertebrates. *Nat Rev Immunol* 10:47–58
34. Kim DH, Ausubel FM (2005) Evolutionary perspectives on innate immunity from the study of *Caenorhabditis elegans*. *Curr Opin Immunol* 17:4–10
35. Ren M-X, Zhao L, Lv X, Wang D-Y (2017) Antimicrobial proteins in the response to graphene oxide in *Caenorhabditis elegans*. *Nanotoxicology* 11:578–590
36. Melber A, Haynes CM (2018) UPR^{mt} regulation and output: a stress response mediated by mitochondrial-nuclear communication. *Cell Res* 28:281–295
37. Rauthan M, Pilon M (2015) A chemical screen to identify inducers of the mitochondrial unfolded protein response in *C. elegans*. *Worm* 4:e1096490
38. Pellegrino MW, Nargund AM, Kirienco NV, Gillis R, Fiorese CJ, Haynes CM (2014) Mitochondrial UPR-regulated innate immunity provides resistance to pathogen infection. *Nature* 516:414–417
39. Haynes CM, Yang Y, Blais SP, Neubert TA, Ron D (2010) The matrix peptide exporter HAF-1 signals a mitochondrial unfolded protein response by activating the transcription factor ZC376.7 in *C. elegans*. *Mol Cell* 37:529–540
40. Nargund AM, Pellegrino MW, Fiorese CJ, Baker BM, Haynes CM (2012) Mitochondrial import efficiency of ATFS-1 regulates mitochondrial UPR activation. *Science* 337:587–590
41. Haynes CM, Petrova K, Benedetti C, Yang Y, Ron D (2007) ClpP mediates activation of a mitochondrial unfolded protein response in *C. elegans*. *Dev Cell* 13:467–480
42. Rauthan M, Ranji P, Abukar R, Pilon M (2015) A mutation in *Caenorhabditis elegans* NDUF-7 activates the mitochondrial stress response and prolongs lifespan via ROS and CED-4. *G3* 5:1639–1648
43. Nargund AM, Fiorese CJ, Pellegrino MW, Deng P, Haynes CM (2015) Mitochondrial and nuclear accumulation of the transcription factor ATFS-1 promotes OXPHOS recovery during the UPR^{mt}. *Mol Cell* 58:123–133

44. Bischof LJ, Kao C-Y, Los FCO, Gonzalez MR, Shen Z, Briggs SP, van der Goot FG, Aroian RV (2008) Activation of the unfolded protein response is required for defenses against bacterial pore-forming toxin *in vivo*. *PLoS Pathog* 4:e1000176
45. Taylor RC, Dillin A (2013) XBP-1 is a cell-nonautonomous regulator of stress resistance and longevity. *Cell* 153:1435–1447
46. Shen X, Ellis RE, Lee K, Liu C, Yang K, Solomon A, Yoshida H, Morimoto R, Kurnit DM, Mori K, Kaufman RJ (2001) Complementary signalling pathways regulate the unfolded protein response and are required for *C. elegans* development. *Cell* 107:893–903
47. Calfon M, Zeng H, Urano F, Till JH, Hubbard SR, Harding HP, Clark SG, Ron D (2001) IRE1 couples endoplasmic reticulum load to secretory capacity by processing the XBP-1 mRNA. *Nature* 415:92–96
48. Richardson CE, Kinkel S, Kim DH (2011) Physiological IRE-1-XBP-1 and PEK-1 signaling in *Caenorhabditis elegans* larval development and immunity. *PLoS Genet* 7:e1002391
49. Kozlowski L, Garvis S, Bedet C, Palladino F (2014) The *Caenorhabditis elegans* HP1 family protein HPL-2 maintains ER homeostasis through the UPR and hormesis. *Proc Natl Acad Sci U S A* 111:5956–5961
50. Sakaki K, Yoshina S, Shen X, Han J, DeSantis MR, Xiong M, Mitani S, Kaufman RJ (2012) RNA surveillance is required for endoplasmic reticulum homeostasis. *Proc Natl Acad Sci U S A* 109:8079–8084
51. Urano F, Calfon M, Yoneda T, Yun C, Kiraly M, Clark SG, Ron D (2002) A survival pathway for *Caenorhabditis elegans* with a blocked unfolded protein response. *J Cell Biol* 158:639–646
52. Singh J, Aballay A (2017) Endoplasmic reticulum stress caused by lipoprotein accumulation suppresses immunity against bacterial pathogens and contributes to immunosenescence. *MBio* 8:e00778–e00717
53. Marza E, Taouji S, Barroso K, Raymond A, Guignard L, Bonneau M, Pallares-Lupon N, Dupuy J, Fernandez-Zapico ME, Rosenbaum J, Palladino F, Dupuy D, Chevet E (2015) Genome-wide screen identifies a novel p97/CDC-48-dependent pathway regulating ER-stress induced gene transcription. *EMBO Rep* 16:332–340
54. Haskins KA, Russell JF, Gaddis N, Dressman HK, Aballay A (2008) Unfolded protein response genes regulated by CED-1 are required for *Caenorhabditis elegans* innate immunity. *Dev Cell* 15:87–97
55. Glover-Cutter KM, Lin S, Blackwell TK (2013) Integration of the unfolded protein and oxidative stress responses through SKN-1/Nrf. *PLoS Genet* 9:e1003701
56. Hou NS, Gutschmidt A, Choi DY, Pather K, Shi X, Watts JL, Hoppe T, Taubert S (2014) Activation of the endoplasmic reticulum unfolded protein response by lipid disequilibrium without disturbed proteostasis *in vivo*. *Proc Natl Acad Sci U S A* 111:E2271–E2280
57. Meléndez A, Levine B (2009) Autophagy in *C. elegans*. *WormBook*. <https://doi.org/10.1895/wormbook.1.147.1>
58. Kuo C, Hansen M, Troemel E (2018) Autophagy and innate immunity: insights from invertebrate model organisms. *Autophagy* 14:233–242
59. Zou C, Ma Y, Dai L, Zhang K (2014) Autophagy protects *C. elegans* against necrosis during *Pseudomonas aeruginosa* infection. *Proc Natl Acad Sci U S A* 111:12480–12485
60. Martinez BA, Kim H, Ray A, Caldwell GA, Caldwell KA (2015) A bacterial metabolite induces glutathione-tractable proteostatic damage, proteasomal disturbances, and PINK1-dependent autophagy in *C. elegans*. *Cell Death Dis* 6:e1908
61. Samokhvalov V, Scott BA, Crowder CM (2008) Autophagy protects from hypoxic injury in *C. elegans*. *Autophagy* 4:1034–1041
62. Visvikis O, Ihuegbu N, Labeled SA, Luhachack LG, Alves AF, Wollenberg AC, Stuart LM, Stormo GD, Irazoqui JE (2014) Innate host defense requires TFEB-mediated transcription of cytoprotective and antimicrobial genes. *Immunity* 40:896–909
63. Chen H, Kao C, Liu B, Huang S, Kuo C, Ruan J, Lin Y, Huang C, Chen Y, Wang H, Aroian RV, Chen C (2017) HLH-30/TFEB-mediated autophagy functions in a cell-autonomous manner for epithelium intrinsic cellular defense against bacterial pore-forming toxin in *C. elegans*. *Autophagy* 13:371–385

64. Das R, Melo JA, Thondamal M, Morton EA, Cornwell AB, Crick B, Kim JH, Swartz EW, Lamitina T, Douglas PM, Samuelson AV (2017) The homeodomain-interacting protein kinase HPK-1 preserves protein homeostasis and longevity through master regulatory control of the HSF-1 chaperone network and TORC1-restricted autophagy in *Caenorhabditis elegans*. *PLoS Genet* 13:e1007038
65. Xiao Y, Liu F, Zhao P, Zou C, Zhang K (2017) PKA/KIN-1 mediates innate immune responses to bacterial pathogens in *Caenorhabditis elegans*. *Innate Immunity* 23:656–666
66. Kumsta C, Chang JT, Schmalz J, Hansen M (2017) Hormetic heat stress and HSF-1 induce autophagy to improve survival and proteostasis in *C. elegans*. *Nat Commun* 8:14337
67. Possik E, Jalali Z, Nouet Y, Yan M, Gingras M, Schmeisser K, Panaite L, Dupuy F, Kharitidi D, Chotard L, Jones RG, Hall DH, Pause A (2014) Folliculin regulates AMPK-dependent autophagy and metabolic stress survival. *PLoS Genet* 10:e1004273
68. Jia K, Thomas C, Akbar M, Sun Q, Adams-Huet B, Gilpin C, Levine B (2009) Autophagy genes protect against *Salmonella typhimurium* infection and mediate insulin signaling-regulated pathogen resistance. *Proc Natl Acad Sci U S A* 106:14564–14569
69. Kirienko NV, Ausubel FM, Ruvkun G (2015) Mitophagy confers resistance to siderophore-mediated killing by *Pseudomonas aeruginosa*. *Proc Natl Acad Sci U S A* 112:1821–1826
70. Li W-J, Wang D-Y, Wang D-Y (2018) Regulation of the response of *Caenorhabditis elegans* to simulated microgravity by p38 mitogen-activated protein kinase signaling. *Sci Rep* 8:857
71. Xiao G-S, Zhao L, Huang Q, Yang J-N, Du H-H, Guo D-Q, Xia M-X, Li G-M, Chen Z-X, Wang D-Y (2018) Toxicity evaluation of Wanzhou watershed of Yangtze Three Gorges Reservoir in the flood season in *Caenorhabditis elegans*. *Sci Rep* 8:6734
72. Yin J-C, Liu R, Jian Z-H, Yang D, Pu Y-P, Yin L-H, Wang D-Y (2018) Di (2-ethylhexyl) phthalate-induced reproductive toxicity involved in DNA damage-dependent oocyte apoptosis and oxidative stress in *Caenorhabditis elegans*. *Ecotoxicol Environ Saf* 163:298–306
73. Zhao L, Rui Q, Wang D-Y (2017) Molecular basis for oxidative stress induced by simulated microgravity in nematode *Caenorhabditis elegans*. *Sci Total Environ* 607–608:1381–1390
74. Wu Q-L, Han X-X, Wang D, Zhao F, Wang D-Y (2017) Coal combustion related fine particulate matter (PM_{2.5}) induces toxicity in *Caenorhabditis elegans* by dysregulating microRNA expression. *Toxicol Res* 6:432–441
75. Shao H-M, Han Z-Y, Krasteva N, Wang D-Y (2018) Identification of signaling cascade in the insulin signaling pathway in response to nanopolystyrene particles. *Nanotoxicology* (in press)
76. Xiao G-S, Zhao L, Huang Q, Du H-H, Guo D-Q, Xia M-X, Li G-M, Chen Z-X, Wang D-Y (2018) Biosafety assessment of water samples from Wanzhou watershed of Yangtze Three Gorges Reservoir in the quiet season in *Caenorhabditis elegans*. *Sci Rep* 8:14102

Chapter 10

Functions of G-Protein-Coupled Receptors and Ion Channels and the Downstream Cytoplasmic Signals in the Regulation of Toxicity of Environmental Toxicants or Stresses



Abstract It is an assumption that environmental toxicants or stresses will first activate or suppress certain G-protein-coupled receptors (GPCRs) and/or ion channels on the surface of targeted cells and then activate a subset of downstream cytoplasmic signaling cascades. Based on this assumption, we here first introduced and discussed the involvement of GPCRs (epidermal DCAR-1, intestinal FSHR-1, neuropeptide receptors, and neuronal SRH-220) and ion channels (cyclic nucleotide-gated ion channel, voltage-gated calcium ion channel, potassium ion channel, and chloride intracellular channel) in the regulation of toxicity of environmental toxicants or stresses and the underlying mechanisms. Moreover, we discussed the potential activation of cytoplasmic signaling cascade, containing ARR-1/arrestin, G-proteins, PLC-DAG-PKD signaling, and Ca^{2+} signaling, upon the exposure to environmental toxicants or stresses and the corresponding important functions.

Keywords G-protein-coupled receptors (GPCRs) · Ion channel · Cytoplasmic signaling cascade · Environmental exposure · *Caenorhabditis elegans*

10.1 Introduction

In nematodes, various environmental toxicants/stresses can induce the alterations in different aspects on animals [1–17]. Upon the exposure to environmental toxicants/stresses, it is assumed that certain G-protein-coupled receptors (GPCRs) or ion channels would be activated or suppressed. After that, a certain downstream cytoplasmic signaling cascade will be affected, and the functions of certain transcriptional factors and their targets will be further altered. If this assumption is correct and the toxic effects of toxicants or stresses can reach the targeted organs (especially the primary targeted organs), both the GPCRs and the ion channels play crucial roles in the induction of toxicity in nematodes exposed to environmental toxicants or stresses.

In this chapter, we first introduced the identified GPCRs involved in the regulation of toxicity of environmental toxicants or stresses and the underlying mechanisms for their important functions. Again, we introduced and discussed the

involvement of several types of ion channels in the regulation of toxicity of environmental toxicants or stresses. Moreover, we focused on ARR-1/arrestin, G-proteins, PLC-DAG-PKD signaling, and Ca²⁺ signaling to discuss the important functions of cytoplasmic signaling cascade in transducing environmental stimuli and mediating the toxicity induction in nematodes exposed to environmental toxicants or stresses.

10.2 GPCRs

In Chaps. 5, 6, and 9, we have discussed the functions of some important GPCRs, such as insulin receptors, Wnt receptors, and neurotransmitter receptors, in regulating the toxicity of environmental toxicants or stresses and the underlying mechanisms. We here further introduced and discussed the involvement of other GPCRs in the regulation of toxicity of environmental toxicants and stresses and the underlying mechanisms.

10.2.1 Epidermal DCAR-1

Infection with environmental pathogens (bacterial pathogens and fungal pathogens) will cause toxicity at various aspects on both human beings and animals, including the nematodes [18–24]. With the fungus *Drechmeria coniospora* as an example, RNAi knockdown was performed on 1150 GPCR-encoding genes to identify the GPCRs required for the control of innate immunity against the fungal infection [25, 26]. Based on the expression of an antimicrobial peptide (AMP) reporter gene (*nlp-29p::gfp*), three clones, targeting *dcar-1* (*dcar-1(RNAi)*), *frpr-11* (*frpr-11(RNAi)*), and *srv-21* (*srv-21(RNAi)*), were found to be able to decrease the expression of the reporter gene (Fig. 10.1) [26]. The *sta-1* (*sta-1(RNAi)*) was used as a control, since it does not affect expression of the gene-encoding GFP. Meanwhile, it was observed that, unlike *frpr-11(RNAi)* or *srv-21(RNAi)*, *dcar-1(RNAi)* did not affect the expression of *nlp-29p::gfp* in nematodes expressing a constitutively active form of the G α protein GPA-12 (Fig. 10.1) [26], suggesting that the DCAR-1 may act upstream or in parallel to GPA-12. *dcar-1(RNAi)* also could not abrogate the *nlp-29* induction by osmotic stress (Fig. 10.1) [26].

In nematodes, DCAR-1 acted in the epidermis to regulate the expression of AMP-encoding genes and the defense against fungal infection [26]. Meanwhile, it was found that mutation of *dcar-1* had a profound effect on the induction of six *nlp* genes in nematodes infected with *D. coniospora* (Fig. 10.1) [26]. Among them, the activation of DCAR-1 was due to the endogenous ligands of NLP-28 and NLP-29, and loss-of-function mutation of *dcar-1* (in a *dpy-10;dcar-1* mutant) reduced the elevated expression of *nlp-29* [26].

In the epidermis, the dihydrocaffeic acid (DHCA) was identified as an exogenous ligand that activates the innate immune response via DCAR-1. The addition of

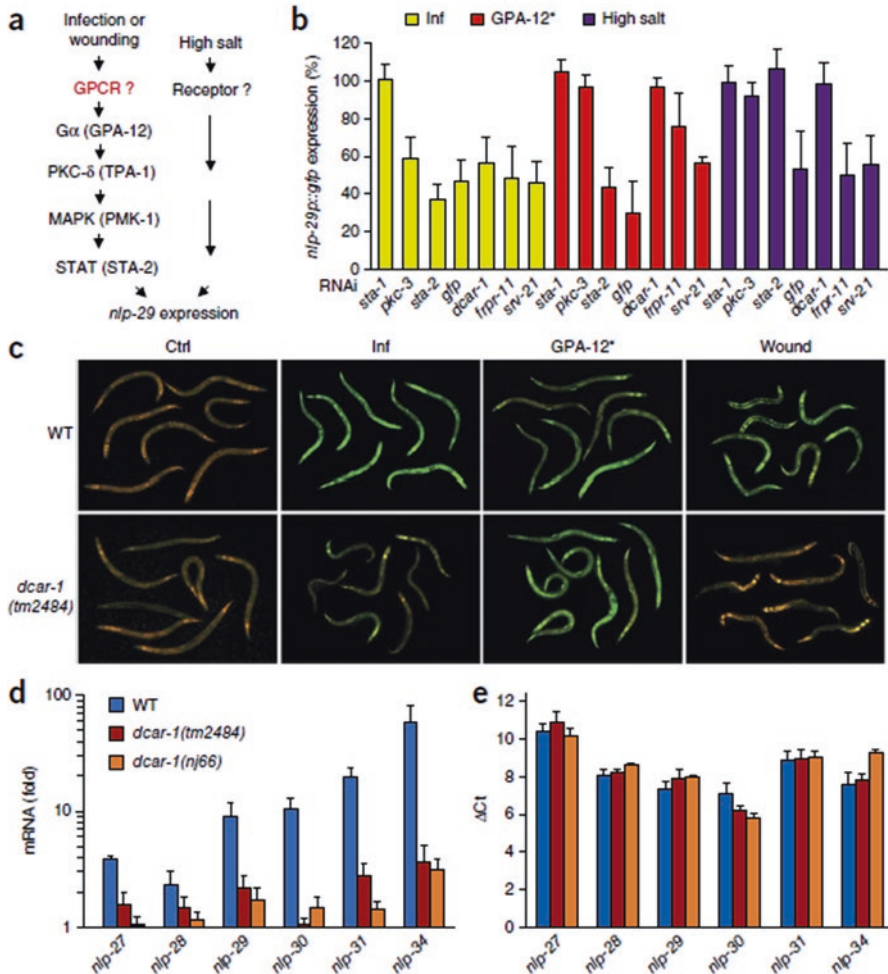


Fig. 10.1 The GPCR DCAR-1 controls the expression of AMP-encoding genes [26]. **(a)** Pathways that lead to the expression of *nlp-29*. **(b)** Expression of *nlp-29p::gfp* by worms carrying the integrated array *frIs7* (which contains the reporter transgenes *nlp-29::gfp* and *col-12::DsRed*) and treated by RNAi directed against control or candidate genes (horizontal axis) and infected with *D. coniospora* (Inf) or expressing the constitutively active GPA-12* in the epidermis (GPA-12*) or exposed to a high salt medium (high salt); results are normalized GFP fluorescence presented relative to results obtained with the negative control *sta-1(RNAi)*, set as 100%. **(c)** Fluorescent images of wild-type (WT) and *dcar-1(tm2484)* worms carrying *frIs7* and assessed without further treatment (control (Ctrl)) or after infection by *D. coniospora* (Inf) or expressing GPA-12* in the epidermis (GPA-12*) or assessed after wounding (wound). Constitutive expression of DsRed in the epidermis is unaffected by these treatments. Original magnification, $\times 600$ (images obtained with a filter set to visualize green and red fluorescence). **(d)** Quantitative RT-PCR analysis of the expression of genes in the *nlp-29* cluster (horizontal axis) in wild-type, *dcar-1(tm2484)*, and *dcar-1(nj66)* worms after infection with *D. coniospora*; results are presented relative to those of uninfected worms. **(e)** Abundance of mRNA of genes in the *nlp-29* cluster in the wild-type, *dcar-1(tm2484)*, and *dcar-1(nj66)* strains, presented as the change in cycling threshold (ΔCt) calculated as the cycling threshold for each *nlp* gene minus that for the gene-encoding actin (*act-1*). Data are from experiments with at least six biological replicates (**b**; with at least 50 worms per condition; mean and s.d.) or are representative of over ten experiments (**c**) or are from three independent experiments (**d**, **e**; average and s.d.)

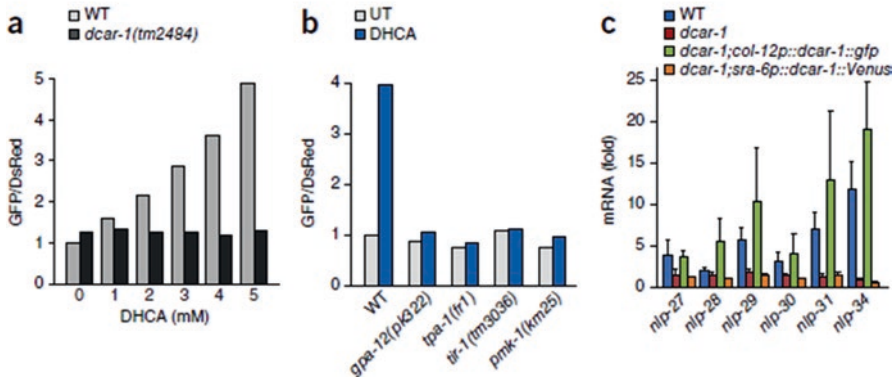


Fig. 10.2 DHCA mimics the effect of infection on the expression of AMP-encoding genes [26]. (a, b) Fluorescence ratio of green (GFP) to red (DsRed) of wild-type and *dcar-1(tm2484)* worms ($n \geq 50$ per condition) carrying *frIs7* and treated with increasing concentrations of DHCA; results are normalized to those of wild-type worms. (b) Fluorescence ratio (as in a, b) of wild-type and various mutant strains ($n > 50$ per condition) carrying *frIs7* and left untreated (UT) or treated with 5 mM DHCA (key). (c) Quantitative RT-PCR analysis of the expression of genes in the *nlp-29* cluster in wild-type, *dcar-1(tm2484)*, *dcar-1;col-12p::dcar-1::gfp*, and *dcar-1;sra-6p::dcar-1::Venus* mutant worms after exposure for 2 h to 5 mM DHCA; results are presented relative to those of uninfected control worms. Data representative of four experiments (a, b) or are from two experiments (c; average and s.d. of three biological replicates)

DHCA to wild-type nematodes could trigger the expression of the *nlp-29p::gfp* reporter gene in a dose-dependent manner (Fig. 10.2) [26]. This increase was blocked in *dcar-1* mutant nematodes or in nematodes in which various elements of regulatory network controlling the *nlp-29* expression were mutant (*gap-12*, *tpa-1*, *tir-1*, or *pmk-1*) (Fig. 10.2) [26]. In addition, treatment with DHCA also triggered an increase in the *nlp-29* expression, and this increase was dependent on *dcar-1* and *pmk-1* (Fig. 10.2) [26]. More importantly, the expression of *dcar-1* in the epidermis, not in the neurons, was sufficient to restore the induction of *nlp* genes by DHCA (Fig. 10.2) [26].

Four molecules (DHPA (3-(2,4-dihydroxyphenyl)propionic acid), DHCA, DPPA, and HPLA) that are structurally related to DHCA were identified as *in vivo* ligands for DCAR-1 and could trigger the *nlp-29p::gfp* expression in a dose-dependent manner (Fig. 10.3) [26]. Nevertheless, DHCA beyond the concentration of 80 mM was toxic, and DPPA, DHPA, and HPLA were toxic at concentrations above 10 mM [26]. Moreover, based on the analysis of high-performance liquid chromatography, the HPLA was present at a low level in control nematodes and could be increased ~3.5-fold by fungal infection (Fig. 10.3) [26].

Additionally, since the HPLA amount was elevated in extracts of pellets of *dpy-10* mutant nematodes, HPLA could be generated as a consequence of alterations in cuticle development [26]. The *nlp-29p::gfp* expression increase induced by HPLA was also dependent on DCAR-1 and various elements of downstream signal transduction cascade (*gpa-12*, *tpa-1*, *tir-1*, and *pmk-1*) (Fig. 10.3) [26], suggesting that

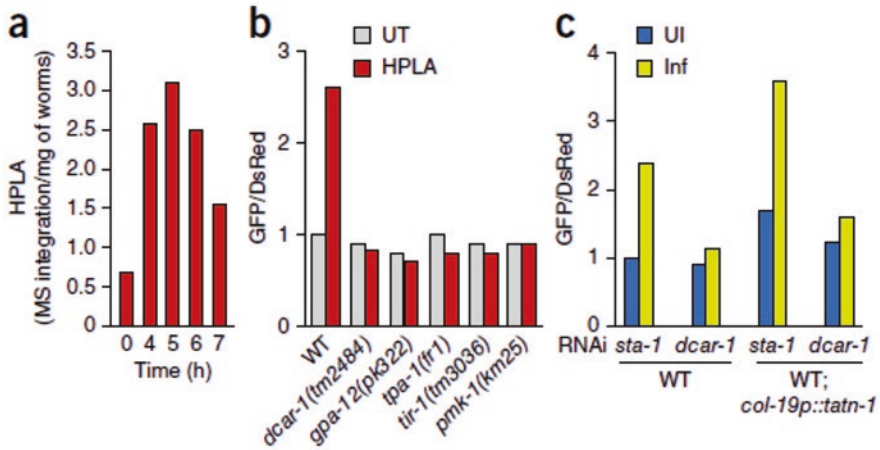


Fig. 10.3 Endogenous HPLA increases upon infection with *D. coniospora* and triggers the expression of *nlp-29* AMP-encoding genes via a DCAR-1–PMK-1 signaling pathway [26]. (a) Abundance of HPLA in wild-type worms at various times (horizontal axis) after infection with *D. coniospora*, presented as integration of high-performance liquid chromatography–mass spectrometry (MS) peaks, normalized to the worm pellet dry weight. (b) Fluorescence ratio of wild-type and mutant worms (horizontal axis) carrying *frIs7*, left untreated or treated with 5 mM HPLA (key). (c) Fluorescence ratio of wild-type worms (left) or wild-type that additionally carry an epidermally expressed construct *col-19p::tatn-1* (right), left uninfected or infected with *D. coniospora* and treated by RNAi with control or *dcar-1*-targeting clones (horizontal axis). Data are representative of two experiments (a) or experiments with at least three (b) or two (c) biological replicates of at least 50 worms per condition

HPLA can act through the DCAR-1 to regulate the epidermal innate immune response in nematodes.

10.2.2 Intestinal FSHR-1

Of the 14 candidate LRR receptors, GPCR FSHR-1 was identified as a putative innate immune receptor. After infection with Gram-negative or Gram-positive bacterial pathogens, the *fshr-1(ok778)* mutant nematodes exhibited more sensitive than wild-type nematodes to the killing (Fig. 10.4) [27]. Meanwhile, the *fshr-1(ok778)* mutant nematodes do not have a reduced lifespan on *E. coli* OP50, suggesting the susceptibility of *fshr-1(ok778)* mutant nematodes to pathogen infection is not due to the nonspecific sickness [27].

More importantly, FSHR-1 regulated transcription of a set of putative antimicrobial genes that can be induced by pathogen infection. Three of five PMK-1-dependent genes (*F56D6.2*, *C17H12.8*, and *F49F1.6*) induced by PA14 were decreased in *fshr-1(ok778)* mutant nematodes (Fig. 10.5) [27]. Besides this, the expression inductions of at least *F01D5.5* and *C32H11.12* upon PA14 exposure

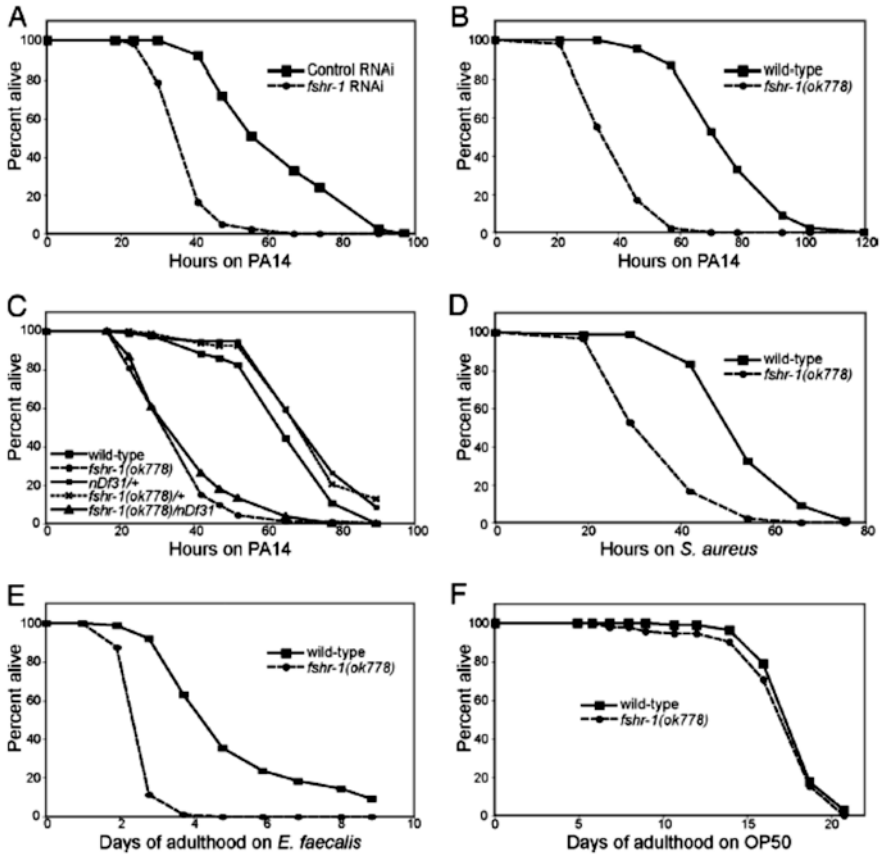


Fig. 10.4 FSHR-1 is required for innate immunity [27]. (a, b) *fshr-1* (RNAi) or *fshr-1(ok778)* mutant worms are sensitive to killing by pathogenic *P. aeruginosa* PA14 relative to wild-type control worms. (c) *fshr-1(ok778)/nDf31* heterozygotes are just as sensitive to PA14 as *fshr-1(ok778)* homozygotes. (d–f) *fshr-1(ok778)* mutants are sensitive to killing by pathogenic *S. aureus* and *E. faecalis* but not to *E. coli* OP50

were reduced in *fshr-1(ok778)* mutant nematodes (Fig. 10.5) [27], suggesting that their expression was independent of PMK-1 but dependent on the FSHR-1 in response to pathogen infection in nematodes.

Tissue-specific activity analysis demonstrated that FSHR-1 functioned in the intestine, the major site of pathogen exposure, to regulate the innate immunity [27]. During the control of innate immunity to pathogen infection, FSHR-1 acted in parallel to both the insulin (*daf-2*) and the p38 MAPK (*tir-1*, *nsy-1*, and *pmk-1*) pathways. It was found that *daf-2(e1368ts); fshr-1(ok778)* double mutants had an immunity phenotype that was intermediate between either of the single mutants (Fig. 10.6) [27]. Additionally, *pmk-1(km25); fshr-1(ok778)* double mutants were even more sensitive than either single mutants, and mutation of *tir-1* or *nsy-1* significantly enhanced the *fshr-1(ok778)* null phenotype (Fig. 10.6) [27].

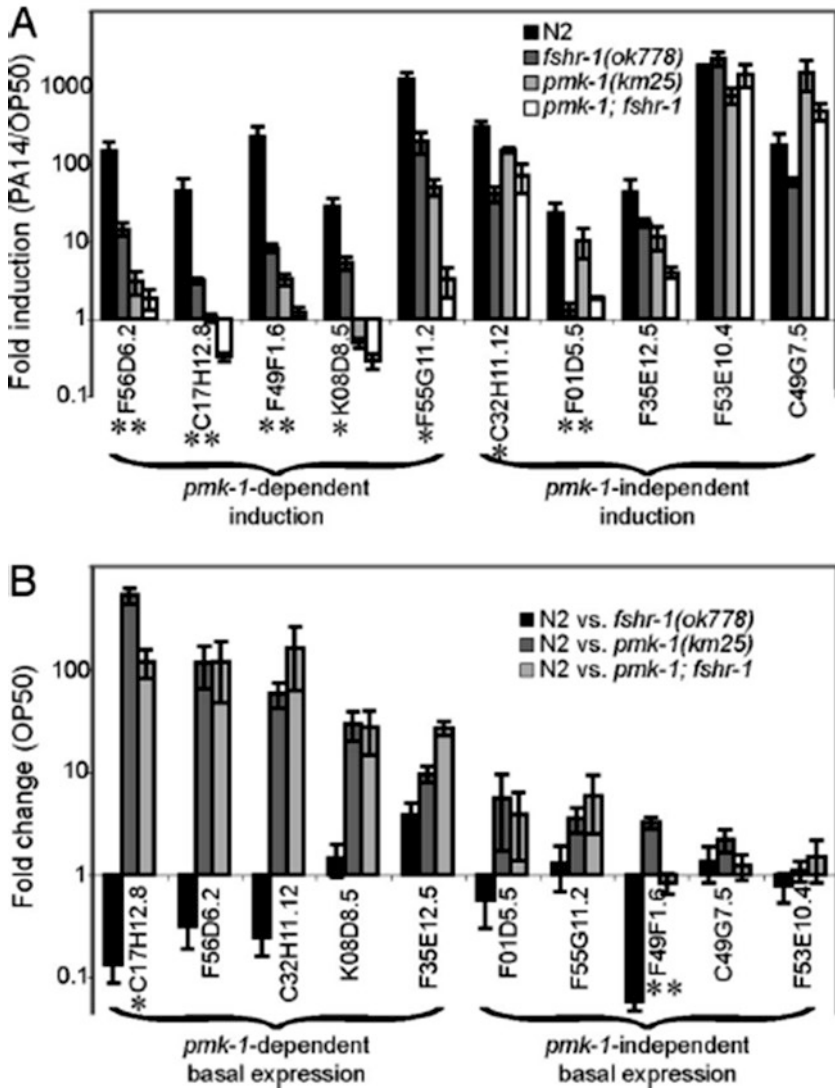
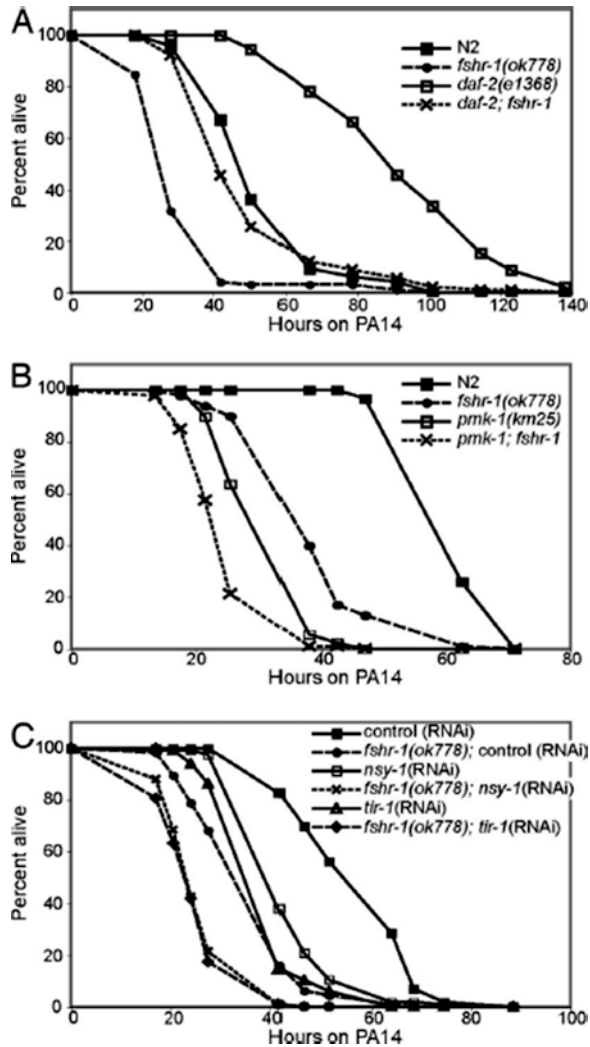


Fig. 10.5 FSHR-1 regulates PA14 response genes [27]. (a, b) qRT-PCR was used to analyze the relative transcription of PA14 response genes in wild-type and mutant worms fed OP50 or PA14. Error bars represent SEM for three independent biologic replicates. (a) Fold induction was calculated as the ratio of normalized expression on PA14 divided by expression on OP50. *Genes with greater than fivefold reduction in their induction in *fshr-1(ok778)* mutant worms relative to wild-type worms with $P < 0.01$. **Genes with greater than tenfold reduction in their induction in *fshr-1(ok778)* mutants relative to wild-type worms with $P < 0.01$. (b) Fold change in basal expression was calculated as the ratio of wild-type expression to mutant expression in worms fed OP50. *Genes with greater than fivefold lower basal expression in wild-type worms relative to *fshr-1(ok778)* mutants. **Genes with greater than tenfold lower basal expression in wild-type worms relative to *fshr-1(ok778)* mutants

Fig. 10.6 FSHR-1 acts in parallel to DAF-2 and the p38 MAPK pathway [27]. (a) *daf-2* and *fshr-1* single and double mutants were raised at 15 °C and then shifted to the restrictive temperature of 25 °C 4 h before exposure to PA14. (b, c) Loss of components of the p38 MAPK pathway, either by genetic mutation (*pmk-1*) or RNAi (*tir-1* and *nsy-1*), enhances the pathogen sensitivity of *fshr-1(ok778)* null mutants. Experiments with *pmk-1* and *fshr-1* single and double mutants were repeated five times, and in all cases the double mutants were significantly more sensitive than either single mutant



10.2.3 Neuropeptide Receptors

10.2.3.1 NPR-1

Based on the mutant screen, it was found that the *npr-1(ad609)* mutant nematodes showed the enhanced susceptibility to *P. aeruginosa*-mediated killing (Fig. 10.7) [28]. Under the normal conditions, no difference in survival was seen between *npr-1(ad609)* mutant and wild-type nematodes [28], suggesting that the *npr-1* mutation affects the innate immune response to pathogenic bacteria without altering the basic lifespan. Additionally, although the lawn avoidance is part of *C. elegans* defense

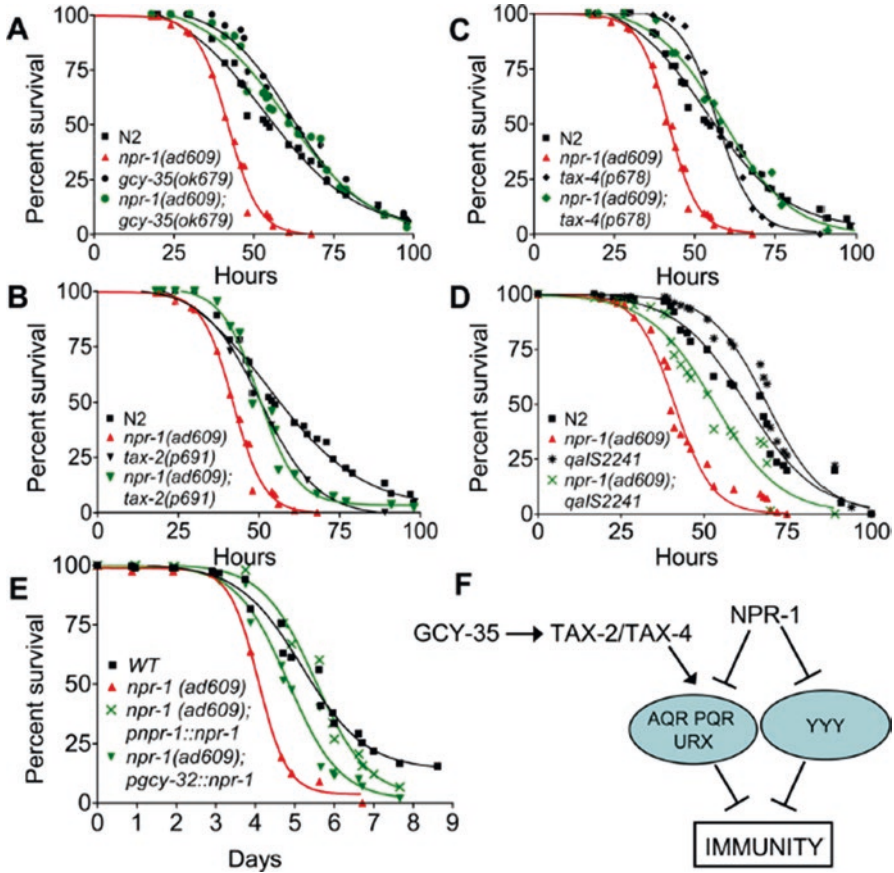


Fig. 10.7 The NPR-1 neural circuit regulates innate immunity [28]. (a) Wild-type N2, *npr-1(ad609)* ($P = 0.0001$), *gcy-35(ok679)* ($P = 0.0125$), and *gcy-35(ok679);npr-1(ad609)* ($P = 0.0639$) were exposed to *P. aeruginosa*. (b) Wild-type N2, *npr-1(ad609)* ($P = 0.1673$), and *tax-4(p678);npr-1(ad609)* ($P = 0.3611$) were exposed to *P. aeruginosa*. (c) Wildtype N2, *npr-1(ad609)* ($P = 0.0001$), *tax-2(p691)* ($P = 0.0930$), and *tax-2(p691);npr-1(ad609)* ($P = 0.0031$) were exposed to *P. aeruginosa*. (d) Wild-type N2; *npr-1(ad609)* ($P = 0.0001$); *qalS2241* ($P = 0.0042$); a strain which lacks AQR, PQR, and URX neurons; and *npr-1(ad609);qalS2241* ($P = 0.0001$) were exposed to *P. aeruginosa*. The graphs represent combined results of at least three independent experiments, $N \geq 40$ adult nematodes per strain. (e) Wild-type N2, *npr-1(ad609)* ($P = 0.0001$), *pgcy-32::npr-1*; *npr-1(ad609)* ($P = 0.0001$), and *pnpr-1::npr-1*; *npr-1(ad609)* ($P = 0.1939$) were exposed to *P. aeruginosa*. The graphs represent combined results of at least two independent experiments, $N \geq 100$ adult nematodes per strain. Killing assays were performed at 17 °C, as low temperatures are known to increase the resolution of killing assays involving *P. aeruginosa*. (f) Model of the neural control of innate immunity in *C. elegans*: NPR-1 inhibits the activity of AQR, PQR, URX and additional neuron(s) designated YYY that suppress innate immunity, while GCY-35, TAX-2, and TAX-4 are required for the activation of AQR, PQR, and URX neurons

response to *P. aeruginosa*, it did not account for the difference between wild-type and *npr-1(ad609)* animals [28]. The susceptibility of nematodes deficient in NPR-1 to *P. aeruginosa* was largely due to the decreased pathogen avoidance and the decreased innate immune responses.

In nematodes, the enhanced susceptibility of *npr-1(ad609)* to *P. aeruginosa* could be rescued by mutations in *gcy-35* soluble guanylate cyclase (Fig. 10.7) [28]. Moreover, *npr-1*- and *gcy-35*-expressing sensory neurons (AQR, PQR, and URX) could actively suppress the innate immune responses of non-neuronal tissues to pathogen infection, since the nematodes lacking AQR, PQR, and URX neurons exhibited an increased survival on *P. aeruginosa* (Fig. 10.7) [28]. In addition, killing the AQR, PQR, and URX neurons also partially rescued the enhanced susceptibility of *npr-1(ad609)* to *P. aeruginosa* (Fig. 10.7) [28]. Expression of *npr-1* in the AQR, PQR, and URX neurons could rescue the enhanced susceptibility of *npr-1(ad609)* to *P. aeruginosa* (Fig. 10.7) [28], suggesting the requirement of NPR-1 activity in sensory neurons for the control of innate immunity.

A full-genome microarray analysis was performed to identify the downstream targets for NPR-1 in regulating innate immunity in nematodes subjecting to pathogen infection. It was found that mutation in *npr-1* caused the alteration of genes that are markers of innate immune responses, including those regulated by a conserved PMK-1/p38 MAPK signaling pathway (Fig. 10.8) [28]. These genes were similarly misregulated in nematodes deficient in NPR-1 or PMK-1 function [28]. Additionally, the *npr-1(ad609)* nematodes showed lower levels of active PMK-1 than wild-type nematodes (Fig. 10.8) [28]. Nevertheless, RNAi knockdown of *pmk-1* in *npr-1(ad609)* mutant nematodes resulted in an increased susceptibility to pathogen infection [28], suggesting that NPR-1 regulates both PMK-1-dependent and independent innate immune responses in nematodes.

10.2.3.2 NPR-4

Using assay system of preference choice on bacterial foods, OP50 and pathogen PA14, it was observed that the ADL sensory neurons were required for the control of preference choice [29]. In nematodes, some neuropeptides encoded by *flp-4*, *flp-21*, *nlp-7*, *nlp-8*, and *nlp-10* are expressed in ADL sensory neurons, and ADL-specific RNAi knockdown of *flp-4* or mutation of *nlp-10* significantly decreased choice index compared with wild-type N2 [29].

The receptor for neuropeptide FLP-4 is NPR-4. Loss-of-function mutation of *npr-4* significantly decreased the choice index compared with wild-type N2 (Fig. 10.9) [29]. In nematodes, the sensory inputs can be released from ADL sensory neurons to AIA, AIB, AVA, AVB, or AVD interneurons (Fig. 10.9) [29]. Expression of NPR-4 in the AVA or AIA interneurons did not recover the deficit in preference choice in *npr-4(tm1782)* mutants (Fig. 10.9) [29]. In contrast, expression of NPR-4 in AIB interneurons could obviously rescue the deficit in preference choice in *npr-4(tm1782)* mutants (Fig. 10.9) [29], suggesting that the FLP-4 released

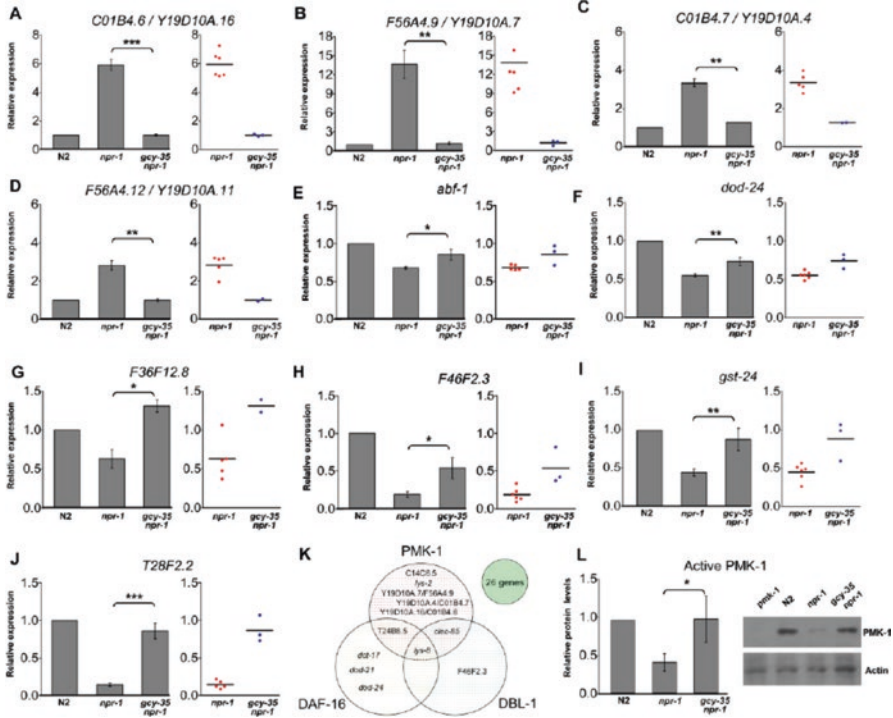


Fig. 10.8 The NPR-1 neural circuit regulates expression of innate immune genes [28]. (a–j) Quantitative reverse transcription–PCR analysis of *C01B4.6/Y19D10A.16*, *F56A4.9/Y19D10A.7*, *C01B4.7/Y19D10A.4*, *F56A4.12/Y19D10A.11*, *abf-1*, *dod-24*, *F36F12.8*, *F46F2.3*, *gst-24*, and *T28F2.2* expression in *npr-1(ad609)* and *gcy-35(ok769);npr-1(ad609)* nematodes relative to wild-type nematodes exposed to *P. aeruginosa*. Data were analyzed by normalization to actin (*act-1, -3, -4*) and relative quantification using the comparative cycle threshold method. Student’s exact *t*-test indicates differences among the groups are significantly different; bar graphs correspond to mean \pm SEM. Point graphs correspond to gene quantification in independent isolations of *npr-1(ad609)* ($N = 6$) and *gcy-35(ok769);npr-1(ad609)* ($N = 3$). (K) The Venn diagram lists the genes identified by microarray analysis to be regulated by both NPR-1 and one or more known innate immune pathways in *C. elegans*. Genes that lie within two or three circles are regulated by multiple innate immune pathways in addition to NPR-1. Twenty-six genes have not been previously connected to any of the innate immune pathways and are depicted in the solitary circle. (L) Immunological detection of active PMK-1. Active PMK-1 was detected in wild-type N2, *npr-1(ad609)*, and *gcy-35(ok769);npr-1(ad609)*. Animals were grown at 20 °C until 1-day-old adult and whole worm lysates were used to detect active PMK-1 by Western blotting using an anti-human p38 antibody. Actin was detected using a polyclonal antibody

from ADL sensory neurons regulates the preference choice through its receptor of NPR-4 in AIB interneurons in nematodes.

To identify candidate targeted genes for *npr-4* in regulating preference choice, the expression patterns of genes expressed in AIB interneurons were examined. Among 24 genes expressed in AIB interneurons, it was found that mutation of *npr-4* caused the significant increase in expression levels of *ptp-3* and *ced-10* and the

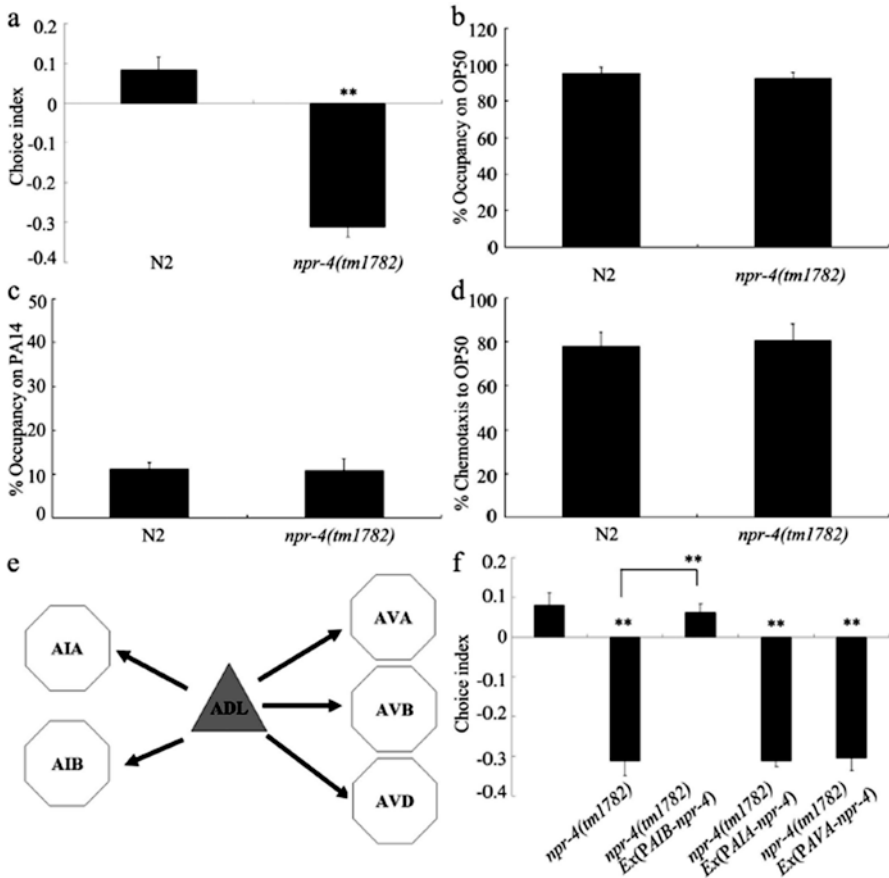


Fig. 10.9 NPR-4 regulated the preference choice in nematodes [29]. (a) Mutation of *npr-4* gene altered preference choice. (b–d) Mutation of *npr-4* gene did not influence leaving behavior from bacterial lawns and chemotaxis to OP50. (e) Schematic diagram for putative neural networks associated with ADL sensory neurons, extracted from the complete circuit. Sensory neurons are shown as triangles and interneurons as hexagons. Arrows indicate chemical synapses. (f) Expression of NPR-4 in AIB interneurons rescued the deficit in preference choice in *npr-4* mutants. Bars represent means \pm S.E.M. ** $P < 0.01$ vs N2 (if not specifically indicated)

significant decrease in expression levels of *glr-2*, *tax-6*, *cdc-42*, and *set-2* (Fig. 10.10) [29]. Using the available mutants for candidate targeted genes of *npr-4* to investigate their possible function in regulating preference choice, it was observed that only mutation of *set-2* caused the significant decrease in choice index compared with wild-type N2 (Fig. 10.10) [29]. In nematodes, *set-2* encodes a histone H3 at lysine 4 (H3K4) methyltransferase. Moreover, preference choice phenotype of double mutant of *set-2(ok952);npr-4(tm1782)* was similar to that of single mutant of *set-2(ok952)* or *npr-4(tm1782)* (Fig. 10.10) [29], suggesting that SET-4 and NPR-4 function in the same pathway to regulate preference choice.

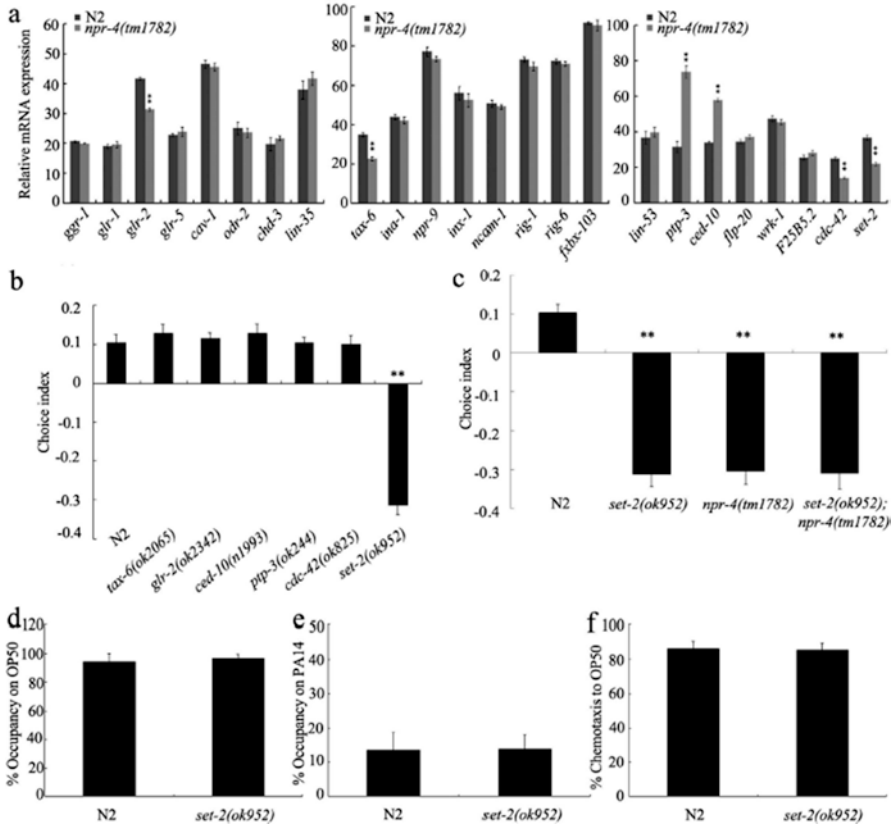


Fig. 10.10 Identification of downstream target for NPR-4 in regulating preference choice in nematodes [29]. (a) Mutation of *npr-4* gene altered expression patterns of some genes expressed in AIB interneurons. (b) Mutation of *set-2* gene induced the deficit in preference choice. (c) Genetic interaction of *npr-4* with *set-2* in regulating preference choice. (d–f) Leaving behavior from bacterial lawns and chemotaxis to OP50 in *set-2* mutants. Bars represent means \pm S.E.M. $**P < 0.01$ vs N2

10.2.3.3 NPR-9

npr-9 encodes a homolog of the gastrin-releasing peptide receptor (GRPR) and is expressed in AIB interneurons. After infection with *P. aeruginosa* PA14, the *npr-9(tm1652)* mutant nematodes showed a resistance to the PA14 infection, a decreased PA14 colonization, and an increased expression of some immunity-related genes (Fig. 10.11) [30]. In contrast, the nematodes overexpressing NPR-9 exhibited an increased susceptibility to infection, an increased PA14 colonization, and a reduced expression of some immunity-related genes [30]. Additionally, the expression of GRPR, the human homolog of NPR-9, could largely mimic the NPR-9 function in regulating the innate immunity against the pathogen infection in nematodes [30].

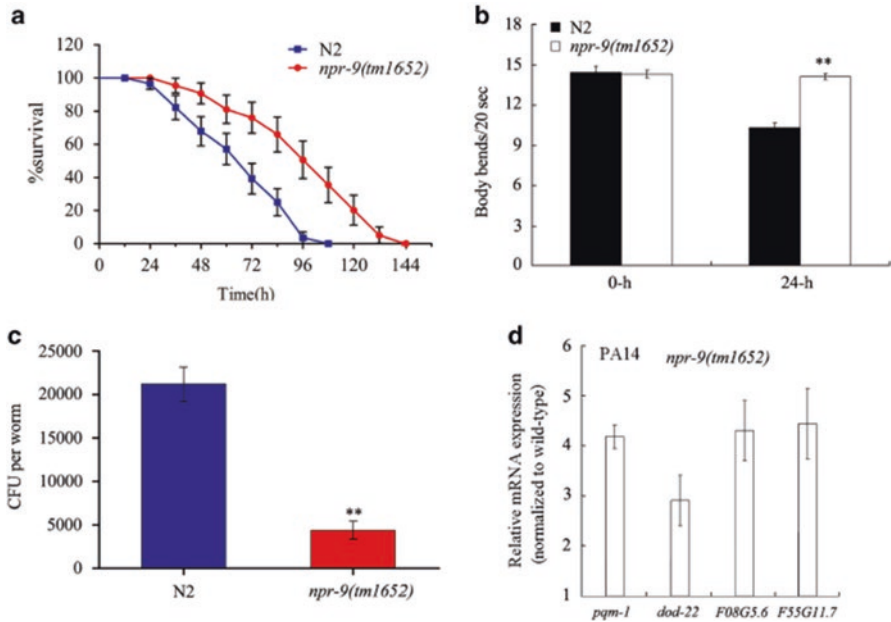


Fig. 10.11 *npr-9* mutants were resistant to *P. aeruginosa* infection [30]. (a) Comparison of survival plots between wild-type N2 and *npr-9* mutants exposed to *P. aeruginosa* PA14. A statistical comparison of the survival plots indicates that survival of the mutant animals was significantly different from that of wild-type N2 animals ($P < 0.0001$). (b) Comparison of body bend between wild-type N2 and *npr-9* mutants exposed to *P. aeruginosa* PA14 for 24 h. Bars represent mean \pm s.d. ** $P < 0.01$ vs N2. (c) Comparison of CFU between wild-type N2 and *npr-9* mutants exposed to *P. aeruginosa* PA14. Bars represent the mean \pm s.d. ** $P < 0.01$ vs N2. (d) Quantitative real-time PCR analysis of expression patterns for immunity-related genes in *npr-9* mutants exposed to *P. aeruginosa* PA14. Normalized expression is presented relative to wild-type expression; bars represent the mean \pm s.d.

Chr2-mediated AIB interneuron activation could strengthen the innate immune response and decrease the PA14 colonization [30]. In nematodes, synaptic transmission can be potentiated by expression of the active protein kinase C homolog (*pkc-1(gf)*) [31, 32]. More importantly, it was observed that the overexpression of NPR-9 suppressed the innate immune response and increased PA14 colonization in nematodes with the activation of AIB interneurons mediated by Chr2 or by expressing *pkc-1(gf)* in AIB interneurons (Fig. 10.12) [30]. Therefore, it is hypothesized that NPR-9 regulates the innate immune response to pathogen infection by antagonizing the activity of AIB interneurons.

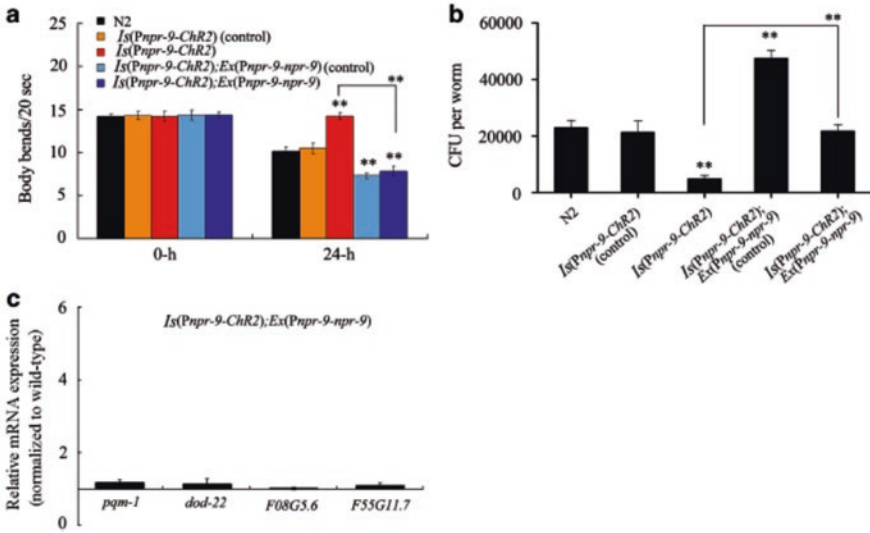


Fig. 10.12 NPR-9 antagonized the function of AIB interneurons to regulate innate immunity [30]. (a) Effects of *npr-9* overexpression on body bend of nematodes with ChR2-mediated activation in AIB interneurons exposed to *P. aeruginosa* PA14. (b) Effects of *npr-9* overexpression on CFU in nematodes with ChR2-mediated AIB interneuron activation exposed to *P. aeruginosa* PA14. (c) Effects of *npr-9* overexpression on expression patterns for immunity-related genes in nematodes with ChR2-mediated activation of AIB interneurons exposed to *P. aeruginosa* PA14. Normalized expression is presented relative to wild-type expression. Bars represent the mean \pm s.d. $^{***}P < 0.01$ vs N2 if not specially indicated. CFU, colony-forming unit

10.2.3.4 NPR-12

NLP-29 is a neuropeptide-like protein expressed in the epidermis. The NLP-29 expression can be induced by infection with pathogens, such as *Drechmeria coniospora* (36-h exposure) [33]. Infection of *D. coniospora* caused significant PVD dendrite degeneration, and mutation of *nlp-29* was able to completely block the infection-induced PVD dendrite degeneration (Fig. 10.13) [33].

The neuronal GPCR NPR-12 was further identified as the receptor of NLP-29 in nematodes [33]. Similarly, mutation of *npr-12* also completely blocked the infection-induced PVD dendrite degeneration (Fig. 10.13) [33]. Compared to aging-associated degeneration, the rate of degeneration induced by infections at day 1 was relatively low (Fig. 10.13) [33], which might be due to protective mechanisms in young animals. Additionally, in infected nematodes, FLP dendrites displayed significantly higher degeneration rates, and mutation of *nlp-29* or *npr-12* also blocked this FLP degeneration caused by infection (Fig. 10.13) [33]. Nevertheless, pathogen infection did not induce obvious degeneration of PLM dendrites/sensory processes (Fig. 10.13) [33]. However, ectopic expression of *npr-12* in PLM neurons was sufficient to cause infection-dependent degeneration, and *nlp-29* mutation could suppress this effect (Fig. 10.13) [33]. Moreover, mutations of *atg-4.1* were able to

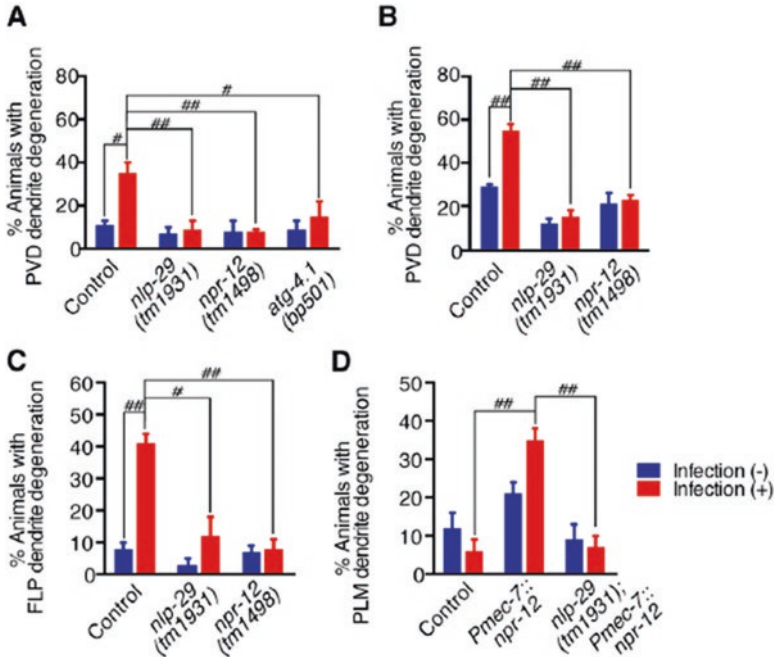


Fig. 10.13 Fungal infection induces dendrite degeneration via NLP-29 and NPR-12 [33]. Animals were either treated with *Drechmeria coniospora* or vehicle solution (NaCl 50 mM) and were quantified for dendrite degeneration after 36-h incubation in the pathogen or vehicle. The mean differences between each strain under different treatment conditions were analyzed by one-way ANOVA, followed by Fisher's LSD post hoc test. (a) Effects of infection on PVD dendrite degeneration; animals were treated on day 3. (b) Effects of infection on PVD dendrite degeneration; animals were treated on day 1. (c) Effects of infection on FLP dendrite degeneration; animals were treated on day 1. (d) Effects of infection on degeneration of PLM dendrite/sensory processes; animals were treated on day 1; ectopic expression of *npr-12* in PLM neurons was driven by the *mec-7* promoter (*Pmec-7::npr-12*). # $p < 0.05$; ## $p < 0.001$. Data are represented as mean \pm SEM

completely block the infection-induced PVD dendrite degeneration (Fig. 10.13) [33], implying that the autophagic machinery may be involved downstream of NPR-12 to transduce the degeneration signals in nematodes.

10.2.4 Neuronal SRH-220

Some genes encoding GPCRs such as SRE-1, SRI-51, SRH-132, and SRH-220 are expressed in the ADL sensory neurons, and, among them, loss-of-function mutation of *srh-220* resulted in an enhanced choice index compared with wild-type N2 (Fig. 10.14) [29], suggesting that the ADL can regulate the preference choice by inhibiting the function of GPCR SRH-220.

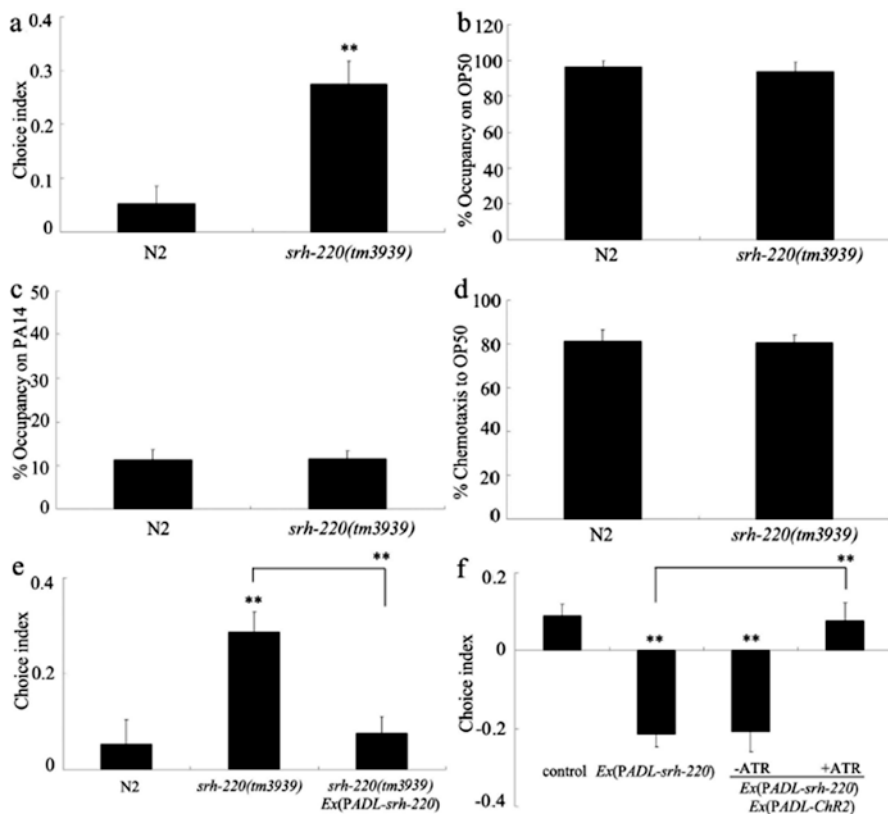


Fig. 10.14 Roles of SRH-220/GPCR in ADL sensory neurons in the control of preference choice in nematodes [29]. (a) Effects of *srh-220* mutation on preference choice. (b–d) Leaving behavior from bacterial lawns and chemotaxis to OP50 in *srh-220* mutants. (e) Rescue assay of preference choice phenotype in *srh-220* mutants. (f) Optogenetically activating ADL sensory neurons suppressed the function of SRH-220 in regulating preference choice. Optogenetical activation was performed under the *lite-1* mutation background. Control, *lite-1(ce314)*. Bars represent means \pm S.E.M. $**P < 0.01$ vs N2 (if not specifically indicated)

In nematodes, *unc-31* encodes a DAG-binding protein that plays a key role in dense core vesicle (DCV) release, and ADL RNAi knockdown of *unc-31* significantly decreased the choice index [29]. *gsa-1* encodes a G α s that enhances exocytosis from DCVs, and *pde-4* encodes a phosphodiesterase to alter cAMP levels. Similarly, ADL RNAi knockdown of *gsa-1* or *pde-4* significantly decreased the choice index [29]. These observations imply that the signaling from ADL sensory neurons may be primarily peptidergic with respect to the control of preference choice. In other words, the ADL sensory neurons might regulate preference choice through peptidergic signals, such as FLP-4 and NLP-10 [29].

Moreover, it was found that the function of FLP-4 or NLP-10 in regulating the preference choice was regulated by SRH-220. The preference choice phenotype in

double mutant of *flp-4(RNAi);srh-220(tm3783)* was similar to that in *flp-4(RNAi)* nematodes, and the preference choice phenotype in double mutant of *nlp-10(tm6232);srh-220(tm3783)* was similar to that in *nlp-10(tm6232)* mutant nematodes [29]. Therefore, *flp-4* or *nlp-10* mutation may suppress the preference choice phenotype in *srh-220* mutant nematodes.

10.3 Ion Channels

10.3.1 Cyclic Nucleotide-Gated Ion Channels

10.3.1.1 TAX-2 and TAX-4

In nematodes, the enhanced susceptibility of *npr-1(ad609)* mutant nematodes to *P. aeruginosa* was rescued by mutations in *tax-2* or *tax-4*, encoding a cyclic GMP-gated ion channel [28], suggesting the involvement of these two ion channels in regulating the function of NPR-1 in controlling the innate immunity to pathogen infection in nematodes.

10.3.1.2 CNG-3

CNG-3 shows high homology with CNG channels of higher animals, as well as the TAX-4 [34]. CNG-3 is restricted in five sensory neurons of amphid, including AFD neurons [34]. Although the *cng-3* null mutant nematodes displayed a normal chemotaxis to volatile odorants, the *cng-3* mutant nematodes exhibited an impaired thermal tolerance (Fig. 10.15) [34]. Moreover, the *tax-4; cng-3* double mutants showed a similar phenotype to *tax-4* mutants (Fig. 10.15) [34], suggesting that TAX-4 may act downstream of CNG-3 to regulate the thermal stress in nematodes.

10.3.2 Voltage-Gated Calcium Ion Channel UNC-2

UNC-2 is an ortholog of voltage-gated calcium ion channel protein. Under the normal conditions, UNC-2 functions to antagonize the transforming growth factor TGF- β pathway to influence the movement rate [35]. This UNC-2/TGF- β pathway was required for the accumulation of normal serotonin levels, because the decreased serotonergic staining in the ADF neurons of *unc-2* mutant nematodes could be suppressed by *daf-4* and *unc-43(gf)* mutations [35]. This UNC-2/TGF- β pathway was further required for the thermal stress-induced tryptophan hydroxylase (TPH-1) expression in serotonergic chemosensory ADF neurons, but not the NSM neurons (Fig. 10.16) [35]. Moreover, this thermal stress-induced *tph-1::GFP* expression could be restored to normal level in the ADF neurons in *unc-2* mutant nematodes by

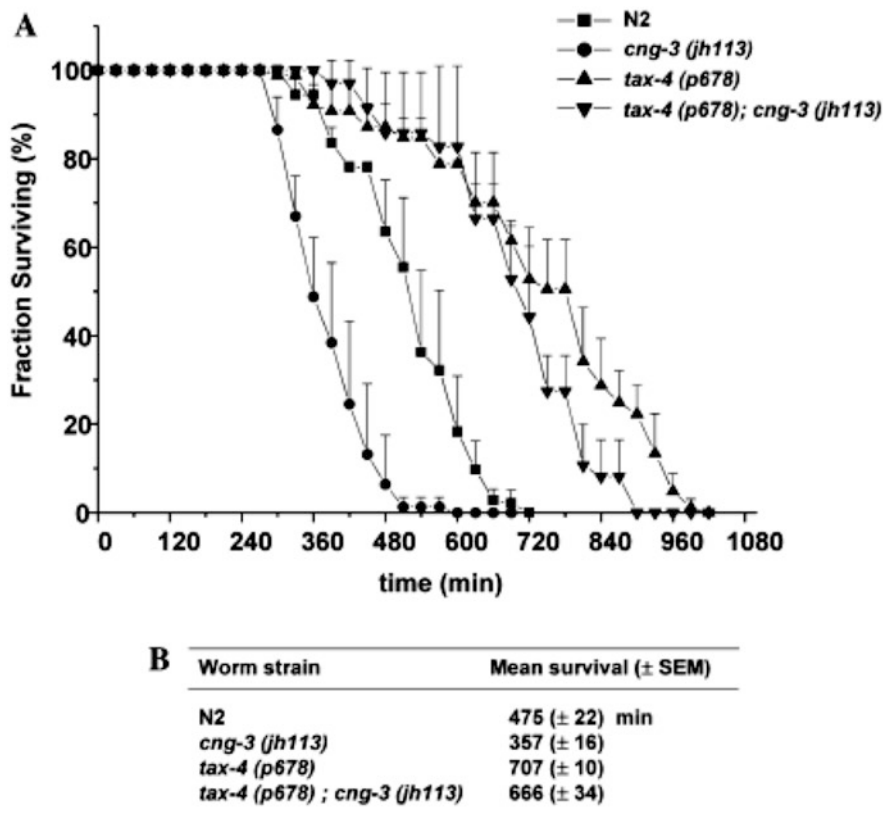


Fig. 10.15 Thermotolerance assay of *cng-3* [34]. (a) Fraction of survived worms was scored during thermal stress of three plates containing 30 animals of each strain. Each data point represents the mean fraction of live worms over three plates at each time point. (b) The survival times of each strain are shown in mean \pm SEM: wild type, 475 \pm 22 min ($n = 73$); *cng-3*, 357 \pm 16 min ($n = 77$); *tax-4*, 707 \pm 10 min ($n = 80$); and *tax-4;cng-3* double mutants, 666 \pm 34 min ($n = 65$). The *cng-3* mutants were significantly more sensitive than wild type ($P < 0.0001$)

mutations in *daf-4* gene in TGF- β pathway or by *unc-43(gf)* mutation [35]. Besides this, it was found that transgenic expression of migraine-associated Ca^{2+} channel, CACNA1A, in *unc-2* mutant nematodes could also functionally substitute for UNC-2 in stress-activated regulation of *tph-1* expression [35].

10.3.3 Potassium Ion Channel KVS-1

KVS-1 is a potassium ion channel protein. In nematodes, the oxidation of KVS-1 during the aging could cause the sensory function loss, and protection of this KVS-1 channel from the oxidation could preserve the neuronal function [36]. Moreover, it

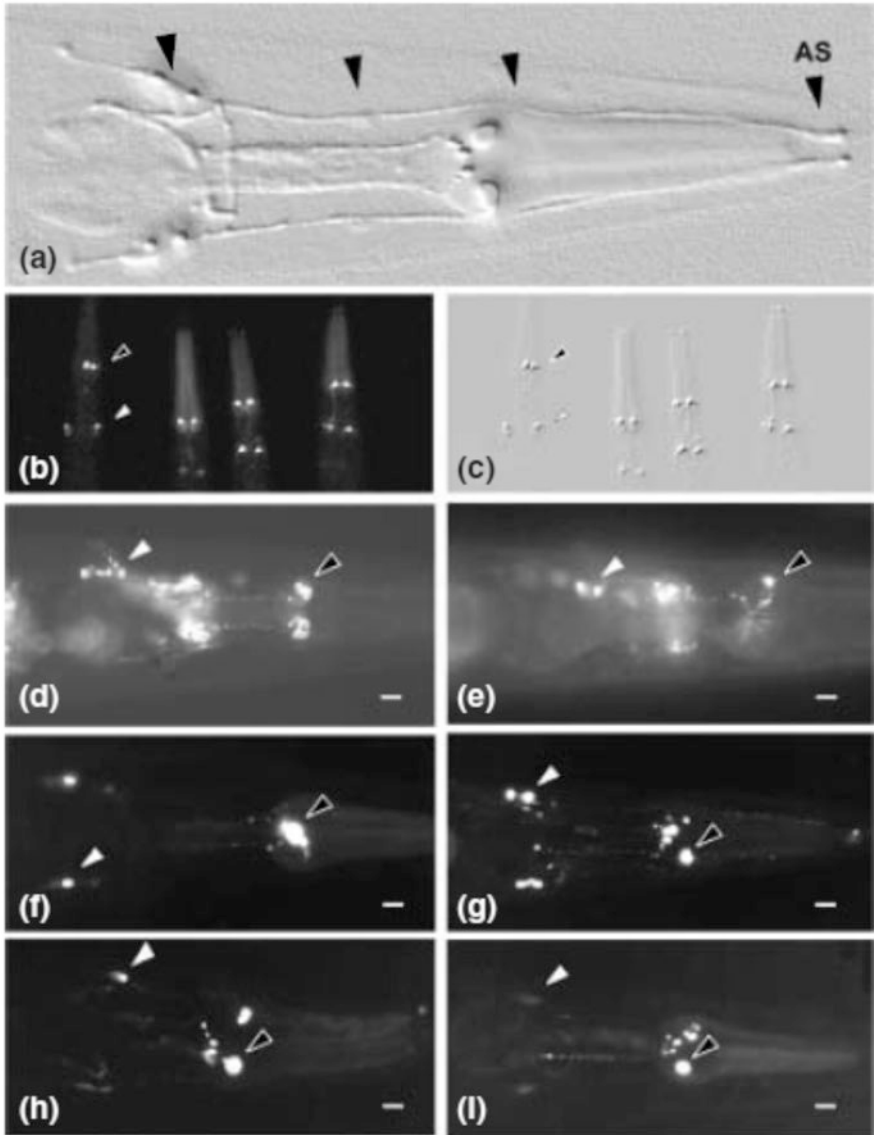


Fig. 10.16 UNC-2 is required for stress-mediated regulation of *tph-1* expression in ADF [35]. (a) The *tph-1* expression in the ADF neuron is emphasized in an embossed fluorescence stereomicroscope image of a WT animal grown at 25 °C. The identity of the cell indicated by the outlined arrowhead as the ADF neuron is confirmed by both the position of the cell body near the distal end of the NSM axonal process and the extension of its dendritic process (black arrowheads) to the amphid sensillum (AS). (b, c) Decreased *tph-1::GFP* expression observed in the ADF neurons of fed *unc-2* adult animals grown at 25 °C is increased by *unc-43(gf)* and *daf-4(m592)*. Animals arranged for fluorescence (b) stereomicroscopy were embossed (c) as described above to emphasize the differences observed between strains in the intensity of the ADF neurons; left to right: WT,

was found that the chemotaxis, a function controlled by KVS-1, was impaired in nematodes exposed to oxidizing agents, but only moderately affected in nematodes with an oxidation-resistant KVS-1 mutant (C113S) (Fig. 10.17) [36]. The endogenous ROS could modify the native KVS-1 channels, and the native KVS-1 currents could be modified by endogenous ROS or by oxidizing agents [36]. In nematodes, the KVS-1 conducted the A-type current in the ASER sensory neurons.

10.3.4 Chloride Intracellular Channel EXL-1

Under the thermal stress conditions, EXL-1, not the EXC-4, responded specifically to the heat stress and translocated from the cytoplasm to the nucleus in intestinal cells in a timely ordered manner from posterior to anterior region and body wall muscle cells (Fig. 10.18) [37]. EXL-1 bears a nonclassical nuclear localization signal (NLS). Meanwhile, it was found that the *exl-1* loss-of-function mutant nematodes were susceptible to heat stress than wild-type nematodes [37].

10.4 ARR-1/Arrestin

ARR-1 is the sole GPCR adaptor protein arrestin-1 in the GPCR signaling. The arrestins can block the G-protein-mediated signaling and itself function as signal transducers [38]. In nematodes, ARR-1 is expressed exclusively and functions within the nervous system to regulate the innate immunity against the pathogen infection (Fig. 10.19) [38]. ARR-1 regulated both the pathogen resistance and the lifespan extension by targeting different pathways [38]. ARR-1 was required for the GPCR signaling in ADF, AFD, ASH, ASI, AQR, PQR, and URX neurons to regulate the innate immune response to pathogen infection (Fig. 10.19) [38]. As indicated by the expressional alteration in *abu* genes, the ER UPR induction in *arr-1(ok401)* mutant nematodes was independent of OCTR-1 in ASH and ASI sensor neurons [38], suggesting that ARR-1 regulates the innate immune response to pathogen infection by activating the ER UPR response in nematodes.



Fig. 10.16 (continued) *unc-2*, *unc-2;unc-43(gf)*, and *unc-2;daf-4(m592)*. **(d, e)** Monoaminergic differentiation of the ADF neurons is normal in *unc-2*. Expression of the monoamine transporter gene reporter *cat-1::GFP* is similar in WT **(d)** and *unc-2* **(e)**. **(f–i)** *tph-1::GFP* expression in the ADF neurons is regulated by temperature and starvation. Expression of the *tph-1* transgene in ADF is weaker than in NSM at 15 °C **(f)** but nearly equal at 25 °C **(g)** in fed WT animals. Fed *unc-2* animals have low levels of *tph-1* transgene expression in the ADF as in **(f)**, at both 15 and 25 °C, but frequently exhibit unilateral **(h)** or absent **(i)** ADF expression when developing to the adult under relative starvation conditions at 25 °C. The location of the ADF and NSM neurons is indicated by white and black arrowheads, respectively. Scale bars, 10 μm

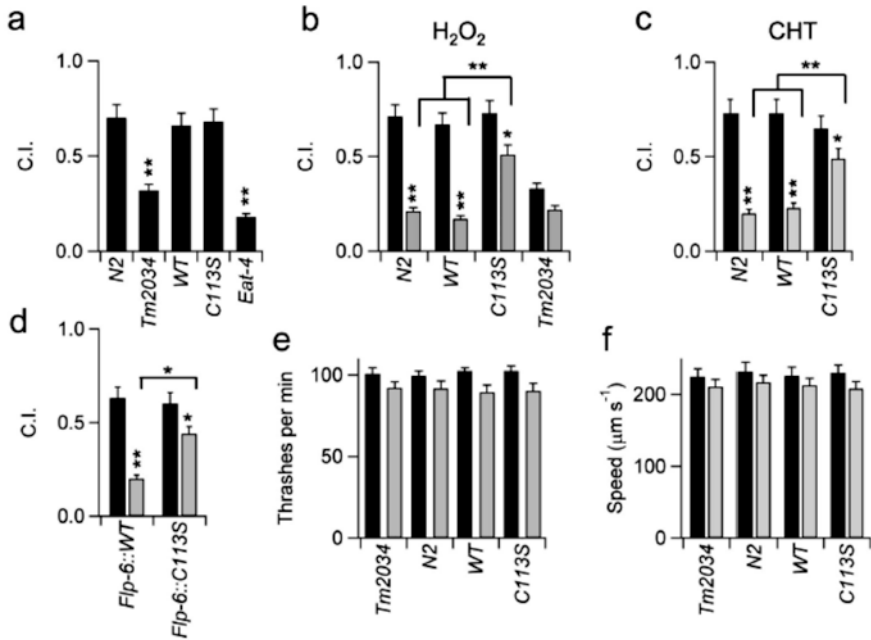


Fig. 10.17 Protected chemosensory function in C113S worms [36]. (a) Chemotaxis to biotin in *N2* (parental control strain), *tm2034* (*kvs-1* null), *wild type-KVS-1* (WT), and *C113S-KVS-1* (C113S), L4 worms. The chemotaxis-defective *eat-4*(*ky5*), which harbors a mutation in a vesicular glutamate transporter necessary for glutamatergic neurotransmission in *C. elegans*, was employed as “sensory-defective” positive control. $n = 4$ experiments. (b) Chemotaxis to biotin in control conditions (black) and in worms exposed to hydrogen peroxide (light gray). Young adult worms were soaked in M9 buffer containing 1 mM H_2O_2 (for 20 min) or M9 buffer (control), allowed to recover for 30 min, transferred to a test plate, and tested for chemotaxis. $n = 5$ experiments for *N2*, *wild type-KVS-1*, and *C113S-KVS-1* and $n = 3$ experiments for *kvs-1* KO. (c) As in B for worms exposed to 0.5 mM CHT for 40 min. $n = 5$ experiments. (d) As in B for *Pflp-6::wild type-KVS-1* and *Pflp-6::C113S-KVS-1* worms. $n = 4$ experiments. (e) Forward movement phenotype in the indicated genotypes in control (black) and after exposure to 1 mM H_2O_2 (light gray). $n \geq 11$ animals/bar. (f) Mean average speeds in the indicated genotypes in control (black) and after exposure to 1 mM H_2O_2 (light gray). $n \geq 10$ animals/bar. Data are presented as mean \pm standard error of the mean (s.e.m). Statistically significant differences are indicated with * ($0.01 < P < 0.05$) and ** ($P < 0.01$)

Fig. 10.18 (continued) (D1–D3) EXL-1::GFP translocates into the nucleus in body wall muscle cells (arrows) under heat shock at 35 °C for 2 h. Inset shows enlarged image of the nucleus. (E1–E3) DAPI staining in L4 animals shows that EXL-1::GFP signal overlaps with DNA staining inside the nucleus. (F1–F3) EXL-1::GFP does not translocate into the nucleus under 200 mM paraquat treatment for 4 h. Images are taken at L4 stage. 1, GFP fluorescence image; 2, Nomarski image (E2: DAPI staining); 3, merged image

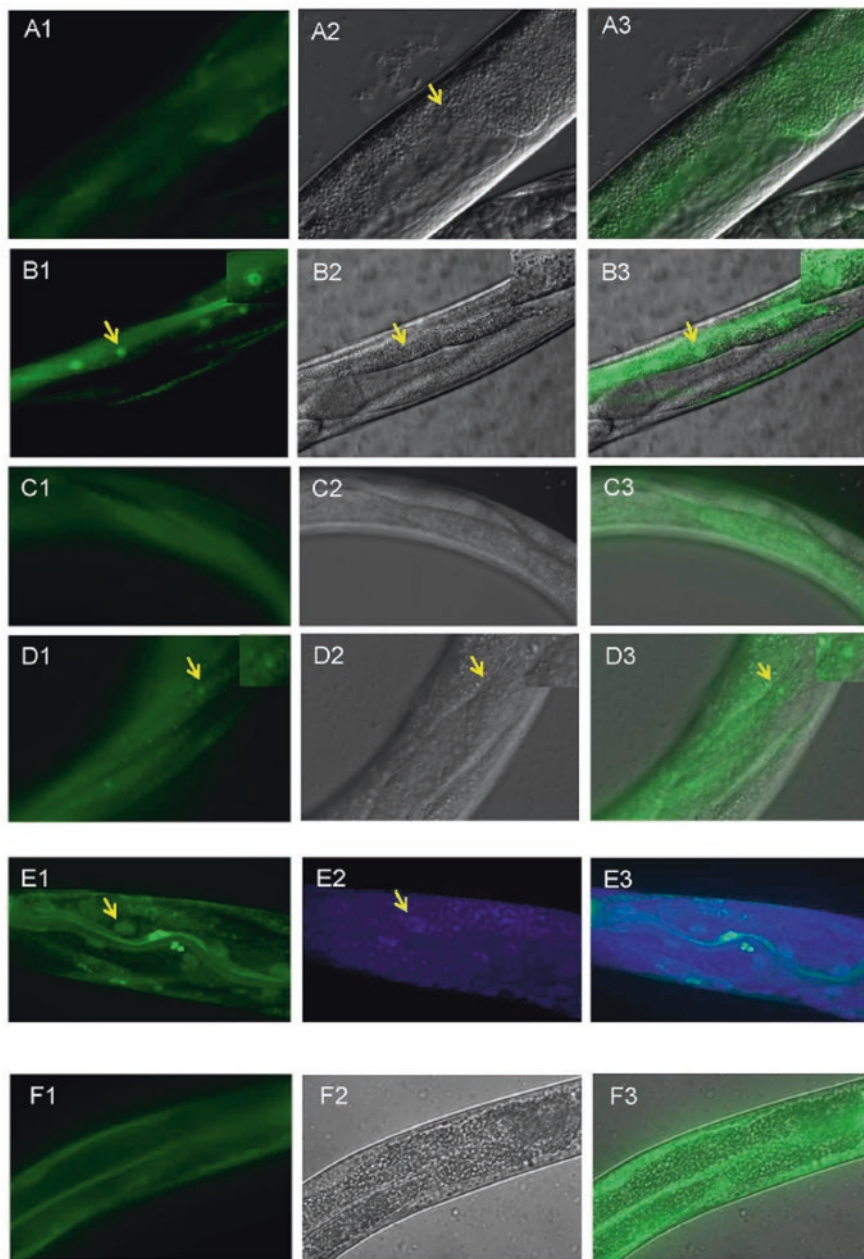


Fig. 10.18 EXL-1 accumulates into the nucleus after heat shock [37]. (A1–A3) EXL-1::GFP is expressed in intestinal cells at standard culture condition (20 °C). The protein is diffuse inside the cells. No exclusion of nuclear expression was observed. (B1–B3) EXL-1::GFP accumulates into the intestinal nuclei (arrows) when animals were subjected to heat shock at 35 °C for 2 h. Inset shows enlarged image of the nucleus. (C1–C3) EXL-1::GFP is expressed in body wall muscle cells.

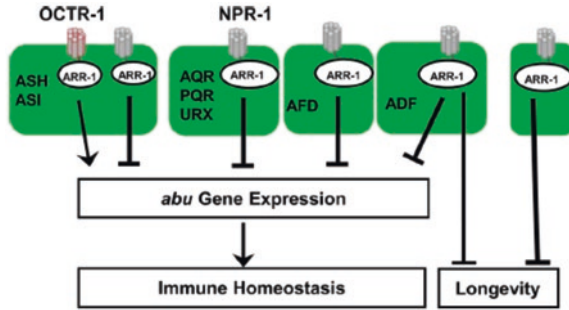


Fig. 10.19 Schematic of neural control of immune homeostasis by ARR-1 signaling [38]. In addition to OCTR-1, at least another receptor may signal through ARR-1 in ASH and ASI neurons to control *abu* gene expression. ARR-1 function in AQR, PQR, and URX neurons appears to play only a small role in the control of *abu* genes, whereas ARR-1 function in ADF and AFD neurons plays a more important role. ARR-1 signaling in ADF neurons also partially regulates longevity. Chemosensory ADF and thermosensory AFD neurons have unidentified receptors that may be regulated by ARR-1 to control *abu* gene expression and immune homeostasis

10.5 G-Proteins

10.5.1 *Gq* Signaling

In organisms, $Gq\alpha$ signaling antagonizes $Go\alpha$ signaling by affecting the levels of diacylglycerol (DAG). In nematodes, the $Gq\alpha$ signaling is mediated by heterotrimeric G-protein α q subunit (EGL-30), and EGL-30 stimulates the phospholipase C β (EGL-8) to produce the DAG [39]. Both the *egl-30* and the *egl-8* mutant nematodes have decreased DAG and decreased neuronal secretion [39]. It was further observed that, besides the constitutive DAF-16 nuclear localization, the elevated expressions of antimicrobial genes (*lys-7*, *thn-2*, and *spp-1*) were observed in *egl-8(n488)*, *egl-30(n686)*, and *egl-8(md1971)* mutant nematodes (Fig. 10.20) [40], suggesting the involvement of $Gq\alpha$ and $PLC\beta$ in the regulation of innate immune response to pathogen infection. The $Gq\alpha$ and $PLC\beta$ mutant nematodes were susceptible to pathogen infection (Fig. 10.20) [40]. Moreover, EGL-30 and EGL-8 were required in the intestine for innate immune response to pathogen infection, but not for longevity [40].

10.5.2 *Go* Signaling

GOA-1 is a neuronal G-protein $Go\alpha$ subunit, and EAT-16 is a regulator of G-protein signaling (RGS) protein, functioning downstream of GOA-1. Under the normal conditions, GOA-1 is involved in the control of locomotion, egg-laying, feeding, and olfactory adaptation. In nematodes, exposure to the pore-forming toxins

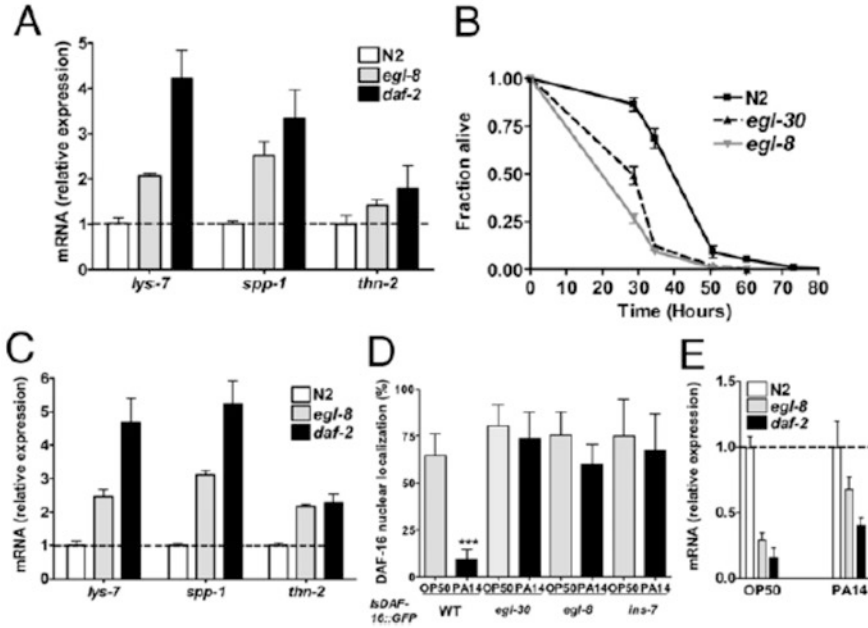


Fig. 10.20 Gq α and PLC β mutants are sensitive to pathogen despite reduced IIS [40]. (a) Elevated expression of IIS-regulated immune genes in *egl-8* mutants. mRNA levels of immune genes in *egl-8(n488)* and wild-type (N2) under conditions of normal growth on *E. coli* as measured by qRT-PCR are shown. (B) Gq α and PLC β mutants are sensitive to pathogen. Fraction of *egl-30(n686)*, *egl-8(n488)*, and wild-type (N2) alive are plotted as a function of time of exposure to *P. aeruginosa*. Shown is a representative of three experiments with 100–120 age-matched adults for each strain, mean time to death of 128.5 ± 4.8 , 83.7 ± 2.5 , and 77.6 ± 2.7 h for N2, *egl-8(n488)*, and *egl-30(n686)*, respectively. Log rank $P < 0.001$ relative to N2. (C–E) *egl-8* mutants maintain reduced IIS upon infection. mRNA levels of *lys-7*, *spp-1*, and *thn-2* (C) and *ins-7* (E) in *egl-8(n488)* and wild-type (N2) after 12 h exposure to *P. aeruginosa* as measured by qRT-PCR. In A, C, and E, mRNA level of each gene was compared with N2, which was set at 1. Shown is the mean \pm SD for a representative of three independent experiments. All datasets were significantly different from wild-type ($P < 0.05$; ANOVA Dunnett’s test). *egl-8* was not significantly different from *daf-2* in A, B, and E ($P > 0.05$, Dunnett’s test). (D) DAF-16::GFP localization in wild-type, *egl-8(n488)*, *egl-30(n686)*, and *ins-7(tm1907)* after exposure to *P. aeruginosa*. The number of nuclei showing distinct DAF-16 localization was enumerated under control (OP50) and infection (PA14) condition. Graph shows a representative of two independent experiments with 20 worms per strain after 21 h of exposure to *P. aeruginosa*. * $P < 0.001$ (Student’s t-test)

(PFTs) induced a feeding cessation [41]. Moreover, it was found that the inhibition of feeding by PFT required both the GOA-1 and the EAT-16 (Fig. 10.21) [41]. Besides this, this G α signaling was also involved in the regulation of PFT defense in nematodes [41].

In nematodes, the serotonin synthesized in the chemosensory neurons play an important function in modulating the innate immune response [42]. Moreover, it was observed that the G α RGS EGL-10 in the rectal epithelium acted downstream of TPH-1-mediated neuronal serotonin signaling released from chemosensory neu-

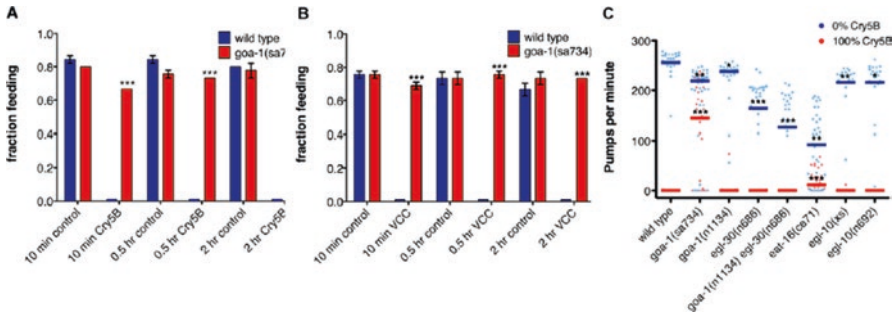


Fig. 10.21 Go α pathway components are required for cessation of feeding in response to PFTs [41]. (a) *goa-1(sa734)* mutant animals constitutively feed on *E. coli*-expressed Cry5B. (b) *goa-1(sa734)* animals constitutively feed on *V. cholerae* expressing VCC. (c) 30 min after transfer to *E. coli*-Cry5B, *goa-1(sa734)* and, to a lesser extent, *eat-16(ce71)* mutant animals have significantly increased feeding rates. Individual measurements of three combined experiments are shown; bars indicate medians

rons to regulate the innate immune response and to affect the pathogen clearance [42]. Different from this, the TPH-1-mediated serotonin signaling might act upstream of, or in parallel to, the EGL-30(G α q) pathway to regulate the innate immune response [42]. A corresponding hypothesis was further raised about this in Fig. 10.22 [42].

10.6 PLC-DAG-PKD Signaling

10.6.1 PLC-PKD-TFEB Signaling Cascade

The transcription factor EB (TFEB) HLH-30 was required for the host defense [43]. It was further found that the activation of HLH-30 required the DKF-1, a homolog of protein kinase D (PKD) in nematodes infected with *Staphylococcus aureus* [43]. The pharmacological activation of PKD was sufficient to activate the HLH-30 [43], which further confirmed this observation. Moreover, the activation of HLH-30 also required the PLC-1, a phospholipase C (PLC), downstream of G α q homolog EGL-30 and upstream of DKF-1 in nematodes infected with *S. aureus* [43]. Therefore, a conserved PLC-PKD-TFEB signaling cascade was identified to be required for the regulation of innate immune response to pathogen infection in nematodes (Fig. 10.23) [43].

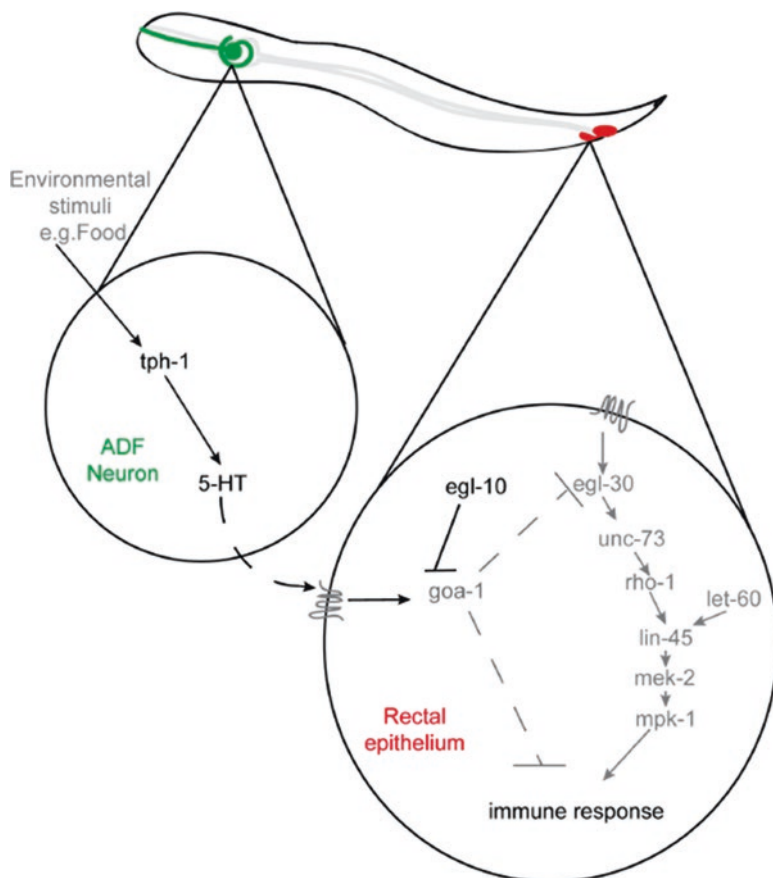
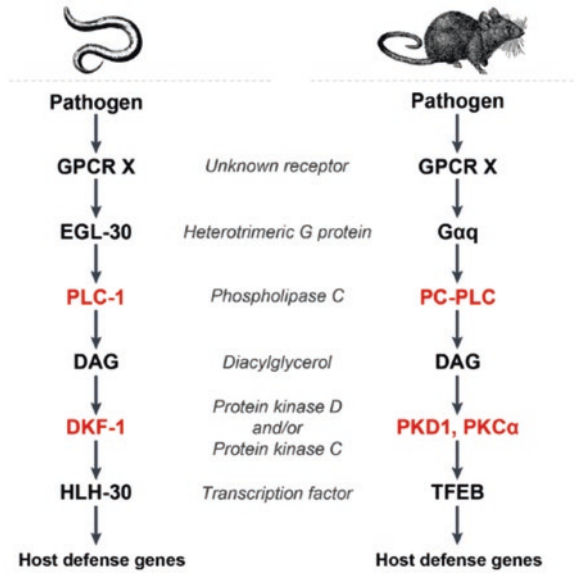


Fig. 10.22 Serotonin synthesis in chemosensory neurons inhibits the immune response by altering rectal epithelial G-protein signaling [42]. In response to environmental cues, such as the presence or absence of food, serotonin, released from ADF chemosensory neurons, acts, directly or indirectly, to regulate GOA-1($G\alpha$) signaling in the rectal epithelium. This signaling suppresses the Dar phenotype that forms part of the innate immune response and limits the rate of pathogen clearance from the rectal opening

10.6.2 DKF-2

DKF-2 is a protein kinase D (PKD). In organisms, the PKD can mediate the signal transduction downstream from phospholipase C and DAG. In nematodes, pathogen infection could potentially activate the DKF-2 expression [44]. Nematodes lacking DKF-2 were hypersensitive to killing by bacteria [44], suggesting that the DKF-2 regulates the innate immunity. Moreover, TPA-1, a PKC δ homolog, was identified to regulate the activation and the functions of DKF-2 in regulating the innate immunity [44]. Therefore, a signaling cascade of DAG-TPA-1-DKF-2 was raised to be required for the control of innate immunity in nematodes (Fig. 10.24) [44].

Fig. 10.23 An evolutionarily conserved PLC-PKD-TFEB pathway for host defense [43]



In nematodes, pathogen infection induced the alteration in expression of >75 mRNAs in *dkf-2* mutant nematodes [44]. The products for these altered genes contained those of antimicrobial peptides and proteins that sustain intestinal epithelium [44]. It was further found that the DKF-2 could promote the activation of PMK-1, and a-loop phosphorylation was required for DKF-2-mediated induction of antimicrobial genes [44]. Therefore, the induction of immune effectors by DKF-2 may proceed via PMK-1-dependent and PMK-1-independent pathways in nematodes.

10.6.3 Association with p38 MAPK Signaling

In nematodes, it was further found that the intestinal Gqα and PLCβ could regulate the innate immunity by affecting the activity of p38 MAPK signaling pathway [40]. The PLCβ mutant nematodes had reduced levels of p38 MAPK-regulated immune genes (Fig. 10.25) [40]. That is, the regulation of innate immunity by Gqα-PLCβ signaling is primarily through the intestinal p38 MAPK signaling pathway. Moreover, the intestinal p38 MAPK activity was regulated by the diacylglycerol levels, a product of PLCβ (Fig. 10.25) [40], suggesting that Gqα and PLCβ may modulate the intestinal p38 MAPK activity and innate immunity by further affecting the levels of DAG.

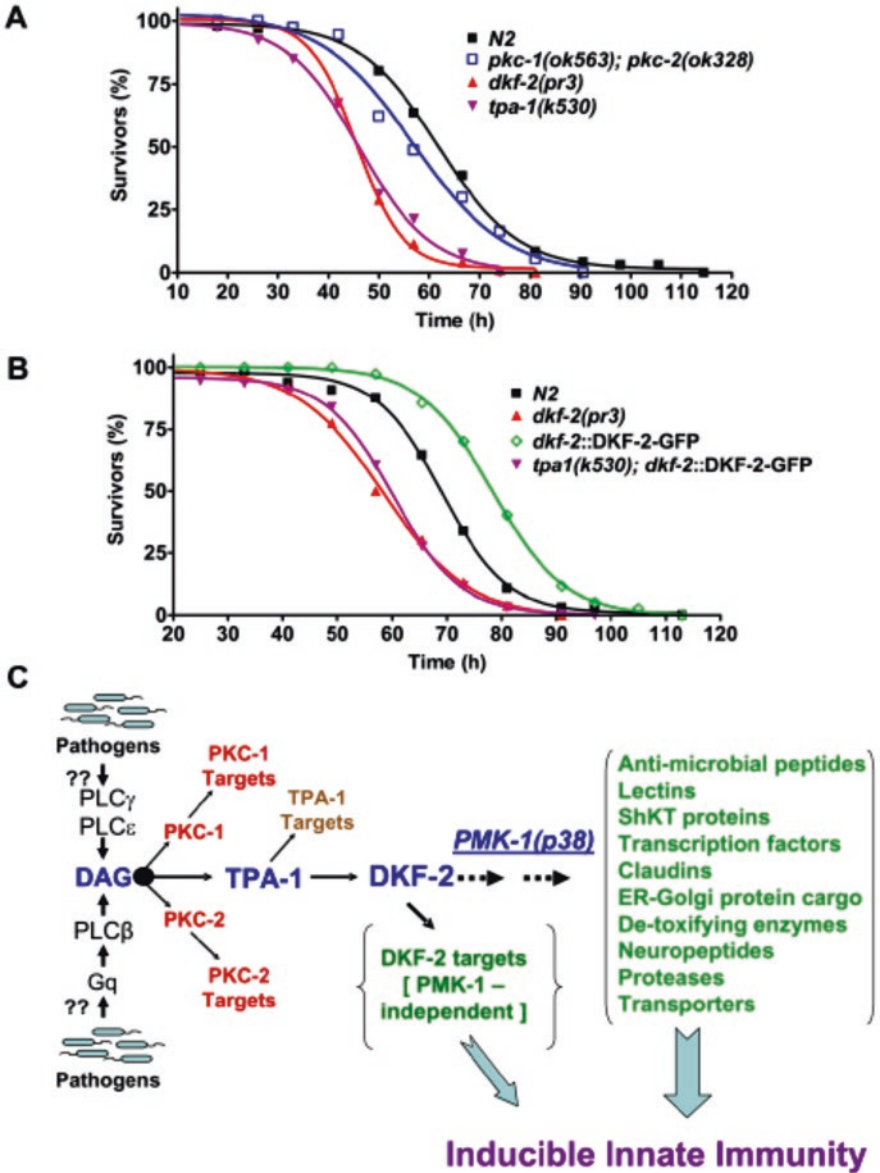


Fig. 10.24 TPA-1 controls DKF-2 [44]. (a) Depicts survival curves for *dkf-2(pr3)* null, *pkc-1(ok563);pkc-2(ok328)* double null, and *tpa-1(k530)* defective *C. elegans* mutants feeding on PA14. (b) Shows survival curves for WT, *dkf-2(pr3)*, and transgenic (*dkf-2::DKF-2-GFP* and *tpa-1(k530);dkf-2::DKF-2-GFP*) nematodes fed PA14. (c) Presents a model for (partial) regulation of immunity by a DAG→TPA-1→DKF-2 signaling pathway in *C. elegans*. It is speculated that pathogens directly/indirectly activate PLCs, thereby increasing DAG levels. DAG recruits and activates TPA-1, which phosphorylates and activates DAG-bound DKF-2. DKF-2, a PKD prototype, induces expression of immune effector mRNAs that defend intestinal cells against pathogens via PMK-1-dependent and PMK-1-independent mechanisms

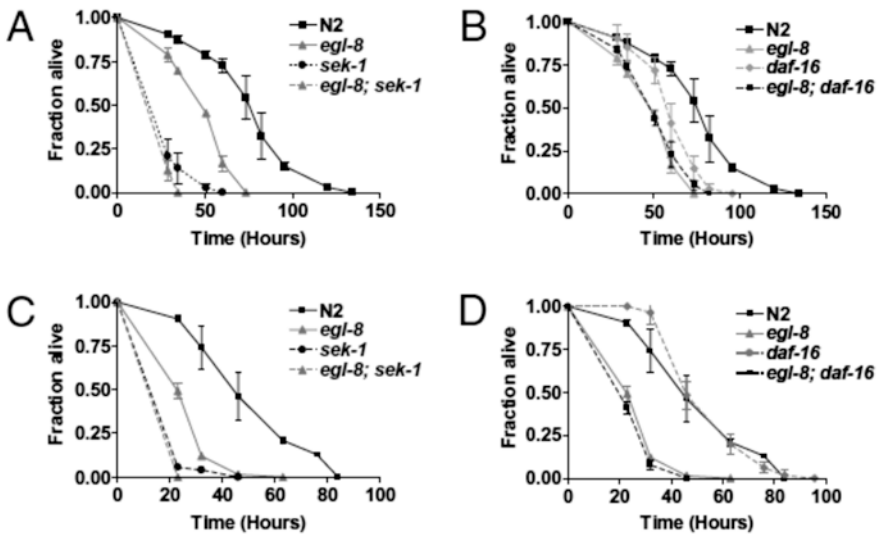


Fig. 10.25 PLC β influences immunity and oxidative stress resistance primarily through the p38 MAPK pathway [40]. p38 MAPK is the primary mediator of oxidative stress (a, b) and pathogen (c, d) sensitivity of *egl-8(n488)*. Graphs show survival of wild-type (N2) and *egl-8(n488)* compared with *sek-1(km4)*, *egl-8(n488); sek-1(km4)* (a, c) and *daf-16(mu86)* and *egl-8(n488); daf-16(mu86)* (b, d) after exposure to 3 mM arsenite (a, b) or *P. aeruginosa* (c, d). Shown is a representative of two independent experiments for a cohort of 100–120 age-matched adults for each strain

10.7 Ca²⁺ Signaling

10.7.1 UNC-31

UNC-31 is a calcium activator. In nematodes, inhibition of feeding by PFT required the neuronally expressed UNC-31 [41]. The inhibition of feeding by PFT in *unc-31(e928)* mutant nematodes was also different from that in wild-type nematodes, and this maintenance of feeding cessation could be restored when *unc-31* was selectively expressed in the neurons [41].

10.7.2 CRT-1

crt-1 encodes a calreticulin (CRT), a Ca²⁺-binding protein with the functions in regulating Ca²⁺ homeostasis and chaperone activity [45]. In nematodes, CRT-1 is expressed in the intestine, pharynx, body wall muscles, head neurons, coelomocytes, and sperm [45]. Besides the reduced mating efficiency, the defects in sperm

development, oocyte development, and/or somatic gonad function in hermaphrodites and the abnormal behavioral rhythms observed in *crt-1* mutant nematodes, the CRT-1 expression was obviously elevated under the stress conditions [45], suggesting the possible involvement of CRT-1 in the regulation of toxicity of environmental toxicants or stresses in nematodes.

10.8 Perspectives

In this chapter, we raised a series of evidence to highlight the crucial roles of GPCRs and ion channels in the toxicity induction of environmental toxicants or stresses. Nevertheless, so far, only very limited GPCRs and ion channels have been identified to be involved in the regulation of toxicity of environmental toxicants or stresses. Actually, there are a huge number of GPCRs existed in the cells of nematodes. However, the exact functions for most of the GPCRs are still unknown even under the normal conditions. Therefore, the systematic elucidation of the functions of GPCRs under both the normal and the stress conditions is needed to be conducted.

At least for nematodes, the responses to environmental toxicants may be very different from those of environmental stresses. The responses of nematodes to environmental toxicants may be closely associated with chemical interaction between toxicants and cells or tissues. However, the response of nematodes to environmental stresses, such as heat shock, UV irradiation, and microgravity, may be more closely associated with the physical interactions. We do not deny that exposure to environmental toxicants and stresses may activate some shared and conserved molecular responses mediated by GPCRs and ion channels. Nevertheless, a certain difference may exist for the molecular responses (mediated by GPCRs and ion channels) to environmental toxicants from those of environmental stresses.

In this chapter, we also tried to introduce and discuss the potential activation of cytoplasmic signaling cascade, especially the signaling cascade containing ARR-1/arrestin, G-proteins, PLC-DAG-PKD signaling, and Ca^{2+} signaling activated in nematodes exposed to environmental toxicants or stresses. Nevertheless, most of the related information about this is still unclear. More detailed and different signaling cascades downstream of the cell membrane GPCRs and ion channels are needed to be further carefully identified, that is, besides the already introduced cytoplasmic signaling cascade here, whether certain GPCRs and especially ion channels will potentially activate or suppress other unknown downstream cytoplasmic signaling cascades. Additionally, it is still unclear how the possible shift will happen between or among different downstream signaling cascades under different conditions in nematodes.

References

1. Wang D-Y (2018) *Nanotoxicology in Caenorhabditis elegans*. Springer, Singapore
2. Ren M-X, Zhao L, Ding X-C, Krasteva N, Rui Q, Wang D-Y (2018) Developmental basis for intestinal barrier against the toxicity of graphene oxide. *Part Fibre Toxicol* 15:26
3. Xiao G-S, Chen H, Krasteva N, Liu Q-Z, Wang D-Y (2018) Identification of interneurons required for the aversive response of *Caenorhabditis elegans* to graphene oxide. *J Nanbiotechnol* 16:45
4. Ding X-C, Rui Q, Wang D-Y (2018) Functional disruption in epidermal barrier enhances toxicity and accumulation of graphene oxide. *Ecotoxicol Environ Saf* 163:456–464
5. Zhao L, Kong J-T, Krasteva N, Wang D-Y (2018) Deficit in epidermal barrier induces toxicity and translocation of PEG modified graphene oxide in nematodes. *Toxicol Res* 7(6):1061–1070. <https://doi.org/10.1039/C8TX00136G>
6. Shao H-M, Han Z-Y, Krasteva N, Wang D-Y (2018) Identification of signaling cascade in the insulin signaling pathway in response to nanopolystyrene particles. *Nanotoxicology* in press
7. Qu M, Xu K-N, Li Y-H, Wong G, Wang D-Y (2018) Using *acs-22* mutant *Caenorhabditis elegans* to detect the toxicity of nanopolystyrene particles. *Sci Total Environ* 643:119–126
8. Dong S-S, Qu M, Rui Q, Wang D-Y (2018) Combinational effect of titanium dioxide nanoparticles and nanopolystyrene particles at environmentally relevant concentrations on nematodes *Caenorhabditis elegans*. *Ecotoxicol Environ Saf* 161:444–450
9. Li W-J, Wang D-Y, Wang D-Y (2018) Regulation of the response of *Caenorhabditis elegans* to simulated microgravity by p38 mitogen-activated protein kinase signaling. *Sci Rep* 8:857
10. Xiao G-S, Zhao L, Huang Q, Yang J-N, Du H-H, Guo D-Q, Xia M-X, Li G-M, Chen Z-X, Wang D-Y (2018) Toxicity evaluation of Wanzhou watershed of Yangtze Three Gorges Reservoir in the flood season in *Caenorhabditis elegans*. *Sci Rep* 8:6734
11. Xiao G-S, Zhao L, Huang Q, Du H-H, Guo D-Q, Xia M-X, Li G-M, Chen Z-X, Wang D-Y (2018) Biosafety assessment of water samples from Wanzhou watershed of Yangtze Three Gorges Reservoir in the quiet season in *Caenorhabditis elegans*. *Sci Rep* 8:14102
12. Yin J-C, Liu R, Jian Z-H, Yang D, Pu Y-P, Yin L-H, Wang D-Y (2018) Di (2-ethylhexyl) phthalate-induced reproductive toxicity involved in DNA damage-dependent oocyte apoptosis and oxidative stress in *Caenorhabditis elegans*. *Ecotoxicol Environ Saf* 163:298–306
13. Xiao G-S, Zhi L-T, Ding X-C, Rui Q, Wang D-Y (2017) Value of *mir-247* in warning graphene oxide toxicity in nematode *Caenorhabditis elegans*. *RSC Adv* 7:52694–52701
14. Zhao L, Wan H-X, Liu Q-Z, Wang D-Y (2017) Multi-walled carbon nanotubes-induced alterations in microRNA *let-7* and its targets activate a protection mechanism by conferring a developmental timing control. *Part Fibre Toxicol* 14:27
15. Zhao L, Rui Q, Wang D-Y (2017) Molecular basis for oxidative stress induced by simulated microgravity in nematode *Caenorhabditis elegans*. *Sci Total Environ* 607–608:1381–1390
16. Wu Q-L, Han X-X, Wang D, Zhao F, Wang D-Y (2017) Coal combustion related fine particulate matter (PM_{2.5}) induces toxicity in *Caenorhabditis elegans* by dysregulating microRNA expression. *Toxicol Res* 6:432–441
17. Ruan Q-L, Qiao Y, Zhao Y-L, Xu Y, Wang M, Duan J-A, Wang D-Y. (2016) Beneficial effects of *Glycyrrhizae radix* extract in preventing oxidative damage and extending the lifespan of *Caenorhabditis elegans*. *J Ethnopharmacol* 177: 101–110
18. Zhi L-T, Yu Y-L, Li X-Y, Wang D-Y, Wang D-Y (2017) Molecular control of innate immune response to *Pseudomonas aeruginosa* infection by intestinal *let-7* in *Caenorhabditis elegans*. *PLoS Pathog* 13:e1006152
19. Zhi L-T, Yu Y-L, Jiang Z-X, Wang D-Y (2017) *mir-355* functions as an important link between p38 MAPK signaling and insulin signaling in the regulation of innate immunity. *Sci Rep* 7:14560
20. Sun L-M, Liao K, Hong C-C, Wang D-Y (2017) Honokiol induces reactive oxygen species-mediated apoptosis in *Candida albicans* through mitochondrial dysfunction. *PLoS ONE* 12:e0172228

21. Sun L-M, Liao K, Wang D-Y (2017) Honokiol induces superoxide production by targeting mitochondrial respiratory chain complex I in *Candida albicans*. PLoS ONE 12:e0184003
22. Sun L-M, Zhi L-T, Shakoor S, Liao K, Wang D-Y (2016) microRNAs involved in the control of innate immunity in *Candida* infected *Caenorhabditis elegans*. Sci Rep 6:36036
23. Sun L-M, Liao K, Li Y-P, Zhao L, Liang S, Guo D, Hu J, Wang D-Y (2016) Synergy between PVP-coated silver nanoparticles and azole antifungal against drug-resistant *Candida albicans*. J Nanosci Nanotechnol 16:2325–2335
24. Wu Q-L, Cao X-O, Yan D, Wang D-Y, Aballay A (2015) Genetic screen reveals link between maternal-effect sterile gene *mes-1* and *P. aeruginosa*-induced neurodegeneration in *C. elegans*. J Biol Chem 290:29231–29239
25. Reboul J, Ewbank JJ (2016) GPCR in invertebrate innate immunity. Biochem Pharmacol 114:82–87
26. Zugasti O, Bose N, Squiban B, Belougne J, Kurz CL, Schroeder FC, Pujol N, Ewbank JJ (2014) Activation of a G protein-coupled receptor by its endogenous ligand triggers the innate immune response of *Caenorhabditis elegans*. Nat Immunol 15:833–838
27. Powell JR, Kim DH, Ausubel FM (2009) The G protein-coupled receptor FSHR-1 is required for the *Caenorhabditis elegans* innate immune response. Proc Natl Acad Sci U S A 106:2782–2787
28. Styer KL, Singh V, Macosko E, Steele SE, Bargmann CI, Aballay A (2008) Innate immunity in *Caenorhabditis elegans* is regulated by neurons expressing NPR-1/GPCR. Science 322:460–464
29. Yu Y-L, Zhi L-T, Guan X-M, Wang D-Y, Wang D-Y (2016) FLP-4 neuropeptide and its receptor in a neuronal circuit regulate preference choice through functions of ASH-2 trithorax complex in *Caenorhabditis elegans*. Sci Rep 6:21485
30. Yu Y-L, Zhi L-T, Wu Q-L, Jing L-N, Wang D-Y (2018) NPR-9 regulates innate immune response in *Caenorhabditis elegans* by antagonizing activity of AIB interneurons. Cell Mol Immunol 15:27–37
31. Sieburth D, Ch'ng Q, Dybbs M, Tavazoie M, Kennedy S, Wang D, Dupuy D, Rual JF, Hill DE, Vidal M, Ruvkun G, Kaplan JM (2005) Systematic analysis of genes required for synapse structure and function. Nature 436:510–517
32. Sieburth D, Madison JM, Kaplan JM (2007) PKC-1 regulates secretion of neuropeptides. Nat Neurosci 10:49–57
33. E L, Zhou T, Koh S, Chuang M, Sharma R, Pujol N, Chisholm AD, Eroglu C, Matsunami H, Yan D (2018) An antimicrobial peptide and its neuronal receptor regulate dendrite degeneration in aging and infection. Neuron 97:125–138
34. Cho S, Choi KY, Park C (2004) A new putative cyclic nucleotide-gated channel gene, *cng-3*, is critical for thermotolerance in *Caenorhabditis elegans*. Biochem Biophys Res Commun 325:525–531
35. Estevez M, Estevez AO, Cowie RH, Gardner KL (2004) The voltage-gated calcium channel UNC-2 is involved in stress-mediated regulation of tryptophan hydroxylase. J Neurochem 88:102–113
36. Cai S, Sesti F (2009) Oxidation of a potassium channel causes progressive sensory function loss during ageing. Nat Neurosci 12:611–617
37. Liang J, Shaulov Y, Savage-Dunn C, Boissinot S, Hoque T (2017) Chloride intracellular channel proteins respond to heat stress in *Caenorhabditis elegans*. PLoS ONE 12:e0184308
38. Singh V, Aballay A (2012) Endoplasmic reticulum stress pathway required for immune homeostasis is neurally controlled by arrestin-1. J Biol Chem 287:33191–33197
39. Lackner MR, Nurrish SJ, Kaplan JM (1999) Facilitation of synaptic transmission by EGL-30 Gq α and EGL-8 PLC β : DAG binding to UNC-13 is required to stimulate acetylcholine release. Neuron 24:335–346
40. Kawli T, Wu C, Tan M (2010) Systemic and cell intrinsic roles of Gq α signaling in the regulation of innate immunity, oxidative stress, and longevity in *Caenorhabditis elegans*. Proc Natl Acad Sci U S A 107:13788–13793

41. Los FCO, Ha C, Aroian RV (2013) Neuronal $G\alpha$ and CAPS regulate behavioral and immune responses to bacterial pore-forming toxins. *PLoS ONE* 8:e54528
42. Anderson A, Laurenson-Schafer H, Partridge FA, Hodgkin J, McMullan R (2013) Serotonergic chemosensory neurons modify the *C. elegans* immune response by regulating G-protein signaling in epithelial cells. *PLoS Pathog* 9:e1003787
43. Najibi M, Labeed SA, Visvikis O, Irazoqui JE (2016) An evolutionarily conserved PLC-PKD-TFEB pathway for host defense. *Cell Rep* 15:1728–1742
44. Ren M, Feng H, Fu Y, Land M, Rubin CS (2009) Protein kinase D (DKF-2), a diacylglycerol effector, is an essential regulator of *C. elegans* innate immunity. *Immunity* 30:521–532
45. Park B, Lee D, Yu J, Jung S, Choi K, Lee J, Lee J, Kim YS, Lee JI, Kwon JY, Lee J, Singson A, Song WK, Eom SH, Park C, Kim DH, Bandyopadhyay J, Ahnn J (2001) Calreticulin, a calcium-binding molecular chaperone, is required for stress response and fertility in *Caenorhabditis elegans*. *Mol Biol Cell* 12:2835–2845

Chapter 11

Discussion on Specificity of Molecular Signals in Response to Certain Environmental Toxicants or Stresses



Abstract In the field of toxicology or environmental science, some researchers are wondering a question. That is, whether specific molecular signaling pathways in response to certain environmental toxicants or stresses exist in organisms. We selected three well-described response signals (heavy metal response, heat shock response, and hypoxia response) to discuss this question. So far, the obtained knowledge does not support the possible existence of specific molecular signaling pathways in response to certain environmental toxicants or stresses at least in nematodes.

Keywords Heavy metal response signaling · Heat shock response signaling · Hypoxia response signaling · Specific molecular signaling · *Caenorhabditis elegans*

11.1 Introduction

In the environment, there are many toxicants or stresses having the potential to cause the toxicity at different aspects on nematodes [1–6]. For a long time, the researchers in the field of toxicology or environmental science have tried to identify the specific molecular signaling pathways for nematodes in response to certain environmental toxicants or stresses. And then, an important question needs us to further carefully judge or evaluate. That is, are there any specific molecular signals for nematodes in response to certain environmental toxicants or stresses?

In this chapter, we selected three well-described response signals (heavy metal response, heat shock response, and hypoxia response) to discuss this question. We first introduced and discussed the widely accepted molecular signals for the control of these three important responses. Again, we will discuss the potential involvement of these molecular signals in the regulation of toxicity from other environmental toxicants or stresses in nematodes.

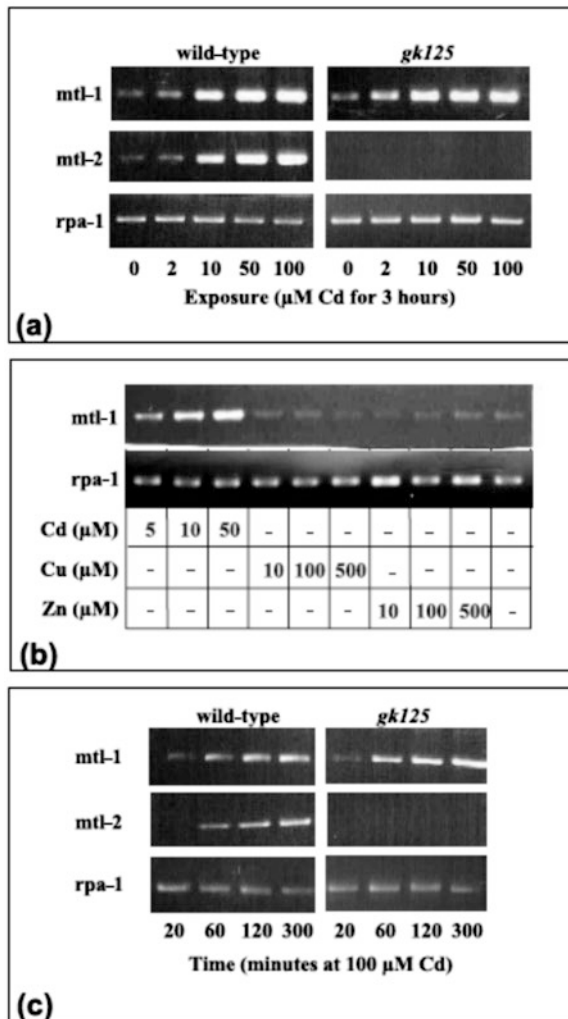
11.2 Heavy Metal Response Signaling

11.2.1 Molecular Signaling for Heavy Metal Response

11.2.1.1 Metallothioneins

Metallothioneins are widely considered as the primary player in the detoxification of and protection from toxicity by the heavy metal of cadmium (Cd) [7]. In nematodes, *mtl-1* and *mtl-2* encode the metallothioneins. A highly sensitive and dose-dependent transcriptional response to Cd, but not Cu or Zn, was observed for both MTL-1 and MTL-2 (Fig. 11.1) [7]. Additionally, Cd exposure induced the

Fig. 11.1 Isoform-specific transcript analysis of *mtl-1* and *mtl-2* [7]. Utilizing a semiquantitative PCR-based approach, it was possible to assess the dose response to cadmium (a), copper, and zinc (b) and the temporal response to cadmium exposure (c) of *mtl-1* and *mtl-2* in wild-type nematodes and *gk125* the *mtl-2* null allele. PCRs were terminated at the half-log phase of amplification and normalized to the invariant ribosomal protein *rpa-1*



sharp induction of both MTL-1::GFP in the pharynx and intestine and MTL-2::GFP in the intestine (Fig. 11.2) [7]. No measurable upregulation of *mtl-1* could be detected in *mtl-2* mutant nematodes [7], suggesting that these two genes are independent and not synergistic action may be formed.

Mutation or RNAi knockdown of *mtl-1* or *mtl-2* induced a susceptibility to Cd toxicity using body size, generation time, brood size, and lifespan as the toxicity assessment endpoints (Fig. 11.3) [7], which provide the functional evidence to demonstrate the important roles of MTL-1 and MTL-2 in regulating the Cd toxicity in nematodes.

11.2.1.2 CDR-1

CDR-1 is a predicted 32-kDa, integral membrane protein. *cdr-1* is transcribed exclusively in intestinal cells of postembryonic nematodes [8]. In the intestine, the CDR-1 is targeted to the cytoplasmic lysosomes [8]. The *cdr-1* transcription was

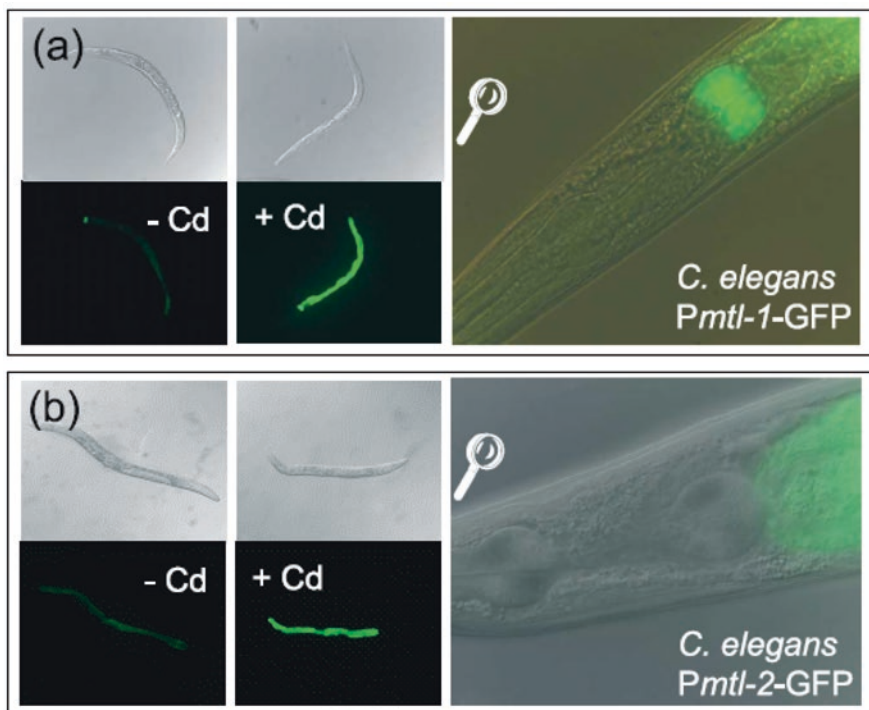


Fig. 11.2 Promoter-GFP fusions of *mtl-1* (a) and *mtl-2* (b) after germ line transformation [7]. The background signal (-Cd) was significantly increased by exposure to 10 mM cadmium (+Cd) for a 24 h period. In both isoforms, the primary site of cadmium responsive induction is the intestine, but note that only *mtl-1* is expressed constitutively in the lower pharyngeal bulb (right-hand panels)

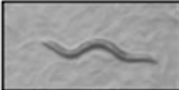

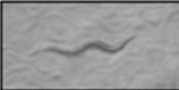


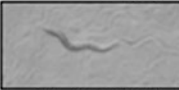
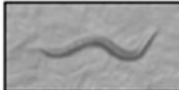




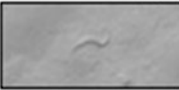
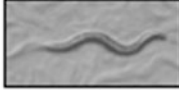


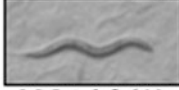
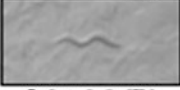

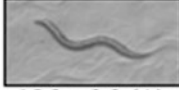
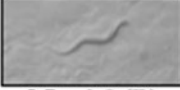

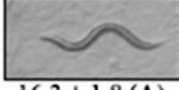


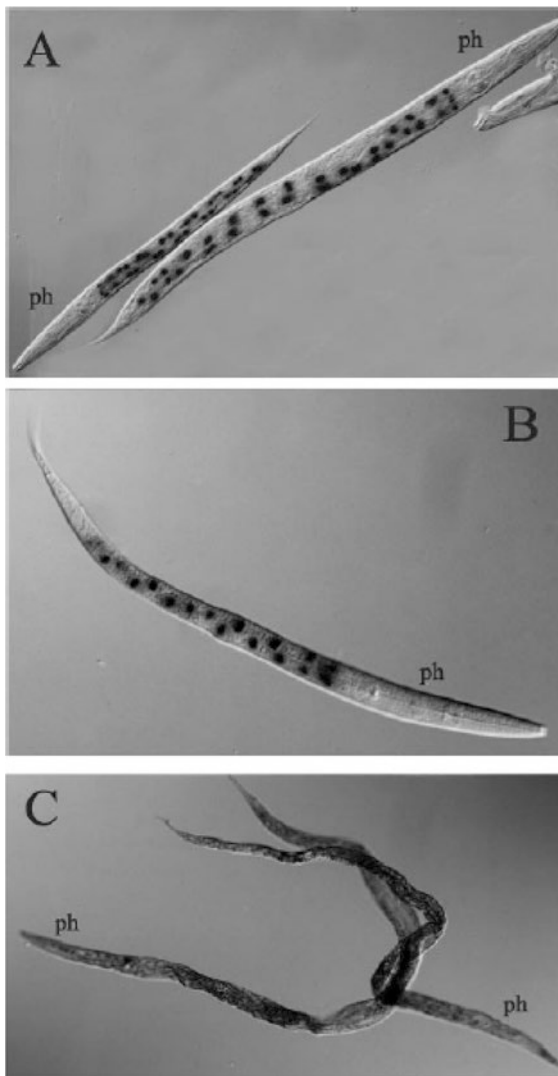
worm strain	RNAi source	cadmium concentration (μM)		
		0	75	150
wild-type	pPD129.36	 15.2 \pm 1.1 (A)	 11.7 \pm 0.4 (B)	 7.9 \pm 0.8 (C)
<i>rff-3</i>	pPD129.36	 14.1 \pm 0.8 (A)	 11.4 \pm 0.3 (B)	 8.3 \pm 0.7 (C)
<i>rff-3</i>	<i>mtl-1</i>	 13.1 \pm 1.9 (A)	 5.1 \pm 0.5 (D)	 3.5 \pm 0.7 (D)
<i>gkl25</i>	<i>mtl-1</i>	 16.6 \pm 0.6 (A)	 6.1 \pm 0.5 (D)	 2.0 \pm 0.4 (E)
<i>rff-3</i>	<i>mtl-2</i>	 15.4 \pm 0.3 (A)	 4.7 \pm 0.4 (D)	 4.9 \pm 0.3 (D)
<i>gkl25</i>	<i>mtl-2</i>	 16.8 \pm 1.3 (A)	 5.6 \pm 0.9 (D)	 3.0 \pm 1.0 (E)
<i>rff-3</i>	<i>mtl-1+2</i>	 15.2 \pm 2.3 (A)	 5.7 \pm 0.8 (D)	 4.5 \pm 0.6 (D)
<i>gkl25</i>	<i>mtl-1+2</i>	 16.3 \pm 1.8 (A)	 5.9 \pm 0.8 (D)	 3.3 \pm 0.3 (E)

Fig. 11.3 Exposure to cadmium slows down development in a dose-responsive manner [7]. This effect is more profound in *gkl25* and particularly during knockdown of *mtl-1*, *mtl-2*, or both by RNAi. All images are representative of 2-day post hatch nematodes. Numbers below the images are average area measurements (G standard error) from four nematodes. Based on a nonparametric Mann–Whitney U-test, identical letters (in brackets) denote that samples are not significantly different ($P \geq 0.05$)

Fig. 11.4 Cell-specific expression of *cdr-1* [8]. (a, b) *C. elegans*, strain JF9 (*mtIs7, cdr-1/lacZ*) was exposed to 100 μM CdCl_2 for 24 h and then stained for β -galactosidase activity. (a) Reporter gene activity in the intestinal cells of a young adult and an L3 larva. (b) *cdr-1* promoter activity in the intestinal cells of an L1 larva. (c) In situ hybridization of cadmium-treated L1 *C. elegans* larvae. CDR-1 mRNA was visualized by exposing wild-type nematodes to a digoxigenin-dUTP-labeled CDR-1 antisense probe. (c) shows that the CDR-1 transcript is expressed throughout the intestine of L1. “*ph*” marks the location of the pharynx in all panels. Nematodes were photographed using Nomarski optics



significantly induced by Cd exposure, but not by other examined stressors (heavy metals of Hg, Cu, and Zn, paraquat, hugalone, and heat shock) (Fig. 11.4) [8], suggesting that CDR-1 expression is under the control of Cd exposure in a cell-specific fashion. In addition, RNAi knockdown of *cdr-1* also induced a susceptibility to Cd [8, 9].

11.2.2 Regulation of Toxicity of Other Environmental Toxicants by *MTL-1* and *MTL-2*

Some engineered nanomaterials (ENMs) have been shown to be toxic for organisms, including the nematodes [10–17]. Among these ENMs, titanium dioxide nanoparticles (TiO₂-NPs) and zinc oxide NPs (ZnO-NPs) are two widely used ENMs. In nematodes, mutation of *mtl-2* resulted in a susceptibility to the TiO₂-NPs toxicity in reducing body length, in reducing brood size, in decreasing locomotion behavior as indicated by the endpoints of head thrash and body bend, and in inducing intestinal autofluorescence and ROS production [18]. In nematodes, *pcs-1* encodes a phytochelatin synthase. Additionally, the severe susceptibility to ZnO-NPs toxicity was observed in the triple mutant of *mtl-1;mtl-2;pcs-1(zs2)* (Fig. 11.5) [19]. Moreover, the *mtl-2::GFP* expression was significantly increased by exposure to ZnO-NPs in nematodes (Fig. 11.5) [19].

Nanopolystyrene particles are another important ENM with the wide commercial uses. In nematodes, prolonged exposure to nanopolystyrene particles caused the toxicity on the functions of both primary and secondary targeted organs [20]. It was further found that the intestinal insulin signaling pathway including the *daf-16* encoding a FOXO transcriptional factor was involved in the control of toxicity of nanopolystyrene particles [21]. *daf-16* has many potential targeted genes during the control of biological processes [22–24], and, among them, *lys-8*, *dct-6*, *nnt-1*, *ftn-1*, *pept-1*, *dod-17*, *klo-1*, *ncx-6*, *cyp-35A3*, *nhx-2*, *vha-6*, *pho-1*, *gale-1*, *cyp-34A9*, *stdh-1*, *nrf-6*, *hsp-16.1*, *hsp-16.2*, *asah-1*, *ges-1*, *cpr-1*, *acd-1*, *vit-5*, *mtl-2*, *dod-22*, *gcy-18*, *vit-2*, *lys-7*, *mtl-1*, *dct-18*, *gpb-2*, *fat-5*, *cyp-35B1*, *sod-3*, *sodh-1*, *icl-1*, *fat-7*, *dod-4*, *fat-7*, *asp-3*, *mdl-1*, *spp-1*, and *dct-1* can be expressed in the intestine. Exposure to nanopolystyrene particles (1 µg/L) only significantly increased the transcriptional expressions of *sod-3*, *mtl-1*, *gpb-2*, *fat-7*, and *sodh-1* in wild-type nematodes (Fig. 11.6) [21]. Meanwhile, *daf-16* mutation significantly decreased the transcriptional expressions of *sod-3*, *mtl-1*, *gpb-2*, *fat-7*, and *sodh-1* after exposure to nanopolystyrene particles (1 µg/L) (Fig. 11.6) [21]. Among these targeted genes, using VP303 as a genetic tool, it was observed that intestine-specific RNAi knockdown of *mtl-1* induced a susceptibility to the toxicity of nanopolystyrene particles in inducing ROS production (Fig. 11.6) [21]. These results suggest that *mtl-1* acts as a targeted gene of *daf-16* in the regulation of toxicity of nanopolystyrene particles.

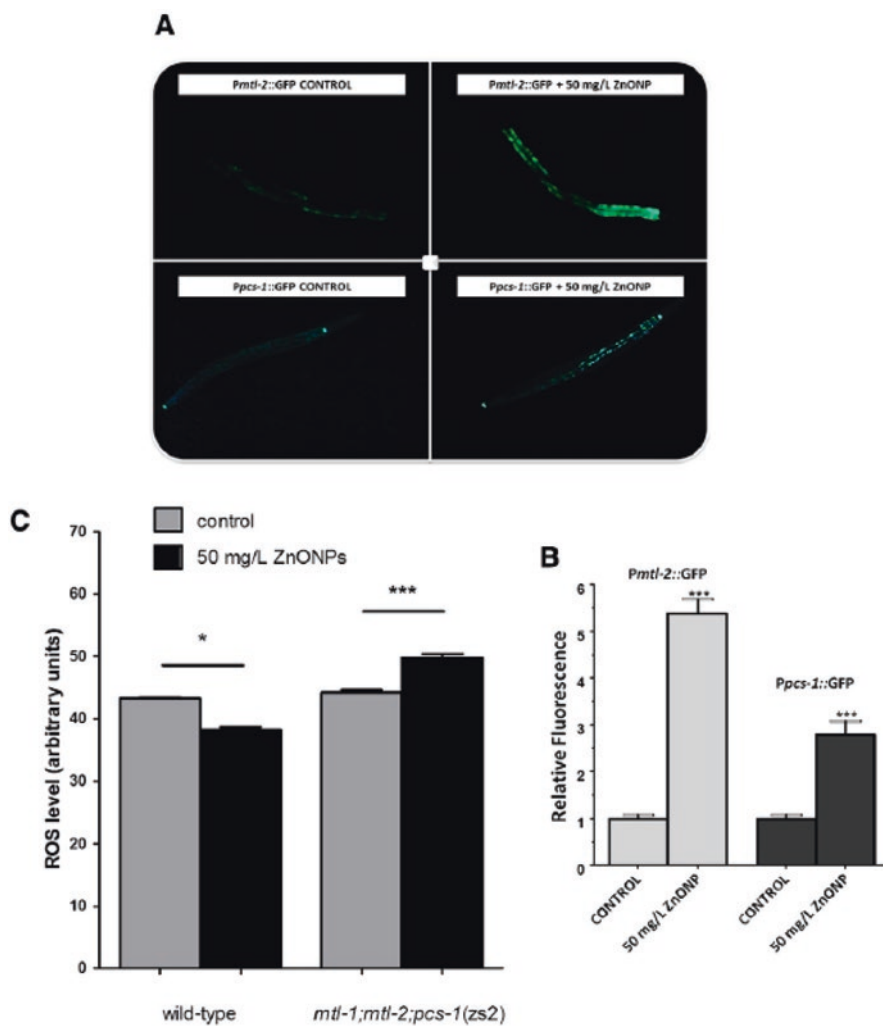


Fig. 11.5 Induction of green fluorescence protein (measured as relative fluorescence units) in *mtl-2::GFP* and *pcs-1::GFP* transgenic *Caenorhabditis elegans* in response to ZnO-NPs [19]. Approximately ten worms were observed in each case. Error bars represent the standard error ($n = 10$). Statistical analysis was performed using the Wilcoxon signed-rank test ($p < 0.05$). Exposure to ZnO-NPs generates high levels of free radical H_2O_2 in *C. elegans*.

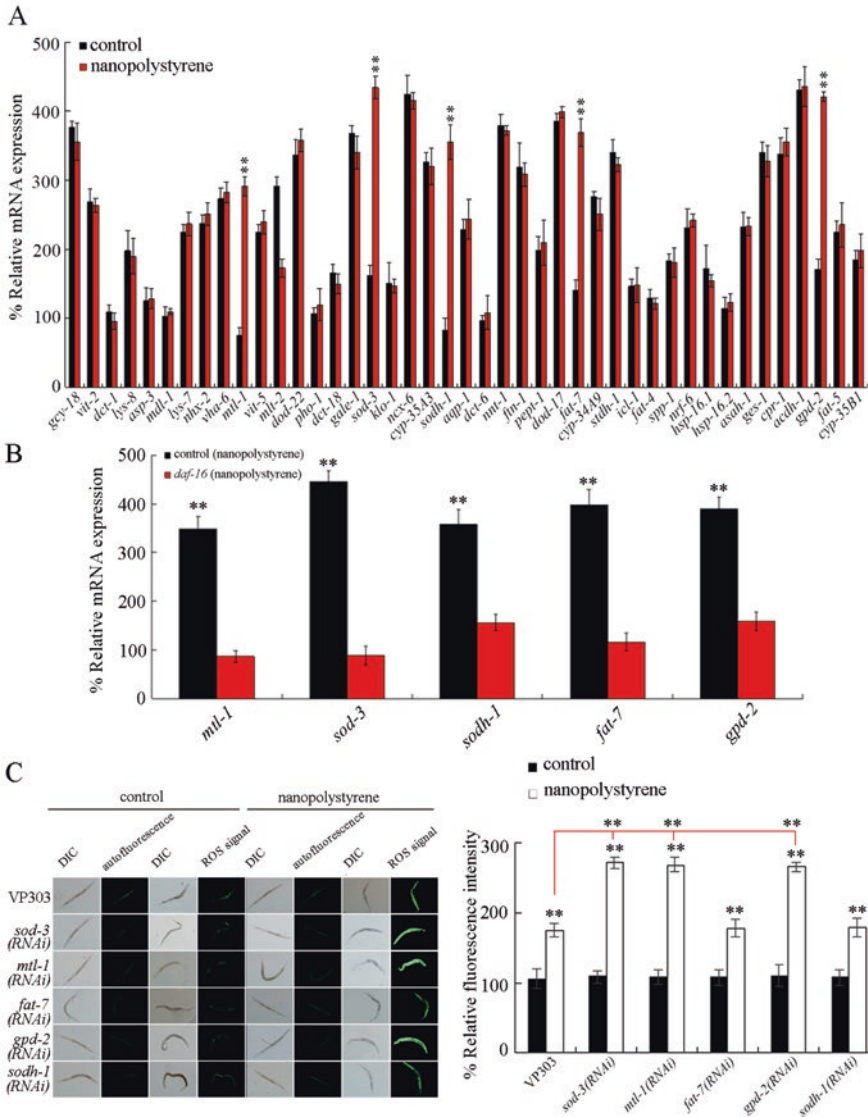


Fig. 11.6 Identification of targeted genes for *daf-16* in the regulation of response to nanopolystyrene particles [21]. (a) Effects of exposure to nanopolystyrene particles on gene expression in wild-type nematodes. (b) Effects of *daf-16* mutation on expression of intestinal targeted genes of *daf-16* after exposure to nanopolystyrene particles. (c) Effect of intestine-specific RNAi knock-down of *sod-3*, *mtl-1*, *gpd-2*, *fat-7*, or *sodh-1* on induction of ROS production in nematodes exposed to nanopolystyrene particles. Nanopolystyrene exposure concentration was 1 $\mu\text{g/L}$. Nanopolystyrene exposure was performed from L1-larvae to adult day 3. Bars represent means \pm SD. $**P < 0.01$ vs control (if not specially indicated)

11.3 Heat Shock Response Signaling

11.3.1 Molecular Signaling for Heat Shock Response

11.3.1.1 Heat Shock Proteins

Early in 1983, it was reported that treatment of the nematodes with elevated temperatures could induce the synthesis of the heat shock proteins [25]. In contrast, synthesis of most other proteins present before the heat shock was suppressed [25]. Additionally, the dauer larvae possess little translatable mRNA but, upon the heat shock, synthesizes a set of messages corresponding to the heat shock proteins [25].

11.3.1.2 HSF-1

hsf-1 encodes a heat shock factor. HSF-1 is a master transcriptional regulator of stress-inducible gene expression, as well as protein-folding homeostasis [26]. *hsf-1* was required for both the longevity control and the temperature-induced dauer larvae formation in nematodes [26, 27]. Heat shock-induced expression of *hsp-16.2* was virtually eliminated in *hsf-1* mutant nematodes (Fig. 11.7) [27], suggesting the potential role of HSF-1 as an inducer of heat shock response.

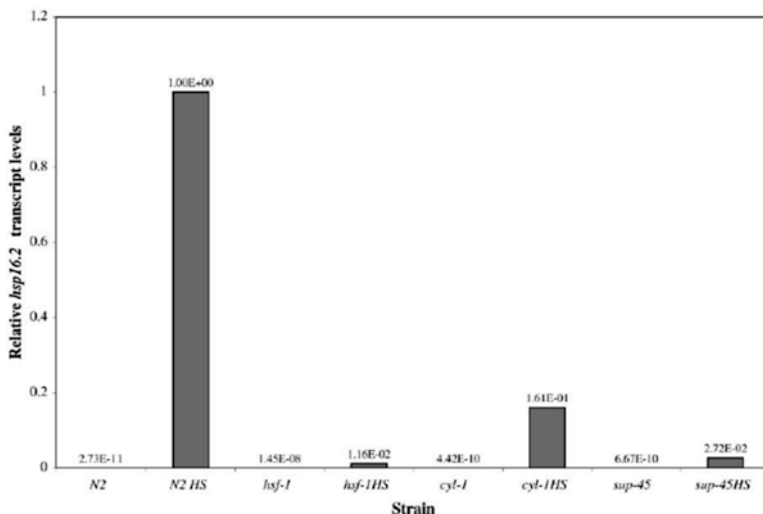


Fig. 11.7 Decreased levels of *hsp-16.2* mRNA in suppressor mutants, as measured by quantitative real-time PCR [27]. Input levels for each sample were normalized with control PCR reactions using 18S rRNA

11.3.2 Regulation of Toxicity of Other Environmental Toxicants by Heat Shock Proteins

In nematodes, heat shock treatment induced the significant increase in HSP-16.1::GFP, HSP-16.2::GFP, HSP-16.41::GFP, and HSP-16.48::GFP (Fig. 11.8) [28]. Meanwhile, hypoxia treatment also induced the significant increase in HSP-16.1::GFP and HSP-16.2::GFP, and ethanol treatment induced the significant increase in HSP-16.1::GFP, HSP-16.2::GFP, HSP-16.41::GFP, and HSP-16.48::GFP (Fig. 11.8) [28].

Moreover, it was found that mutation of *hsp-16.48* could further result in a susceptibility to the TiO₂-NPs toxicity in reducing body length, in reducing brood size, in decreasing locomotion behavior, and in inducing intestinal autofluorescence and ROS production [18]. Similarly, mutation of *hsp-16.48* caused the susceptibility to graphene oxide (GO) toxicity in reducing brood size, in decreasing locomotion behavior, and in inducing intestinal ROS production, and the enhanced accumulation of GO in the body of nematodes (Fig. 11.9) [29]. In addition, mutation of *hsp-70* or *hsp-3* increased the susceptibility of nematodes to Mn toxicity in reducing lifespan, and mutation of *hsp-70* enhanced neurotoxicity of Mn in inducing the degradation of dopaminergic neurons in nematodes [30].

11.3.3 Regulation of Toxicity of Other Environmental Toxicants by HSF-1

Environmental pathogen infection can potentially cause the toxicity as different aspects on organisms, including the nematodes [31–39]. It was observed that RNAi knockdown of *hsf-1* induced a susceptibility to *P. aeruginosa* PA14 infection in reducing the lifespan, whereas overexpression of HSF-1 induced a resistance to *P.*

Fig. 11.8 (continued) expression of HSP16-1. HSP16-1 is minimally expressed without stress. The second row represents the result of exposure to 7% ethanol for 30 min. The third row represents the result of exposure to 1 mM of sodium azide for 30 min. The fourth row represents the result of exposure to 200 mM of NaCl solution for 30 min, and the last row represents the result of starvation for 12 h. The figures of the first and third column are Nomarski images, and the second and fourth are GFP fluorescence driven by the *hsp-16-1* promoter. HSP-16.1 was more strongly induced by starvation than by other stresses and appeared as punctuated spots. The scale bar represents 50 μm. **(b)** Hypoxia response of the *hsp-16* genes in a hypoxia chamber. Each column represents the expression of *hsp-16.1*, *hsp-16.2*, *hsp-16.41*, and *hsp-16.48*, respectively. Upper panels are control animals and lower panels, the animals incubated in the hypoxia chamber. Only *hsp-16.1* and *hsp-16.2* responded to hypoxia. **(c)** Hypoxia response of the *hsp-16* genes in the animals soaked in the M9 buffer. Each column represents the expression of *hsp-16.1*, *hsp-16.2*, *hsp-16.41*, and *hsp-16.48*, respectively. All four genes are responsive to heat shock and ethanol stress, but only *hsp-16.1* and *hsp-16.2* responded to hypoxia. We observed more than 30 animals from at least two independent transgenic lines for each gene and obtained similar results shown in this figure. This figure shows representative animals. The scale bars in **(b, c)** represent 0.2 mm

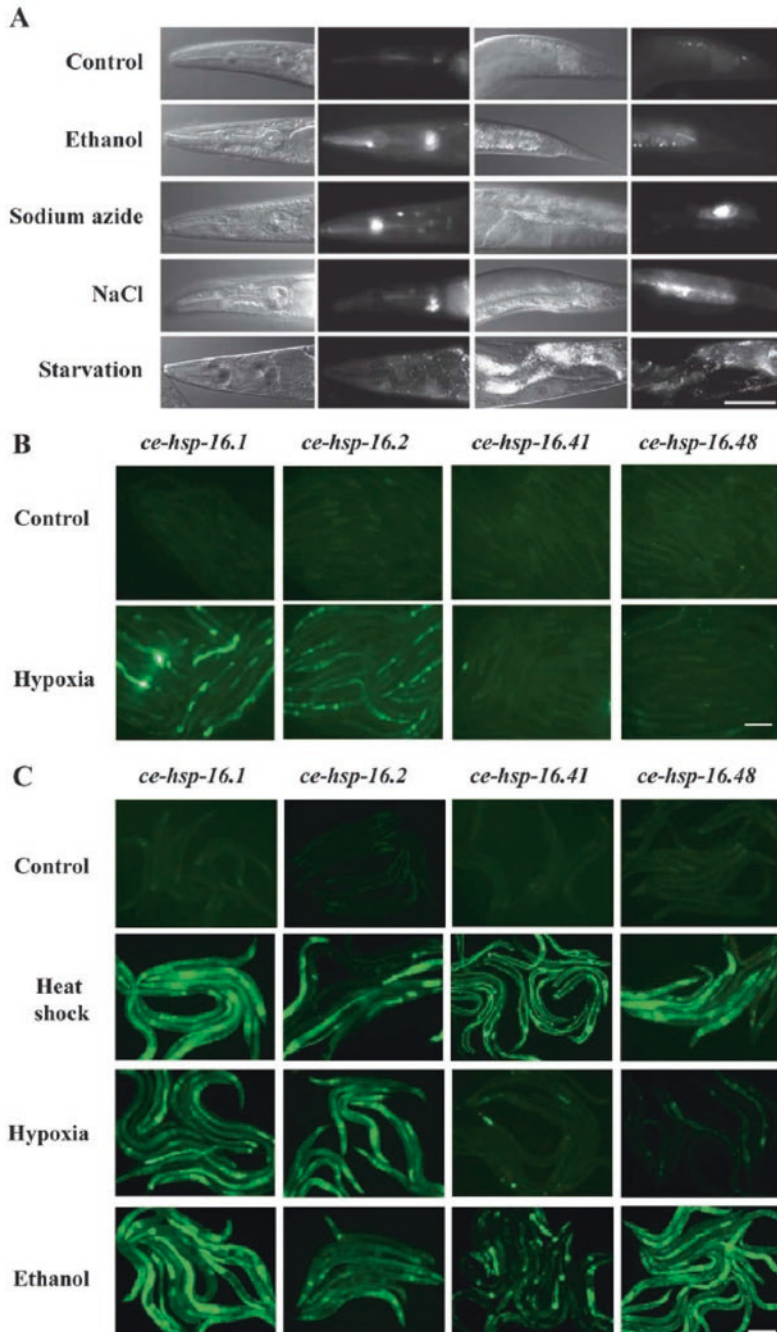


Fig. 11.8 The hypoxia responses of the *hsp-16* genes in *C. elegans* are distinct [28]. (a) The expression of HSP-16.1 is induced by several types of stress. The first row represents the basal

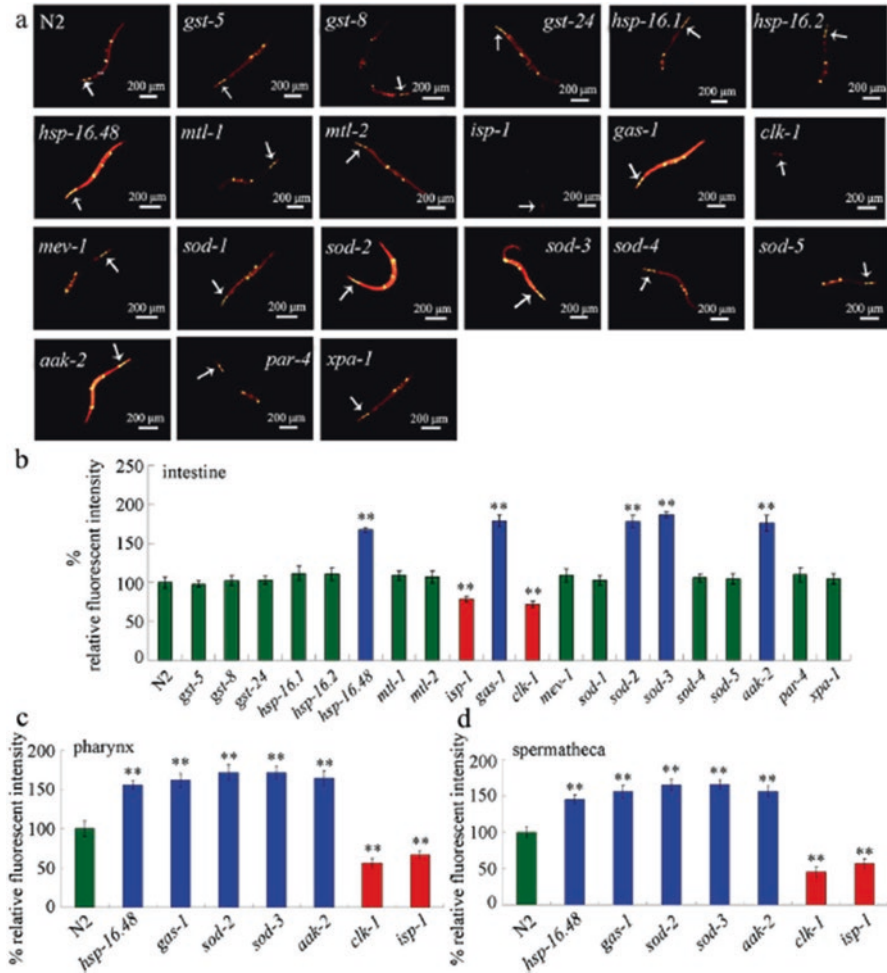


Fig. 11.9 Distributions of GO-Rho B in wild-type and mutant nematodes [29]. (a) Pictures showing the distributions of GO-Rho B in wild-type and mutant nematodes. (b) Comparison of relative fluorescence of GO-Rho B in the intestine between wild-type and mutant nematodes. (c) Comparison of relative fluorescence of GO-Rho B in the pharynx between wild-type and mutant nematodes. (d) Comparison of relative fluorescence of GO-Rho B in the spermatheca between wild-type and mutant nematodes. The arrowheads indicate the pharynx. The intestine (***) and the spermatheca (*) are also indicated. GO exposure was performed from L1-larvae to young adult. The exposure concentration of GO was 100 mg/L. Bars represent means \pm SEM. $**P < 0.01$ vs. N2

aeruginosa PA14 infection in reducing the lifespan (Fig. 11.10) [40]. The susceptibility of *hsf-1* mutant nematodes to *P. aeruginosa* PA14 infection in reducing the lifespan could be further enhanced by RNAi knockdown of *pmk-1* encoding a p38 MAPK in p38 MAPK signaling pathway (Fig. 11.10) [40].

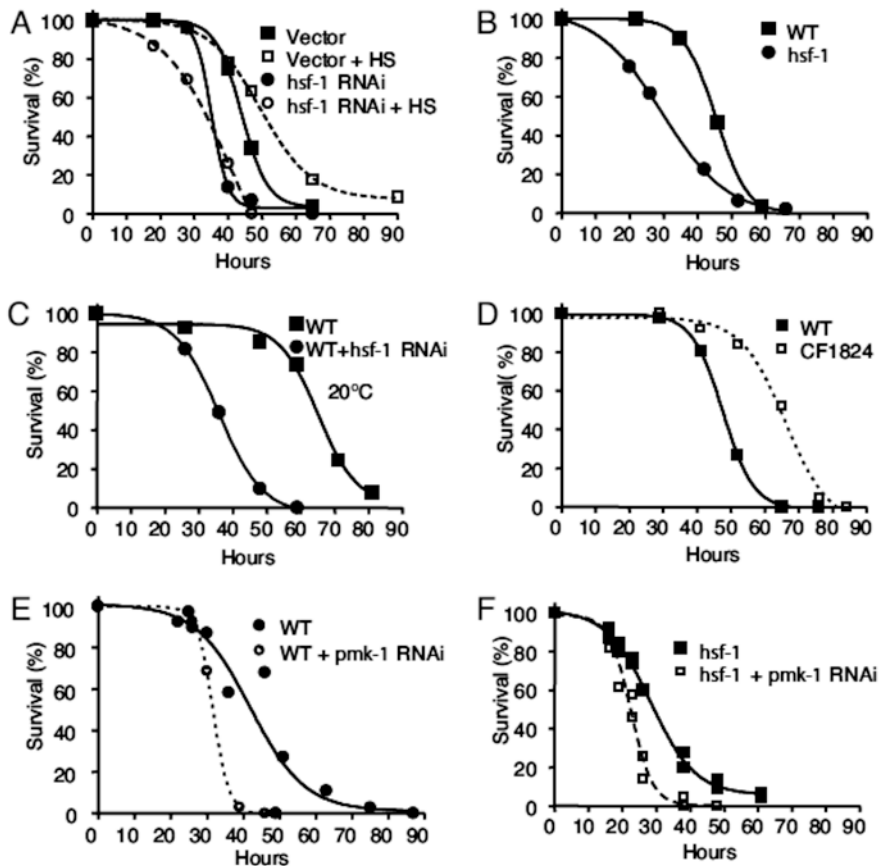


Fig. 11.10 HSF is required for *C. elegans* immunity to *P. aeruginosa* [40]. (a) Wild-type worms grown on *E. coli* carrying a vector control were untreated or HS-treated and exposed to *P. aeruginosa* ($P < 0.03$). In addition, wild-type animals grown on *E. coli* expressing *hsf-1* double-stranded RNA were untreated or HS-treated and exposed to *P. aeruginosa* ($P = 0.2660$). *hsf-1* RNAi animals were more susceptible to *P. aeruginosa* compared with vector RNAi controls ($P < 0.005$). (b) Wild-type or *hsf-1*(*sy441*) animals were grown on *E. coli* carrying a vector control and exposed to *P. aeruginosa* ($P < 0.0001$). (c) Wild-type animals grown on vector control or *hsf-1* double-stranded RNA were exposed to *P. aeruginosa* at 20 °C ($P < 0.0001$). (d) Wild-type or CF1824 (*hsf-1* overexpression) animals were exposed to *P. aeruginosa* ($P < 0.001$). (e) Wild-type animals grown on *E. coli* carrying a vector control or expressing *pmk-1* double-stranded RNA were exposed to *P. aeruginosa* ($P < 0.0001$). (f) *hsf-1*(*sy441*) animals grown on *E. coli* carrying a vector control or expressing *pmk-1* double-stranded RNA were exposed to *P. aeruginosa* ($P = 0.0023$). For each condition, 80–200 animals were used

In nematodes, it was further observed that RNAi knockdown of *hsf-1* could suppress the resistance of *daf-2* mutant nematodes to pathogen infection (Fig. 11.11) [40], suggesting that HSF-1 may act downstream of insulin signaling pathway to regulate the innate immune response to pathogen infection in nematodes. That is,

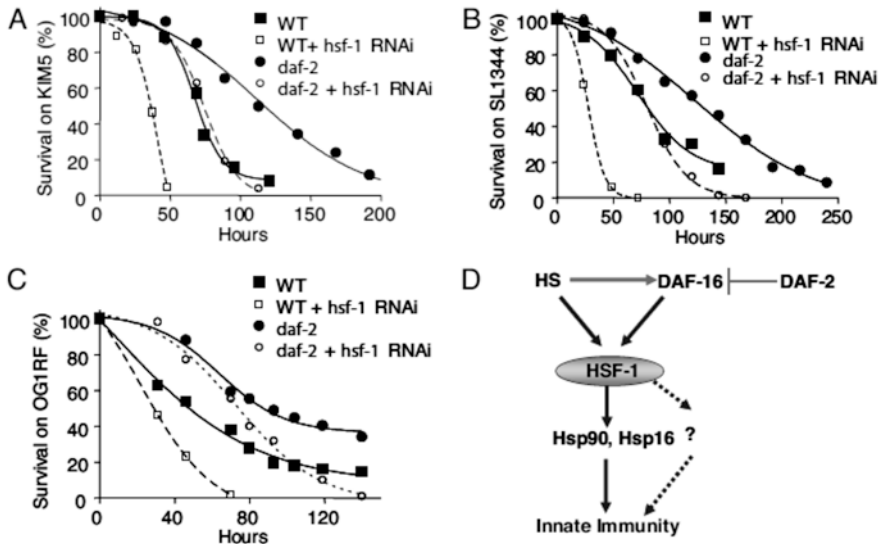


Fig. 11.11 HSF-1 is required for immunity to Gram-negative and Gram-positive pathogens [40]. (a) Wild-type worms grown on *E. coli* carrying a vector control or on *E. coli* expressing *hsf-1* double-stranded RNA were exposed to *Y. pestis* KIM5 ($P < 0.0001$). *daf-2*(*e1370*) worms grown on *E. coli* carrying a vector control or on *E. coli* expressing *hsf-1* double-stranded RNA were exposed to *Y. pestis* KIM5 ($P < 0.001$). (b) Wild-type worms grown on *E. coli* carrying a vector control or on *E. coli* expressing *hsf-1* double-stranded RNA were exposed to *S. enterica* SL1344 ($P < 0.0001$). *daf-2*(*e1370*) worms grown on *E. coli* carrying a vector control or on *E. coli* expressing *hsf-1* double-stranded RNA were exposed to *S. enterica* SL1344 ($P < 0.0001$). (c) Wild-type worms grown on *E. coli* carrying a vector control or on *E. coli* expressing *hsf-1* double-stranded RNA were exposed to *En. faecalis* OG1RF ($P < 0.0001$). *daf-2*(*e1370*) worms grown on *E. coli* carrying a vector control or on *E. coli* expressing *hsf-1* double-stranded RNA also were exposed to *En. faecalis* OG1RF ($P < 0.0001$). (d) HSF-1 activated by HS and the DAF-2/DAF-16 pathway enhances *C. elegans* immunity. HSF-1 mediates protection via induction of Hsp90 and small HSPs in a PMK-1-independent manner

the increased temperature activated HSF-1 will enhance the innate immunity, and this HSF-1 defense response is mediated by the further induction of a system of chaperones.

11.4 Hypoxia Response Signaling

11.4.1 Molecular Signaling for Hypoxia Response

11.4.1.1 HIF-1 and EGL-9

hif-1 encodes a bHLH-PAS hypoxia-inducible transcription factor. During the response to hypoxia stress, a physical complex is formed, and this complex contains HIF-1 and AHA-1, which are encoded by *C. elegans* homologs of hypoxia-inducible factor

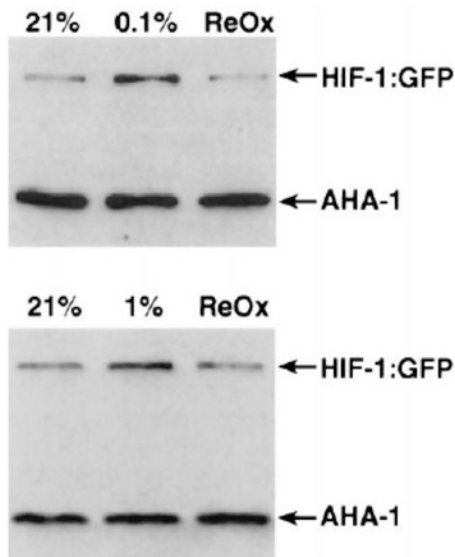


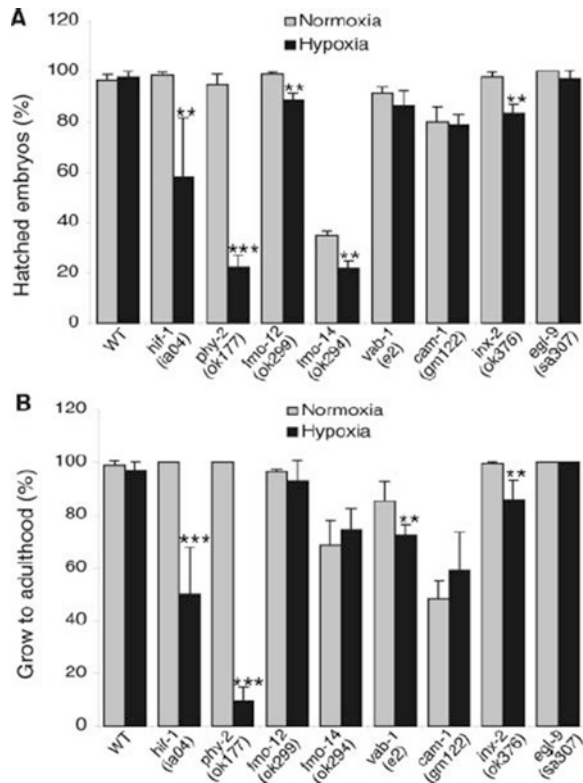
Fig. 11.12 HIF-1:GFP protein levels are increased by hypoxia [41]. The transgenic *C. elegans* strain pHJ06 Ex6, which expresses the complete HIF-1 protein fused to GFP, was harvested before (21% O₂) and after incubation in 0.1% oxygen (*upper*) or 1% oxygen (*lower*) for 8 h. In each experiment, a fraction of the hypoxia-treated worms was reoxygenated for 10 min (ReOx). Worms were lysed by boiling in loading buffer, and equal amounts of total protein were loaded in each lane. The expression of HIF-1:GFP and AHA-1 was assayed by probing the immunoblot with a GFP-specific antibody and the AHA-1-specific mAb 10H8

(HIF) α and β subunits, respectively [41]. The expression of HIF-1:GFP could be highly induced by hypoxia and was subsequently reduced upon reoxygenation (Fig. 11.12) [41]. In addition, the subcellular localization of AHA-1 was disrupted in the *hif-1* (*ia04*) mutant nematodes [41], suggesting that HIF-1 acts upstream of AHA-1 to regulate the hypoxia stress in a complex.

HIF-1 is a critical regulator for the responses to low oxygen levels. The *hif-1* mutant nematodes exhibited no adaptation to hypoxia stress, and the majority of *hif-1*-defective nematodes would die under these conditions (Fig. 11.13) [41, 42]. Additionally, it was found that some HIF-1 target genes could negatively regulate the formation of stress-resistant dauer larvae [42], suggesting the potential involvement of HIF-1 in the regulation of other stresses in nematodes.

A summary for the basics molecular basis for the hypoxia response signaling is provided in Fig. 11.14 [42]. During the control of response to hypoxia stress, EGL-9/PHD modifies the HIF-1, thereby increasing its affinity for VHL-1/E3 ligase to target the HIF-1 for proteasomal degradation (Fig. 11.14) [42]. That is, the proteasomal degradation of HIF-1 is mediated by both the EGL-9 and the VHL-1 (Fig. 11.14) [42]. Meanwhile, the expression of *egl-9* could also be regulated by *hif-1* mutation [42]. This suggests that the positive regulation of *egl-9* transcription by HIF-1 will further help to maintain the EGL-9 activity when oxygen substrate is

Fig. 11.13 Viability assays in normoxia (21% oxygen) and hypoxia (0.5% oxygen) [42]. Animals carrying strong loss-of-function mutations in downstream targets of HIF-1 were incubated in 0.5% oxygen (hypoxia) or room air (normoxia) for 24 h and then assayed for successful completion of embryogenesis (a) and survival to adulthood (b). Asterisks indicate that the viability of hypoxia-treated mutants is significantly lower than that of wild-type (WT)

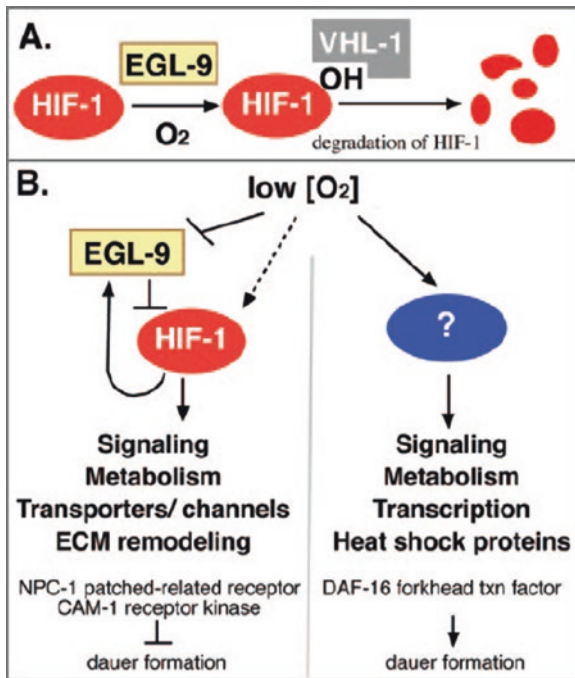


limiting, and a feedback loop will be activated to attenuate the HIF-1 activation (Fig. 11.14) [42]. In addition, the response to hypoxia is mediated by HIF-1-dependent or by HIF-1-independent pathway(s) (Fig. 11.14) [42]. HIF-1 can further positively regulate the expression of *npc-1* and *cam-1*, regulators of dauer formation [42]. The increased expression in *daf-16* is a common feature of the hypoxia response and of the perturbations in insulin signaling pathway [42].

11.4.1.2 Aminoacyl-tRNA Synthetase RRT-1

rrt-1 encodes a arginyl-transfer RNA (tRNA) synthetase, an enzyme essential for protein translation. Mutation or RNAi knockdown of *rrt-1* or other genes encoding the aminoacyl-tRNA synthetase could rescue the nematodes from the hypoxia-induced death [43]. More importantly, this hypoxia resistance was inversely correlated with the protein translation rate [43]. The ER unfolded protein response (UPR) induced by hypoxia was required for the resistance of *rrt-1* mutant nematodes to the hypoxia stress [43], suggesting that the translational suppression can induce the hypoxia resistance in part by reducing the unfolded protein toxicity in nematodes.

Fig. 11.14 Models for hypoxia signaling and response [42]



11.4.2 Regulation of Toxicity of Other Environmental Toxicants by HIF-1 and EGL-9

In nematodes, it was found that loss-of-function mutation of *hif-1* promoted the resistance of nematodes to exogenous mitochondrial stressor ethidium bromide (EtBr) and suppressed the EtBr-induced ROS production (Fig. 11.15) [44]. Similarly, mutation of *hif-1* also induced a resistance to high-glucose diets stress in reducing lifespan in nematodes [45]. During the control of EtBr toxicity, p38 MAPK signaling was identified as an indispensable factor for the survival against mitochondrial stress in *hif-1* mutant nematodes [45].

Moreover, it was observed that mutation of *hif-1* induced a susceptibility to pore-forming toxins (PFTs) toxicity in reducing the lifespan (Fig. 11.16) [46]. In contrast, the Cry21A PFT resistance was observed in *egl-9* mutant nematodes (Fig. 11.16) [46]. In nematodes, the intestinal specific expression of *egl-9* was sufficient to rescue the Cry21A PFT resistance [46]. Two of the downstream effectors of this pathway were identified, and they were nuclear receptor NHR-57- and XBP-1-mediated ER UPR signaling during the control of PFTs toxicity in nematodes.

Furthermore, it was found that mutation of *hif-1* induced a susceptibility to pathogen infection, whereas mutation of *egl-9* induced a resistance to pathogen infection (Fig. 11.17) [47]. Moreover, the HIF-1 α was dispensable for the host defense gene induction, and SWAN-1-mediated noncanonical pathway inhibited this HIF-1 induced defense gene repression in nematodes [47].

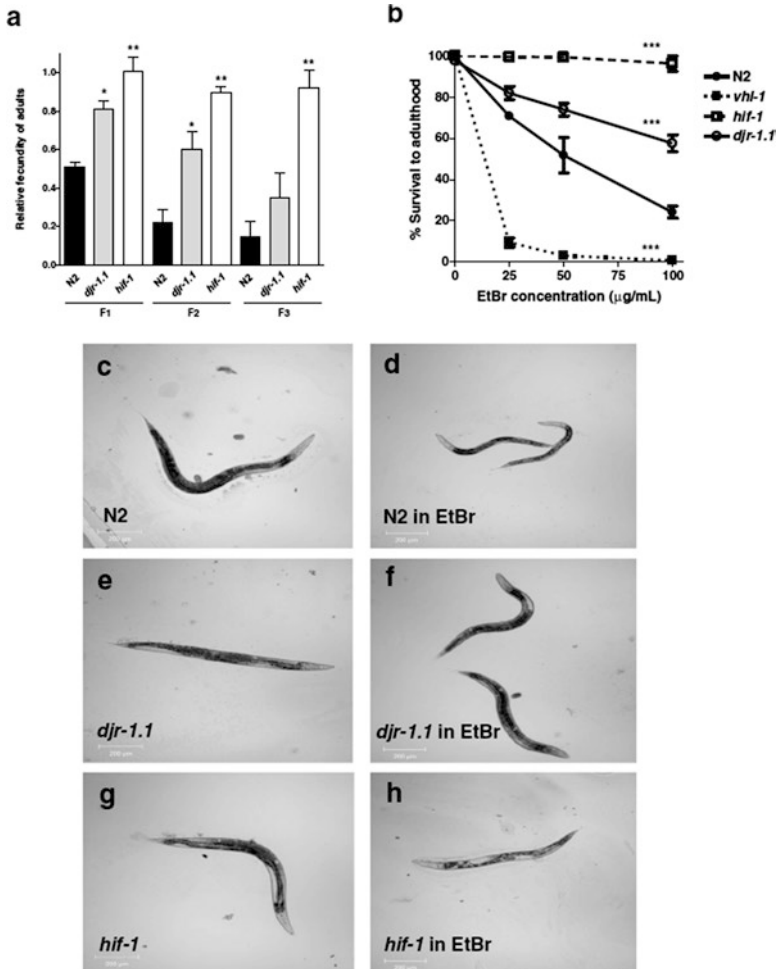
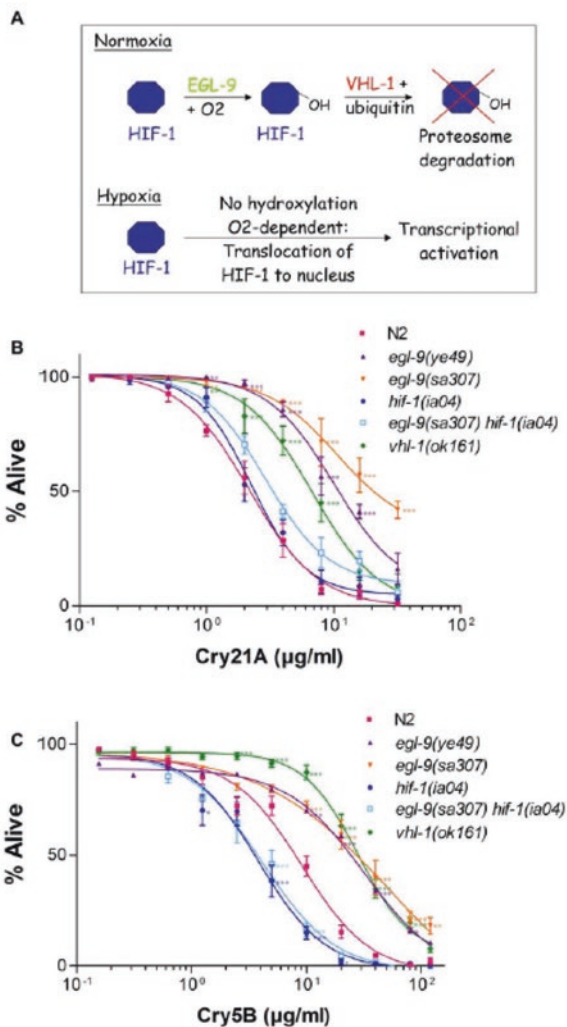


Fig. 11.15 *hif-1* and *djr-1.1* mutants are highly resistant to EtBr [44]. (a) *hif-1* animals exposed to EtBr have no effect on fecundity over three generations, while wild-type worms showed a significant decrease in brood size. Brood size of N2 (wild-type), *djr-1.1*, and *hif-1* animals in 25 µg/mL EtBr were counted for three generations: F1, F2, and F3. Relative fecundity is measured as the number of progeny grown to adulthood on EtBr divided by the number of progeny grown to adulthood in the absence of EtBr and would include animals that arrest at the L3 stage. Animals with ruptured vulva were not counted. Asterisk marks denote significant difference of fecundity between P0 (normalized to 1.0) and the following generations for each strain (* denotes $p < 0.05$ and ** $p < 0.01$) using one-way ANOVA. (b) Concentration dependence of EtBr. N2, *hif-1*, *vhl-1*, and *djr-1.1* mutant animals (first generation) were grown on worm plates containing nematode growth media and various concentrations of EtBr (0, 25, 50, and 100 µg/mL). The number of worms that grew to adulthood was determined and plotted. To determine significant differences between strains, the data were subjected to two-way ANOVA comparing groups (different strains) over different concentrations of EtBr. All strains showed a significant difference compared to N2 (***) ($p < 0.001$). (c–h) Growth of strains on EtBr. N2, *djr-1.1* and *hif-1* worms (as labeled) 4 days after egg-laying in plates containing either no EtBr (c, e, g) or 50 µg/mL EtBr (d, f, h)

Fig. 11.16 Quantitative response of *egl-9* and HIF-1 pathway mutants to Cry PFTs [46]. (a) Schematic illustrating O₂-dependent regulation of HIF-1 activity. The O₂-dependent prolyl hydroxylation of HIF-1 by EGL-9/PHD increases its affinity to VHL-1, leading to ubiquitylation and destruction. (b, c) Dose-dependent mortality assays were performed using (b) Cry21A spore crystal lysates or (c) purified Cry5B to quantitatively compare sensitivities of wild-type N2, *egl-9* mutants, and HIF-1 pathway mutants to PFTs. Each data point shows the mean and standard errors of the mean of results from three independent experiments (three wells per experiment; on average, 180 animals per data point). Statistical differences between mutant strains and N2 are given for each concentration using P values represented by asterisks as follows: * *P* < 0.05; ** *P* < 0.01; *** *P* < 0.001



11.5 Perspectives

In this chapter, we selected three well-described response signals (heavy metal response, heat shock response, and hypoxia response) to discuss the question on the specificity of molecular signals in response to certain environmental toxicants or stresses in nematodes. Actually, there are still other relevant evidence on the study of UV irradiation, osmotic stress, etc. As introduced and discussed in this chapter, so far the obtained data in nematodes does not support the existence of specific molecular signals in response to certain environmental toxicants or stresses. The molecular basis for the response to heavy metal response, heat shock response, or

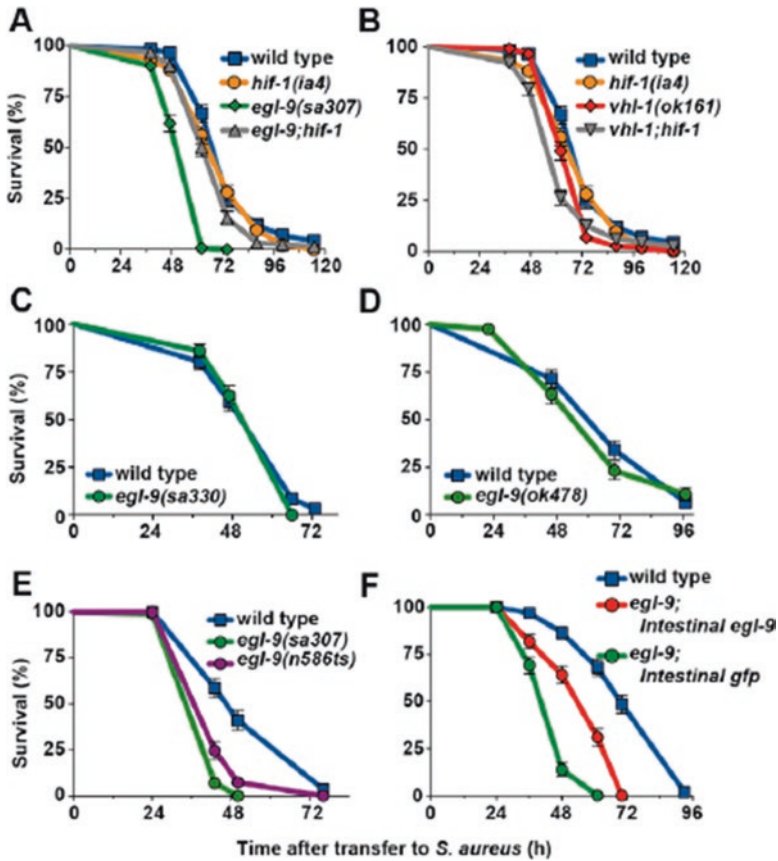


Fig. 11.17 *egl-9* inactivation causes enhanced susceptibility to *S. aureus*-mediated killing [47]. (a) *egl-9(sa307)* animals exhibited enhanced susceptibility, whereas *egl-9(sa307);hif-1(ia4)* mutants exhibited near wild-type susceptibility. Survival analysis: *egl-9* Kaplan–Meier median survival (MS) = 62 h, time to 50% death by nonlinear regression analysis (LT50) = 48.78 h, number of animals (N) = 142, $p < 0.0001$ (log-rank test, compared with wild-type); *egl-9;hif-1* MS = 68 h, LT50 = 62.10 h, $N = 122/2$, $p = 0.0030$ (compared with wild-type). (b) *vhl-1(ok161)* and *hif-1(ia4)* animals exhibited near wild-type susceptibility. Survival analysis: wild-type MS = 74 h, LT50 = 67.03 h, $N = 117/5$; *vhl-1* MS = 62 h, LT50 = 61.86 h, $N = 118$, $p < 0.0001$ (compared with wild-type); *hif-1* MS = 74 h, LT50 = 64.77 h, $N = 136$, $p = 0.0943$ (compared with wild-type). (c) *egl-9(sa330)* animals and (d) *egl-9(ok478)* animals exhibit wild-type susceptibility. (e) *egl-9(n586ts)* animals are hypersusceptible to *S. aureus*. Survival analysis: *egl-9(sa307)* MS = 43 h, $N = 95/1$, $p < 0.0001$ (compared with wild-type); *egl-9(n586ts)* MS = 43 h, $N = 96/15$, $p < 0.0001$ (compared with wild-type); wild-type MS = 50 h, $N = 92/9$. (f) Wild-type, *egl-9(sa307);crp-1::egl-9* (Intestinal *egl-9*), and *egl-9(sa307);crp-1::gfp* (Intestinal *gfp*) animals show that intestinal expression of EGL-9, but not GFP, rescues the *egl-9(sa307)* enhanced susceptibility phenotype. Survival analysis: wild-type MS = 70 h, $N = 108/7$; Intestinal *egl-9* MS = 61 h, $N = 115/14$, $p < 0.0001$ (compared with wild-type), $p < 0.0001$ (compared with Intestinal *gfp*); Intestinal *gfp* MS = 48 h, $N = 102/3$, $p < 0.0001$ (compared with wild-type). Results are representative of two independent trials, performed in triplicate. Animals were subjected to *cdc-25* RNAi to prevent reproduction and subsequently transferred to *S. aureus* killing assay plates

hypoxia response can also involve in the regulation of toxicity of other environmental toxicants or stresses under certain conditions. However, this also not means that the nematodes share the completely same molecular signaling pathways in response to different environmental toxicants or stresses. The further studies are suggested to focus on the definition of direct or primary molecular signals involved in the regulation of certain environmental toxicants or stresses in nematodes.

References

1. Wang D-Y (2018) Nanotoxicology in *Caenorhabditis elegans*. Springer, Singapore
2. Li W-J, Wang D-Y, Wang D-Y (2018) Regulation of the response of *Caenorhabditis elegans* to simulated microgravity by p38 mitogen-activated protein kinase signaling. *Sci Rep* 8:857
3. Xiao G-S, Zhao L, Huang Q, Yang J-N, Du H-H, Guo D-Q, Xia M-X, Li G-M, Chen Z-X, Wang D-Y (2018) Toxicity evaluation of Wanzhou watershed of Yangtze Three Gorges Reservoir in the flood season in *Caenorhabditis elegans*. *Sci Rep* 8:6734
4. Xiao G-S, Zhao L, Huang Q, Du H-H, Guo D-Q, Xia M-X, Li G-M, Chen Z-X, Wang D-Y (2018) Biosafety assessment of water samples from Wanzhou watershed of Yangtze Three Gorges Reservoir in the quiet season in *Caenorhabditis elegans*. *Sci Rep* 8:14102
5. Yin J-C, Liu R, Jian Z-H, Yang D, Pu Y-P, Yin L-H, Wang D-Y (2018) Di (2-ethylhexyl) phthalate-induced reproductive toxicity involved in DNA damage-dependent oocyte apoptosis and oxidative stress in *Caenorhabditis elegans*. *Ecotoxicol Environ Saf* 163:298–306
6. Wu Q-L, Han X-X, Wang D, Zhao F, Wang D-Y (2017) Coal combustion related fine particulate matter (PM_{2.5}) induces toxicity in *Caenorhabditis elegans* by dysregulating microRNA expression. *Toxicol Res* 6:432–441
7. Swain SC, Keusekotten K, Baumeister R, Sturzenbaum SR (2004) *C. elegans* metallothioneins: new insights into the phenotypic effects of cadmium toxicosis. *J Mol Biol* 341:951–959
8. Liao VH, Dong J, Freedman JH (2002) Molecular characterization of a novel, cadmium-inducible gene from the nematode *Caenorhabditis elegans*. *J Biol Chem* 277:42049–42069
9. Hall J, Haas KL, Freedman JH (2012) Role of MTL-1, MTL-2, and CDR-1 in mediating cadmium sensitivity in *Caenorhabditis elegans*. *Toxicol Sci* 128:418–426
10. Ren M-X, Zhao L, Ding X-C, Krasteva N, Rui Q, Wang D-Y (2018) Developmental basis for intestinal barrier against the toxicity of graphene oxide. *Part Fibre Toxicol* 15:26
11. Xiao G-S, Chen H, Krasteva N, Liu Q-Z, Wang D-Y (2018) Identification of interneurons required for the aversive response of *Caenorhabditis elegans* to graphene oxide. *J Nanobiotechnol* 16:45
12. Ding X-C, Rui Q, Wang D-Y (2018) Functional disruption in epidermal barrier enhances toxicity and accumulation of graphene oxide. *Ecotoxicol Environ Saf* 163:456–464
13. Zhao L, Kong J-T, Krasteva N, Wang D-Y (2018) Deficit in epidermal barrier induces toxicity and translocation of PEG modified graphene oxide in nematodes. *Toxicol Res* 7(6):1061–1070. <https://doi.org/10.1039/C8TX00136G>
14. Qu M, Xu K-N, Li Y-H, Wong G, Wang D-Y (2018) Using *acs-22* mutant *Caenorhabditis elegans* to detect the toxicity of nanopolystyrene particles. *Sci Total Environ* 643:119–126
15. Dong S-S, Qu M, Rui Q, Wang D-Y (2018) Combinational effect of titanium dioxide nanoparticles and nanopolystyrene particles at environmentally relevant concentrations on nematodes *Caenorhabditis elegans*. *Ecotoxicol Environ Saf* 161:444–450
16. Xiao G-S, Zhi L-T, Ding X-C, Rui Q, Wang D-Y (2017) Value of *mir-247* in warning graphene oxide toxicity in nematode *Caenorhabditis elegans*. *RSC Adv* 7:52694–52701

17. Zhao L, Wan H-X, Liu Q-Z, Wang D-Y (2017) Multi-walled carbon nanotubes-induced alterations in microRNA *let-7* and its targets activate a protection mechanism by conferring a developmental timing control. *Part Fibre Toxicol* 14:27
18. Rui Q, Zhao Y-L, Wu Q-L, Tang M, Wang D-Y (2013) Biosafety assessment of titanium dioxide nanoparticles in acutely exposed nematode *Caenorhabditis elegans* with mutations of genes required for oxidative stress or stress response. *Chemosphere* 93:2289–2296
19. Polak N, Read DS, Jurkschat K, Matzke M, Kelly FJ, Spurgeon DJ, Stürzenbaum SR (2014) Metalloproteins and phytochelatin synthase may confer protection against zinc oxide nanoparticle induced toxicity in *Caenorhabditis elegans*. *Comp Biochem Physiol C* 160:75–85
20. Zhao L, Qu M, Wong G, Wang D-Y (2017) Transgenerational toxicity of nanopolystyrene particles in the range of $\mu\text{g/L}$ in nematode *Caenorhabditis elegans*. *Environ Sci Nano* 4:2356–2366
21. Shao H-M, Han Z-Y, Krasteva N, Wang D-Y (2018) Identification of signaling cascade in the insulin signaling pathway in response to nanopolystyrene particles. *Nanotoxicology in press*
22. Murphy CT, McCarroll SA, Bargmann CI, Fraser A, Kamath RS, Ahringer J, Li H, Kenyon C (2003) Gene that act downstream of DAF-16 to influence the lifespan of *Caenorhabditis elegans*. *Nature* 424:277–284
23. Pinkston-Gosse J, Kenyon C (2007) DAF-16/FOXO targets genes that regulate tumor growth in *Caenorhabditis elegans*. *Nat Genet* 39:1403–1409
24. Tepper RG, Ashraf J, Kaletsky R, Kleemann G, Murphy CT, Bussemaker HJ (2013) PQM-1 complements DAF-16 as a key transcriptional regulator of DAF-2-mediated development and longevity. *Cell* 154:676–690
25. Snutch TP, Baillie DL (1983) Alterations in the pattern of gene expression following heat shock in the nematode *Caenorhabditis elegans*. *Can J Biochem Cell Biol* 61:480–487
26. Morley JF, Morimoto RL (2004) Regulation of longevity in *Caenorhabditis elegans* by heat shock factor and molecular chaperones. *Mol Biol Cell* 15:657–664
27. Hajdu-Cronin YM, Chen WJ, Sternberg PW (2004) The L-type cyclin CYL-1 and the heat-shock-factor HSF-1 are required for heat-shock-induced protein expression in *Caenorhabditis elegans*. *Genetics* 168:1937–1949
28. Hong M, Kwon JY, Shim J, Lee J (2004) Differential hypoxia response of *hsp-16* genes in the nematode. *J Mol Biol* 344:369–381
29. Wu Q-L, Zhao Y-L, Li Y-P, Wang D-Y (2014) Molecular signals regulating translocation and toxicity of graphene oxide in nematode *Caenorhabditis elegans*. *Nanoscale* 6:11204–11212
30. Avila DS, Benedetto A, Au C, Bornhorst J, Aschner M (2016) Involvement of heat shock proteins on Mn induced toxicity in *Caenorhabditis elegans*. *BMC Pharmacol Toxicol* 17:54
31. Zhi L-T, Yu Y-L, Li X-Y, Wang D-Y, Wang D-Y (2017) Molecular control of innate immune response to *Pseudomonas aeruginosa* infection by intestinal *let-7* in *Caenorhabditis elegans*. *PLoS Pathog* 13:e1006152
32. Zhi L-T, Yu Y-L, Jiang Z-X, Wang D-Y (2017) *mir-355* functions as an important link between p38 MAPK signaling and insulin signaling in the regulation of innate immunity. *Sci Rep* 7:14560
33. Sun L-M, Liao K, Hong C-C, Wang D-Y (2017) Honokiol induces reactive oxygen species-mediated apoptosis in *Candida albicans* through mitochondrial dysfunction. *PLoS ONE* 12:e0172228
34. Sun L-M, Liao K, Wang D-Y (2017) Honokiol induces superoxide production by targeting mitochondrial respiratory chain complex I in *Candida albicans*. *PLoS ONE* 12:e0184003
35. Sun L-M, Zhi L-T, Shakoob S, Liao K, Wang D-Y (2016) microRNAs involved in the control of innate immunity in *Candida* infected *Caenorhabditis elegans*. *Sci Rep* 6:36036
36. Sun L-M, Liao K, Li Y-P, Zhao L, Liang S, Guo D, Hu J, Wang D-Y (2016) Synergy between PVP-coated silver nanoparticles and azole antifungal against drug-resistant *Candida albicans*. *J Nanosci Nanotechnol* 16:2325–2335

37. Wu Q-L, Cao X-O, Yan D, Wang D-Y, Aballay A (2015) Genetic screen reveals link between maternal-effect sterile gene *mes-1* and *P. aeruginosa*-induced neurodegeneration in *C. elegans*. *J Biol Chem* 290:29231–29239
38. Yu Y-L, Zhi L-T, Guan X-M, Wang D-Y, Wang D-Y (2016) FLP-4 neuropeptide and its receptor in a neuronal circuit regulate preference choice through functions of ASH-2 trithorax complex in *Caenorhabditis elegans*. *Sci Rep* 6:21485
39. Yu Y-L, Zhi L-T, Wu Q-L, Jing L-N, Wang D-Y (2018) NPR-9 regulates innate immune response in *Caenorhabditis elegans* by antagonizing activity of AIB interneurons. *Cell Mol Immunol* 15:27–37
40. Singh V, Aballay A (2006) Heat-shock transcription factor (HSF)-1 pathway required for *Caenorhabditis elegans* immunity. *Proc Natl Acad Sci U S A* 103:13092–13097
41. Jiang H, Guo R, Powell-Coffman JA (2001) The *Caenorhabditis elegans hif-1* gene encodes a bHLH-PAS protein that is required for adaptation to hypoxia. *Proc Natl Acad Sci U S A* 98:7916–7921
42. Shen C, Nettleton D, Jiang M, Kim SK, Powell-Coffman JA (2005) Roles of the HIF-1 hypoxia-inducible factor during hypoxia response in *Caenorhabditis elegans*. *J Biol Chem* 280:20580–20588
43. Anderson LL, Mao X, Scott BA, Crowder CM (2009) Survival from hypoxia in *C. elegans* by inactivation of aminoacyl-tRNA synthetases. *Science* 323:630–633
44. Kamal M, D'Amora DR, Kubiseski TJ (2016) Loss of *hif-1* promotes resistance to the exogenous mitochondrial stressor ethidium bromide in *Caenorhabditis elegans*. *BMC Cell Biol* 17:34
45. AlcaÂntar-FernaÂndez J, Navarro RE, Salazar-MartÃ³nez AM, PeÃ±ez-Andrade ME, Miranda-RÃ³s J (2018) *Caenorhabditis elegans* respond to high-glucose diets through a network of stress- responsive transcription factors. *PLoS ONE* 13:e0199888
46. Bellier A, Chen C-S, Kao C-Y, Cinar HN, Aroian RV (2009) Hypoxia and the hypoxic response pathway protect against pore-forming toxins in *C. elegans*. *PLoS Pathog* 5:e1000689
47. Luhachack LG, Visvikis O, Wollenberg AC, Lacy-Hulbert A, Stuart LM, Irazoqui JE (2012) EGL-9 controls *C. elegans* host defense specificity through prolyl hydroxylation-dependent and -independent HIF-1 pathways. *PLoS Pathog* 8:e1002798

Chapter 12

Epigenetic Regulation of Toxicity of Environmental Toxicants or Stresses



Abstract The epigenetic regulation mechanisms can provide us a possibility that a small set of molecules potentially govern many important molecular signaling pathways to regulate the biological processes. We here focused on the methylation, acetylation, microRNAs (miRNAs), and long noncoding RNAs (lncRNAs) to introduce and to discuss the contributions of epigenetic regulation to toxicity induction of environmental toxicants or stresses and the underlying mechanisms. These investigations may open a new window to understand the full story on the toxicity induction in nematodes exposed to environmental toxicants or stresses.

Keywords Methylation · Acetylation · MicroRNAs · Long noncoding RNAs · Environmental exposure · *Caenorhabditis elegans*

12.1 Introduction

Besides the important roles and functions of molecular signaling pathways encoded by genes, in recent years, the epigenetic control of toxicity of environmental toxicants or stresses has gradually received the attention. The epigenetic regulation can be formed and reflected by several forms, such as methylation, acetylation, and small RNA control. The epigenetic regulation mechanisms provide such a possibility that a small set of molecules can act upstream and govern many important molecular signaling pathways to regulate the toxicity of environmental toxicants or stresses.

In this chapter, we first introduced and discussed the contributions of methylation regulation and acetylation regulation to the toxicity induction of environmental toxicants or stresses and the underlying mechanisms. Moreover, we further introduced and discussed the roles of microRNAs (miRNAs) and long noncoding RNAs (lncRNAs) in regulating the toxicity of environmental toxicants and stresses and the underlying mechanisms. The investigations on the epigenetic regulation mechanisms open a new window for us to understand the possible full story on the toxicity induction in nematodes exposed to environmental toxicants or stresses.

12.2 Methylation Regulation

12.2.1 Methylation of Histone H3K4

12.2.1.1 Function of ASH-2 Trithorax Complex

In nematodes, environmental pathogens, including the *Pseudomonas aeruginosa*, can potentially result in toxic effects on animals and even kill the animals [1–7]. *E. coli* OP50 is the normal food source for nematodes. Using *P. aeruginosa* PA4 and *E. coli* OP50, a preference choice model can be established [8]. In this preference choice model, it was found that the ADL sensory neurons regulated the preference choice by inhibiting function of a G protein-coupled receptor (GPCR)/SRH-220 [8]. Moreover, the ADL sensory neurons regulated the preference choice through peptidergic signals of FLP-4 and NLP-10, and the function of FLP-4 or NLP-10 in regulating preference choice was under the regulation of GPCR SRH-220 [8]. The FLP-4 released from the ADL sensory neurons further affected the preference choice through its receptor of NPR-4 in the AIB interneurons [8].

In nematodes, ASH, WDR-5, and SET-2 constitute an ASH-2 trithorax complex, which trimethylates the histone H3K4. ASH-2 is a trithorax group protein, WDR-5 is a WD40 repeat-containing protein, SET-2 is a histone H3 at lysine 4 (H3K4) methyltransferase, and RBR-2 is a H3K4 demethylase. In the AIB interneurons, NPR-4 regulated the preference choice by activating the function of SET-2 [8]. Mutation of *set-2*, *ash-2*, or *wdr-5* caused the significant decrease in choice index; however, mutation of *rbr-2* did not significantly affect the preference choice behavior (Fig. 12.1) [8], suggesting the involvement of ASH-2 trithorax complex in the control of preference choice behavior. In this ASH-2 trithorax complex, genetic interactions demonstrated that SET-2 functioned in the same pathway with ASH-2 and WDR-5 in regulating the preference choice (Fig. 12.1) [8]. Additionally, expression of *set-2*, *ash-2*, or *wdr-5* in AIB interneurons could rescue the deficit in preference choice in corresponding mutant nematodes [8]. Therefore, the GPCR NPR-4 is involved in the control of preference choice by activating the functions of ASH-2 trithorax complex consisting of SET-2, ASH-2, and WDR-5. These results also highlight the important function of the ASH-2 trithorax complex-mediated molecular machinery for trimethylation of histone H3K4 in the regulation of toxicity of environmental toxicants or stresses in nematodes.

12.2.1.2 S-Adenosyl Methionine (SAM) and SET-16-Mediated Complex

SAM, the sole methyl donor, modifies the molecules including the histones, and its fluctuation is associated with the variations in histone methylation. In nematodes, it was observed that RNAi knockdown of *sams-1* encoding a SAM synthase resulted in the activation of innate immune genes and the constitutively activation of p38 MAPK signaling pathway under the normal conditions [9], suggesting that the low SAM can

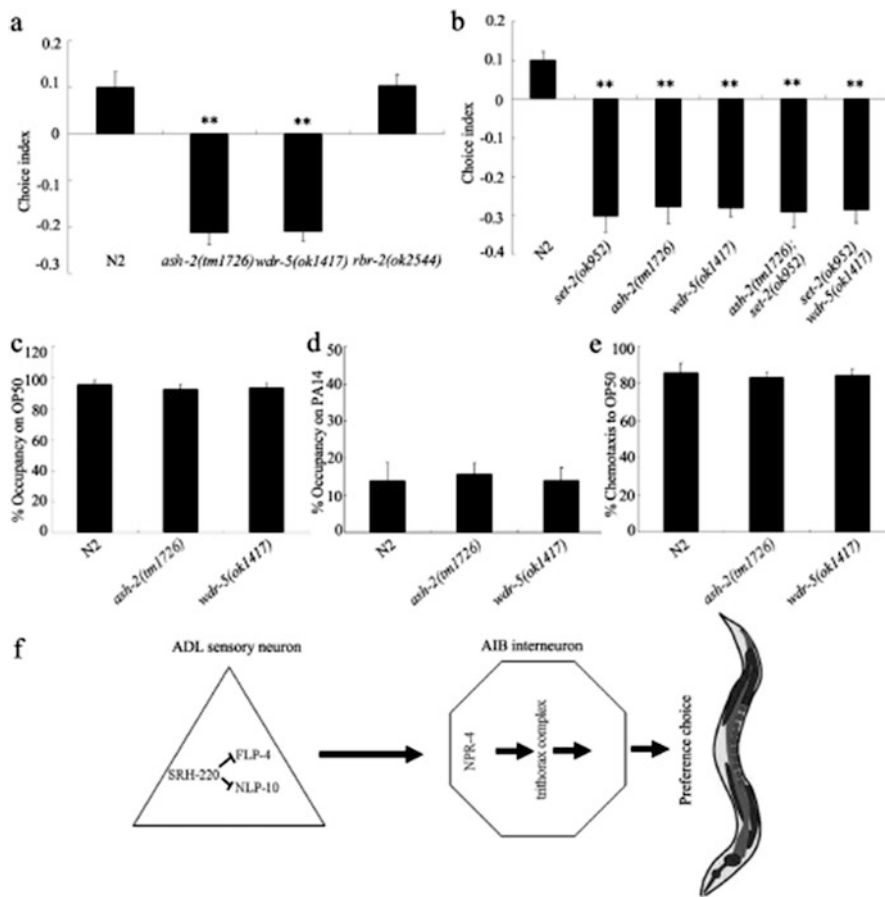


Fig. 12.1 SET-2 functioned together with ASH-2 and WDR-5 to regulate preference choice in nematodes [8]. (a) Preference choice phenotype in *ash-2*, *wdr-5*, or *rbr-2* mutants. (b) Genetic interaction of SET-2 with ASH-2 or WDR-5 in regulating preference choice. (c) Leaving behavior from bacterial lawns and chemotaxis to OP50 in *ash-2* or *wdr-5* mutants. (d) The molecular signals regulating preference choice in the neuronal circuit of ADL sensory neuron-AIB interneuron. Sensory neurons are shown as triangles and interneurons as hexagons. Arrows indicate chemical synapses. Bars represent means \pm S.E.M. ** $P < 0.01$ vs N2

activate or attenuate the innate immune response. Additionally, the innate immune activation was formed downstream of the phosphatidylcholine (PC) in the *sams-1(RNAi)* nematodes [9]. Moreover, it was found that the *sams-1(lof)* mutant nematodes died rapidly after infection with *Pseudomonas*, and the failure of transcriptional response to *Pseudomonas* was observed in the *sams-1(lof)* mutant nematodes [9]. The analysis on the H3K4 methylation further demonstrated that the infection response genes could not cause the increase in histone methylation marks in *sams-1(lof)* mutant nematodes after *Pseudomonas* infection, and the low SAM restricted the H3K4me3, thereby limiting their expression in *sams-1* mutant nematodes (Fig. 12.2) [9].

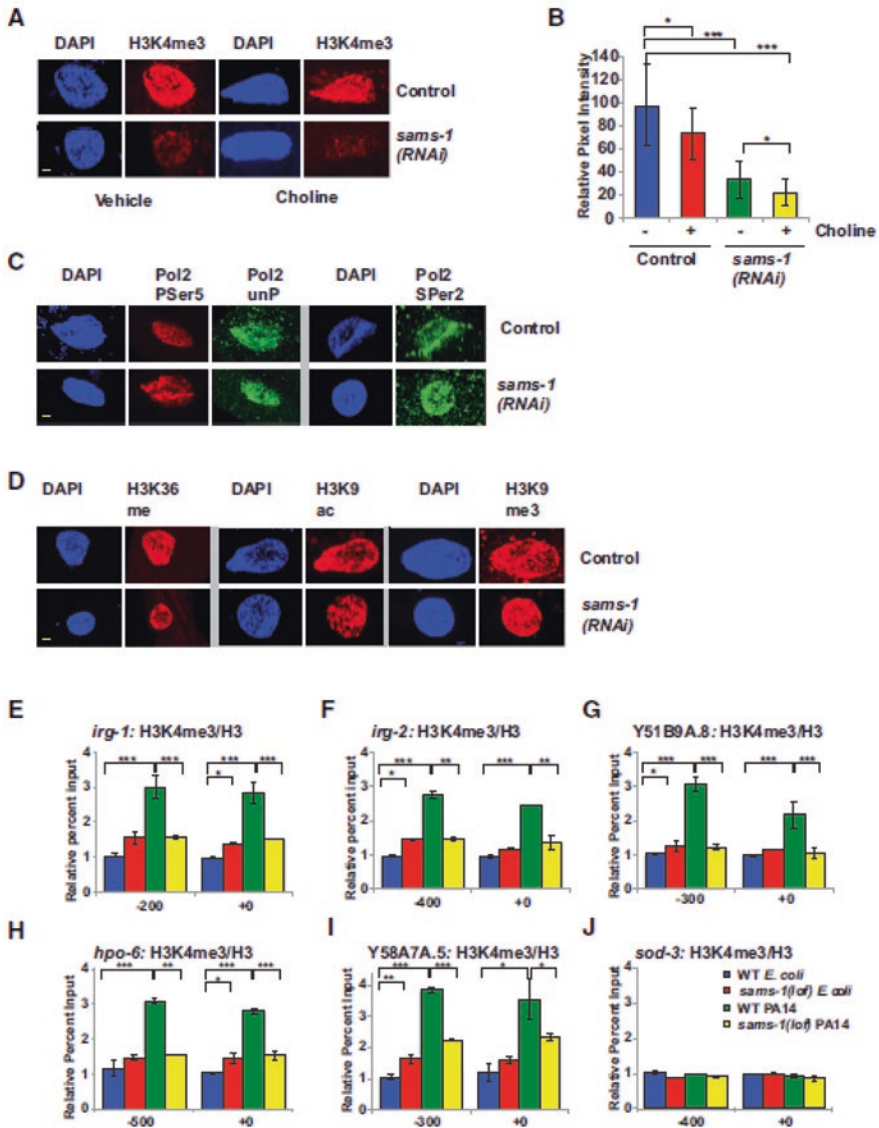


Fig. 12.2 Infection response genes do not accumulate activating histone methylation marks in *sams-1(lof)* mutants exposed to *Pseudomonas* [9]. (a) H3K4me3 is diminished in nuclei of intestinal cells after *sams-1*(RNAi) and in choline-treated *sams-1*(RNAi). Yellow bar shows 2 μ m. (b) Quantitation of immunofluorescence showing an average of pixel intensity over the area for 8–12 nuclei per sample. (c) Immunostaining comparing markers of active phosphorylated RNA polymerase II (Pol II PSer 5, PSer 2) with total Pol II (unP). (d) Other histone modifications associated with active transcription (H3K36me and H3K9ac) or with heterochromatin (H3K9me3) within intestinal nuclei in control or *sams-1*(RNAi) animals. (e–j) Chromatin immunoprecipitation comparing levels of H3K4me3 on infection response or control genes grown on *E. coli* (OP50) or *Pseudomonas* (PA14) in wild-type (WT) or *sams-1(lof)* mutants. Input levels were normalized to the WT *E. coli* value on the upstream primer pair. Numerical representation of primer location is based on translational start site. Legend in (j) refers to all images. Error bars show SD. Results from Student's *t*-test shown by * <0.05 , ** <0.01 , *** <0.005

The H3K4 modification occurs through the action of methyltransferases with the functions in COMPASS methyltransferase complex. The nematodes contain the orthologs of catalytic COMPASS complex components such as *set-2*/SETD1A/KMT2F/Set1 and *set-16*/MLL/KMT2A [10]. It was further found that the genes requiring *set-16*/MLL-dependent methylation were preferentially affected by SAM depletion during the transcriptional response to pathogen infection (Fig. 12.3) [9]. That is, the *set-16*/MLL was critical for the transcriptional response to pathogenic infection, and this response depended on the H3K4 methyltransferase *set-16*/MLL (Fig. 12.3) [9].

BLMP-1 is the BLIMP-1 ortholog. The BLMP-1 was necessary for controlling the histone methylation level in *daf-7* mutant nematodes, and the BLMP-1 regulated the expression of SAMS-1 [11]. Therefore, BLMP-1 can further act upstream of SAMS-1 to regulate the histone methylation and the stress responses, such as the dauer formation.

12.2.1.3 The Possible Downstream Molecular Response After H3K4 Trimethylation

In nematodes, it was observed that the chronic exposure to MeHg (10 μ M) could cause the epigenetic landscape modifications of histone H3K4 trimethylation (H3K4me3) marks based on the chromatin immunoprecipitation sequencing (ChIP-seq) analysis (Fig. 12.4) [12]. These modifications corresponded to the locations of 1467 upregulated genes and 508 downregulated genes [12]. The upregulated genes contain those encoding glutathione S-transferases, lipocalin-related protein, and a cuticular collagen (Fig. 12.4) [12]. Among these genes, RNAi knockdown of lipocalin-related protein gene *lpr-5*, which is involved in intercellular signaling, or cuticular collagen gene *dpy-7*, structural component of the cuticle, led to the increased lethality in nematodes exposed to MeHg [12].

12.2.2 Methylation of Histone H3K9

12.2.2.1 MET-2 and Nuclear Co-factor LIN-65

In nematodes, LIN-65 was identified as a new regulator for the activation of mitochondrial UPR response, because the neuronal polyglutamine expression could induce a *lin-65* dependent activation of the mitochondrial UPR response [13]. Histone H3K9 methylation plays an important role in regulating the gene expression, and the histone H3K9 is methylated sequentially by methyltransferases MET-2/SETDB1 and SET-25 in nematodes [14]. MET-2 potentially mono- and di-methylate the H3K9 in the cytoplasm, and the nuclear SET-25 acts as a trimethylation methyltransferase for the H3K9 [14]. It was further observed that the MET-2 was required for the LIN-65 nuclear accumulation induced by mitochondrial UPR response [13].

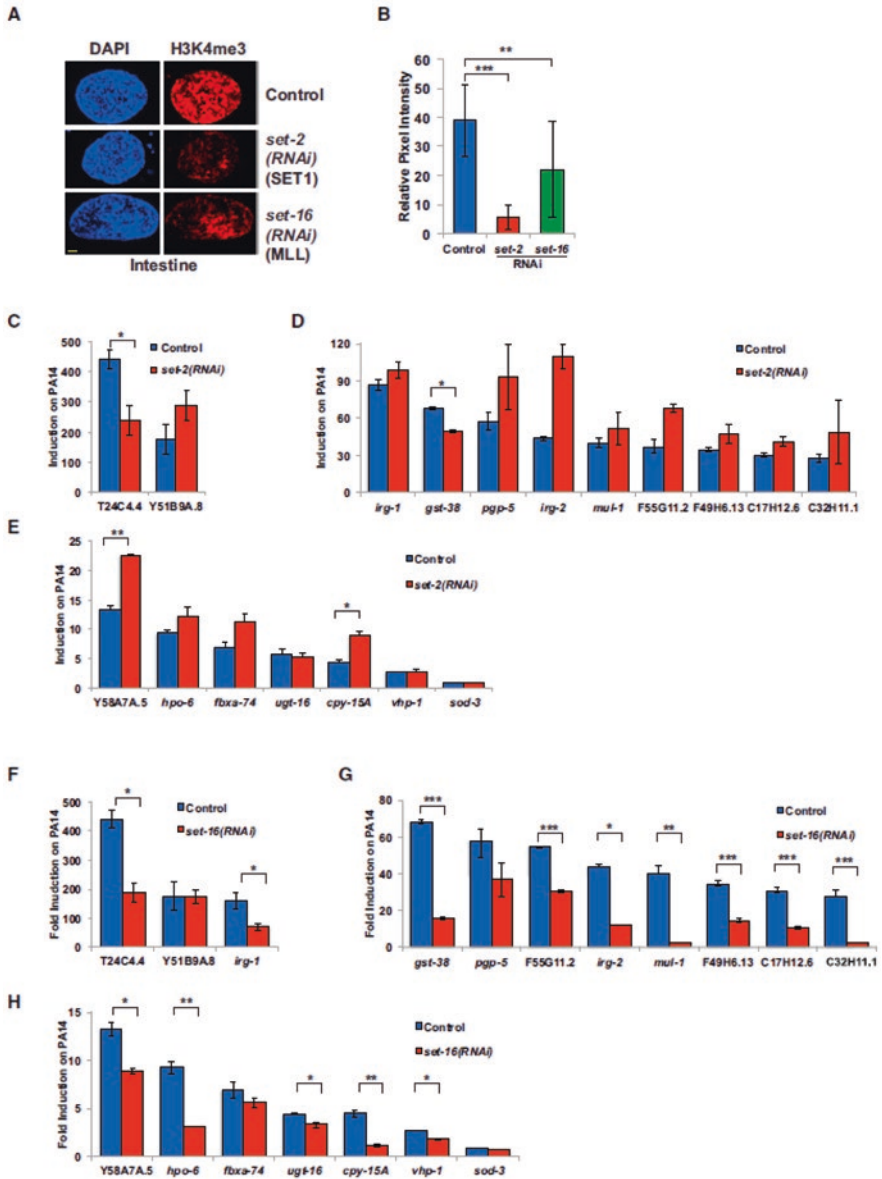


Fig. 12.3 *set-16*/MLL is important for expression of infection response genes upon *Pseudomonas* exposure [9]. (a) Immunostaining of intestinal nuclei with antibodies to H3K4me3 after RNAi of *set-2* or *set-16*. Yellow bar shows 2 mm. (b) Quantitation of immunofluorescence showing an average of pixel intensity over area for 8–12 nuclei per sample. Requirement for *set-2*/SET1 (b–d) or *set-16*/MLL (e–h) for induction of infection response genes upon a 6 h exposure to PA14 compared to *E. coli* (HT115). Error bars show SD. Results from Student’s *t*-test shown by * <0.05 , ** <0.01 , *** <0.005

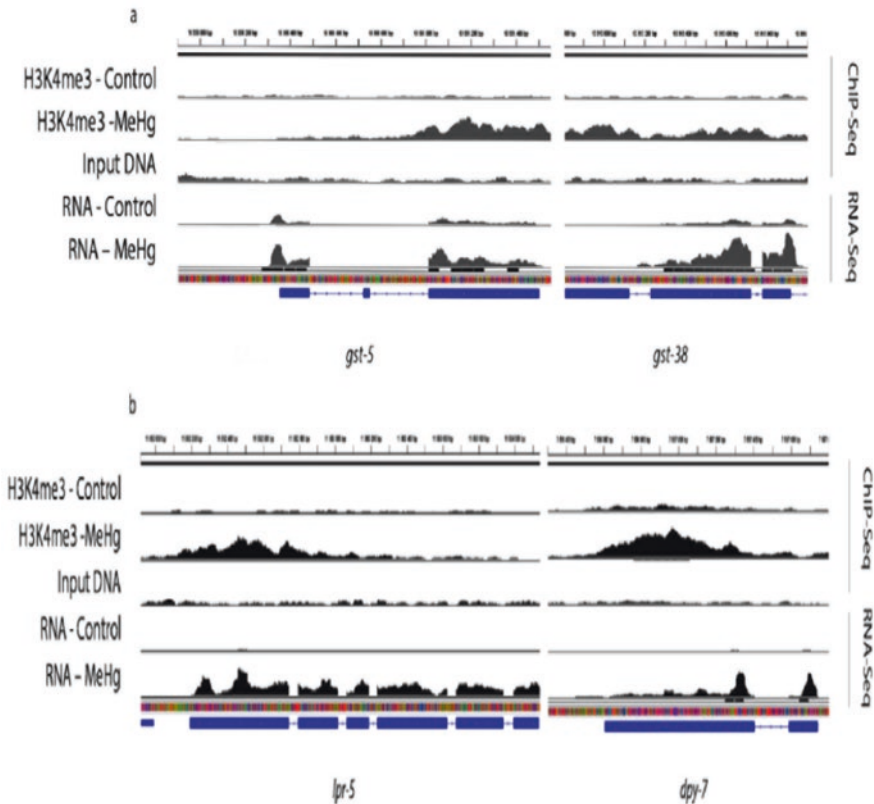


Fig. 12.4 ChIP-seq and RNA-seq in control treated and MeHg-treated animals [12]. (a) ChIP-seq peaks were identified using H3K4Me3 antibody or input DNA as a control. MeHg treatment increased H3K4me3 signals in genes *gst-5*, *gst-38*. (b) Peaks from *lpr-5* and *dpy-7* genes. ChIP-Seq data (lines 1–3) and the corresponding genes were compared with RNA-Seq data (lines 4–5). Gene structure is shown at the bottom. Images were generated by Integrated Genome Viewer 2.3

In nematodes, the full activation of mitochondrial UPR required both the remodeling of chromatin and the di-methylation of histone H3K9 (Fig. 12.5) [13]. Additionally, the global chromatin reorganization induced by mitochondrial stress was dependent on both MET-2 and LIN-65 (Fig. 12.5) [13], suggesting that *lin-65* and *met-2* are required for the regulation of transcriptional response to mitochondrial stress and chromatin reorganization induced by mitochondrial stress in nematodes.

In nematodes, the full induction of mitochondrial UPR response requires the nuclear localization of transcription factor DVE-1 and co-factor UBL-5, as well as the activity of protease CLPP-1. The nuclear localization of LIN-65 was further found to be partially dependent on CLPP-1/DVE-1 and independent of ATFS-1

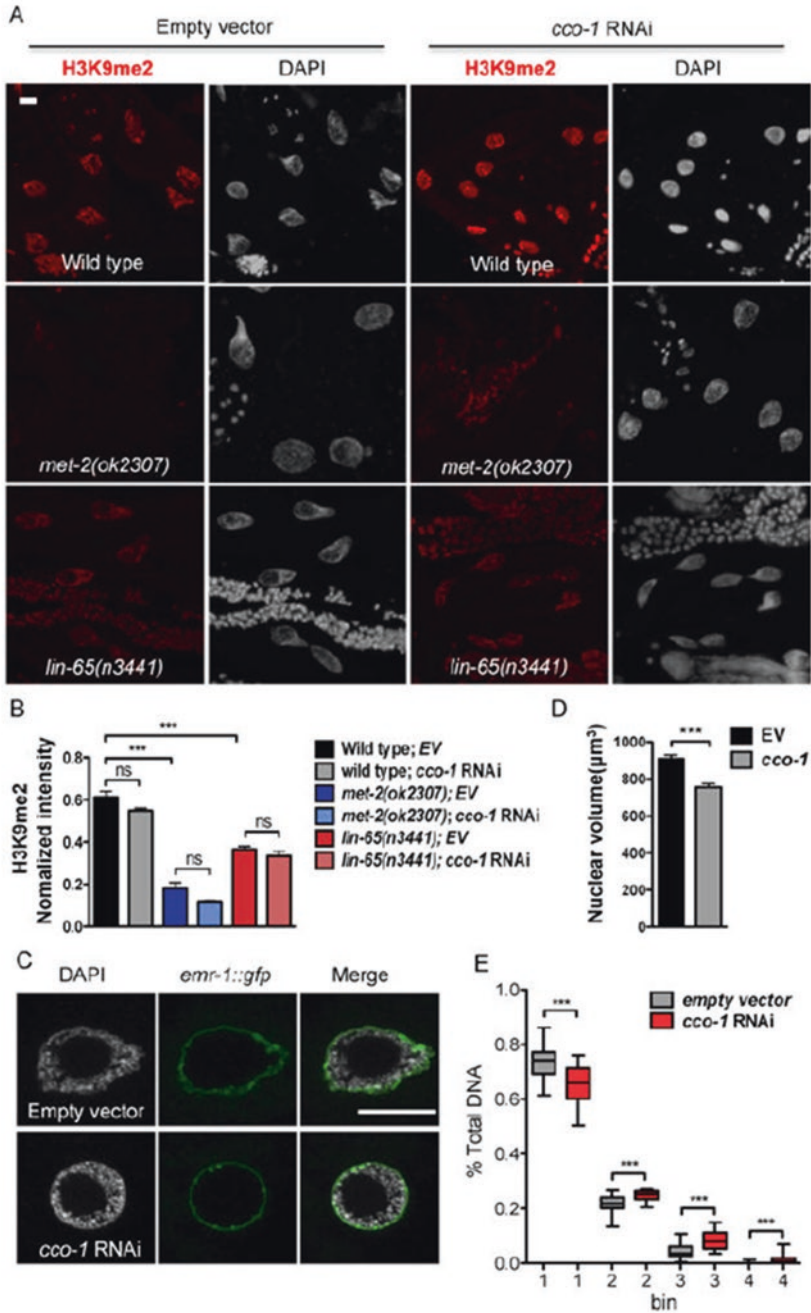


Fig. 12.5 Mitochondrial stress-induced chromatin reorganization [13]. (a) Representative maximal intensity projection images of H3K9me2 immunostaining of intestinal nuclei in Day 1

[13]. Meanwhile, the H3K9me2 was required for the mitochondrial stress-induced DVE-1 nuclear puncta formation [13]. Based on the so far obtained data, a model for the epigenetic regulation of mitochondrial UPR response was summarized in Fig. 12.6 [13].

12.2.2.2 JMJD-1.2 and JMJD-3.1

In nematodes, JMJD-1.2, a member of the KDM7 family, is a demethylase toward lysine residues on histone 3 (H3). The *jmjd-1.2* potentially controlled the level of histone 3 lysine 9, lysine 23, and lysine 27 di-methylation (H3K9/K23/K27me2) [15]. Moreover, it was found that mutation of *jmjd-1.2* induced a susceptibility to replication stress (Fig. 12.7) [15]. The progeny of *jmjd-1.2* mutant nematodes exposed to hydroxyurea showed an increased embryonic lethality and an increased mutational rate compared to those in wild-type nematodes (Fig. 12.7) [15].

Moreover, both JMJD-1.2 and JMJD-3.1, two histone lysine demethylases, were identified to be required for the induction of mitochondrial UPR response [16]. Reduction of function of JMJD-1.2 or JMJD-3.1 suppressed the longevity and mitochondrial UPR induction, whereas the overexpression of *jmjd-1.2* or *jmjd-3.1* was sufficient for the lifespan extension and the mitochondrial UPR induction in nematodes [16].

12.2.3 Methylation of HIS-24K14

HIS-24 is a linker histone (H1) variant, and HPL-1 and HPL-2 are heterochromatin protein 1 (HP1)-like proteins. These proteins are essential components of heterochromatin and contribute to the transcriptional repression of genes. In nematodes, it was observed that pathogen infection could increase the cellular levels of HIS-24K14me1 [17]. Meanwhile, the HIS-24K14me1 localization was changed from being mostly nuclear to both nuclear and cytoplasmic in intestinal cells by



Fig. 12.5 (continued) adult WT, *met-2* or *lin-65* mutant animals grown on EV or *cco-1* RNAi from hatch (as indicated). H3K9me2 (red); DAPI (gray). Scale bar represents 10 μ m. **(b)** Quantification of H3K9me2 level. The genotypes and treatments are as in **(a)**. H3K9me2 intensity is normalized to DAPI intensity. (***) denotes $p < 0.0001$; ns denotes $p > 0.05$ via *t*-test, error bars indicate SEM, $n \geq 15$ nuclei). **(c)** Representative of three center images of DAPI staining with *lmn-1p::emr-1::gfp* of intestinal nuclei in Day 1 adult animals grown on EV or *cco-1* RNAi from hatch as indicated. *lmn-1p::emr-1::gfp* (green); DAPI (gray). Scale bar represents 10 μ m. **(d)** Quantification of the intestinal nuclear size at Day 1 adulthood using *lmn-1p::emr-1::gfp* as a marker. Animals grown on EV or *cco-1* RNAi from hatch (***) denotes $p < 0.0001$ via *t*-test, error bars indicate SEM, $n \geq 20$ nuclei). **(e)** Quantification of the distribution of DAPI staining signal in intestinal nuclei at Day 1 of adulthood in animals grown on EV or *cco-1* RNAi from hatch. The distributions of fractions from the top four bins are shown as boxplots. (***) denotes $p < 0.0001$ via Mann–Whitney test, error bars indicate SEM, $n \geq 25$ nuclei)

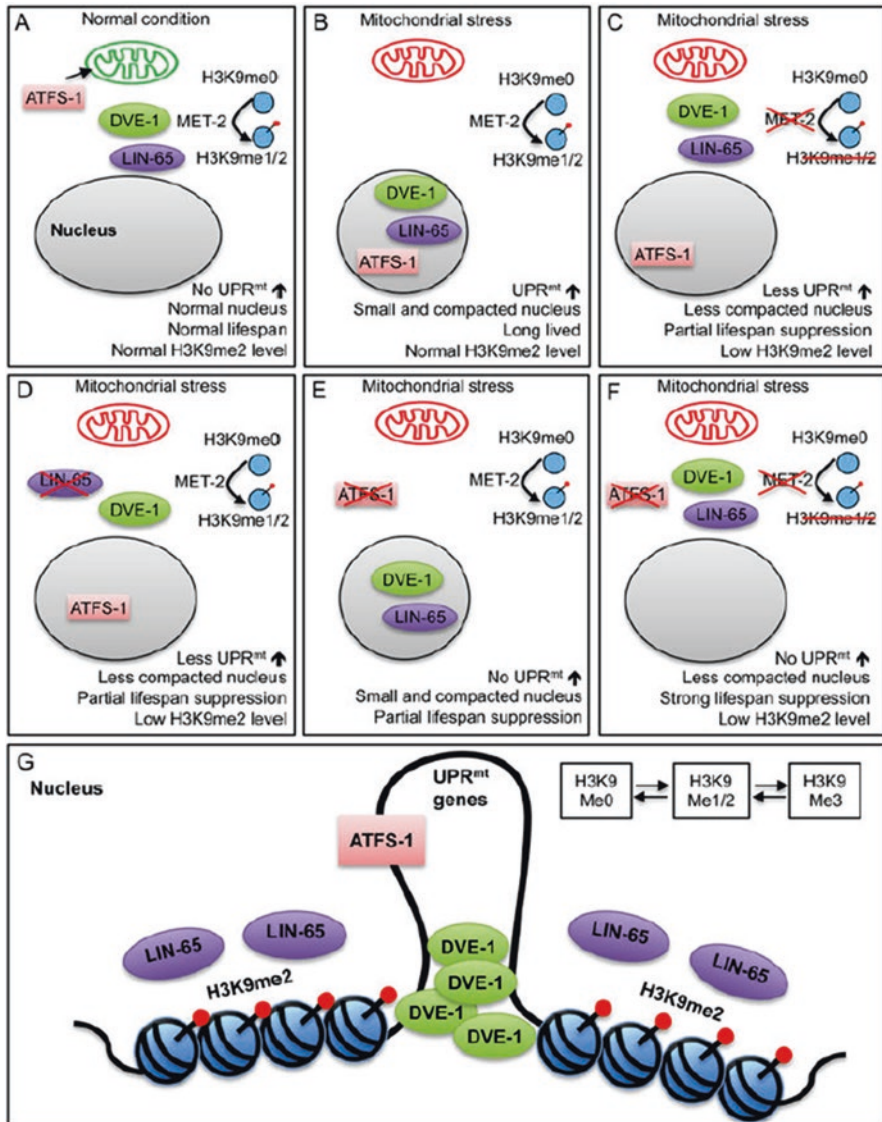


Fig. 12.6 Model for mitochondrial stress signaling pathway [13]. (a) Under non-stressed conditions, MET-2 produces H3K9me1/2 histone subunits in the cytoplasm. ATFS-1 translocates to the mitochondria and is degraded. DVE-1 and LIN-65 do not accumulate in the nucleus, and the UPR^{mt} is not induced, animals are normal lived, and the nucleus is not compacted. (b) During mitochondrial stress, MET-2 continues to produce H3K9me2 histone subunits, ATFS-1 now translocates to the nucleus to induce UPR^{mt}. DVE-1 and LIN-65 accumulate in the nucleus. Animals are long-lived, the UPR^{mt} is induced, nuclei become compacted, and H3K9me2 levels remain unchanged. (c) Loss of *met-2* during mitochondrial stress results in reduced nuclear H3K9me2 levels, nuclei that are less compacted, reduced DVE-1 and LIN-65 nuclear accumulation, reduced UPR^{mt} induction and partial suppression of increased lifespan. (d) Loss of *lin-65* during mitochondrial stress

pathogen infection [17]. Moreover, HIS-24 recruited the HPL proteins to the promoters of genes involved in the defense response against the pathogen infection [17]. The HPL-1 was further found to interact with the HIS-24 monomethylated at the lysine 14 (HIS-24K14me1) [17].

12.2.4 Methylated Glycans

The tectonin 2 of the mushroom *Laccaria bicolor* (Lb-Tec2) has been shown to agglutinate the Gram-negative bacteria and to exert the toxicity toward nematodes [18]. Additionally, both the bacterial agglutination and the Lb-Tec2 depended on the recognition of methylated glycans (*O*-methylated mannose and fucose residues) as part of bacterial lipopolysaccharide (LPS) and cell-surface glycans in nematodes (Fig. 12.8) [18]. Moreover, the Lb-Tec2 was toxic for nematodes, and this toxicity formation depended on the binding to N-glycans (Fig. 12.8) [18]. SAMT-1, a membrane transport protein for presumptive donor substrate of glycan methylation from cytoplasm to Golgi, was identified to be required for the regulation of Lb-Tec2 toxicity, and mutation of *samt-1* induced a Lb-Tec2 resistance in nematodes [18].

12.3 Histone Acetylation Regulation

12.3.1 MYST Family Histone Acetyltransferase Complex

The MYST family histone acetyltransferase complex contains MYS-1 and TRR-1. Both MYS-1 and TRR-1 were found to promote rather than inhibit the stress resistance and the longevity in nematodes (Fig. 12.9) [19]. Both single mutants and double mutants of *mys-1* and *trr-1* were resistant to environmental stress (Fig. 12.9) [19]. Mutation of *mys-1* or *trr-1* suppressed the induction of *sod-3* induced by environmental stress (Fig. 12.9) [19]. Under the stress conditions, mutation of



Fig. 12.6 (continued) results in reduced nuclear H3K9me2 levels, nuclei that are less compacted, reduced DVE-1 nuclear accumulation, reduced UPR^{mt} induction, and partial suppression of increased lifespan. **(e)** Loss of *atfs-1* during mitochondrial stress results in suppressed UPR^{mt} induction and partial suppression of lifespan extension. This is independent of compacted nuclei and nuclear accumulation of DVE-1 and LIN-65. **(f)** Loss of both *met-2* and *atfs-1* during mitochondrial stress results in nuclei that are less compacted, reduced nuclear accumulation of DVE-1 and LIN-65, no UPR^{mt} induction, and complete suppression of lifespan extension. **(g)** During mitochondrial stress, LIN-65 and DVE-1 accumulate in the nucleus, chromatin becomes remodeled, and DVE-1 is able to form puncta at the loose regions of the chromatin, activating transcription of UPR^{mt} targets. This remodeling works in parallel to the relocation of mitochondrial-specific transcription factor ATFS-1 to initiate UPR^{mt} and regulate longevity

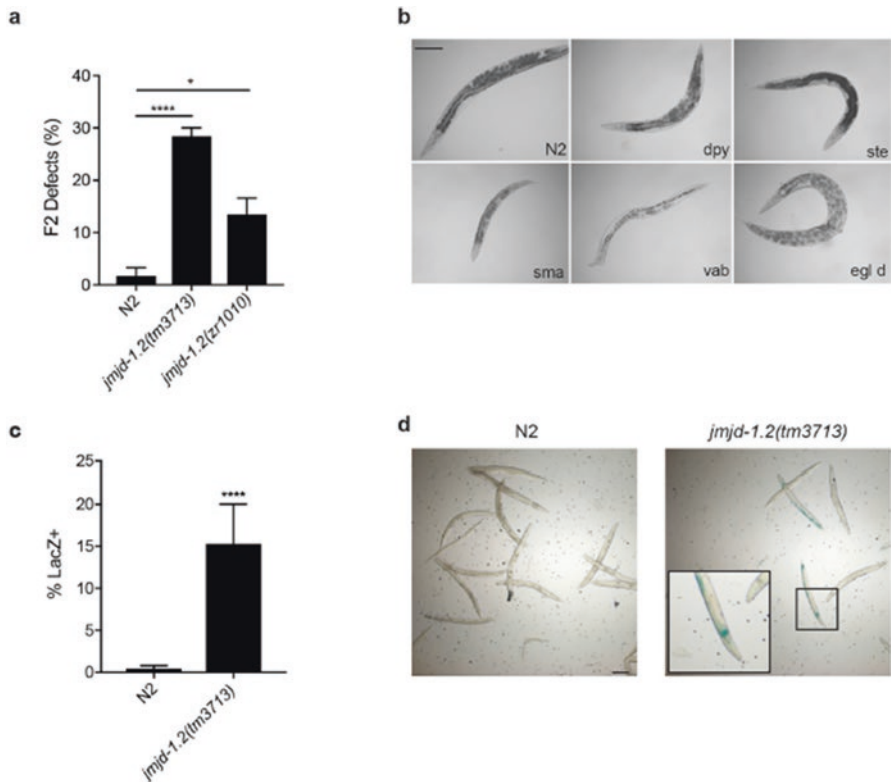


Fig. 12.7 *jmjd-1.2* mutants have increased mutational rate after HU [15]. **(a)** Quantification of the percentage of abnormalities identified in F2 progeny derived from animals of indicated genotypes exposed to HU (25 mM, 16 h). The percentage of F2 abnormalities was determined based on the number of plates that had at least one F2 abnormal animal. **(b)** Representative images of *jmjd-1.2* F2 progeny derived from animals exposed to HU (25 mM, 16 h). Dpy, dumpy; ste, sterile; sma, small; vab, organism morphology variant; egl d, egg-laying defective. A wild-type animal (N2) is shown, for comparison. **(c)** Quantification of the percentage of *lacZ*-positive animals in F1 generation after parental HU treatment (25 mM, 16 h). N2 and *jmjd-1.2(tm3713)* carrying the pKIs1604 transgene are used. **(d)** Representative images of the F1 generation after parental HU treatment, (25 mM, 16 h) stained by X-gal. N2 and *jmjd-1.2(tm3713)*, carrying the pKIs1604 transgene, are shown. A magnification of a *lacZ*-positive animal is shown. In **(a)** and **(c)** the graphics show the average of two independent experiments, and data are presented as mean \pm SD. * $p \leq 0.05$, **** $p \leq 0.0001$, with χ^2 test. Scale bars, 100 μ m

mys-1 or *trr-1* suppressed the resistance of *daf-2* mutant nematodes to environmental stress (Fig. 12.9) [19], suggesting that MYS-1 and TRR-1 act downstream of DAF-2 to regulate the toxicity of environmental toxicants or stresses.

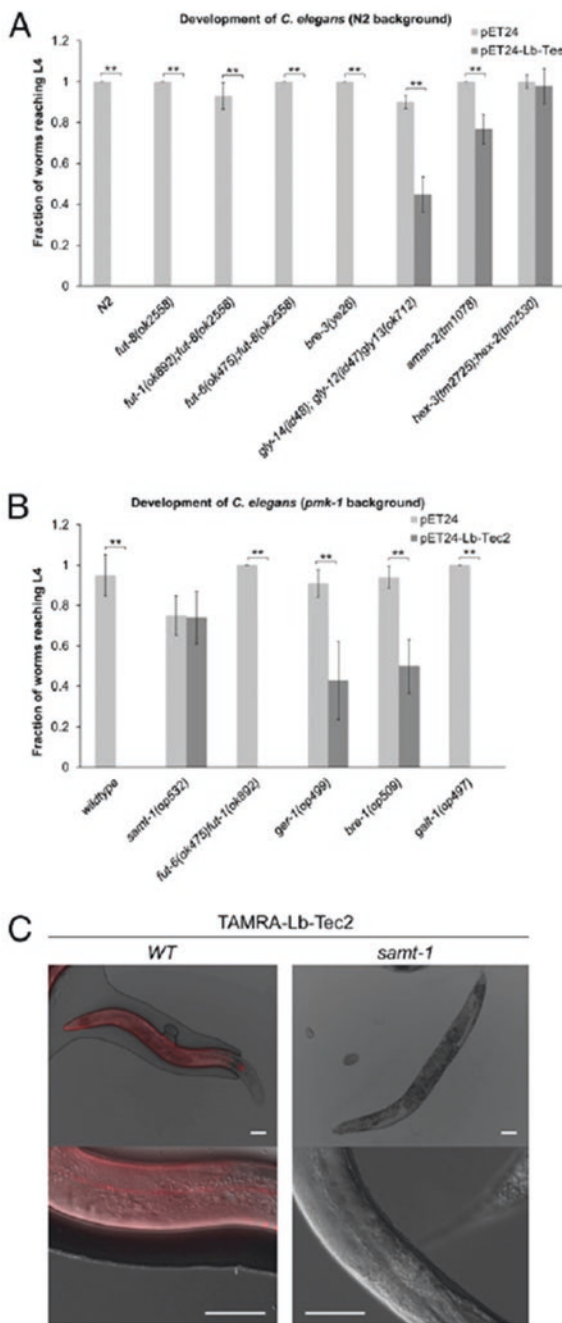
The beneficial effects of MYS-1 and TRR-1 were largely mediated through the transcriptional upregulation of FOXO transcription factor DAF-16 and its targets [19]. More importantly, it was found that MYS-1 and TRR-1 could be recruited to the promoter regions of *daf-16*, where they functioned in the histone acetylation, including the H4K16 acetylation (Fig. 12.10) [19].

Fig. 12.8 Carbohydrate-binding-dependent toxicity of Lb-Tec2 toward *C. elegans* [18]. (a)

Development of *C. elegans* wild-type (N2) and various glycosylation mutants feeding on Lb-Tec2-expressing *E. coli* (dark gray) or empty pET24 vector containing *E. coli* (light gray) ($n = 5$). Error bars indicate SD. Comparisons between Lb-Tec2 and vector control for each *C. elegans* strain were performed using the Mann–Whitney U test (** $P < 0.01$).

(b) Development of *C. elegans* *pmk-1(km25)* strain (wild-type) and various glycosylation mutants with *pmk-1(km25)* background feeding on Lb-Tec2-expressing *E. coli* (dark gray) or empty pET24 vector containing *E. coli* (light gray) ($n = 5$). Error bars indicate SD. Comparisons between Lb-Tec2 and vector control for each *C. elegans* strain were performed using the Mann–Whitney U test (** $P < 0.01$).

(c) Binding of TAMRA–Lb-Tec2 to the cuticle of *C. elegans* *pmk-1(km25)* (WT) and *samt-1(op532)pmk-1(km25)* (*samt-1*) at lower (upper) and higher magnification (lower). (Scale bars, 60 μm)



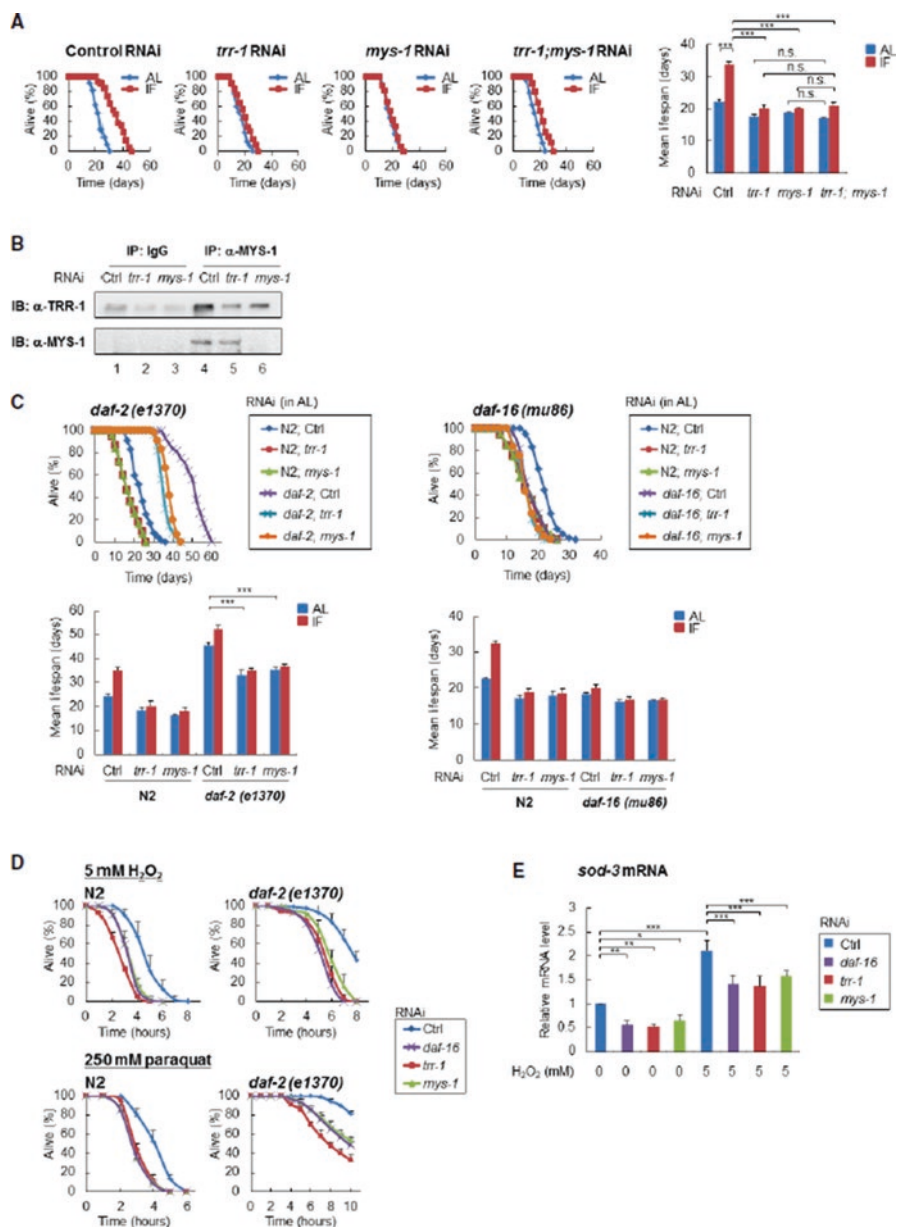


Fig. 12.9 The MYS-1 HAT complex regulates longevity and oxidative stress resistance [19]. (a) Survival curves of the indicated RNAi-treated N2 worms under AL and IF are shown [control RNAi, $n = 117$ (AL), 98 (IF); *trr-1* RNAi, $n = 117$ (AL), 107 (IF); *mys-1* RNAi, $n = 118$ (AL), 104 (IF); *trr-1; mys-1* RNAi, $n = 111$ (AL), 106 (IF)]. The bars represent the mean lifespan of three independent experiments. n, total number of worms in three independent experiments. Error bars, SD. *** $P < 0.001$, n.s. not significant; one-way ANOVA followed by Tukey's test. (b) Immunoprecipitates with anti-Tip60/MYS-1 antibody from extracts of the indicated RNAi-treated

12.3.2 *N-Terminal Acetyltransferase C (NAT) Complex*

In nematodes, *natc-1* encodes a N-a-acetyltransferase 35, an auxiliary subunit of the N-terminal acetyltransferase C (NAT) complex. NATC-1 is expressed in many cells and tissues and localizes to the cytoplasm [20]. The *natc-1(am138)* mutant nematodes showed a zinc resistance in multiple genetic backgrounds [20]. Additionally, loss-of-function mutations in *natc-1* caused the resistance to a broad spectrum of stressors, including heat stress and oxidation stress [20]. DAF-16 was predicted to directly bind the *natc-1* promoter, and the *natc-1* mRNA levels were suppressed by DAF-16 activity (Fig. 12.11) [20], indicating that NATC-1 is a physiological target of DAF-16. *natc-1* was epistatic to *daf-16* in resistance to both the heat stress and the zinc stress [20]. That is, NATC-1 functions downstream of insulin/IGF-1 signaling pathway to regulate the toxicity of environmental toxicants or stresses in nematodes.

12.3.3 *CBP-1*

In nematodes, the sirtuin SIR-2.4 can promote the DAF-16-dependent transcription and the stress-induced DAF-16 nuclear localization. It was further observed that the DAF-16 was hyperacetylated in the *sir-2.4* mutants [21]. SIR-2.4 regulated both the acetylation and the localization of DAF-16 independently of its catalytic function (Fig. 12.12) [21]. Additionally, SIR-2.4 blocked the acetyltransferase CBP1-dependent DAF-16 acetylation, since DAF-16 was acetylated by CBP-1 and

←

Fig. 12.9 (continued) N2 worms at day 2 adulthood were subjected to immunoblot analysis using anti-TRR-1 antibody. Representative images of two independent experiments are shown. (c) Survival curves of the indicated RNAi-treated *daf-2(e1370)* mutants (left) or *daf-16(mu86)* mutants (right) under AL are shown [*daf-2(e1370)* mutants $n = 180$ (control RNAi), 180 (*trr-1*RNAi), 180 (*mys-1*RNAi); *daf-16(mu86)* mutants $n = 178$ (control RNAi), 180 (*trr-1*RNAi), 180 (*mys-1*RNAi)]. The bars represent the mean lifespan from three independent experiments. n , total number of worms in three independent experiments. Error bars, SD *** $P < 0.001$, one-way ANOVA followed by Tukey's test. (d) Survival curves of the indicated RNAi-treated N2 worms or *daf-2(e1370)* mutants, which were exposed to 5 mM hydrogen peroxide (H₂O₂) [N2 worms $n = 180$ (control RNAi), 180 (*trr-1*RNAi), 180 (*mys-1*RNAi); *daf-2(e1370)* mutants $n = 180$ (control RNAi), 180 (*trr-1*RNAi), 180 (*mys-1*RNAi)] or 250 mM paraquat [N2 worms $n = 128$ (control RNAi), 128 (*trr-1*RNAi), 128 (*mys-1*RNAi); *daf-2(e1370)* mutants $n = 90$ (control RNAi), 90 (*trr-1*RNAi), 90 (*mys-1*RNAi)] at the young adult stage, are shown. The number of surviving worms was counted every hour. Error bars represent the SD derived from three independent experiments. n , total number of worms in three independent experiments. (e) Indicated RNAi-treated N2 worms at the young adult stage were exposed to 5 mM H₂O₂ for 30 min, and *sod-3* mRNA expression levels were determined by qRT-PCR. The value of the control RNAi-treated N2 worms (0 mM H₂O₂) was set to 1. Error bars represent the SD derived from three independent experiments. * $P < 0.05$, ** $P < 0.01$, *** $P < 0.001$, one-way ANOVA followed by Tukey's test

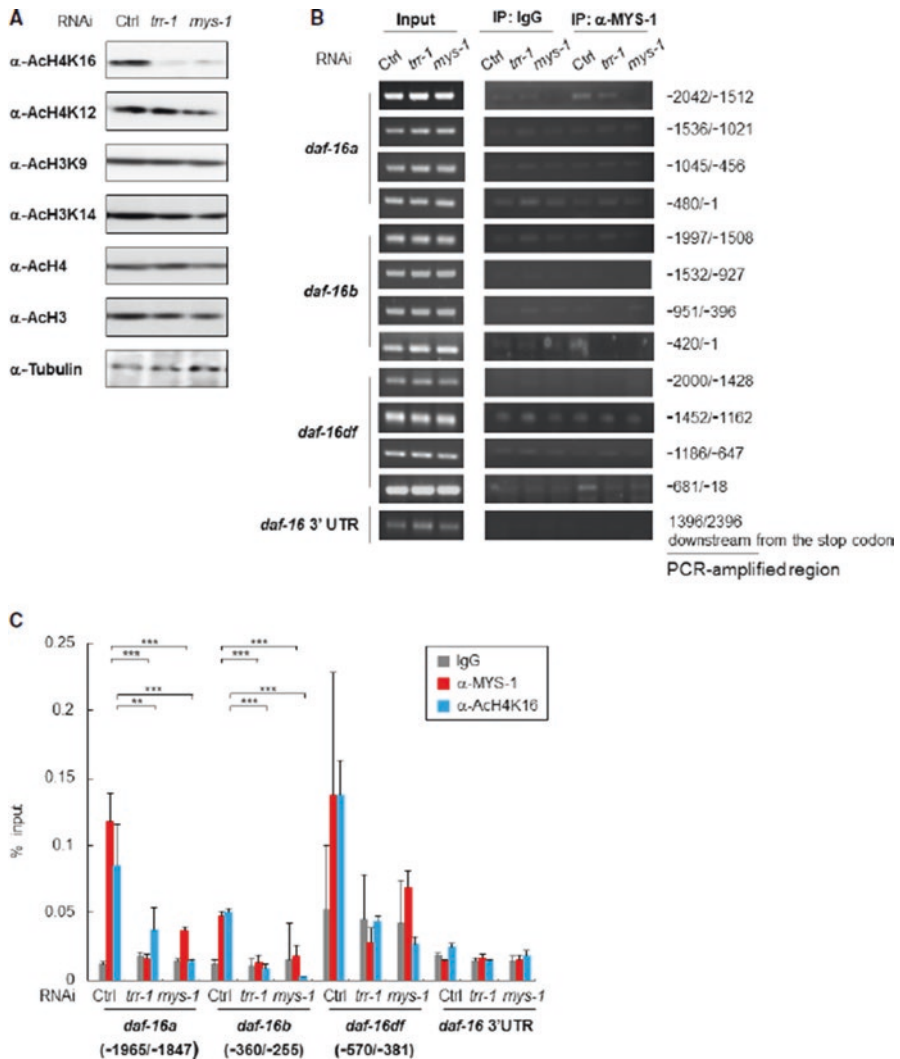


Fig. 12.10 The MYS-1 HAT complex is recruited to the *daf-16* promoter region and contributes to histone acetylation [19]. (a) Whole-worm lysates isolated from the indicated RNAi-treated N2 worms at day 2 adulthood were subjected to immunoblot analysis using the indicated antibodies. Representative images of three independent experiments are shown. (b) MYS-1 binding was examined by ChIP-PCR using cross-linked DNA-protein complexes isolated from the indicated RNAi-treated N2 worms at day 2 adulthood with anti-Tip60/MYS-1 and control IgG antibody. PCR amplification was done with specific primers for the *daf-16* promoter region and the *daf-16* 3'UTR. Representative images of two independent experiments are shown. Genomic DNA in the input samples was used as a positive control. (c) MYS-1 binding and histone H4K16 acetylation status were examined by ChIP-qPCR using cross-linked DNA-protein complexes isolated from the indicated RNAi-treated N2 worms at day 2 adulthood with anti-Tip60/MYS-1, anti-AcH4K16, and control IgG antibody. The bars represent the percentage of total input DNA for each ChIP sample, and error bars represent the SD derived from three independent experiments. ** $P < 0.01$, *** $P < 0.001$, one-way ANOVA followed by Tukey's test

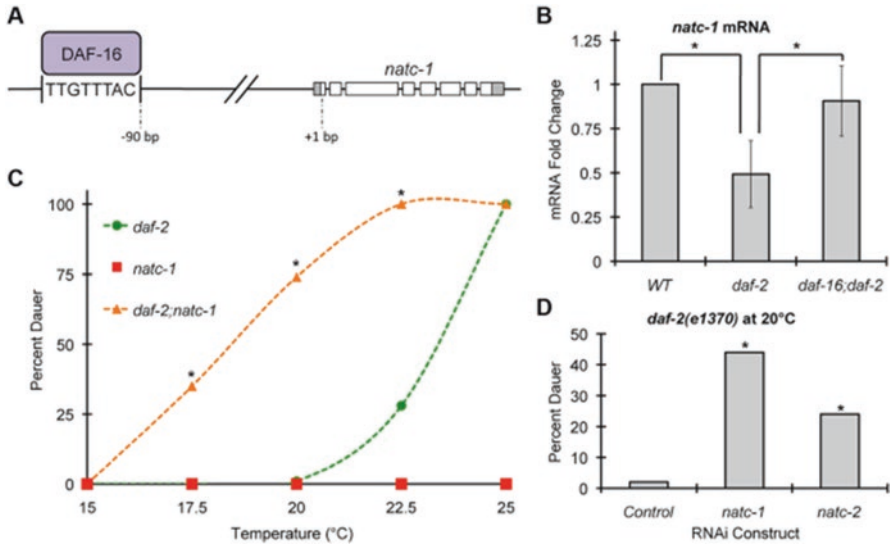


Fig. 12.11 *natc-1* is regulated by *daf-16* and functions in dauer formation [20]. (a) A model of the *natc-1* promoter and open reading frame showing DAF-16 protein binding an evolutionarily conserved DAF-16 binding site positioned 90 base pairs upstream of the *natc-1* start codon. (b) Wild-type, *daf-2(e1370)*, and *daf-16(mu86);daf-2(e1370)* animals were synchronized at the L1 stage of development and cultured for 2 days at 20 °C on NGM. For each genotype, mRNA was extracted, analyzed by qRT-PCR, and *natc-1* mRNA levels were normalized to the control gene *rps-23*. Bars show mRNA fold-change values calculated by comparing *daf-2* and *daf-16;daf-2* to WT by the comparative CT method ($N = 4-6$ biological replicates). Error bars indicate standard deviation. *natc-1* mRNA levels were significantly reduced in *daf-2(e1370)* animals compared to WT but were not significantly different from WT in *daf-16;daf-2* animals (*, $p < 0.05$). The *mtl-1* gene was utilized as a positive control, since it is an established target of DAF-16, and *mtl-1* mRNA levels were significantly increased in *daf-2(e1370)* compared to WT ($p < 0.05$), and this effect was *daf-16* dependent ($p < 0.05$). (c) *daf-2(e1370)*, *natc-1(am138)*, and *daf-2(e1370);natc-1(am138)* embryos were cultured for 4 days on NGM at the indicated temperature and scored as either dauer or non-dauer ($N = 200-341$). Values for *daf-2;natc-1* were significantly higher than *daf-2* at 17.5 °C, 20 °C, and 22.5 °C (* $p < 0.05$). (d) *daf-2(e1370)* embryos were cultured on NGM at 20 °C, fed *E. coli* expressing dsRNA targeting *natc-1*, *natc-2*, or an empty vector control and scored as dauer or non-dauer after 4 days ($N = 590-627$). *natc-1* and *natc-2* RNAi significantly increased dauer formation compared to control (* $p < 0.05$).

DAF-16 was hypoacetylated and constitutively nuclear in response to *cbp-1* inhibition (Fig. 12.12) [21]. The in vitro assay further suggested that SIR-2.4 regulated the DAF-16 acetylation indirectly by preventing the CBP-1-mediated acetylation under the stress conditions [21]. Therefore, a novel role for acetylation in modulating DAF-16 localization and function was revealed, and this acetylation was modulated by the antagonistic activities of CBP-1 and SIR-2.4 in nematodes.

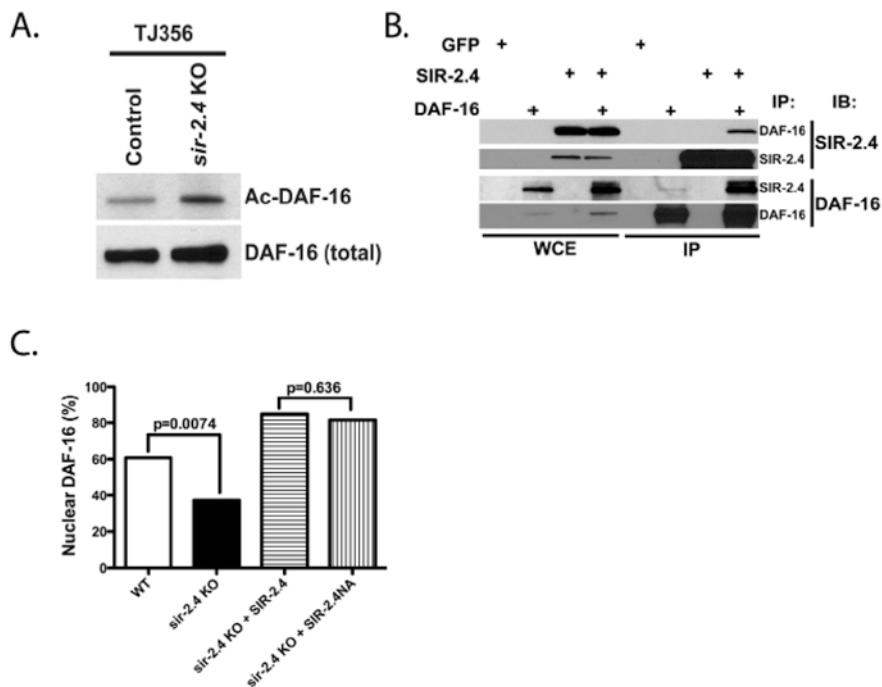


Fig. 12.12 SIR-2.4 interacts with DAF-16 and promotes DAF-16 deacetylation and function independently of catalytic activity [21]. (a) *sir-2.4* deletion promotes DAF-16 hyperacetylation. DAF-16 acetylation was assessed in control or *sir-2.4* KO worms by acetyl-lysine immunoprecipitation followed by GFP immunoblot. (b) SIR-2.4 and DAF-16 interact. Plasmids encoding FLAG-tagged SIR-2.4 and HA-tagged DAF-16 were transfected into 293T cells as indicated (GFP, negative control). Immunoprecipitation and immunoblotting were performed as shown. (c) Rescue of DAF-16 nuclear localization with a catalysis-defective *sir-2.4* mutant. Stable transgenic strains of *sir-2.4(n5137)* were generated expressing either wild-type SIR-2.4 or the *sir-2.4* N124A mutant. Worms were scored for GFP accumulation within the head hypodermic nuclei as day 1 adult ($n = 50$ or greater) after 20 min of heat-shock at 35 °C. P -values were calculated by Pearson's χ^2 test

12.4 miRNA Regulation

12.4.1 Dysregulated miRNAs by Environmental Toxicants or Stresses

It has been recognized that some engineered nanomaterials (ENMs) can potentially cause the toxicity on organisms, including the nematodes [22–30]. The dysregulated miRNAs have been systematically identified in nematodes exposed to certain ENMs [31, 32]. The dysregulated miRNAs have also been examined and identified in nematodes exposed to other toxicants or stresses [33–35]. With graphene oxide (GO), a carbon-based ENM, as an example, it was observed that GO (10 mg/L)

exposure induced 31 dysregulated expressed miRNAs (23 upregulated miRNAs and 8 downregulated miRNAs) (Fig. 12.13) [31].

Based on gene ontology analysis, these dysregulated miRNAs were associated with some important biological processes (such as cell metabolism, immune response, response to stimulus, cell communication, cell cycle, cell adhesion, reproduction, and development) in GO-exposed nematodes (Fig. 12.14) [31]. Based on KEGG pathway analysis, these dysregulated miRNAs were associated with some important signaling pathways (such as those related to cell metabolism, immune response, vesicle transportation, DNA damage and repair, oxidative stress response, transcription regulation, neuronal degeneration, cell death, cell cycle, and development) in GO-exposed nematodes (Fig. 12.14) [31]. These bioinformatics analysis data provide important clues for the further elucidation of the underlying mechanisms for GO toxicity induction in nematodes.

Among these dysregulated miRNAs, *mir-244* or *mir-235* mutation could induce a susceptibility to GO toxicity, whereas *mir-247/797*, *mir-73/74*, or *mir-231* mutation could induce a resistance to GO toxicity [31]. In contrast, mutation of *mir-360*, *mir-81/82*, *mir-246*, or *mir-259* did not obviously affect the GO toxicity in reducing lifespan in nematodes [31].

12.4.2 Functions of miRNAs in Response to Environmental Toxicants or Stresses and the Underlying Molecular Mechanisms

The important function of *let-7* in the regulation of toxicity of environmental toxicants or stresses has been introduced and discussed in Chap. 6. We further introduced and discussed the important functions of other miRNAs in response to environmental toxicants or stresses and the underlying molecular mechanisms.

12.4.2.1 Biological Function of *mir-73*

In *C. elegans*, SEK-1, a mitogen-activated protein kinase kinase (MAPKK), is an important member of the p38 MAPK signaling pathway. Using locomotion behavior as the toxicity assessment endpoint, mutation of *mir-73* induced a resistance to GO toxicity, and mutation of *sek-1* induced a susceptibility to GO toxicity (Fig. 12.15) [36]. Moreover, it was found that *sek-1* mutation could inhibit the resistance of *mir-73* mutant to GO toxicity (Fig. 12.15) [36], implying the role of SEK-1 as target of *mir-73* in regulating GO toxicity. *mir-73* expression could be decreased by GO exposure [36], suggesting the alteration in *mir-73* expression mediates a protective response to GO exposure.

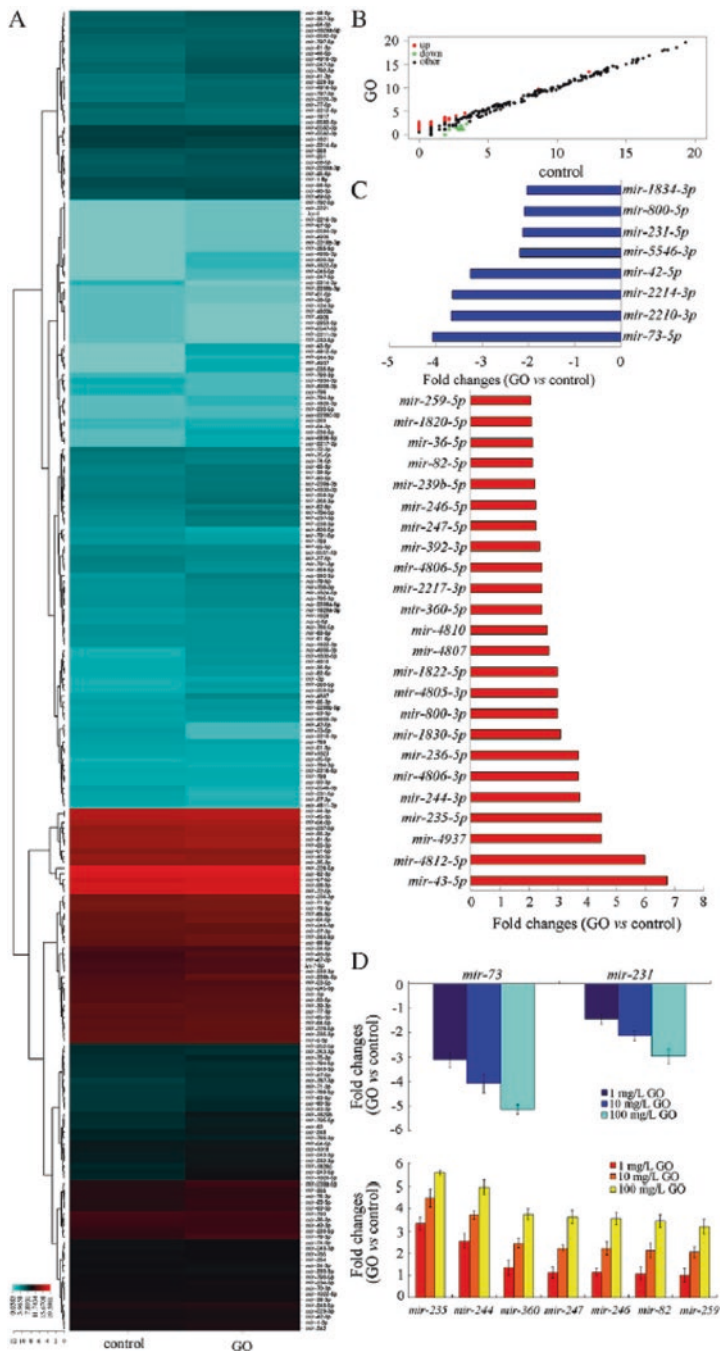


Fig. 12.13 Results of SOLiD sequencing for GO exposure [31]. (a) miRNA gene expression analysis by hierarchical clustering assay to reveal a characteristic molecular signature for GO (10 mg/L)-exposed nematodes. (b) Scatter diagram of miRNA coverage of the control group and GO treatment group. (c) Fold changes of up- and downregulated miRNAs in GO (10 mg/L)-exposed nematodes. (d) Expression pattern of mature miRNAs detected by real-time PCR after exposure to different concentrations of GO. Bars represent means \pm S.E.M

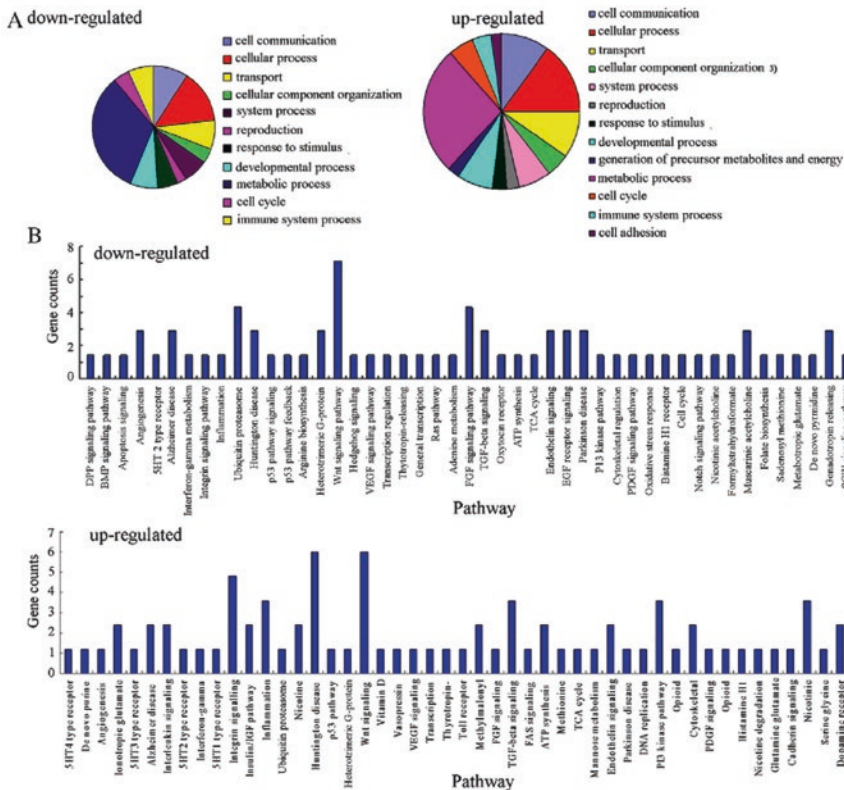


Fig. 12.14 Assessment of gene ontology terms and signal pathways [31]. (a) Gene ontology terms with gene counts based on dysregulated miRNAs in GO-exposed nematodes. (b) The predicted KEGG signal pathways based on dysregulated miRNAs in GO-exposed nematodes

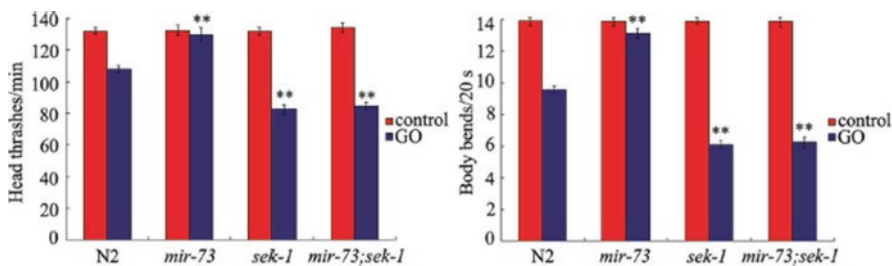


Fig. 12.15 Genetic interaction of *mir-73* and *sek-1* in regulating GO toxicity on locomotion behavior in nematodes [36]. Bars represent the mean \pm S.E.M. ****** $P < 0.01$ vs wild-type N2. GO (10 mg/L) was exposed from L1-larvae to adult day 1

12.4.2.2 Biological Function of *mir-84* and *mir-241*

In nematodes, the nuclear receptor DAF-12 negatively regulated the defense against pathogens, because mutation of *daf-12* induced a resistance to pathogen infection and enhanced the expressions of antimicrobial gene expression [37]. Mutation of *nsy-1* or *pmk-1* suppressed the resistance of *daf-12* mutant nematodes to pathogen infection [37], suggesting that the DAF-12 acts upstream of p38 MAPK signaling pathway to regulate the innate immune response to pathogen infection. *mir-84* and *mir-241* are members of *let-7* family. Mutation of *daf-12* decreased the expression of *mir-84* and *mir-241* after pathogen infection, and mutation of *mir-84* or *mir-241* induced a resistance to pathogen infection [37]. Moreover, SKN-1 was identified as a direct functional target of *let-7s* miRNAs (*mir-84* and *mir-241*), and mutation of *skn-1* suppressed the resistance of *mir-84* or *mir-241* mutant nematodes to pathogen infection (Fig. 12.16) [37], indicating that *mir-84* and *mir-241* regulate the innate immunity by suppressing the expression and function of their target SKN-1 in nematodes.

12.4.2.3 Biological Function of *mir-231*

In nematodes, *mir-231* acted in the intestine to regulate GO toxicity [38]. Additionally, nematodes overexpressing intestinal *mir-231* showed a susceptibility to GO toxicity [37]. *smk-1*, a predict targeted gene of *mir-231*, encodes a homolog of SMEK (suppressor of MEK null) protein. After GO exposure, *mir-231* mutation increased *smk-1* expression [38]. *mir-231* mutants showed a susceptibility to GO toxicity [38]. Genetic analysis has indicated that *smk-1* mutation could inhibit the resistance of *mir-231*(*n4571*) mutants to GO toxicity (Fig. 12.17) [38].

SMK-1 acted in the intestine to regulate GO toxicity, and DAF-16 further acted as a downstream target of SMK-1 during the regulation of GO toxicity [38]. That is, an intestinal signaling cascade (*mir-231*-SMK-1-DAF-16) was formed during the control of GO toxicity. *mir-231* expression could be decreased by GO exposure [31], suggesting that the alteration in *mir-231* expression mediates a protective response to GO exposure in nematodes.

12.4.2.4 Biological Function of *mir-233*

In nematodes, *P. aeruginosa* infection upregulated the expression of *mir-233* [39]. Meanwhile, the *mir-233* mutant nematodes were more sensitive to *P. aeruginosa* infection [39]. SCA-1, a homolog of sarco-/endoplasmic reticulum Ca²⁺-ATPase, was identified as a target of *mir-233* during the control of innate immune response to pathogen infection (Fig. 12.18) [39]. During the *P. aeruginosa* PA14 infection, *mir-233* repressed the protein levels of SCA-1, which might in turn lead to the activation of XBP-1-mediated ER UPR response, since the *mir-233* was required for the activation of ER UPR (Fig. 12.18) [39]. RNAi knockdown of *sca-1* caused

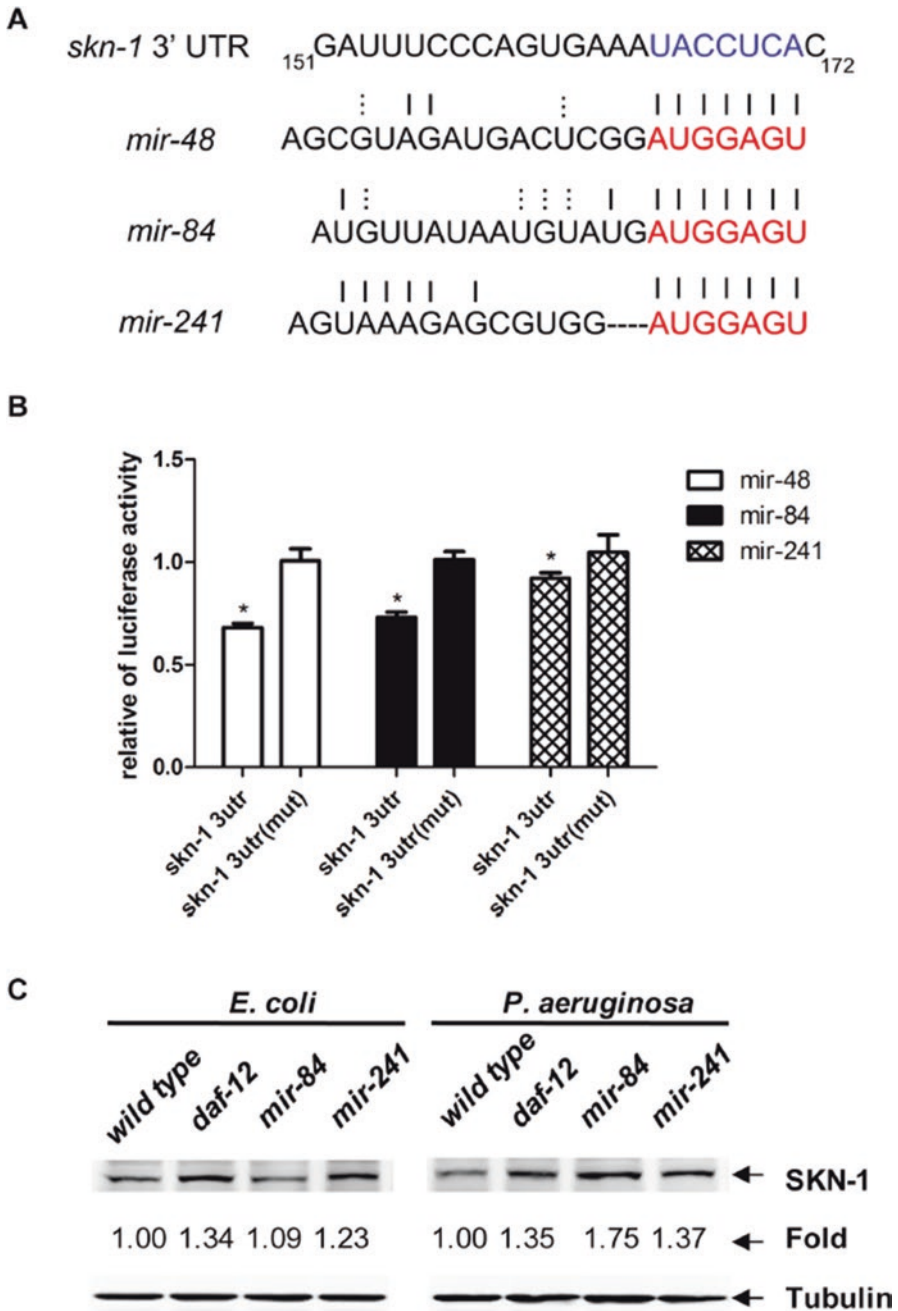


Fig. 12.16 SKN-1 is a direct functional target of *let-7s* miRNAs [37]. (a) Bioinformatics alignment of *let-7s* miRNAs and the 3'UTR of SKN-1. (b) Luciferase assays using the *skn-1* 3'UTR or the *skn-1* 3'UTR (mut) with *let-7s* mimics in HEK293T cells. The data shown are the mean \pm SEM of three independent experiments, each of which was performed in triplicate, * $P < 0.05$. (c) Immunoblot analysis of the lysates from N2, *daf-12(RNAi)*, *mir-84(n4037)*, and *mir-241(n4316)* worms on *E. coli* or *P. aeruginosa* using anti-SKN-1 antibody and anti-tubulin antibody (loading control)

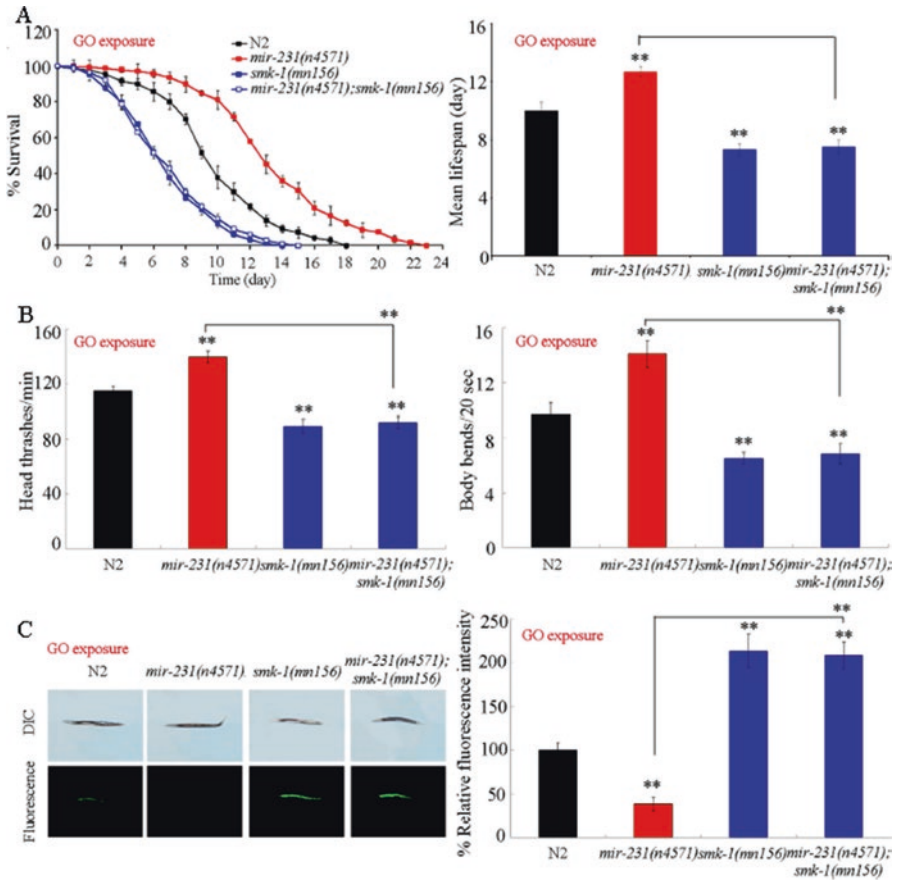


Fig. 12.17 Genetic interaction between *mir-231* and SMK-1 in regulating GO toxicity in nematodes [38]. **(a)** Genetic interaction between *mir-231* and SMK-1 in regulating GO toxicity in reducing lifespan. **(b)** Genetic interaction between *mir-231* and SMK-1 in regulating GO toxicity in decreasing locomotion behavior. **(c)** Genetic interaction between *mir-231* and SMK-1 in regulating GO toxicity in inducing intestinal ROS production. GO exposure concentration was 100 mg/L. Prolonged exposure was performed from L1-larvae to young adults. Bars represent means \pm SD. ****** $P < 0.01$ vs N2 (if not specially indicated)

the enhanced resistance to the killing by *P. aeruginosa* and suppressed the susceptibility of *mir-233* mutant nematodes to pathogen infection [39]. The *mir-233*/SCA-1 signaling cascade was further found to act downstream of p38 MAPK signaling to activate the ER UPR and to regulate the innate immunity in nematodes [39].

12.4.2.5 Biological Function of *mir-247*

In nematodes, GO exposure could increase the expression of *mir-247*, and the *mir-247/797* mutant nematodes showed a resistance to GO toxicity on lifespan and aging-related phenotypes [31]. Moreover, it was found that the *mir-247* acted in neurons, but not in pharynx, to regulate the GO toxicity in reducing lifespan and in inducing intestinal ROS production (Fig. 12.19) [40]. In contrast, the neuronal overexpression of *mir-247* induced a susceptibility to GO toxicity in reducing lifespan and in inducing intestinal ROS production [40]. Furthermore, the significant increase in *mir-247* could be detected in wild-type nematodes exposed to GO at concentrations of more than 10 mg/L, and the GO toxicity in a transgenic strain overexpressing neuronal *mir-247* after exposure to GO at concentrations of more than 10 µg/L was observed [40]. This implies the potential of *mir-247* in warning of the GO toxicity in the range of µg/L.

12.4.2.6 Biological Function of *mir-259*

Multiwalled carbon nanotubes (MWCNTs) exposure could increase the expression of *mir-259* [32], and MWCNTs exposure induced an increase in *mir-259::GFP* in pharyngeal/intestinal valve and reproductive tract [41]. Meanwhile, mutation of *mir-259* induced a susceptibility to MWCNTs toxicity [32], implying that *mir-259* mediates a protection mechanism for nematodes against the MWCNTs toxicity. The expression of *mir-259* in pharynx/intestinal valve could suppress the susceptibility of *mir-259(n4106)* mutant nematodes to MWCNTs toxicity on lifespan, suggesting that *mir-259* acts in the pharynx/intestinal valve to regulate the MWCNTs toxicity [41]. RSKS-1, a putative ribosomal protein S6 kinase, was identified as a target of *mir-259* in regulating the MWCNTs toxicity, and the *rsk-1(ok1255)* mutant nematodes had a resistance to the MWCNTs toxicity (Fig. 12.20) [41]. In nematodes, mutation of *rsk-1* suppressed the susceptibility of *mir-259* mutant nematodes to the MWCNTs toxicity (Fig. 12.20) [41]. RSKS-1 functioned in the pharynx to regulate the MWCNTs toxicity [41]. Moreover, the resistance of *rsk-1(ok1255)* mutant nematodes to MWCNTs toxicity on lifespan and aging-related properties could be inhibited by *aak-2* mutation [41], indicating that RSKS-1 acts upstream of AAK-2 to regulate the MWCNTs toxicity. Additionally, AAK-2 acted together with DAF-16 in the same genetic pathway to regulate the MWCNTs toxicity [41]. Therefore, RSKS-1 regulated the MWCNTs toxicity by suppressing the function of AAK-2-DAF-16 signaling cascade in nematodes.

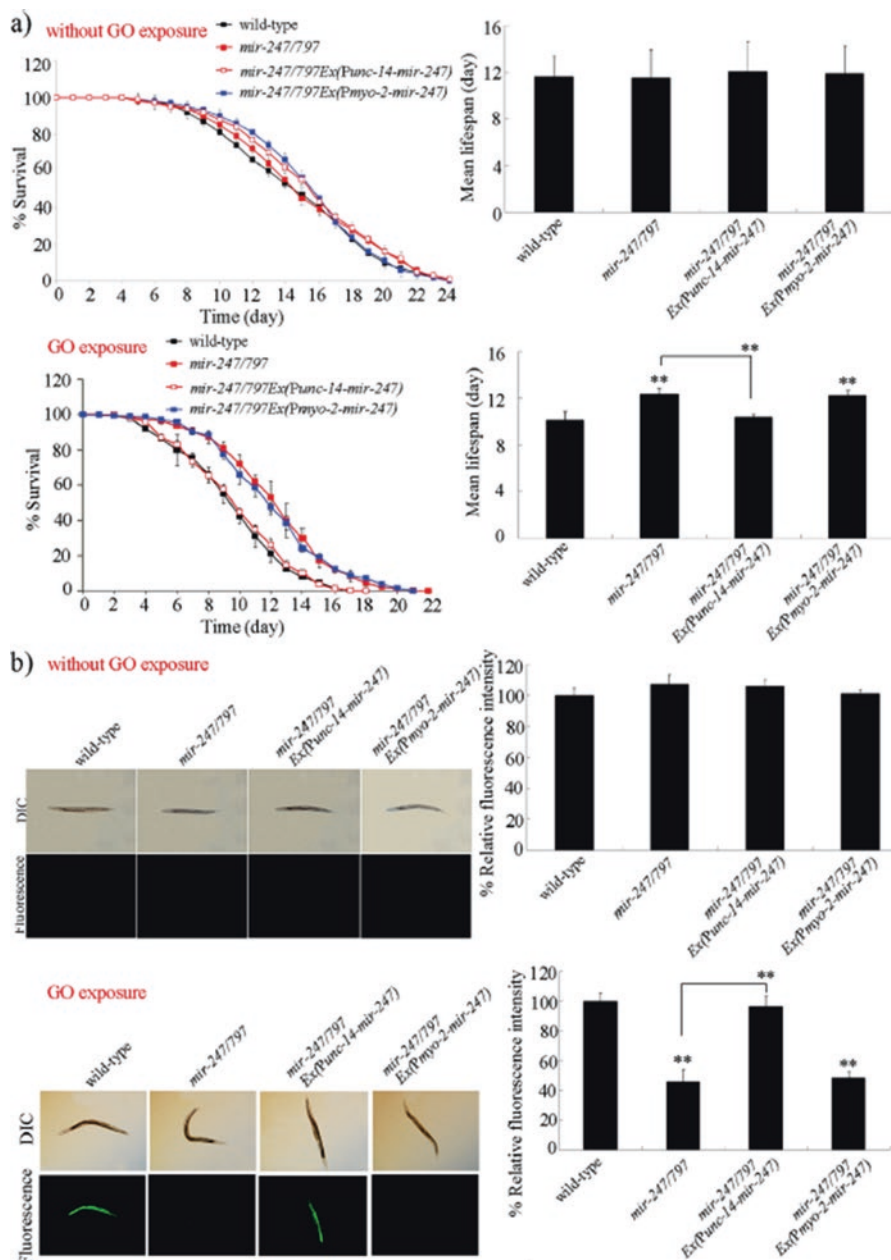


Fig. 12.19 Tissue-specific activity of *mir-247* in the regulation of GO toxicity [40]. **(a)** Tissue-specific activity of *mir-247* in the regulation of GO toxicity on lifespan. **(b)** Tissue-specific activity of *mir-247* in the regulation of GO toxicity in inducing intestinal ROS production. Prolonged exposure was performed from L1-larvae to adult day 1. Bars represent means \pm SD. ** $P < 0.01$ vs wild-type (if not specially indicated)

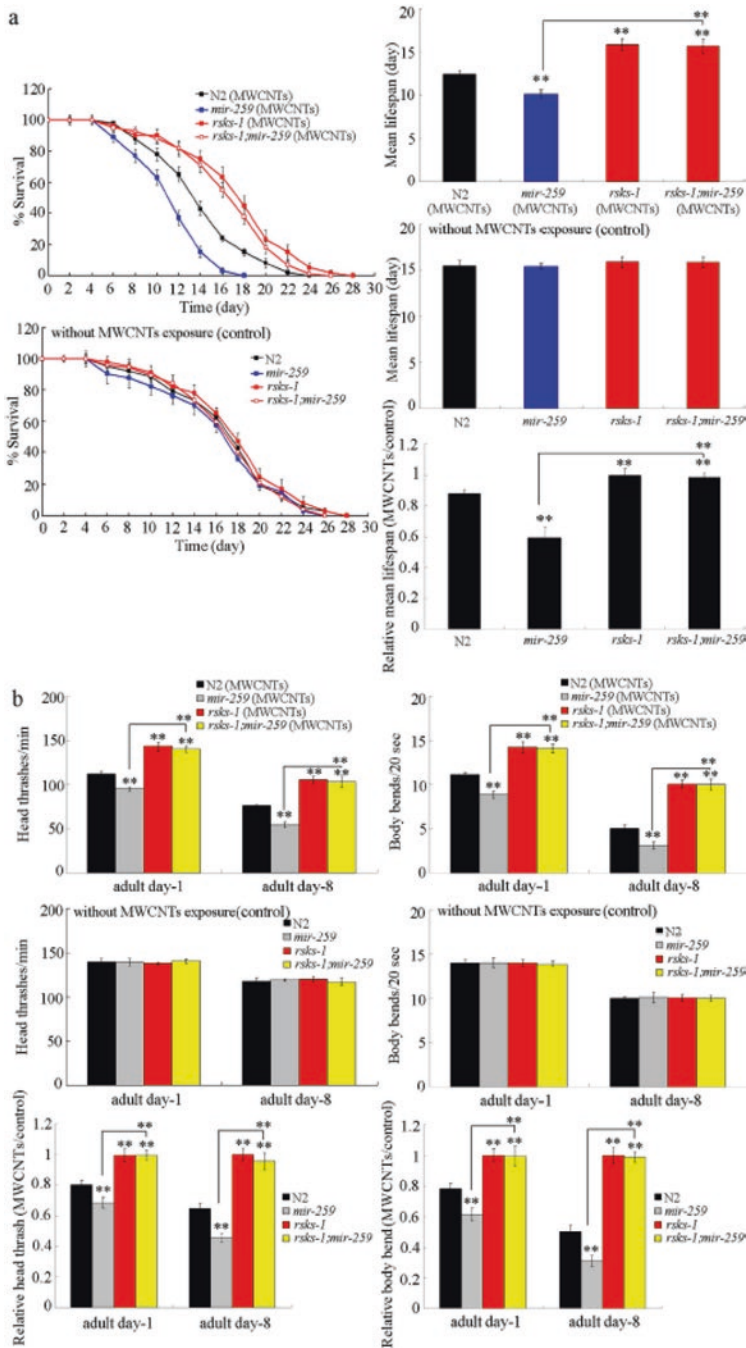


Fig. 12.20 Genetic interaction between *mir-259* and *rsk-1* in regulating MWCNTs toxicity in nematodes [41]. (a) Genetic interaction between *mir-259* and *rsk-1* in regulating MWCNTs toxicity in reducing lifespan in nematodes. (b) Genetic interaction between *mir-259* and *rsk-1* in regulating MWCNTs toxicity in decreasing locomotion behavior in nematodes. Exposure concentration of MWCNTs was 1 mg/L. Prolonged exposure was performed from L1-larvae to young adults. Bars represent means \pm SD. $**P < 0.01$ vs N2 (if not specially indicated)

12.4.2.7 Biological Function of *mir-355*

In nematodes, infection with *Pseudomonas aeruginosa* could dysregulate some miRNAs [42]. Among these miRNAs, loss-of-function mutation of *mir-45*, *mir-75*, *mir-246*, *mir-256*, or *mir-355* induced a resistance to *P. aeruginosa* infection, whereas loss-of-function mutation of *mir-63* or *mir-360* induced a susceptibility to *P. aeruginosa* infection [42]. Based on the prediction, SMA-3 in the TGF- β signaling pathway might function as a potential target for *mir-246* in the regulation of innate immunity [42]. Moreover, the effects of intestinal overexpression of *daf-2* lacking 3' UTR or containing 3' UTR on innate immune response of nematodes overexpressing intestinal *mir-355* to *P. aeruginosa* PA14 infection, as well as the in vivo 3'-UTR binding assay, demonstrated that the DAF-2 in the insulin signaling pathway acted as a target for intestinal *mir-355* to regulate the innate immunity (Fig. 12.21) [42]. Mutation of *daf-2* resulted in a resistance to pathogen infection and suppressed the susceptibility of *mir-355(n4618)* mutant nematodes to pathogen infection [42]. In nematodes, *mir-355* acted downstream of PMK-1 to regulate the innate immune response to *P. aeruginosa* PA14 infection [42]. Additionally, *mir-355* acted upstream of DAF-16 and SKN-1 to regulate the innate immune response to *P. aeruginosa* PA14 infection [42]. Therefore, *mir-355* functions as an important link between p38 MAPK signaling pathway and insulin signaling pathway in the regulation of innate immunity in nematodes. Similarly, DAF-2 was also found to act as a target of *mir-355* in regulating the MWCNTs toxicity in nematodes [43].

12.4.2.8 Biological Function of *mir-360*

Among the dysregulated miRNAs induced by GO, *mir-360* mutation enhanced reproductive toxicity of GO; however, *mir-360* overexpression inhibited reproductive toxicity of GO (Fig. 12.22) [44]. CEP-1 was identified as the target of *mir-360* during the control of reproductive toxicity of GO in inducing germline apoptosis (Fig. 12.22) [44]. *mir-360* expression could be increased by GO exposure [31], suggesting that the alteration in *mir-360* expression mediates a protective response to GO exposure in nematodes.

12.4.3 The mRNAs–miRNA Network Involved in the Regulation of Toxicity of Environmental Toxicants or Stresses

The mRNAs–miRNA network has been raised to be involved in the regulation of GO toxicity [36]. Based on the prediction, *mir-259*, *mir-1820*, *mir-36*, *mir-82*, *mir-239*, *mir-246*, *mir-392*, *mir-2217*, *mir-360*, *mir-4810*, *mir-4807*, *mir-4805*, *mir-800*, *mir-1830*, *mir-236*, *mir-4806*, *mir-244*, *mir-235*, *mir-4812*, *mir-43*, *mir-231*,

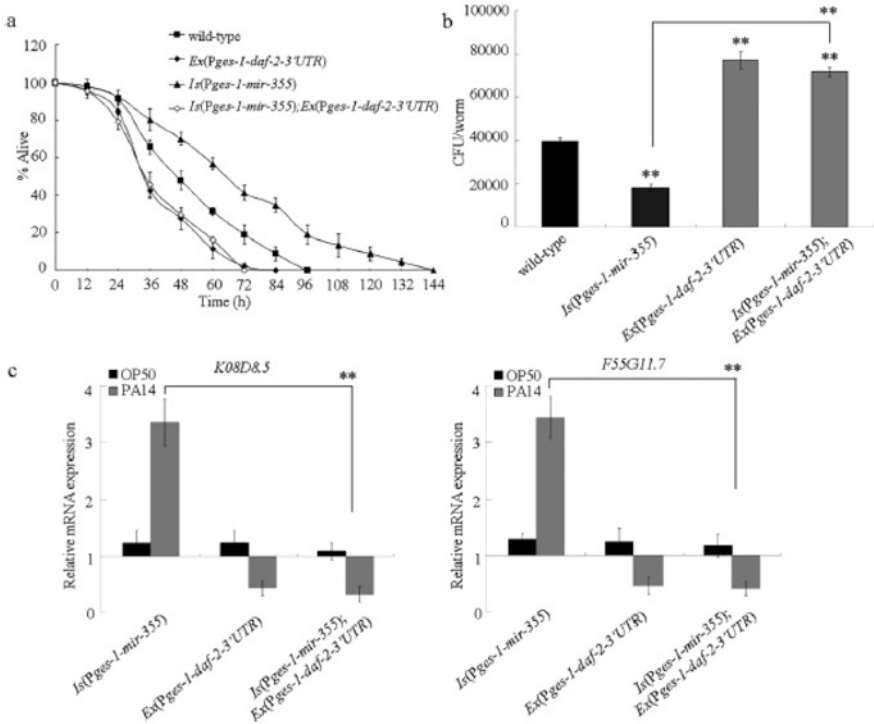


Fig. 12.21 Effects of intestinal overexpression of *daf-2* lacking 3' UTR on innate immune response to *P. aeruginosa* PA14 infection in nematodes overexpressing intestinal *mir-355* [42]. (a) Effects of intestinal overexpression of *daf-2* lacking 3' UTR on survival of nematodes overexpressing intestinal *mir-355* after *P. aeruginosa* PA14 infection. Statistical comparisons of the survival plots indicate that, after the *P. aeruginosa* PA14 infection, the survival of transgenic strain *Is(Pges-1-mir-355);Ex(Pges-1-daf-2-3'UTR)* was significantly different from that of transgenic strain *Is(Pges-1-mir-355)* ($P < 0.001$). Bars represent mean \pm SD. (b) Effects of intestinal overexpression of *daf-2* lacking 3' UTR on *P. aeruginosa* PA14 CFU in the body of nematodes overexpressing intestinal *mir-355*. Bars represent mean \pm SD. $**P < 0.01$ vs wild-type (if not specially indicated). (c) Effects of intestinal overexpression of *daf-2* lacking 3' UTR on expression patterns of putative antimicrobial genes of nematodes overexpressing intestinal *mir-355* after *P. aeruginosa* PA14 infection. Normalized expression is presented relative to wild-type expression. Bars represent mean \pm SD. $**P < 0.01$

mir-42, *mir-2210*, and *mir-73* might be involved in the control of GO toxicity with some of the dysregulated genes as their targets in GO-exposed nematodes [36]. Among these potential targeted genes, *gas-1* might act as a molecular target for *mir-4810* to regulate the activation of oxidative stress in GO-exposed nematodes, and *par-6* might act as a molecular target for *mir-1820* to regulate intestinal development and function in GO-exposed nematodes [36]. Additionally, *mir-231*, *mir-236*,

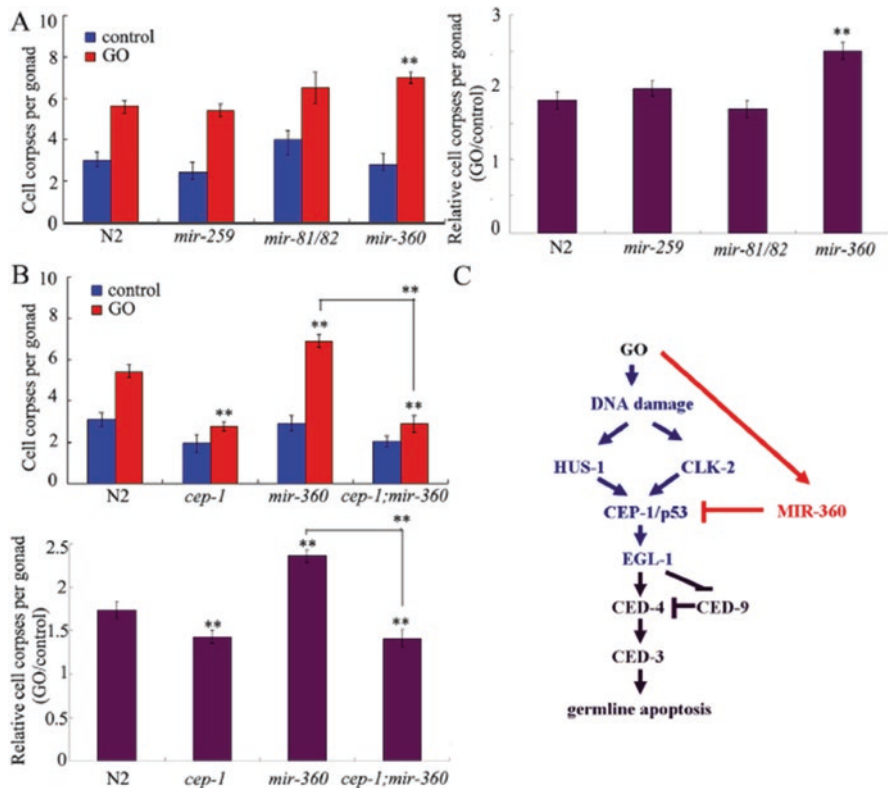


Fig. 12.22 *mir-360* negatively regulated the functions of signaling pathways of DNA damage checkpoints and apoptosis in the control of reproductive toxicity in GO-exposed nematodes [44]. (a) Germline apoptosis in *mir-259*, *mir-81/82*, or *mir-360* mutant exposed to GO. The used mutants were wild-type N2, *mir-360*(n4635), *mir-259*(n4106), and *mir-81&82*(nDf54). (b) Genetic interaction of *mir-360* with *cep-1* in regulating germline apoptosis in nematodes exposed to GO. The used strains were wild-type N2, *mir-360*(n4635), *cep-1*(RNAi), and *cep-1*(RNAi);*mir-360*(n4635). (c) A summary model for the molecular control of reproductive toxicity of GO in inducing germline apoptosis in nematodes. GO exposure concentration was 10 mg/L. Prolonged exposure to GO was performed from L1-larvae to young adults. Bars represent means \pm S.E.M. ** $P < 0.01$

mir-259, *mir-36*, *mir-42*, *mir-43*, *mir-73*, *mir-82*, and *mir-4805* might act through the functions of *unc-44*, *mig-2*, *itr-1*, *ced-10*, *unc-93*, *fat-2*, *smp-1*, and/or *cab-1* to regulate the defecation behavior in GO-exposed nematodes [36]. Therefore, certain miRNA–mRNA networks may exist to regulate the toxicity of environmental toxicants or stresses by influencing some important biological processes, such as oxidative stress, intestinal development and function, and defecation behavior, in nematodes.

12.5 lncRNA Regulation

Long noncoding RNAs (lncRNAs) are normally defined as the noncoding RNAs having at least 200 nucleotides and no (or weak) protein coding ability, which have been shown to potentially regulate various biological processes [45–48].

12.5.1 *Dysregulation of lncRNAs by Environmental Toxicants or Stresses*

With the GO as an example, the Illumina HiSeq 2000 sequencing was performed for nematodes after prolonged exposure (L1-larvae stage to young adults) to GO (100 mg/L). Among the dysregulated 39 lncRNAs, 10 known lncRNAs were 1 upregulated lncRNA (*linc-3*) and 9 downregulated lncRNAs (*linc-14*, *anr-24*, *linc-68*, *linc-103*, *linc-83*, *linc-24*, *anr-36*, *linc-5*, and *linc-37*) (Fig. 12.23) [49]. *linc-14*, *linc-68*, *linc-103*, *linc-83*, *linc-24*, *linc-5*, *linc-37*, and *linc-3* are intergenic lncRNAs, and *anr-36* and *anr-24* are antisense lncRNAs (Fig. 12.23) [49]. Besides this, 29 novel lncRNAs were also identified in GO-exposed nematodes (Fig. 12.23) [49]. Among these lncRNAs, 34 differentially expressed lncRNAs could be confirmed by qRT-PCR analysis in GO-exposed nematodes [49].

12.5.2 *Effect of Ascorbate or Paraquat Treatment on lncRNA Profiling in Nematodes Exposed to Environmental Toxicants or Stresses*

After pretreatment with paraquat (2 mM), a ROS generator, the expression of candidate 34 lncRNAs was more severely affected in GO-exposed nematodes (Fig. 12.24) [49]. Different from this, ascorbate (10 mM) treatment could recover the dysregulation in expressions of some lncRNAs caused by GO exposure (Fig. 12.24) [49].

12.5.3 *Effects of PEG Modification or FBS Surface Coating on Graphene Oxide-Induced lncRNA Profiling*

After the comparison of 34 candidate long noncoding RNAs (lncRNAs) in control, GO-, or GO-PEG-exposed nematodes, expression patterns of some dysregulated lncRNAs induced by GO exposure could be reversed by PEG surface modification (Fig. 12.25) [49]. PEG surface modification could increase the expressions of

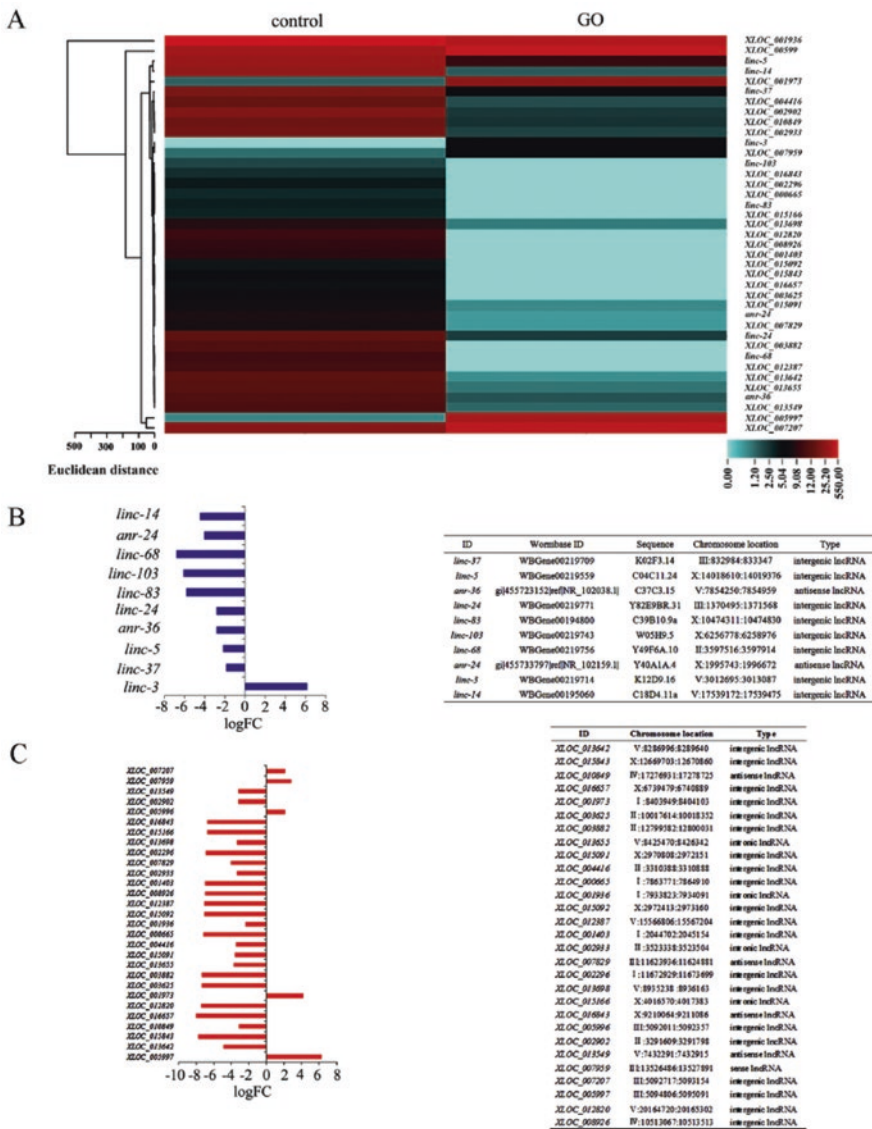


Fig. 12.23 Dysregulated lncRNAs induced by GO exposure in nematodes [49]. (a) Hierarchical clustering assay to show the characteristic molecular signature of 39 dysregulated lncRNAs in GO-exposed nematodes. (b) Dysregulated known lncRNAs induced by GO exposure in nematodes. $\logFC > 2$ and $p < 0.05$. (c) Dysregulated novel lncRNAs induced by GO exposure in nematodes. $\logFC > 2$ and $p < 0.05$

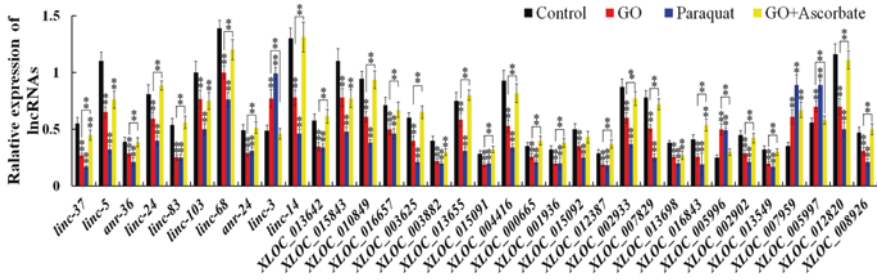


Fig. 12.24 Effects of ascorbate or paraquat treatment on lincRNA expression in nematodes [49]. L4-larval nematodes were treated with 2 mM paraquat for 12 h in the 12-well sterile tissue culture plates. Nematodes were exposed to GO (100 mg/L) first from L1-larvae to L4-larvae and then treated with 10 mM ascorbate for 24 h. Bars represent means \pm S.E.M. ** $P < 0.01$

linc-37, *linc-5*, *linc-24*, *linc-14*, *XLOC_013642*, *XLOC_010849*, and *XLOC_004416* and decrease the expression of *XLOC_007959* in GO-exposed nematodes (Fig. 12.25) [49]. Similarly, FBS surface coating could suppress the increase in the expressions of *linc-37*, *linc-24*, *linc-14*, *XLOC_004416*, *XLOC_013698*, and *XLOC_012820*, and the decrease in the expression of *XLOC_007959* induced by GO exposure (Fig. 12.25) [49]. More importantly, it was found that both the FBS surface coating and the PEG surface modification could decrease the expressions of *linc-37*, *linc-24*, *linc-14*, and *XLOC_004416* and increase the expression of *XLOC_007959* in GO-exposed nematodes (Fig. 12.25) [49], which implies that FBS surface coating or PEG surface modification may potentially reduce the GO toxicity by influencing the functions of some certain conserved molecular basis mediated by same lincRNAs in nematodes.

12.5.4 The lincRNA–miRNA Network Involved in the Regulation of Toxicity of Environmental Toxicants or Stresses

Based on the identified dysregulated miRNAs and lincRNAs, a lincRNA–miRNA network that responds to GO exposure was raised in nematodes using a bioinformatics analysis algorithm. In this lincRNA–miRNA network, lincRNAs may regulate the GO toxicity by affecting or altering the function of certain targeted miRNA(s) [49]. These identified 34 lincRNAs might potentially only bind to a very limited number of miRNAs to regulate the GO toxicity in nematodes [49]. The lincRNA–miRNA networks provide important clues for further elucidation of underlying mechanisms for candidate lincRNAs in the regulation of toxicity of environmental toxicants or stresses in nematodes.

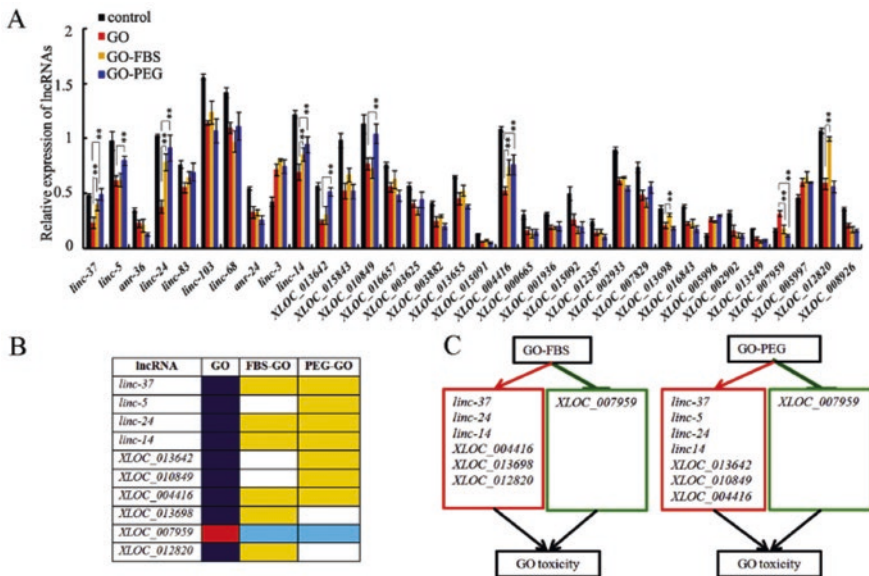


Fig. 12.25 Surface modification altered the expression patterns of some lncRNAs in GO-exposed wild-type nematodes [49]. (a) lncRNA expression patterns in GO-, GO-FBS-, or GO-PEG-exposed nematodes. GO-, GO-FBS-, or GO-PEG exposure concentration was 100 mg/L. Prolonged exposure to GO was performed from L1-larvae to young adults. Bars represent means ± S.E.M. ** $P < 0.01$. (b) Summary on the expression patterns of lncRNAs in GO-, GO-FBS-, or GO-PEG-exposed nematodes. Dark blue color indicates the decreased lncRNAs by GO, red color indicates the increased lncRNA by GO, yellow color indicate the increased lncRNAs by modification, and light blue color indicate the decreased lncRNA by modification. (c) Diagram for molecular mechanism of FBS coating or PEG surface modification to reduce the GO toxicity through the regulation of functions of lncRNAs in nematodes

12.5.5 Functional Analysis of *linc-37* and *linc-14* in Regulating the Toxicity of Environmental Toxicants or Stresses

In nematodes, RNAi knockdown of *linc-37* or *linc-14* could induce a resistance to GO toxicity in reducing lifespan, in inducing intestinal ROS production, and in decreasing locomotion behavior [49]. In contrast, nematodes overexpressing *linc-37* or *linc-14* showed a susceptibility to GO toxicity [49]. Based on the screen of candidate binding transcriptional factors (TFs) for *linc-37*, it was found that *linc-37* RNAi knockdown increased the expressions of *ama-1*, *daf-16*, *nhr-28*, *elt-3*, *fos-1*, and *gmeb-1* in GO-exposed nematodes (Fig. 12.26) [49]. DAF-16 is the FOXO TF in the insulin signaling pathway. *linc-37* RNAi knockdown also enhanced expression and translocation of DAF-16::GFP into intestinal nucleus (Fig. 12.26) [49]. Genetic analysis has indicated that *linc-37* regulates GO toxicity by modulating DAF-16 function in nematodes.

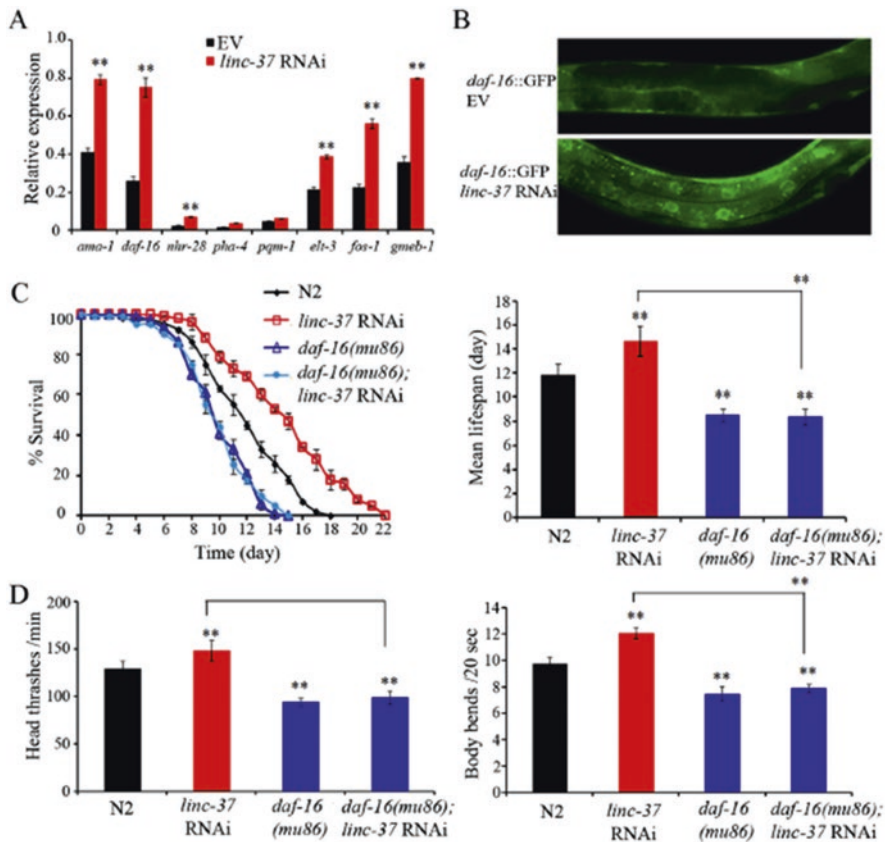


Fig. 12.26 Interaction of DAF-16/TF with *linc-37* in the regulation of GO toxicity [49]. (a) TFs expression patterns in *linc-37* RNAi knockdown nematodes. (b) Subcellular localization of DAF-16::GFP fusion protein in GO-exposed *linc-37* RNAi knockdown nematodes. (c) Lifespan of wild-type N2, *daf-16(mu86)*, *linc-37* RNAi, and *daf-16(mu86);linc-37* RNAi nematodes exposed to GO. (d) Locomotion behavior in wild-type N2, *daf-16(mu86)*, *linc-37* RNAi, and *daf-16(mu86);linc-37* RNAi nematodes exposed to GO. GO exposure concentration was 100 mg/L. Prolonged exposure to GO was performed from L1-larvae to young adults. Bars represent means \pm S.E.M. ** $P < 0.01$

linc-37 RNAi knockdown altered expressions of *sod-1*, *sod-2*, *sod-3*, *sod-4*, *isp-1*, *clk-1*, *nhx-2*, *pkc-3*, *jkk-1*, *jnk-1*, *ced-3*, *ced-4*, *cep-1*, and *daf-16* [49], demonstrating the possible important roles of *linc-37* in affecting oxidative stress, stress response, intestinal development, and cell apoptosis and DNA damage in GO-exposed nematodes. *linc-14* RNAi knockdown also altered expressions of *sod-3*, *sod-4*, *isp-1*, *nhx-2*, *par-6*, *pkc-3*, *jnk-1*, *mek-1*, *ced-3*, *ced-4*, *clk-2*, *cep-1*, *daf-16*, *akt-1*, and *daf-18* [49], suggesting the similar functions of *linc-14* in affecting oxidative stress, stress response, intestinal development, and cell apoptosis and DNA damage in GO-exposed nematodes.

12.6 Perspectives

In nematodes, in this chapter, we only focused on the methylation, acetylation, microRNAs (miRNAs), and long noncoding RNAs (lncRNAs) to discuss the involvement of epigenetic mechanisms in the regulation of toxicity of environmental toxicants or stresses. Actually, there are still some other forms of epigenetic regulation, such as the circular RNAs. Therefore, more efforts are needed to elucidate the molecular basis for epigenetic control of toxicity of environmental toxicants or stresses.

Nevertheless, so far, the researchers still do not pay more attention to the epigenetic control of biological processes, as done on genes encoding molecular signaling pathways, that is, whether the epigenetic signals can play a pivotal role in regulating the biological processes, including the stress response or, in other words, whether the contribution of epigenetic signals is equally important to the genes encoding molecular signaling pathways in regulating the biological processes. A further possibility also exist that certain forms of epigenetic control are only very important at certain aspects in the regulation of biological processes. More convincing data are still needed to prove the possible or potential pivotal roles of different forms of epigenetic signals in regulating different biological processes at least in nematodes.

In nematodes, it is assumed that a small set of epigenetic signals can govern many important molecular signaling pathways to regulate the toxicity of environmental toxicants or stresses. If this assumption is correct, the study on the epigenetic regulation at least can help us identify more important signaling pathways involved in the regulation of toxicity of environmental toxicants or stresses. But, this should not be the real focus of work on the epigenetic regulation itself.

References

1. Zhi L-T, Yu Y-L, Li X-Y, Wang D-Y, Wang D-Y (2017) Molecular control of innate immune response to *Pseudomonas aeruginosa* infection by intestinal *let-7* in *Caenorhabditis elegans*. *PLoS Pathog* 13:e1006152
2. Sun L-M, Liao K, Hong C-C, Wang D-Y (2017) Honokiol induces reactive oxygen species-mediated apoptosis in *Candida albicans* through mitochondrial dysfunction. *PLoS One* 12:e0172228
3. Sun L-M, Liao K, Wang D-Y (2017) Honokiol induces superoxide production by targeting mitochondrial respiratory chain complex I in *Candida albicans*. *PLoS One* 12:e0184003
4. Sun L-M, Zhi L-T, Shakoor S, Liao K, Wang D-Y (2016) microRNAs involved in the control of innate immunity in *Candida* infected *Caenorhabditis elegans*. *Sci Rep* 6:36036
5. Sun L-M, Liao K, Li Y-P, Zhao L, Liang S, Guo D, Hu J, Wang D-Y (2016) Synergy between PVP-coated silver nanoparticles and azole antifungal against drug-resistant *Candida albicans*. *J Nanosci Nanotechnol* 16:2325–2335
6. Wu Q-L, Cao X-O, Yan D, Wang D-Y, Aballay A (2015) Genetic screen reveals link between maternal-effect sterile gene *mes-1* and *P. aeruginosa*-induced neurodegeneration in *C. elegans*. *J Biol Chem* 290:29231–29239

7. Yu Y-L, Zhi L-T, Wu Q-L, Jing L-N, Wang D-Y (2018) NPR-9 regulates innate immune response in *Caenorhabditis elegans* by antagonizing activity of AIB interneurons. *Cell Mol Immunol* 15:27–37
8. Yu Y-L, Zhi L-T, Guan X-M, Wang D-Y, Wang D-Y (2016) FLP-4 neuropeptide and its receptor in a neuronal circuit regulate preference choice through functions of ASH-2 trithorax complex in *Caenorhabditis elegans*. *Sci Rep* 6:21485
9. Ding W, Smulan LJ, Hou NS, Taubert S, Watts JL, Walker AK (2015) s-Adenosylmethionine levels govern innate immunity through distinct methylation-dependent pathways. *Cell Metab* 22:633–645
10. Wenzel D, Palladino F, Jedrusik-Bode M (2011) Epigenetics in *C. elegans*: facts and challenges. *Genesis* 49:647–661
11. Hyun M, Kim J, Dumur C, Schroeder FC, You Y (2016) BLIMP-1/BLMP-1 and metastasis-associated protein regulate stress resistant development in *Caenorhabditis elegans*. *Genetics* 203:1721–1732
12. Rudgalvyte M, Peltonen J, Lakso M, Wong G (2017) Chronic MeHg exposure modifies the histone H3K4me3 epigenetic landscape in *Caenorhabditis elegans*. *Comp Biochem Physiol C* 191:109–116
13. Tian Y, Garcia G, Bian Q, Steffen KK, Joe L, Wolff S, Meyer BJ, Dillin A (2016) Mitochondrial stress induces chromatin reorganization to promote longevity and UPR^{mt}. *Cell* 165:1197–1208
14. Towbin BD, González-Aguilera C, Sack R, Gaidatzis D, Kalck V, Meister P, Askjaer P, Gasser SM (2012) Step-wise methylation of histone H3K9 positions heterochromatin at the nuclear periphery. *Cell* 150:934–947
15. Myers TR, Amendola PG, Lussi YC, Salcini AE (2018) JMJD-1.2 controls multiple histone post-translational modifications in germ cells and protects the genome from replication stress. *Sci Rep* 8:3765
16. Merkwirth C, Jovaisaite V, Durieux J, Matilainen O, Jordan SD, Quiros PM, Steffen KK, Williams EG, Mouchiroud L, Uhlein SN, Murillo V, Wolff SC, Shaw RJ, Auwerx J, Dillin A (2016) Two conserved histone demethylases regulate mitochondrial stress-induced longevity. *Cell* 165:1209–1223
17. Studencka M, Konzer A, Moneron G, Wenzel D, Opitz L, Salinas-Riester G, Bedet C, Krüger M, Hell SW, Wisniewski JR, Schmidt H, Palladino F, Schulze E, Jedrusik-Bode M (2012) Novel roles of *Caenorhabditis elegans* heterochromatin protein HP1 and linker histone in the regulation of innate immune gene expression. *Mol Cell Biol* 32:251–265
18. Wohlschläger T, Butschi A, Grassi P, Sutov G, Gauss R, Hauck D, Schmieder SS, Knobel M, Titz A, Dell A, Haslam SM, Hengartner MO, Aebi M, Künzler M (2014) Methylated glycans as conserved targets of animal and fungal innate defense. *Proc Natl Acad Sci U S A* 111:E2787–E2796
19. Ikeda T, Uno M, Honjoh S, Nishida E (2017) The MYST family histone acetyltransferase complex regulates stress resistance and longevity through transcriptional control of DAF-16/FOXO transcription factors. *EMBO Rep* 18:1716–1726
20. Warnhoff K, Murphy JT, Kumar S, Schneider DL, Peterson M, Hsu S, Guthrie J, Robertson JD, Kornfeldt K (2014) The DAF-16 FOXO transcription factor regulates *natc-1* to modulate stress resistance in *Caenorhabditis elegans*, linking insulin/IGF-1 signaling to protein N-terminal acetylation. *PLoS Genet* 10:e1004703
21. Chiang W-C, Tishkoff DX, Yang B, Wilson-Grady J, Yu X, Mazer T, Eckersdorff M, Gygi SP, Lombard DB, Hsu A (2012) *C. elegans* SIRT6/7 homolog SIR-2.4 promotes DAF-16 relocalization and function during stress. *PLoS Genet* 8:e1002948
22. Wang D-Y (2018) *Nanotoxicology in Caenorhabditis elegans*. Springer, Singapore
23. Wu Q-L, Han X-X, Wang D, Zhao F, Wang D-Y (2017) Coal combustion related fine particulate matter (PM_{2.5}) induces toxicity in *Caenorhabditis elegans* by dysregulating microRNA expression. *Toxicol Res* 6:432–441

24. Ren M-X, Zhao L, Ding X-C, Krasteva N, Rui Q, Wang D-Y (2018) Developmental basis for intestinal barrier against the toxicity of graphene oxide. *Part Fibre Toxicol* 15:26
25. Xiao G-S, Chen H, Krasteva N, Liu Q-Z, Wang D-Y (2018) Identification of interneurons required for the aversive response of *Caenorhabditis elegans* to graphene oxide. *J Nanobiotechnol* 16:45
26. Ding X-C, Rui Q, Wang D-Y (2018) Functional disruption in epidermal barrier enhances toxicity and accumulation of graphene oxide. *Ecotoxicol Environ Saf* 163:456–464
27. Zhao L, Kong J-T, Krasteva N, Wang D-Y (2018) Deficit in epidermal barrier induces toxicity and translocation of PEG modified graphene oxide in nematodes. *Toxicol Res* 7(6):1061–1070. <https://doi.org/10.1039/C8TX00136G>
28. Qu M, Xu K-N, Li Y-H, Wong G, Wang D-Y (2018) Using *acs-22* mutant *Caenorhabditis elegans* to detect the toxicity of nanopolystyrene particles. *Sci Total Environ* 643:119–126
29. Dong S-S, Qu M, Rui Q, Wang D-Y (2018) Combinational effect of titanium dioxide nanoparticles and nanopolystyrene particles at environmentally relevant concentrations on nematodes *Caenorhabditis elegans*. *Ecotoxicol Environ Saf* 161:444–450
30. Shao H-M, Han Z-Y, Krasteva N, Wang D-Y (2018) Identification of signaling cascade in the insulin signaling pathway in response to nanopolystyrene particles. *Nanotoxicology* (in press)
31. Wu Q-L, Zhao Y-L, Zhao G, Wang D-Y (2014) microRNAs control of in vivo toxicity from graphene oxide in *Caenorhabditis elegans*. *Nanomedicine* 10:1401–1410
32. Zhao Y-L, Wu Q-L, Li Y-P, Nouara A, Jia R-H, Wang D-Y (2014) In vivo translocation and toxicity of multi-walled carbon nanotubes are regulated by microRNAs. *Nanoscale* 6:4275–4284
33. Taki FA, Pan X, Zhang B (2014) Chronic nicotine exposure systemically alters microRNA expression profiles during post-embryonic stages in *Caenorhabditis elegans*. *J Cell Physiol* 229:79–89
34. Rudgalvyte M, VanDuyn N, Aarnio V, Heikkinen L, Peltonen J, Lakso M, Nass R, Wong G (2013) Methylmercury exposure increases lipocalin related (*lpr*) and decreases activated in blocked unfolded protein response (*abu*) genes and specific miRNAs in *Caenorhabditis elegans*. *Toxicol Lett* 222:189–196
35. Saul N, Chakrabarti S, Stürzenbaum SR, Menzel R, Steinberg CEW (2014) Neurotoxic action of microcystin-LR is reflected in the transcriptional stress response of *Caenorhabditis elegans*. *Chem Biol Interact* 223:51–57
36. Zhao Y-L, Wu Q-L, Wang D-Y (2015) A microRNAs-mRNAs network involved in the control of graphene oxide toxicity in *Caenorhabditis elegans*. *RSC Adv* 5:92394–92405
37. Liu F, He C, Luo L, Zou Q, Zhao Y, Saini R, Han S, Knölker H, Wang L, Ge B (2013) Nuclear hormone receptor regulation of microRNAs controls innate immune responses in *C. elegans*. *PLoS Pathog* 9:e1003545
38. Yang R-L, Ren M-X, Rui Q, Wang D-Y (2016) A *mir-231*-regulated protection mechanism against the toxicity of graphene oxide in nematode *Caenorhabditis elegans*. *Sci Rep* 6:32214
39. Dai L, Gao J, Zou C, Ma Y, Zhang K (2015) *mir-233* modulates the unfolded protein response in *C. elegans* during *Pseudomonas aeruginosa* infection. *PLoS Pathog* 11:e1004606
40. Xiao G-S, Zhi L-T, Ding X-C, Rui Q, Wang D-Y (2017) Value of *mir-247* in warning graphene oxide toxicity in nematode *Caenorhabditis elegans*. *RSC Adv* 7:52694–52701
41. Zhuang Z-H, Li M, Liu H, Luo L-B, Gu W-D, Wu Q-L, Wang D-Y (2016) Function of RSKS-1-AAK-2-DAF-16 signaling cascade in enhancing toxicity of multi-walled carbon nanotubes can be suppressed by *mir-259* activation in *Caenorhabditis elegans*. *Sci Rep* 6:32409
42. Zhi L-T, Yu Y-L, Jiang Z-X, Wang D-Y (2017) *mir-355* functions as an important link between p38 MAPK signaling and insulin signaling in the regulation of innate immunity. *Sci Rep* 7:14560
43. Zhao Y-L, Yang J-N, Wang D-Y (2016) A microRNA-mediated insulin signaling pathway regulates the toxicity of multi-walled carbon nanotubes in nematode *Caenorhabditis elegans*. *Sci Rep* 6:23234

44. Zhao Y-L, Wu Q-L, Wang D-Y (2016) An epigenetic signal encoded protection mechanism is activated by graphene oxide to inhibit its induced reproductive toxicity in *Caenorhabditis elegans*. *Biomaterials* 79:15–24
45. Rinn JL, Chang HY (2012) Genome regulation by long noncoding RNAs. *Annu Rev Biochem* 81:145–166
46. Guttman M, Rinn JL (2012) Modular regulatory principles of large non-coding RNAs. *Nature* 482:339–346
47. Ulitsky I, Bartel DP (2013) LincRNAs: genomics, evolution, and mechanisms. *Cell* 154:26–46
48. Chen LL, Carmichael GG (2010) Decoding the function of nuclear long non-coding RNAs. *Curr Opin Cell Biol* 22:357–364
49. Wu Q-L, Zhou X-F, Han X-X, Zhuo Y-Z, Zhu S-T, Zhao Y-L, Wang D-Y (2016) Genome-wide identification and functional analysis of long noncoding RNAs involved in the response to graphene oxide. *Biomaterials* 102:277–291

Chapter 13

Strategies to Screen and to Identify New Genetic Loci Involved in the Regulation of Toxicity of Environmental Toxicants or Stresses



Abstract It is necessary to employ powerful strategies to screen and to identify new genetic loci involved in the regulation of toxicity of environmental toxicants or stresses in nematodes. We here introduced the usefulness of transcriptomic analysis, proteomic analysis, forward genetics, and reverse genetics in screening and in identifying new genetic loci involved in the regulation of toxicity of environmental toxicants or stresses. Meanwhile, we discussed the related limitations for these strategies in nematodes.

Keywords Transcriptomic analysis · Proteomic analysis · Forward genetics · Reverse genetics · Screen · *Caenorhabditis elegans*

13.1 Introduction

So far, most of the works on the elucidation of underlying molecular mechanisms for toxicity of environmental toxicants or stresses are relevant to those well-known signaling pathways. In nematode *Caenorhabditis elegans*, many environmental toxicants or stresses can potentially result in the toxicity at different aspects on animals [1–8]. Actually, during the toxicity induction of environmental toxicants or stresses, a complex network may exist and contain many relevant signaling pathways. Therefore, it is necessary to employ effective strategies to screen and to identify new genetic loci involved in the regulation of toxicity of environmental toxicants or stresses.

In this chapter, we first introduced the importance of transcriptomic analysis and proteomic analysis for the screen and the identification of new genetic loci involved in the regulation of toxicity of environmental toxicants or stresses. Moreover, we further introduced the importance of forward and reverse genetic screen techniques in screening and in identifying new genetic loci involved in the regulation of toxicity of environmental toxicants or stresses. The related advantages and limitations for these strategies were further discussed.

13.2 Transcriptomic Screen and Identification of New Genetic Loci Involved in the Regulation of Toxicity of Environmental Toxicants or Stresses

In nematodes, the transcriptomic technique has been widely and frequently employed to screen and to identify the new genetic loci involved in the regulation of toxicity of environmental toxicants or stresses [9–23]. The nanotoxicological studies have demonstrated that some of the engineered nanomaterials (ENMs) can potentially induce the toxic effects on the functions of both primary and secondary targeted organs in organisms, including the nematodes [24–30]. We here selected the multiwalled carbon nanotubes (MWCNTs), a carbon-based ENM, as an example to discuss the use of transcriptomic technique in screening and in identifying new genetic loci involved in the regulation of toxicity of environmental toxicants or stresses [31].

Using Illumina HiSeq™ 2000 sequencing technique, transcriptomes from both control and MWCNT exposure groups were sequenced to obtain clean read data after filtering raw sequence data containing adaptor fragments [31]. The analysis based on statistical significance and use of a 2.0-fold change cutoff was performed, and the acquired annotations of differentially expressed genes were compared with the databases of gene bank (Fig. 13.1) [31]. Among the detected 13,752 genes, totally, 1903 genes were differentially expressed in MWCNT-exposed nematodes compared with control (Fig. 13.1) [31]. Among these 1903 mRNAs, 924 mRNAs were upregulated, and 993 mRNAs were downregulated by MWCNT exposure [31]. Among these dysregulated genes, some genes were associated with the control of oxidative stress or intestinal development [31]. The dysregulated genes associated with the control of oxidative stress were *sod-2*, *sod-3*, *mev-1*, *isp-1*, *gas-1*, and *clk-1*, and the dysregulated genes associated with the control of intestinal development were *pqp-3*, *gem-4*, *par-3*, *pkc-3*, *ajm-1*, *lin-7*, *inx-3*, and *abts-4* [31].

To determine the biological processes mediated by the dysregulated genes in MWCNT-exposed nematodes, gene ontology analysis was performed. Based on the dysregulated mRNAs, the significantly influenced gene ontology terms could be mainly classified into several categories, which were at least associated with biological processes of development, reproduction, cell adhesion, apoptosis, enzyme activity, cellular component, cellular localization and transportation, response to stimulus, immune response, cell metabolism, macromolecular complex, transcription, and translation in organisms (Fig. 13.2) [31]. The KEGG pathway mapping, a bioinformatics resource used to map molecular data sets in genomics, was further

Fig. 13.1 (continued) expression levels are represented as blue, and relatively high expression levels are represented in red. **(b)** Scatter diagram of relationship between mRNA coverage of the control group and the MWCNT exposure group. **(c)** qRT-PCR analysis of the expressions of some genes encoding insulin signaling pathway in nematodes exposed to MWCNTs. **(d)** MWCNT exposure influenced the nuclear translocation of DAF-16::GFP in nematodes. Scale bar, 150 μm . MWCNT (1 mg/L) exposure was performed from L1-larvae to young adult. Bars represent means \pm SEM ** $P < 0.01$ vs control

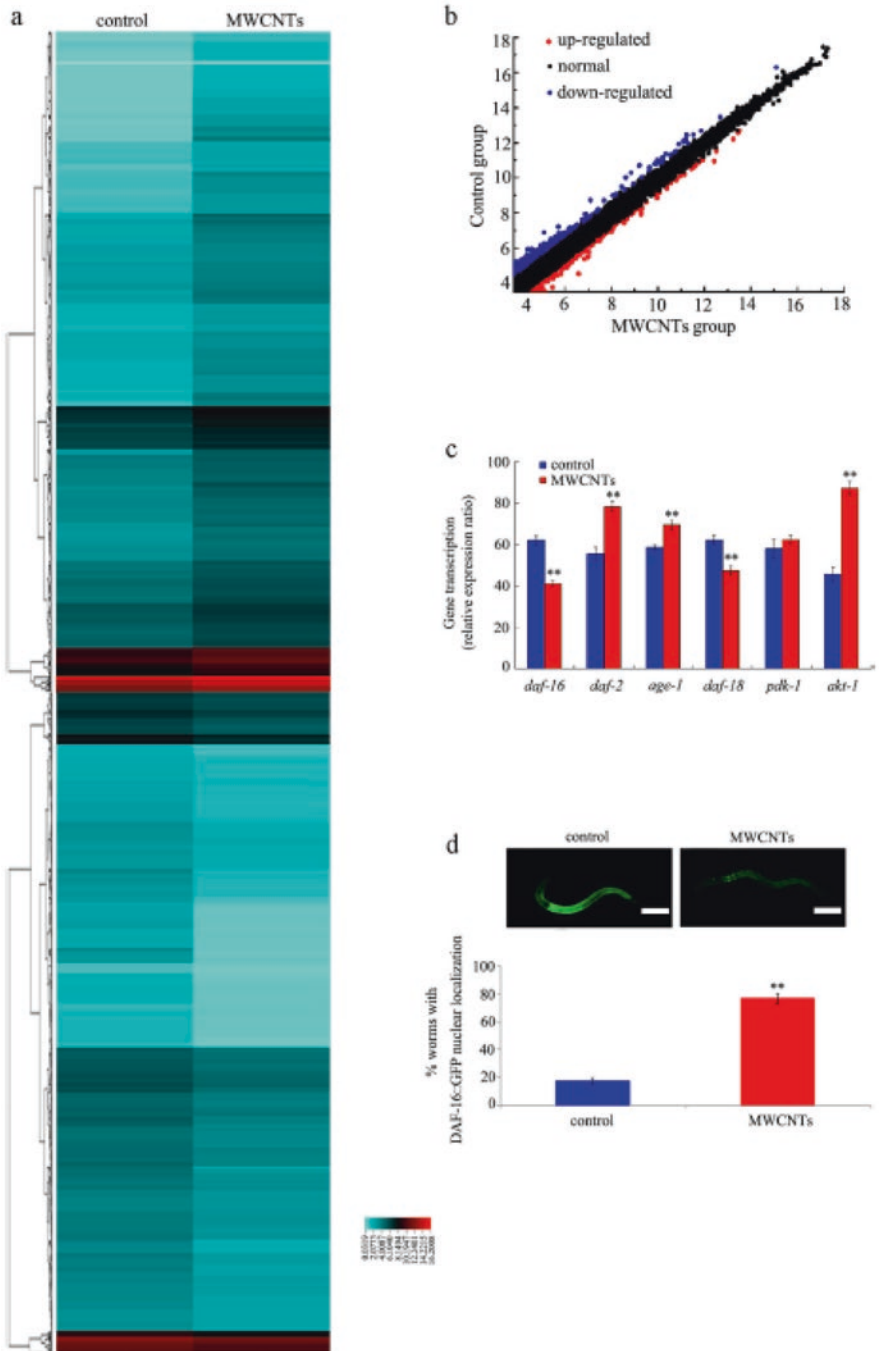


Fig. 13.1 Dysregulated mRNAs induced by MWCNT exposure [31]. (a) Heat map showing the expression of mRNAs obtained from control and MWCNT-exposed nematodes. Relatively low

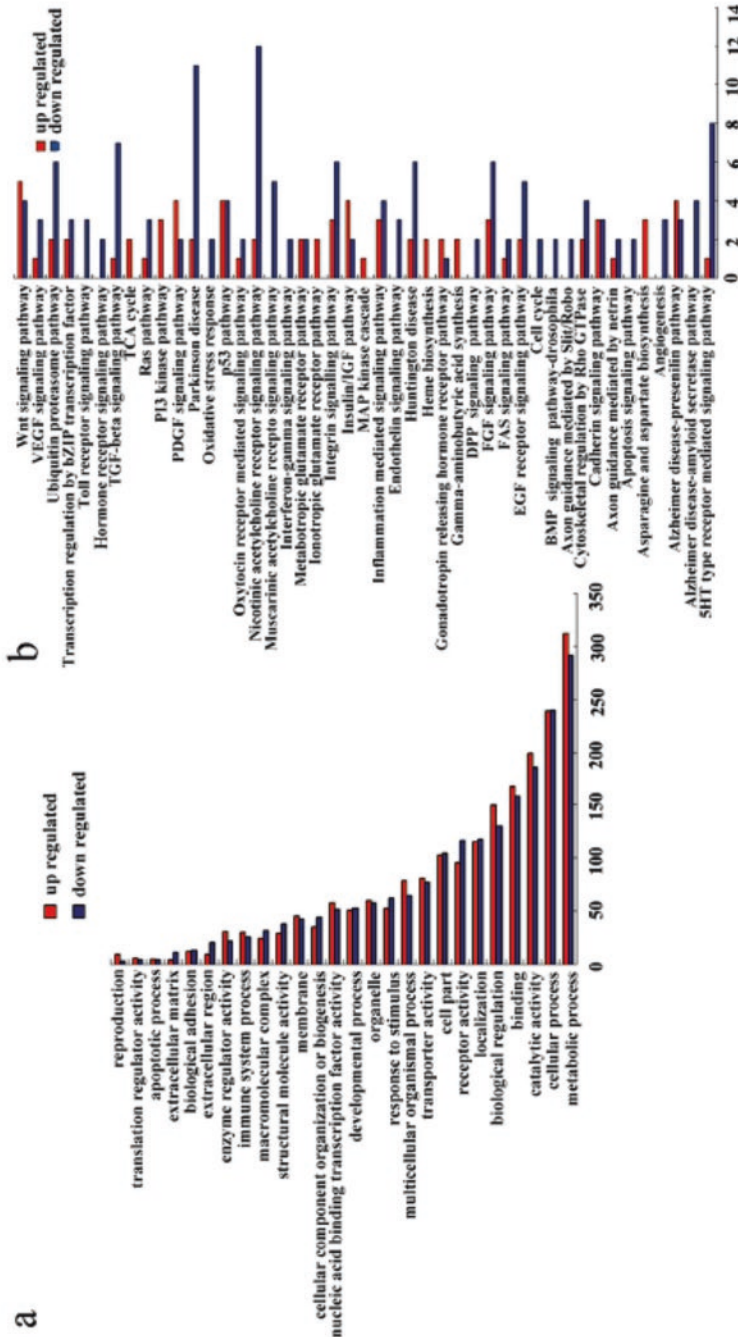


Fig. 13.2 Analysis of gene ontology terms and signaling pathways [31]. (a) Gene ontology terms with gene counts based on both down- and upregulated mRNAs in MWCNT-exposed nematodes. (b) Predicted KEGG signal pathways based on both down- and upregulated mRNAs in MWCNT-exposed nematodes

analyzed. The signaling pathways for the MWCNT toxicity control at least contained signaling pathways related to development, cell cycle, cell death, oxidative stress response, cellular component, immune response, neuronal development and neurodegeneration, and cell metabolism (Fig. 13.2) [31]. These results provide important clues for further understanding or elucidating the potential functions of dysregulated genes in the MWCNT toxicity induction in nematodes.

In nematodes, MWCNT exposure could induce the dysregulation of a series of miRNAs [32]. Among the dysregulated miRNAs, the bioinformatics analysis further demonstrated that *lin-4*, *mir-228*, *mir-249*, *mir-47*, *mir-355*, *mir-45*, *mir-2210*, *mir-57*, *mir-1018*, *mir-360*, *mir-64*, *mir-2209*, *mir-793*, *mir-1830*, *mir-2210*, *mir-83*, *mir-789*, and *mir-806* might be involved in the regulation of MWCNT toxicity through affecting the functions of identified dysregulated genes in exposed nematodes [31]. For example, *isp-1* gene might serve as a molecular target for *mir-249* to regulate the induction of oxidative stress in MWCNT-exposed nematodes [31]. Mutation of *mir-249* enhanced the induction of ROS production in MWCNT-exposed nematodes [31]. Mutation of *isp-1* inhibited the induction of ROS production in MWCNT-exposed nematodes, and mutation of *isp-1* gene suppressed the enhanced induction of ROS production observed in MWCNT-exposed *mir-249(n4983)* mutant nematodes [31]. The raised miRNA–mRNA network provides another important clue for the further elucidation of underlying molecular mechanisms of MWCNT toxicity induction in nematodes.

In nematodes, the insulin signaling pathway plays a crucial role in the regulation of toxicity of environmental toxicants or stresses [1, 33–35]. Among the genes encoding the insulin signaling pathway, the transcriptional expressions of *daf-16* and *daf-18* were decreased, and the transcriptional expressions of *age-1*, *daf-2*, *pdk-1*, and *akt-1* were increased in MWCNT (1 mg/L)-exposed nematodes compared with control (Fig. 13.1) [31]. The qRT-PCR assay confirmed these changes (Fig. 13.1) [31]. *daf-2* encodes a protein that is homologous to human insulin receptor InR, *age-1* encodes a protein that is homologous to human phosphoinositide 3-kinase PI3K, *daf-18* encodes a protein that is homologous to human lipid phosphatase PTEN, *akt-1* encodes a protein that is homologous to human serine/threonine kinase Akt/PKB, and *daf-16* encodes a protein that is homologous to human transcription factor FOXO. Meanwhile, it was observed that the percentage of nematodes with DAF-16::GFP in nucleus was significantly increased compared with control after the exposure to MWCNTs (Fig. 13.1) [31].

Moreover, it was found that mutation of *daf-2*, *age-1*, or *akt-1* led to the obvious inhibition in induction of ROS production in the intestine and the significant increase in brood size or locomotion behavior in MWCNT (1 mg/L)-exposed nematodes; however, mutation of *daf-16* or *daf-18* resulted in the enhanced induction of ROS production in the intestine and the more severe decrease in brood size or locomotion behavior in MWCNT (1 mg/L)-exposed nematodes (Fig. 13.3) [31]. Therefore, the functional analysis demonstrated the crucial role of the insulin signaling pathway in regulating the MWCNT toxicity in nematodes.

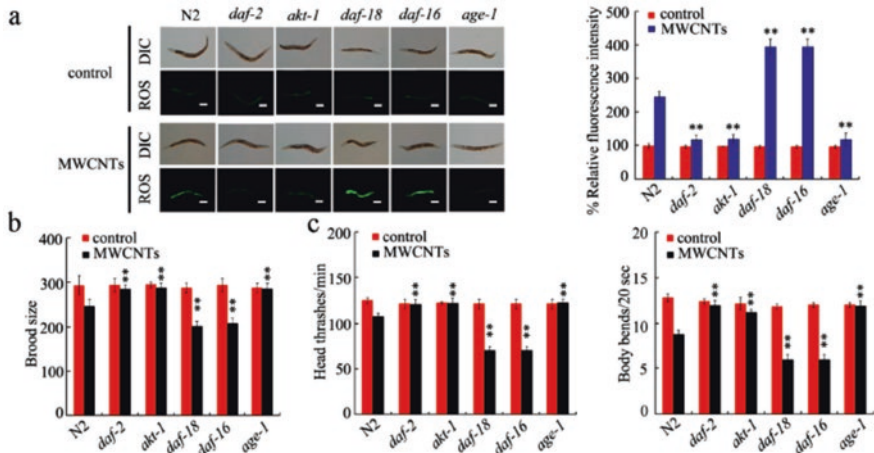


Fig. 13.3 Genes encoding insulin signaling pathway were involved in the control of MWCNT toxicity in nematodes [31]. (a) Intestinal ROS production assay in mutants for genes encoding insulin signaling pathway. Scale bar, 150 μ m. (b) Brood size assay in mutants for genes encoding insulin signaling pathway. (c) Locomotion behavior assay in mutants for genes encoding insulin signaling pathway. Locomotion behavior was assessed by the endpoints of head thrash and body bend. The used nematode strains were wild-type N2, *daf-16(mu86)*, *daf-2(e1370)*, *daf-1(hx546)*, *daf-18(e1375)*, and *akt-1(ok525)*. MWCNT (1 mg/L) exposure was performed from L1-larvae to young adult. Bars represent means \pm SEM $**P < 0.01$ vs N2

13.3 Proteomic Screen and Identification of New Genetic Loci Involved in the Regulation of Toxicity of Environmental Toxicants or Stresses

With the acrylamide as an example, the second-dimension SDS-PAGE was performed to analyze the differences in protein expressions in acrylamide-exposed nematodes. Totally 274 ± 31 spots from the control extracts and 334 ± 29 spots from acrylamide (500 mg/l)-treated extracts were detected (Fig. 13.4) [36]. Among these spots, 14 spots were identified as dysregulated spots by MALDI-TOF mass spectrometer (Fig. 13.4) [36]. Moreover, four proteins were clearly upregulated by 500 mg/l of acrylamide, and these were all GSTs [36].

It was further observed that the GST expressions were induced by acrylamide (500 mg/l) exposure for 12, 24, and 48 h (Fig. 13.5) [36]. Especially, the obvious alteration in expressions of GST-4, GST-7, GST-38, and GST-30 could be induced by acrylamide (500 mg/l) [36]. After acrylamide (500 mg) exposure for 48 h, the GST-4 expression was strongest, and RNAi knockdown of *skn-1* suppressed this expression induction in the pharynx and in the body wall muscle [36].

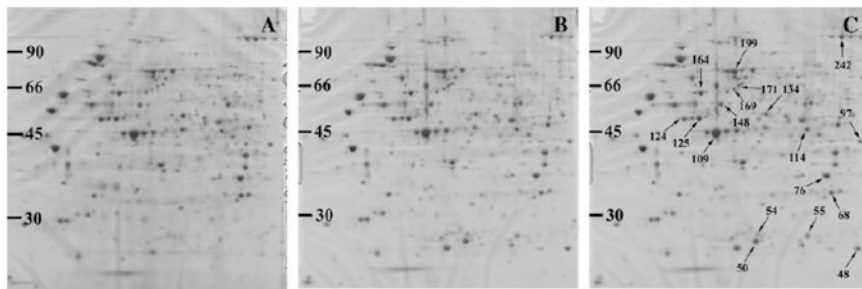


Fig. 13.4 2-DE gel images of *Caenorhabditis elegans* total protein [36]. Five hundred microgram of protein was separated in the first dimension by pH gradient (pH 4–7, 18 cm) and in the second dimension by molecular weight. (a) Proteins from animals grown on control plates without acrylamide; 277 ± 31 (mean \pm SD) protein spots were detected from four independent experiments. (b) Proteins from animals grown on 500 mg/l acrylamide; 334 ± 29 (mean \pm SD) protein spots were detected from four independent experiments. (c) Eighteen identified spots are indicated on a 2-DE gel image

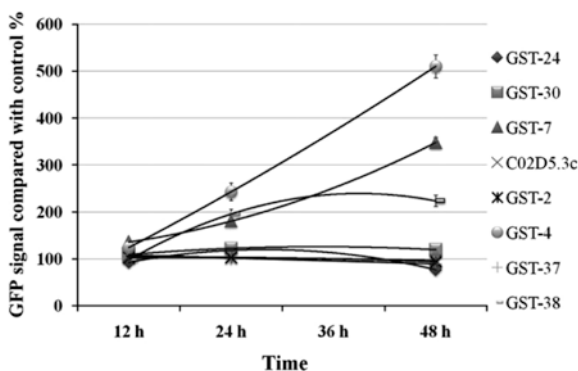


Fig. 13.5 Changes in the GST expression of the eight transgenic animals exposed from the L1 stage to 500 mg/l of acrylamide for 12, 24, and 48 h [36]. Animals were alive after all measurements. Data points indicate mean values \pm SEM of three independent experiments. Statistical significance was shown by the GFP signals from 12 h for GST-4, GST-7, and GST-30 and from 24 h for GST-38 ($p < 0.05$)

13.4 Forward Genetic Screen and Identification of New Genetic Loci Involved in the Regulation of Toxicity of Environmental Toxicants or Stresses

The forward genetic screen is a powerful genetic tool to identify new genetic loci involved in the regulation of toxicity of environmental toxicants or stresses in nematodes [37, 38]. In nematodes, the excess iodide caused pleiotropic defects on animals [39]. We here selected the iodide toxicity as an example to introduce the use of

forward genetics for the screen and the identification of new genetic loci involved in the regulation of toxicity of environmental toxicants or stresses.

The P0 nematodes were mutagenized with ethyl methanesulfonate, and the phenotypes were screened in 5000 F1 animals [39]. The mutants that could survive in 5 mM NaI were saved, and 12 independent isolates were obtained [39]. After mapping using SNPs and genetic complementation tests of all 12 mutations, these mutations might affect at least 4 genes [39].

Using nuclear-binding fluorescence dye Hoechst 33258, five isolates (*mac33*, *mac38*, *mac40*, *mac42*, and *mac43*) exhibited a defective cuticle integrity (Fig. 13.6) [39], suggesting the genetic lesions affecting cuticle formation. In nematodes, mutations affecting cuticles usually cause blisters on cuticle (Bli), dumpy (Dpy), long (Lon), roller (Rol), and/or squat (Sqt). Because only an obviously Bli phenotype

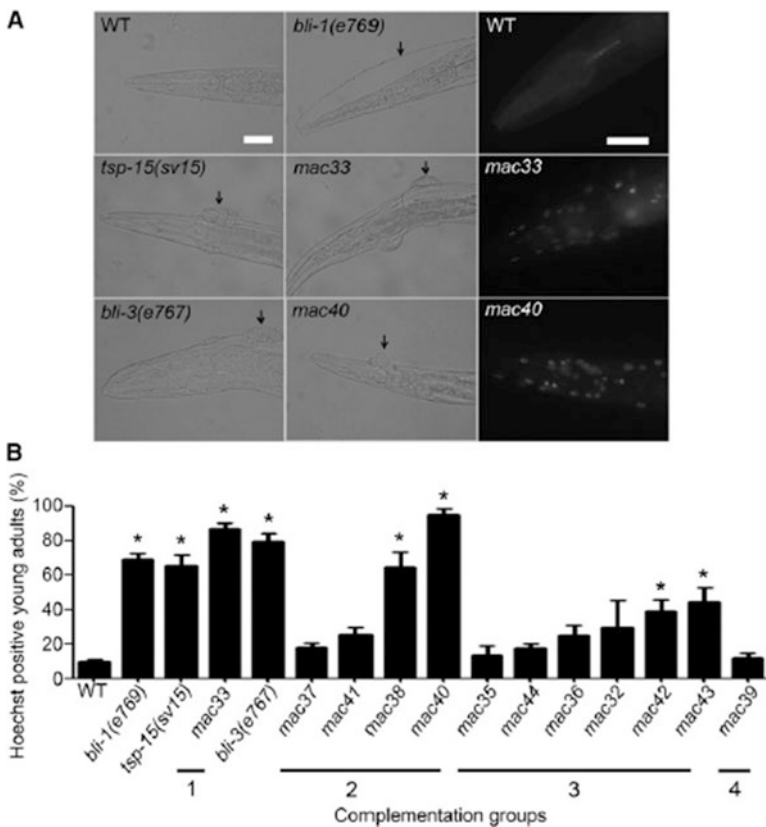


Fig. 13.6 Mutants that survive in 5 mM NaI have defective cuticle integrity [39]. (a) Cuticle blisters (arrows) of *bli* mutants, *tsp-15(sv15)* mutants, and two *mac* mutants (left and middle panels). Hoechst 33258 labels numerous nuclei in *mac33* and *mac40* mutants (right panels). Scale bars, 20 μ m. (b) Ratios of Hoechst 33258-positive animals. Statistics, different from wild type. Bars, SEs of four biological replicates ($n = 50$ for each replicate). * $P < 0.01$ (Bonferroni test with one-way ANOVA)

was detected in *mac* isolates, it was postulated that the Bli mutants might potentially survive in excess iodide [39]. Nevertheless, the further test on a series of Bli mutants (*bli-1(e769)*, *bli-2(e768)*, *bli-3(e767)*, *bli-4(e937)*, *bli-5(e518)*, *bli-6(n776)*, *sc16*), and *tsp-15(sv15)*) indicated that only *bli-3(e767)* and *tsp-15(sv15)* mutant nematodes could survive in the excess iodide [39].

It was found that three of four complementation groups were mapped to chromosome I, on which both *bli-3* and *tsp-15* locate [39]. Moreover, *mac40* is an allele of *bli-3*, *mac33* is an allele of *tsp-15*, and *mac32* represents an unknown gene (Fig. 13.7) [39]. Meanwhile, the blisters of *mac33* and *mac40* mutant nematodes resemble those of *tsp-15(sv15)* and *bli-3(e767)* mutant nematodes but are still different from the clear blisters of *bli-1(e769)* mutants (Fig. 13.7) [39]. Additionally, nematodes with RNAi knockdown of *bli-3* or *tsp-15* could survive in 5 mM NaI [39].

In nematodes, the DOXA-1, an ortholog of mammalian dual oxidase maturation factor, forms a complex with BLI-3 and TSP-15, and each component of BLI-3/TSP-15/DOXA-1 dual oxidase complex was found to be required for the development-arresting effect of excess iodide [39]. The nematodes with RNAi knockdown of *mtl-7* encoding a ShkT (Shk toxin)-domain-containing heme peroxidase were Bli but failed to survive in 5 mM NaI [39]. Meanwhile, RNAi knockdown of *mlt-7* and each *skpo* gene (*skpo-1*, *skpo-2*, or *skpo-3*) encoding other

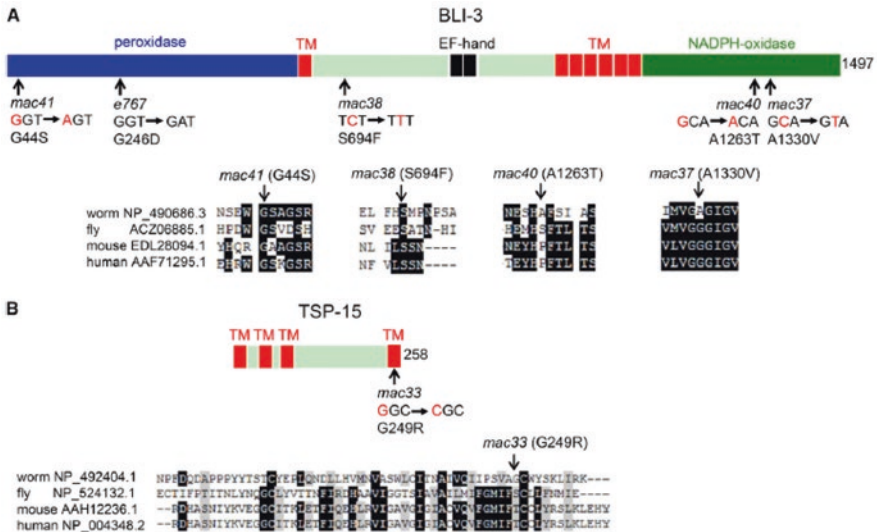


Fig. 13.7 Some *mac* mutations affect *bli-3* and *tsp-15* [39]. (a) The *mac* mutations in *bli-3* affect conserved (*mac41*, G44S; *mac38*, S694F) or nonconserved (*mac40*, A1263T; *mac37*, A1330V) amino acids in different domains of BLI-3. Nucleotide changes, amino acid changes, and BLI-3 DUOX1 partial sequence alignments of different species were presented. TM, transmembrane domain. (b) *mac33* affects a nonconserved amino acid residue in the fourth transmembrane domain of TSP-15. Nucleotide change, amino acid change, and TSP-15 partial sequence alignment were presented

ShkT-domain-containing peroxidases individually or in combination did not result in the survival phenotype in excess iodide [39], suggesting that MLT-7 and each of the SKPO proteins might not be redundantly required for development-arresting effect in response to the excess iodide.

13.5 Reverse Genetic Screen and Identification of New Genetic Loci Involved in the Regulation of Toxicity of Environmental Toxicants or Stresses

13.5.1 *Using a Certain Number of Mutants to Screen and to Identify Genetic Loci Involved in the Regulation of Toxicity of Environmental Toxicants or Stresses*

The mutant resources for nematodes are very rich, and thus, using a certain number of mutants is frequently employed to screen and to identify genetic loci involved in the regulation of toxicity of environmental toxicants or stresses [40–42]. Environmental pathogens can potentially cause the toxicity or even kill the host organisms, including the nematodes [43–50]. We here further select the pathogen infection as an example to introduce the use of mutants to screen and to identify microRNAs (miRNAs) involved in the regulation of toxicity of environmental toxicants or stresses in nematodes [51].

Using deletion mutants, a large-scale screen was performed to identify the miRNAs involved in the control of *P. aeruginosa* PA14 infection and the corresponding innate immune response [51]. Based on the phenotypic analysis of survival in miRNA mutants infected with *P. aeruginosa* PA14, totally 11 out of the examined 82 miRNA mutants with the abnormal survival phenotype were identified (Fig. 13.8) [51]. These miRNA mutants were *let-7(mg279)*, *mir-45(n4280)*, *mir-63(n4568)*, *mir-75(n4472)*, *mir-84(n4307)*, *mir-233(n4761)*, *mir-241(n4316)*, *mir-246(n4636)*, *mir-256(n4471)*, *mir-355(n4618)*, and *mir-360(n4635)* (Fig. 13.8) [51]. Loss-of-function mutation of *let-7*, *mir-45*, *mir-75*, *mir-84*, *mir-241*, *mir-246*, or *mir-256* caused a resistance to *P. aeruginosa* PA14 infection in reducing survival (Fig. 13.8) [51]. In contrast, loss-of-function mutation of *mir-63*, *mir-233*, *mir-360*, or *mir-355* resulted in a susceptibility to *P. aeruginosa* PA14 infection in reducing survival (Fig. 13.8) [51].

Colony-forming unit (CFU) was employed to determine the PA14 colony formation in the body of miRNA mutant after *P. aeruginosa* infection. After *P. aeruginosa* PA14 infection, loss-of-function mutation of *mir-63*, *mir-360*, or *mir-355* enhanced the PA14 colony formation in the body of nematodes; however, loss-of-function mutation of *mir-45*, *mir-75*, *mir-246*, or *mir-256* suppressed the PA14 colony formation in the body of nematodes (Fig. 13.9) [51].

P. aeruginosa PA14 infection can increase the transcriptional expression of antimicrobial genes. Some putative antimicrobial genes (*lys-1*, *lys-8*, *clec-85*, *dod-22*,

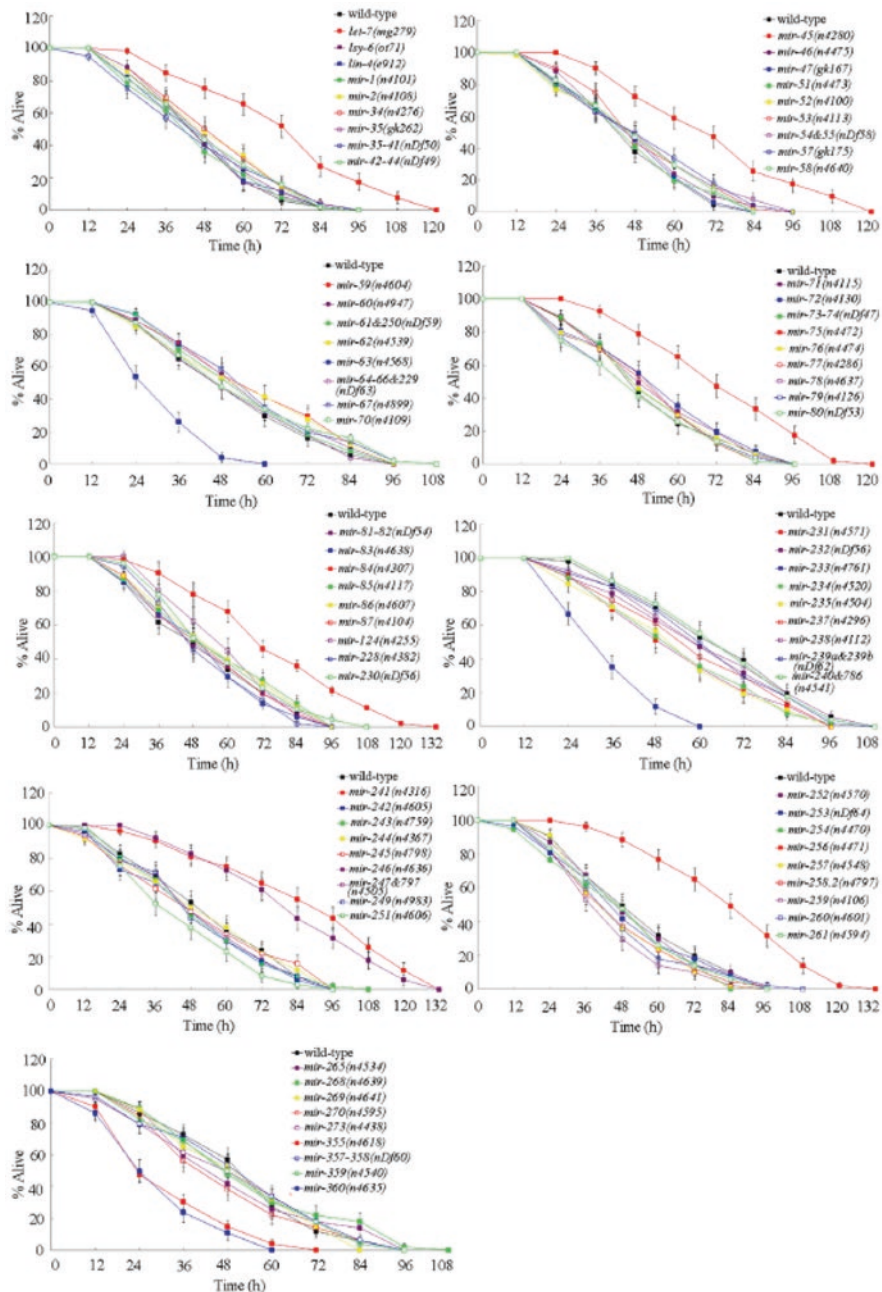


Fig. 13.8 Survival in miRNA mutants infected with *P. aeruginosa* PA14 [51]. Bars represent mean \pm SD

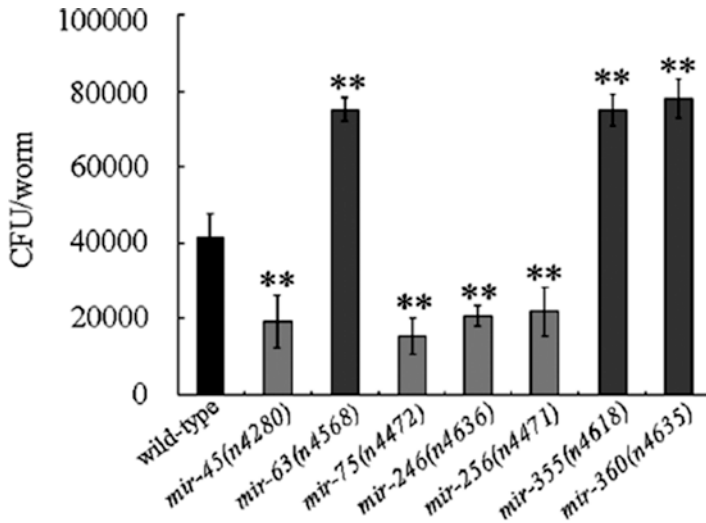


Fig. 13.9 *P. aeruginosa* PA14 CFU in the body of miRNA mutants infected with *P. aeruginosa* PA14 [51]. Bars represent mean \pm SD. ** $P < 0.01$ vs wild type

K08D8.5, *F55G11.7*, and *F55G11.4*) were selected to determine the innate immune response in *P. aeruginosa* PA14 infected miRNA mutants. *lys-1* and *lys-8* encode lysozymes, *clec-85* encodes a C-type lectin protein, *dod-22* and *F55G11.7* encode orthologs of human epoxide hydrolase 1, and *K08D8.5* and *F55G11.4* encode CUB-like domain-containing proteins. After *P. aeruginosa* PA14 infection, mutation of *mir-45* increased the expressions of *lys-8*, *clec-85*, *dod-22*, *F55G11.7*, and *F55G11.4*; mutation of *mir-75* increased the expressions of *lys-1*, *lys-8*, *dod-22*, *F55G11.7*, and *F55G11.4*; mutation of *mir-246* increased the expressions of *lys-8*, *clec-85*, *dod-22*, *K08D8.5*, and *F55G11.7*; and mutation of *mir-256* increased the expressions of *lys-1*, *lys-8*, *clec-85*, *dod-22*, and *K08D8.5* (Fig. 13.10) [51]. Different from these, mutation of *mir-63* decreased the expressions of *lys-1*, *dod-22*, *F55G11.7*, and *F55G11.4*; mutation of *mir-355* decreased the expressions of *lys-1*, *lys-8*, *K08D8.5*, *F55G11.7*, and *F55G11.4*; and mutation of *mir-360* decreased the expressions of *lys-8*, *dod-22*, *K08D8.5*, and *F55G11.7* (Fig. 13.10) [51]. These results suggest that loss-of-function mutation of these seven miRNAs alters the innate immune response of nematodes to *P. aeruginosa* PA14 infection in nematodes.

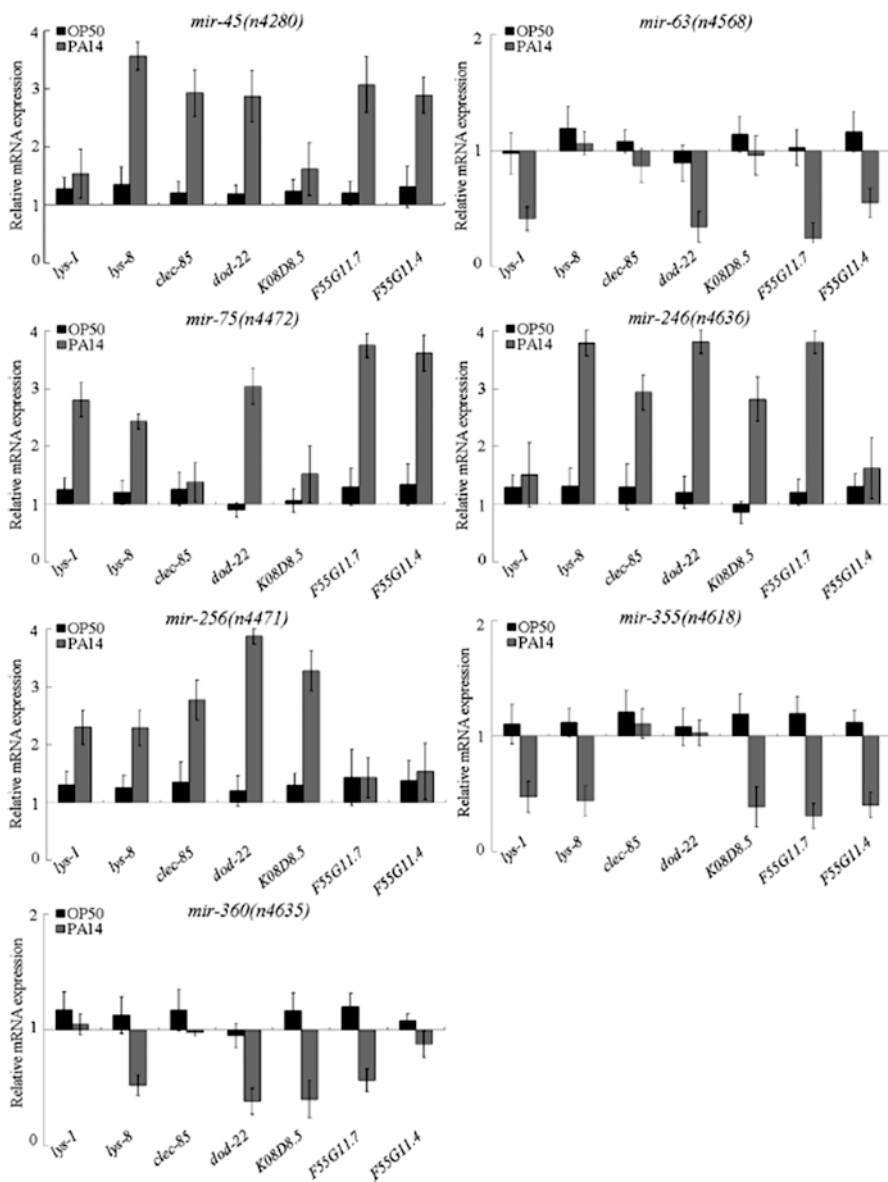


Fig. 13.10 Expression patterns of putative antimicrobial genes in *P. aeruginosa* PA14 infected miRNA mutant nematodes [51]. Normalized expression is presented relative to wild-type expression. Bars represent mean \pm SD

13.5.2 Using RNAi Knockdown Technique to Screen and to Identify Genetic Loci Involved in the Regulation of Toxicity of Environmental Toxicants or Stresses

Myotonic dystrophy disorders can be induced by expanded CUG repeats in noncoding regions. The reporter constructs without any CUG repeats in the 384-nt 3' UTR from *let-858* (0CUG) showed a strong GFP fluorescence, whereas the presence of 123 CUG repeats in the 3' UTR (123CUG) resulted in a sharp decline in GFP fluorescence [52]. Using the decline in adult-stage GFP fluorescence in 123CUG transgenic nematodes, RNAi screen was performed to identify the gene inactivations that can modify toxicity of expanded-CUG-repeat RNA [52]. After an initial fluorescence-based RNAi screen, a secondary motility-based screen of hits from the primary screen was further performed [52]. An RNAi library of 403 clones targeting genes that encode RNA-binding proteins and factors implicated in small-RNA pathways was screened. After the rescreening in triplicate, 84 gene inactivations were observed to induce an increase in late-developmental-stage GFP fluorescence in the 123CUG strain without affecting the control 0CUG strain (Fig. 13.11) [52]. Among these genes, 14 gene inactivations could further significantly increase or decrease the velocity of 123CUG animals without affecting the control (0CUG) animals (Fig. 13.11) [52].

13.6 Perspectives

No doubt, all the four introduced strategies in this chapter are powerful and effective for the screen and the identification of new genetic loci involved in the regulation of toxicity of environmental toxicants or stresses. Nevertheless, meanwhile, these strategies have certain limitations.

With the concern on the transcriptomic analysis, it has at least two aspects of limitations. Firstly, this strategy cannot reflect the alterations at the translational level. Secondly, this strategy itself cannot tell us the biological or toxicological function of candidate genes. Nevertheless, this strategy can provide us a large number of candidate genes for further consideration.

With the concern on the proteomic analysis, it has also at least two aspects of limitations. Firstly, largely due to the 2-D SDS-PAGE technical limitation, usually only very limited dysregulated proteins can be identified. Secondly, data from this strategy still need the further functional analysis and confirmation.

With the concern on the forward genetics, these two aspects should be paid attention to. On the one hand, the number of obtained candidate mutants is usually largely affected by the examined phenotype or endpoint. The subtle phenotype or sensitive endpoint may be helpful for us to obtain more candidate mutants. On the other hand, this strategy still needs the further examination on the expression of candidate genes corresponding to the obtained mutants in nematodes exposed to

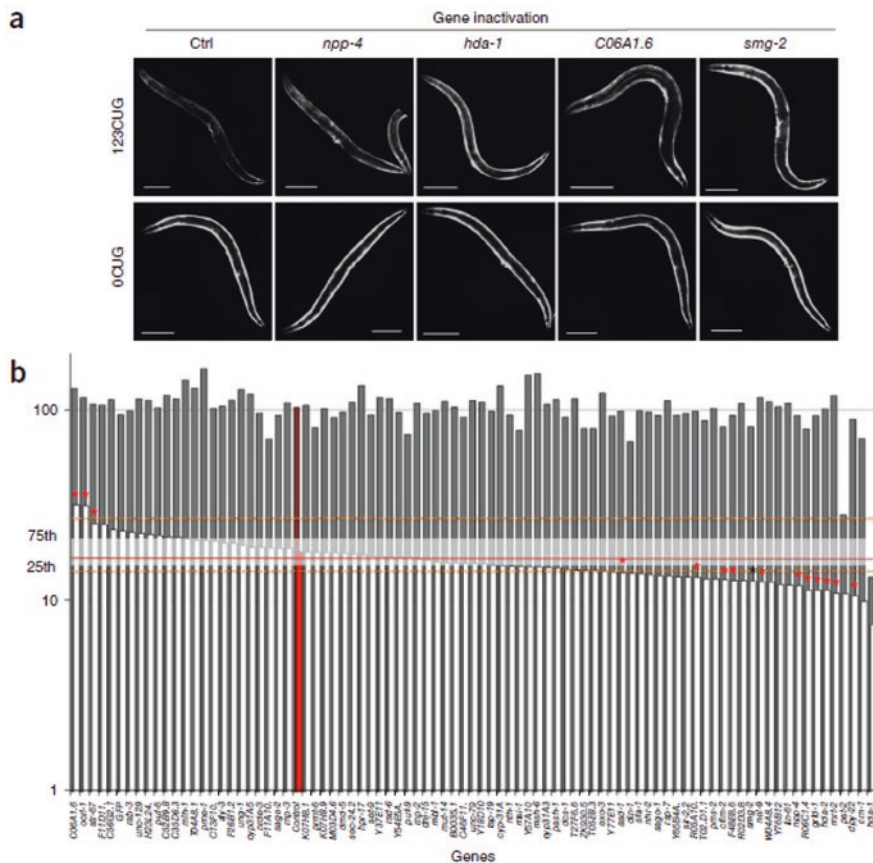


Fig. 13.11 Identification of gene inactivations that modulate expanded-CUG-repeat toxicity [52]. **(a)** Gene inactivations that disrupt the late-stage downregulation of GFP fluorescence mediated by 123CUG in the 3' UTR. Fluorescence microscopy images of the strains 123CUG and the control 0CUG, on different RNAi gene inactivations: empty vector control (ctrl), *npp-4*, *hda-1*, *C06A1.6*, and *smg-2*. Images were taken at the 3-day-old adult stage. Bar, 200 μm . **(b)** Genetic suppressors and enhancers of expanded-CUG-repeat toxicity. Graph of velocity measurements of 0CUG (gray) and 123CUG (white) animals fed on different gene inactivations. The plotted velocities (x-axis, in $\mu\text{m/s}$) correspond to the median values of three independent experiments for *aly-3*, *asd-1*, *C52B9.8*, *C06A1.6*, *cfm-2*, *dpy-2*, *F26B1.2*, *F48E8.6*, *grld-1*, *hda-1*, *hda-2*, *mrt-2*, *msh-6*, *nhr-2*, *nol-9*, *nth-1*, *pst-2*, *puf-6*, *puf-9*, *R05D10.1*, *R06C1.4*, *rmp-3*, *sago-1*, *sec-24.2*, *sfa-1*, *sir-2.2*, *smg-2*, *str-67*, *ung-1*, and *Y65B4A1* of 2 experiments for all other tested genes and of 22 experiments for control L4440. Red bars, strains fed on control vector; red line, median velocity; white shading, 25th and 75th percentiles, as indicated, for the 123CUG animals fed on control vector; dotted orange lines, maximum (upper) and minimum (lower) of the median velocity for 123CUG animals fed on control vector; and red asterisks, significant gene inactivations, as determined by Kolmogorov–Smirnov *P* value. The number of animals analyzed varied from 50 to 250 animals depending on the RNAi clone (further described in Online Methods), with a total of 1384 animals analyzed for the L4440 control. The black asterisk indicates the gene *smg-2*

environmental toxicants or stresses. The important advantage for this strategy is to be able to obtain the mutants with the anticipated phenotypes.

With the concern on the reverse genetics, it has at least two aspects of limitations. Firstly, this strategy also needs the further examination on the expression of candidate genes corresponding to the obtained mutants in nematodes exposed to environmental toxicants or stresses. Secondly, the powerfulness of this strategy to identify new genetic loci involved in the regulation of toxicity of environmental toxicants or stresses is somewhat limited. Usually, for the screened mutants, the functions of corresponding genes are already known. That is, for this strategy, a large-scale screen is suggested.

Taken together, to screen and to identify new genetic loci involved in the regulation of toxicity of environmental toxicants or stresses, we should consider both of these two aspects simultaneously. On the one hand, we hope to be able to identify candidate genetic loci with the functions in regulating the toxicity of environmental toxicants or stresses. On the other hand, we need to carefully examine the alterations in expression of these candidate genetic loci in nematodes exposed to environmental toxicants or stresses. Lacking any one aspect is not reasonable for the elucidation of underlying molecular mechanisms for the observed toxicity induced by certain environmental toxicants or stresses in nematodes.

References

1. Wang D-Y (2018) *Nanotoxicology in Caenorhabditis elegans*. Springer, Singapore
2. Qu M, Xu K-N, Li Y-H, Wong G, Wang D-Y (2018) Using *acs-22* mutant *Caenorhabditis elegans* to detect the toxicity of nanopolystyrene particles. *Sci Total Environ* 643:119–126
3. Dong S-S, Qu M, Rui Q, Wang D-Y (2018) Combinational effect of titanium dioxide nanoparticles and nanopolystyrene particles at environmentally relevant concentrations on nematodes *Caenorhabditis elegans*. *Ecotoxicol Environ Saf* 161:444–450
4. Li W-J, Wang D-Y, Wang D-Y (2018) Regulation of the response of *Caenorhabditis elegans* to simulated microgravity by p38 mitogen-activated protein kinase signaling. *Sci Rep* 8:857
5. Xiao G-S, Zhao L, Huang Q, Yang J-N, Du H-H, Guo D-Q, Xia M-X, Li G-M, Chen Z-X, Wang D-Y (2018) Toxicity evaluation of Wanzhou watershed of Yangtze Three Gorges Reservoir in the flood season in *Caenorhabditis elegans*. *Sci Rep* 8:6734
6. Xiao G-S, Zhao L, Huang Q, Du H-H, Guo D-Q, Xia M-X, Li G-M, Chen Z-X, Wang D-Y (2018) Biosafety assessment of water samples from Wanzhou watershed of Yangtze Three Gorges Reservoir in the quiet season in *Caenorhabditis elegans*. *Sci Rep* 8:14102
7. Yin J-C, Liu R, Jian Z-H, Yang D, Pu Y-P, Yin L-H, Wang D-Y (2018) Di (2-ethylhexyl) phthalate-induced reproductive toxicity involved in DNA damage-dependent oocyte apoptosis and oxidative stress in *Caenorhabditis elegans*. *Ecotoxicol Environ Saf* 163:298–306
8. Wu Q-L, Han X-X, Wang D, Zhao F, Wang D-Y (2017) Coal combustion related fine particulate matter (PM_{2.5}) induces toxicity in *Caenorhabditis elegans* by dysregulating microRNA expression. *Toxicol Res* 6:432–441
9. Starnes DL, Lichtenberg SS, Unrine JM, Starnes CP, Oostveen EK, Lowry GV, Bertsch PM, Tsyusko OV (2016) Distinct transcriptomic responses of *Caenorhabditis elegans* to pristine and sulfidized silver nanoparticles. *Environ Pollut* 213:314–321

10. Lewis JA, Gehman EA, Baer CE, Jackson DA (2013) Alterations in gene expression in *Caenorhabditis elegans* associated with organophosphate pesticide intoxication and recovery. *BMC Genomics* 14:291
11. McElwee MK, Ho LA, Chou JW, Smith MV, Freedman JH (2013) Comparative toxicogenomic responses of mercuric and methyl-mercury. *BMC Genomics* 14:698
12. Chatterjee N, Kim Y, Yang J, Roca CP, Joo S, Choi J (2016) A systems toxicology approach reveals the Wnt-MAPK crosstalk pathway mediated reproductive failure in *Caenorhabditis elegans* exposed to graphene oxide (GO) but not to reduced graphene oxide (rGO). *Nanotoxicology* 11:76–86
13. Menzel R, Yeo HL, Rienau S, Li S, Steinberg CEW, Stürzenbaum SR (2007) Cytochrome P450s and short-chain dehydrogenases mediate the toxicogenomic response of PCB52 in the nematode *Caenorhabditis elegans*. *J Mol Biol* 370:1–13
14. Lewis JA, Szilagyi M, Gehman E, Dennis WE, Jackson DA (2009) Distinct patterns of gene and protein expression elicited by organophosphorus pesticides in *Caenorhabditis elegans*. *BMC Genomics* 10:202
15. Roh J, Sim SJ, Yi J, Park K, Chung KH, Ryu D, Choi J (2009) Ecotoxicity of silver nanoparticles on the soil nematode *Caenorhabditis elegans* using functional ecotoxicogenomics. *Environ Sci Technol* 43:3933–3940
16. Eom H, Kim H, Kim B, Chon T, Choi J (2014) Integrative assessment of benzene exposure to *Caenorhabditis elegans* using computational behavior and toxicogenomic analyses. *Environ Sci Technol* 48:8143–8151
17. Menzel R, Swain SC, Hoess S, Claus E, Menzel S, Steinberg CEW, Reifferscheid G, Stürzenbaum SR (2009) Gene expression profiling to characterize sediment toxicity – a pilot study using *Caenorhabditis elegans* whole genome microarrays. *BMC Genomics* 10:160
18. Vin uela A, Snoek LB, Riksen JAG, Kammenga JE (2010) Genome-wide gene expression analysis in response to organophosphorus pesticide chlorpyrifos and diazinon in *C. elegans*. *PLoS ONE* e12145:5
19. Sahu SN, Lewis J, Patel I, Bozdag S, Lee JH, Sprando R, Cinar HN (2013) Genomic analysis of stress response against arsenic in *Caenorhabditis elegans*. *PLoS ONE* 8:e66431
20. Boehler CJ, Raines AM, Sunde RA (2014) Toxic-selenium and low-selenium transcriptomes in *Caenorhabditis elegans*: toxic selenium up-regulates oxidoreductase and down-regulates cuticle-associated genes. *PLoS ONE* 9:e101408
21. Rudgalvyte M, VanDuyn N, Aarnio V, Heikkinen L, Peltonen J, Lakso M, Nass R, Wong G (2013) Methylmercury exposure increases lipocalin related (*lpr*) and decreases activated in blocked unfolded protein response (*abu*) genes and specific miRNAs in *Caenorhabditis elegans*. *Toxicol Lett* 222:189–196
22. Cui Y, McBride SJ, Boyd WA, Alper S, Freedman JH (2007) Toxicogenomic analysis of *Caenorhabditis elegans* reveals novel genes and pathways involved in the resistance to cadmium toxicity. *Genome Biol* 8:R122
23. Tsyusko OV, Unrine JM, Spurgeon D, Blalock E, Starnes D, Tseng M, Joice G, Bertsch PM (2012) Toxicogenomic responses of the model organism *Caenorhabditis elegans* to gold nanoparticles. *Environ Sci Technol* 46:4115–4124
24. Ren M-X, Zhao L, Ding X-C, Krasteva N, Rui Q, Wang D-Y (2018) Developmental basis for intestinal barrier against the toxicity of graphene oxide. *Part Fibre Toxicol* 15:26
25. Xiao G-S, Chen H, Krasteva N, Liu Q-Z, Wang D-Y (2018) Identification of interneurons required for the aversive response of *Caenorhabditis elegans* to graphene oxide. *J Nanobiotechnol* 16:45
26. Ding X-C, Rui Q, Wang D-Y (2018) Functional disruption in epidermal barrier enhances toxicity and accumulation of graphene oxide. *Ecotoxicol Environ Saf* 163:456–464
27. Zhao L, Kong J-T, Krasteva N, Wang D-Y (2018) Deficit in epidermal barrier induces toxicity and translocation of PEG modified graphene oxide in nematodes. *Toxicol Res* 7(6):1061–1070. <https://doi.org/10.1039/C8TX00136G>

28. Shao H-M, Han Z-Y, Krasteva N, Wang D-Y (2018) Identification of signaling cascade in the insulin signaling pathway in response to nanopolystyrene particles. *Nanotoxicology in press*
29. Xiao G-S, Zhi L-T, Ding X-C, Rui Q, Wang D-Y (2017) Value of *mir-247* in warning graphene oxide toxicity in nematode *Caenorhabditis elegans*. *RSC Adv* 7:52694–52701
30. Wang Q-Q, Zhao S-Q, Zhao Y-L, Rui Q, Wang D-Y (2014) Toxicity and translocation of graphene oxide in *Arabidopsis* plants under stress conditions. *RSC Adv* 4:60891–60901
31. Zhao Y-L, Yang J-N, Wang D-Y (2016) A microRNA-mediated insulin signaling pathway regulates the toxicity of multi-walled carbon nanotubes in nematode *Caenorhabditis elegans*. *Sci Rep* 6:23234
32. Zhao Y-L, Wu Q-L, Li Y-P, Nouara A, Jia R-H, Wang D-Y (2014) In vivo translocation and toxicity of multi-walled carbon nanotubes are regulated by microRNAs. *Nanoscale* 6:4275–4284
33. Ren M-X, Zhao L, Lv X, Wang D-Y (2017) Antimicrobial proteins in the response to graphene oxide in *Caenorhabditis elegans*. *Nanotoxicology* 11:578–590
34. Zhuang Z-H, Li M, Liu H, Luo L-B, Gu W-D, Wu Q-L, Wang D-Y (2016) Function of RSKS-1-AAK-2-DAF-16 signaling cascade in enhancing toxicity of multi-walled carbon nanotubes can be suppressed by *mir-259* activation in *Caenorhabditis elegans*. *Sci Rep* 6:32409
35. Zhao Y-L, Yang R-L, Rui Q, Wang D-Y (2016) Intestinal insulin signaling encodes two different molecular mechanisms for the shortened longevity induced by graphene oxide in *Caenorhabditis elegans*. *Sci Rep* 6:24024
36. Hasegawa K, Miwa S, Isomura K, Tsutsumiuchi K, Taniguchi H, Miwa J (2008) Acrylamide-responsive genes in the nematode *Caenorhabditis elegans*. *Toxicol Sci* 101:215–225
37. Bruinsma JJ, Schneider DL, Davis DE, Kornfeld K (2008) Identification of mutations in *Caenorhabditis elegans* that cause resistance to high levels of dietary zinc and analysis using a genomewide map of single nucleotide polymorphisms scored by pyrosequencing. *Genetics* 179:811–828
38. Munoz MJ, Riddle DL (2003) Positive selection of *Caenorhabditis elegans* mutants with increased stress resistance and longevity. *Genetics* 163:171–180
39. Xu Z, Luo J, Li Y, Ma L (2015) The BLI-3/TSP-15/DOXA-1 dual oxidase complex is required for iodide toxicity in *Caenorhabditis elegans*. *G3* 5:195–203
40. Rui Q, Zhao Y-L, Wu Q-L, Tang M, Wang D-Y (2013) Biosafety assessment of titanium dioxide nanoparticles in acutely exposed nematode *Caenorhabditis elegans* with mutations of genes required for oxidative stress or stress response. *Chemosphere* 93:2289–2296
41. Ahn J, Eom H, Yang X, Meyer JN, Choi J (2014) Comparative toxicity of silver nanoparticles on oxidative stress and DNA damage in the nematode, *Caenorhabditis elegans*. *Chemosphere* 108:343–352
42. Wu Q-L, Zhao Y-L, Li Y-P, Wang D-Y (2014) Susceptible genes regulate the adverse effects of TiO₂-NPs at predicted environmental relevant concentrations on nematode *Caenorhabditis elegans*. *Nanomedicine* 10:1263–1271
43. Wu Q-L, Cao X-O, Yan D, Wang D-Y, Aballay A (2015) Genetic screen reveals link between maternal-effect sterile gene *mes-1* and *P. aeruginosa*-induced neurodegeneration in *C. elegans*. *J Biol Chem* 290:29231–29239
44. Yu Y-L, Zhi L-T, Guan X-M, Wang D-Y, Wang D-Y (2016) FLP-4 neuropeptide and its receptor in a neuronal circuit regulate preference choice through functions of ASH-2 trithorax complex in *Caenorhabditis elegans*. *Sci Rep* 6:21485
45. Sun L-M, Zhi L-T, Shakoov S, Liao K, Wang D-Y (2016) microRNAs involved in the control of innate immunity in *Candida* infected *Caenorhabditis elegans*. *Sci Rep* 6:36036
46. Sun L-M, Liao K, Li Y-P, Zhao L, Liang S, Guo D, Hu J, Wang D-Y (2016) Synergy between PVP-coated silver nanoparticles and azole antifungal against drug-resistant *Candida albicans*. *J Nanosci Nanotechnol* 16:2325–2335
47. Sun L-M, Liao K, Hong C-C, Wang D-Y (2017) Honokiol induces reactive oxygen species-mediated apoptosis in *Candida albicans* through mitochondrial dysfunction. *PLoS ONE*. 2017 12:e0172228

48. Sun L-M, Liao K, Wang D-Y (2017) Honokiol induces superoxide production by targeting mitochondrial respiratory chain complex I in *Candida albicans*. PLoS ONE 12:e0184003
49. Zhi L-T, Yu Y-L, Li X-Y, Wang D-Y, Wang D-Y (2017) Molecular control of innate immune response to *Pseudomonas aeruginosa* infection by intestinal *let-7* in *Caenorhabditis elegans*. PLoS Pathog 13:e1006152
50. Yu Y-L, Zhi L-T, Wu Q-L, Jiang L-N, Wang D-Y (2018) NPR-9 regulates innate immune response in *Caenorhabditis elegans* by antagonizing activity of AIB interneurons. Cell Mol Immunol 15:27–37
51. Zhi L-T, Yu Y-L, Jiang Z-X, Wang D-Y (2017) *mir-355* functions as an important link between p38 MAPK signaling and insulin signaling in the regulation of innate immunity. Sci Rep 7:14560
52. Garcia SMDA, Tabach Y, Lourenço GF, Armakola M, Ruvkun G (2014) Identification of genes in toxicity pathways of trinucleotide-repeat RNA in *C. elegans*. Nat Struct Mol Biol 21:712–720

Chapter 14

Molecular Basis for Adaptive Response to Environmental Toxicants or Stresses



Abstract In nematodes, pretreatment with a mild stress or toxicant will induce an adaptive response to the following severe environmental toxicant or stress. In this chapter, we introduced the molecular alterations during the formation of adaptive response and the relevant molecular signaling pathways involved in the regulation of adaptive response induction. The future research focuses were further suggested and discussed.

Keywords Molecular basis · Adaptive response · *Caenorhabditis elegans*

14.1 Introduction

In nematode *Caenorhabditis elegans*, various environmental toxicants or stresses can potentially cause the toxic effects on different aspects on animals [1–14]. In the environment, it is further observed that pretreatment with a mild stress or toxicant can induce an adaptive response for nematodes against the following severe toxicity of same or different environmental toxicant or stress [15]. The related information has been summarized in a review [15]. In nematodes, the adaption has been widely investigated in response to same or different environmental toxicant or stress [16–18].

In this chapter, we first introduced the molecular alterations during the formation of adaptive response. Moreover, we introduced and discussed the relevant molecular signaling pathways involved in the regulation of adaptive response induction. The obtained information so far provides important clues for the further elucidation of the underlying mechanism for this complex response behavior in nematodes.

14.2 Molecular Alterations During the Formation of Adaptive Response

In nematodes, pretreatment with methylmercury (MeHg) could render the nematodes more resistant to the subsequent exposure to the toxicant [19]. Meanwhile, it was observed that all the expressions of *gst-4::GFP*, *hsp-4::GFP*, *mtl-1::GFP*, and *mtl-2::GFP* could be further significantly increased to different degrees during the formation of adaptive response (Fig. 14.1) [19]. That is, some protective responses,

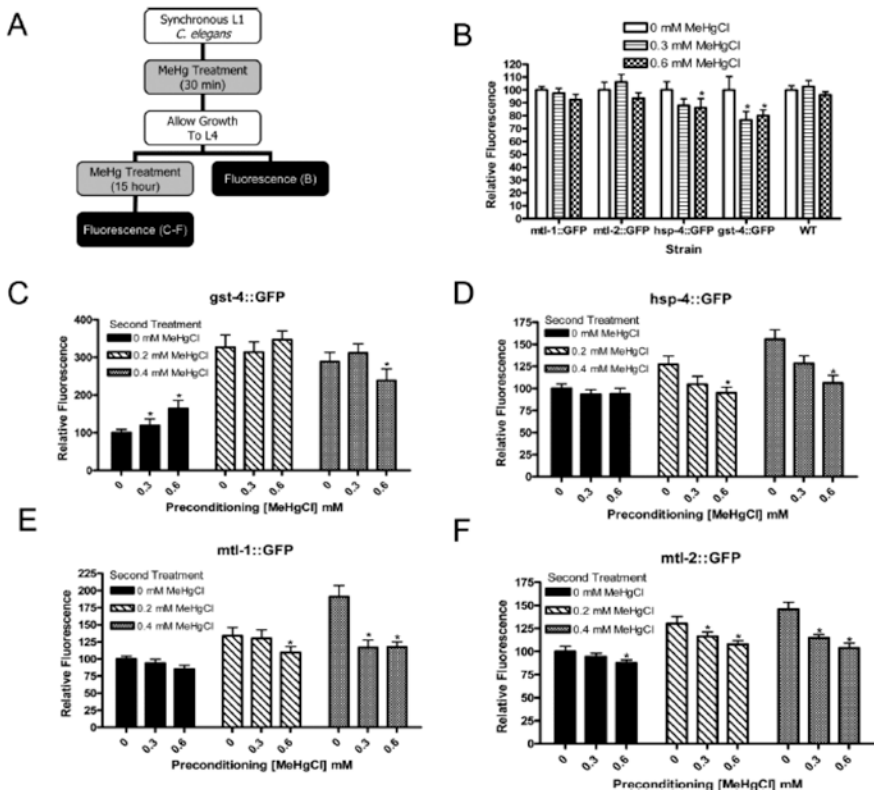


Fig. 14.1 Fluorescence of *gst-4::GFP*, *hsp-4::GFP*, *mtl-1::GFP*, and *mtl-2::GFP* strains following hormesis treatments [19]. Treatment paradigm includes animals treated at the L1 stage for 30 min, allowed to grow to the L4 stage, assessed for fluorescence or treated again, and assessed for fluorescence after second treatment (a). Decreases were noted in fluorescence in *gst-4::GFP* and *hsp-4::GFP* animals after a single treatment and recovery (B, $n = 4$). After an initial treatment with MeHg and subsequent exposure to control treatment conditions, *gst-4::GFP* animals showed an increase in fluorescence ($p < 0.05$). At higher subsequent MeHg levels and in all conditions of *hsp-4::GFP*, *mtl-1::GFP*, and *mtl-2::GFP* worms, only decreases in fluorescence at increasing MeHg concentrations were noted (C-F, $n = 4$)

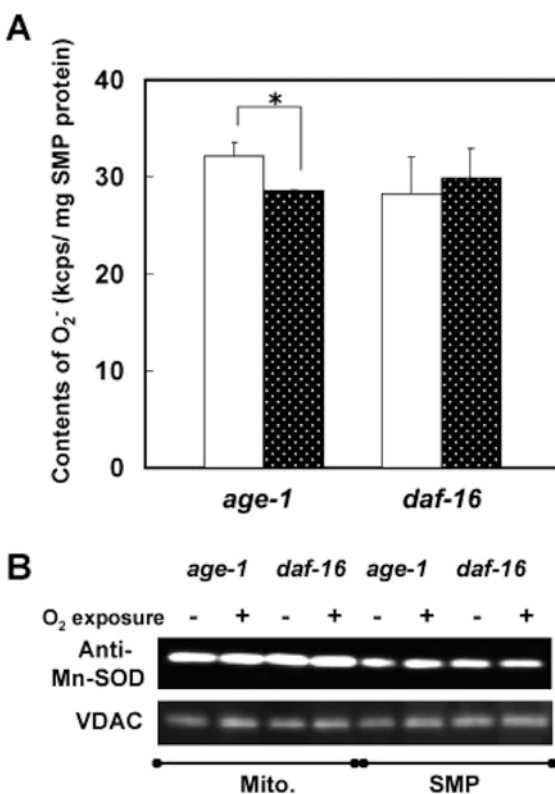
at least including the UPR response, can be activated during the pretreatment with mild stress in nematodes.

14.3 Molecular Signaling Pathways Involved in the Regulation of Adaptive Response Induction

14.3.1 Insulin Signaling Pathway

In nematodes, it was found that the oxidative stress resistance in nematodes with the mutation of *age-1* encoding a kinase in the insulin signaling pathway was associated with the adaptive response induction [20]. For the underlying mechanism, it was observed that the mitochondrial superoxide radical ($\cdot\text{O}_2^-$) level was decreased by *age-1* mutation in nematodes after intermittent hypoxia exposure (Fig. 14.2) [20]. This reduction in $\cdot\text{O}_2^-$ level could be even detected if the mitochondrial Mn-SODs were reduced (Fig. 14.2) [20]. In contrast, no alteration in $\cdot\text{O}_2^-$ level could be detected in nematodes with mutation of *daf-16* encoding a FOXO transcriptional

Fig. 14.2 $\cdot\text{O}_2^-$ contents in SMP fractions of *age-1* and *daf-16* strains [20]. (a) Left-hand open bar for each strain indicates $\cdot\text{O}_2^-$ level in SMP without daily exposure to hypoxia, and right-hand shaded bar indicates levels with exposure. (b) Contents of VDAC and Mn-SOD proteins were confirmed in mitochondrial and SMP fractions by Western blot analysis



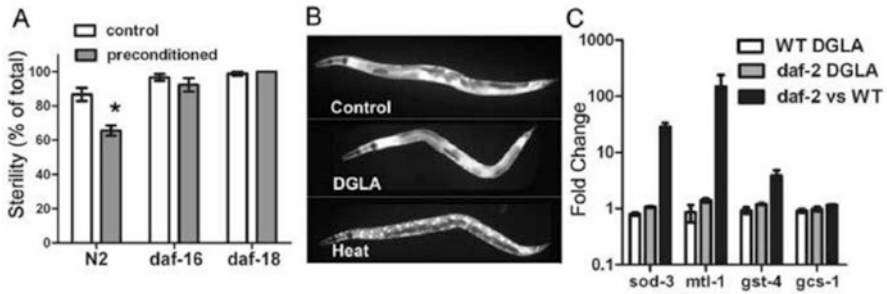


Fig. 14.3 Preconditioning suppresses germ cell loss [21]. (a) Synchronized L1 worms were raised on standard NGM plates to the eight-cell gonad stage, then preconditioned with a mild heat stress of 35 °C for 25 min, and plated on 0.25 mM DGLA-supplemented plates until worms reach adulthood. Graph displays the percentage of sterile worms in the population. (b) DAF-16::GFP transgenic worms show no noticeable GFP nuclear localization when fed a DGLA-supplemented diet from L1 through adulthood (DGLA), indistinguishable from the unsupplemented control. Heat stress preconditioning positive control (heat) shows strong nuclear localization of DAF-16::GFP. (c) Quantitative real-time RT-PCR analysis of targets of DAF-16 (*mtl-1* and *sod-3*) and targets of SKN-1 (*gcs-1* and *gst-4*). WT DGLA and *daf-2* DGLA represent the fold change of worms when grown on 0.3 mM DGLA compared to the same strains grown on unsupplemented plates. Error bars, SEM

factor in the insulin signaling pathway after intermittent hypoxia exposure (Fig. 14.2) [20]. Meanwhile, no difference in contents of VDAC, a mitochondrial membrane marker, was detected between hypoxia exposure and without exposure (Fig. 14.2) [20]. Therefore, the induction of adaptive response may be mediated by the suppression in mitochondrial $\cdot\text{O}_2^-$ production in nematodes.

In nematodes, it was also observed that pretreatment with a mild heat stress (35 °C for 25 min) could suppress the induction of sterility by treatment with dihomo-gamma-linolenic acid (DGLA) (an omega-6 fatty acid, 0.25 mM) (Fig. 14.3) [21]. Meanwhile, pretreatment with a mild heat stress induced the obvious nuclear localization of DAF-16::GFP; however, DGLA treatment alone did not obviously affect the localization of DAF-16::GFP (Fig. 14.3) [21]. In the insulin signaling pathway, mutation of *daf-16* or *daf-18* disrupted this induction of adaptive response to DGLA treatment (Fig. 14.3) [21]. In contrast, mutation of *daf-2* could increase the expressions of *daf-16*-targeted genes (*sod-3* and *mtl-1*) and *skn-1*-targeted gene (*gst-4*) in DGLA-exposed nematodes (Fig. 14.3) [21].

Similarly, it was also observed that pretreatment with isoamyl alcohol (IAA) or acetic acid (AA) odor could induce an adaptive response to the aging stress, and this induction of adaptive stress was suppressed by mutation of *daf-16* (Fig. 14.4) [22]. Meanwhile, pretreatment with IAA or AA odor could significantly increase the expressions of targeted genes (*sod-3*, *hsp-12.6*, *hsp-16.2*, and *hsp-70*) of DAF-16 or HSF-1 under the odor stimuli in nematodes [22].

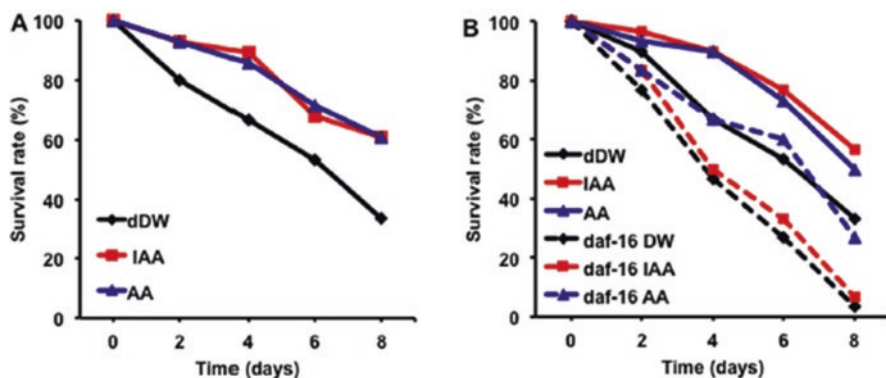


Fig. 14.4 Lifespan of worms stimulated by odor of isoamyl alcohol (IAA) or acetic acid (AA) [22]. (a) Age-synchronized L1 larvae were transferred onto nematode growth medium (NGM) plates seeded with OP50 and cultured at 20 °C for 72 h. After 3 days of culture, the worms were exposed to odor stimulus and cultured at 20 °C for 24 h. Subsequently, the worms were transferred onto NGM plates dribbled with 100 μ L OP50 and cultured at 37 °C for 3.5 h (20 worms/plate). After heat stress treatment, the odor stimulus was given again, and the plates were cultured at 20 °C. The number of living individuals was counted every 2 days. Statistical significance was analyzed with the log-rank test ($N = 60$). $*p < 0.05$. (b) Age-synchronized wild-type or *daf-16* mutant L1 larvae were transferred onto NGM plates seeded with OP50 and cultured at 20 °C for 72 h. After 3 days of culture, the worms were exposed to odor stimulus and cultured at 20 °C for 24 h. Next, the worms were transferred onto NGM plates dribbled with 100 μ L OP50 and cultured at 37 °C for 3.5 h (20 worms/plate). After heat stress treatment, the odor stimulus was given again, and the plates were cultured at 20 °C. The number of living individuals was counted every 2 days. Statistical significance was analyzed with the log-rank test ($N = 60$). $*p < 0.05$. *dDW* double-distilled water

14.3.2 *SKN-1/Nrf*

In nematodes, pretreatment with mild H_2O_2 could induce an adaptive response to the subsequent toxicity of severe H_2O_2 exposure in reducing the survival [23]. It was observed that the pretreatment with mild H_2O_2 could induce the accumulation of SKN-1::GFP in intestinal nuclei (Fig. 14.5) [23]. Mutation of *skn-1* inhibited this induction of adaptive response to H_2O_2 exposure in reducing the survival (Fig. 14.5) [23]. Additionally, pretreatment with mild H_2O_2 could increase the expression of *pas-7*, one of the targeted genes of *skn-1*, whereas mutation of *skn-1* inhibited this *pas-7* increase in H_2O_2 -exposed nematodes (Fig. 14.5) [23].

14.3.3 *ERK MAPK Signaling Pathway*

In nematodes, pretreatment with UVB or IR can induce an adaptive response to the subsequent treatment with heat shock (HS, 35 °C) (Fig. 14.6) [24]. Mutation of *pmk-1* encoding a p38 MAPK or *jnk-1* encoding a JNK MAPK did not affect this

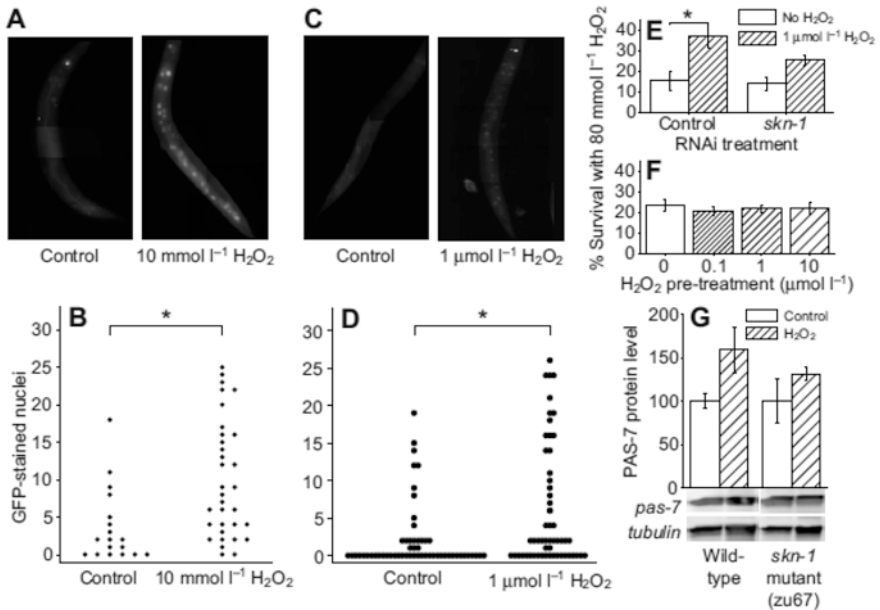


Fig. 14.5 Role of SKN-1 in regulating the adaptive response to H_2O_2 exposure [23]. (a) Pretreatment with 10 mM H_2O_2 causes an adaptive increase in SKN-1 nuclear localization. Representative images of L4 stage worms expressing an SKN-1::GFP transgene (*idIS7*) in intestinal nuclei following treatment with 10 mM H_2O_2 . (b) Quantification of the number of fluorescent nuclei observed per worm following 10 mM H_2O_2 treatment ($N = 20\text{--}30$ worms). (c) Treatment with 1 μM H_2O_2 also causes an adaptive increase in SKN-1::GFP nuclear fluorescence. Worms were prepared as in (a), except worms were treated with 1 μM H_2O_2 . (D) Quantification of the number of fluorescent nuclei observed per worm following 1 μM H_2O_2 treatment ($N = 50\text{--}60$ worms). (E) RNAi knockdown of SKN-1 blunts the pretreatment-induced adaptive increase in oxidative stress tolerance. Percentage survival of either control or *skn-1* RNAi-treated worms was measured following H_2O_2 pretreatment and challenge. (F) *skn-1(zu67)* mutants do not appear to have an H_2O_2 pretreatment-induced adaptive increase in oxidative stress tolerance. Adult *skn-1* mutant worms were pretreated and subsequently challenged with H_2O_2 . (G) H_2O_2 pretreatment causes a *skn-1*-dependent adaptive increase in 20S subunit protein abundance, which is blunted in *skn-1(zu67)* mutants. Shown are representative Western blots and quantification of PAS-7 protein abundance in wild-type or *skn-1* mutants 24 h after pretreatment with 1 μM H_2O_2 and in controls. Values are plotted as means (normalized to tubulin) \pm SEM, $N = 3$. Values marked with an asterisk indicate statistically significant differences ($P \leq 0.05$) compared with controls using Student's *t*-test

induction of adaptive response (Fig. 14.6) [24]. In contrast, mutation of *mpk-1* encoding an ERK MAPK in the ERK MAPK signaling pathway suppressed this induction of adaptive response (Fig. 14.6) [24]. Moreover, it was observed that pretreatment with IR significantly increased the expression of phospho-ERK, and mutation of *mpk-1* blocked this induction (Fig. 14.6) [24].

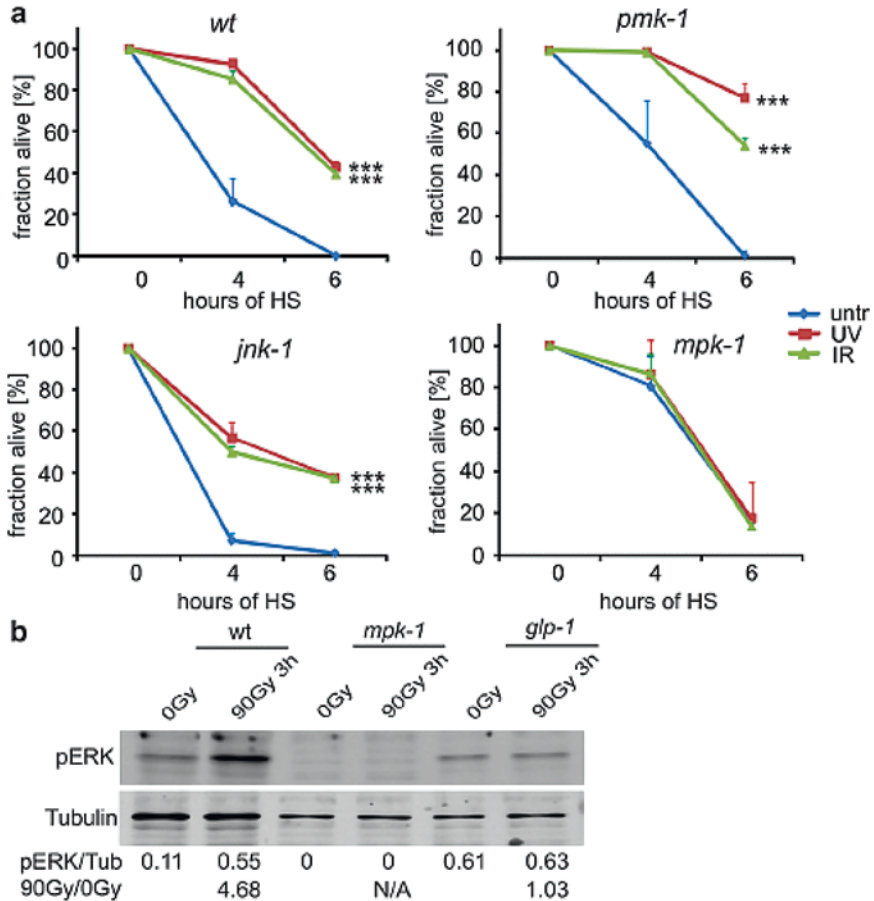


Fig. 14.6 Stress resistance induced by germline DNA damage is mediated through MPK-1 [24]. (a) L4 larvae were exposed to 520 mJ/cm² UVB or 90 Gy IR and subjected to heat stress. (b) Worms were grown at 25 °C and IR treated on day 1 of adulthood. Respective phospho-ERK signal was compared to tubulin. (Error bars = SD. In (a, b) *n* ≥ 100 for each experimental condition; ****P* < 0.0001, log-rank test)

14.3.4 Apoptosis Signaling Pathway

The core apoptosis signaling pathway contains CED-9/Bcl2, CED-4/Apaf1, and CED-3/Casp9, which can be triggered by CED-13, an alternative BH3-only protein. In nematodes, it was observed that pretreatment with paraquat (0.1 mM) could induce an adaptive response for nematodes against the following aging stress (Fig. 14.7) [25]. Moreover, it was found that mutation of *ced-4*, *ced-3*, or *ced-9* disrupted this induction of adaptive response against the aging stress (Fig. 14.7) [25]. In contrast, mutation of *ced-13* or *egl-1* did not affect this induction of adaptive

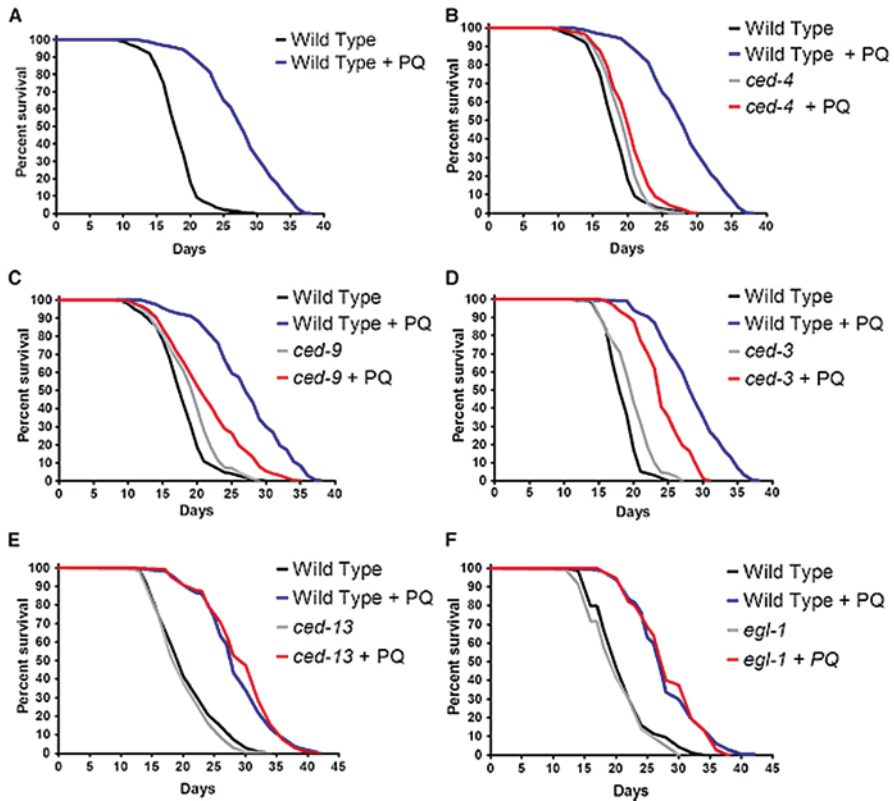


Fig. 14.7 Lifespan extension by 0.1 mM paraquat (PQ) requires the intrinsic apoptosis pathway [25]. (a) Effect of 0.1 mM PQ treatment on the wild type. (b–f) Effects of 0.1 mM PQ treatment on: (b) *ced-4*(n1162), (c) *ced-9*(n1950 *gf*), (d) *ced-3*(n717), (e) *ced-13*(sv32), and (f) *egl-1*(n1084n3082)

response against the aging stress (Fig. 14.7) [25]. These observations suggest the involvement of core apoptosis signaling pathway in the regulation of adaptive response in nematodes.

14.3.5 Catalases and RNA Interference

It was found that pretreatment with a mild H_2O_2 could induce a thermotolerance, a certain form of adaptive response [26]. In nematodes, *ctl-2* encodes a catalase, a peroxisomal enzyme involved in the H_2O_2 elimination, and mutation of *ctl-2* could suppress the induction of this adaptive response (Fig. 14.8) [25]. Meanwhile, mutation of *dcr-1* encoding an ortholog of Dicer required for the RNA interference did not affect the induction of this adaptive response, and inhibited the function of

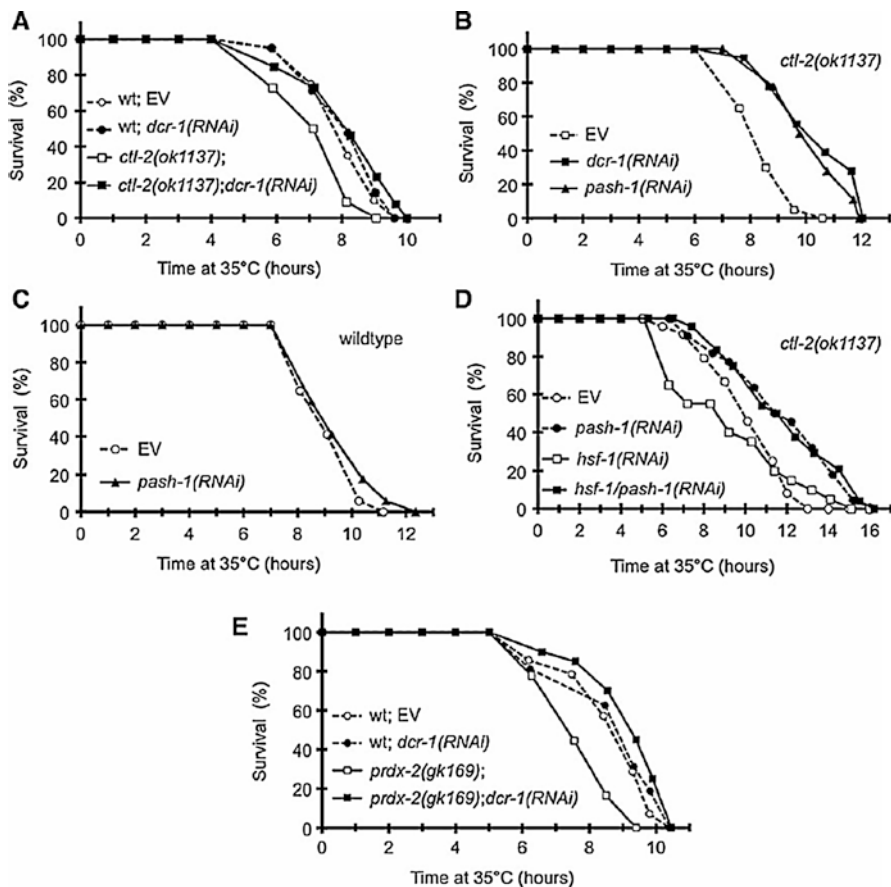


Fig. 14.8 Loss of RNA interference rescues thermotolerance in nematodes with genetic defects of H_2O_2 disposal [26]. (a) Effect of *dcr-1(RNAi)* on thermotolerance of N2 and *ctl-2(ok1137)* worms. *ctl-2(ok1137)* worms exhibited significantly shorter survival ($p < 0.001$), while other survivals were not significantly different ($p > 0.2$), compared to N2 control. (b) *pash-1(RNAi)* phenocopies *dcr-1(RNAi)* by inducing a significant increase in thermotolerance of *ctl-2(ok1137)* ($p < 0.0001$) compared to that of the EV control. (c) *pash-1(RNAi)* does not change thermotolerance of wild-type worms ($p > 0.1$) compared to that of the EV control. (d) *pash-1(RNAi)* extends thermotolerance independently of *hsf-1* in *ctl-2(ok1137)* worms [$p < 0.01$ vs. *pash-1/hsf-1(RNAi)*]. (e) Effect of *dcr-1(RNAi)* on thermotolerance of N2 and *prdx-2(gk169)* worms. *prdx-2(gk169)* worms fed by EV exhibited significantly shorter ($p < 0.0001$), while those fed by *dcr-1(RNAi)* exhibited slightly longer survival ($p < 0.05$) compared to N2 control. Survival curves are representatives of three independent experiments giving similar results

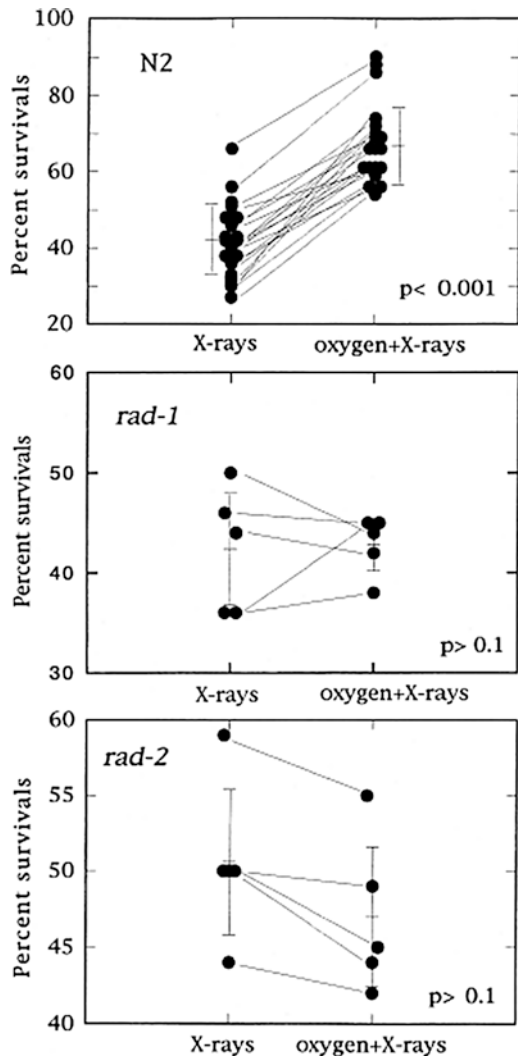
ctl-2 mutation in suppressing the induction of adaptive response (Fig. 14.8) [25], suggesting that CTL-2 acts upstream of DCR-1 to regulate the induction of adaptive response. Similarly, *pash-1(RNAi)* with the function to phenocopy the *dcr-1(RNAi)* also inhibited the function of *ctl-2* mutation in suppressing the induction of adaptive response (Fig. 14.8) [25]. Therefore, various mild environmental toxicants- or

stresses-activated oxidative stress may induce the adaptive response to the subsequent toxicant or stress by modulating the RNA interference event in nematodes.

14.3.6 RAD-1 and RAD-2

In nematodes, pretreatment with oxygen could confer an adaptive response for nematodes against the lethality imposed by the subsequent X-irradiation (Fig. 14.9) [27]. The mutants of *rad-1* and *rad-2* were susceptible to the UV and ionizing

Fig. 14.9 Sensitivity of wild-type N2, *rad-1* and *rad-2* to X-rays with and without pre-exposure to 90% of oxygen for 1 h [27]. N2, *rad-1* and *rad-2* strains were irradiated at a dose of 300, 100 and 60 Gy, respectively. Doses of X-rays were chosen to give an approximately equal survival in the two mutants and the wild-type animals. Vertical bars represent standard deviations. A total of 40–190 animals were scored for each experiment. The circles represent the range of experimental values obtained for percent survival in a series of repeat experiments. Student's *t*-test was used in statistical comparisons



radiation, but not to the oxygen, and these two mutant nematodes did not show the induction of this adaptive response (Fig. 14.9) [27]. Moreover, it was found that treatment with oxygen could increase the expression of two heat shock protein genes (*hsp16-1* and *hsp16-48*); however, mutation of *rad-1* or *rad-2* caused the decrease in the expression of these two genes [27], which implies that mutation of *rad-1* or *rad-2* may be attributed to inappropriate gene expression for the induction of adaptive response.

14.3.7 Metallothioneins (MTs)

In nematodes, it was observed that pretreatment with a mild heat-shock at L2-larva stage could effectively prevent the formation of neurobehavioral defects in metal (Pb) exposed nematodes at concentrations of 50 and 100 mM [28]. During the formation of adaptive response, the induction of *mtl-1* and *mtl-2* promoter activity and subsequent GFP expression were sharply increased in Pb (50 or 100 mM) exposed *Pmtl-1::GFP* and *Pmtl-2::GFP* transgenic adult nematodes after mild heat-shock treatment compared with those treated with mild heat-shock or metal exposure alone (Fig. 14.10) [28].

In nematodes, after pretreatment with a mild heat-shock, no noticeable increase of locomotion behaviors could be observed in Pb exposed *mtl-1* or *mtl-2* mutant nematodes (Fig. 14.11) [28], suggesting the crucial role of MTs in the regulation of induction of adaptive response. To confirm the crucial role of MTs in regulating the induction of adaptive response, rescue assays were performed. It was found that the defects of adaptive response to neurobehavioral toxicity induced by Pb exposure formed in *mtl-1* and *mtl-2* mutants could be rescued by the expression of *mtl-1* and *mtl-2* with the aid of their native promoters (Fig. 14.11) [28]. The overexpression of MTL-1 and MTL-2 at the L2-larval stage could suppress the toxicity on locomotion behaviors in Pb exposed nematodes [28], which further demonstrates the important protective function of MTs for nematodes.

14.3.8 20S Proteasome

During the induction of adaptive response to H₂O₂ exposure, pretreatment of mild H₂O₂ could increase the expression of PAS-7, a 20S proteasome subunit, but not the RPN-10, proteasome regulatory particle non-ATPase-like 10, a key component of the 26S proteasome (Fig. 14.12) [23], suggesting that the 20S but not the 26S proteasome may be involved in the regulation of adaptive response induction. Moreover, RNAi knockdown of other genes (*pas-5*, *pbs-3*, *pbs-5*, and *pbs-6*) encoding the 20S proteasome could further suppress the induction of adaptive response to the toxicity of H₂O₂ exposure in reducing survival (Fig. 14.12) [23],

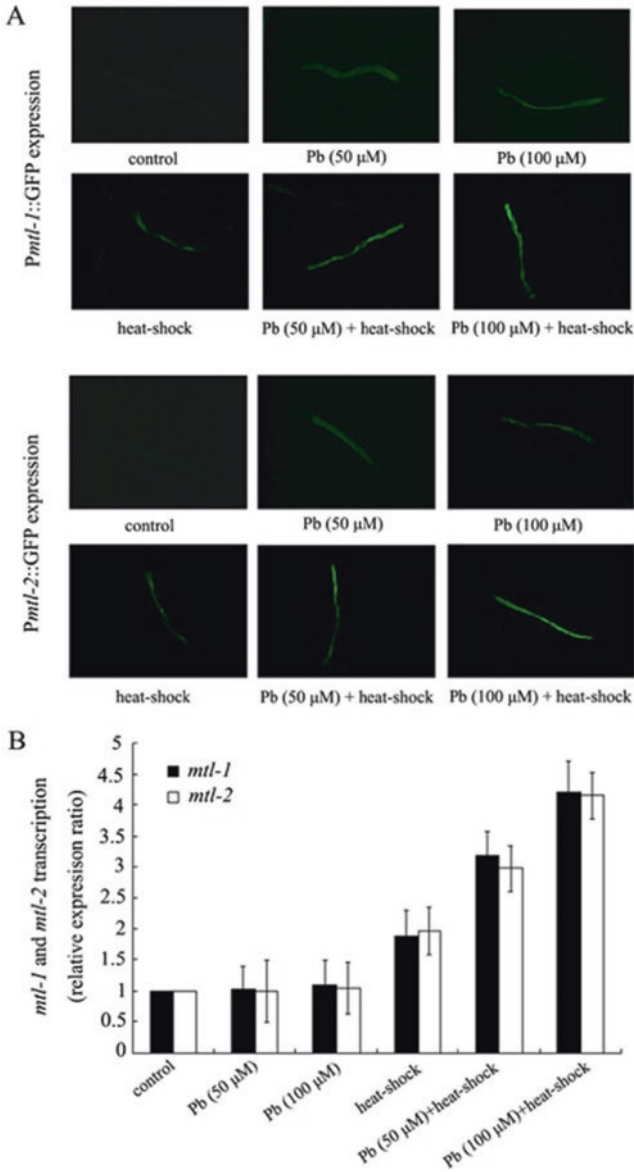


Fig. 14.10 Induction of metallothionein gene expression during the formation of cross-adaptation response to neurobehavioral toxicity induced by Pb exposure [28]. (a) Induction of green fluorescence protein in the *Pmlt-1::GFP* and *Pmlt-2::GFP* transgenic nematodes. (b) *mtl-1* and *mtl-2* transcription assay. Relative expression ratio (between *mtl-1* or *mtl-2* gene and *ubq-1* reference gene) in treatments are normalized to the control. L2-stage larvae animals were heat stressed for 1 h at 36 °C. The exposed metal concentrations were 50 and 100 mM. Bars represent means \pm S.D

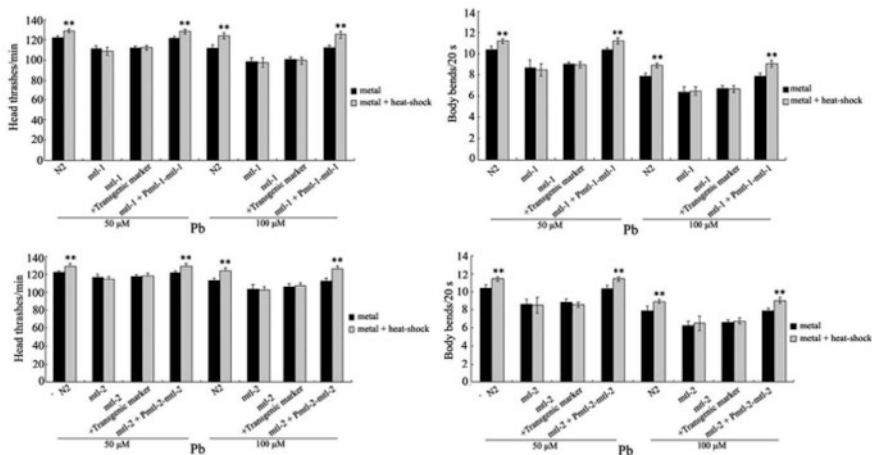


Fig. 14.11 The defects of adaptive response to neurobehavioral toxicity induced by Pb exposure in *mtl-1(tm1770)* and *mtl-2(gk125)* mutants can be rescued by the expression of *mtl-1* and *mtl-2* with their native promoters [28]. L2-stage larvae animals were heat stressed for 1 h at 36 °C. The exposed metal concentrations were 50 and 100 mM. The plasmids were injected as a mix at 20 ng/ml using *Pdop-1::rfp* as a transgenic marker. Bars represent means 6 S.D. ** $p < 0.01$ vs metal

which further supports the important role of 20S proteasome in the regulation of adaptive response induction in nematodes.

14.3.9 HPL-2 and Endoplasmic Reticulum Unfolded Protein Response (ER UPR)

In nematodes, a mild ER stress could protect against the subsequent acute stress (Fig. 14.13) [29]. HPL-2, homolog of heterochromatin protein 1 (HP1), downregulated the UPR in the intestine, and this induction of adaptive response could not be observed in *hpl-2* mutant nematodes (Fig. 14.13) [29]. One of the underlying mechanisms is that the inactivation of HPL-2 already resulted in an enhanced resistance to the ER stress [29]. Another possible underlying mechanism is that mutation of *hpl-2* was associated with the increase in expressions of XBP-1 and ER chaperone under physiological conditions [29]. Meanwhile, it was observed that the ER stress preconditioning induced the increase in expressions of UPR reporters of both *hsp-4p::GFP* and *ckb-2p::GFP* (Fig. 14.13) [29]. These results suggest the important roles of HPL-2 and ER UPR in inducing the adaptive response in nematodes.

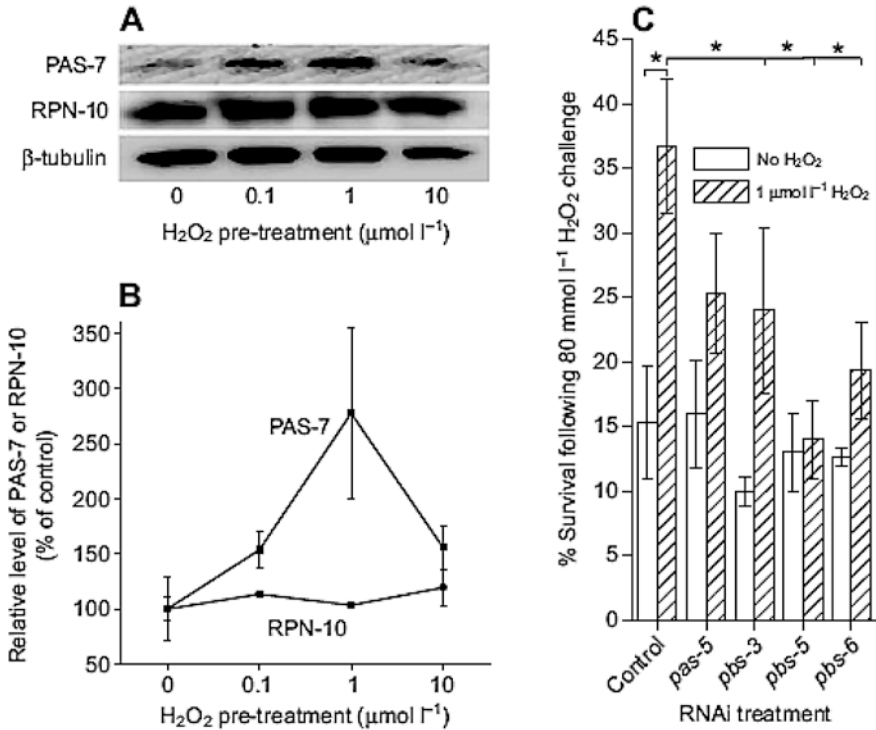


Fig. 14.12 Role of 20S proteasome in the regulation of adaptive response to H_2O_2 [23]. (a) H_2O_2 pretreatment causes an adaptive increase in the expression of the 20S proteasome (PAS-7) but not the 26S proteasome (19S regulator RPN-10). Triplicate samples of N2 worms were pretreated with the indicated concentrations of H_2O_2 . Worms were then lysed 24 h later, and the lysate was analyzed by Western blotting. (b) Samples were prepared as in (a), in triplicate. Values are plotted as means (normalized to β -tubulin) \pm SEM, $N = 3$. (c) Blocking the H_2O_2 -induced adaptive increase in the 20S proteasome blunts the pretreatment-induced increase in oxidative stress tolerance. Worms were cultured on the indicated RNA interference (RNAi) plates for 6 h and then pretreated with $1 \mu\text{M}$ H_2O_2 for 1 h, after which worms were returned to RNAi plates for 24 h. Worms were then challenged with H_2O_2 , and survival was scored. All values are means \pm SEM, $N = 3$. Values marked with an asterisk indicate statistically significant differences ($P \leq 0.05$) using Student's t -test

14.3.10 Germline Signals

It was found that no elevated heat stress resistance upon UV or IR pretreatment could be formed in germline-less *glp-1* mutant nematodes (Fig. 14.14) [24]. Meanwhile, pretreatment with IR significantly increased the expression of phospho-ERK, and mutation of *glp-1* blocked this induction (Fig. 14.6) [24], which suggests that the stress resistance induced by germline DNA damage is mediated through the function of MPK-1 in ERK MAPK signaling pathway.

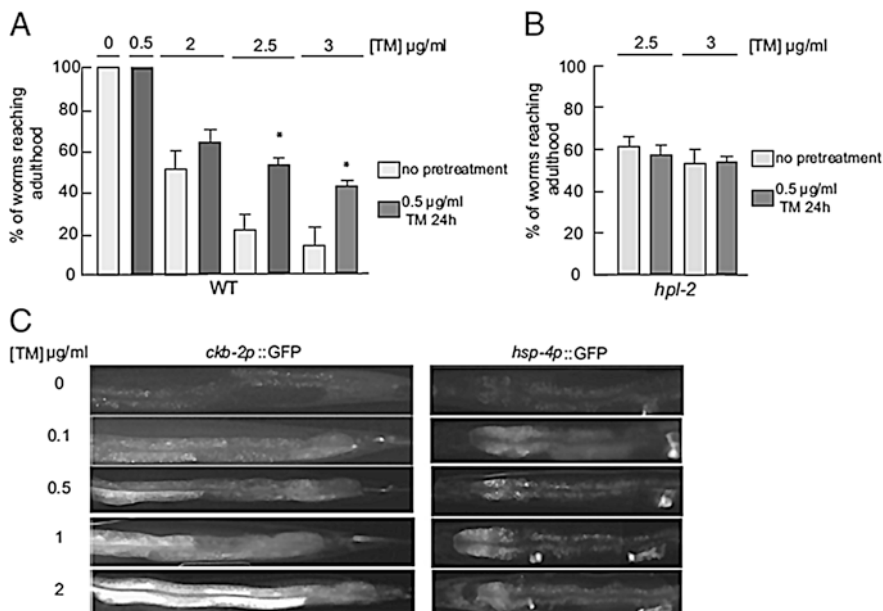


Fig. 14.13 Mild ER stress protects against subsequent acute stress [29]. (a) WT young adult worms were grown on plates containing sublethal doses of TM (0.5 µg/mL, pretreatment) or control plates without TM (no pretreatment) for 24 h and then transferred onto fresh plates containing the indicated concentrations of TM and allowed to lay eggs. The graph represents the mean of three independent experiments. Two-way ANOVA with factor treatment (various doses of TM) and pretreatment (none vs 0.5 µg/mL TM) (**P* value ≤0.05). (b) Preconditioning does not further enhance survival of *hpl-2* animals. (c) ER stress preconditioning induces the UPR. Animals expressing *hsp-4p::GFP* and *ckb-2p::GFP* UPR reporters were treated with the indicated dose of TM for 24 h and observed with a Zeiss AxioPlan. For both reporters, strongest expression was observed in the intestine. All images were taken with the same exposure time using MetaMorph software. Individual panels were assembled from two or more images using Adobe Photoshop.

In nematodes, pathogen infection can potentially cause the toxicity and the innate immune response as indicated by the alterations in antimicrobial proteins [30–35]. It was further observed that the gene expression changes upon the UV and the IR were significantly correlated with the alteration in pathogen infection-induced transcriptomes (Fig. 14.14) [24], implying the possible similarities between the DNA damage and the innate immune responses. Both the *glp-1* and the *mpk-1* mutations failed to induce their expression following the UV or the IR treatment (Fig. 14.14) [24]. Meanwhile, these immune factors could be strongly induced in the germlines isolated from UV and IR treated nematodes (Fig. 14.14) [24]. Therefore, the DNA damage-induced MPK-1 activation in germline may lead to the induction of putative secreted immune peptides in UV or IR treated nematodes. Moreover, it was found that the innate immune responses triggered the UPS activation (as indicated by *sur-5::UbV-GFP* reporter expression) to confer the stress resistance [24], which further confirms this assumption.

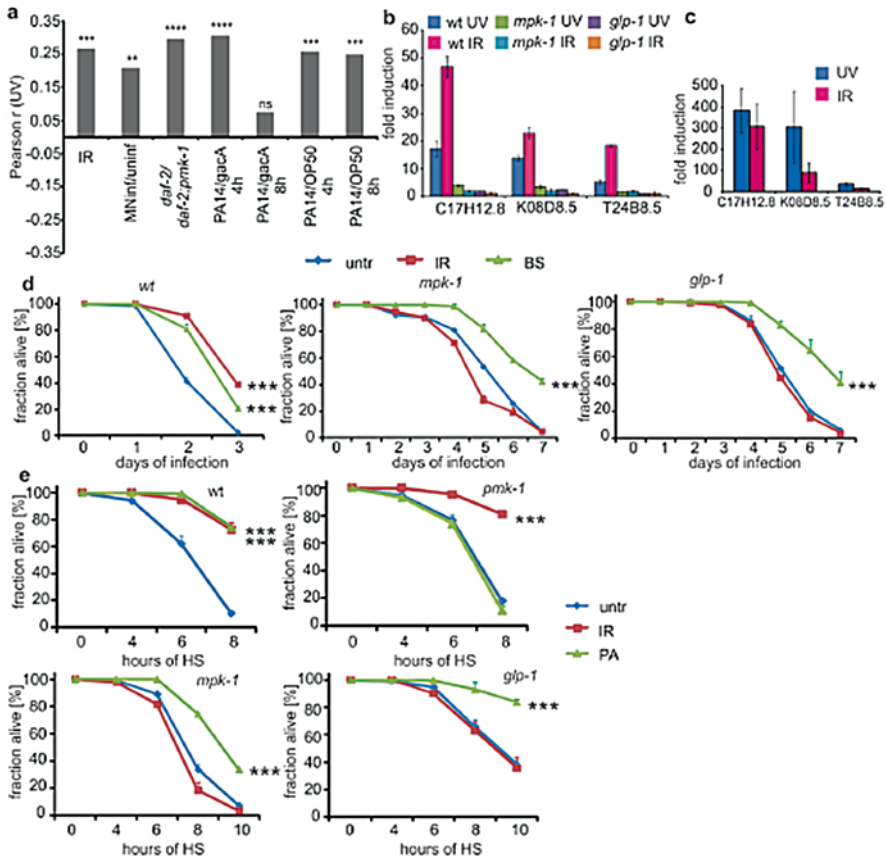


Fig. 14.14 Somatic stress resistance upon DNA damage in germ cells is mediated through MPK-1-induced functional innate immune response [24]. (a) Pearson correlation analysis of significantly induced genes upon UV treatment with transcriptomes upon IR, pathogen infections (*MN M. nematophilum*, *PA P. aeruginosa*, *BS B. subtilis*), and *pmk-1* mutants. (b) Gene expression was assayed by qPCR 6 h post-UV and IR treatment. (c) Germlines were dissected 1–2 h post-UVB (520 mJ/cm²) or IR (90 Gy) for qPCR analysis. (d) L4 larvae were treated with 90 Gy IR or placed for 10 h on *B. subtilis* and 24 h later exposed to *P. aeruginosa*. (e) Young adults were treated with 90 Gy IR or *P. aeruginosa* for 4 h and 24 h later exposed to heat stress. (Error bars = SD. $N \geq 10$ for each experimental condition (d, e); *** $P < 0.0001$, log-rank test)

14.4 Perspectives

It has been widely accepted that the adaption can be activated in response to various environmental toxicants or stresses in nematodes. Some relevant important molecular signaling pathways involved in the regulation of adaptive response induction have also been identified in nematodes. Nevertheless, it is still largely unclear whether pretreatment with a mild toxicant or stress can induce an adaptive response to all subsequent environmental toxicants or stresses. If the answer is YES,

the conserved molecular mechanisms for the induction of adaptive response are needed to be further determined. If the answer is NO, how the nematodes recognize the subsequent different environmental toxicants or stresses through the adaptive response? Besides these, the transition between the adaptive response induction and the toxicity induction from certain doses of environmental toxicants or stresses and the possible underlying mechanisms are also an important and tough question needed to be further solved.

References

1. Wang D-Y (2018) Nanotoxicology in *Caenorhabditis elegans*. Springer, Singapore
2. Ren M-X, Zhao L, Ding X-C, Krasteva N, Rui Q, Wang D-Y (2018) Developmental basis for intestinal barrier against the toxicity of graphene oxide. *Part Fibre Toxicol* 15:26
3. Xiao G-S, Chen H, Krasteva N, Liu Q-Z, Wang D-Y (2018) Identification of interneurons required for the aversive response of *Caenorhabditis elegans* to graphene oxide. *J Nanobiotechnol* 16:45
4. Ding X-C, Rui Q, Wang D-Y (2018) Functional disruption in epidermal barrier enhances toxicity and accumulation of graphene oxide. *Ecotoxicol Environ Saf* 163:456–464
5. Zhao L, Kong J-T, Krasteva N, Wang D-Y (2018) Deficit in epidermal barrier induces toxicity and translocation of PEG modified graphene oxide in nematodes. *Toxicol Res* 7(6):1061–1070. <https://doi.org/10.1039/C8TX00136G>
6. Shao H-M, Han Z-Y, Krasteva N, Wang D-Y (2018) Identification of signaling cascade in the insulin signaling pathway in response to nanopolystyrene particles. *Nanotoxicology in press*
7. Qu M, Xu K-N, Li Y-H, Wong G, Wang D-Y (2018) Using *acs-22* mutant *Caenorhabditis elegans* to detect the toxicity of nanopolystyrene particles. *Sci Total Environ* 643:119–126
8. Dong S-S, Qu M, Rui Q, Wang D-Y (2018) Combinational effect of titanium dioxide nanoparticles and nanopolystyrene particles at environmentally relevant concentrations on nematodes *Caenorhabditis elegans*. *Ecotoxicol Environ Saf* 161:444–450
9. Li W-J, Wang D-Y, Wang D-Y (2018) Regulation of the response of *Caenorhabditis elegans* to simulated microgravity by p38 mitogen-activated protein kinase signaling. *Sci Rep* 8:857
10. Xiao G-S, Zhao L, Huang Q, Yang J-N, Du H-H, Guo D-Q, Xia M-X, Li G-M, Chen Z-X, Wang D-Y (2018) Toxicity evaluation of Wanzhou watershed of Yangtze Three Gorges Reservoir in the flood season in *Caenorhabditis elegans*. *Sci Rep* 8:6734
11. Xiao G-S, Zhao L, Huang Q, Du H-H, Guo D-Q, Xia M-X, Li G-M, Chen Z-X, Wang D-Y (2018) Biosafety assessment of water samples from Wanzhou watershed of Yangtze Three Gorges Reservoir in the quiet season in *Caenorhabditis elegans*. *Sci Rep* 8:14102
12. Yin J-C, Liu R, Jian Z-H, Yang D, Pu Y-P, Yin L-H, Wang D-Y (2018) Di (2-ethylhexyl) phthalate-induced reproductive toxicity involved in DNA damage-dependent oocyte apoptosis and oxidative stress in *Caenorhabditis elegans*. *Ecotoxicol Environ Saf* 163:298–306
13. Xiao G-S, Zhi L-T, Ding X-C, Rui Q, Wang D-Y (2017) Value of *mir-247* in warning graphene oxide toxicity in nematode *Caenorhabditis elegans*. *RSC Adv* 7:52694–52701
14. Wu Q-L, Han X-X, Wang D, Zhao F, Wang D-Y (2017) Coal combustion related fine particulate matter (PM_{2.5}) induces toxicity in *Caenorhabditis elegans* by dysregulating microRNA expression. *Toxicol Res* 6:432–441
15. Zhao Y-L, Wang D-Y (2012) Formation and regulation of adaptive response in nematode *Caenorhabditis elegans*. *Oxidat Med Cell Longev* 2012:564093
16. Wang D-Y, Liu P-D, Xing X-J (2010) Pretreatment with mild UV irradiation increases the resistance of nematode *Caenorhabditis elegans* to toxicity on locomotion behavior from metal exposure. *Environ Toxicol Pharmacol* 29:213–222

17. Wang D-Y, Xing X-J (2010) Pre-treatment with mild UV irradiation suppresses reproductive toxicity induced by subsequent cadmium exposure in nematodes. *Ecotoxicol Environ Saf* 73:423–429
18. Wang D-Y, Xing X-J (2009) Pre-treatment with mild metal exposure suppresses the neurotoxicity on locomotion behavior induced by the subsequent severe metal exposure in *Caenorhabditis elegans*. *Environ Toxicol Pharmacol* 28:459–464
19. Helmcke K, Aschner M (2010) Hormetic effect of methylmercury on *Caenorhabditis elegans*. *Toxicol Appl Pharmacol* 248:156–164
20. Yanase S, Ishii N (2008) Hypoxia exposure induced hormesis decreases mitochondrial superoxide radical levels via Ins/IGF-1 signaling pathway in a long-lived *age-1* mutant of *Caenorhabditis elegans*. *J Radiat Res* 49:211–218
21. Webster CM, Deline ML, Watts JL (2013) Stress response pathways protect germ cells from omega-6 polyunsaturated fatty acid-mediated toxicity in *Caenorhabditis elegans*. *Dev Biol* 373:14–25
22. Kurino C, Furuhashi T, Sudoh K, Sakamoto K (2017) Isoamyl alcohol odor promotes longevity and stress tolerance via DAF-16 in *Caenorhabditis elegans*. *Biochem Biophys Res Commun* 485:395–399
23. Pickering AM, Staab TA, Tower J, Sieburth D, Davies KJ (2013) A conserved role for the 20S proteasome and Nrf2 transcription factor in oxidative stress adaptation in mammals, *Caenorhabditis elegans* and *Drosophila melanogaster*. *J Exp Biol* 216:543–553
24. Ermolaeva MA, Segref A, Dakhovnik A, Ou HL, Schneider JI, Utermöhlen O, Hoppe T, Schumacher B (2013) DNA damage in germ cells induces an innate immune response that triggers systemic stress resistance. *Nature* 501:416–420
25. Yee C, Yang W, Hekimi S (2014) The intrinsic apoptosis pathway mediates the pro-longevity response to mitochondrial ROS in *C. elegans*. *Cell* 157:897–909
26. Spiro Z, Arslan MA, Somogyvari M, Nguyen MT, Smolders A, Dancso B, Nemeth N, Elek Z, Braeckman BP, Csermely P, Soti C (2012) RNA interference links oxidative stress to the inhibition of heat stress adaptation. *Antioxid Redox Signal* 17:890–901
27. Yanase S, Hartman PS, Ito A, Ishii N (1999) Oxidative stress pretreatment increases the X-radiation resistance of the nematode *Caenorhabditis elegans*. *Mutat Res* 426:31–39
28. Ye B-P, Rui Q, Wu Q-L, Wang D-Y (2010) Metallothioneins are required for formation of cross-adaptation response to neurobehavioral toxicity from lead and mercury exposure in nematodes. *PLoS ONE* 5:e14052
29. Kozłowski L, Garvis S, Bedet C, Palladino F (2014) The *Caenorhabditis elegans* HPI family protein HPL-2 maintains ER homeostasis through the UPR and hormesis. *Proc Natl Acad Sci U S A* 111:5956–5961
30. Wu Q-L, Cao X-O, Yan D, Wang D-Y, Aballay A (2015) Genetic screen reveals link between maternal-effect sterile gene *mes-1* and *P. aeruginosa*-induced neurodegeneration in *C. elegans*. *J Biol Chem* 290:29231–29239
31. Sun L-M, Zhi L-T, Shakoov S, Liao K, Wang D-Y (2016) microRNAs involved in the control of innate immunity in *Candida* infected *Caenorhabditis elegans*. *Sci Rep* 6:36036
32. Yu Y-L, Zhi L-T, Guan X-M, Wang D-Y, Wang D-Y (2016) FLP-4 neuropeptide and its receptor in a neuronal circuit regulate preference choice through functions of ASH-2 trithorax complex in *Caenorhabditis elegans*. *Sci Rep* 6:21485
33. Zhi L-T, Yu Y-L, Jiang Z-X, Wang D-Y (2017) *mir-355* functions as an important link between p38 MAPK signaling and insulin signaling in the regulation of innate immunity. *Sci Rep* 7:14560
34. Zhi L-T, Yu Y-L, Li X-Y, Wang D-Y, Wang D-Y (2017) Molecular control of innate immune response to *Pseudomonas aeruginosa* infection by intestinal *let-7* in *Caenorhabditis elegans*. *PLoS Pathog* 13:e1006152
35. Yu Y-L, Zhi L-T, Wu Q-L, Jing L-N, Wang D-Y (2018) NPR-9 regulates innate immune response in *Caenorhabditis elegans* by antagonizing activity of AIB interneurons. *Cell Mol Immunol* 15:27–37

Chapter 15

Molecular Basis for Transgenerational Toxicity Induction of Environmental Toxicants or Stresses



Abstract In the recent years, the underlying mechanisms for transgenerational toxicity of environmental toxicants or stresses have received more and more attention. We here introduced the molecular alterations during the formation of transgenerational toxicity of environmental toxicants or stresses. We also introduced molecular signal- and epigenetic signal-mediated molecular mechanisms for transgenerational toxicity of environmental toxicants or stresses. Moreover, we discussed the crucial role of intestinal barrier against the formation of transgenerational toxicity of environmental toxicants or stresses in nematodes.

Keywords Molecular basis · Transgenerational toxicity · *Caenorhabditis elegans*

15.1 Introduction

In nematode *Caenorhabditis elegans*, many environmental toxicants or stresses can cause the toxicity at different aspects and to different degrees on animals [1–13]. Moreover, it has been observed that some aspects of toxicity formed in environmental toxicant- or stress-exposed nematodes can be further transferred from the parents to their progeny [14–25]. In the recent years, the underlying molecular mechanisms for the induction of transgenerational toxicity of environmental toxicants or stresses have gradually received the attention in nematodes.

In this chapter, we first introduced the molecular alterations during the formation of transgenerational toxicity of environmental toxicants or stresses. Again, we discussed the crucial role of intestinal barrier against the formation of transgenerational toxicity of environmental toxicants or stresses. Moreover, we introduced and discussed both the molecular signals and the epigenetic signals involved in the regulation of transgenerational toxicity of environmental toxicants or stresses. The systematic determination on the mechanisms of transgenerational toxicity of environmental toxicants or stresses may help us open another important window to understand the molecular mechanisms of toxicity induction from environmental toxicants or stresses.

15.2 Molecular Alterations During the Formation of Transgenerational Toxicity of Environmental Toxicants or Stresses

15.2.1 Environmental Toxicant- or Stress-Induced Transgenerational Gene Expression Profiles

Bisphenol A (BPA) exposure could cause the transgenerational toxicity on nematodes [26]. In the first generation, BPA could increase the expressions of most of the examined genes required for the control of oxidative stress and stress response, and the increased genes included those of *hsp*, *sod*, and *mtl* genes (Fig. 15.1) [26]. In the fourth generation of BPA-exposed nematodes, although many of the examined genes were still upregulated, BPA exposure induced the more obvious increase in the expressions of tested genes in the first generation than those in the fourth generation (Fig. 15.1) [26], which may reflect an adaptive response or evolutionary response formed in the fourth generation.

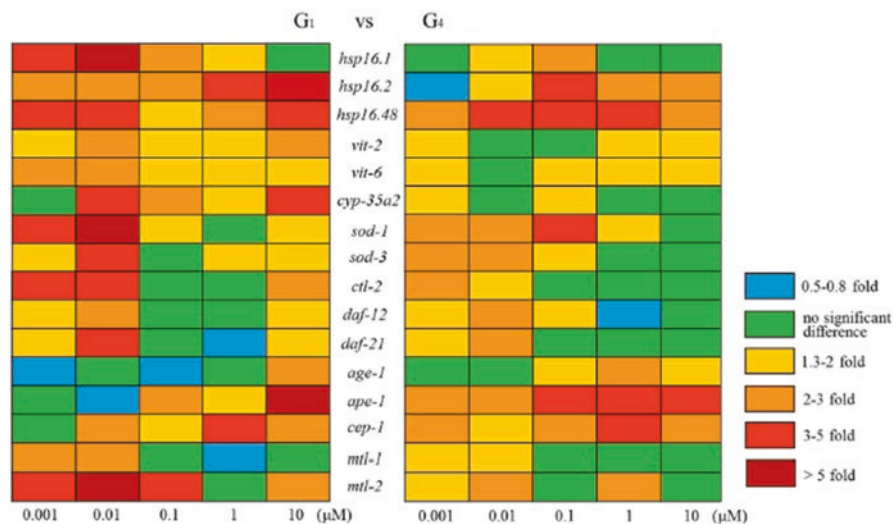


Fig. 15.1 Integrated gene expression profiles tested in *C. elegans* from the G1 and G4 generation [26]. Values of stress-related gene expression were normalized using actin mRNA and represent means ($n = 3$) relative to the control

15.2.2 Environmental Toxicant- or Stress-Induced Transgenerational microRNA (miRNA) Expression Profiles

Environmental exposure to nicotine could cause adverse effects on nematodes [27]. Meanwhile, exposure to nicotine even at the low dose induced a globally dysregulated expression profiles of miRNAs (Fig. 15.2) [27]. Moreover, in the F1 and the F2 generation of nicotine-exposed nematodes, the dysregulated expression profiles of miRNAs could also be detected (Fig. 15.2) [27]. The dysregulation of some miRNAs could be observed across two or more generations from the beginning of nicotine-exposed nematodes [27]. These observations suggest the potential involvement of miRNAs in the regulation of transgenerational toxicity induction of environmental toxicants or stresses in nematodes.

15.3 Crucial Role of Intestinal Barrier Against the Formation of Transgenerational Toxicity of Environmental Toxicants or Stresses

The intestinal barrier plays a key role in being against the toxicity of environmental toxicants or stresses in nematodes [28, 29]. With CdTe quantum dots (CdTe QDs), an engineered nanomaterial, as an example, exposure to CdTe QDs (2.5–20 mg/L) could result in the transgenerational toxicity [30]. In CdTe QD-exposed nematodes, CdTe QD particles were accumulated in the pharynx, the intestine, the reproductive organs such as the gonad, and the embryos of the exposed animals, and the CdTe QD signals could be detected in the F1 generation [30]. ZnS coating could reduce the toxicity of CdTe QDs, and the main cellular basis for this beneficial function was to maintain the normal function of intestinal barrier [30], suggesting the crucial role of intestinal barrier against the transgenerational toxicity of CdTe QDs.

In nematodes, *clk-1* encodes a demethoxyubiquinone hydroxylase required for the biosynthesis of ubiquinone, *isp-1* encodes a subunit of mitochondrial complex III, and *daf-2* encodes an insulin receptor. Exposure to CdTe QDs (20 mg/L) could increase the transcriptional expressions of *clk-1*, *isp-1*, or *daf-2* in wild-type nematodes [30]. Meanwhile, mutation of *clk-1*, *isp-1*, or *daf-2* caused the resistance to the toxicity of CdTe QDs in decreasing locomotion behavior and in inducing intestinal ROS production (Fig. 15.3) [30], suggesting that CLK-1-, ISP-1-, and DAF-2-mediated signaling pathways act as important molecular basis for transgenerational toxicity induction of CdTe QDs. Moreover, it was found that intestinal-specific RNAi knockdown of *clk-1*, *isp-1*, or *daf-2* also led to the resistance of nematodes to the toxicity of CdTe QDs in decreasing locomotion behavior and in inducing intestinal ROS production (Fig. 15.3) [30]. Additionally, no obvious toxicity of CdTe QDs in inducing intestinal ROS production was observed in the progeny of exposed

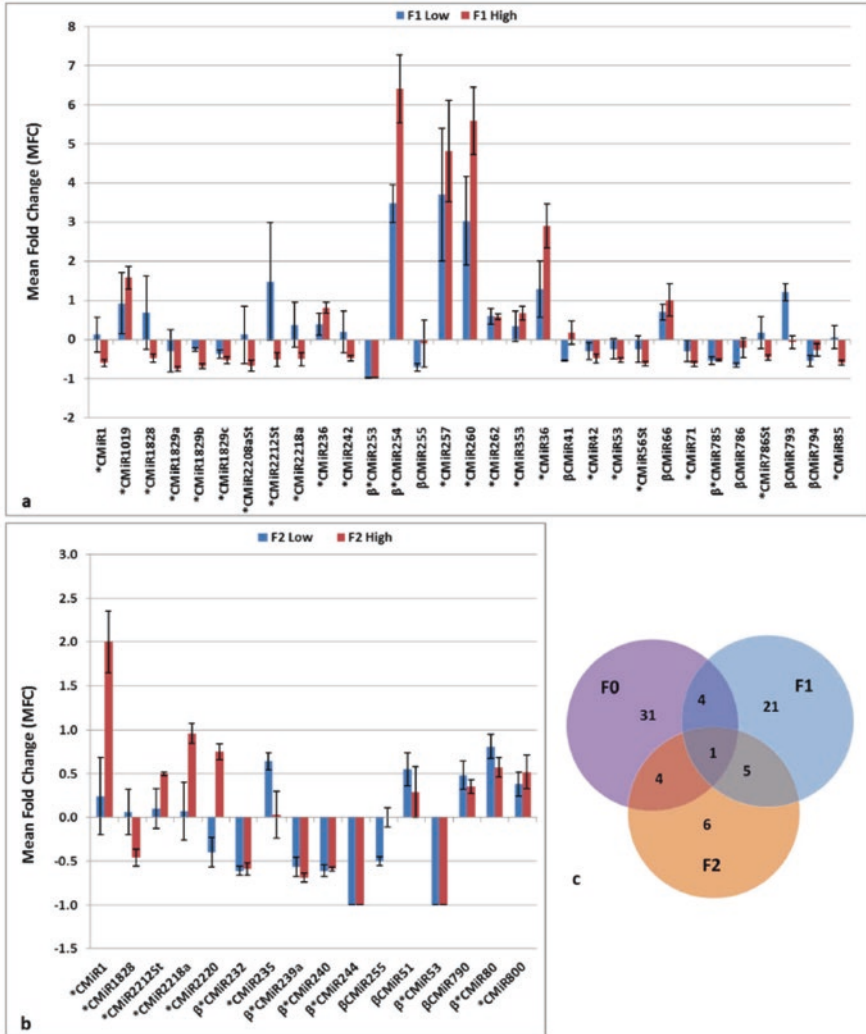


Fig. 15.2 Nicotine altered the miRNA expression profiles across generations in a dose-dependent manner [27]. (a) Nicotine significantly altered the expression levels of 31 miRNAs in the F1 worm population. (b) Nicotine significantly altered the expression levels of 16 miRNAs in the F2 worm population. (c) A Venn diagram showing the number of the miRNAs with differentially altered expression levels shared in L4 larvae belonging to the three generations (F0, F1, and F2). $P < 0.05$. (*, β denote statistically significant changes in response to high (20 mM) and low (20 mM) nicotine concentrations, respectively). All comparisons were based on control

nematodes with intestinal-specific RNAi knockdown of *clk-1*, *isp-1*, or *daf-2* [30]. Therefore, intestinal CLK-1, ISP-1, and DAF-2 regulate the induction of transgenerational CdTe QDs toxicity by modulating the functional state of intestinal barrier in nematodes.

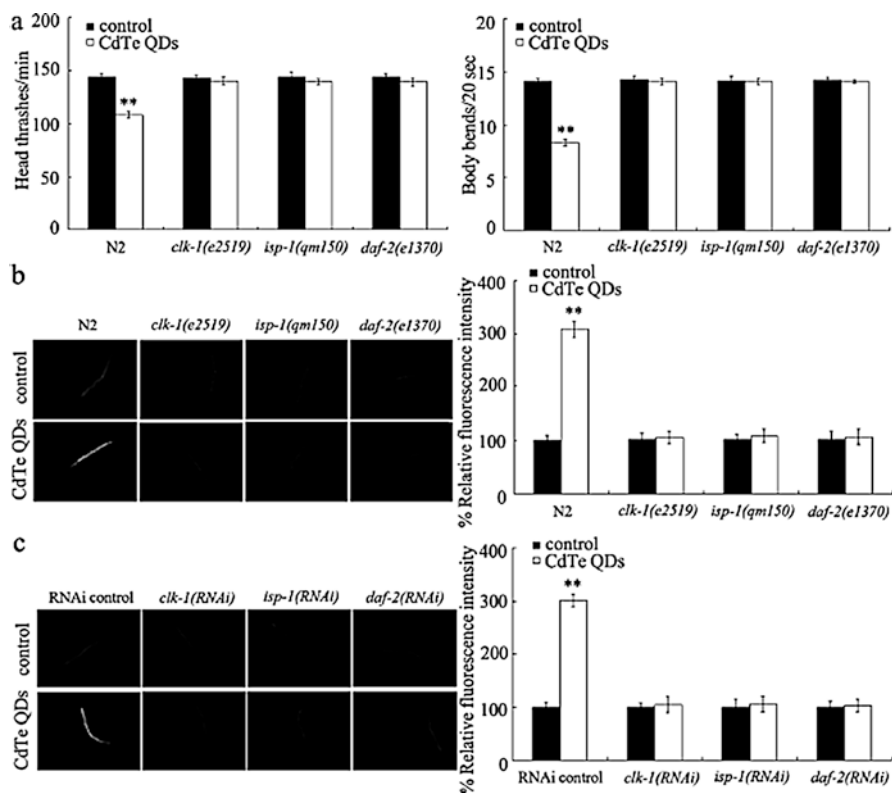


Fig. 15.3 Effects of *clk-1*, *isp-1*, or *daf-2* gene mutation on toxicity formation of CdTe QDs in nematodes [30]. (a) Effects of *clk-1*, *isp-1*, or *daf-2* gene mutation on toxicity of CdTe QDs on locomotion behavior in nematodes. (b) Effects of *clk-1*, *isp-1*, or *daf-2* gene mutation on toxicity of CdTe QDs in inducing intestinal ROS production in nematodes. (c) Effects of intestine-specific RNAi of *clk-1*, *isp-1*, or *daf-2* gene on toxicity of CdTe QDs in inducing intestinal ROS production in nematodes. RNAi control, VP303. Exposure concentration of CdTe QDs was 20 mg/L. QDs quantum dots. Bars represent means \pm SEM. *** $P < 0.01$ vs. control

Moreover, it was observed that intestinal-specific RNAi knockdown of *clk-1*, *isp-1*, or *daf-2* only caused the moderate accumulation of CdTe QDs particles in the intestine of exposed nematodes (Fig. 15.4) [30]. Additionally, no obvious CdTe QDs signals were detected in the progeny of CdTe QDs expose nematodes with intestinal-specific RNAi knockdown of *clk-1*, *isp-1*, or *daf-2* (Fig. 15.4) [30]. That is, the intestinal-specific RNAi knockdown of *clk-1*, *isp-1*, or *daf-2* can prevent the translocation of CdTe QDs from exposed nematodes to their progeny by maintaining the normal physiological state of intestinal barrier.

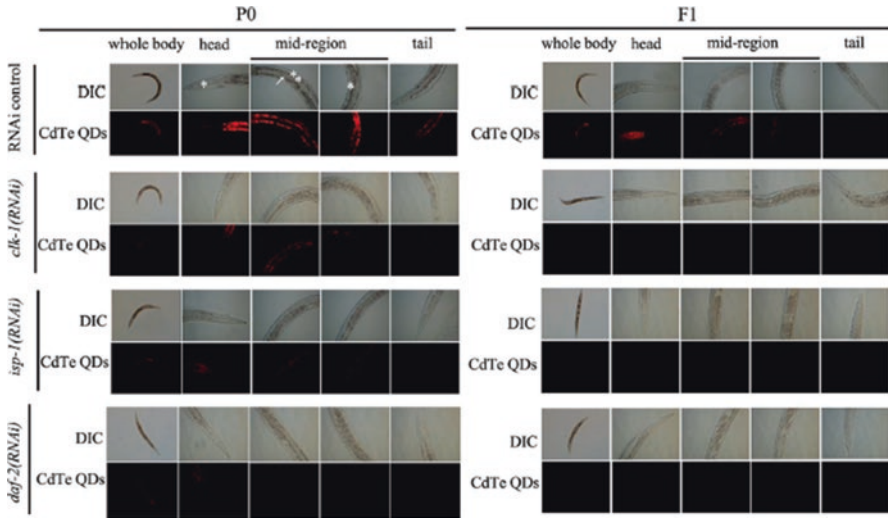


Fig. 15.4 Effects of intestine-specific RNAi of *clk-1*, *isp-1*, or *daf-2* gene on the distribution and translocation of CdTe QDs in nematodes [30]. Arrowheads indicate the intestine. Pharynx (*) in the head, embryos (*) in the mid-region, and gonad (**) in the mid-region were also indicated. RNAi control, VP303. Exposure concentration of CdTe QDs was 20 mg/L. P0, parents; F1, the filial generation. *QDs* quantum dots

15.4 Molecular Signals for RNA Inheritance Are Involved in the Regulation of Transgenerational Toxicity of Environmental Toxicants or Stresses

15.4.1 RNA Inheritance and Transgenerational Toxicity of Heat Stress

The siRNA functions in mediating transgenerational gene silencing through a germline nuclear RNAi pathway. In nematodes, HRDE-1 is a germline nuclear AGO protein. Based on the 12-generation temperature-shift experiments, HRDE-1 might play an epigenetic role in repressing the heat stress-induced transcriptional activation of over 280 genes, and many of the related genes were in or near LTR (long-terminal repeat) retrotransposons [31]. Moreover, some of the heat stress-induced transcriptional activation in *hrde-1* mutant nematodes was intensified in the late generations under heat stress condition and could be heritable for at least two generations after the shift back to lower temperature [31]. Therefore, the germline nuclear RNAi may regulate heat stress response by antagonizing the temperature effect at the transcriptional level in nematodes.

15.4.2 RNA Inheritance and Transgenerational Toxicity of Pathogen Infection

Environmental pathogens can potentially cause the adverse effects at different aspects on organisms, including the nematodes [32–40]. The nematodes were recently found to enter the diapause state in the F2 generation as a defense strategy against the moderate pathogen infection [41]. The formation of a diapause stage in the second generation was a response for nematodes to the infection by pathogens with moderate virulences, since the pathogen-induced dauer formation in the second generation was found to be dependent on the bacterial virulence [41]. In the second generation of nematodes infected with pathogen, the developmental transition to dauer formation occurred, and the dauer formation in response to pathogenesis required the persistent intestinal pathogen colonization [41]. Moreover, it was observed that the information for dauer formation could be transmitted transgenerationally to the progeny through the maternal germline (Fig. 15.5) [41].

Moreover, it was found that the RNA interference was required for defense against pathogen infection. The growth of more than half of the RNAi-defective mutant nematodes tested was affected on *P. aeruginosa* PAO1 (Fig. 15.6) [41], suggesting that the RNAi machinery is necessary for the defense against pathogen infection. Furthermore, the RNAi machinery was required for communicating the dauer formation information transgenerationally [41]. Pathogen infection could induce the nuclear expression of DAF-16::GFP in the late F1 larvae and the F2 embryos; however, this DAF-16 activation was independent of the RNA interference

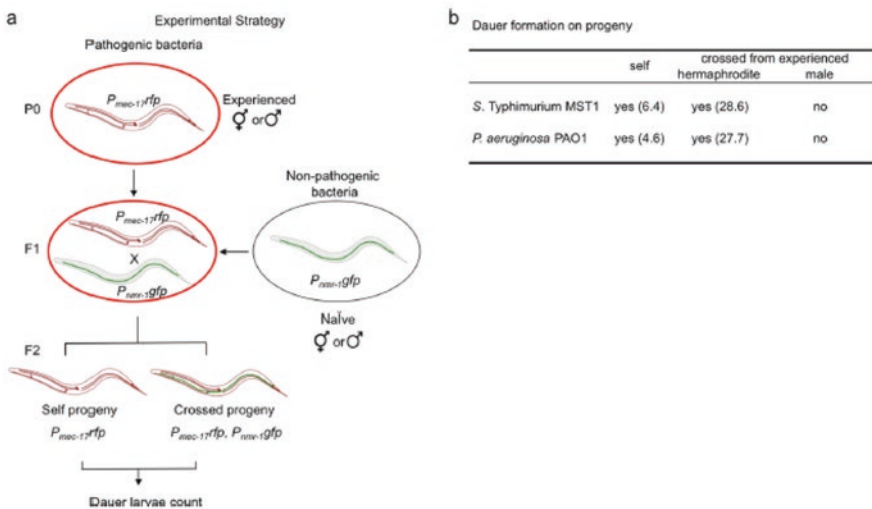


Fig. 15.5 Dauer formation under pathogenesis is transmitted to the progeny through the maternal germline [41]. (a) Schematic representation of the experimental strategy used for identifying which germline carries the information to form dauers in the progeny. (b) Dauer formation on self- and crossed progeny

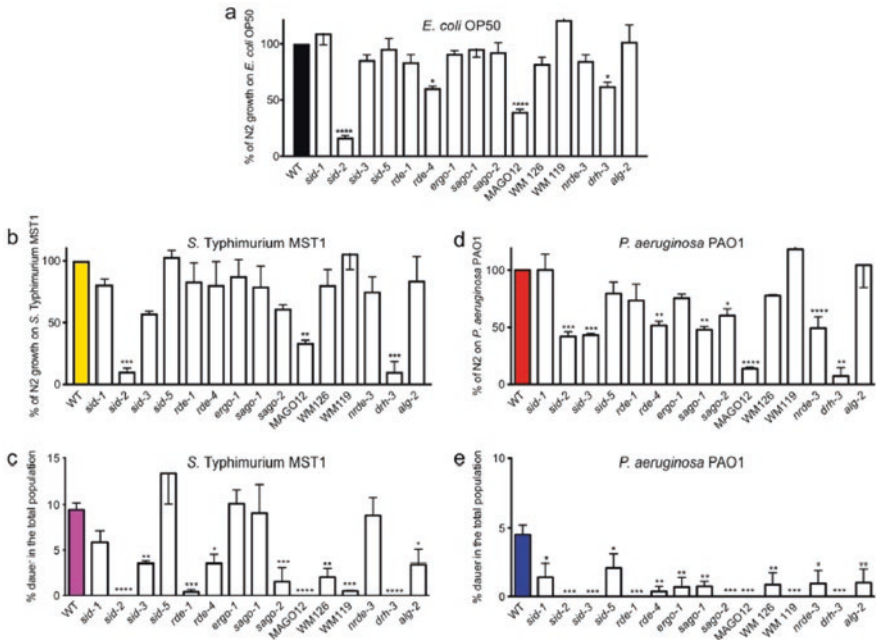


Fig. 15.6 RNAi effectors are needed for pathogen resistance and dauer formation as a transgenerational defense [41]. (a–c) Growth of RNAi mutant animals on *E. coli* OP50 (a), *S. Typhimurium* MST1 (b), and *P. aeruginosa* PAO1 (c) as the percentage of wild-type N2 growth under each condition. (d, e) Dauer formation of RNAi mutant animals on *S. Typhimurium* MST1 (d) and *P. aeruginosa* PAO1 (e). ****, $P < 0.0001$; ***, $P < 0.001$; **, $P < 0.005$; *, $P < 0.05$. Error bars indicate SEM of at least three biological replicas done in triplicates

pathway [41]. These results suggest that the information encoding this survival strategy to enter the diapause state can be transmitted transgenerationally to the progeny via the maternal germline in nematodes.

15.5 Epigenetic Regulation of Transgenerational Toxicity of Environmental Toxicants or Stresses

15.5.1 Role of H3K4 Dimethylation

Exposure to arsenite could cause the transgenerational toxicity at least in reducing the brood size in nematodes [42]. Meanwhile, it was observed that the transcriptional expression of *spr-5* encoding a H3K4me2 demethylase LSD/KDM1 was significantly reduced in F0-exposed generation and the subsequent F1–F3 generations of arsenite-exposed nematodes [42]. Moreover, it was found that the dimethylation of global H3K4 was increased in F0–F3 generations of arsenite-exposed nematodes

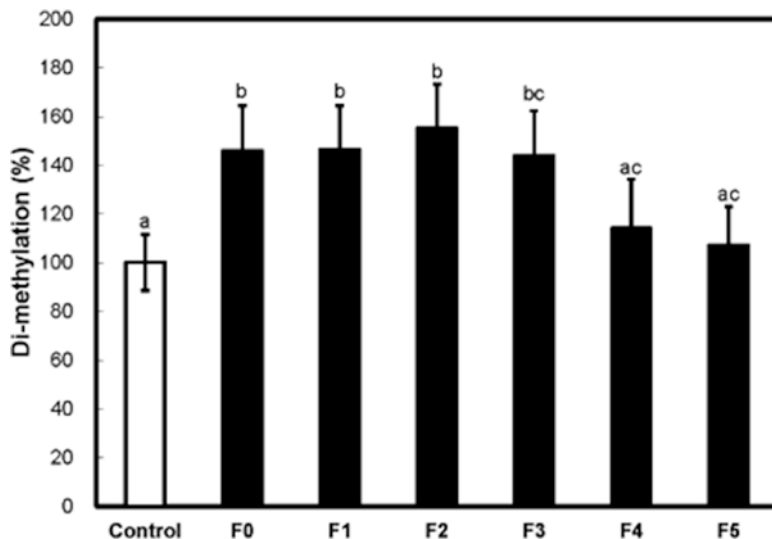


Fig. 15.7 Multigenerational effect of arsenite exposure on dimethylated histone H3K4 level in *C. elegans* for all generations (F0–F5) [42]. F0–F5 generation nematodes were cultured as described in the text. Total histones were extracted from adult worms (F0–F5), and the dimethylated histone H3K4 level was analyzed by use of the EpiQuik global dimethyl histone H3K4 quantification kit. Normalization was ensured by adding 500 ng of total histones for each sample. Nonexposed control nematodes were also followed over six generations. Exposed individuals (F1–F5) were compared to the pool of nonexposed controls of all generations. Statistical significance was calculated by Tukey's test, and bars represent standard errors of the mean (SEM), with different lowercase letters representing statistical differences ($p < 0.05$)

(Fig. 15.7) [42]. These observations imply the possible association between transgenerational toxicity of arsenite and H3K4 dimethylation in nematodes.

In nematodes, the transcriptional factors of DAF-16/FOXO and HSF-1 in the parental somatic tissues were found to mediate the formation of epigenetic memory of transgenerational response (Fig. 15.8) [43]. The histone H3K4me3 regulatory complex contains ASH-2, WDR-5, and SET-2. It was further found that the function of DAF-16 and HSF-1 was maintained through the histone H3 lysine 4 trimethylase complex in the germline across the generations (Fig. 15.8) [43], suggesting the requirement of histone modifiers for the transgenerational inheritance.

The germ-to-soma communications existed for the control of transgenerational response in nematodes [43]. The elicitation of epigenetic memory also required the transcription factor SKN-1/Nrf [43]. Tissue-specific activity analysis indicated that DAF-16 and HSF-1 acted in several somatic tissues other than intestine and neurons to regulate the transgenerational response, and SKN-1 acted in somatic tissues, especially in intestine and neurons, to regulate the transgenerational response [43]. Different from these, the H3K4me3 complex acted in the germline to maintain and to transmit the epigenetic memory for transgenerational response [43]. An overview

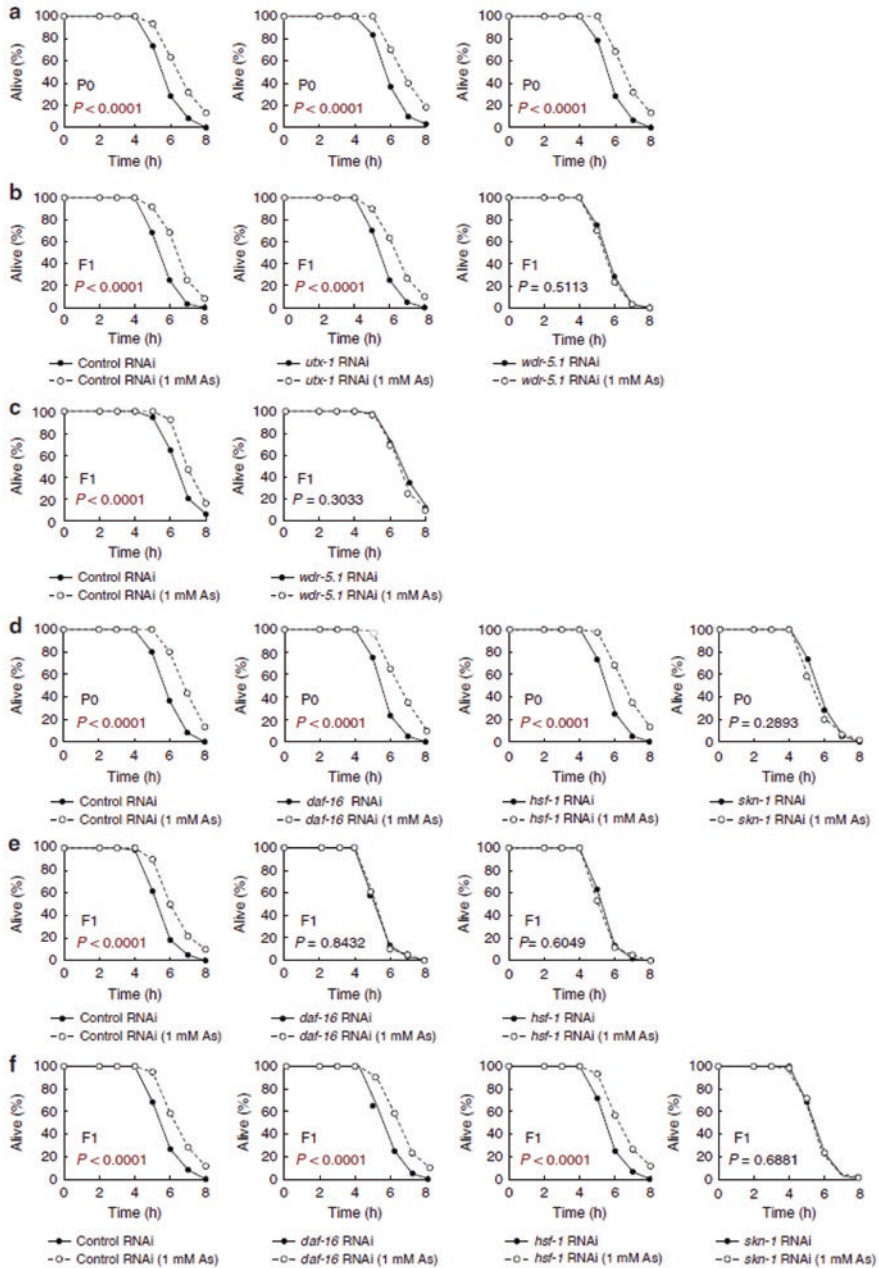


Fig. 15.8 The H3K4me3 complex and two transcription factors are required for the transgenerational inheritance [43]. (a, b) Oxidative stress resistance (1.7 mM H₂O₂) of the stressed P0 parents treated with RNAi (left, empty vector (control); middle, *utx-1*; right, *wdr-5.1* on day 2 adulthood (a) and the self-fertilized F1 descendants on day 1 adulthood (b) compared with control groups. Two independent experiments are integrated into each survival curve ($n = 60$). (c) *wdr-5.1* RNAi

model for the control of epigenetic memory for transgenerational response to environmental stimuli was summarized in Fig. 15.9 [43].

15.5.2 Role of H3K9 Methylation

In nematodes, exposure to Iranian heavy crude oil (IHC) could induce the transgenerational toxicity at least in reducing the reproduction capacity [44]. Meanwhile, the decreased methylation of histone H3 (H3K9), not the H3K4, H3K27, and H3K36, was detected in IHC-exposed nematodes (Fig. 15.10) [44]. The transgenerational toxicity of IHC in reducing brood size was not found in a H3K9 histone methyltransferase (HMT) mutant, *met-2(n4256)* [44], suggesting a potential role of H3K9 HMT in regulating the transgenerational toxicity of environmental toxicants or stresses in nematodes.

In nematodes, it was further observed that the temperature-induced change in expression from a heterochromatic gene array could endure for at least 14 generations (Fig. 15.11) [45]. In details, the 14 generation memory of high temperature could be detected in nematodes (Fig. 15.11) [45].

In nematodes, the transgenerational inheritance was primarily in cis with locus and occurred through both the oocytes and the sperm [45]. The analysis on the H3K9me changes indicated that this transgenerational inheritance was associated with the altered trimethylation of histone H3 lysine 9 (H3K9me3) before the onset of zygotic transcription [45]. The high temperature during germline development could result in the depletion of H3K9me3 [45]. SET-25, a putative histone methyltransferase, is responsible for H3K9me3 and required for the maintenance of piRNA-initiated stable gene silencing in nematodes. It was found that inactivating *set-25* could increase the expression from the heterochromatic gene array (Fig. 15.12) [45], which suggests that the repression of heterochromatic gene array at low temperature and the epigenetic expression memory of endogenous loci required the SET-25. These results imply that the long-lasting epigenetic memory of environmental toxicants or stresses is possible in nematodes. During this process, SET-25 activity is reduced at high temperature, resulting in the derepression of loci in the genome [45]. Different from this, after a return to low temperature, SET-25 activity needs multiple generations for the repression to be completely reestablished [45].



Fig. 15.8 (continued) treatment in F1 descendants from the stressed P0 parents leads to the suppression of the increase in the oxidative stress resistance. Three independent experiments are integrated into each survival curve ($n = 90$). **(d, e)** Oxidative stress resistance (1.7 mM H₂O₂) of the stressed P0 parents on day 2 adulthood treated with RNAi of indicated genes **(d)** and the self-fertilized F1 descendants on day 1 adulthood **(e)** compared with control groups. **(f)** *daf-16* or *hsf-1* RNAi treatment performed in the F1 descendants does not compromise the increased resistance, whereas *skn-1* RNAi leads to the suppression of the increase in the oxidative stress resistance. Two independent experiments are integrated into each survival curve ($n = 60$). P values were calculated by log-rank test

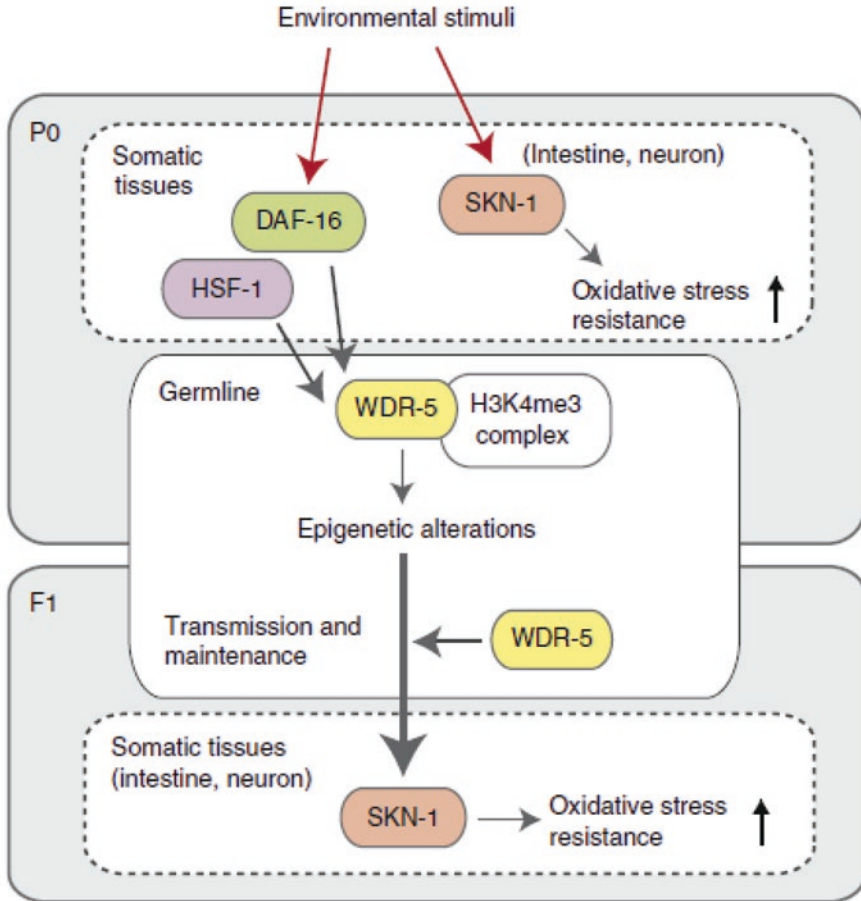


Fig. 15.9 Overview model of transgenerational inheritance of epigenetic memory in response to environmental stimuli [43]. In the P0 generation, somatic DAF-16 and HSF-1 communicate with the H3K4me3 complex in the germline so as to regulate and maintain epigenetic alterations associated with inheritable acquired traits, and the H3K4me3 complex in the filial germline then transfers hormetic information to SKN-1 of the somatic tissues

15.6 Transgenerational Hormesis and Insulin Signaling Pathway

In nematodes, it was observed that parental exposure to mild osmotic stress could protect the progeny from the effects of strong osmotic stress, and this transgenerational hormesis required the DAF-2 activation [46]. Like parental exposure to the mild osmotic stress, reduction in maternal intestinal insulin signaling protected the progeny from the effects of strong osmotic stress [47], suggesting a link between maternal insulin signaling and progeny physiology in nematodes.

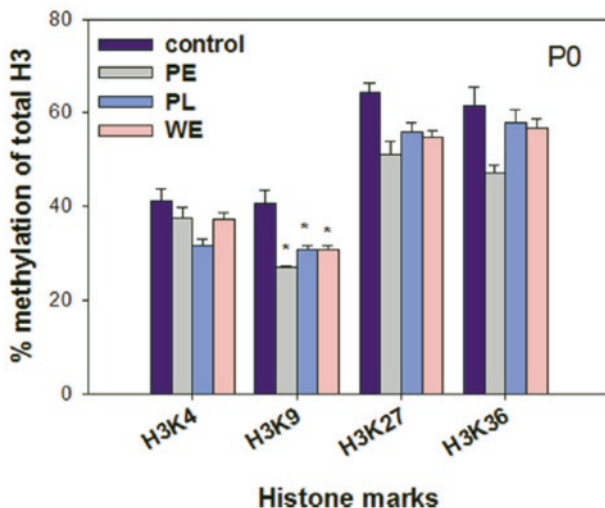


Fig. 15.10 Total methylation status of histone H3 (H3K4, H3K9, H3K27, and H3K36) in *C. elegans* exposed to IHC in the three treatment groups (PE, PL, and WE) [44]. Methylation of each histone residue was normalized according to the total histone 3 value (total H3 = 1, $n = 3$; mean \pm standard error of the mean; * $p < 0.05$)

It was found that the glycerol biosynthetic enzyme GPDH-2 was required for parental exposure to 300 mM NaCl to protect the progeny from 500 mM NaCl (Fig. 15.13) [47], suggesting that the increased level of glycerol is required for the adaptation to osmotic stress. The *daf-2* mutant nematodes do not deposit more glycerol into the embryos [47]. Moreover, GPDH-2 was required for the reduced maternal insulin signaling to protect the progeny from the developmental arrest (Fig. 15.13), implying that the inhibition of maternal insulin signaling results in an increased glycerol production in the embryos. This observation further reveals a link between maternal insulin signaling and progeny metabolism in nematodes. For the underlying molecular mechanism, it was further found that the insulin signaling to the maternal germline modified the progeny response to osmotic stress by regulating the signaling cascade of RAS-ERK [47].

15.7 Perspectives

In this chapter, we introduced and discussed the molecular basis for the transgenerational toxicity of environmental toxicants or stresses in nematodes. As introduced above, so far, the related information for the molecular basis of transgenerational toxicity of environmental toxicants or stresses is still limited in nematodes. The obtained or detected molecular alterations during the formation of transgenerational

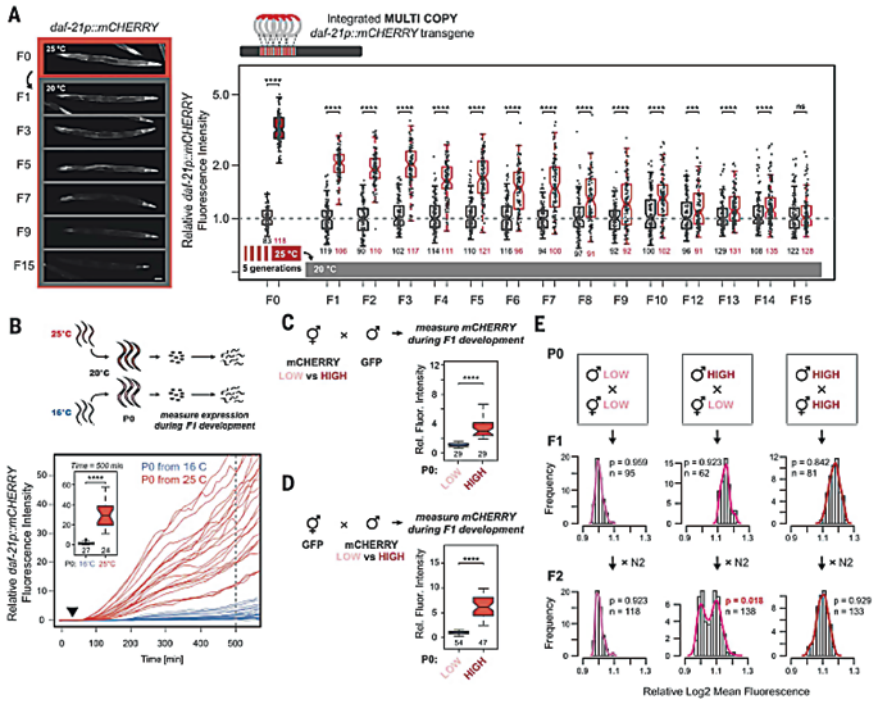


Fig. 15.11 Fourteen generation memory of high temperature [45]. (a) Adult expression of a *daf-21p::mCHERRY*-integrated multicopy transgene at 20 °C after five generations at 25 °C. Scale bar, 0.1 mm. Stage-matched worms at 20 °C are used as a reference for normalization (black). False discovery rates (FDR) q values: **** $q < 0.0001$; *** $q < 0.001$; ns, $q > 0.05$ (Wilcoxon test). Sample size indicated. (b) Expression in embryos from animals transferred to 20 °C at the L4 larval stage (inset: quantification at 500 min). Arrowhead indicates start of zygotic transcription of the transgene. Transmission occurs through oocytes (c) and sperm (d) and in cis with the locus (e). Intensities normalized to the “low” (low-expression) population; sample size and P value for Hartigans’ dip test for unimodality. (b) (Inset), (c, d) **** $P < 0.0001$

toxicity of environmental toxicants or stresses may provide some useful clues for the further elucidation.

Among the obtained information for molecular basis of transgenerational toxicity of environmental toxicants or stresses, most of them are on the epigenetic regulation. The core molecular network organized by epigenetic signals and molecular signals is suggested to be further examined during the induction of transgenerational toxicity of environmental toxicants or stresses.

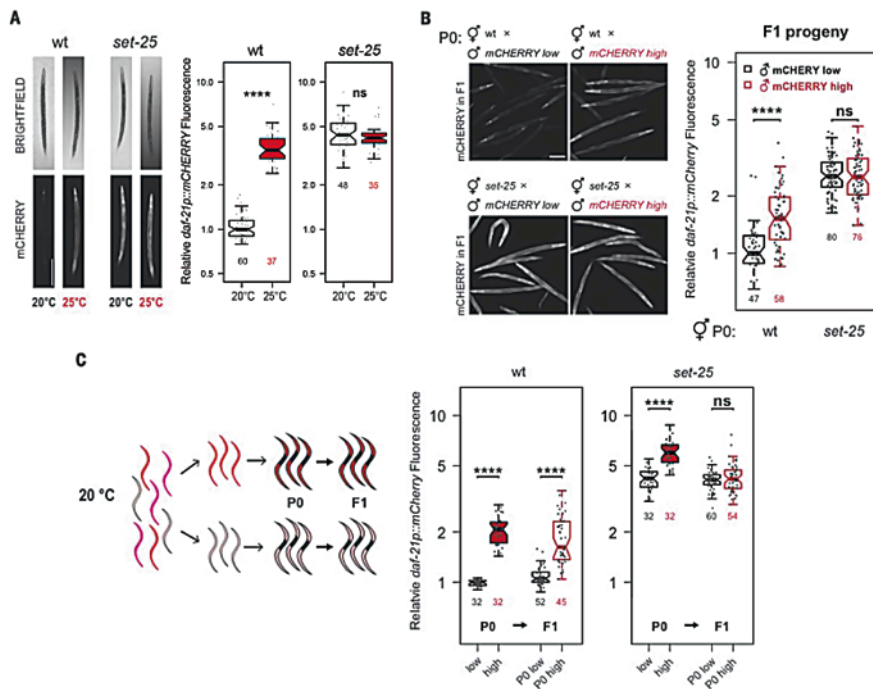


Fig. 15.12 Requirement for SET-25 [45]. **(a)** Quantification of *daf-21p::mCherry* expression in L4 larvae at 20 and 25 °C in WT and *set-25* mutants. **(b)** Expression of a paternally derived transgene in the adult progeny of WT and *set-25* mutant mothers. A common batch of low- and (temperature-induced) high-expressing males was used. **(c)** Quantification of *daf-21p::mCherry* expression in the self-progeny (F1) of parental (P0) animals sorted into high and low groups based on transgene expression at the L4 stage in WT and *set-25* mutants. **** $P < 0.0001$; ns not significant. **(a, b)** Scale bars, 0.2 mm

We here further discussed the crucial role of intestinal barrier for the nematodes against transgenerational toxicity of environmental toxicants or stresses. Nevertheless, the potential crucial roles of other biological barriers, such as reproduction related biological barrier(s), in being against the transgenerational toxicity of environmental toxicants or stresses is still largely unclear in nematodes.

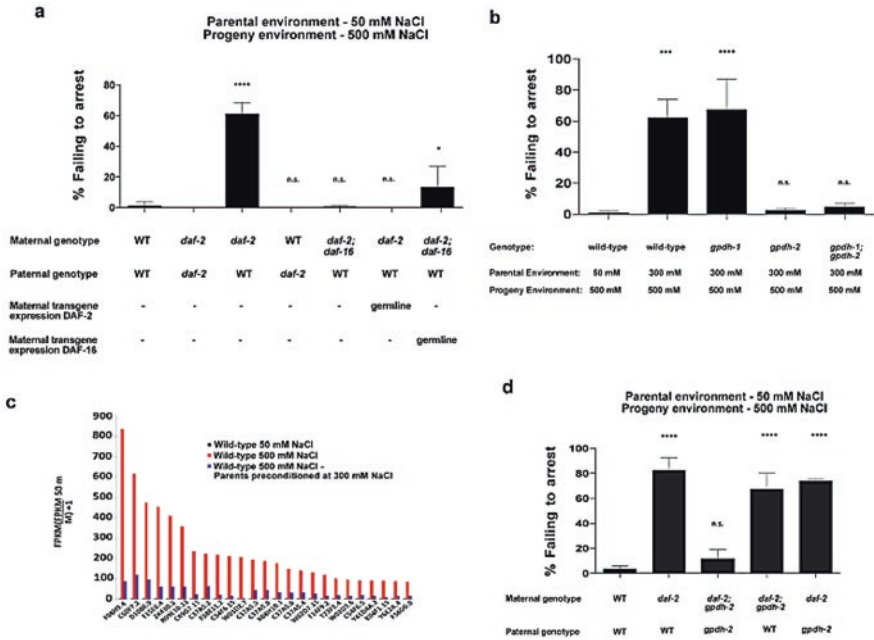


Fig. 15.13 Insulin-like signaling to the maternal germline regulates progeny response to osmotic stress [47]. (a) Percent of wild-type, *daf-2(e1370)* and *daf-2(e1370); daf-16(mu86)* cross progeny failing to arrest development after 48 h at 500 mM NaCl. Males contained (*Pegl-1::4xNLS::GFP*); *him-5(e1490); nIs349 (Pceh-28::4xNLS::mCherry)* for the identification of cross progeny. The *pie-1* promoter was used to drive germline-specific expression of DAF-2, and the *mex-5* promoter was used to drive germline-specific expression of DAF-16. Error bars, s.d. (b) Percent of wild-type, *gpdh-1(ok1558)*, and *gpdh-2(ok1733)* animals failing to arrest development at 500 mM NaCl after 48 h. Error bars, s.d. $n = 3$ experiments of >100 animals. (c) Average fold change of 2 replicates of the 25 most upregulated genes in embryos in response to osmotic stress after 6 h. (d) Percent of wild-type, *daf-2(e1370)* and *gpdh-2(ok1733)* cross progeny failing to arrest development after 48 h at 500 mM NaCl. Males contained *otIs39 (Punc-47::GFP); him-5(e1490)* for the identification of cross progeny. Error bars, s.d. $n = 3$ experiments of >20 animals. The quantified results are presented as mean \pm s.d. using ANOVA. * $P < 0.05$, *** $P < 0.001$, and **** $P < 0.0001$ were considered significant. n.s. not significant

References

1. Wang D-Y (2018) Nanotoxicology in *Caenorhabditis elegans*. Springer, Singapore
2. Ren M-X, Zhao L, Ding X-C, Krasteva N, Rui Q, Wang D-Y (2018) Developmental basis for intestinal barrier against the toxicity of graphene oxide. Part Fibre Toxicol 15:26
3. Xiao G-S, Chen H, Krasteva N, Liu Q-Z, Wang D-Y (2018) Identification of interneurons required for the aversive response of *Caenorhabditis elegans* to graphene oxide. J Nanbiotechnol 16:45
4. Ding X-C, Rui Q, Wang D-Y (2018) Functional disruption in epidermal barrier enhances toxicity and accumulation of graphene oxide. Ecotoxicol Environ Saf 163:456–464

5. Zhao L, Kong J-T, Krasteva N, Wang D-Y (2018) Deficit in epidermal barrier induces toxicity and translocation of PEG modified graphene oxide in nematodes. *Toxicol Res* 7(6):1061–1070. <https://doi.org/10.1039/C8TX00136G>
6. Shao H-M, Han Z-Y, Krasteva N, Wang D-Y (2018) Identification of signaling cascade in the insulin signaling pathway in response to nanopolystyrene particles. *Nanotoxicology in press*
7. Qu M, Xu K-N, Li Y-H, Wong G, Wang D-Y (2018) Using *acs-22* mutant *Caenorhabditis elegans* to detect the toxicity of nanopolystyrene particles. *Sci Total Environ* 643:119–126
8. Dong S-S, Qu M, Rui Q, Wang D-Y (2018) Combinational effect of titanium dioxide nanoparticles and nanopolystyrene particles at environmentally relevant concentrations on nematodes *Caenorhabditis elegans*. *Ecotoxicol Environ Saf* 161:444–450
9. Xiao G-S, Zhao L, Huang Q, Yang J-N, Du H-H, Guo D-Q, Xia M-X, Li G-M, Chen Z-X, Wang D-Y (2018) Toxicity evaluation of Wanzhou watershed of Yangtze Three Gorges Reservoir in the flood season in *Caenorhabditis elegans*. *Sci Rep* 8:6734
10. Xiao G-S, Zhao L, Huang Q, Du H-H, Guo D-Q, Xia M-X, Li G-M, Chen Z-X, Wang D-Y (2018) Biosafety assessment of water samples from Wanzhou watershed of Yangtze Three Gorges Reservoir in the quiet season in *Caenorhabditis elegans*. *Sci Rep* 8:14102
11. Yin J-C, Liu R, Jian Z-H, Yang D, Pu Y-P, Yin L-H, Wang D-Y (2018) Di (2-ethylhexyl) phthalate-induced reproductive toxicity involved in DNA damage-dependent oocyte apoptosis and oxidative stress in *Caenorhabditis elegans*. *Ecotoxicol Environ Saf* 163:298–306
12. Xiao G-S, Zhi L-T, Ding X-C, Rui Q, Wang D-Y (2017) Value of *mir-247* in warning graphene oxide toxicity in nematode *Caenorhabditis elegans*. *RSC Adv* 7:52694–52701
13. Wu Q-L, Han X-X, Wang D, Zhao F, Wang D-Y (2017) Coal combustion related fine particulate matter (PM_{2.5}) induces toxicity in *Caenorhabditis elegans* by dysregulating microRNA expression. *Toxicol Res* 6:432–441
14. Wang Y, Xie W, Wang D-Y (2007) Transferable properties of multi-biological toxicity caused by cobalt exposure in *Caenorhabditis elegans*. *Environ Toxicol Chem* 26:2405–2412
15. Wang D-Y, Shen L-L, Wang Y (2007) The phenotypic and behavioral defects can be transferred from zinc exposed nematodes to their progeny. *Environ Toxicol Pharmacol* 24:223–230
16. Wang D-Y, Yang P (2007) The multi-biological defects caused by lead exposure exhibit transferable properties from exposed parents to their progeny in *Caenorhabditis elegans*. *J Environ Sci* 19:1367–1372
17. Wang D-Y, Wang Y (2008) Nickel sulfate induces numerous defects in *Caenorhabditis elegans* that can also be transferred to progeny. *Environ Pollut* 151:585–592
18. Kim SW, Kwak JI, An YJ (2013) Multigenerational study of gold nanoparticles in *Caenorhabditis elegans*: transgenerational effect of maternal exposure. *Environ Sci Technol* 47:5393–5399
19. Zhao Y-L, Lin Z-Q, Jia R-H, Li G-J, Xi Z-G, Wang D-Y (2014) Transgenerational effects of traffic-related fine particulate matter (PM_{2.5}) on nematode *Caenorhabditis elegans*. *J Hazard Mater* 274:106–114
20. Schultz CL, Wamuko A, Tsyusko OV, Unrine JM, Crossley A, Svendsen C, Spurgeon DJ (2016) Multigenerational exposure to silver ions and silver nanoparticles reveals heightened sensitivity and epigenetic memory in *Caenorhabditis elegans*. *Proc Biol Sci B* 283:20152911
21. Wu Q-L, Zhao Y-L, Li Y-P, Wang D-Y (2014) Molecular signals regulating translocation and toxicity of graphene oxide in the nematode *Caenorhabditis elegans*. *Nanoscale* 6:11204–11212
22. Yu Z, Chen X, Zhang J, Wang R, Yin D (2013) Transgenerational effects of heavy metals on L3 larva of *Caenorhabditis elegans* with greater behavior and growth inhibitions in the progeny. *Ecotoxicol Environ Saf* 88:178–184
23. Taki FA, Pan X, Zhang B (2013) Nicotine exposure caused significant transgenerational heritable behavioral changes in *Caenorhabditis elegans*. *EXCLI J* 12:793–806
24. Min H, Sung M, Son M, Kawasaki I, Shim YH (2017) Transgenerational effects of proton beam irradiation on *Caenorhabditis elegans* germline apoptosis. *Biochem Biophys Res Commun* 490:608–615

25. Buisset-Goussen A, Goussen B, Della-Vedova C, Galas S, Adam-Guillermin C, Lecomte-Pradines C (2014) Effects of chronic gamma irradiation: a multigenerational study using *Caenorhabditis elegans*. *J Environ Radioact* 137:190–197
26. Dong Zhou D, Yang J, Li H, Lu Q, Liu Y, Lin K (2016) Ecotoxicity of bisphenol A to *Caenorhabditis elegans* by multigenerational exposure and variations of stress response in vivo across generations. *Environ Pollut* 208:767–773
27. Taki FA, Pan X, Lee MH, Zhang B (2014) Nicotine exposure and transgenerational impact: a prospective study on small regulatory microRNAs. *Sci Rep* 4:7513
28. Zhi L-T, Fu W, Wang X, Wang D-Y (2016) ACS-22, a protein homologous to mammalian fatty acid transport protein 4, is essential for the control of toxicity and translocation of multi-walled carbon nanotubes in *Caenorhabditis elegans*. *RSC Adv* 6:4151–4159
29. Zhao Y-L, Yu X-M, Jia R-H, Yang R-L, Rui Q, Wang D-Y (2015) Lactic acid bacteria protects *Caenorhabditis elegans* from toxicity of graphene oxide by maintaining normal intestinal permeability under different genetic backgrounds. *Sci Rep* 5:17233
30. Liu Z-F, Zhou X-F, Wu Q-L, Zhao Y-L, Wang D-Y (2015) Crucial role of intestinal barrier in the formation of transgenerational toxicity in quantum dots exposed nematodes *Caenorhabditis elegans*. *RSC Adv* 5:94257–94266
31. Ni JZ, Kalinava N, Chen E, Huang A, Trinh T, Gu SG (2016) A transgenerational role of the germline nuclear RNAi pathway in repressing heat stress-induced transcriptional activation in *C. elegans*. *Epigenetics Chromatin* 9:3
32. Wu Q-L, Cao X-O, Yan D, Wang D-Y, Aballay A (2015) Genetic screen reveals link between maternal-effect sterile gene *mes-1* and *P. aeruginosa*-induced neurodegeneration in *C. elegans*. *J Biol Chem* 290:29231–29239
33. Yu Y-L, Zhi L-T, Guan X-M, Wang D-Y, Wang D-Y (2016) FLP-4 neuropeptide and its receptor in a neuronal circuit regulate preference choice through functions of ASH-2 trithorax complex in *Caenorhabditis elegans*. *Sci Rep* 6:21485
34. Sun L-M, Zhi L-T, Shakoor S, Liao K, Wang D-Y (2016) microRNAs involved in the control of innate immunity in *Candida* infected *Caenorhabditis elegans*. *Sci Rep* 6:36036
35. Sun L-M, Liao K, Li Y-P, Zhao L, Liang S, Guo D, Hu J, Wang D-Y (2016) Synergy between PVP-coated silver nanoparticles and azole antifungal against drug-resistant *Candida albicans*. *J Nanosci Nanotechnol* 16:2325–2335
36. Sun L-M, Liao K, Hong C-C, Wang D-Y (2017) Honokiol induces reactive oxygen species-mediated apoptosis in *Candida albicans* through mitochondrial dysfunction. *PLoS ONE* 12:e0172228
37. Sun L-M, Liao K, Wang D-Y (2017) Honokiol induces superoxide production by targeting mitochondrial respiratory chain complex I in *Candida albicans*. *PLoS ONE* 12:e0184003
38. Zhi L-T, Yu Y-L, Li X-Y, Wang D-Y, Wang D-Y (2017) Molecular control of innate immune response to *Pseudomonas aeruginosa* infection by intestinal *let-7* in *Caenorhabditis elegans*. *PLoS Pathog* 13:e1006152
39. Zhi L-T, Yu Y-L, Jiang Z-X, Wang D-Y (2017) *mir-355* functions as an important link between p38 MAPK signaling and insulin signaling in the regulation of innate immunity. *Sci Rep* 7:14560
40. Yu Y-L, Zhi L-T, Wu Q-L, Jing L-N, Wang D-Y (2018) NPR-9 regulates innate immune response in *Caenorhabditis elegans* by antagonizing activity of AIB interneurons. *Cell Mol Immunol* 15:27–37
41. Palominos MF, Verdugo L, Gabaldon C, Pollak B, Ortíz-Severín J, Varas MA, Chávez FP, Calixto A (2017) Transgenerational diapause as an avoidance strategy against bacterial pathogens in *Caenorhabditis elegans*. *MBio* 8:e01234–e01217
42. Yu C, Liao VH (2016) Transgenerational reproductive effects of arsenite are associated with H3K4 dimethylation and SPR-5 downregulation in *Caenorhabditis elegans*. *Environ Sci Technol* 50:10673–10681

43. Kishimoto S, Uno M, Okabe E, Nono M, Nishida E (2016) Environmental stresses induce transgenerationally inheritable survival advantages via germline-tosoma communication in *Caenorhabditis elegans*. *Nat Commun* 8:14031
44. Yang J, Chatterjee N, Kim Y, Roh J, Kwon J, Park M, Choi J (2018) Histone methylation-associated transgenerational inheritance of reproductive defects in *Caenorhabditis elegans* exposed to crude oil under various exposure scenarios. *Chemosphere* 200:358–365
45. Klosin A, Casas E, Hidalgo-Carcedo C, Vavouri T, Lehner B (2017) Transgenerational transmission of environmental information in *C. elegans*. *Science* 356:320–323
46. Frazier HN III, Roth MB (2009) Adaptive sugar provisioning controls survival of *C. elegans* embryos in adverse environments. *Curr Biol* 19:859–863
47. Burton NO, Furuta T, Webster AK, Kaplan REW, Baugh LR, Arur S, Horvitz HR (2017) Insulin-like signalling to the maternal germline controls progeny response to osmotic stress. *Nat Cell Biol* 19:252–257